Journal of Food Quality

Bioactive Food Components and their Chronic Diseases Prevention Effects 2021

Lead Guest Editor: Quancai Sun
Guest Editors: Ye Peng, Shengbao Cai, and Biao Yuan

Bioactive Food Components and their Chronic Diseases Prevention Effects 2021

Journal of Food Quality

Bioactive Food Components and their Chronic Diseases Prevention Effects 2021

Lead Guest Editor: Quancai Sun
Guest Editors: Ye Peng, Shengbao Cai, and Biao Yuan

Chief Editor

Associate Editors

Academic Editors

Contents

Contents

Hindawi
Journal of Food Quality
Volume 2022, Article ID 5797727, 10 pages
https://doi.org/10.1155/2022/5797727

Research Article

Phytochemical Compounds, Antioxidant, and Digestive Enzymes Inhibitory Activities of Different Fractions from *Ginkgo biloba L.* Nut Shells

Luo Liu,[1] **Yiyi Shang**,[1] **Yan Zhang**,[2] **and Mingjie Pang**[1,3]

[1]*The Affiliated Hospital of/College of Medical, Kunming University of Science and Technology, Department of Cardiology, The First People's Hospital of Yunnan Province, Kunming 650032, Yunnan, China*
[2]*Department of Magnetic Resonance Imaging, The First People's Hospital of Yunnan Province, The Affiliated Hospital of Kunming University of Science and Technology, Kunming 650032, Yunnan, China*
[3]*Department of Cardiology, The First People's Hospital of Yunnan Province, The Affiliated Hospital of Kunming University of Science and Technology, Kunming 650032, Yunnan, China*

Correspondence should be addressed to Mingjie Pang; mjpangkmust@163.com

Received 26 July 2021; Revised 4 September 2021; Accepted 21 September 2022; Published 6 October 2022

Academic Editor: Shengbao Cai

This study was designed to investigate the phytochemical compounds, antioxidant, and digestive enzymes inhibitory activities of the free (F), esterified (E), and insoluble-bound (IB) fractions from *Ginkgo biloba* L. nut shells. Results showed that a total of twelve compounds were detected in *G. biloba* nut shells by using UHPLC-ESI-HRMS/MS, including two kinds of organic acids, three kinds of phenolic acids, three kinds of flavonoids, and four kinds of terpene lactones. The F fraction contained all identified compounds and had the highest contents of the total phenolics and total flavonoids. All of the three different fractions exhibited good DPPH radical and ABTS radical cation scavenging activities and strong inhibitory effects on the generation of intracellular reactive oxygen species (ROS). Moreover, these three fractions also had good inhibitory effects towards α-glucosidase and pancreatic lipase. Among the three fractions, the F fraction possessed the strongest bioactivities. The findings obtained in the current study may provide some insights and bases for the further investigation and application of *G. biloba* nut shells in clinical medicine or the nutraceutical industry.

1. Introduction

Ginkgo biloba L., a mesozoic and valuable tree species, was widely cultivated in China. Ancient people knew that ginkgo nutlets are edible and possess benefits for the heart and lungs [1]. Modern studies have shown that the main active substances of ginkgo nut include ginkgo lactone, ginkgo flavonoids, and ginkgo phenolic acids [2, 3]. Among those phytochemicals, ginkgo lactones possess the effects of preventing platelet aggregation, delaying arteriosclerosis, and anti-inflammatory [4, 5]. Ginkgo phenolic acid has anti-inflammatory, antibacterial, and antitumor activities [6]. *G. biloba* extract is also reported to have neuroprotective effects [7]. *G. biloba* and its extracts are widely used in traditional Chinese medicine, daily health care, and clinical treatment nowadays [8]. With the extensive usage of gingko nutlets, the shells are not fully exploited and utilized, resulting in a great waste. A previous study confirmed that lignin in ginkgo nut shells exhibited outstanding antioxidant activity, even much higher than commercial antioxidants [9]. However, information about the phytochemical compounds and bioactivities of different fractions from *G. biloba* nut shells is scarce.

Recently, metabolic diseases, such as obesity, hypertension, hyperlipidemia, diabetes, and coronary heart disease, have risen rapidly and been a challenge around the world, which are related to unhealthy life habits and high-fat and high-carbohydrate dietary patterns [10]. As is well known, large amounts of carbohydrate and fat intake will contribute to the formation of fat, resulting in obesity and

diabetes [11]. Besides, these metabolic diseases are related to cell oxidative stress, which is also produced by excess fat and carbohydrate to some extent [12, 13]. For instance, oxidized low-density lipoprotein (ox-LDL) plays an important role in the formation of atherosclerotic plaque, which is produced by the oxidation of excessive free radicals in the body [14, 15]. Therefore, it is vital to control high-carbohydrate and high-fat intake and free radical generation in our daily life. Dietary fat and carbohydrate could only be absorbed after being hydrolyzed by the corresponding enzyme, and pancreatic lipase and α-glucosidase are the most important enzymes in this process [16, 17]. Inhibiting the activities of these two enzymes could effectively restrain or slow down the absorption of fat and carbohydrate, which are the action mechanisms of the clinical drugs of orlistat and acarbose, respectively. However, these two drugs possess side effects, which could not be ignored. Therefore, it is necessary to exploit some natural products that possess those bioactivities with few side effects. In this study, the digestive enzyme inhibitory activities and antioxidant activities of different extracts from *G. biloba* nut shells were investigated with the aim to provide a scientific basis for further exploiting the medicinal or nutraceutical value of *G. biloba* nut shells.

2. Materials and Methods

2.1. Materials and Chemical Reagents. Fresh *G. biloba* nuts were purchased from a local market in Kunming city, Yunnan Province, China. Human umbilical vein cell fusion cells (EA.hy926) were supplied by the Kunming Animal Research Institute (Kunming, Yunnan, China). 2,2-Diphenyl-1-picrylhydrazyl (DPPH), 2,2′-azino-bis (3-ethylbenzothiazoline-6- sulphonic acid) (ABTS), porcine pancreatic lipase (from porcine pancreas, 163 U/mg, EC: 3.1.1.3), α-glucosidase (from Saccharomyces cerevisiae, EC: 3.2.1.20; Type I, lyophilized powder, ≥10 units/mg protein), *p*-nitrophenyl laurate (purity ≥99.0%), *p*-nitrophenyl-α-D-glucopyranoside (pNPG, purity ≥99.0%), methylthiazol-2-yl-2,5- diphenyltetrazolium bromide (MTT), and 2′,7′-dichlorofluorescein diacetate (DCFH- DA, purity ≥97%) were obtained from Sigma (Sigma-Aldrich, Shanghai, China). Fetal bovine serum (FBS), streptomycin, penicillin, and Dulbecco's modified Eagle's medium (DMEM) were supplied by Gibco (Grand Island, NY). All of the other chemicals used in this study were of analytical grade.

2.2. Sample Extraction. Fresh *G. biloba* nuts were steamed for 30 min. The nut shells were manually gathered and lyophilized. The free (F), esterified (E), and insoluble-bound (IB) fractions of the nut shells were extracted by referring to the methods reported previously [18]. Briefly, the dried shells were powdered to pass through a 60-mesh sieve. Then, 50 g of shell powder was defatted by petroleum ether three times (1 : 5, w/v) and subsequently ultrasonically extracted with 250 mL of mixture solution of 70% acetone and 70% methanol (1 : 1, v/v) for 30 min at room temperature. After the centrifugation, the supernatant phase was used to extract F and *E* fractions, and the residue was used to extract the IB fraction. For the extraction of F and E fractions, the supernatant phase was evaporated by using a rotary evaporator (Hei-VAP, Heidolph, Germany) at 40°C to get an aqueous phase. After adjusting the aqueous phase to pH 2 by 6 MHCl, the aqueous phase was extracted three times with diethyl ether-ethyl acetate (1 : 1, v/v). After being evaporated and lyophilized in the diethyl ether-ethyl acetate phase, the F fraction was obtained. The remaining aqueous phase was added 4 M of NaOH (1 : 10 v/v) to hydrolyze at room temperature for 4 h; the following operation was similar to that of F, and the E fraction was obtained. For the extraction of the IB fraction, the remained residue was hydrolyzed with 4 M of NaOH (1 : 10, v/v) for 4 h at room temperature. After centrifugation, the supernatant was adjusted to pH 2, and the following operation was the same as that of the F fraction to get the IB fraction.

2.3. Determination of the Total Phenolic and Total Flavonoid Contents. The total phenolic contents (TPCs) and total flavonoid contents (TFCs) of different fractions from *G. biloba* nut shells were measured according to the previous methods [19]. In brief, all freeze-dried samples were dissolved separately in 80% methanol. For TPC measurement, the reaction mixture was recorded at 765 nm by using a Spectra Max M5 reader (Molecular Device, Sunnyvale, CA, USA). TPCs were expressed as mg gallic acid equivalent (GAE)/g of dry extract. When determining TFC, the absorbance of the reaction solution was measured at 510 nm. TFCs were displayed as mg rutin equivalent (RE)/g of dry extract.

2.4. Phytochemical Identification with UHPLC-ESI-HRMS/MS. The phytochemicals in the three fractions were identified by using a Thermo Fisher Ultimate 3000 system with a Thermo Fisher Scientific Q-Exactive Orbitrap mass spectrometer (Bremen, Germany) in the negative mode. Phytochemicals were separated by using an Agilent Zorbax SB-C18 column (2.1 × 100 mm, 1.7 μm). Acidified water (0.1% formic acid) and acetonitrile were used as the mobile phases A and B, respectively, and the elution gradient was as follows: 0–2 min, 5% B; 2–20 min, 5%–50% B; 20–30 min, 50%–70% B; 30–32 min, 70% B; 32–34 min, 70%–5% B; and 34–40 min, 5% B. The injection volume and the flow rate were 3.0 μL and 0.2 mL/min, respectively, and the column temperature was set at 30°C. The mass spectrometry conditions were the same as in the previous study [20].

2.5. DPPH Radical and ABTS Radical Cation Scavenging Activities. DPPH radical and ABTS radical cation scavenging activities of all fractions were determined according to a previously reported method [21, 22]. The optical density (OD) value was measured by using a Spectra Max M5 reader at 517 nm and 745 nm, respectively. Each scavenging activity was calculated by using the following formula: DPPH radical or ABTS radical cation scavenging ratio (%) = $[(OD_{control}-OD_{sample})/OD_{control}] \times 100\%$.

2.6. Inhibition on H2O2-Induced Intracellular Reactive Oxygen Species (ROS) Production in EA.hy926 Cells. The measurement of intracellular ROS in EA.hy926 triggered by H2O2 was conducted according to a method reported earlier [23] with a slight modification. Cells were seeded in a 6-well plate at 2.0×10^5 cells per well. After being cultivated for 24 hours, 200 μL of fresh DMEM containing 50 μg/mL of the sample and 10 μg/mL of vitamin C (Vc) were added into the corresponding well, and the cells in the control group (CK) and the H_2O_2 group were still cultured in fresh DMEM. All groups were incubated for another 24 hours. Then, 1.0 mM H_2O_2 was added to groups of H2O2, Vc, F, E, and IB for 5 hours. Thereafter, cells were washed, harvested, and labeled with DCFH-DA. Finally, the fluorescence of each group was detected with a flow cytometer (Guava easy Cyte 6-2L, Millipore, Billerica, USA). The content of intracellular ROS in CK was regarded as 100%.

2.7. Determination of α-Glucosidase Inhibition. The inhibitory abilities of the three fractions against α-glucosidase were evaluated as per the previously reported method [24] with a minor modification. In brief, 10 μL of α-glucosidase (200 μg/mL) and 10 μL of sample solution were mixed with 110 μL of phosphate buffer saline (pH 6.8) and incubated for 30 min at 37°C. Then, 20 μL of pNPG (2.5 mM) was added as a substrate and incubated for another 30 min at 37°C. The reaction was stopped by adding 60 μL of Na_2CO_3 (0.2 mol/L). A reaction mixture without a sample was used as a control. The OD value of each reaction mixture was measured by using a Spectra Max M5 reader at 405 nm. The inhibition ratio (%) was calculated as follows: $[(OD_{control}\text{-}OD_{sample})/OD_{control}] \times 100\%$.

2.8. Determination of Pancreatic Lipase Inhibition. The inhibitory effects of the three fractions against pancreatic lipase were evaluated according to the previously reported method [25]. Briefly, 100 mM of Tris buffer (pH 8.2) and 0.1% of *p*-nitrophenyl laurate were used as reaction buffer and substrate, respectively. A sample (100 μL) with appropriate concentrations was mixed with reaction buffer (200 μL) and the substrate (250 μL), and then, lipase solution (50 μL) was added to start the reaction. The reaction mixture without a sample was used as a control. All reaction mixtures were incubated at 37°C for 120 minutes. The OD value of each reaction mixture was measured by using a Spectra Max M5 reader at 400 nm. The inhibition of pancreatic lipase activity (%) was calculated as follows: $[(OD_{control}\text{-}OD_{sample})/OD_{control}] \times 100\%$.

2.9. Statistical Analysis. Each experiment was carried out at least three times. The data are expressed as mean ± standard deviation (SD) and analyzed with Origin 8.5 software (OriginLab, Northampton, Massachusetts, USA). The significant differences between groups were analyzed by one-way ANOVA with the Tukey test ($p < 0.05$).

3. Results and Discussion

3.1. TPCs and TFCs of Different Fractions. TPCs and TFCs of all fractions in *G. biloba* nut shells are summarized in Table 1. For TPCs, the F fraction had the highest content, followed by the E fraction, while the IB fraction contained the lowest content of phenolic compounds ($p < 0.05$). The TPC in the F fraction was almost four times higher than that in the IB fraction. A similar phenomenon was also observed in TFCs. The F fraction contained the highest TFC, followed by the E fraction, and the IB fraction had the lowest TFC ($p < 0.05$). Moreover, the TFC in the F fraction was approximately five times higher than that in the IB fraction. A previous study also reported that the free fraction of *Rhus chinensis* Mill. fruits had the highest content of phenolic compounds among three different fractions [18]. Previous studies confirmed that the different extracts from leaves of *G. biloba* are rich in polyphenols and flavonol glycosides [26, 27]. The present results indicated that *G. biloba* nut shells may be a good source of dietary phenolic compounds.

3.2. Characterization of Phytochemical Compounds. The phytochemical compounds in each fraction of *G. biloba* nut shells were characterized by UHPLC-ESI-HRMS/MS, and the results are presented in Figure 1 and Table 2. In the current work, phytochemical compounds in each fraction were characterized by comparing their mass data with the corresponding commercial standard or with the available data reported earlier. Figure 1 and Table 2show that a total of 12 phytochemical substances were identified, including two organic acids (peaks **1** and **2**), three kinds of phenolic acids (peaks **3**, **4**, and **5**), three kinds of flavonoids (peaks **6**, **7**, and **9**), and four kinds of terpene lactones (peaks **8**, **10**, **11**, and **12**). Among the three fractions, the F fraction was found to contain all of those 12 phytochemical compounds, while both of the E and IB fractions only had six substances. A previous study also confirmed that some flavonoid glycosides, such as derivatives of quercetin, kaempferol, and isorhamnetin, were detected in the extract of *G. biloba* leaves [27]. Ginkgolides are the characteristic phytochemical compounds of *G. biloba*, and in the current work, four different ginkgolides were detected, namely, ginkgolide C (peak **8**), bilobalide (peak **10**), ginkgolide A (peak **11**), and ginkgolide B (peak **12**). A previous study reported that ginkgolide B, isolated from the leaves and root bark of *G. biloba*, exhibited good antioxidant, anti-inflammatory, and other activities with potential capacities to prevent many diseases [28]. Ginkgolide C has been considered to possess a potential capacity to inhibit adipogenesis in adipocytes, thereby improving metabolic syndrome [29].

In addition, according to Figure 1, the F fraction almost contained the most abundant phytochemical compounds. Therefore, the relative content of each substance in *E* and IB fractions was compared with that in the F fraction (set as 100%) based on the peak area. Table 1shows that IB possessed the highest gluconic acid content ($p < 0.05$). For the malic acid content, the *E* and IB fractions accounted for about 55.65% and 62.55% of that in the F fraction,

Table 1: Total phenolic contents (TPCs) and total flavonoid contents (TFCs) of different fractions from *Ginkgo biloba* L. nut shells.

	F	E	IB
Total phenolic contents (mg gallic acid/g dry extract)	443.64 ± 1.99^{a}	152.85 ± 1.03^{b}	112.86 ± 0.58^{c}
Total flavonoid contents (mg rutin/g dry extract)	190.49 ± 1.50^{a}	61.91 ± 0.02^{b}	41.98 ± 0.15^{c}

All values are expressed as mean ± S.D. ($n = 3$). Different letters in the same row indicate significant differences at the $p < 0.05$ level.

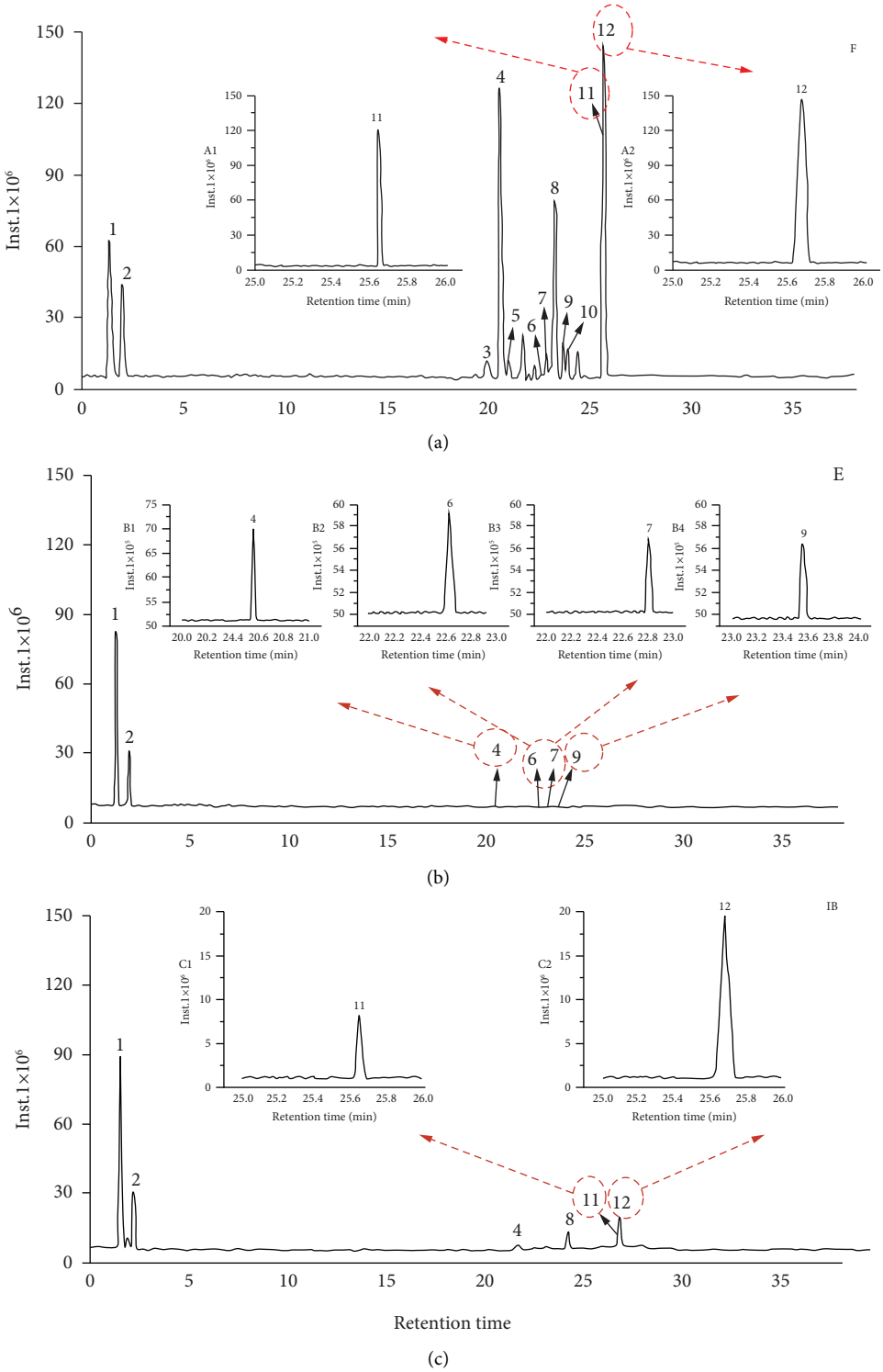

Figure 1: Base peak and extracted ion chromatograms of phytochemical compounds in different fractions of *Ginkgo biloba L.* nut shells. F: free fraction (a); E: esterified fraction (b); IB: insoluble-bound fraction (c). Peak identification and their MS data are shown in Table 2.

Table 2: Characterization of phytochemical compounds in three different fractions of *Ginkgo biloba* L. nut shells.

Peak no.	Compounds	Rt[a] (min)	[M-H]− m/z	Molecular formula	MS/MS fragment ions	Fractions (%)[b]			References
						F	E	IB	
1	Gluconic acid	1.48	195.0506	$C_6H_{12}O_7$	75.0074 (100), 129.0191 (9.37)	100	233.03	262.55	[30]
2	Malic acid	2.12	133.0132	$C_4H_6O_5$	71.0125 (100),72.9918 (74.75)	100	55.65	62.55	[31]
3	4-Hydroxybenzoic acid	19.90	137.0235	$C_7H_6O_3$	99.0334 (100)	100	ND	ND	Standard
4	Eucomic acid	20.56	239.0562	$C_{11}H_{12}O_6$	107.0493 (100), 133.0649(27.46)	100	4.67	7.94	[32]
5	Caffeic acid	21.00	179.0344	$C_9H_7O_4$	134.0364 (100), 135.0445(63.69)	100	ND	ND	Standard
6	Kaempferol-3-*O*-2″-glucosylrhamnoside	22.69	593.1525	$C_{15}H_{18}O_8$	285.0406(100)	100	42.02	ND	[33]
7	Isorhamnetin-3-*O*-rutinoside	22.82	623.1632	$C_{46}H_{23}O_{11}$	315.0514 (100), 314.0438(40.51)	100	12.03	ND	Standard
8	Ginkgolide C	23.27	439.1252	$C_{20}H_{24}O_{11}$	383.0127(88.75),365.9188(11.54)	100	ND	20.48	[33]
9	Quercetin-3-*O*-2″-(6″-*p*-coumaroyl) glucosylrhamnoside	23.55	755.1846	$C_{36}H_{36}O_{18}$	609.1474(100), 301.0341(22.03)	100	18.32	ND	[33]
10	Bilobalide	23.63	325.0935	$C_{15}H_{18}O_8$	163.1121(100)	100	ND	ND	[34]
11	Ginkgolide A	25.65	407.1353	$C_{20}H_{24}O_9$	245.1550 (11.73)	100	ND	6.54	[34]
12	Ginkgolide B	25.67	423.1204	$C_{20}H_{24}O_{10}$	113.0233(89.76)	100	ND	14.21	[34]

[a]Rt: retention time; [b]ND: no detected; the peak areas of each compound in *E* and IB fractions were normalized with that in the F fraction (100%).

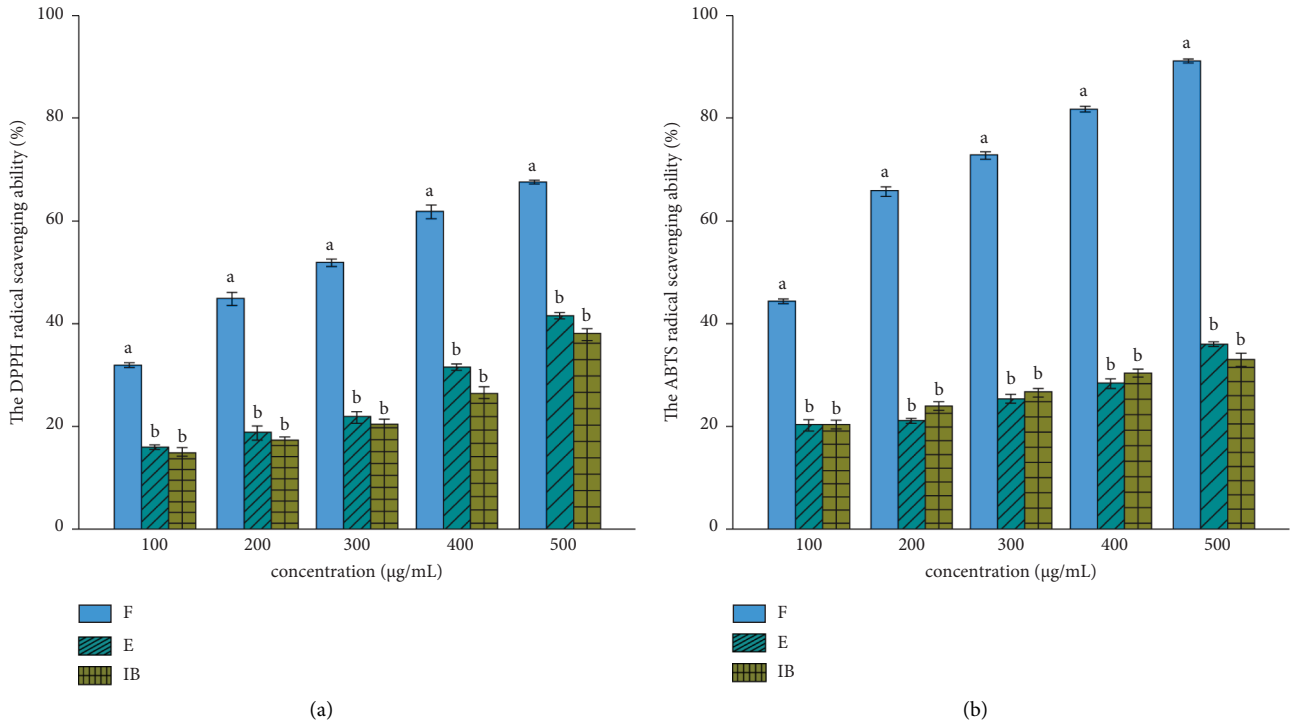

Figure 2: DPPH radical (a) and ABTS radical cation (b) scavenging activities of three fractions of *Ginkgo biloba L.* nut shells. All values are expressed as mean ± S.D. $n = 3$. Different letters at the same concentration indicate significant differences at the $p < 0.05$ level. F: free fraction; E: esterified fraction; IB: insoluble-bound fraction.

respectively. The content of eucomic acid in the E and IB fractions accounted for approximately 4.67% and 7.94% of that in the F fraction, respectively. The relative content of isorhamnetin-3-O-rutinoside, which was not detected in the IB fraction, in the E fraction accounted for about 12.03% of that in the F fraction. For four ginkgolides, only ginkgolide B and ginkgolide C were detected in the IB and accounted for about 20.48% and 14.21% of that in the F fraction, respectively.

3.3. Antioxidant Capacity

3.3.1. DPPH Radical Scavenging Activity. The DPPH radical scavenging abilities of the three different fractions of *G. biloba* nut shells are shown in Figure 2(a). All fractions exhibited good DPPH radical scavenging capacities in a dose-dependent manner. Among three fractions, the F fraction possessed the strongest DPPH radical scavenging activity at each tested concentration ($p < 0.05$), while the E

and IB fractions had similar scavenging activity without a significant difference at each tested concentration ($p > 0.05$). The half-maximal inhibitory concentration (IC_{50}) values of the F, E, and IB fractions were 273.57 ± 20.56, 573.18 ± 43.99, and $635.44 \pm 11.68\,\mu$g/mL, respectively. Pearson's correlation analysis between the phenolic contents and DPPH radical scavenging activities indicated that the phenolic contents of the three fractions were closely related to their DPPH radical scavenging ratios ($r = 0.84$, $p < 0.05$). Vc, used as the positive control in this study, possessed the lowest IC_{50} value of $6.43 \pm 0.17\,\mu$g/mL. This result was inconsistent with that of the previous study that the insoluble-bound fraction of palm oil possessed the strongest antioxidant activity [35]. This phenomenon occurs due to their different phytochemical compositions.

3.3.2. ABTS Radical Cation Scavenging Activity. The ABTS radical cation scavenging abilities of three different fractions of *G. biloba* nut shells are shown in Figure 2(b). The overall trend of scavenging capacities was similar to that of DPPH radical. All three fractions also exhibited good ABTS radical cation scavenging capacities in a dose-dependent manner. The F fraction had the strongest ABTS radical cation scavenging activity ($p < 0.05$), followed by the E fraction and IB fraction, and the latter two fractions had no significant difference with each other ($p > 0.05$). The IC_{50} values of the F, E, and IB fractions were 273.57 ± 20.56, 573.18 ± 43.99, and $635.44 \pm 11.68\,\mu$g/mL, respectively. Pearson's correlation analysis between the phenolic contents and ABTS radical cation scavenging activities also indicated that the phenolic contents of the three fractions significantly contributed to their ABTS radical cation scavenging ratios ($r = 0.97$, $p < 0.05$). The IC_{50} value of Vc, used as a positive control, was $8.68 \pm 0.25\,\mu$g/mL in the current work. A previous study also showed that three different fractions of *Rhus chinensis* Mill. fruits exhibited good scavenging activities against ABTS radical cation, and the free fraction was the strongest [18], which was consistent with the current work.

3.3.3. Inhibitory Effect on Intracellular ROS Generation. Overproduction of intracellular ROS will lead to tissue or organ damage in the organism and cause many chronic diseases [36]. H_2O_2, which could pass through the cell membrane and generate free radicals, was normally used as an ROS generator. A previous study has confirmed that H_2O_2 could induce an increase in the ROS level to trigger oxidative stress in EA.hy926 cells [23]. Therefore, the H_2O_2-induced oxidative damaged cell model in EA.hy926 cells was used in this study, and the inhibitory effects of different fractions of *G. biloba* nut shells on intracellular ROS generation are shown in Figure 3. The intracellular ROS level of the H_2O_2 group was more than 1.5 times that of the control group (CK), indicating that the H_2O_2-induced oxidative model was successfully established in EA.hy926 cells by 0.8 mM of H_2O_2. Compared with the H_2O_2 group, all samples could significantly inhibit intracellular ROS production ($p < 0.05$). Among the three samples, the F fraction displayed the strongest inhibition on intracellular ROS generation at $50.0\,\mu$g/mL ($p < 0.05$), which was similar with Vc at $10.0\,\mu$g/mL ($p > 0.05$). The E fraction and the IB fraction exhibited a similar inhibition with no significant difference ($p > 0.05$). Previous studies have also reported that both phenolic compounds of grapefruit peels and *Astragalus* polysaccharide had good inhibitory effects on intracellular ROS generation in EA.hy926 cells [37, 38].

3.4. α-Glucosidase Inhibitory Activities. α-Glucosidase, one of the most vital carbohydrate digestive enzymes, catalyzes the hydrolysis of dietary starch into simple sugars for absorption, resulting in the increase of the postprandial blood glucose level. Inhibiting the activities of α-glucosidase could control the postprandial blood glucose level effectively, which is one of the important mechanisms of the clinical drug, acarbose [39]. Results of inhibitory effects of the different fractions of *G. biloba* nut shells on α-glucosidase are shown in Figure 4. The inhibitory effects of three different fractions on α-glucosidase are all in a dose-dependent manner. Among the three fractions, the F fraction possessed the strongest inhibitory capacity with an IC_{50} value of $434.03 \pm 22.57\,\mu$g/mL ($p < 0.05$). The IC_{50} values of the *E* and IB fractions are 629.87 ± 15.37 and $644.76 \pm 12.62\,\mu$g/mL, respectively. In addition, Pearson's correlation analysis showed a positive correlation between the TPCs and the inhibition rate of α-glucosidase ($r = 0.583$, $p < 0.05$), indicating that the phenolic compounds in *G. biloba* nut shells may be the main bioactive compounds for inhibiting the α-glucosidase activity. Previous literature also found that phenolic compounds may be the main contributor to the inhibitory activity of α-glucosidase [40, 41]. For example, a high correlation between the phenolic contents and α-glucosidase inhibitory ratios was observed in *Prinsepia utilis* Royle fruits [40]. Another study also observed a strong correlation between the total phenolic content and α-glucosidase inhibitory activity of the extracts of *G. biloba* leaf [41]. Acarbose, the clinical drug as a α-glucosidase inhibitor, was used as the positive control in this study and possessed the lowest IC_{50} value of $0.21 \pm 0.02\,\mu$g/mL.

3.5. Pancreatic Lipase Inhibitory Activities of the Three Fractions. Pancreatic lipase, the most important enzyme that hydrolyzes dietary fat, makes triglycerides degradation into diglycerides, monoglycerides, glycerols, and fatty acids [42]. Inhibiting the activities of pancreatic lipase could effectively reduce the absorption of dietary fat, thereby reducing the incidence of some cardiovascular diseases, such as hyperlipidemia. The inhibition results of three fractions of *G. biloba* nut shells against pancreatic lipase are presented in Figure 4. Figure 4shows that three different fractions of *G. biloba* nut shells possess strong inhibitory effects against pancreatic lipase, and inhibitory capacities gradually upgraded with the increased concentrations. The inhibitory effect of the F fraction was much stronger than that of the E fraction and IB fraction ($p < 0.05$). The inhibitory effects of E and IB fractions did not have significant difference with each other at each tested concentration ($p > 0.05$). At the

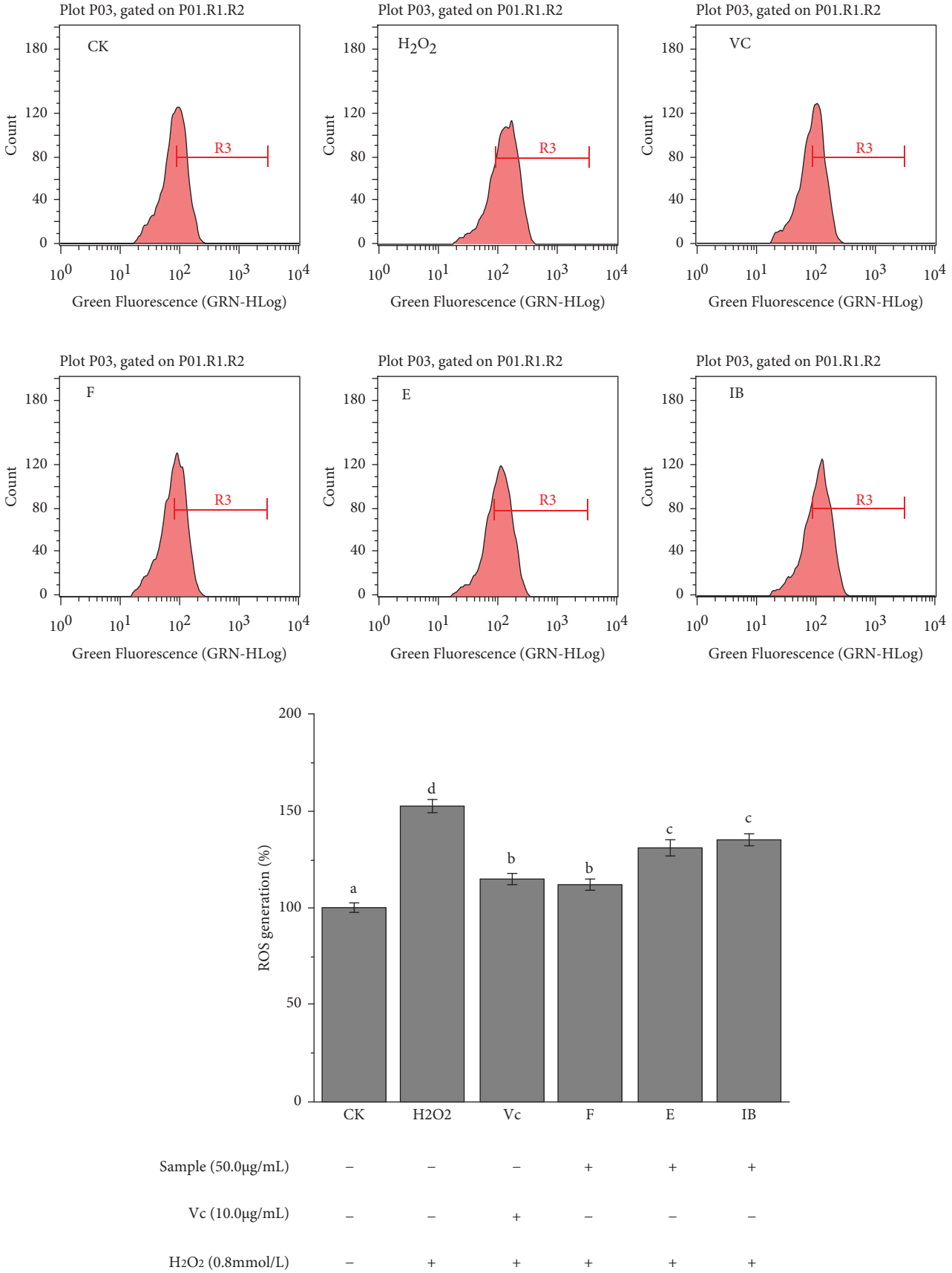

Figure 3: Inhibitory effects of three fractions of *Ginkgo biloba L.* nut shells on intracellular ROS production of H_2O_2-induced EA.hy926. All values are expressed as mean ± S.D. ($(n) = 3$). Different letters indicate significant differences at the $p < 0.05$ level. CK: control group; H_2O_2: H_2O_2-induced group; Vc: positive group; F: free fraction; E: esterified fraction; IB: insoluble-bound fraction.

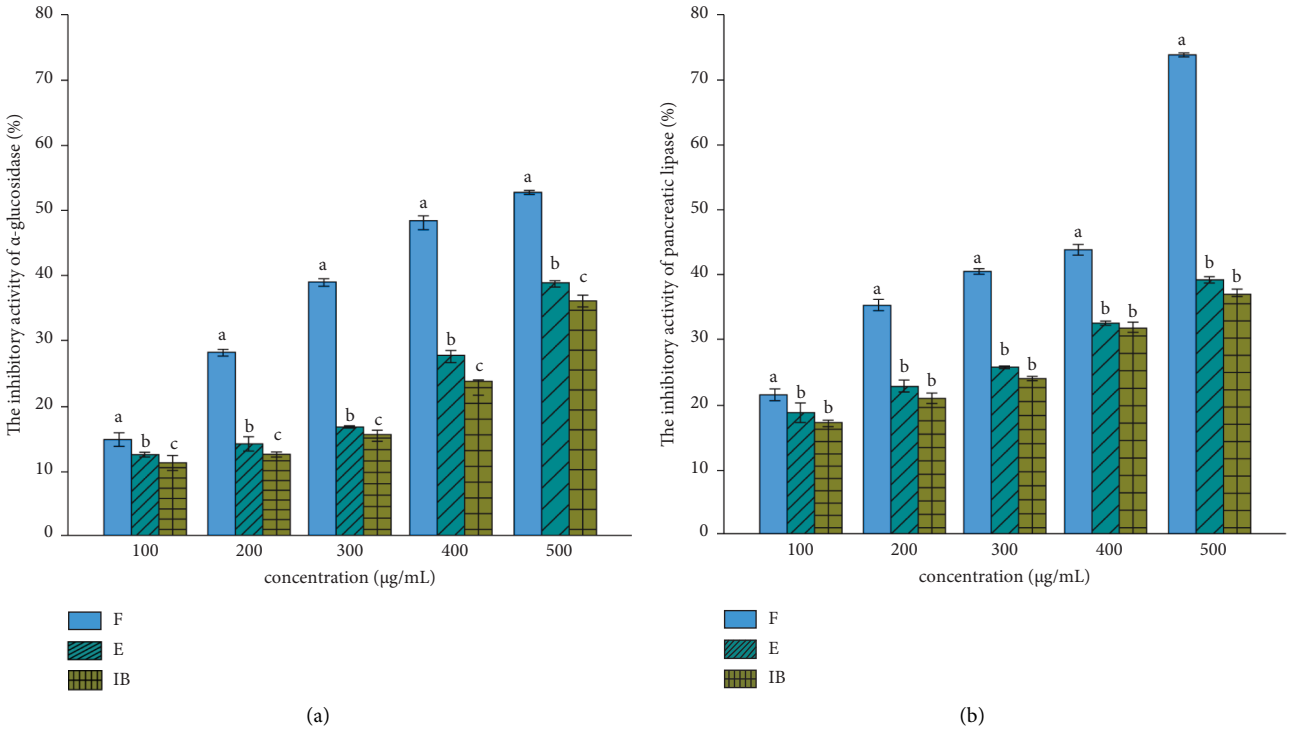

Figure 4: The inhibitory activities of the different fractions of *Ginkgo biloba L.* nut shells towards α-glucosidase (a) and pancreatic lipase (b). All values are expressed as mean ± S.D. ($(n) = 3$). Different letters indicate significant differences at the $p < 0.05$ level. F: free fraction; E: esterified fraction; IB: insoluble-bound fraction.

maximum concentration in the experiment, the pancreatic lipase inhibition rate of the F fraction was more than 70%. IC_{50} values of F, E, and IB fractions were 386.62 ± 18.91, 621.69 ± 18.28, and 668.04 ± 28.04 μg/ml, respectively. Moreover, Pearson analysis was used to measure the correlation coefficient between the TPCs and lipase inhibitory abilities of three fractions, and the result exhibited a good positive correlation between the two parameters ($r = 0.94$, $p < 0.05$), suggesting that phenolic compounds may play a crucial role in pancreatic lipase inhibition. Many previous studies have shown that plants with high content of polyphenols have good lipase inhibitory effects, such as Chinese sumac (*Rhus chinensis* Mill.) fruits [18] and *Prinsepia utilis* Royle fruits [34], which were consistent with the finding of this study. Orlistat, a positive control, had the lowest IC_{50} value of 35.47 ± 1.26 μg/mL.

4. Conclusions

This study analyzed phytochemical compounds in different fractions of *G. biloba* nut shells and their antioxidant and digestive enzymes inhibitory activities. The TPCs and TFCs of the F fraction were significantly higher than those of the E and IB fractions. Twelve different phytochemical compounds were identified by LC-MS. The three fractions had good DPPH radical and ABTS radical cation scavenging activities, and the F fraction exhibited the strongest activity, followed by the E and IB fractions. The F fraction also showed the strongest effect on inhibiting the generation of intracellular ROS. Moreover, results displayed that the three fractions had good inhibitory effects towards α-glucosidase and pancreatic lipase, and the F fraction had the strongest inhibitory capacities. A positive correlation between TPCs and digestive enzyme inhibitions implied that the phenolic compounds in *G. biloba* nut shells might be the main bioactive compounds. These findings may provide insights and bases for the further application of *G. biloba* nut shells in clinical medicine or the nutraceutical industry.

Data Availability

All data included in this study are available upon request from the corresponding author.

Conflicts of Interest

The authors declare that there are no conflicts of interest regarding the publication of this article.

Authors' Contributions

Luo Liu and Yiyi Shang contributed equally to this work.

Acknowledgments

This work was financially supported by the famous doctor project of the "Ten Thousand People Plan" in Yunnan Province (Grant No. YNWR-MY-2020-017) and the National Natural Science Foundation of China (Grant no. 82160079).

References

[1] F. Lang, R. Hoerr, M. Noeldner, and E. Koch, "Ginkgo biloba extract EGb 761®: from an ancient Asian plant to a modern European herbal medicinal product," *Evidence and Rational Based Research on Chinese Drugs*, pp. 431–470, Springer, Berlin, Germany, 2013.

[2] J. L. Luo, F. L. Lu, Y. C. Liu, and Y. C. Shih, "Fingerprint analysis of Ginkgo biloba extract and Ginkgo semen in preparations by LC-Q-TOF/MS," *Journal of Food and Drug Analysis*, vol. 21, pp. 27–39, 2013.

[3] P. Chen, M. Ozcan, and J. Harnly, "Chromatographic fingerprint analysis for evaluation of Ginkgo biloba products," *Analytical and Bioanalytical Chemistry*, vol. 389, no. 1, pp. 251–261, 2007.

[4] A. K. Dutta-Roy, M. J. Gordon, C. Kelly et al., "Inhibitory effect of Ginkgo biloba extract on human platelet aggregation," *Platelets*, vol. 10, no. 5, pp. 298–305, 1999.

[5] K. J. Chen, "Chinese expert consensus on clinical application of oral ginkgo biloba preparations," *Chinese Journal of Integrative Medicine*, vol. 27, no. 3, pp. 163–169, 2021.

[6] S. H Jujm and S. H. Qian, "Dynamic changes of the total ginkgolic acid in ginkgo biloba leaf from different growing seasons," *Chinese Traditional and Herbal Drugs*, vol. 41, no. 2, pp. 305–307, 2010.

[7] B. Ahlemeyer and J. Krieglstein, "Neuroprotective effects of Ginkgo biloba extract," *Cellular and Molecular Life Sciences*, vol. 60, no. 9, pp. 1779–1792, 2003.

[8] T. Isah, "Rethinking *Ginkgo biloba L.*: medicinal uses and conservation," *Pharmacognosy Reviews*, vol. 9, no. 18, p. 140, 2015.

[9] B. Jiang, H. Chen, H. Zhao, W. Wu, and Y. Jin, "Structural features and antioxidant behavior of lignins successively extracted from ginkgo shells (Ginkgo biloba L)," *International Journal of Biological Macromolecules*, vol. 163, pp. 694–701, 2020.

[10] E. E. Canfora, R. CR. Meex, K. Venema, and E. E. Blaak, "Gut microbial metabolites in obesity, NAFLD and T2DM," *Nature Reviews Endocrinology*, vol. 15, no. 5, pp. 261–273, 2019.

[11] X. Liu, J. Shi, J. Yi, X. Zhang, Q. Ma, and S. Cai, "The effect of in vitro simulated gastrointestinal digestion on phenolic bioaccessibility and bioactivities of Prinsepia utilis Royle fruits," *LWT*, vol. 138, Article ID 110782, 2021.

[12] V. Rani, G. Deep, R. K. Singh, K. Palle, and U. C. Yadav, "Oxidative stress and metabolic disorders: pathogenesis and therapeutic strategies," *Life Sciences*, vol. 148, pp. 183–193, 2016.

[13] J. Zhu and C. B. Thompson, "Metabolic regulation of cell growth and proliferation," *Nature Reviews Molecular Cell Biology*, vol. 20, no. 7, pp. 436–450, 2019.

[14] A. J. Kattoor, N. V. K. Pothineni, D. Palagiri, and J. L. Mehta, "Oxidative stress in atherosclerosis," *Current Atherosclerosis Reports*, vol. 19, no. 11, p. 42, 2017.

[15] D. A. Chistiakov, A. N. Orekhov, and Y. V. Bobryshev, "LOX-1-mediated effects on vascular cells in atherosclerosis," *Cellular Physiology and Biochemistry*, vol. 38, no. 5, pp. 1851–1859, 2016.

[16] Q. You, F. Chen, X. Wang, Y. Jiang, and S. Lin, "Anti-diabetic activities of phenolic compounds in muscadine against alpha-glucosidase and pancreatic lipase," *LWT—Food Science and Technology*, vol. 46, no. 1, pp. 164–168, 2012.

[17] R. Sultana, A. M. Alashi, K. Islam, M. Saifullah, C. E. Haque, and R. E. Aluko, "Inhibitory activities of polyphenolic extracts of Bangladeshi vegetables against α-amylase, α-glucosidase, pancreatic lipase, renin, and angiotensin-converting enzyme," *Foods*, vol. 9, no. 7, p. 844, 2020.

[18] C. Zhang, Y. Ma, F. Gao, Y. Zhao, S. Cai, and M. Pang, "The free, esterified, and insoluble-bound phenolic profiles of Rhus chinensis Mill. fruits and their pancreatic lipase inhibitory activities with molecular docking analysis," *Journal of Functional Foods*, vol. 40, pp. 729–735, 2018.

[19] J. Zhou, Y. Ma, Y. Jia, M. Pang, G. Cheng, and S. Cai, "Phenolic profiles, antioxidant activities and cytoprotective effects of different phenolic fractions from oil palm (*Elaeis guineensis* Jacq.) fruits treated by ultra-high pressure," *Food Chemistry*, vol. 288, pp. 68–77, 2019.

[20] Q. Ma, S. B. Cai, Y. Jia, X. Sun, J. Yi, and J. Du, "Effects of hot-water extract from vine tea (Ampelopsis grossedentata) on acrylamide formation, quality and consumer acceptability of bread," *Foods*, vol. 9, no. 3, p. 373, 2020.

[21] I. Sedej, M. Sakač, A. mandic, A. Misan, V. Tumbas, and J. Canadanovic-Brunet, "Buckwheat (*Fagopyrum esculentum* Moench) grain and fractions: antioxidant compounds and activities," *Journal of Food Science*, vol. 77, no. 9, pp. 954–C959, 2012.

[22] R. Re, N. Pellegrini, A. Proteggente, A. Pannala, M. Yang, and C. Rice-Evans, "Antioxidant activity applying an improved ABTS radical cation decolorization assay," *Free Radical Biology and Medicine & Medicine*, vol. 26, pp. 1231–1237, 1999.

[23] F. Jia, L. Mou, and H. Ge, "RETRACTED: protective effects of ginsenoside Rb1 on H_2O_2-induced oxidative injury in human endothelial cell line (EA.hy926) via miR-210," *International Journal of Immunopathology & Pharmacology*, vol. 33, Article ID 205873841986602, 2019.

[24] A. B. Justino, N. C. Miranda, R. R. Franco, M. M. Martins, N. Md Silva, and F. S. Espindola, "Annona muricata Linn. leaf as a source of antioxidant compounds with in vitro antidiabetic and inhibitory potential against -amylase, -glucosidase, lipase, non-enzymatic glycation and lipid peroxidation," *Biomedicine & Pharmacotherapy*, vol. 100, pp. 83–92, 2018.

[25] S. B. Cai, O. Wang, M. Wang et al., "In vitro inhibitory effect on pancreatic lipase activity of subfractions from ethanol extracts of fermented oats (*avena sativa L.*) and synergistic effect of three phenolic acids," *Journal of Agricultural and Food Chemistry*, vol. 60, no. 29, pp. 7245–7251, 2012.

[26] J. Kobus, E. Flaczyk, A. Siger, M. Nogala-Kalucka, J. Korczak, and R. B. Pegg, "Phenolic compounds and antioxidant activity of extracts of Ginkgo leaves," *European Journal of Lipid Science and Technology*, vol. 111, no. 11, pp. 1150–1160, 2009.

[27] T. A. van Beek and P. Montoro, "Chemical analysis and quality control of Ginkgo biloba leaves, extracts, and phytopharmaceuticals," *Journal of Chromatography A*, vol. 1216, no. 11, pp. 2002–2032, 2009.

[28] S. H. Xia and D. C. Fang, "Pharmacological action and mechanisms of ginkgolide B," *Chinese Medical Journal*, vol. 120, no. 10, pp. 922–928, 2007.

[29] L. Chian-Jiun, X. Y. Lai, Y. L. Chen, C. L. Wang, C. H. Wei, and W. C. Huang, "Ginkgolide C suppresses adipogenesis in 3T3-L1 adipocytes via the AMPK signaling pathway," *Evidence-Based Complementary and Alternative Medicine*, vol. 201510 pages, 2015.

[30] F. Piana, M. Ciulu, R. Quirantes-Piné et al., "Simple and rapid procedures for the extraction of bioactive compounds from Guayule leaves," *Industrial Crops and Products*, vol. 116, pp. 162–169, 2018.

[31] J. Y. Zhong, N. Chen, S. Huang et al., "Chemical profiling and discrimination of green tea and Pu-erh raw tea based on

UPLC–Q–Orbitrap–MS/MS and chemometrics," *Food Chemistry*, vol. 326, Article ID 126760, 2020.

[32] S. S. El-Hawary, H. A. El-Kammar, M. A. Farag, D. O. Saleh, and R. S. El Dine, "Metabolomic profiling of five Agave leaf taxa via UHPLC/PDA/ESI-MS inrelation to their anti-inflammatory, immunomodulatory and ulceroprotective activities," *Steroids*, vol. 160, Article ID 108648, 2020.

[33] L. Guo, L. L. Dou, L. Duan et al., "Comprehensive analysis of chemical constituents in Xingxiong injection by high performance liquid chromatography coupled with mass spectrometry," *Chinese Journal of Natural Medicines*, vol. 13, no. 9, pp. 711–720, 2015.

[34] E. Pereira, L. Barro, C. Santos-Buelga, and I. Ferreira, "Phenolic compounds among the bioactive molecules in *Ginkgo biloba L.*" *2nd Symposium on Medicinal Chemistry of University of Minho*, vol. 40, pp. 108–113, 2015.

[35] Y. P. Neo, A. Ariffin, C. P. Tan, and Y. A. Tan, "Phenolic acid analysis and antioxidant activity assessment of oil palm (E. guineensis) fruit extracts," *Food Chemistry*, vol. 122, no. 1, pp. 353–359, 2010.

[36] S. B. Cai, O. Wang, W. Wu et al., "Comparative study of the effects of solid-state fermentation with three filamentous fungi on the total phenolics content (TPC), flavonoids, and antioxidant activities of subfractions from oats (*Avena sativa* L.)," *Journal of Agricultural and Food Chemistry*, vol. 60, no. 1, pp. 507–513, 2012.

[37] W. M. Huang, Y. Q. Liang, L. J. Tang, Y. Ding, and X. H. Wang, "Antioxidant and anti-inflammatory effects of Astragalus polysaccharide on EA. hy926 cells," *Experimental and Therapeutic Medicine*, vol. 6, no. 1, pp. 199–203, 2013.

[38] A. O. Ademosun, G. Oboh, S. Passamonti et al., "Phenolics from grapefruit peels inhibit HMG-CoA reductase and angiotensin-I converting enzyme and show antioxidative properties in endothelial EA. Hy 926 cells," *Food Science and Human Wellness*, vol. 4, no. 2, pp. 80–85, 2015.

[39] A. E. Martin and P. A. Montgomery, "Acarbose: an α-glucosidase inhibitor," *American Journal of Health-System Pharmacy*, vol. 53, no. 19, pp. 2277–2290, 1996.

[40] X. Zhang, Y. Jia, Y. Ma, G. Cheng, and S. Cai, "Phenolic composition, antioxidant properties, and inhibition toward digestive enzymes with molecular docking analysis of different fractions from Prinsepia utilis Royle fruits," *Molecules*, vol. 23, no. 12, p. 3373, 2018.

[41] M. Da Silva Pinto, Y. I. Kwon, E. Apostolidis, F. M. Lajolo, M. I. Genovese, and K. Shetty, "Potential of Ginkgo biloba L. leaves in the management of hyperglycemia and hypertension using in vitro models," *Bioresource Technology*, vol. 100, no. 24, pp. 6599–6609, 2009.

[42] M. E. Lowe, "Structure and function of pancreatic lipase and colipase," *Annual Review of Nutrition*, vol. 17, no. 1, pp. 141–158, 1997.

Hindawi
Journal of Food Quality
Volume 2022, Article ID 5526810, 7 pages
https://doi.org/10.1155/2022/5526810

Research Article

Species-Specific Gene, *spt5*, in the Qualitative and Quantitative Detection of *Boletus reticulatus*

Zhan Lei, Chen Zhang, Yinjiao Li, Lunzhao Yi, and Ying Shang

Faculty of Agriculture and Food, Kunming University of Science and Technology, Kunming 650500, Yunnan, China

Correspondence should be addressed to Ying Shang; shangying1986@163.com

Received 27 January 2021; Accepted 7 March 2022; Published 1 April 2022

Academic Editor: Efstathios Giaouris

Boletus reticulatus is a wild edible fungus with high nutritional value in Yunnan Province. In this study, *B. reticulatus* was used as the research object to diagnose the species characteristics. A commercial kit was used to extract the DNA of various fungi, and the quality of DNA was determined by using universal fungus primers. Through sequence alignment, the *spt5* gene was selected as the species-specific gene of *B. reticulatus*. This gene was then qualitatively and quantitatively analyzed by PCR. In the qualitative detection, the *spt5* amplification products were only found in *B. reticulatus* which proved its good specificity. Meanwhile, SYBR Green I based quantitative PCR results were highly sensitive, and the limit of detection was 0.04 ng of genomic DNA. These experiments illustrated that *spt5* is an ideal species-specific gene for the quantitative and qualitative detection of *B. reticulatus*. This method is also suitable for the analysis of the processed samples of *B. reticulatus* and the determination of the adulteration of edible wild mushrooms.

1. Introduction

The fruiting body of *Boletus reticulatus* is thick and delicate [1], and the nutritional value is extremely rich [2, 3]. *B. reticulatus* is not only edible but also has certain health effects [4], such as the treatment of numbness of the hands and feet [5], lumbago and leg pain, and infertility [6]. In the market, the price of *B. reticulatus* is more expensive than that of other fungi, food adulteration may occur, and food poisoning may even be reported in severe cases. Therefore, *B. reticulatus* should be identified to avoid this phenomenon. To improve the current situation of adulteration and protect the rights and interests of consumers, an efficient and rapid wild edible fungus detection method should be established.

Traditional detection methods include morphological identification, zoological detection, and physical and chemical detection. Morphological identification is based on the determination of the shape, odor, color, and secretions of fruiting bodies [7]. However, many types of wild fungi exist in Yunnan, and many wild fungi are highly similar in shape and cannot be directly distinguished [8]. Some deep-processed products can also severely damage the morphology of wild fungi, so morphological identification has certain limitations. Zoological detection refers to the use of animals to test whether edible fungi are toxic, which is not representative. The physical and chemical techniques are based on the analysis of unique markers in food to achieve product identification, and it is widely used in the field of food detection. With the continuous development and application of various technologies such as chromatography, mass spectrometry, and spectroscopy, chemical methods have been rapidly developed and perfected, playing an active and effective role in monitoring poor manufacturers [9–11]. However, with the advancement of science and technology, food adulteration technology is becoming increasingly sophisticated [12, 13]. By artificially adding chemical components, ordinary physical and chemical detection methods cannot easily identify the authenticity of food ingredients [14].

With the rapid development of modern biotechnology, molecular biological detection has been widely used to identify food sources [15, 16]. DNA-based forgery detection mainly relies on polymerase chain reaction (PCR) to amplify highly specific DNA fragments in the genome to achieve

detection purposes [17, 18]. The techniques that fall under DNA-based forgery detection mainly include single-strand conformation polymorphism technology (SSCP), random amplified polymorphic DNA technology (RAPD), simple sequence repeat technology (SSR), intersimple sequence repeat technology (ISSR), and DNA amplification fingerprinting technology [19–21]. However, these technologies either need to design multiple pairs of primers and amplify multiple targets in the early stage or sequence the amplified products in the later stage. The purpose of detection can be achieved by sequence comparison, which takes a long time. Compared with the above techniques, detection technology based on amplifying species-specific gene (also called endogenous reference gene) is more convenient, specific, and economical [22].

Normal qualitative PCR has the advantages of low-cost, convenience, and wide applicability. Real-time fluorescent quantitative PCR technology has the advantages of high sensitivity, strong specificity and accuracy, short detection time, data visualization, and high automation. It is widely used in the fields of genetic modification detection, clinical medicine, and research and development of new disease-resistant crops. This study mainly used normal PCR and real-time fluorescent quantitative PCR technology to achieve qualitative and quantitative detection of species-specific gene of *spt5* in *B. reticulatus*.

In this study, the DNA of various edible fungi was extracted using a commercial kit, and the DNA quality was determined by PCR using universal fungus primers. Through multiple sequence alignment, the *spt5* gene is selected as the species-specific gene of *B. reticulatus*. This gene was then qualitatively and quantitatively analyzed by PCR using substrate genomic DNA of *B. reticulatus* and other species. The minimum detection limit was 0.04 ng of genomic DNA by SYBR Green fluorescence quantitative PCR, and the *spt5* amplification products were not found in the 10 other species. Allelic variation was not detected in *B. reticulatus*. These experiments proved that *spt5* is an excellent species-specific gene for the quantitative and qualitative detection of *B. reticulatus*. It can be used to analyze *B. reticulatus* and its processed samples and determine the adulteration of wild mushrooms.

2. Materials and Methods

2.1. Materials and Reagents. This study used 11 species of fungus samples, such as *Boletus reticulatus*, *Boletus magnificus* W.F.Chiu, *Lentinus edodes*, *Agrocybe aegirit*, *Leccinum extremiorientale* (L.Vass.) Singer, *Boletus griseus* Frost, *Boletus sinicus* W.F.Chiu, *Russula virescens*, *Collybia albuminosa*, *Lactarius volemus*, and *Pleurotus eryngii*. These samples were purchased from local markets in Yunnan Province, China.

The following reagents were used in the study: Ezup column fungal genomic DNA extraction kit purchased from Sangon Biotech (Shanghai) Co., Ltd.; 50× TAE buffer; EDTA (pH 8.0); 10 mg/mL RNase A, 20 mg/mL proteinase K, ethidium bromide (10 mg/mL), and DNA marker DL 2000 purchased from Tiangen Biotech (Beijing) Co., Ltd.; and 6× loading buffer purchased from Takara Biomedical Technology (Beijing) Co., Ltd. The primers used in the PCR reaction were synthesized by Sangon Biotech (Shanghai) Co., Ltd.

2.2. DNA Extraction and Purification. About 50–100 mg of each fresh fungus was ground into powder with liquid nitrogen and transferred into a 1.5 mL centrifuge tube. The steps in the kit were followed to perform the experiment. The purity and concentration of the extracted DNA were measured by using the microconcentration analyzer NanoDrop 2000. Each sample was measured three times. Finally, the extracted DNA was placed at −20°C till used for the subsequent experiments.

2.3. Qualitative Detection of the Extracted Genomic DNA Using ITS Universal Fungal Primer. To verify whether the extracted DNA can be used for PCR amplification, the universal primers of fungal internal transcribed spacer (ITS) rDNA (Table 1) were used to amplify the genomic DNA of the 11 samples.

PCR assays were conducted in a total volume of 25 μL on an ABI SimpliAmp thermal cycler (Applied Biosystems, USA) (Table 2). The PCR amplification conditions were as follows: predenaturation (95°C, 5 min); 30 cycles of denaturation (95°C, 30 s), annealing (58°C, 30 s), and extension (72°C, 30 s); and termination extension (72°C, 10 min). The 5 μL of each PCR product was then analyzed by 2% agarose gel electrophoresis (containing 0.1 g/mL EB) [23].

2.4. Screening of Species-Specific Gene in B. reticulatus. The gene information of *B. reticulatus* was searched in the nucleotide database of NCBI (https://blast.ncbi.nlm.nih.gov/Blast.cgi), and BLASTN alignment analysis was performed. The gene with low homologous sequences and high species specificity was selected as the candidate of endogenous reference gene.

Aiming at the sequence of candidate genes, Primer Premier 5.0 software (PREMIER Biosoft, San Francisco, USA) was used to design primers. BLASTN comparative analysis was performed on the designed primers to ensure the specificity, and the detailed sequences are given in Table 1.

2.5. Verification of the Specificity of the Selected Species-Specific Gene. The genomic DNA of the 11 mushroom species was used as the template to qualitatively verify the interspecies specificity of the species-specific gene in *B. reticulatus*. The PCR amplification system and conditions were the same with those of ITS amplification.

2.6. Detection Sensitivity of the Species-Specific Gene in B. reticulatus. The genomic DNA of *B. reticulatus* was selected as the target, and the sample was diluted tenfold in a gradient of 20, 2, 0.2, 0.02, 0.002, and 0.0002 ng/μL; ddH_2O was used as a negative control. The qualitative and

Table 1: Primers used in qualitative and quantitative PCR.

Primer name	Primer sequence (5′⟶3′)	Length	Product size (bp)	Reference
ITS-F	TCCGTAGGTGAACCTGCGG	19	189	This study
ITS-R	TCCTCCGCTTATTGATATGC	20		
spt5-F	GGTCTTGTTGTGTCTGTTTCGG	22		
spt5-R	TTGCCTACAATGTTTGTGCCA	21		

Table 2: PCR amplification system.

Reagent	Final concentration	Volume (μL)
10× buffer	1×	2.5
dNTPs	0.2 mM	2
Forward primer	0.4 μM	1
Reverse primer	0.4 μM	1
Taq DNA polymerase	2.5 units	0.2
DNA template	5 ng/μL	2
Water		16.3
Total volume		25

quantitative detection was performed to determine the detection sensitivity.

In the qualitative detection, the PCR conditions were the same with those of ITS amplification. The quantitative detection sensitivity of the species-specific gene was evaluated in a final volume of 25 μL. Each reaction mixture contained 1× SYBR Green Mix, 200 nm of each primer, and 2 μL of genomic DNA. Real-time PCR reactions were performed on an ABI Step One Plus detection system (Applied Biosystems, Foster City, USA) with the following program: 2 min at 50°C, 10 min at 95°C, 40 cycles of 30 s at 95°C, 30 s at 60°C, and 30 s at 68°C. Then, melting curve analysis was performed as follows: 15 s at 95°C, 20 s at 60°C, and 95°C at a heating rate of 0.5°C/s. The specificity of the species-specific gene can be verified by checking whether the melting curve has a single peak at the appropriate Tm value. The samples of each biological replicate were quantified, and the process was replicated twice. A standard curve relating the DNA quantities to the detection thresholds (Ct) was constructed.

3. Results and Discussion

3.1. Qualitative Verification of the Extracted Genomic DNA. In this experiment, the genomic DNA of 11 species of wild mushrooms was extracted by using the kits and detected by electrophoresis in 1% agarose gel. The test results are shown in Figure 1(a); although there are no visible bands in some lanes, this does not mean that DNA has not been successfully extracted. The lack of bands in electrophoresis results may be due to the low DNA concentration. As long as the target genomic DNA can be successfully amplified by PCR using universal primers of fungal, the extracted DNA can be used for the subsequent experiments.

The purity of DNA extraction plays a prerequisite role for subsequent PCR reactions. Extracting high-quality DNA is a key step in molecular biology tests. NanoDrop 2000 was used to determine the concentration and purity of the genomic DNA of the 11 wild bacteria, and each sample was repeatedly measured three times. The test results are given in Table 3. In general, the $OD_{260/280}$ values among 1.7–1.9 can be judged as DNA, but the small fragment of degraded DNA cannot be observed in the electrophoretic diagram, and the concentration can still be measured when analyzed the absorbance value. When the $OD_{260/280}$ value is out of the range mentioned above, it may be generated by other substances, such as protein, RNA, or impurities. In this table, the $OD_{260/280}$ of the DNA of these 11 wild bacteria was between 1.7 and 2.0, indicating that the purity of the DNA was relatively high.

The genomic DNA of the 11 species of wild fungi was amplified by PCR using universal primers of fungal ITS rDNA, and the amplification results were detected by 2% agarose gel electrophoresis. The test results are shown in Figure 1(b). The ITS rDNA was effectively amplified from the genomic DNA of the 11 wild fungi, showing electrophoretic bands different from the blank. The bands were clear and tidy, which meets the requirements of PCR experiments. The electrophoretic results of *A. aegirit* (lanes 7-8) were shallow but not absent.

3.2. Selection of Species-Specific Genes in B. reticulatus. A qualified species-specific gene should have a low and constant copy number because low-copy genes tend to be relatively conserved, and their mutation rates are low; meanwhile, it also should exhibit low heterogeneity within the same species. The nucleotide of *B. reticulatus* was searched in NCBI, and 209 results were produced; every DNA sequence was analyzed by BLAST alignment. After the analysis, the *spt5* gene (accession number: LC084605.1, *Boletus reticulatus spt5* genes for *spt5* protein) was selected as the candidate of species-specific gene. As shown in Figure 2, the *spt5* gene exhibits low homology, and no other DNA sequences were aligned.

3.3. Species Specificity Verification of spt5 Gene in B. reticulatus. To verify the species specificity of the *spt5* gene in *B. reticulatus*, the genomic DNA of 11 of mushrooms

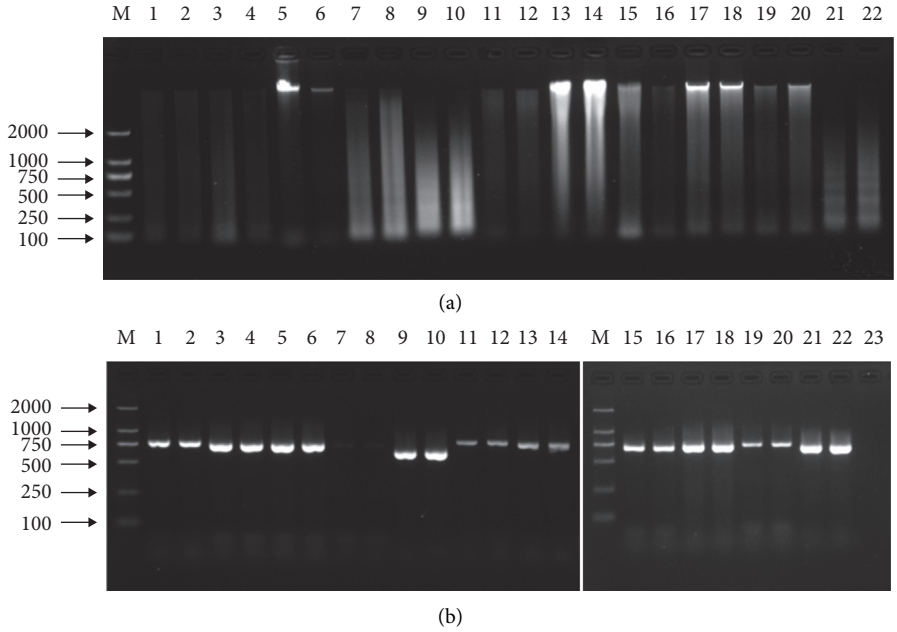

Figure 1: The DNA extraction results by the kit method. (a) The electrophoresis profile of genomic DNA extracted from the 11 tested species of fungi. (b) The electrophoresis profile of the PCR products amplified by ITS primers. M DNA marker DL 2000; lanes 1-2, *Boletus magnificus* W.F.Chiu; 3-4, *Lentinus edodes*; 5-6, *Boletus reticulatus*; 7-8, *Agrocybe aegirit*; 9-10, *Leccinum extremiorientale* (L.Vass.) Singer; 11-12, *Boletus griseus* Frost; 13-14, *Boletus sinicus* W.F.Chiu; 15-16, *Russula virescens*; 17-18, *Collybia albuminosa*; 19-20, *Lactarius volemus*; 21-22, *Pleurotus eryngii*.

Table 3: The purity and concentration of the DNA extracted by the kit method ($\overline{a} \pm$ SD, $n = 3$).

Fungi	OD260/280	Concentration (ng/μL)
Boletus magnificus W.F.Chiu	1.79	24.5 ± 2.5
Lentinus edodes	1.98	31.05 ± 1.7
Boletus reticulatus	1.82 ± 0.01	23.1 ± 2.1
Agrocybe aegirit	1.86	36.3 ± 1.6
Leccinum extremiorientale (L.Vass.) Singer	1.78 ± 0.02	24.8 ± 1.1
Boletus griseus Frost	1.85 ± 0.01	23.6 ± 1.6
Boletus sinicus W.F.Chiu	1.97	33.5 ± 1.2
Russula virescens	1.88	36.7 ± 1
Collybia albuminosa	1.96	39.6 ± 0.6
Lactarius volemus	2.00 ± 0.01	40.8 ± 1.2
Pleurotus eryngii	1.69 ± 0.02	67.2 ± 3.1

was used as samples, and the primer pair *spt5*-F/R was used for common PCR amplification detection. The PCR products were analyzed by 2% agarose gel electrophoresis (containing 0.1 μg/mL EB). The results are shown in Figure 3.

The *spt5* gene was successfully amplified from the genomic DNA of *B. reticulatus*, and the band was obvious, while the other mushrooms did not obtain the amplified products.

3.4. Detection Sensitivity of spt5 Gene in B. reticulatus

3.4.1. Qualitative Detection Results of spt5 Gene in B. reticulatus. To obtain the qualitative detection limit of the *spt5* gene of *B. reticulatus*, the genomic DNA of *B. reticulatus* was series diluted. The amplified products were analyzed by 2% agarose gel electrophoresis, and the result is shown in Figure 4.

When the DNA template contents of *B. reticulatus* were 40, 4, and 0.4 ng, a clear and specific band appeared on the electrophoresis map, and the brightness gradually decreased. When the template content decreased to 0.04 ng, no product was appeared, which indicated that the detection limit of qualitative PCR was 0.4 ng.

3.4.2. Quantitative Detection Results of spt5 Gene in B. reticulatus. The SYBR Green real-time PCR amplification curve and standard curve are shown in Figure 5. In Figure 5(a), the amplification curve still occurred when the template content was as low as 0.04 ng, and the Ct value was significantly lower than the negative control. Thus, the detection limit of SYBR Green quantitative PCR was 0.04 ng.

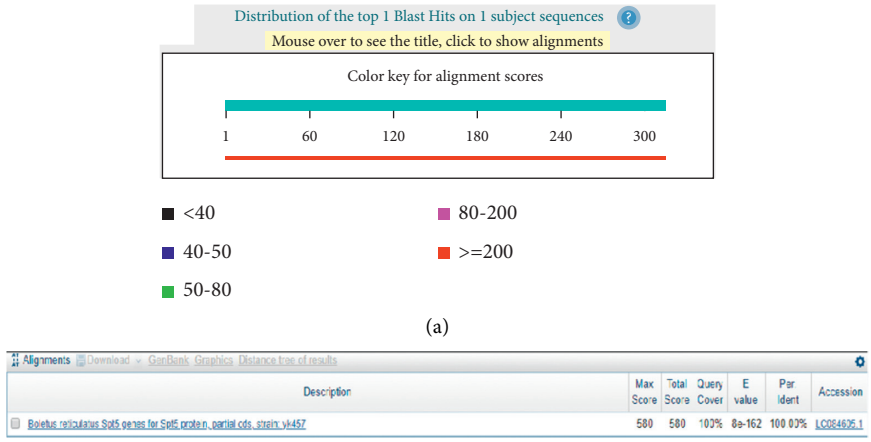

Figure 2: The homology analysis of *spt5* gene. (a) The BLAST analysis of *spt5* in the nucleotide collection database. (b) The detail information about the BLAST result.

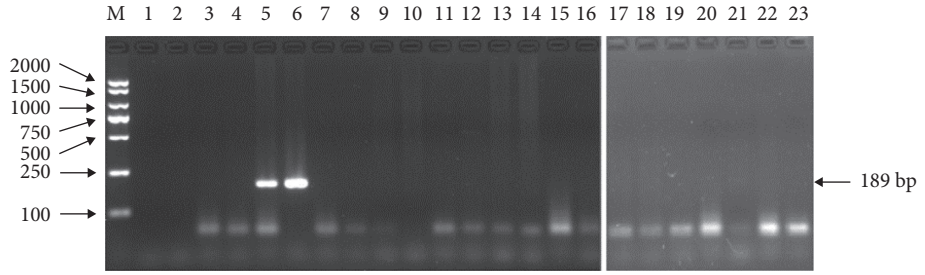

Figure 3: Specificity of the *spt5* gene detected by qualitative PCR. M DNA marker DL 2000; lanes 1-2, *Boletus magnificus* W.F.Chiu; 3-4, *Lentinus edodes*; 5-6, *Boletus reticulatus*; 7-8, *Agrocybe aegirit*; 9-10, *Leccinum extremiorientale* (L.Vass.) Singer; 11-12, *Boletus griseus* Frost; 13-14, *Boletus sinicus* W.F.Chiu; 15-16, *Russula virescens*; 17-18, *Collybia albuminosa*; 19-20, *Lactarius volemus*; 21-22, *Pleurotus eryngii*; 23, negative control.

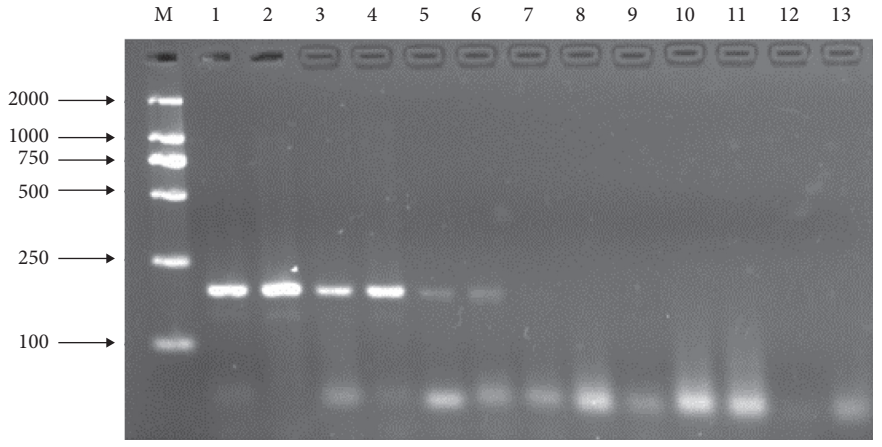

Figure 4: The detection sensitivity of the spt5 gene detection in qualitative PCR. The initial amount of DNA in each PCR reaction is as follows: 1-2, 40 ng; 3-4, 4 ng; 5-6, 0.4 ng; 7-8, 0.04 ng; 9-10, 0.004 ng; 11-12, 0.0004 ng; 13, negative control; M DNA marker DL 2000.

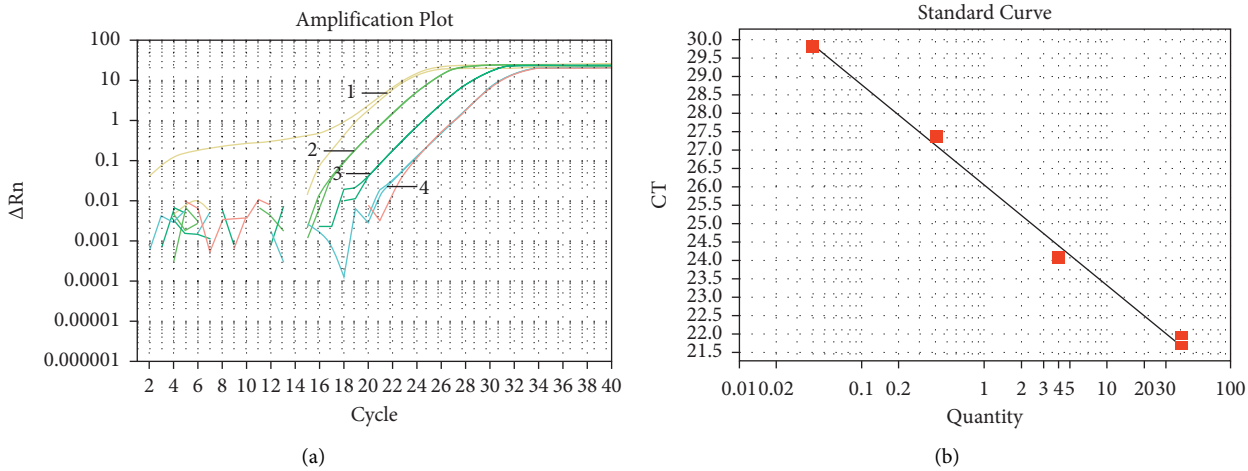

Figure 5: The detection sensitivity of the spt5 gene detection in SYBR Green I quantitative PCR. (a) The final content of DNA in each reaction is as follows: 1, 40 ng; 2, 4 ng; 3, 0.4 ng; 4, 0.04 ng. (b) The standard curve of the quantitative PCR.

As shown in Figure 5(b), we could obtain the linear formula of the Ct value and the content of the DNA template: $Y = -2.728X + 26.048$ (The value range of X is: > 0.04), and the correlation coefficient R^2 was 0.995.

4. Conclusion

In this study, we screened and verified the species-specific gene, *spt5*, of *B. reticulatus*, and the results showed that the *spt5* gene exhibited excellent species specificity, which are suitable for practical use in the qualitative and quantitative monitoring of *B. reticulatus* component. This method showed good specificity and sensitivity, and limit of detection was 0.04 ng of genomic DNA by SYBR Green fluorescence quantitative PCR. The results showed that this method can be used to evaluate the processed products of *B. reticulatus* or other types of products containing small amounts of *B. reticulatus*, and the DNA quantities of it reached the detection thresholds.

Data Availability

The data used to support the findings of this study are available from the corresponding author upon request.

Ethical Approval

This article does not contain any studies with human participants or animals performed by any of the authors.

Conflicts of Interest

The authors declare that they have no conflicts of interest.

Acknowledgments

This work was supported by the National Natural Science Foundation of China (31801635) and the Yunnan Education Department Scientific Research Fund Project (2018JS020).

References

[1] G. Jaworska, E. Bernaś, A. Biernacka, and I. Maciejaszek, "Comparison of the texture of fresh and preserved Agaricus bisporus and Boletus edulis mushrooms," *International Journal of Food Science and Technology*, vol. 45, no. 8, pp. 1659–1665, 2010.

[2] I. Janco, M. Snirc, M. Hrstkova, I. Tirdil'Ova, T. Losak, and J. Arvay, "The relationship between risk elements contamination of wild edible mushrooms (Boletus reticulatus schaeff.) and underlying soil substrate," *Journal of Microbiology, Biotechnology and Food Sciences*, vol. 9, pp. 657–660, 2019.

[3] M. Rasalanavho, R. Moodley, and S. B. Jonnalagadda, "Elemental distribution including toxic elements in edible and inedible wild growing mushrooms from South Africa," *Environmental Science and Pollution Research*, vol. 26, no. 8, pp. 7913–7925, 2019.

[4] N. Nikolic, J. Stojanovic, J. Mitrovic, M. Lazic, I. Karabegovic, and G. Stojanovic, "The antioxidant activity and the composition of free and bound phenolic acids in dough of wheat flour enriched by Boletus edulis after mixing and thermal processing," *International Journal of Food Science and Technology*, vol. 51, pp. 2019–2025, 2016.

[5] S. Santoyo, A. C. Ramírez-Anguiano, G. Reglero, and C. Soler-Rivas, "Improvement of the antimicrobial activity of edible mushroom extracts by inhibition of oxidative enzymes," *International Journal of Food Science and Technology*, vol. 44, no. 5, pp. 1057–1064, 2009.

[6] X. Yuan, *Molecular Identification and Phylogeny Research on Commercial Boletes in Yunnan*Yunnan University, 2016.

[7] K Plouznikoff, M. J Asins, H. D De Boulois, E. A Carbonell, and S Declerck, "Genetic analysis of tomato root colonization by arbuscular mycorrhizal fungi," *Annals of Botany*, vol. 124, pp. 933–946, 2019.

[8] J. Zhang, D. Barałkiewicz, A. Hanć, J. Falandysz, and Y. Wang, "Contents and health risk assessment of elements in three edible ectomycorrhizal fungi (boletaceae) from polymetallic soils in yunnan Province, SW China," *Biological Trace Element Research*, vol. 195, no. 1, pp. 250–259, 2020.

[9] J. Gayo and S. A. Hale, "Detection and quantification of species authenticity and adulteration in crabmeat using visible and near-infrared spectroscopy," *Journal of Agricultural and Food Chemistry*, vol. 55, no. 3, pp. 585–592, 2007.

[10] Y Peng, R Gan, H Li et al., "Absorption, metabolism, and bioactivity of vitexin: recent advances in understanding the efficacy of an important nutraceutical," *Critical Reviews in Food Science and Nutrition*, vol. 61, pp. 1–16, 2020.

[11] A. I. Ruiz-Matute, S. Rodríguez-Sánchez, M. L. Sanz, and I. Martínez-Castro, "Detection of adulterations of honey with high fructose syrups from inulin by GC analysis," *Journal of Food Composition and Analysis*, vol. 23, no. 3, pp. 273–276, 2010.

[12] I. Khalil, W. A. Yehye, N. Muhd Julkapli et al., "Dual platform based sandwich assay surface-enhanced Raman scattering DNA biosensor for the sensitive detection of food adulteration," *The Analyst*, vol. 145, no. 4, pp. 1414–1426, 2020.

[13] S. Lohumi, S. Lee, H. Lee, and B.-K. Cho, "A review of vibrational spectroscopic techniques for the detection of food authenticity and adulteration," *Trends in Food Science & Technology*, vol. 46, no. 1, pp. 85–98, 2015.

[14] J. Tian, H. Chu, Y. Zhang et al., "TiO2 nanoparticle-enhanced linker recombinant strand displacement amplification (LRSDA) for universal label-free visual bioassays," *ACS Applied Materials & Interfaces*, vol. 11, no. 50, pp. 46504–46514, 2019.

[15] S. Gianì, V. Di Cesare, F. Gavazzi, L. Morello, and D. Breviario, "Tubulin-based polymorphism genome profiling: a novel method for animal species authentication in meat and poultry," *Food Control*, vol. 110, Article ID 107010, 2020.

[16] Y. Liu, N. Liu, and Y. Zhang, "Research progress of food authentication technology," *Science and Technology of Food Industry*, vol. 37, pp. 374–383+393, 2016.

[17] E. Bonerba, A. Di Pinto, L. Novello et al., "Detection of potentially enterotoxigenic food-related Bacillus cereus by PCR analysis," *International Journal of Food Science and Technology*, vol. 45, no. 6, pp. 1310–1315, 2010.

[18] K. Hong, "Application of nucleic ACID sequence analysis in fungi taxonmy," *Journal of Tropical Biology*, vol. 2, pp. 39–43, 2006.

[19] G. P. Danezis, A. S. Tsagkaris, F. Camin, V. Brusic, and C. A. Georgiou, "Food authentication: techniques, trends & emerging approaches," *TRAC Trends in Analytical Chemistry*, vol. 85, pp. 123–132, 2016.

[20] W. Powell, M. Morgante, C. Andre et al., "The comparison of RFLP, RAPD, AFLP and SSR (microsatellite) markers for germplasm analysis," *Molecular Breeding*, vol. 2, no. 3, pp. 225–238, 1996.

[21] J. Welsh and M. Mcclelland, "Fingerprinting genomes using PCR with arbitrary primers," *Nucleic Acids Research*, vol. 18, no. 24, pp. 7213–7218, 1990.

[22] Y Xu, W Xiang, Q Wang et al., "A smart sealed nucleic acid biosensor based on endogenous reference gene detection to screen and identify mammals on site," *Scientific Reports*, vol. 7, pp. 43453–43510, 2017.

[23] X. Liu, J. Guo, S. Wang, Y. Li, and R. Na, "Identification of several edible mushrooms in Inner Mongolia by rDNA-ITS," *Edible and Medicinal Mushrooms*, vol. 23, pp. 301–306, 2015.

Hindawi
Journal of Food Quality
Volume 2022, Article ID 9739851, 9 pages
https://doi.org/10.1155/2022/9739851

Research Article

Phytochemical Characterization and Antioxidant and Enzyme Inhibitory Activities of Different Parts of *Prinsepia utilis* Royle

Yue Zheng,[1] **Lei Zhao**,[2] **and Junjie Yi**[1]

[1]*Faculty of Food Science and Engineering, Kunming University of Science and Technology, Kunming, Yunnan Province 650500, China*
[2]*Beijing Engineering and Technology Research Center of Food Additives, Beijing Technology and Business University, Beijing 100048, China*

Correspondence should be addressed to Junjie Yi; junjieyi@kust.edu.cn

Received 28 May 2021; Accepted 25 January 2022; Published 21 February 2022

Academic Editor: Maria Concetta Strano

The objective of this study was to evaluate the phenolic composition and antioxidant and enzyme inhibitory activities of the flowers, leaves, and stems of *Prinsepia utilis* Royle. In the work, their total phenol content and flavonoid content were determined. In addition, the scavenging effects of DPPH and ABTS free radicals and ferric reducing antioxidant power were measured. The results showed the flowers had the highest total phenol and flavonoid content, followed by the leaves and stems. A total of 11 phenolic substances were identified and quantified using UHPLC-ESI-HRMS/MS, of which rutin was the dominant phenolic compound in all samples. All three samples had good antioxidant activity and dose dependently inhibited the activity of α-glucosidase, pancreatic lipase, and tyrosinase. In summary, the ethanol extracts of the flowers have the best antioxidant and enzyme inhibitory ability among three samples. The outcome could provide support for the development and utilization of *P. utilis*.

1. Introduction

Polyphenols are naturally occurring compounds that are widely distributed in different parts of plants including flowers, leaves, stems, fruits, and bark. Polyphenols play an important role in plant growth and development and protecting plants from insect damage, ultraviolet light, and wound infections [1]. In addition, they have biological functions and benefits to human health [2]. Humans ingest polyphenols mainly from fruits, vegetables, and beverages, especially tea, coffee, and red wine for good health, whereas the body cannot synthesize them by its own [3]. Therefore, it is important to adhere to daily eat a certain amount of polyphenol-rich food.

Nowadays, the incidence of chronic noncommunicable diseases (CNCDs) is increasing and the age of patients has shown a trend of getting younger, resulting from changes of diet habits, living environment, and lifestyle, for example, high-calorie food intake, industrial pollution, smoking, alcoholism, staying up late, and lack of exercise [4, 5]. Researchers have increasingly focused on the prevention and alleviation of the diseases through diets with little side effects. More and more research projects indicated that polyphenols have the potential to prevent or treat metabolic syndromes and many noninfectious diseases *in vivo* [4], so as to enhance human health. According to the previous reports, polyphenols could exhibit various biological activities including antioxidant [6, 7], anti-inflammatory [8], and anticancer [9], as well as the prevention of cardiovascular and Parkinson's diseases [10].

Prinsepia utilis Royle is a deciduous shrub of the *Rosaceae* family. It is perennial and mainly distributed in high-altitude areas, such as some areas in China and India [11]. The *P. utilis* usually grow among bushes, along depressions and roadsides, and on both sides of mountain slopes or valleys. They are cultivated as windproof and sand-fixing plants that show strong adaptability to the environment. Residents in Yunnan, China, usually consume *P. utilis* as vegetables. Many parts of *P. utilis* (e.g., leaves, fruits, and roots) can be used as traditional Chinese medicine to treat

various diseases, such as skin-related diseases, fracture, and rheumatism [12]. Previous studies have separated and identified the chemical constituents of *P. utilis*, which reported it contains hydroxybutyronitrile glucoside, diterpene glucoside, hydrocyanic acid, triterpenoids, etc [13]. However, there are few reports on the phenolic composition and biological activities of *P. utilis* flowers, leaves, and stems, which hinders the development and utilization of *P. utilis*. Therefore, the objective of this study is to compare the phenolic composition and antioxidant and enzyme (e.g., glycosidase, pancreatic lipase, and tyrosinase) inhibitory properties of different parts of *P. utilis*, namely flowers, leaves, and stems.

2. Materials and Methods

2.1. Chemical and Reagents. Acetonitrile, formic acid, Folin phenol reagent, and methanol were purchased from Darmstadt Merck, Germany. 2,2-Diphenyl-1-picrylhydrazyl radical (DPPH), 2,2′-azo-bis (3-ethylbenzothiazole-6-sulfonic acid) (ABTS), pancreatic lipase (from pig pancreas, 163 U/mg, EC: 3.1.1.3), α-glycosidase from *Saccharomyces cerevisiae* (type I, ≥10 units/mg protein), *p*-nitrobenzene α-D-glucopyranoside (pNPG, purity ≥99.0%), acarbose (purity ≥95%), and orlistat (purity ≥97.0%) were purchased from Sigma-Aldrich (Shanghai, China). Tyrosinase (derived from mushrooms, 500 U/mg) was purchased from Shanghai Ruiyang (Shanghai, China). Kojic acid (purity ≥99.0%) was purchased from Aladdin (Shanghai, China). Levodopa (L-DOPA, purity ≥99.0%) was purchased from Braunway (Beijing, China). Phenolic compound standards (purity ≥98.0%) were purchased from Chengdu Bide Biotechnology Co., Ltd. (Chengdu, China). The other reagents used are of analytical grade.

2.2. Materials and Treatment. *P. utilis* flowers, leaves, and stems were collected from Kunming, Yunnan Province, in April 2019. After picking, they were dried and ground with a grinder (30,000 rpm; Lingdan LD-T300; Shanghai, China). A total of 100 g powders of the flowers, stems, and leaves were defatted with petroleum ether at a material/solvent ratio of 1 : 5 (w/v) for five times and then extracted three times (30 min for each time) with 80% ethanol (v/v) in an ultrasonic bath. After extraction, the mixture was centrifuged at 25°C and 4000*g* for 15 min. The supernatant was collected and evaporated using a rotary evaporator (Hei-VAP, Heidolph, Germany) under vacuum at −40°C to remove the organic reagent and excess water. Then, the concentrated solution was lyophilized to obtain the ethanol extracts of the flowers, stems, and leaves.

2.3. Determination of Total Phenol Content (TPC). The total phenol content of the ethanol extracts of *P. utilis* flowers, leaves, and stems was determined by using the Folin–Ciocalteu method [12]. The absorbance was measured with a microplate reader (SpectraMax M5; Molecular Device, San Jose, CA, USA) at 765 nm, and gallic acid was used to establish the standard curve. The TPC of each sample was expressed as mg of GAE/g, where GAE was gallic acid equivalents.

2.4. Determination of Total Flavonoid Content (TFC). The total flavonoid content of three ethanol extracts was determined according to the methods reported in the literature [12]. The absorbance value was measured with a SpectraMax M5 microplate reader at 510 nm, and rutin was used to establish the standard curve. The TFC of each sample was expressed as mg RE/g, where RE was rutin equivalents.

2.5. Identification and Quantification of Phenolics with UHPLC-ESI-HRMS/MS. The Thermo Fisher Ultimate 3000 UHPLC system (Thermo Fisher Scientific, Bremen, Germany) with an Agilent Zorbax SB-C18 column (2.1 × 100 mm, 1.7 μm) was utilized for the qualitative and quantitative analysis of phenolic substances in the ethanol extracts of flowers, leaves, and stems from *P. utilis*. In the current study, the identified phenolic compounds were quantified by the calibration curve of the corresponding authentic standard or by the calibration curve of the standard shared a similar aglycone. The injection volume was 3 μL, the flow rate was 0.2 mL/min, and the column temperature was 35°C. Acidified ultrapure water (0.1% formic acid, phase A) and acetonitrile (phase B) were used as the mobile phases. The gradient elution condition was 0–2 min, 5% B; 2–15 min, 50% B; 15-16 min, 70% B. The mass spectrometry conditions were set according to the study of Sun et al. [14].

2.6. Evaluation of Antioxidant Activity

2.6.1. DPPH Free Radical Scavenging Experiment. The DPPH free radical scavenging ability of ethanol extracts was evaluated according to the methods of Sun et al. [14]. The absorbance of each sample was measured at 517 nm with a SpectraMax M5 microplate reader. The free radical scavenging capacity of DPPH is calculated by using equation (1).

$$\text{DPPH free radical scavenge ratio (\%)} = \frac{(A_0 - A_0') - (A_1 - A_1')}{A_0 - A_0'} \times 100, \quad (1)$$

where A_1 represents the absorbance of sample solution and DPPH free radical, A_1' represents the absorbance of sample solution and methanol, A_0 is the absorbance of methanol and DPPH free radical, and A_0' is the absorbance of methanol and distilled water.

2.6.2. ABTS Free Radical Scavenging Experiment. The ABTS free radical scavenging ability of ethanol extracts was evaluated by the methods of Sun et al. [14]. The absorbance of each group was measured at 734 nm with a SpectraMax M5 microplate reader. The following is the calculation formula of ABTS (equation (2)):

$$\text{ABTS free radical scavenge ratio (\%)} = \frac{(A_0 - A_0') - (A_1 - A_1')}{A_0 - A_0'} \times 100, \quad (2)$$

where A_1 represents the absorbance of sample solution and ABTS free radical, A_1' represents the absorbance of sample solution and methanol, A_0 is the absorbance of methanol and ABTS free radical, and A_0' is the absorbance of methanol and distilled water.

2.6.3. Ferric Reducing Antioxidant Power (FRAP) Method. The FRAP values of three ethanol extracts were evaluated according to the reported method with some modifications [15]. Trolox $FeSO_4{\cdot}7H_2O$ was used to prepare the calibration curve, ranging from 0.1 mmol/L to 0.5 mmol/L. This curve was used to calculate the antioxidant values of each sample.

2.7. Determination of α-Glucosidase Inhibitory Effect. The α-glucosidase inhibitory activities of the ethanol extracts of *P. utilis* spikes, leaves, and stems were measured with the methods reported by Zhang et al. [16]. The absorbance of each reaction solution was measured at 405 nm with a SpectraMax M5 microplate reader. The following is the calculation formula for the α-glucosidase inhibition (%) (equation (3)):

$$\text{glucosidase inhibition (\%)} = \frac{\left(\text{OD}_{\text{control}} - \text{OD}_{\text{sample}}\right)}{\text{OD}_{\text{control}}} \times 100. \quad (3)$$

2.8. Determination of Pancreatic Lipase Inhibitory Effect. The pancreatic lipase inhibitory activities of the extracts of *P. utilis* flowers, leaves, and stems were measured according to the study of Cai et al. [17]. The absorbance of each reaction solution was measured at 405 nm with a SpectraMax M5 microplate reader. The following is the calculation formula for the pancreatic lipase inhibition (%) (equation (4)):

$$\text{Pancreatic lipase inhibition (\%)} = \frac{\left(\text{OD}_{\text{control}} - \text{OD}_{\text{sample}}\right)}{\text{OD}_{\text{control}}} \times 100. \quad (4)$$

2.9. Determination of Tyrosinase Inhibitory Effect. The tyrosinase inhibitory activity of ethanol extracts of *P. utilis* flowers, leaves, and stems were measured according to the previously reported method with some modifications [18]. The volume of the reaction system was reduced from 1 mL to 200 μL, and the added volume of each reagent was reduced in proportion.

2.10. Statistical Analysis. All experiments were measured in triplicate, and the experimental data results were expressed as mean ± standard deviation (SD). One-way analysis of variance and Tukey's test were used to determine the significance of difference ($p < 0.05$). All analyses were performed using Origin 8.5 software (OriginLab, Northampton, MA, USA).

3. Results and Discussion

3.1. Determination of Total Phenolic and Total Flavonoid Content. Table 1 shows the total phenolic and total flavonoid contents in the *P. utilis* flowers, leaves, and stems. Sánchez et al. [19] reported that the positive correlations between total phenol content and antioxidant capacity measured according to $ABTS^{\bullet+}$, $DPPH^{\bullet}$, ORAC, and β-carotene-linoleate model system. It indicates that the total phenol content can reflect the strength of antioxidant activity of extract to a certain extent. In this study, the TPCs in the ethanol extracts of the flowers, leaves, and stems of *P. utilis* were not significantly different ($p > 0.05$), while the TPCs of dried flowers and leaves were significantly higher than that of dried stems ($p < 0.05$). The dried flowers of *P. utilis* had the highest TPC, which was 1.7 times of that of the stems.

As shown in Table 1, the TFC of *P. utilis* flower ethanol extract was significantly higher than that of leaves and stems ($p < 0.05$). The dried flowers, leaves, and stems of *P. utilis* have significant differences in TFC ($p < 0.05$), and the dried flowers had the highest TFC, followed by leaves. The TFC of the dried flowers was as about twice as that of the dried stems. According to previous reports [20], the ethyl acetate component extracted from tubers of *Stachys affinis* had good antioxidant activity, and the concentrations of phenols and flavonoids are positively correlated with the antioxidant activity.

3.2. Identification and Quantitation of Phenolic Compounds. The phenolic components of the ethanol extracts of flowers, leaves, and stems of *P. utilis* were analyzed using UHPLC-ESI-HRMS/MS in a negative ion mode. The ion flow chromatogram is shown in Figure 1. In addition, the relevant data such as retention time, molecular mass, molecular formula, and secondary ion fragments are shown in Table 2. The composition and content of polyphenols in the ethanol extracts of three samples were investigated by comparing the information, including secondary MS fragments with a large number of references or public mass spectrometry databases (MassBank, http://www.massbank.jp/QuickSearch.htmL). The extracts were subjected to preliminary qualitative and quantitative analysis. According to the qualitative data, appropriate standards were selected to perform further quantitative analysis on the corresponding substances. As known, the negative ion mode is usually used to detect phenolic acids and flavonoids [22]. In negative ion mode, a total of 11 compounds were analyzed including 1 phenolic acid, 10 flavonoids, and their derivatives (Table 2 and Figure 1). The retention time of flavonoids was mainly between 7 and 15 min. In the flower extracts, the peak areas of compounds 6 and 10 were relatively high, indicating that the

Table 1: Total phenolic contents (TPCs) and total flavonoid contents (TFCs) in the flower, leaf, and stem of *Prinsepia utilis* Royle.

	Extraction rate (%)	TPC (mg GAE/g)		TFC (mg RE/g)	
		DWS	DWE	DWS	DWE
Flower	$26.49 \pm 1.32\%^{b}$	6.40 ± 0.07^{a}	24.00 ± 0.23^{a}	31.43 ± 0.95^{a}	117.86 ± 2.92^{a}
Leaf	$27.59 \pm 1.37\%^{a}$	6.26 ± 0.50^{a}	23.48 ± 1.54^{a}	24.36 ± 0.47^{b}	91.36 ± 1.44^{b}
Stem	$17.45 \pm 0.86\%^{c}$	3.77 ± 0.18^{b}	21.49 ± 0.83^{a}	15.75 ± 0.97^{c}	89.77 ± 4.53^{b}

All the values are expressed as mean ± SD ($n = 3$). Values with different superscript letters in each column indicate significant differences among samples ($p < 0.05$). DWS = dry weight of sample, DWE = dry weight of extract, GAE = gallic acid equivalent, RE = rutin equivalents.

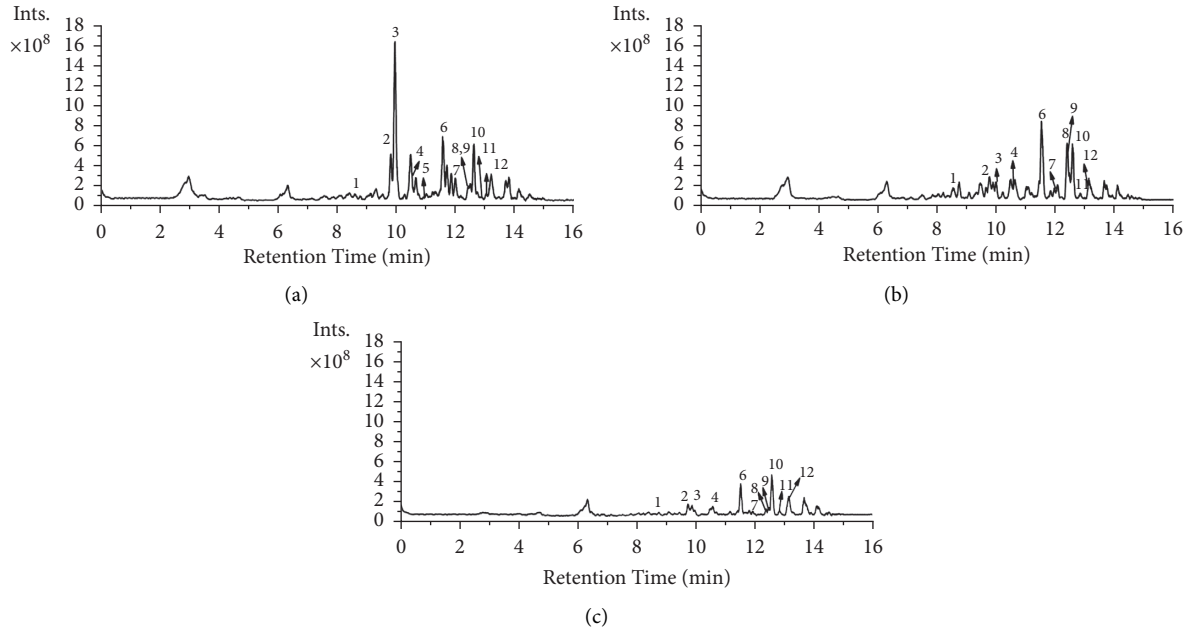

Figure 1: Total ion chromatograms (TICs) for the ethanol extracts of the (a) flowers, (b) leaves, and (c) stems of *Prinsepia utilis* Royle in negative mode. 1–12 refers to the corresponding compounds in Tables 1 and 2.

Table 2: Identification of major polyphenols in the flower, leaf, and stem of *Prinsepia utilis* Royle using the negative ion mode of UPLC-ESI-HRMS/MS.

Peak no.	Compounds	RT (min)	$[M-H]^-$ (m/z)	Molecular formula	MS/MS fragment ions	Reference	Flower	Leaf	Stem
1	*p*-Coumaric acid	8.57	163.0395	$C_9H_8O_3$	119.0493(100)	Standard	✓	✓	✓
2	Catechin	9.79	289.0726	$C_{15}H_{14}O_6$	123.0443(83), 109.0285(100)	Standard	✓	✓	✓
3	Unknown	9.93	447.1882	$C_{20}H_{31}O_{11}$	165.0919(100), 220.1104(73)		✓	✓	✓
4	Isoschaftoside	10.53	563.1423	$C_{26}H_{28}O_{14}$	563.1414(100), 353.0666(20)	Standard	✓	✓	✓
5	Kaempferol-3-*O*-glucoside	10.95	447.0945	$C_{21}H_{20}O_{11}$	284.0331(21), 285.0418(51)	Standard	✓	✓	✓
6	Rutin	11.54	609.1474	$C_{27}H_{32}O_{16}$	300.0283(52), 609.1478(100)	Standard	✓	✓	✓
7	Quercetin-3-*O*-glucoside	11.97	463.0897	$C_{21}H_{20}O_{12}$	300.0284(100), 271.0253(5)	Standard	✓	✓	✓
8	Kaempferol-3-*O*-rhamnosylhexose	12.40	593.1535	$C_{27}H_{30}O_{15}$	284.0334(32), 593.1530(64)	[21]	✓	✓	✓
9	Quercetin 3-(6-*O*-acetyl-beta-glucoside)	12.45	505.1004	$C_{23}H_{22}O_{13}$	300.0283(100), 301.0347(49)	Mass bank	✓	✓	✓
10	Isorhamnetin-3-*O*-rutinoside	12.60	623.1636	$C_{28}H_{32}O_{16}$	315.0518(100), 623.1638(50)	Standard	✓	✓	✓
11	Kaempferol-3-*O*-hexoside	12.87	447.0947	$C_{21}H_{20}O_{11}$	285.0391(36), 284.0334(100)	[21]	✓	✓	✓
12	Isorhamnetin-3-*O*-glucoside	13.05	477.1052	$C_{22}H_{22}O_{12}$	314.0442(100), 477.1052(25)	Standard	✓	✓	✓

RT = retention time, ✓ = contains the substance.

two phenolic substances are the main compounds in the ethanol extract of *P. utilis* flowers. Compound 6 ($[M\text{-}H]^-$ at m/z 609.1474) was determined as rutin by comparison with the corresponding standard. The characteristic ion fragment of compound 6 ($m/z = 300.0283$) was caused by the partial loss of rutinose. Compound 10 ($[M\text{-}H]^-$ at m/z 623.1636) was identified as isorhamnetin-3-*O*-rutinoside by comparison with the standard and the presence of m/z 315.0518, which represent the loss of a rutinose in isorhamnetin-3-*O*-rutinoside produces this characteristic ion. Among all the identified components, rutin (compound 6) was the predominate phenol in the leaf and stem extracts. Additionally, the peak areas of catechin, kaempferol-3-*O*-glucoside, and quercetin-3-*O*-glucoside were higher than that of the other components.

The quantitative analysis results of all phenolic components in the ethanol extracts of *P. utilis* flowers, leaves, and stems are shown in Table 3. Among them, there were 8 compounds (1, 2, 4, 5, 6, 7, 10, and 12) that can be analyzed by comparison with the corresponding standards. The rest of the phenolic substances (8, 9, and 11) can use similar aglycone standards for their quantitation. As shown in Table 3, rutin was the dominant phenolic compound in all the extracts. However, the rutin content was different among three extracts, that the highest content was detected in flowers, followed by leaves and stems. It indicates that phenol contents and species in the ethanol extracts of *P. utilis* flowers, leaves, and stems were abundant, which may have good biological activity. Zhang et al. [16] studied the composition and biological activity of the total phenols, total flavonoids, and anthocyanin components in *P. utilis* fruits. A total of 20 phenolic compounds were identified, of which composition was similar to that of ethanol extracts of *P. utilis* flowers, leaves, and stems. Zhang et al. found that three main components (rutin, isorhamnetin-3-*O*-rutinoside, and cyanidin-3-*O*-glucoside) in *P. utilis* fruits have a good inhibitory effect on α-glycosidase and lipase. The ethanol extracts of the flowers, leaves, and stems of *P. utilis* also contain rutin and isorhamnetin-3-*O*-rutinoside.

3.3. In Vitro Antioxidant Activity. Free radicals are inevitably produced in biological systems and taken into the body from the environment. They are known to cause a variety of degenerative diseases, such as mutagenesis, carcinogenesis, cardiovascular disorders, and aging [23]. An antioxidant is a compound that inhibits free radicals by interfering with the three main steps of the free radical-mediated oxidation process, namely initiation, proliferation, and termination [24]. The balance between oxidants and antioxidants determined inside the human body is important to protect against the occurrence of many diseases [25].

Generally, plant polyphenols have been reported to show many important biological activities, which is believed to be partially or largely related to their antioxidant activity [15]. At present, some *in vitro* antioxidant methods (e.g. DPPH, ABTS, and FRAP) are usually used to measure the antioxidant capacity of a substance. The obtained results are used as a reference index for the antioxidant effect *in vivo*. In the work, DPPH, ABTS, and FRAP methods were used to evaluate the antioxidant activity of the ethanol extracts of *P. utilis* flowers, leaves, and stems.

3.3.1. DPPH Free Radical Scavenging Activity. The DPPH free radical scavenging activity of ethanol extracts from different parts of *P. utilis* is shown in Figure 2(a). In the concentration range of 20–100 μg/mL, the DPPH free radical scavenging activity of all samples was concentration-dependent. The DPPH free radical scavenging activity of the flower extract of *P. utilis* was significantly stronger than that of the other two samples ($p < 0.05$). The IC_{50} values of the ethanol extracts of *P. utilis* flowers, leaves, and stems were 46.07 ± 2.42, 82.08 ± 0.97, and 71.46 ± 2.85 μg/mL, respectively. The scavenging rate of DPPH free radicals of three samples is lower than that of Vc (positive control, $IC_{50} = 3.75 \pm 0.02$ μg/mL). The flower extract has the strongest DPPH scavenging ability among the three components ($p < 0.05$), which may be attributed to its highest polyphenol content.

3.3.2. ABTS Free Radical Scavenging Activity. Figure 2(b) shows the ABTS free radical scavenging ability of the ethanol extract of *P. utilis* flowers, leaves, and stems. The IC_{50} values of the ethanol extracts of *P. utilis* flowers, leaves, and stems for scavenging ABTS free radicals were 22.07 ± 0.94, 27.14 ± 0.28, and 20.29 ± 0.57 μg/mL, respectively. The IC_{50} values of the ethanol extracts of flowers, leaves, and stems of *P. utilis* for ABTS scavenging assay were 22.07 ± 0.94, 27.14 ± 0.28, and 20.29 ± 0.57 μg/mL, respectively. It shows that the ethanol extract of leaves had the best scavenging effect on ABTS free radicals among all ethanol extracts. The IC_{50} value of Vc was 3.56 ± 0.07 μg/mL, and its ABTS scavenging effect is better than that of the *P. utilis* extracts. Overall, the ethanol extracts of flowers, leaves, and stems from *P. utilis* had strong free radical scavenging activity. Three extracts had different IC_{50} values for their DPPH and ABTS free radical scavenging activities, which may be caused by the differences in free radical species, polyphenol compositions, and contents.

3.3.3. FRAP Evaluation. FRAP is a relatively efficient and sensitive method to determine the antioxidant capacity of samples, which is widely used in food, chemical, and other fields. The antioxidant capacity of a sample evaluated using this method is expressed by the equivalent value of $FeSO_4$. The concentration of $FeSO_4$ was in the range of 0.1~0.5 mmol/L, and the concentration has a good linear relationship with the absorbance at 593 nm. Figure 2(c) shows the ferrous reduction capacity of the ethanol extracts of *P. utilis*. The concentration of three group samples filled in the range of 20–60 μg/mL. The flower extract had the highest FRAP value ($p < 0.05$), followed by the leaf extract and the stem extract. For example, the ferrous reduction activity of flower extract was significantly higher than that of leaf and stem extracts ($p < 0.05$) at 60 μg/mL. The FRAP values of flower, leaf, and stem extracts were 0.60 ± 0.01,

Table 3: Quantitation of phenolic substances in the flower, leaf, and stem of *Prinsepia utilis* Royle by UPLC-ESI-HRMS/MS.

Peak no.	Compounds	Flower (μg/g)	Leaf (μg/g)	Stem (μg/g)
1	*p*-Coumaric acid	381.60 ± 19.08^{a}	265.60 ± 13.28^{a}	22.85 ± 1.14^{b}
2	Catechin	742.60 ± 37.13^{a}	448.86 ± 22.44^{b}	227.99 ± 11.40^{c}
4	Isoschaftoside	463.58 ± 23.18^{b}	352.65 ± 17.63^{c}	537.65 ± 26.88^{a}
5	Kaempferol-3-*O*-glucoside	9.39 ± 0.47^{a}	ND	ND
6	Rutin	8822.63 ± 441.13^{a}	8484.19 ± 424.21^{a}	1801.33 ± 90.07^{b}
7	Quercetin-3-*O*-glucoside	744.64 ± 37.23^{a}	237.85 ± 11.89^{b}	33.54 ± 1.68^{c}
8	Kaempferol-3-*O*-rhamnosylhexose	269.34 ± 13.47^{b}	1069.80 ± 53.49^{a}	29.14 ± 1.46^{c}
9	Quercetin 3-(6-*O*-acetyl-beta-glucoside)	668.61 ± 33.43^{a}	46.00 ± 2.30^{b}	8.08 ± 0.40^{b}
10	Isorhamnetin-3-*O*-rutinoside	1944.96 ± 97.25^{a}	1108.94 ± 55.45^{b}	529.00 ± 26.45^{c}
11	Kaempferol-3-*O*-hexoside	65.72 ± 3.29^{a}	23.81 ± 1.19^{b}	3.91 ± 0.20^{c}
12	Isorhamnetin-3-*O*-glucoside	30.34 ± 1.52^{c}	57.71 ± 2.89^{a}	37.60 ± 1.88^{b}

All the values are expressed as mean ± SD ($n = 3$). Values with different superscript letters in each column indicate significant differences among samples. Compounds 1, 2, 4, 5, 6, 7, 10, and 12 were quantified by the calibration curve of the corresponding commercial standard; compounds 8 and 11 were quantified by the calibration curve of compound 5; and compound 9 was quantified by the calibration curve of compound 7. The result is expressed as μg/g dry matter. ND = not detected.

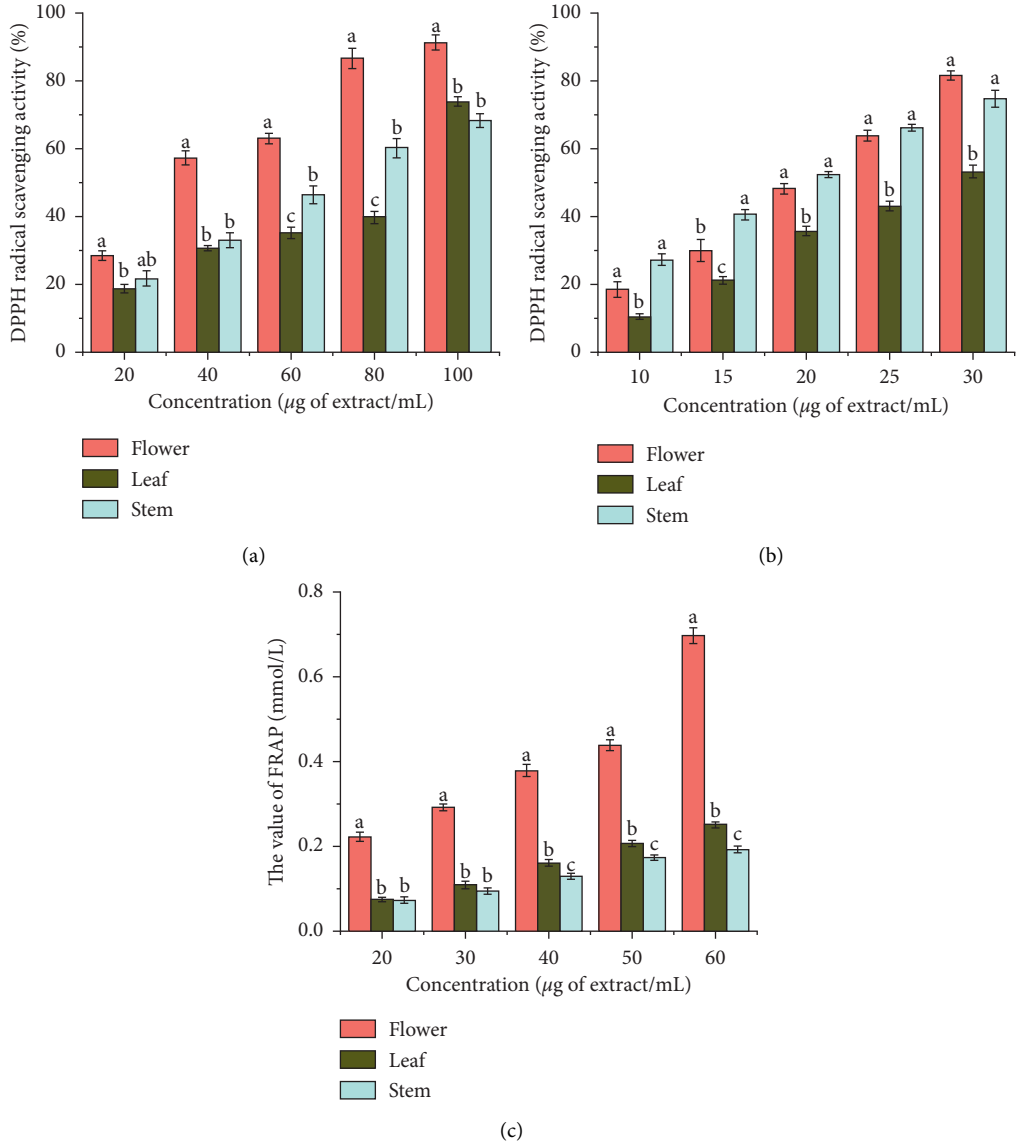

Figure 2: The antioxidant activities of the flower, leaf, and stem extracts of *Prinsepia utilis* Royle. (a) DPPH radical scavenging activity, (b) ABTS radical scavenging ability, and (c) ferric reducing antioxidant power (FRAP). All the values are expressed as mean ± SD ($n = 3$). Values with different superscript letters in each column indicate significant differences among samples ($p < 0.05$).

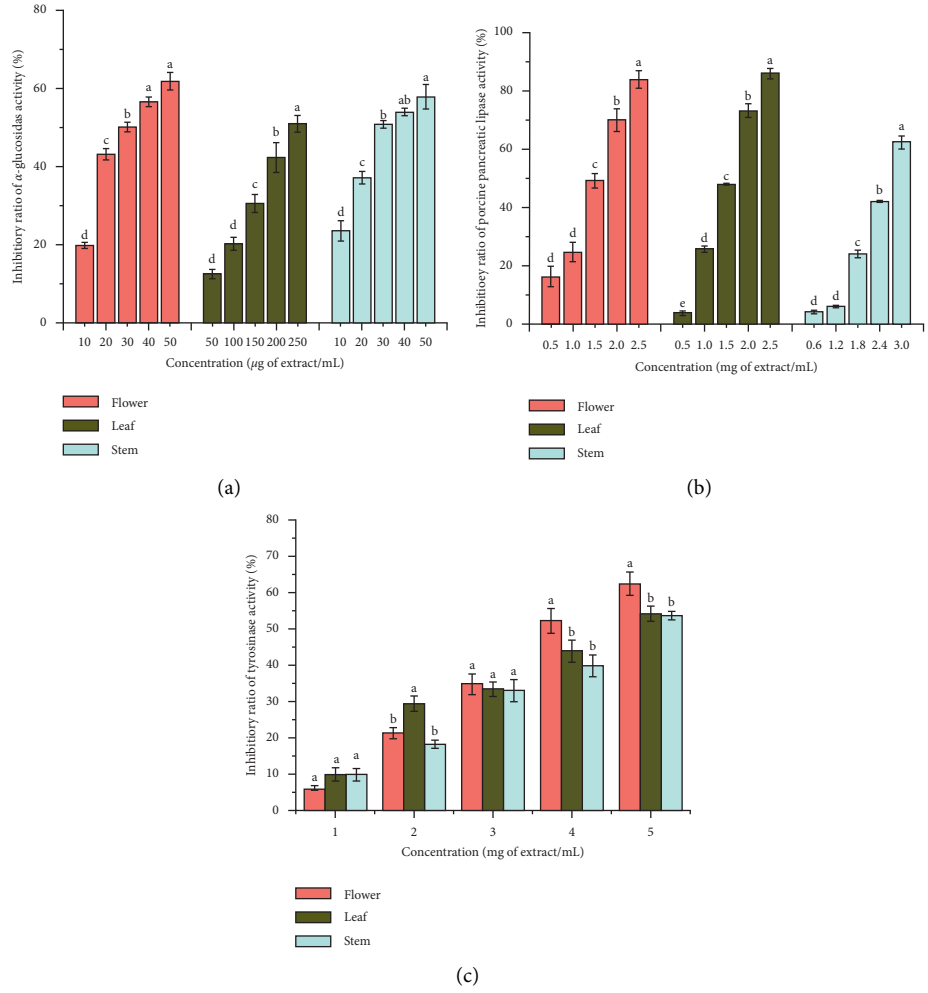

Figure 3: (a) α-glucosidase inhibitory rates, (b) porcine pancreatic lipase inhibitory rates, and (c) tyrosinase inhibitory rates of the flower, leaf, and stem extracts from *Prinsepia utilis* Royle. All the values are expressed as mean ± SD ($n = 3$). Values with different superscript letters in each column indicate significant differences among samples ($p < 0.05$).

0.25 ± 0.003, and 0.19 ± 0.01 mmol/L, respectively. The ferrous reduction activity of flower extract was 3 times higher than that of stem extract and 2.4 times higher than that of leaf extract. In addition, it can be observed that the samples with high total phenol content have high FRAP values.

In general, the antioxidant activity of the *P. utilis* flower ethanol extract was the highest among all three samples. It may be due to the fact that the total phenol and total flavonoid contents of flower extract was higher than other samples. Huang et al. [11], Zhang et al. [26], and Zhang et al. [16] reported that *P. utilis* fruits showed a higher antioxidant capacity than flowers, leaves, and stems. Although the total phenol and total flavonoid contents in leaves are higher than those in stems, the ethanol stem extract had a stronger free radical scavenging ability than that of leaf extract. It was found that the content of isoschaftoside in the ethanol extract of stem was higher than that of leaf, but the other components of the ethanol extract of stems were lower than that of the leaf extract. Compared with the leaf extract, the better scavenging effect of stem extract against DPPH and ABTS free radicals may attribute to its higher content of isoschaftoside. A previous study reported a similar finding that the DPPH scavenging activity of ethanol extract from Okinawa Taumu (*Colocasia esculenta* S.) was higher than that of the water extract [27]. In addition to phenolic compounds, some other components also exhibited a good antioxidant activity, such as peptides [28]. Therefore, the total antioxidant activity of a sample was contributed from a combination of several components.

3.4. α-Glucosidase Inhibitory Activity. Figure 3(a) shows the inhibitory effect of ethanol extracts of *P. utilis* flowers, leaves, and stems on α-glucosidase. The α-glucosidase inhibitory effects of three extracts were concentration-dependent. As shown in Figure 3(a), the IC_{50} values for the α-glucosidase inhibitory activity of ethanol extracts from *P. utilis* spike flowers, leaves, and stems were 35.71 ± 0.58, 231.12 ± 6.59, and 37.29 ± 1.59 μg/mL, respectively. The IC_{50} value of the positive control acarbose was 0.16 ± 0.04 μg/mL, which was significantly lower than that of three extracts ($p < 0.05$). The flower extracts had the highest inhibitory effect on

α-glucosidase, followed by stem and leaf extracts, which may be due to the different polyphenol composition. Several studies [29, 30] reported that plants rich in polyphenols have good inhibitory activity on α-glucosidase. It suggested that phenolic compounds are considered to be the main compounds that contribute to the α-glucosidase inhibitory activity. Zhang et al. [16] have reported that the *P. utilis* fruits were rich in rutin and isorhamnetin-3-*O*-rutinoside, and those phenolic compounds exhibited a good inhibitory activity towards α-glucosidase.

3.5. Pancreatic Lipase Inhibitory Activity. Figure 3(b) shows the pancreatic lipase inhibitory activity of *P. utilis* flower, leaf, and stem ethanol extracts. As shown in Figure 3(b), each extract had a good inhibitory effect on pancreatic lipase. As the concentration increased, the pancreatic lipase inhibition rates of three extracts gradually increased. The IC_{50} values for pancreatic lipase inhibitory activity of the ethanol extracts from *P. utilis* flowers, leaves, and stems were 1.72 ± 0.03, 1.82 ± 0.15, and 2.56 ± 0.02 mg/mL, respectively. It can be seen that the flower extract had the highest inhibitory activity on pancreatic lipase, followed by the leaf and stem extracts. However, orlistat, as a positive control, inhibited almost 50% of lipase activity at 40.00 μg/mL in the current work, indicating that orlistat may possess much stronger inhibitory effect against lipase than the three extracts. Considering the total phenol content of three samples, it was found that the sample with higher polyphenol content had better inhibitory activity on pancreatic lipase. Many studies have shown that plant food extracts rich in phenols generally have good inhibitory activity against lipases [31]. Dorota et al. reported the inhibitory effects of the crude extract of black chokeberry fruit and its ethyl acetate fraction and polyphenol-rich fraction on pancreatic lipase activity [31]. The results showed that the polyphenol-rich fraction exhibited higher antilipase activity than other components. In general, the composition and content of phenolics in the extract may play an important role in pancreatic lipase inhibitory activity.

3.6. Tyrosinase Inhibitory Activity. Figure 3(c) shows the inhibition of tyrosinase activity of ethanol extracts of *P. utilis* flowers, leaves, and stems. As the concentration increased, the inhibitory effect of each extract on tyrosinase gradually increased. The IC_{50} values of the *P. utilis* flower, leaf, and stem extracts for tyrosinase inhibitory activity were 4.11 ± 0.11, 4.33 ± 0.04, and 4.58 ± 0.11 mg/mL, respectively, which were higher than that of the positive control kojic acid ($IC_{50} = 0.39 \pm 0.02$ μg/mL) ($p < 0.05$). It can be seen that the tyrosinase inhibitory activity of the *P. utilis* flower extract is the highest, followed by the leaf extract, and the stem extract had the lowest tyrosinase inhibitory activity. In addition, the inhibitory activity of three samples on tyrosinase was related to the total phenol and total flavonoid content, by comparing their corresponding total phenol and total flavonoid content. Our results showed that the ethanol extracts of flowers, leaves, and stems contained *p*-coumaric acid, which has been reported to have a good inhibitory effect on mushroom polyphenol oxidase, human tyrosinase, and cell melanin [32]. Therefore, the utilization of flower extracts with high content of coumaric acid may be helpful for fruit browning prevention and human skin whitening.

4. Conclusions

This study investigated the total phenols, total flavonoids, and polyphenol composition of ethanol extracts from flowers, leaves, and stems of *P. utilis*. Their antioxidant capacity and inhibitory activities against α-glycosidase, lipase, and tyrosinase were also determined *in vitro*. The total phenols and total flavonoids were detected with the highest contents in flowers followed by leaves and stems. Among polyphenol compounds, rutin and isorhamnetin-3-*O*-rutinoside were the dominant compounds in flower and leaf ethanol extracts. As for the stem ethanol extract, rutin and isoschaftoside were the most abundant substances. Moreover, the antioxidant capacity and enzyme inhibitory capacity were detected with the highest value in the flower ethanol extract compared with others. The outcome of the work could provide support to the development and utilization of *P. utilis* in food and health products.

Data Availability

All data included in this study are available upon request by contacting the corresponding author.

Conflicts of Interest

There are no conflicts of interest regarding the publication of this article.

Acknowledgments

The present work was financially supported by the Science and Technology Project of Yunnan Province (202002AE320006-01-03 and 2019ZG001-4-1) and the Key Research and Development Program of Kunming City (No. 2019-1-N-25318000003141).

References

[1] D. Šamec, E. Karalija, I. Šola, V. Vujčić Bok, and B. Salopek-Sond, "The role of polyphenols in abiotic stress response: the influence of molecular structure," *Pan*, vol. 10, no. 1, p. 118, 2021.

[2] F. Shahidi and P. Ambigaipalan, "Phenolics and polyphenolics in foods, beverages and spices: antioxidant activity and health effects—a review," *Journal of Functional Foods*, vol. 18, pp. 820–897, 2015.

[3] V. Ponzo, I. Goitre, M. Fadda et al., "Dietary flavonoid intake and cardiovascular risk: a population-based cohort study," *Journal of Translational Medicine*, vol. 13, no. 1, pp. 218–313, 2015.

[4] Boua, B. Benson, L. Traoré, D. C. Ouattara, J.-A. Mamyrbekova-Békro, and Y.-A. Békro, "The changes in the contents of polyphenolic compounds of taro (Colocasia *esculenta*) upon domestic processing," *World Journal of Pharmaceutical Research*, vol. 10, pp. 102–111, 2021.

[5] H. Cory, S. Passarelli, J. Szeto, M. Tamez, and J. Mattei, "The role of polyphenols in human health and food systems: a mini-review," *Frontiers in Nutrition*, vol. 5, p. 87, 2018.

[6] M. Sobhani, M. H. Farzaei, S. Kiani, and R. Khodarahmi, "Immunomodulatory; anti-inflammatory/antioxidant effects of polyphenols: a comparative review on the parental compounds and their metabolites," *Food Reviews International*, vol. 37, no. 8, pp. 759–811, 2021.

[7] J. Xiang, M. Zhang, F. B. Apea-Bah, and T. Beta, "Hydroxycinnamic acid amide (HCAA) derivatives, flavonoid C-glycosides, phenolic acids and antioxidant properties of foxtail millet," *Food Chemistry*, vol. 295, pp. 214–223, 2019.

[8] B. A. Nikfarjam, F. Hajiali, M. Adineh et al., "Anti-inflammatory effects of quercetin and vitexin on activated human peripheral blood neutrophils: - the effects of quercetin and vitexin on human neutrophils," *Journal of Pharmacopuncture*, vol. 20, no. 2, pp. 127–131, 2017.

[9] R. Rituparna, A. Saha, P. Barua, and Atish, "Tea polyphenols egcg and tf restrict tongue and liver carcinogenesis simultaneously induced by *N*-nitrosodiethylamine in mice," *Toxicology and Applied Pharmacology*, vol. 300, pp. 34–46, 2016.

[10] X.-Q. Chen, T. Hu, Y. Han et al., "Preventive effects of catechins on cardiovascular disease," *Molecules*, vol. 21, no. 12, p. 1759, 2016.

[11] S. Huang, Y. Ma, C. Zhang, S. Cai, and M. Pang, "Bioaccessibility and antioxidant activity of phenolics in native and fermented Prinsepia utilis Royle seed during a simulated gastrointestinal digestion in vitro," *Journal of Functional Foods*, vol. 37, pp. 354–362, 2017.

[12] Q. Zhang, H.-X. Liu, H.-B. Tan, and S.-X. Qiu, "Novel highly oxygenated and B-Ring-Seco-Ent-Diterpene glucosides from the seeds of *Prinsepia utilis*," *Tetrahedron*, vol. 71, no. 50, pp. 9415–9419, 2015.

[13] Y. Q. Xu, Z. Yao, J. Y. Hu, J. Teng, Y. Takaishi, and H. Q. Duan, "Immunosuppressive terpenes from *Prinsepia utilis*," *Journal of Asian Natural Products Research*, vol. 9, no. 6–8, pp. 637–642, 2007.

[14] D. Sun, S. Huang, S. Cai, J. Cao, and P. Han, "Digestion property and synergistic effect on biological activity of purple rice (*Oryza sativa* L.) anthocyanins subjected to a simulated gastrointestinal digestion in vitro," *Food Research International*, vol. 78, pp. 114–123, 2015.

[15] J. Zhou, Y. Ma, Y. Jia, M. Pang, G. Cheng, and S. Cai, "Phenolic profiles, antioxidant activities and cytoprotective effects of different phenolic fractions from oil palm (elaeis guineensis jacq.) fruits treated by ultra-high pressure," *Food Chemistry*, vol. 288, pp. 68–77, 2019.

[16] X. Zhang, Y. Jia, Y. Ma, G. Cheng, and S. Cai, "Phenolic composition, antioxidant properties, and inhibition toward digestive enzymes with molecular docking analysis of different fractions from *Prinsepia utilis* Royle fruits," *Molecules*, vol. 2312 pages, 2018.

[17] S. Cai, O. Wang, M. Wang et al., "In vitro inhibitory effect on pancreatic lipase activity of subfractions from ethanol extracts of fermented oats (*Avena sativa* L.) and synergistic effect of three phenolic acids," *Journal of Agricultural and Food Chemistry*, vol. 60, no. 29, pp. 7245–7251, 2012.

[18] N. Baurin, E. Arnoult, T. Scior, Q. T. Do, and P. Bernard, "Preliminary screening of some tropical plants for anti-tyrosinase activity," *Journal of Ethnopharmacology*, vol. 82, no. 2-3, pp. 155–158, 2002.

[19] C. S. Sánchez, A. M. T. González, M. C. García-Parrilla, J. J. Q. Granados, H. López García De La Serrana, and M. C. López Martínez, "Different radical scavenging tests in virgin olive oil and their relation to the total phenol content," *Analytica Chimica Acta*, vol. 593, no. 1, pp. 103–107, 2007.

[20] H. Guo, S. Kandasamy, and M. H. Wang, "Total phenolic, flavonoid contents and free radical scavenging capacity of extracts from tubers of Stachys affinis," *Biocatalysis and Agricultural Biotechnology*, vol. 15, 2018.

[21] L. Zhang, Z.-c. Tu, H. Wang, Z.-f. Fu, Q.-h. Wen, and D. Fan, "Metabolic profiling of antioxidants constituents in artemisia selengensis leaves," *Food Chemistry*, vol. 186, pp. 123–132, 2015.

[22] P. Milica, D. Dragana, M. Saša et al., "Chemical characterization of fruit wine made from oblačinska sour cherry," *The Scientific World Journal*, vol. 2014, Article ID 454797, 9 pages, 2014.

[23] Z. Liu, Z. Ren, C. C. Chuang, E. Kandaswamy, T. Zhou, and L. Zuo, "Role of ROS and nutritional antioxidants in human diseases," *Frontiers in physiology*, vol. 9, p. 477, 2018.

[24] K. Cui, X. Luo, K. Xu, and M. R. Ven Murthy, "Role of oxidative stress in neurodegeneration: recent developments in assay methods for oxidative stress and nutraceutical antioxidants," *Progress in Neuro-Psychopharmacology and Biological Psychiatry*, vol. 28, no. 5, pp. 771–799, 2004.

[25] S. Cuevas and P. Pelegrín, "Pyroptosis and redox balance in kidney diseases," *Antioxidants and Redox Signaling*, vol. 35, no. 1, pp. 40–60, 2021.

[26] C. Zhang, Y. Ma, F. Gao, Y. Zhao, S. Cai, and M. Pang, "The free, esterified, and insoluble-bound phenolic profiles of rhus chinensis mill. Fruits and their pancreatic lipase inhibitory activities with molecular docking analysis," *Journal of Functional Foods*, vol. 40, pp. 729–735, 2018.

[27] A. C.-N. Leong, Y. Kinjo, M. Tako, H. Iwasaki, H. Oku, and H. Tamaki, "Flavonoid glycosides in the shoot system of Okinawa Taumu (*Colocasia esculenta* S.)," *Food Chemistry*, vol. 119, no. 2, pp. 630–635, 2010.

[28] R. Gao, Q. Yu, Y. Shen et al., "Production, bioactive properties, and potential applications of fish protein hydrolysates: developments and challenges," *Trends in Food Science & Technology*, vol. 110, no. 1, pp. 687–699, 2021.

[29] M. J. Rahman, P. Ambigaipalan, and F. Shahidi, "Biological activities of camelina and sophia seeds phenolics: inhibition of LDL oxidation, DNA damage, and pancreatic lipase and α-glucosidase activities," *Journal of Food Science*, vol. 83, no. 1–3, pp. 237–245, 2018.

[30] Y. Wu, Q. Zhou, X.-y. Chen, X. Li, Y. Wang, and J.-l. Zhang, "Comparison and screening of bioactive phenolic compounds in different blueberry cultivars: evaluation of anti-oxidation and α-glucosidase inhibition effect," *Food Research International*, vol. 100, no. 1, pp. 312–324, 2017.

[31] S. Dorota, P. Anna, R. Małgorzata, and Z. Kucharska Alicja, "Inhibitory effect of black chokeberry fruit polyphenols on pancreatic lipase—searching for most active inhibitors," *Journal of Functional Foods*, vol. 49, pp. 196–204, 2018.

[32] C. B. Yong, "P-coumaric acid as an active ingredient in cosmetics: a review focusing on its antimelanogenic effects," *Antioxidants*, vol. 8, no. 8, p. 275, 2019.

Hindawi
Journal of Food Quality
Volume 2021, Article ID 9541725, 13 pages
https://doi.org/10.1155/2021/9541725

Research Article

Selective Fermentation of *Lactobacillus* and *Streptococcus In Vitro*: Effects of Chinese Fermented Glutinous Rice on the Growth Promotion of Potential Probiotics

Wenliang Ma,[1] Xiao Ni,[1] Ying Guo,[1] Yu Zhang,[1] Chaojie Zhu,[1] Yinping Li,[1] Chi Shen,[1] Biao Yuan ,[2] and Xiao Xu [1,3]

[1]*School of Life Science, Shaoxing University, Shaoxing, Zhejiang 312000, China*
[2]*Department of Food Quality and Safety, National R&D Center for Chinese Herbal Medicine Processing, College of Engineering, China Pharmaceutical University, Nanjing, Jiangsu 211198, China*
[3]*National Engineering Laboratory for Cereal Fermentation Technology, Jiangnan University, Wuxi, Jiangsu 214122, China*

Correspondence should be addressed to Biao Yuan; yuanbiao@cpu.edu.cn and Xiao Xu; xiaolexu@126.com

Received 30 July 2021; Revised 15 October 2021; Accepted 12 November 2021; Published 23 December 2021

Academic Editor: Alessandra Durazzo

A functional Chinese fermented glutinous rice has been developed with the supplementation of Fu brick tea (CRW-FBT). In this study, we aimed to evaluate its effect on the growth of potential probiotic strains in the *Lactobacillus*, *Streptococcus*, and *Weissella* genus, compared with traditional Chinese fermented glutinous rice (CRW). The growth profiles of lactic acid bacteria were analyzed based on fermentations *in vitro*, and the optical densities were recorded at 600 nm during the whole fermentation. Growth curve, maximum $OD_{600\,nm}$, and growth rate were measured and compared among samples with different ratios of CRW-FBT and CRW addition. Through the multiple analysis of growth parameters, we found that all the tested strains obtained better growth results when CRW-FBT was supplemented to the media, compared with the CRW and basic media. The bacterial growth was promoted by exhibiting the shortened lag time, prolonged logarithmic phase and stationary phase, and increased growth rate and cell density, as well as the better performance after 24 h and 48 h fermentation. Besides, short-chain fatty acids and organic acids in CRW-FBT were founded. Our work demonstrated the positive effect of Fu brick tea supplemented in the CRW and illustrated its beneficial role in the food fermentation industry for the purpose of microorganism enrichment and the improvement of microbial metabolism.

1. Introduction

In recent years, prebiotics have been received increasing attention as 'a substrate that is selectively utilized by host microorganisms conferring a health benefit' [1]. The consumption of food-based prebiotics is one of the practicable approaches to modulate the composition and structure of human intestinal microbiota. These prebiotics reach the large intestine and were selectively metabolized by certain intestinal bacterial species, such as lactobacilli and galactococcus [2]. In general, the prebiotics could promote short-chain fatty acids, resulting in various health benefits [3]. Nowadays, numerous new functional foods emerged endlessly aiming at improving host health, while novel beneficial food supplements achieve rapid development in possession of stimulating the growth of probiotics and leading to intestinal microflora homeostasis.

Polyphenols have been found to have the capabilities of influencing cell growth of microorganisms and their metabolisms. Zhou et al. showed the addition of gallic and protocatechuic acids significantly reduced the concentration of ethyl carbamate during Chinese glutinous rice wine fermentation [4]. Chen et al. reported the finding that one type of polyphenols in oolong tea influenced the protein expression and meliorated alcohol-induced intoxication of *Saccharomyces cerevisiae* [5]. Figueiredo et al. presented the

finding that the phenolic aldehydes, coniferaldehyde, 3,4-dihydroxybenzaldehyde, p-hydroxybenzaldehyde, and sinapaldehyde significantly affected the growth of *Oenococcus oeni*, while flavonoids showed slight differences such as myricetin and the flavan-3-ols studied (catechin and epicatechin) [6, 7]. Thus, polyphenols played crucial roles in food fermentation and were used to contribute to the population adjustment of microorganism, leading to the enhanced fermentation efficiency and food quality.

Fermented foods and beverages have been developed for nearly 14,000 years as irreplaceable staples and drinks of human diets. In recent years, fermented foods and beverages has been increasingly popular for their functional properties. Lactic acid bacteria and their metabolites in fermented foods, such as exopolysaccharide, organic acids, galactooligosaccharides, and phenolic acids, have many positive effects on human health [8]. Hence, it needed to establish relationships among lactic acid bacteria in fermented foods, their metabolites, and gut health. Chinese fermented glutinous rice wine (CRW), as one of the oldest alcoholic beverages, was brewed dating as far as 5000 BCE in China and recently is consumed widely in the world. CRW usually appears in daily diet as a drinking or seasoning matter during cooking. CRW was a primary source of polyphenols intake in eastern diets, just like beer in western diets. Phenolic acids, flavonoids, tannins, and flavan-3-ols were biotransformed by microorganisms and released from materials during the fermentation. Furthermore, CRW had many pharmacological benefits and value as its various nutritional compounds including polysaccharides, peptides, and amino acids [9, 10]. CRW was also used to supplement as one of foodstuffs during the food fermentation process with an effect to promote microbial growth, ameliorate flavor, and participate in substance metabolism. A certain type of Chinese glutinous rice wine in the region of Shaoxing city (Zhejiang province, China) called "*xiangxue*" was made by mixing with fermented glutinous rice wine during the primary fermentation. The flavor of *xiangxue* was special and this processing technique was popular, but few studies focus on the effect of fermented glutinous rice wine supplementation, especially on microbial growth and their metabolism. It is also difficult to ascertain the biological effects on microbial metabolism and the promotion of the special species growth.

Chinese glutinous rice wine has been reported to contain ten individual phenolic compounds such as syringic acid, rutin, (−)-epicatechin, (+)-catechin, gallic acid, and vanillic acid [11]. Xu et al. studied the promoted fermentation efficiency exhibited by Chinese fermented glutinous rice when supplementation with Fu brick tea (CRW-FBT) in the primary fermentation, because of an increased concentration of polyphenols leading to an increased population of yeasts and enzyme activities [8, 12]. Thus, it is rational that Fu brick tea as a supplement of polyphenols was utilized into fermentation process to modulate microbial community. In this study, Chinese fermented glutinous rice with Fu brick tea was pressed to collect the low-alcohol juice, and its ability of supporting the growth of potential intestinal probiotics and lactic acid bacteria was analyzed. A series of substrate utilization examinations were carried out, by pure cultures of strains, such as *Streptococcus thermophilus*, *Lactobacillus plantarum*, *Lactobacillus rhamnosus*, and other 8 species. The dynamic changes of microorganism in various fermentation stages were displayed based on the growth curves, maximum microorganism population, growth rates, and lag parameters. We compared the microbial growth rate when growing at original media with those growing at which carbohydrate was partially replaced with CRW-FBT or CRW. We aimed to obtain information about the growth profiles of potential probiotics under different conditions based on the model analysis, along with the influence CRW-FBT and CRW may have on the fermentation ability of lactic acid bacteria during fermentation process.

2. Method

2.1. Materials and Reagents. Glutinous rice (*Oryza sativa* var.) was bought from a local market. Fu brick tea (*Camellia sinensis* L.) was obtained from a tea factory in Yiyang city, Hunan province, China. The starter this study used was commercial starter (Angel Yeast Co., Yichang, Hubei Province, China). Media components were purchased from Sinopharm Chemical Reagent Co. (Shanghai, China). MRS (Man-Rogosa and Sharp) was utilized as a basic media for the growth of *Lactobacillus* and *Streptococcus* strains, enriched with carbohydrates, nitrogen sources, mineral elements, and 0.1% (v/v) Tween 80. Besides, 2% (w/v) of the experimental fraction was supplemented into basic media. The standards were as follows: oxalic acid, tartaric acid, succinic acid, pyruvic acid, malic acid, lactic acid, citric acid, formic acid, acetic acid, propionic acid, and butyric acid were obtained from Aladdin Chemical Reagent Co. (Shanghai, China). LC-grade methanol was from Merck (Darmstadt, Germany). All the other reagents were of analytical grade.

All strains in this study were isolated from traditional fermented foods in our lab. *Lactobacillus helveticus* MB2-1 and *Streptococcus thermophilus* MB5-1 were isolated from Sayram ropy yogurt in Xinjiang [13]. *Weissella hellenica* D1501 was obtained from Dongzu fermented meat [7]. *L. plantarum* 70810 and *L. rhamnosus* LS-8 were isolated from Chinese pickle [14]. *L. delbrueckii* subsp. *bulgaricus* 1-4 was obtained from fermented dzho milk. *L. plantarum* B1-6 was isolated from a type of fermented cereal beverage in Xinjiang province of China called Kirgiz boza. *L. plantarum* 17-1 was obtained from Zhalaba, a special type of fermented vegetable in Guizhou province of China.

2.2. Preparation of Chinese Fermented Glutinous Rice with Fu Brick Tea. Chinese fermented glutinous rice was fermented with/without Fu brick tea (CRW-FBT/CRW) according to the method of our previous study [12]. In brief, Fu brick tea extract was performed by extracting with water at 100°C for 5 min in a ratio of 2 : 100 (g/mL). Glutinous rice was soaked and steamed for 30 min firstly and then mixed with starters and Fu brick tea extracts at a ratio of 2%, followed by incubating at 30°C. The liquor was collected after 4-day

fermentation by pressing and filtered with 0.45 μm membrane for the following analysis.

2.3. Microorganisms and Culture Media. Bacterial strains in our work belong to *Lactobacillus* and *Lactococcus* genera. The strains were cultured in MRS broth and incubated at 37°C in a 5% CO_2 atmosphere under anaerobic conditions (Thermo Forma 3111, Thermo Fisher Scientific Co., USA). The CRW-FBT extracts were supplemented into basic media into different ratios of 1%, 2%, 5%, and 10% as the experiment groups. The CRW extracts were prepared as a control group that was supplemented at ratio of 1%. The blank group was MRS basic media. The whole lactic acid bacteria were cultured and revived twice before the measurement of bacterial growth.

2.4. Measurement of Organic Acids in the Fermented Samples. The organic acids were detected according to a HPLC analysis. All CRW-FBT and CRW samples were prepared by centrifuging at 10000 × g for 10 min at 4°C (Allegra64R, Beckman Coulter, Inc., Brea, USA). The supernatant was collected and filtrated with 0.22 μm membrane and then injected into a HPLC system (Agilent Technologies, Wilmington, DE, USA) equipped with a XSelect HSS T3 analysis column (4.6 mm × 250 mm, 5 mm, Agilent) and a diode-array detector. The injection volume was 20 μL. Each sample was eluted at a flow rate of 0.7 mL/min for 20 min by mobile phases (96% 0.01 M $(NH_4)_2HPO_4$ and 4% methanol). The column temperature was maintained at 30°C. Lactic acid and other 9 organic acids were monitored at the wavelength of 215 nm. The concentrations of identified compounds in samples were quantified due to standards.

2.5. Evaluation of Bacterial Growth. The microbial strains were cultured in MRS for 36 h, and then the cells were harvested by centrifuging at 8000 × g for 10 min at 4°C. After washing twice with 0.85% NaCl solution, the cells were used as seed cultures of each strain and were diluted 1 : 100 into media for the assays described below. The media used in this study included basic media, MRS plus CRW-FBT and MRS plus CRW. According to the method of Ahn et al., bacterial growth was performed in 300 μL wells of sterile 100-well honeycomb microplates by repeating three replicates [15]. Each strain was inoculated into 300 μL fresh medium in individual wells and grown at 37°C for 50 h. To monitor growth patterns, the optical densities at 600 nm ($OD_{600\,nm}$) were recorded at 20 min intervals using a BioScreen C automated growth curve analysis system (Oy Growth Curves AB Ltd., Helsinki, Finland).

2.6. Statistical Analysis. All the results in the present study were presented as means ± standard deviation. One-way analysis of variance (ANOVA) and t-tests were implemented to consider the significant differences ($p < 0.05$), using SPSS version 24.0 (SPSS Inc., Chicago, IL, USA). In order to analyze the microplate assays comprehensively, the representative results were expressed as maximum growth rate (μ_{max}, h^{-1}) and lag time (lag, h) calculated by fitting the curves to a growth model using Microsoft Excel [14].

3. Results and Discussion

To understand the effects of Chinese fermented glutinous rice fermented with Fu brick tea (CRW-FBT) and Chinese fermented glutinous rice (CRW) on the growth of lactic acid bacteria, the selected strains of the genera *Lactobacillus* and *Streptococcus* were used due to their widespread utilization in fermented foods [16]. The growth curves of representative strains grown on supplementation of CRW-FBT at ratios of 1%, 2%, 5%, and 10%, as well as 1% CRW, are depicted in Figure 1. The growth curves showed the growth phases of bacteria, covering the lag phase, logarithmic phase, and stationary phase. All the strains did not meet their decline phases during the 50 h incubation, and thus the overall stationary phases were not exhibited in order to compare differences of other three growth phases evidently.

As shown in Figure 1(a) and Figure 1(b), *L. plantarum* 17-1 and *L. plantarum* 70810 reached their stationary phases earlier compared with other 6 bacteria. Similarly, the needed time that *L. delbrueckii* subsp. *bulgaricus* 1-4 reached the stationary phase was a little shorter than that of the other groups. The $OD_{600\,nm}$ values still preserved a slight raising tendency during its stationary phase, especially in the supplementation groups of 10% CRW-FBT and 5% CRW-FBT (shown in Figure 1(f)). Moreover, the $OD_{600\,nm}$ values in these two experiment groups at different growth periods displayed higher results than those in the control group, 2% CRW-FBT, 1% CRW-FBT, and 1% CRW groups. These results illustrated that the growth and reproduction of lactic acid bacteria were promoted by the supplementation of high content of CRW-FBT. This phenomenon appeared significantly in the growth of *L. plantarum* B1-6, in which a longer lag phase and logarithmic phase were needed, while reaching stationary phase cost about another 5 h compared with experiment groups (Figure 1(c)). Interestingly, the densities of *L. rhamnosus* LS-8 bacteria in 10% CRW-FBT group at any time were higher than those in 5% CRW-FBT, followed by those in 2% CRW-FBT and 1% CRW-FBT, while the much lower were exhibited in the control group.

To analyze the characteristics of the proliferation under the effect of nutrient supplements, the growth rates were calculated (Figure 2). Usually, in the lag phase, the growth rates increase laggingly and then increase fleetly to the maximum when reaching the logarithmic phase There were plenty of differences displayed by the growth profiles of *L. helveticus* MB2-1 in different media (Figure 2(e)). Obviously, the CRW actuated a promotion of microbial growth, leading to shortening lag phase period and costing less time for the maximum growth rates. The influences of CRW-FBT caught better results, in which the least time of the lag phase was spent by the selected strains culturing in the media with the supplementation of 10% CRW-FBT, as well as costing the least time to reach the maximum growth rate. The trends of growth rates of 5% CRW-FBT, 2% CRW-FBT, and 1% CRW-FBT were semblable and spent a little more time staying on lag phase and reaching the maximum growth rates than the 10% CRW-FBT group. As for

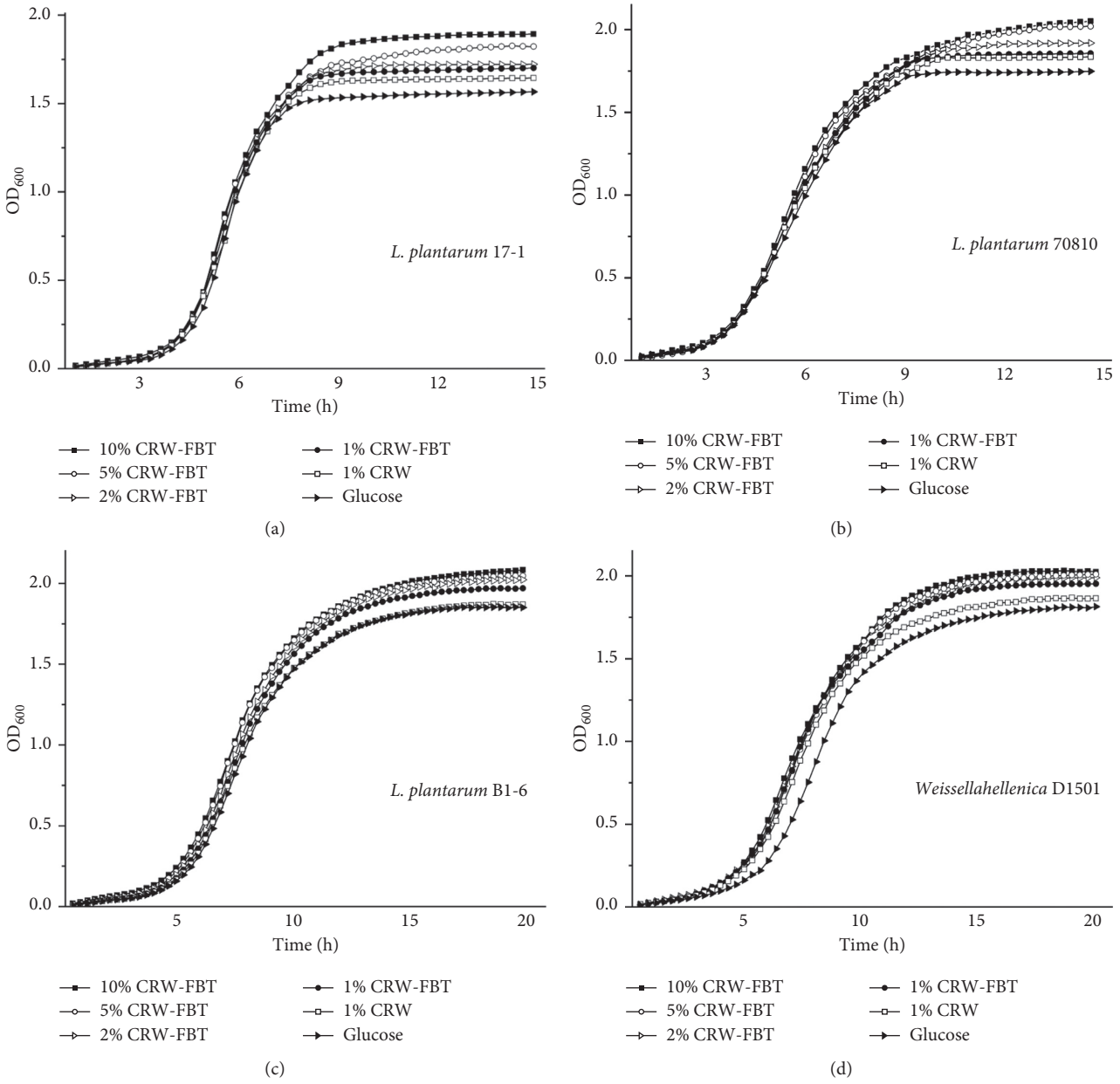

Figure 1: Continued.

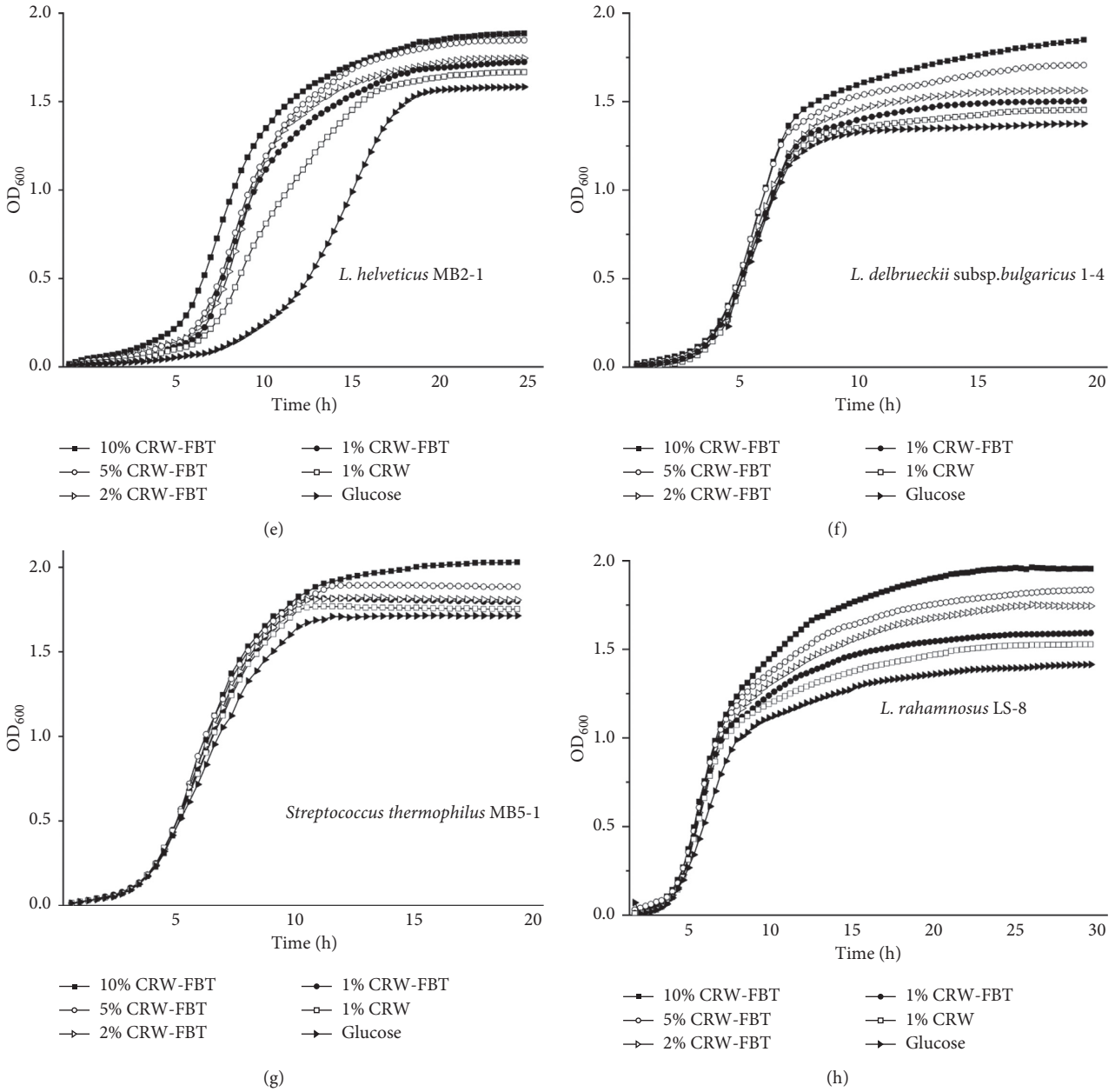

Figure 1: Growth curves of representative selected strains with the supplementation of Chinese fermented glutinous rice with Fu brick tea (CRW-FBT) and Chinese fermented glutinous rice (CRW). *L. plantarum* 17-1 (a), *L. plantarum* 70810 (b), *L. plantarum* B1-6 (c), *Weissella hellenica* D1501 (d), *Lactobacillus helveticus* MB2-1 (e), *L. delbrueckii* subsp. *bulgaricus* 1-4 (f), *Streptococcus thermophilus* MB5-1 (g), and *L. rhamnosus* LS-8 (h) during 50 h fermentation.

W. hellenica D1501 (Figure 2(d)) and *L. delbrueckii* subsp. *bulgaricus* 1-4 (Figure 2(f)), these phenomena could be noted, but the influences were insignificant compared with *L. helveticus* MB2-1. Furthermore, it was inconsistent in all strains that a high concentration of CRW-FBT had a high growth rate. For example, the least time was spent by *W. hellenica* D1501 with the supplementation of 1% CRW-FBT running to the maximum growth rates, followed by 2% CRW-FBT and 5% CRW-FBT. This may be because some microorganisms were sensitive to higher concentration of acids and polyphenols in the supplementation, whereas a synchronous trends were displayed in the growth rate of *L. plantarum* 17-1 grown in all samples (Figure 2(a)). To better describe the effect of all samples on the growth of *L. plantarum* 17-1, we analyzed another two parameters, the maximum growth rate (μ_{max}) and lag time (lag), which were used to compare the substrates preferences of microorganism [17].

As shown in Table 1, through fitting the curves to a sigmoid growth model, the fastest growth rate (μ_{max}) of *L. plantarum* 17-1 was 0.69 h^{-1} with the supplementation of 1% CRW-FBT and 1% CRW, followed by the control group, and other high concentrations of CRW-FBT. However, in

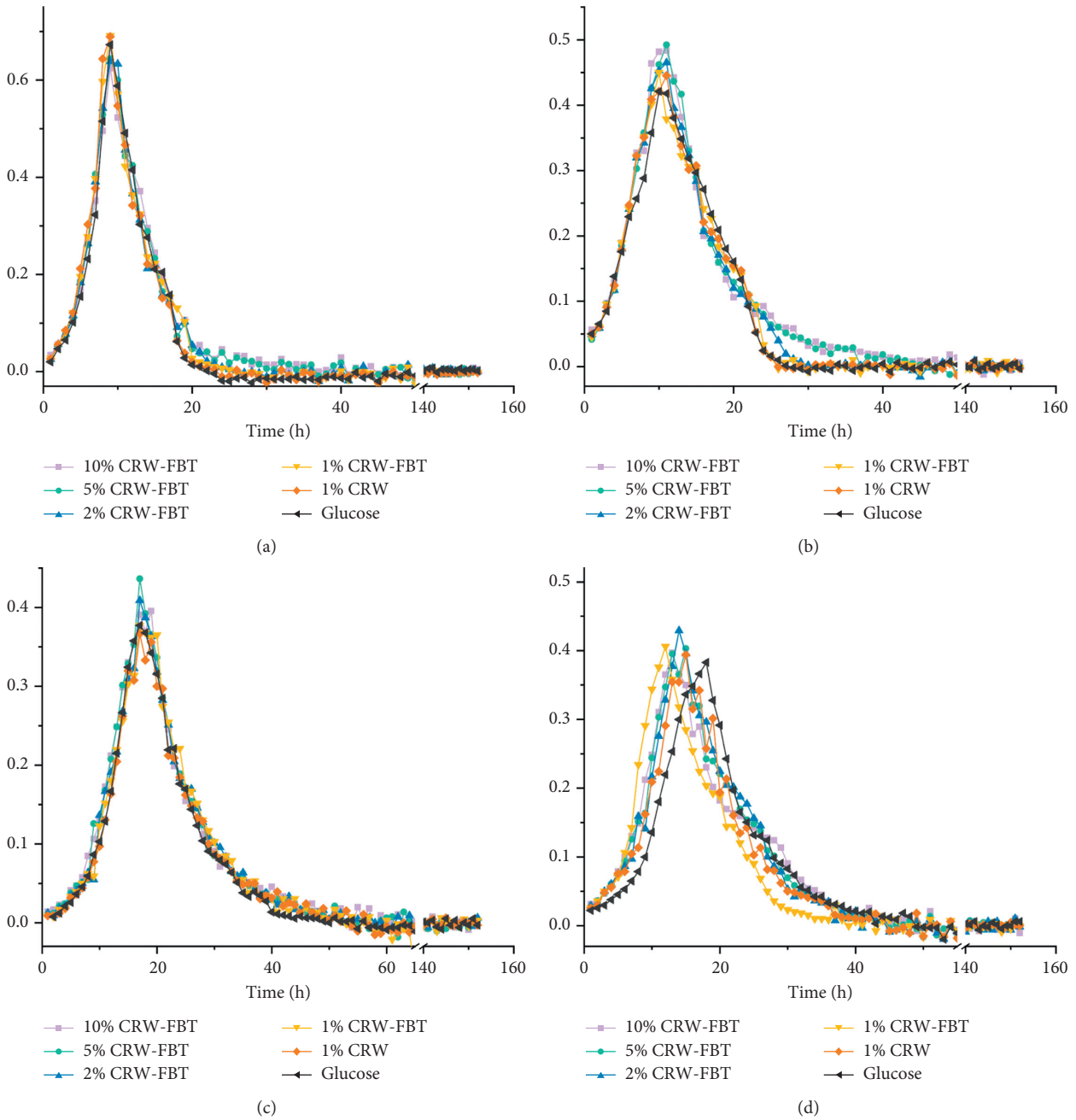

Figure 2: Continued.

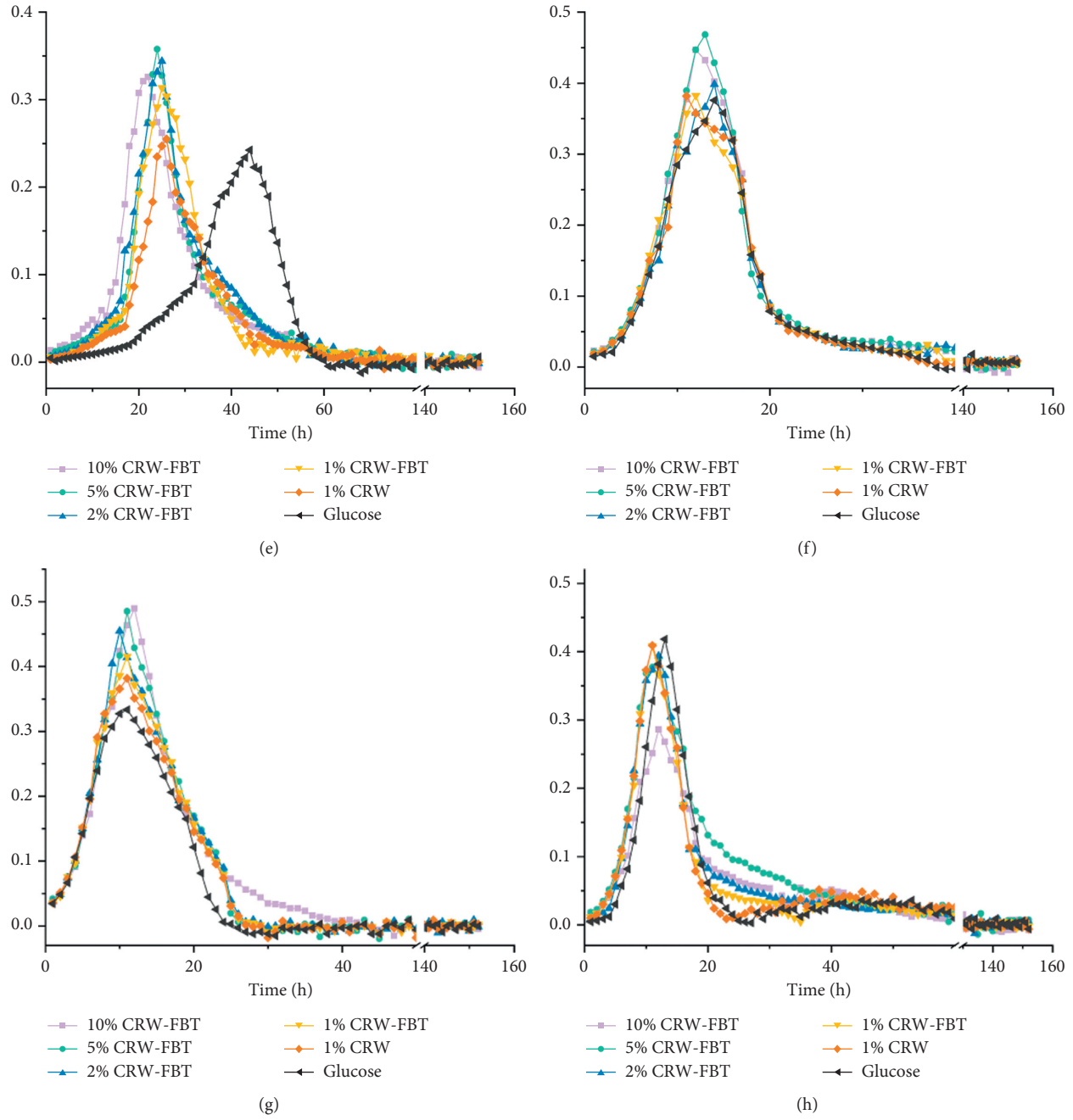

Figure 2: Growth rates of representative selected strains at each time during the whole fermentation with the supplementation of CRW-FBT and CRW. *L. plantarum* 17-1 (a), *L. plantarum* 70810 (b), *L. plantarum* B1-6 (c), *Weissella hellenica* D1501 (d), *Lactobacillus helveticus* MB2-1 (e), *L. delbrueckii* subsp. *bulgaricus* 1-4 (f), *Streptococcus thermophilus* MB5-1 (g), and *L. rhamnosus* LS-8 (h).

the case of *W. hellenica* D1501 and *S. thermophilus* MB5-1, the highest μ_{max} was 0.40 $h^{-1}$and 0.49 h^{-1}, endowed by both 5% CRW-FBT and 10% CRW-FBT. As for these two strains, the higher μ_{max} parameters emerged in the high concentrations of CRW-FBT. That illustrated the finding that less than 5% of the addition proportion would be enough to perform an optimal role to promote the bacterial growth in the culture of these species. Similarly, the fastest growth rate endowed by 5% CRW-FBT occurred with *L. plantarum* 70810, *L. plantarum* B1-6, *L. helveticus* MB2-1, and *L. delbrueckii* subsp. *bulgaricus* 1-4 reaching values of 0.49 h^{-1}, 0.44 h^{-1}, 0.36 h^{-1}, and 0.47 h^{-1}, followed by 0.48 h^{-1} of 10% CRW-FBT, 0.41 h^{-1} of 2% CRW-FBT, 0.34 h^{-1} of 2% CRW-FBT, and 0.45 of h^{-1} 10% CRW-FBT, respectively.

In general, a higher μ_{max} implied that growth of the strains keeps a higher rate, while indirectly reflecting a stronger capability of all samples. But possessing the fastest growth rate could not be a necessary and sufficient condition for the strongest bioactivity; therefore, the lag time (lag) was used to present the profiles of microbial lag phases. The

Table 1: The lag time (lag, h) and the fastest growth rate (μ_{max}, h^{-1}) of representative selected strains during 50 h fermentation with the supplementation of CRW-FBT and CRW.

	17-1		70810		B1-6		D1501		MB2-1		1-4		MB5-1		LS-8	
	lag	μ_{max}	lag	μ_{max}	lag	μ_{max}	lag	μ_{max}	lag	μ_{max}	lag	μ_{max}	lag	μ_{max}	lag	μ_{max}
10% CRW-FBT	2.60	0.62	3.89	0.48	4.61	0.40	4.73	0.40	5.73	0.33	3.69	0.45	3.85	0.49	4.38	0.29
5% CRW-FBT	2.64	0.64	3.81	0.49	4.54	0.44	4.84	0.40	4.67	0.36	3.33	0.47	3.59	0.49	4.43	0.39
2% CRW-FBT	2.28	0.64	3.73	0.47	4.60	0.41	4.76	0.43	5.37	0.34	3.29	0.40	3.45	0.45	4.58	0.39
1% CRW-FBT	2.23	0.69	3.56	0.45	4.68	0.38	4.63	0.40	5.40	0.31	3.18	0.38	3.44	0.42	4.58	0.41
1% CRW	2.20	0.69	3.64	0.45	4.70	0.38	4.42	0.39	5.31	0.26	2.93	0.38	3.44	0.38	4.63	0.41
Control	1.90	0.67	3.31	0.42	4.82	0.37	4.15	0.38	6.31	0.24	3.02	0.38	3.76	0.33	4.71	0.42

L. plantarum 17-1, *L. plantarum* 70810, *L. plantarum* B1-6, *Weissella hellenica* D1501, *Lactobacillus helveticus* MB2-1, *L. delbrueckii subsp. bulgaricus* 1-4, *Streptococcus thermophilus* MB5-1, and *L. rhamnosus* LS-8.

fermentation of basic medium by *L. helveticus* MB2-1 with a long lag time (6.31 h) and the lowest μ_{max} values (0.24 h^{-1}) was characterized as being much slower than fermentation in the sample-supplemented medium, with 4.57 h of lag time by 5% CRW-FBT and 5.31 h of lag time by 1% CRW. However, the positive effect of CRW-FBT and CRW would not be achieved during the fermentation of other lactic acid bacteria, such as *W. hellenica* D1501, in which control group (1.90 h) with the shortest lag time indicated that supplementing experimental samples could prolong the lag phase of bacterial growth. In addition, as for *L. plantarum*, different subspecies exhibited different bioactivities. We found that the lag times of *L. plantarum* 17-1 and *L. plantarum* 70810 were prolonged, while the lag times of *L. plantarum* B1-6 were shortened by various constituents of samples. Tang et al. also reported their distinct performance when different subspecies of *L. plantarum* grow on the exopolysaccharide fractions [18]. In fact, the shortening lag time was considered as a way to accelerate the reproduction of microorganisms, as well as to push the process of microbial metabolism and substrate utilization [19].

In terms of the comprehensive comparison among samples, Figure 3 shows the time of lag phases and logarithmic phases and reaching the maximum $OD_{600\,nm}$ (OD_{max}) during the stationary phases. The addition of CRW-FBT and CRW observed with *L. rhamnosus* LS-8 resulted in the significant longer time of logarithmic phases, which were prolonged about ten hours compared with the control MRS medium. A longer time was spent by *L. delbrueckii* subsp. *bulgaricus* 1-4 for obtaining OD_{max} when it was grown in the supplementation of 10% CRW-FBT and 5% CRW-FBT. That was also the reason why significant higher OD_{max} values were endowed with the high concentrations of CRW-FBT compared to other medias. During the prolonged stationary phase, the growth rates were positive till reaching the OD_{max} value, and further leading to the delayed decline phase. It would be a beneficial result to food industry, particularly to a long-time fermentation process. In the cases of three *L. plantarum* samples, different effects were made by adding the experimental samples. *L. plantarum* 17-1 spent a longer time reaching the OD_{max} value in 10% CRW-FBT and 5% CRW-FBT supplemented media, while the OD_{max} values were obtained quickly after the end of logarithmic phase when grown in other media. *L. plantarum* 70810 had a shorter time to reach OD_{max}, but a longer time of logarithmic phase, as a reason of obtaining the highest OD_{max} in the shortest time. *L. plantarum* B1-6 were the least affected by the samples, exhibiting a little shorter lag time and longer stationary time in the high concentrations of CRW-FBT. Furthermore, the *L. helveticus* MB2-1 was influenced with the shorter time in the three periods we detected, indicating that CRW-FBT promoted the bacterial proliferation. Thus, 2% CRW-FBT could be utilized to shorten the production time and improve the fermentation efficiency.

With respect to mirroring the growth performance through microbial densities during the fermentation, the maximum $OD_{600\,nm}$ (OD_{max}) was recorded (Figure 4), and the $OD_{600\,nm}$ values at 24 h and 48 h fermentation were summarized (Table 2). Obviously, the highest OD_{max} was obtained by supplementing experimental samples. *S. thermophilus* MB5-1 and *L. helveticus* MB2-1 cultured in 10% CRW-FBT fraction possessed the highest OD_{max}, which were much higher than those in 1% CRW and basic media. Meanwhile, these two strains obtained the higher $OD_{600\,nm}$ at both 24 h and 48 h in the media supplemented with CRW-FBT, whose effect was in a dose-dependent manner. Similarly, three *L. plantarum* strains reached better significant growth results when 10% CRW-FBT was added to MRS broth than with a low concentration of CRW-FBT and CRW. In the case of *L. plantarum* 17-1, the highest OD_{max} (2.17) was observed in 10% CRW-FBT fermentation, which was much higher than 1.97 of OD_{max} in 1% CRW-FBT, 1.94 of OD_{max} in 1% CRW and 1.88 of OD_{max} in basic MRS media. Thereby, 10% CRW-FBT addition had a positive effect on obtaining a better bacterial growth behavior during a long-time fermentation, especially after 24 h fermentation. Otherwise, the growth performances of *L. rhamnosus* LS-8 and *W. hellenica* D1501, by the supplementation of 5% CRW-FBT, reached 2.19 and 2.21 of $OD_{600\,nm}$ after 24 h fermentation, as well as 2.21 and 2.18 of $OD_{600\,nm}$ after 48 h fermentation, which were a little higher compared with those grown in other media. Meanwhile, at the supplementation concentration of 10%, these two strains, coupled with *L. delbrueckii* subsp. *bulgaricus* 1-4, gave a similar performance in the $OD_{600\,nm}$ values at 24 h and 48 h, as well as OD_{max}.

All the data demonstrated that CRW-FBT and CRW fractions stimulated the growth of the tested lactic acid bacteria in the typical food fermentation environment. The occurrence of components in CRW-FBT and CRW seems to influence the μ_{max} values, lag time, and maximum $OD_{600\,nm}$

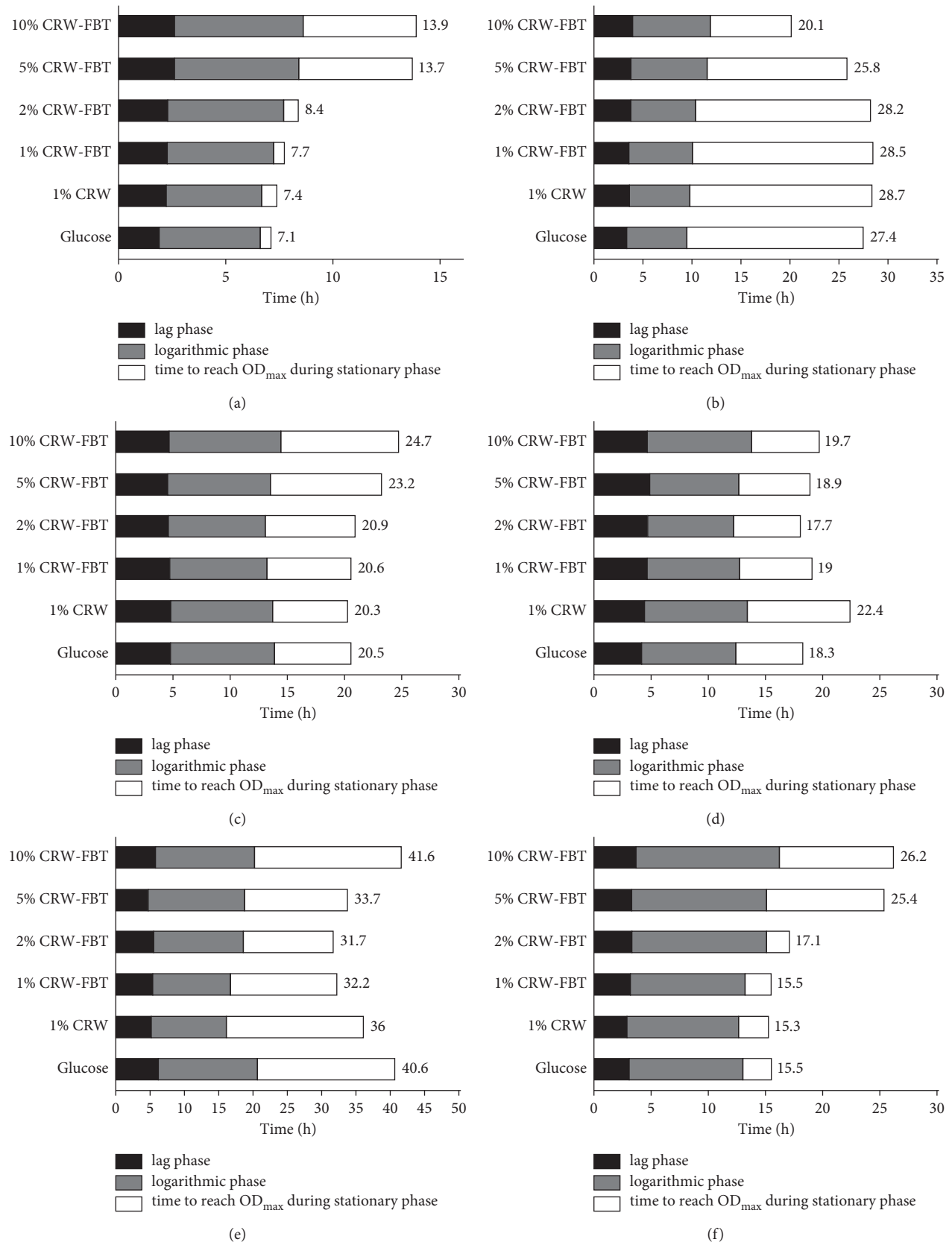

Figure 3: Continued.

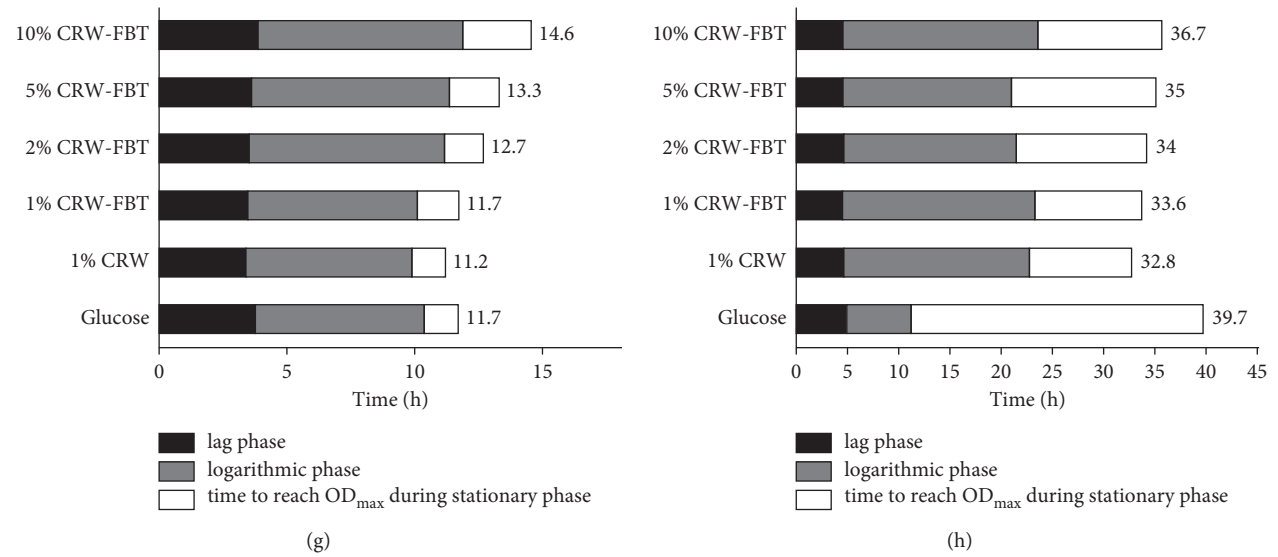

Figure 3: The time of lag phase and logarithmic phase and to reach OD_{max} during stationary phase of selected fermentation of representative strains with the supplementation of CRW-FBT and CRW. *L. plantarum* 17-1 (a), *L. plantarum* 70810 (b), *L. plantarum* B1-6 (c), *Weissella hellenica* D1501 (d), *Lactobacillus helveticus* MB2-1 (e), *L. delbrueckii* subsp. *bulgaricus* 1-4 (f), *Streptococcus thermophilus* MB5-1 (g), and *L. rhamnosus* LS-8 (h).

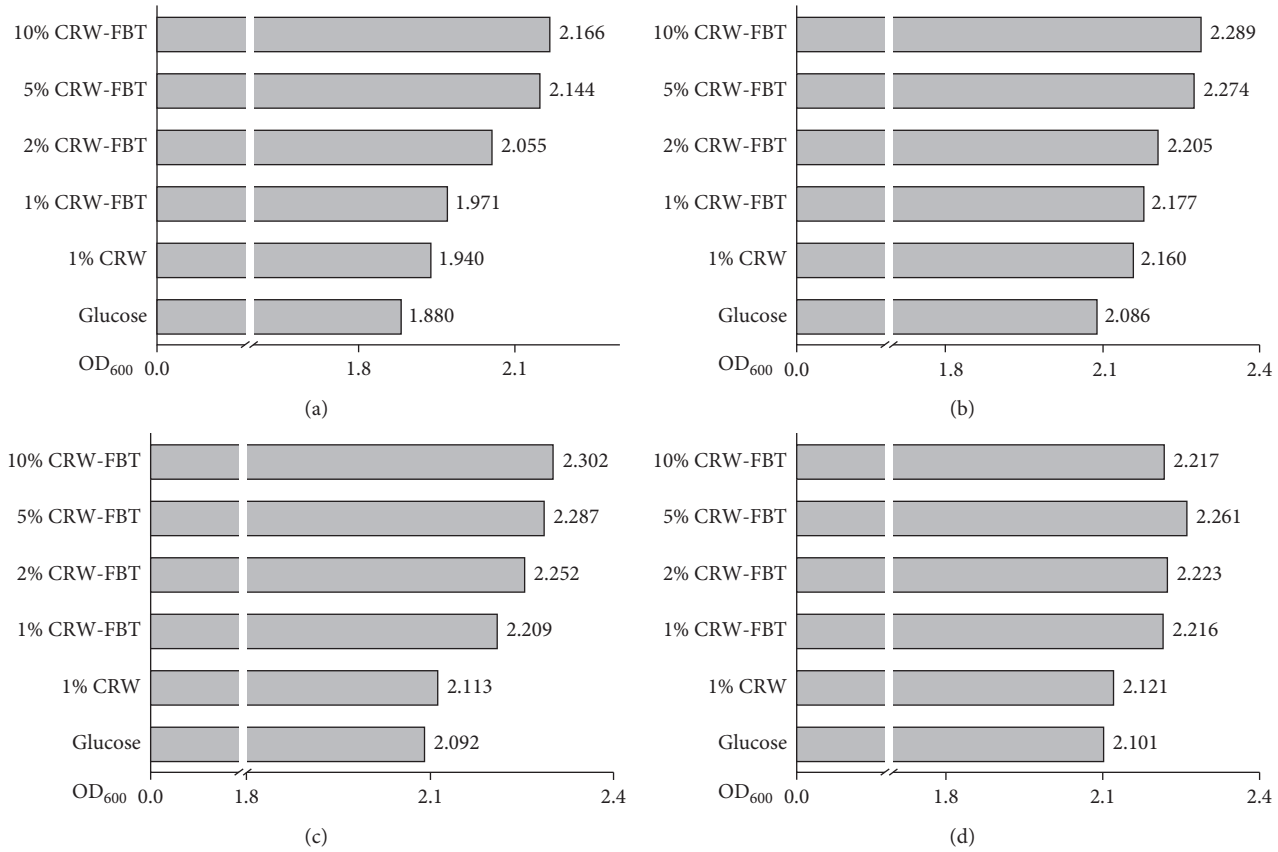

Figure 4: Continued.

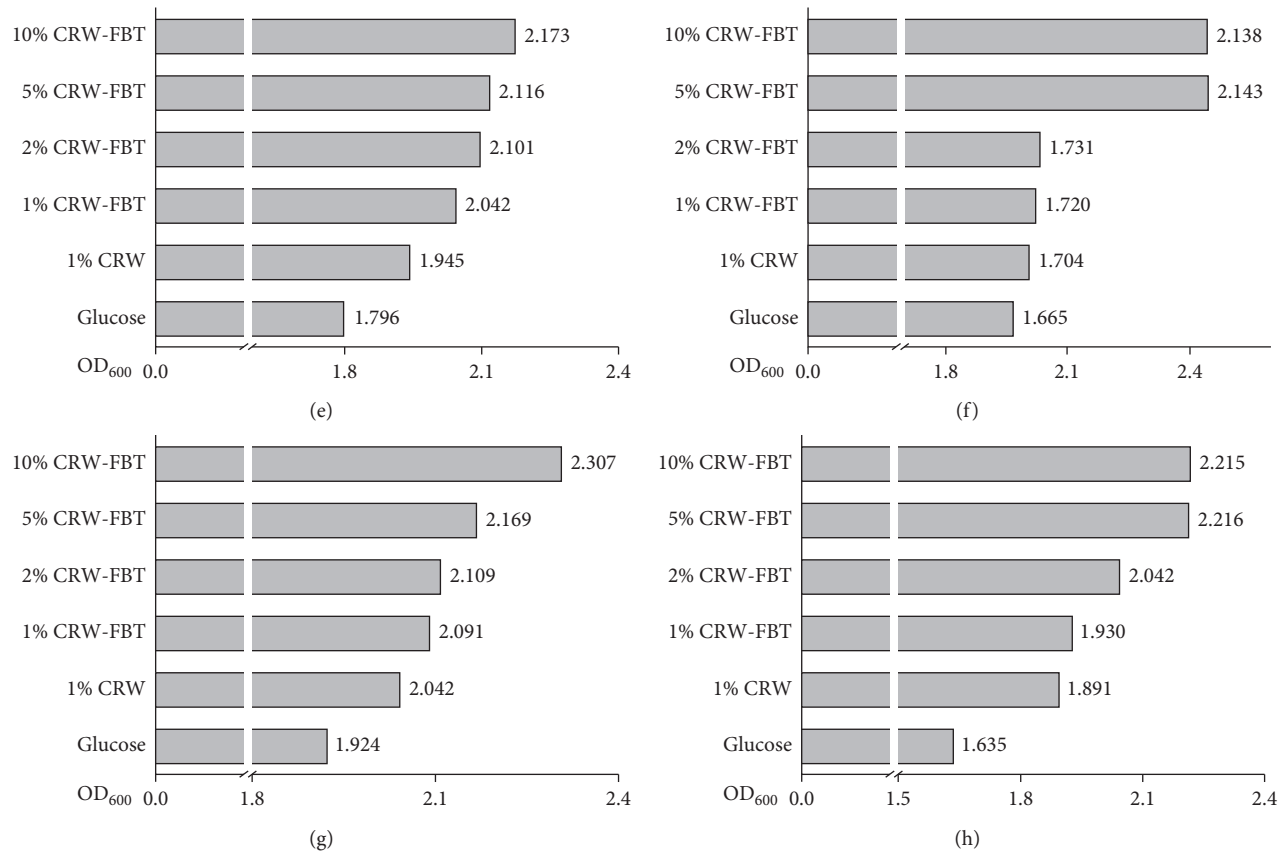

Figure 4: The maximum $OD_{600\,nm}$ (OD_{max}) of representative selected strains during 50 h fermentation with the supplementation of CRW-FBT and CRW. *L. plantarum* 17-1 (a), *L. plantarum* 70810 (b), *L. plantarum* B1-6 (c), *Weissella hellenica* D1501 (d), *Lactobacillus helveticus* MB2-1 (e), *L. delbrueckii* subsp. *bulgaricus* 1-4 (f), *Streptococcus thermophilus* MB5-1 (g), and *L. rhamnosus* LS-8 (h).

Table 2: The $OD_{600\,nm}$ values of representative selected strains after 24 h and 48 h fermentation with the supplementation of CRW-FBT and CRW.

	17-1		70810		B1-6		D1501		MB2-1		1-4		MB5-1		LS-8	
	24 h	48 h	24 h	48 h	24 h	48 h	24 h	48 h	24 h	48 h	24 h	48 h	24 h	48 h	24 h	48 h
10% CRW-FBT	2.09	2.16	2.27	2.26	2.30	2.21	2.19	2.13	2.10	2.17	2.10	2.14	2.27	2.27	2.12	2.20
5% CRW-FBT	2.02	2.14	2.25	2.23	2.27	2.19	2.21	2.18	2.06	2.11	2.08	2.13	2.13	2.17	2.19	2.21
2% CRW-FBT	1.89	2.05	2.17	2.20	2.24	2.16	2.15	2.15	2.10	2.09	1.70	1.72	2.05	2.11	1.99	2.04
1% CRW-FBT	1.84	1.97	2.11	2.18	2.16	2.14	2.06	2.12	1.98	2.04	1.65	1.70	2.03	2.09	1.86	1.92
1% CRW	1.78	1.85	2.09	2.16	2.06	2.05	2.03	2.07	1.91	1.94	1.65	1.69	2.00	2.04	1.83	1.89
Control	1.74	1.85	2.04	2.08	2.04	2.08	2.00	2.06	1.76	1.78	1.63	1.65	1.90	1.92	1.54	1.64

L. plantarum 17-1, *L. plantarum* 70810, *L. plantarum* B1-6, *Weissella hellenica* D1501, *Lactobacillus helveticus* MB2-1, *L. delbrueckii subsp. bulgaricus* 1-4, *Streptococcus thermophilus* MB5-1, and *L. rhamnosus* LS-8.

values of the individual strains, such as the polysaccharides, polyphenols, and short-chain fatty acids (SCFAs). In the survival of the model probiotic *L. plantarum*, Ramos et al. reported that the presence of the exopolysaccharides β-glucans enhanced the beneficial properties of probiotic bacteria [20]. In addition, Gomez et al. evaluated the low-molecular-weight pectic oligosaccharides according to the selective fermentation by potential probiotic *Lactobacillus* and *Bifidobacterium* strains, and the fermentation capability of probiotic bacteria was modified [17]. The stimulatory effects on the growth and malolactic activity of lactic acid bacteria were exhibited by fermentation with low concentrations of gallic acid [21]. We also found CRW-FBT contained a low concentration of gallic acid [12]. That was one of reasons why the better growth parameters were observed in the selective fermentation when supplementing with CRW-FBT.

The metabolism of lactic acid bacteria produces the short-chain fatty acids (SCFAs), which have been confirmed to contain several healthy benefits, especially to the improvement of colonic health, like reducing the growth of potential pathogenic bacteria and ameliorating probiotics [22, 23]. As shown in Table 3, the contents of acetic acid were the highest (0.095 ± 0.003 g/L), followed by the propionic acid (0.138 ± 0.007 g/L) in CRW-FBT, and 0.015 ± 0.004 g/L and 0.033 ± 0.008 g/L, respectively in CRW. Acetic acid

Table 3: The contents (g/L) of organic acids and short-chain fatty acids in CRW-FBT and CRW.

		CRW-FBT	CRW	p value
Organic acids	Succinic acid	0.281 ± 0.008	0.280 ± 0.010	0.97
	Tartaric acid	0.082 ± 0.002	0.050 ± 0.004	0.0003
	Oxalic acid	0.013 ± 0.001	0.002 ± 0.001	< 0.0001
	Malic acid	0.090 ± 0.001	n.d.	< 0.0001
	Citric acid	0.348 ± 0.008	0.353 ± 0.007	0.44
	Pyruvic acid	0.006 ± 0.001	n.d.	0.0001
	Lactic acid	0.886 ± 0.031	1.472 ± 0.034	< 0.0001
	Total	1.706 ± 0.051	2.157 ± 0.056	0.0001
Short-chain fatty acids	Formic acid	0.095 ± 0.003	0.091 ± 0.008	0.44
	Acetic acid	0.155 ± 0.006	0.015 ± 0.004	< 0.0001
	Propionic acid	0.138 ± 0.007	0.033 ± 0.008	< 0.0001
	Butyric acid	0.011 ± 0.001	0.006 ± 0.001	0.0015
	Total	0.399 ± 0.017	0.145 ± 0.021	< 0.0001

** and * exhibit significant differences at $p < 0.01$ and $p < 0.05$ levels between CRW-FBT and CRW after the same fermentation time. "nd." represented "not detected." Each value was expressed as means ± standard error ($n = 3$).

usually could serve as a source of energy for human body tissues, such as brain, heart, and peripheral tissues [24]. Propionic acid has various beneficial effects and was reported to affect the cell metabolism and immune system, thus reducing hepatic and serum cholesterol content *in vivo* [25]. Butyrate can regulate the precursors of M2 macrophages and T cells, regulate oxidative stress, and contribute to intestinal homeostasis [22]. The content of butyric acid in CRW-FBT was 0.011 ± 0.001 g/L, which was higher than in CRW significantly with 0.006 ± 0.001 g/L. Campos et al. also reported that special strains could produce butyric acid during food fermentation [26]. The total content of organic acids (in Table 3) except for SCFAs in CRW-FBT (1.706 ± 0.051 g/L) was a little lower than CRW (2.157 ± 0.056 g/L), covering the significant differences of lactic acid contents and constituent proportion. Malic acid and pyruvic acid were not found in CRW, while they were quantified by 0.090 ± 0.001 g/L and 0.006 ± 0.001 g/L in CRW-FBT. Malic acid is one of the major organic compounds which contribute to the flavor and taste of wine, juices, and other drinks [27]. Malolactic fermentation was usually studied in red wine fermentation because of its benefits of increasing flowery aroma and adjusting the balance of saccharinity and acidity [28]. In our work, the significant differences were also present in the contents of tartaric acid (0.082 ± 0.002 g/L in CRW-FBT and 0.050 ± 0.004 g/L in CRW).

4. Conclusion

This study evaluated the potential beneficial role of fermented glutinous rice with Fu brick tea (CRW-FBT) by establishing a pure culture system. Eight strains used in traditional fermented foods were selected for bacterial fermentation *in vitro*. Our results suggested CRW-FBT may have a great potential as supplementation to shorten lag time, raise the growth rate, and prolong the proliferation period, leading to a higher cell density. A high concentration of CRW-FBT was considered to possess the bioactive capability of stimulating the growth of probiotic strains related to the human intestinal health. In sum, these results could provide a novel perspective for fermented glutinous rice development in food fermentation industry.

Data Availability

The raw data used to support the findings of this study are currently under embargo while the research findings are commercialized. Requests for data, 6 months after publication of this article, will be considered by the corresponding author.

Ethical Approval

This article does not contain any studies with human participants or animals performed by any of the authors.

Conflicts of Interest

All authors declare that they have no conflicts of interest.

Authors' Contributions

Xiao Xu conceived the project idea and obtained fundings. Xiao Xu and Biao Yuan were assigned the project and wrote this article. Wenliang Ma and Xiao Ni finished all the researches. Chi Shen, Ying Guo, and Biao Yuan revised the paper. Other authors were participants in the method optimization and review. All authors approved the final manuscript draft.

Acknowledgments

Financial support from the Natural Science Foundation of Zhejiang Province, China (LQ21C200003), Natural Science Foundation of Shaoxing University (2019LG1012), and Scientific Research Start-Up Fund of Shaoxing University (20195015) was acknowledged.

References

[1] G. R. Gibson, R. Hutkins, M. E. Sanders et al., "The International scientific association for probiotics and prebiotics (ISAPP) consensus statement on the definition and scope of

prebiotics," *Nature Reviews Gastroenterology & Hepatology*, vol. 14, no. 8, pp. 491–502, 2017.

[2] L. B. Bindels, N. M. Delzenne, P. D. Cani, and J. Walter, "Towards a more comprehensive concept for prebiotics," *Nature Reviews Gastroenterology & Hepatology*, vol. 12, no. 5, pp. 303–310, 2015.

[3] A. Peredo-Lovillo, H. E. Romero-Luna, and M. Jimenez-Fernandez, "Health promoting microbial metabolites produced by gut microbiota after prebiotics metabolism," *Food Research International*, vol. 136, 2020.

[4] W. Zhou, R. Fang, and Q. Chen, "Effect of gallic and protocatechuic acids on the metabolism of ethyl carbamate in Chinese yellow rice wine brewing," *Food Chemistry*, vol. 233, pp. 174–181, 2017.

[5] C. Chen, X. Chen, M. Jiang, X. Rui, W. Li, and M. Dong, "A newly discovered bacteriocin from Weissella hellenica D1501 associated with Chinese dong fermented meat (Nanx Wudl)," *Food Control*, vol. 42, pp. 116–124, 2014.

[6] A. R. Figueiredo, F. Campos, V. de Freitas, T. Hogg, and J. A. Couto, "Effect of phenolic aldehydes and flavonoids on growth and inactivation of Oenococcus oeni and Lactobacillus hilgardii," *Food Microbiology*, vol. 25, no. 1, pp. 105–112, 2008.

[7] F. Liu, P. Li, M. Chen et al., "Fructooligosaccharide (FOS) and galactooligosaccharide (GOS) increase Bifidobacterium but reduce butyrate producing bacteria with adverse glycemic metabolism in healthy young population," *Scientific Reports*, vol. 7, Article ID 11789, 2017.

[8] X. Xu, S. Zhou, D. Julian McClements et al., "Multistarter fermentation of glutinous rice with Fu brick tea: effects on microbial, chemical, and volatile compositions," *Food Chemistry*, vol. 309, Article ID 125790, 2020.

[9] Q.-Y. Lu, R.-P. Lee, J. Huang et al., "Quantification of bioactive constituents and antioxidant activity of Chinese yellow wine," *Journal of Food Composition and Analysis*, vol. 44, pp. 86–92, 2015.

[10] C. Shen, J. Mao, Y. Chen, X. Meng, and Z. Ji, "Extraction optimization of polysaccharides from Chinese rice wine from the Shaoxing region and evaluation of its immunity activities," *Journal of the Science of Food and Agriculture*, vol. 95, no. 10, pp. 1991–1996, 2015.

[11] Q. Fei, L. Mao, and P. Xin, "Antioxidant activities of five Chinese rice wines and the involvement of phenolic compounds," *Food Research International*, vol. 39, no. 5, pp. 581–587, 2006.

[12] X. Xu, W. Hu, S. Zhou et al., "Increased phenolic content and enhanced antioxidant activity in fermented glutinous rice supplemented with Fu brick tea," *Molecules*, vol. 24, no. 4, p. 671, 2019.

[13] W. Li, M. Mutuvulla, X. Chen, M. Jiang, and M. Dong, "Isolation and identification of high viscosity-producing lactic acid bacteria from a traditional fermented milk in Xinjiang and its role in fermentation process," *European Food Research and Technology*, vol. 235, no. 3, pp. 497–505, 2012.

[14] M. Feng, X. Chen, C. Li, R. Nurgul, and M. Dong, "Isolation and identification of an exopolysaccharide-producing lactic acid bacterium strain from Chinese paocai and biosorption of Pb(II) by its exopolysaccharide," *Journal of Food Science*, vol. 77, no. 6, pp. T111–T117, 2012.

[15] S. J. Ahn, W. Hull, S. Desai, K. C. Rice, and D. Culp, "Understanding LrgAB regulation ofStreptococcus mutansMetabolism," *Frontiers in Microbiology*, vol. 11, p. 2119, 2020.

[16] S. Parvez, K. A. Malik, S. Ah Kang, and H.-Y. Kim, "Probiotics and their fermented food products are beneficial for health," *Journal of Applied Microbiology*, vol. 100, no. 6, pp. 1171–1185, 2006.

[17] B. Gómez, C. Peláez, M. C. Martínez-Cuesta, J. C. Parajó, J. L. Alonso, and T. Requena, "Emerging prebiotics obtained from lemon and sugar beet byproducts: evaluation of their in vitro fermentability by probiotic bacteria," *Lwt*, vol. 109, pp. 17–25, 2019.

[18] W. Tang, S. Han, J. Zhou et al., "Selective fermentation of Lactobacillus delbrueckii ssp. Bulgaricus SRFM-1 derived exopolysaccharide by Lactobacillus and Streptococcus strains revealed prebiotic properties," *Journal of Functional Foods*, vol. 69, Article ID 103952, 2020.

[19] M. Berga, A. J. Székely, and S. Langenheder, "Effects of disturbance intensity and frequency on bacterial community composition and function," *PLoS One*, vol. 7, no. 5, Article ID e36959, 2012.

[20] A. P. Romas, M. L. Mohedano, P. López et al., "In situ β-glucan fortification of cereal-based matrices by pediococcus parvulus 2.6: technological aspects and prebiotic potential," *International Journal of Molecular Sciences*, vol. 18, p. 1588, 2017.

[21] H. Rodríguez, J. A. Curiel, J. M. Landete et al., "Food phenolics and lactic acid bacteria," *International Journal of Food Microbiology*, vol. 132, no. 2-3, pp. 79–90, 2009.

[22] B. Gómez, B. Gullón, C. Remoroza, H. A. Schols, J. C. Parajó, and J. L. Alonso, "Purification, characterization, and prebiotic properties of pectic oligosaccharides from orange peel wastes," *Journal of Agricultural and Food Chemistry*, vol. 62, pp. 9769–9782, 2014.

[23] L. Paparo, R. Nocerino, E. Ciaglia et al., "Butyrate as a bioactive human milk protective component against food allergy," *Allergy*, vol. 76, no. 5, pp. 1398–1415, 2021.

[24] G. den Besten, K. van Eunen, A. K. Groen, K. Venema, D.-J. Reijngoud, and B. M. Bakker, "The role of short-chain fatty acids in the interplay between diet, gut microbiota, and host energy metabolism," *Journal of Lipid Research*, vol. 54, no. 9, pp. 2325–2340, 2013.

[25] S. a. Al-Lahham, H. Roelofsen, F. Rezaee et al., "Propionic acid affects immune status and metabolism in adipose tissue from overweight subjects," *European Journal of Clinical Investigation*, vol. 42, no. 4, pp. 357–364, 2011.

[26] J. Rodriguez-Campos, H. B. Escalona-Buendía, I. Orozco-Avila, E. Lugo-Cervantes, and M. E. Jaramillo-Flores, "Dynamics of volatile and non-volatile compounds in cocoa (Theobroma cacao L.) during fermentation and drying processes using principal components analysis," *Food Research International*, vol. 44, no. 1, pp. 250–258, 2011.

[27] R. Monosik, M. Streďanský, G. Greif, and E. Šturdík, "Malic acid Comparison of biosensors based on gold and nanocomposite electrodes for monitoring of malic acid in wine," *Central European Journal of Chemistry*, vol. 10, pp. 157–164, 2012.

[28] Z. D. Celik, T. Cabaroglu, and S. Krieger-Weber, "Impact of malolactic fermentation on the volatile composition of Turkish Kalecik karası red wines," *Journal of the Institute of Brewing*, vol. 125, no. 1, pp. 92–99, 2019.

Hindawi
Journal of Food Quality
Volume 2021, Article ID 9247998, 9 pages
https://doi.org/10.1155/2021/9247998

Research Article

Protease Catalyzed Production of Spent Hen Meat Hydrolysate Powder for Health Food Applications

Deepak Kumar,[1] **Aishwarya Mishra**,[1] **Ayon Tarafdar**,[2] **Abdullah Anwar**,[1] **Athiya Salagram**,[1] **Siraz Alam**,[1] **Ashish K. Sahoo**,[1] **Raveendran Sindhu**,[3] **and Prarabdh C. Badgujar**[1]

[1]*Department of Food Science and Technology, National Institute of Food Technology Entrepreneurship and Management, Kundli, Sonipat 131028, Haryana, India*
[2]*Livestock Production and Management Section, ICAR-Indian Veterinary Research Institute, Izatnagar, Bareilly 243122, Uttar Pradesh, India*
[3]*Microbial Processes and Technology Division, CSIR-National Institute for Interdisciplinary Science and Technology (CSIR-NIIST), Trivandrum 695019, India*

Correspondence should be addressed to Prarabdh C. Badgujar; prarabdh.badgujar@gmail.com

Received 2 July 2021; Accepted 29 September 2021; Published 12 October 2021

Academic Editor: Biao Yuan

Whole spent hen meat of Indian commercial layer bird (BV-300 breed) was enzymatically hydrolyzed using Flavourzyme® derived from *Aspergillus oryzae*. Different time, temperature, and pH combinations generated through response surface methodology (RSM) were tested to find the optimal hydrolysis condition at which maximum antioxidant potential and degree of hydrolysis can be achieved. Hydrolysis for 30 min at a temperature of 53.9°C and pH of 6.56 was found suitable for achieving high degree of hydrolysis and antioxidant activity. Antioxidant potential at optimized conditions was estimated at 93.26% by DPPH radical scavenging assay and 2.32 mM TEAC by FRAP assay. Amino acid profiling of the hydrolysate correlated very well with SDS-PAGE profiling. SDS-PAGE results confirmed that 30 min hydrolysis time was enough to produce low molecular weight peptides (2–5 kDa) with high antioxidant potential. Antioxidant rich Indian spent hen meat hydrolysate powder was economically produced using spray drying. Sensory analysis revealed that 10% hydrolysate powder had satisfactory overall acceptability and has potential to be used in health/functional foods at this concentration. This is the first study wherein optimum hydrolysis conditions for Indian spent hen meat have been reported.

1. Introduction

Indian layer industry is growing at the rate of 6-7% per annum with current population of layer birds estimated at 240 million [1]. As time passes, the hens progress in age and develop cross linkages in their collagen network manifested in less juicy, tougher, and chewier meat [2]. Hens that lose their capacity to lay eggs efficiently are referred to as "spent." Approximately 140 million spent hens are generated annually, taking their laying cycle and moulting into consideration. The increasing number of spent hens is raising a concern for their disposal. Due to the tough texture of spent hen meat, they are often disposed of as landfill, thereby limiting their utilization as a source of food. An efficient alternative for the utilization of spent hen has to be thought of.

Protein hydrolysis employing proteases like Alcalase (endoenzyme) and Flavourzyme (endo- and exoproteases) is emerging as an attractive alternative for food waste utilization. The generated hydrolysates have been shown to possess enhanced nutritional and therapeutic activities including but not limited to antioxidant activity [3, 4], antihypertensive activity [5], hypoglycaemic effect [6], antimicrobial properties [7], and antitumor activity [8]. Functional characteristics of these hydrolysates are due to bioactive peptides formed during hydrolysis of native

proteins. The extent of bioactivity depends on the source of substrate, nature of enzyme, and hydrolysis conditions. Hydrolysate consists of soluble and insoluble protein fractions among which insoluble portion is generally dried and used for cattle feed. Soluble portion consists of small and medium chain peptides [9]. Pharmaceutical industries incorporate an additional purification step to obtain low molecular weight peptides which are in demand, but the process results in lower yield of hydrolysate and increased production cost. Generally, whole or nonpurified peptides exert higher antioxidant activity than purified peptides [10].

In the current work, we aimed to optimize hydrolysis conditions for the production of spent hen meat hydrolysate with maximum degree of hydrolysis and antioxidant potential. The study also dealt with production of spent hen meat hydrolysate powder with the help of spray drying which can be used for the development of functional food products and nutraceuticals by the processed food industry.

2. Materials and Methods

2.1. Materials. Stable free radical: 1,1-diphenyl-2-picrylhydrazyl (DPPH); FRAP reagent: 2,4,6-tri(2-pyridyl)-s-triazine (TPTZ); and Flavourzyme® [a mixture of exo- and endopeptidases (from *Aspergillus oryzae*), with a declared activity of ≥500 U/g] were purchased from Sigma-Aldrich (India). All other chemicals used were of high analytical/ACS grade.

2.2. Sample Preparation. Spent hens (BV-300 breed) were procured from the local commercial layer farm and slaughtered by neck cut (bleeding) method as per the regulations prevalent in the country (stunning by electrocuted water) in a nearby butcher shop to obtain boneless meat, which was immediately frozen at −20°C. To maintain uniformity in the batch of spent hen meat used, spent hens were procured from the commercial layer farm instead of directly sourcing its meat from the butcher shops. Since no experimental trials were done on the live animals/birds (spent hens), prior approval from Institutional Animal Ethics Committee (IAEC) was not required. Meat was transported to lab in the frozen form which was then converted to smaller meat cuts using frozen block cutter (Sanco, Indonesia) and kept in polyethylene bags at −20°C. Prior to experimentation, frozen meat was kept at refrigeration temperature (4°C) overnight for thawing. Small meat blocks were then minced using a lab scale meat mincer (Sanco, Indonesia). Minced meat was defatted 3 times using hexane (1 : 10; meat: hexane). The defatted meat was then mixed with distilled water (1 : 3 w/w) followed by homogenization at 10,000 rpm for a duration of 5 min using a high speed tissue homogenizer (POLYTRON, Kinematica AG, Switzerland).

2.3. Preparation of Hydrolysate. The homogenized meat-water mixture was transferred to a 1 L bioreactor and heated at a desired temperature. pH was maintained using 0.1 N NaOH. The mixture was hydrolyzed using a protease enzyme, Flavourzyme®, which was used at an enzyme to substrate ratio of 3% (v/w) under appropriate conditions. Amount of enzyme required for hydrolysis was determined on the basis of crude protein content in the substrate. The experimental levels of independent variables (temperature, X_1; pH, X_2; time, X_3) were selected based on preliminary trials, and their effect on the dependent parameters such as degree of hydrolysis (Y_1) and functional properties, as measured by radical scavenging assays, viz., DPPH (Y_2) and FRAP (Y_3), was analyzed. After hydrolysis at different temperatures and pH, the reaction was terminated by heating the mixture at 85°C for 20 min followed by cooling and centrifugation at 6000 g for 10 min. The resulting supernatant was immediately stored at 4°C for further processing.

2.4. Determination of Degree of Hydrolysis. pH-stat method was employed, in which the ratio of number of peptide bonds cleaved to the total number of peptide bonds available for hydrolysis was calculated according to Adler-Nissin [11] using the following equation:

$$\mathrm{DH}\,(\%) = \frac{B \times N_b}{M_p \times \alpha \times h_{\mathrm{total}}} \times 100. \quad (1)$$

Here, B is the NaOH consumed during hydrolysis (in mL), N_b is the normality of base, M_p is the mass of protein (in g), α represents the average degree of dissociation (α-NH_2 groups), and h_{total} is the total number of peptide bonds in the protein substrate.

2.5. Estimation of Antioxidant Potential

2.5.1. DPPH Radical Scavenging Assay. DPPH radical scavenging activity was estimated according to the procedure reported by Tang et al. [12] with slight modifications. Briefly, liquid hydrolysate (500 μL, 10 mg/ml) was mixed with 500 μL of 0.1 mM ethanolic DPPH. The mixture was vortexed for 5 min to ensure thorough mixing and left in dark for 30 min. The reaction mixture was then centrifuged at 5,000 g for 10 min to remove turbidity. Absorbance of the resulting supernatant was measured at 517 nm wavelength. Radical scavenging activity was determined using the following equation:

$$\text{scavenging ability}\,(\%) = \left(1 - \frac{A_1 - A_2}{A_0}\right) \times 100. \quad (2)$$

Here, A_1 is absorbance of 500 μL sample + 500 μL DPPH in ethanol; A_2 is absorbance of 500 μL sample + 500 μL ethanol; and A_0 is the absorbance of 500 μL DPPH in ethanol + 500 μL distilled water

2.5.2. Ferric Reducing Antioxidant Power (FRAP) Assay. FRAP was assessed according to the method reported by Verma et al. [13] with slight modification. Fresh FRAP reagent (300 mM acetate buffer (pH 3.6) + 20 mM ferric chloride + 10 mM TPTZ prepared in 40 mM HCl) was prepared in the ratio of 10 : 1 : 1 and incubated at 37°C. From this reagent, 900 μL was taken, mixed with 100 μL (25 mg/ml) of hydrolysate, and incubated again at 37°C for 40 min.

Absorbance was recorded at 593 nm. Trolox was used for preparing the standard curve (5–200 μm).

2.6. Process Optimization. Optimization of hydrolysis conditions was accomplished by response surface methodology (RSM) using face-centered central composite design (FCCCD) and derivative based optimization technique in the Design-Expert software v.10.0.1.

2.7. SDS-PAGE of Optimized Liquid Hydrolysate. Molecular weight distribution of marker and optimized liquid hydrolysate sample were determined by the method given by Laemmli [14]. Samples (5 μL) were diluted by Tris-HCl buffer (4% SDS, 0.2 mol/L DTT, 0.125 mol/L Tris-HCl, 0.02% bromophenol blue, 20% v/v glycerol, pH 6.8). To cleave all noncovalent bonds, samples were boiled for 2 minutes. Gel was casted with 15% resolving gel and 5% stacking gel. Electrophoretic separation was done in SE300 miniVE integrated vertical protein electrophoresis and blotting unit assembly (Hoefer, Massachusetts, United States) using power supply of 120 V in PS300B (Hoefer, Massachusetts, United States). Seven microliters of molecular weight marker of 2–250 kDa (Precision Plus Protein Dual Xtra Standards, Bio-Rad Laboratories Inc., Hercules, CA, USA) range was used.

2.8. Spray Drying of Optimized Hydrolysate. Liquid hydrolysate was mixed with maltodextrin (5DE) at 10% concentration. Inlet and outlet temperature were maintained at 160°C and 70°C, respectively, in pilot scale spray drier (SMST, India). Feed was supplied to spray drier using a peristaltic pump maintained at 10 rpm. Nozzle pressure was maintained at 10 psi. The spray dried powder was collected in an airtight LDPE Polypack and stored in a desiccator till further analysis.

2.9. Analysis of Spray Dried Hydrolysate Powder

2.9.1. Antioxidant Activity. For DPPH assay, sample concentration of 10 mg/ml was used, and the procedure described in Section 2.5.1 was followed. For FRAP assay, sample concentration used was 25 mg/ml. The same procedure mentioned in Section 2.5.2 was followed.

2.9.2. Amino Acid Profiling. Amino acid composition was estimated by Pico-Tag method as per Kurozawa et al. [9] with slight modification. Protein hydrolysates were digested using 6 N HCl/0.1% phenol at 110°C for 24 h and then derivatized with 20 μL of ethanol:water:trimethylamine: phenylisothiocyanate solution (7 : 1 : 1 : 1, v/v). Amino acid composition was then analyzed with HPLC system (Nova-Pak C18, 4 μm, Waters, Milford, MA) equipped with reverse phase column.

2.9.3. Essential Amino Acid Score and Protein Efficiency Ratio. Nutritional quality of protein is measured from protein efficiency ratio (PER) and essential amino acid (EA) score. Essential amino acid score was determined by comparing the essential amino acids in hydrolysate with the standard amino acid content requirement for adults [15]. Protein efficiency ratio was calculated by the following equations given by Lee et al. [16]:

$$\mathrm{PER}_7 = 0.08084 \times \sum AA_7 - 0.1094, \quad (3)$$

$$\mathrm{PER}_{10} = 0.0320 \times \sum AA_{10} - 0.1539, \quad (4)$$

where $\sum AA_7$ is the sum of threonine, valine, methionine, isoleucine, leucine, phenylalanine, and lysine contents (g/100g protein); $\sum AA_{10}$ is the sum of $\sum AA_7$, histidine, arginine, and tryptophan contents (g/100 g protein).

2.9.4. Sensory Evaluation. Spent hen hydrolysate powder was added to potable drinking water at H_1 (5%), H_2 (10%), and H_3 (15%) to prepare a drink for sensory evaluation. Sensory analysis was done on 9-point hedonic scale, and the quality attributes selected were appearance, aroma, taste, bitterness, and overall acceptability as done by Kumar et al. [17]. Panellists were chosen from the Food Science and Technology and Food Engineering Department of our institute and subjected to training to familiarize them with hydrolysate samples. The three preparations were presented to 15 semi-trained (9 male + 6 female) panellists in the age group of 20–30 years.

2.10. Statistical Analysis. The number of experiments was 19 following a face-centered central composite design. Experimental data were analyzed and optimized using Design-Expert v.10.0.1 (Stat-Ease Inc.). For proximate studies, all analyses were performed in triplicate. Results of the analyses were reported as mean ± standard deviation ($n = 3$). Data were analyzed with the help of independent sample t-test using SPSS statistical software v.20 at 5% level of significance ($p < 0.05$).

3. Results and Discussion

3.1. Degree of Hydrolysis. Higher degree of hydrolysis is essential for enhancing the solubility of lower molecular weight protein fractions which directly influence the antioxidant potential of the resulting hydrolysate [18]. Experimental values for degree of hydrolysis varied in the range of 15.29–54.23 (Table 1) which was in agreement with that reported by Bhaskar et al. [19] for meat industry waste. Kurozawa et al. [9] reported a maximum degree of hydrolysis of ~38% for enzymatic hydrolysis of chicken meat with Alcalase®, while Zhang and coworkers reported that enzymatic hydrolysis of chicken breast meat with trypsin could produce ~19% degree of hydrolysis after 8 h hydrolysis time [20]. On close comparison of literature reports to this study, it is clear that Flavourzyme could show higher performance in yielding lower molecular weight peptides than other proteolytic enzymes for chicken meat hydrolysis. Hydrolysis temperature, time, and pH had no significant effect ($p > 0.05$) on the degree of hydrolysis when

Table 1: Hydrolysis experiments and corresponding responses.

Run	Independent variables			Response		
	Temperature (X_1)	pH (X_2)	Time (X_3)	DH (Y_1)	DPPH (Y_2)	FRAP (Y_3)
1	50	7	90	34.41	73.82	0.54
2	40	5	30	41.70	96.48	0.52
3	50	6	150	21.98	90.21	2.38
4	40	7	150	26.82	76.80	0.34
5	50	6	90	27.83	95.53	2.01
6	40	7	30	18.50	87.65	0.48
7	50	6	90	20.79	97.07	2.38
8	50	5	90	22.47	94.41	2.39
9	50	6	90	20.45	91.75	2.23
10	50	6	30	29.52	91.38	2.27
11	40	5	150	54.23	93.13	1.14
12	60	6	90	21.50	92.87	2.07
13	50	6	90	17.94	94.30	2.65
14	60	7	150	27.87	74.68	0.14
15	60	5	150	25.98	93.40	0.60
16	50	6	90	15.29	92.97	2.14
17	60	5	30	25.80	93.19	0.95
18	40	6	90	26.40	93.35	0.97
19	60	7	30	52.90	71.54	0.38

X: independent variable, Y: dependent variable.

considered individually (Table 2). However, the interaction between these variables was found significant ($p \leq 0.05$). For instance, the interaction effect of temperature and pH had a positive influence on the degree of hydrolysis. Simultaneous increase or decrease in temperature-pH combination generated favorable conditions causing increase in the degree of hydrolysis (Figure 1(a)). Since higher temperature and pH conditions could facilitate breakdown of the tightly bound chicken meat fibres, more active sites for the enzyme are available. Lower hydrolysis temperature and pH allow for optimum enzymatic activity which could contribute to significant increase in degree of hydrolysis (Figure 1(a)). The interaction effect of pH and hydrolysis time also affected degree of hydrolysis significantly ($p \leq 0.05$) (Figure 1(b)).

3.2. Antioxidant Potential

3.2.1. DPPH Radical Scavenging Activity. Hydrolysis temperature and pH significantly affected DPPH free radical scavenging activity ($p \leq 0.05$). It was found that free radical scavenging activity (FRSA) ranged from 71.54% to 97.07%. Model plots (Figures 1(d)–1(f)) revealed a relatively constant FRSA with increase in pH up to 5.5 followed by a gradual decrease in FRSA which continued to a pH of 7.0. Wang et al. [21] also reported a decrease in DPPH scavenging potential for duck meat protein hydrolysates beyond a pH of 5.5. During hydrolysis, chicken meat protein breaks down into lower molecular weight peptides that have functional attributes and contribute to antioxidant potential. When pH of the medium surrounding these peptides increases, they undergo structural modification and thereby lose their capability to scavenge free radicals. Negative model coefficient for pH (Table 2) confirmed the hypothesis that increase in pH would result in reduced FRSA. Increase in temperature also showed a similar decrease in FRSA (Figures 1(d)–1(f)). It was observed that increasing the temperature from 40°C to 60°C resulted in 5–25% decrease in FRSA (Table 1). Our finding is in parallel with those of other researchers who have given a plausible reason that, at elevated temperatures, denaturation of Flavourzyme could lead to lower degree of hydrolysis resulting in decreased formation of bioactive peptides, consequently reducing the FRSA [22]. Hydrolysis time was found to insignificantly affect the DPPH radical scavenging activity ($p > 0.05$) which shows that lower time of hydrolysis can be selected to reduce the energy consumed during the process without

Table 2: Second order model coefficients obtained after regression analysis between experimental variables and responses.

Model coefficient	DPPH		FRAP		DH	
	Coeff.	p value	Coeff.	p value	Coeff.	p value
Intercept	93.260	≤0.001	2.320	≤0.001	20.950	≤0.001
A- hydrolysis temp	−2.180	≤0.030	0.068	≤0.630	−1.360	≤0.460
B- hydrolysis pH	−8.610	≤0.001	−0.371	≤0.020	−0.968	≤0.600
C- hydrolysis time	−1.200	≤0.190	−0.000	≤0.990	−1.150	≤0.530
AB	−1.900	≤0.070	−0.023	≤0.880	9.950	≤0.001
AC	2.190	≤0.040	−0.133	≤0.400	−5.710	≤0.010
BC	−0.571	≤0.560	-0.083	≤0.590	−3.680	≤0.090
A^2	1.190	≤0.480	-0.829	≤0.010	2.380	≤0.500
B^2	−7.800	≤0.001	−0.882	≤0.001	6.870	≤0.070
C^2	−1.120	≤0.500	−0.021	≤0.930	4.180	≤0.250
r	0.972		0.939		0.930	
R^2	0.946		0.883		0.864	
SD	2.700		0.433		5.640	

r: correlation coefficient, R^2: regression coefficient, SD: standard deviation, Coeff.: coefficient.

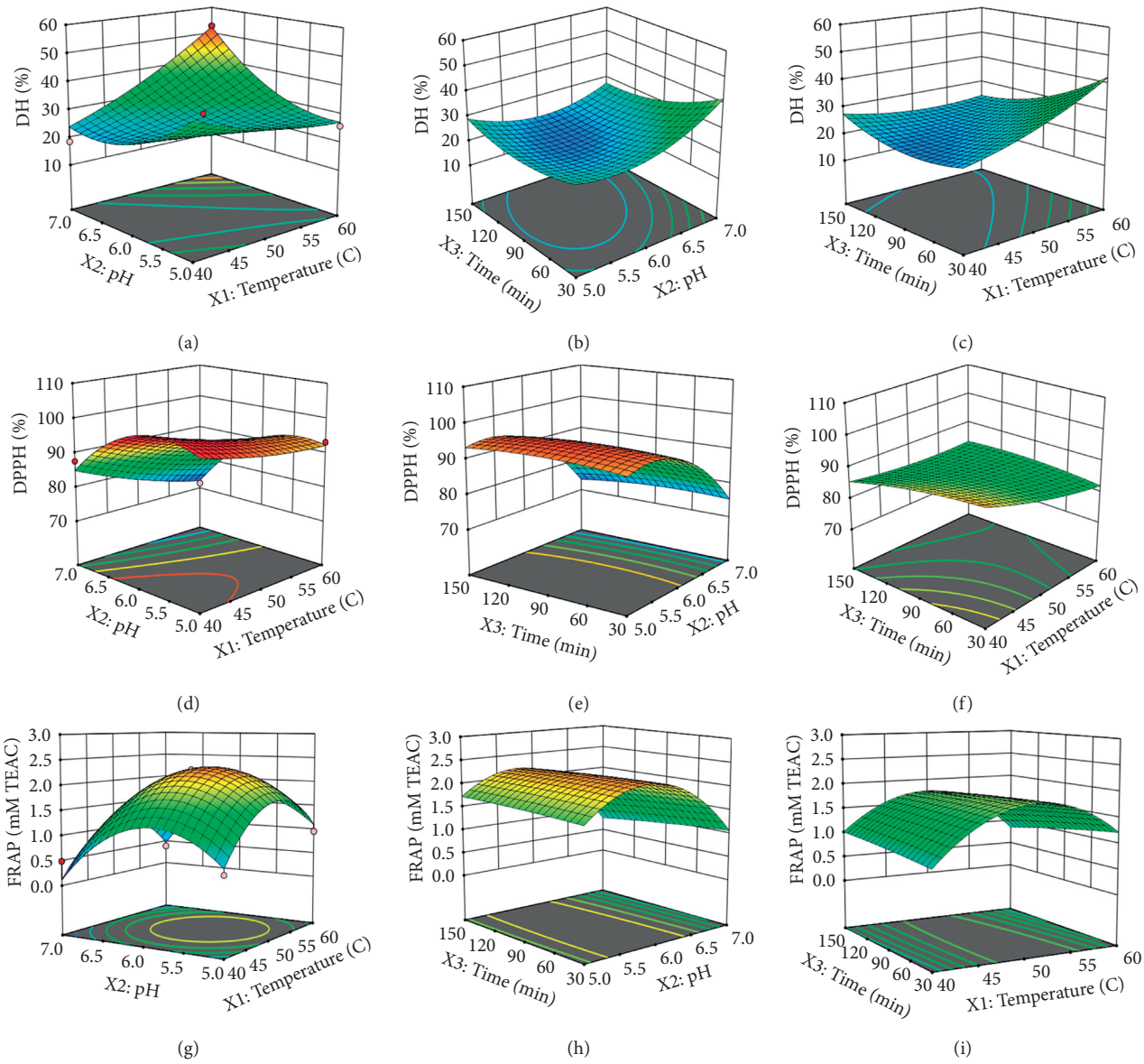

Figure 1: Response surface plots for degree of hydrolysis (a-c), DPPH scavenging activity (d-f), and FRAP (g-i) for spent hen meat hydrolysates.

compromising the antioxidant potential of the hydrolysate. Literature suggests that antioxidant potential of hydrolysates varies significantly up to 1 h of hydrolysis [23]. On the contrary, the results of this study show no distinct change in FRSA, perhaps due to a change in substrate under consideration.

3.2.2. FRAP. Temperature and pH significantly affected the ferric reducing antioxidant power ($p \leq 0.05$). Increasing pH up to 6.0 and temperature up to 50°C enhanced FRAP (Figures 1(g)–1(i)). At higher pH and temperatures, a steep decrease in FRAP was observed possibly due to enzyme denaturation. Wang and Shahidi [24] also reported a similar trend in reducing power of Turkey meat protein hydrolysates. Decrease in FRAP with increased pH and temperature was consistent with negative model coefficient for the variables (Table 2). In addition to a quadratic coefficient, the linear coefficient of pH was also found to be significant. This indicated that decrease in FRAP with pH was more gradual as compared to its decrease with temperature which only had a significant quadratic coefficient. A quadratic nature of the results also indicate that the size of peptides can influence the rate of hydrolysis since smaller molecular weight peptides can diffuse faster in the medium which can be only generated up to a specific hydrolysis condition. Hydrolysis time affected FRAP insignificantly ($p > 0.05$). Estimated effects of variables in FRAP were similar to those observed for FRSA, which indirectly shows a strong positive correlation between the former and the latter. Similar effect of hydrolysis time on FRAP and DPPH scavenging activity also proves that antioxidants will not be greatly influenced if hydrolysis times

are reduced generating a possibility of process cost reduction by reduction in operating time.

3.3. Process Optimization. Optimization of hydrolysis processing conditions was carried out using the regression models developed for the dependent variables (Table 2). The purpose of optimization algorithm was to search for processing conditions that would offer maximum degree of hydrolysis and antioxidant potential with fastest hydrolysis time. The algorithm generated 37 solutions, of which the solution with the highest desirability was selected. Optimum temperature for hydrolysis was observed as 53.9°C with a hydrolysis time of 30 min at pH 6.56. Extended experiments were conducted at the optimized hydrolysis conditions, and the resulting hydrolysates were subsequently dried to form a powder.

3.4. SDS-PAGE of Optimized Liquid Hydrolysate. SDS-PAGE profiling of optimized liquid hydrolysate was done to analyze the molecular weight distribution of peptides in the hydrolysate and to confirm the extent of hydrolysis which has taken place. When SDS-PAGE profile of the sample was compared with marker, it showed that enzymatic treatment was effective in breaking large peptide chains into very smaller peptides of molecular weight of 2–5 kDa (Figure 2). Peptide bands in the molecular weight region of 75 kDa, 55 kDa, 50 kDa, and 25 kDa were also observed. After extensive literature survey, we could not find any report of spent hen meat/chicken meat hydrolysis using Flavourzyme. This is the first report of molecular weight profiling of spent hen meat hydrolysate by SDS-PAGE technique. Since Flavourzyme is both endo- and exopeptidase, it generated a very good number of small peptides. However, in parallel to our findings, Nchienzia et al. [25] reported low molecular weight peptides after 30 min hydrolysis of poultry meal with 20.95% degree of hydrolysis and resultantly good antioxidant activity.

3.5. Analysis of Spray Dried Hydrolysate Powder

3.5.1. Antioxidant Activity. Spray dried hydrolysate powder showed significantly higher ($p \leq 0.05$) DPPH value as compared to liquid hydrolysate. Similar results were obtained for FRAP assay. Spray dried hydrolysate powder showed Fe^{3+} reducing power of 2.42 ± 0.21 mM TEAC over 1.71 ± 0.55 mM TEAC for liquid hydrolysate. Since spray drying removes most of the moisture present in the liquid feed, the concentration of low and medium molecular weight peptides increases. This in turn increases the free radical scavenging activity exhibited by the low molecular weight peptides present in the powdered hydrolysate [26]. Results of amino acid profiling also prove that high amount of histidine (3.59 g/100 g) present in the hydrolysate powder could be responsible for higher antioxidant activity obtained in this study probably due to decomposition of imidazole moiety of histidine as suggested by Wang et al. [21]. Higher antioxidant activity of the hydrolysate powder than its liquid state translates well into its potential utilization in the functional foods and nutraceuticals.

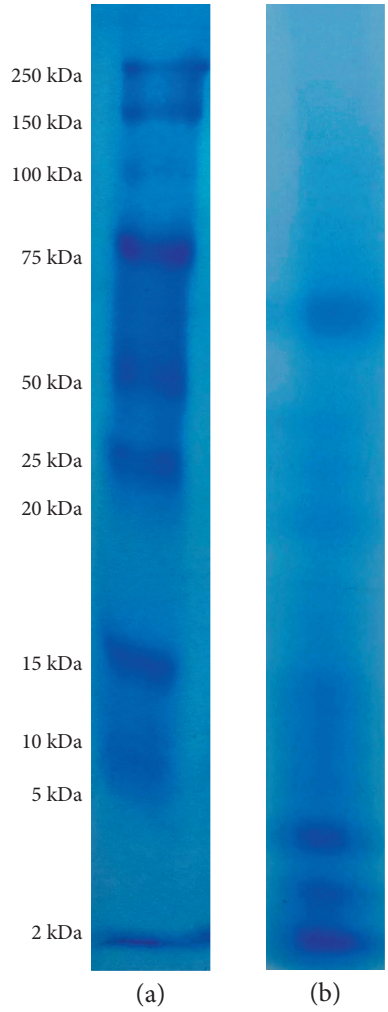

Figure 2: SDS-PAGE profile of (a) molecular weight marker and (b) optimized liquid hydrolysate.

3.5.2. Amino Acid Profiling. Amino acid composition of spray dried spent hen meat hydrolysate powder was analyzed to observe possible effect of amino acid profiling on its antioxidant potential. Results of amino acid profiling are presented in Table 3. Amount of amino acids such as glutamic acid, histidine, lysine, and tryptophan was found to be comparatively higher in the developed hydrolysate powder. It has been reported that histidine shows strong antioxidant activity owing to decomposition of imidazole ring [21, 27]; however, amino acids such as tryptophan, histidine, tyrosine, lysine, and methionine are also known to exhibit good antioxidant potential [28]. Essential amino acid (EA) accounts for 59.56% of all the amino acids shown in Table 3. Thus, results of amino acid profiling also hold significance with respect to the nutritional quality of the hydrolysate powder.

3.5.3. Essential Amino Acid Score and Protein Efficiency Ratio. EA score and PER are two criteria to judge the nutritional quality of protein hydrolysate. The higher the PER and EA score are, the better the nutritional quality will

Table 3: Amino acid composition (g/100 g protein) of spent hen meat and spray dried spent hen meat hydrolysate powder.

Amino acid	Spent hen meat	SD-SHMH powder	FAO/WHO (2002)*	EA score (spent hen meat)	EA score (spray dried hydrolysate powder)
Nonessential					
Alanine	5.41	4.12	—	—	—
Arginine	5.37	6.96	—	—	—
Aspartic acid	7.15	5.78	—	—	—
Cystine	1.19	0.14	—	—	—
Glutamic acid	13.81	11.89	—	—	—
Glycine	3.51	3.44	—	—	—
Proline	2.33	2.02	—	—	—
Serine	3.19	2.06	—	—	—
Tyrosine	2.94	2.77	—	—	—
Essential					
Histidine	3.67	3.59	1.5	2.45	2.39
Isoleucine	7.94	7.81	3	2.65	2.60
Leucine	7.56	6.64	5.9	1.28	1.13
Lysine	7.55	7.15	4.5	1.68	1.59
Methionine	8.25	6.19	2.2**	3.75	2.81
Phenylalanine	3.35	3.22	3***	1.12	1.07
Threonine	4.15	6.56	2.3	1.80	2.85
Tryptophan	9.32	11.29	0.6	15.53	18.15
Valine	5.41	5.27	3.9	1.39	1.35

*Reference FAO/WHO (2002) pattern (essential amino acid for adults), **methionine + cysteine, ***phenylalanine + tyrosine, and EA: essential amino acid.

be. Table 3 shows that the EA scores of all the essential amino acids of spray dried spent hen meat hydrolysate powder were fairly good (EA >1), which means all the essential amino acids are present in adequate amounts, while tryptophan was found to be present in excess (EA score >>1). EA values were calculated by considering the adult requirement. EA values of more than 1 signify that protein contains specific essential amino acid in excess of the requirement of adult. This excess amino acid can serve to complement any food limiting in that specific amino acid.

PER_7 and PER_{10} were calculated by considering the 7 and 10 amino acids, respectively. PER_7 was found to be higher for spent hen meat (3.46) than that of spray dried hydrolysate powder (3.35), while PER_{10} of spray dried hydrolysate powder was higher (3.93) as compared to the spent hen meat (3.80) due to the inflated value of tryptophan. PER_{10} of spray dried developed hydrolysate was found to be higher than the chicken protein hydrolysate (3.49) [9] and shrimp protein hydrolysate (2.99) [29]. The high PER and EA values of spray dried hydrolysate powder render it perfect candidate for use in protein supplement or for functional food development [30, 31].

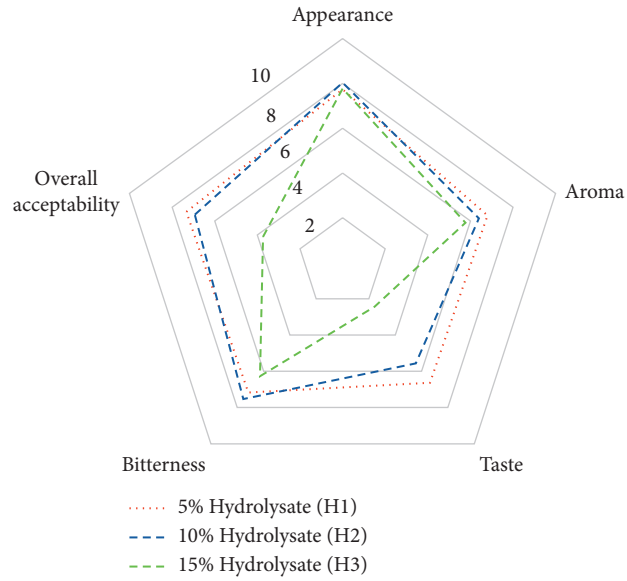

Figure 3: Sensory analysis of spent hen meat hydrolysate powder formulations.

3.5.4. Sensory Evaluation. For sensory evaluation, three different formulations were prepared in water using spray dried hydrolysate powder. Samples H_1 and H_2 were found satisfactory with H_2 being the highest acceptable concentration when compared among all three samples. Overall acceptability was reduced drastically from H_2 to H_3 scoring 6.9 and 3.7 on hedonic scale, respectively (Figure 3). Taste attribute of H_3 was "disliked very much" when compared with H_2 which was "liked slightly." Bitterness of all three samples was acceptable as hydrolysis was done only for 30 min (optimized time). Bitter peptides in hydrolysates are known to develop only after extensive hydrolysis of 6–24 h [27]. Based on sensory evaluation, it was evident that 10% hydrolysate concentration (H_2) can be suitably used for the development of nutraceuticals and functional foods which can be easily and economically disseminated in the form spray dried powders [32]. Again, we are the first to report sensory analysis of spent hen meat hydrolysate powder (or that of chicken meat hydrolysate powder, for that matter) and its acceptable percentage to be added/mixed in the functional foods. Furthermore, the maltodextrin (its type,

i.e., %DE) and its concentration to be used in spray drying of spent hen meat hydrolysate will help food industry to use the same at commercial scale. The bitterness of such powders has been reported to be lower when maltodextrin is used as a carrier agent in spray drying of whey protein hydrolysate and casein protein hydrolysate [33].

4. Conclusions

Temperature of 53.9°C with 30 min hydrolysis time and pH of 6.56 was found optimum for spent hen meat protein hydrolysis using Flavourzyme®. SDS-PAGE profile of spent hen meat protein hydrolysate showed good resolution of low molecular weight peptides at optimized conditions which were associated with antioxidant potential. Spray dried spent hen meat hydrolysate powder exhibited good functional properties when compared with its liquid counterpart. Amino acid profiling substantiated findings of high antioxidant activity shown by hydrolysate powder as some of the amino acids such as histidine, lysine, and methionine were present in good quantity. Sensory analysis of spent hen meat hydrolysate powder revealed that it can be suitably used in egg/chicken-based protein supplements and health foods. The results of this study hold significance to the nutraceutical and functional food industry for the potential exploitation of the developed hydrolysate powder.

Data Availability

All the data pertaining to this study have been provided within the manuscript.

Conflicts of Interest

The authors declare that there are no conflicts of interest.

Authors' Contributions

Deepak Kumar and Aishwarya Mohan contributed equally to this work.

Acknowledgments

The authors are grateful to the Vice Chancellor, National Institute of Food Technology Entrepreneurship and Management (NIFTEM), Kundli, Sonipat, for providing necessary facilities and funds to carry out this research work. The first author, Deepak Kumar, thanks UGC (India) for providing fellowship vide NTA reference no. 190510017474.

References

[1] T. Kotaiah, "Poultry production in India—the current scenario," *Food and Beverage News*, http://www.fnbnews.com/Poultry/poultry-production-in-india--the-current-scenario-38620, 2016.

[2] E. N. Frankel and A. J. Baily, "Recent advances in the chemistry of meat," *Food Chemistry*, vol. 15, no. 4, pp. 315-316, 1984.

[3] S. Prajapati, S. Koirala, and A. K. Anal, "Bioutilization of chicken feather wastes by newly isolated keratinolytic bacteria into protein hydrolysates with improved functionalities," *Applied Biochemistry and Biotechnology*, vol. 193, pp. 2497–2515, 2021.

[4] J. O. Onuh, A. T. Girgih, R. E. Aluko, and M. Aliani, "In vitro antioxidant properties of chicken skin enzymatic protein hydrolysates and membrane fractions," *Food Chemistry*, vol. 150, pp. 366–373, 2014.

[5] T. A. Aderinola, T. N. Fagbemi, V. N. Enujiugha, A. M. Alashi, and R. E. Aluko, "In vitro antihypertensive and antioxidative properties of alcalase-derived *Moringa oleifera* seed globulin hydrolysate and its membrane fractions," *Journal of Food Processing and Preservation*, vol. 43, no. 2, Article ID e13862, 2019.

[6] R. Nasri, O. Abdelhedi, I. Jemil et al., "Ameliorating effects of goby fish protein hydrolysates on high-fat-high-fructose diet-induced hyperglycemia, oxidative stress and deterioration of kidney function in rats," *Chemico-Biological Interactions*, vol. 242, pp. 71–80, 2015.

[7] J. Salampessy, M. Phillips, S. Seneweera, and K. Kailasapathy, "Release of antimicrobial peptides through bromelain hydrolysis of leatherjacket (meuchenia sp.) insoluble proteins," *Food Chemistry*, vol. 120, no. 2, pp. 556–560, 2010.

[8] Z. Xue, J. Gao, Z. Zhang, W. Yu, H. Wang, and X. Kou, "Antihyperlipidemic and antitumor effects of chickpea albumin hydrolysate," *Plant Foods for Human Nutrition*, vol. 67, no. 4, pp. 393–400, 2012.

[9] L. E. Kurozawa, K. J. Park, and M. D. Hubinger, "Optimization of the enzymatic hydrolysis of chicken meat using response surface methodology," *Journal of Food Science*, vol. 73, no. 5, pp. C405–C412, 2008.

[10] B. H. Sarmadi and A. Ismail, "Antioxidative peptides from food proteins: a review," *Peptides*, vol. 31, no. 10, pp. 1949–1956, 2010.

[11] J. Adler-Nissen, *Enzymic Hydrolysis of Food Proteins*, Elsevier Applied Science Publishers, London, UK, 1986.

[12] W. L. Tang, M. Zhang, B. Adhikari, and A. S. Mujumdar, "Effects of preparation and drying methods on the antioxidant activity of enzymatically hydrolyzed porcine placenta hydrolysates," *Drying Technology*, vol. 31, no. 13-14, pp. 1600–1610, 2013.

[13] A. K. Verma, M. K. Chatli, P. Kumar, and N. Mehta, "Antioxidant and antimicrobial activity of protein hydrolysate extracted from porcine liver," *The Indian Journal of Animal Sciences*, vol. 87, no. 6, pp. 711–717, 2017.

[14] U. K. Laemmli, "Cleavage of structural proteins during the assembly of the head of bacteriophage T4," *Nature*, vol. 227, no. 5259, pp. 680–685, 1970.

[15] [FAO/WHO] Food and Agriculture Organization/World Health Organization, "Evaluation of protein quality. joint FAO/WHO report," *FAO Food Nutrition*, Rome, 2002.

[16] Y. B. Lee, J. G. Elliott, D. A. Rickansrud, and E. Y. C. Hagberg, "Predicting protein efficiency ratio by the chemical determination of connective tissue content in meat," *Journal of Food Science*, vol. 43, no. 5, pp. 1359–1362, 1978.

[17] Y. Kumar, A. Tarafdar, D. Kumar, and P. C. Badgujar, "Effect of Indian brown seaweed Sargassum wightii as a functional ingredient on the phytochemical content and antioxidant activity of coffee beverage," *Journal of Food Science and Technology*, vol. 56, no. 10, pp. 4516–4525, 2019.

[18] S. Dong, M. Zeng, D. Wang, Z. Liu, Y. Zhao, and H. Yang, "Antioxidant and biochemical properties of protein hydrolysates prepared from silver carp (*Hypophthalmichthys molitrix*)," *Food Chemistry*, vol. 107, no. 4, pp. 1485–1493, 2008.

[19] N. Bhaskar, V. K. Modi, K. Govindaraju, C. Radha, and R. G. Lalitha, "Utilization of meat industry by products: protein hydrolysate from sheep visceral mass," *Bioresource Technology*, vol. 98, no. 2, pp. 388–394, 2007.

[20] Y. Zhang, Y. Wang, F. Jiang, and H. Jin, "Sensory characteristics of maillard reaction products from chicken protein hydrolysates with different degrees of hydrolysis," *CyTA—Journal of Food*, vol. 17, no. 1, pp. 221–227, 2019.

[21] J. Wang, M. Zhao, Q. Zhao, and Y. Jiang, "Antioxidant properties of papain hydrolysates of wheat gluten in different oxidation systems," *Food Chemistry*, vol. 101, no. 4, pp. 1658–1663, 2007.

[22] J. Roslan, M. S. Kamal, M. K. Yunos, and N. Abdullah, "Optimization of enzymatic hydrolysis of tilapia (*Oreochromis niloticus*) byproduct using response surface methodology," *International Food Research Journal*, vol. 22, no. 3, p. 1117, 2015.

[23] D. Wang, M. Zhang, Y. Zou, Z. Sun, and W. Xu, "Optimization of flavourzyme hydrolysis condition for the preparation of antioxidant peptides from duck meat using response surface methodology," *The Journal of Poultry Science*, vol. 55, pp. 217–223, Article ID 0160155, 2018.

[24] D. Wang and F. Shahidi, "Protein hydrolysate from Turkey meat and optimization of its antioxidant potential by response surface methodology," *Poultry Science*, vol. 97, no. 5, pp. 1824–1831, 2018.

[25] H. A. Nchienzia, R. O. Morawicki, and V. P. Gadang, "Enzymatic hydrolysis of poultry meal with endo-and exopeptidases," *Poultry Science*, vol. 89, no. 10, pp. 2273–2280, 2010.

[26] C. Chen, Y. J. Chi, and W. Xu, "Comparisons on the functional properties and antioxidant activity of spray-dried and freeze-dried egg white protein hydrolysate," *Food and Bioprocess Technology*, vol. 5, no. 6, pp. 2342–2352, 2012.

[27] B. Y. Liu, K. X. Zhu, W. Peng, X. N. Guo, and H. M. Zhou, "Effect of sequential hydrolysis with endo-and exo-peptidase on bitterness properties of wheat gluten hydrolysates," *RSC Advances*, vol. 6, no. 33, pp. 27659–27668, 2016.

[28] L. You, M. Zhao, C. Cui, H. Zhao, and B. Yang, "Effect of degree of hydrolysis on the antioxidant activity of loach (*Misgurnus anguillicaudatus*) protein hydrolysates," *Innovative Food Science & Emerging Technologies*, vol. 10, no. 2, pp. 235–240, 2009.

[29] S. S. Dey and K. C. Dora, "Optimization of the production of shrimp waste protein hydrolysate using microbial proteases adopting response surface methodology," *Journal of Food Science and Technology*, vol. 51, no. 1, pp. 16–24, 2014.

[30] D. Kumar, A. Jyoti, A. Tarafdar, A. Kumar, and P. C. Badgujar, "Comparative functional and spectroscopic analysis of spent hen meat hydrolysate by individual and combined treatment of microbial proteases," *Preparative Biochemistry & Biotechnology*, vol. 51, no. 6, pp. 618–627, 2021.

[31] D. Kumar, A. Mishra, A. Tarafdar et al., "In vitro bioaccessibility and characterisation of spent hen meat hydrolysate powder prepared by spray and freeze-drying techniques," *Process Biochemistry*, vol. 105, pp. 128–136, 2021.

[32] P. Unnikrishnan, B. Puthenveetil Kizhakkethil, M. Anant Jadhav et al., "Protein hydrolysate from yellowfin tuna red meat as fortifying and stabilizing agent in mayonnaise," *Journal of Food Science and Technology*, vol. 57, no. 2, pp. 413–425, 2020.

[33] P. S. Rao, R. K. Bajaj, B. Mann, S. Arora, and S. K. Tomar, "Encapsulation of antioxidant peptide enriched casein hydrolysate using maltodextrin–gum Arabic blend," *Journal of Food Science and Technology*, vol. 53, no. 10, pp. 3834–3843, 2016.

Hindawi
Journal of Food Quality
Volume 2021, Article ID 3271727, 19 pages
https://doi.org/10.1155/2021/3271727

Review Article

Chemical Components and Biological Effects of Genus *Origanum*

Li Zhou[1], **Fatma Al-Zahra Kamal Kamel Attia**[1,2,3], **Lijun Meng**[1], **Sitan Chen**[1], **Zhenhua Liu**[1,2,4], **Changyang Ma**[1,2,4], **Lijun Liu**[1,5] and **Wenyi Kang**[1,2]

[1]*National R&D Center for Edible Fungus Processing Technology, Henan University, Kaifeng 475004, China*
[2]*Joint International Research Laboratory of Food & Medicine Resource Function, Henan, Kaifeng 475004, China*
[3]*Department of Ornamental Medicinal and Aromatic Plants, Faculty of Agriculture, Assiut University, Asyut 71515, Egypt*
[4]*Kaifeng Key Laboratory of Functional Components in Health Food, Kaifeng 475004, China*
[5]*Huaihe Hospital, Henan University, Kaifeng 475004, China*

Correspondence should be addressed to Zhenhua Liu; liuzhenhua623@163.com, Changyang Ma; macaya1024@vip.henu.edu.cn, Lijun Liu; funiuxzr2001@163.com, and Wenyi Kang; kangweny@hotmail.com

Received 6 May 2021; Revised 18 August 2021; Accepted 20 August 2021; Published 6 September 2021

Academic Editor: Quancai Sun

The plants from genus *Origanum* are common folk Chinese herbs used to treat a variety of diseases. They are also used as a spice, a seasoning, and an ornament. *Origanum* plants are rich in essential oils and also have other compounds including terpenoids, flavonoids, organic acids, and sterols. They have a variety of biological activities such as antispasmodic, anti-inflammatory, growth-promoting, antibacterial, antioxidant, and anticancer properties. The chemical components and biological effects of genus *Origanum* were summarized by different scientific databases such as Web of Science, SciFinder, Baidu Scholar, PubMed, ScienceDirect, and SpringerLink. In conclusion, recent studies were mainly focused on the activities of their essential oils. The research studies for nonvolatile constituents and their pharmacological activities are few. Therefore, research on compounds in genus *Origanum* plants can be strengthened and their application prospect can be explored so as to make better use of the resources of these plants.

1. Introduction

The genus *Origanum* (Lamiaceae) is an annual, perennial, and shrubby herb. It comprises about 15 to 20 species and is widely distributed throughout the world. There is only one species of genus *Origanum* (*O. vulgare*) in China, mainly distributed in Xinjiang, Gansu, Shanxi, Hubei, and Henan Provinces, etc. [1].

The whole plants of the genus *Origanum* can be used medicinally throughout the world. For example, *O. majorana* has been used in ancient Egypt as antiseptic, insect repellent, and expectorant and for arthritis, muscle pain, rheumatism, and other diseases and is now widely used in cooking seasonings and cosmetics. *O. vulgare* subsp. *glandulosum* (syn. *O. glandulosum*) is named 'Zaâter moulouk' in Tunisia. It is one of the most important plants of Lamiaceae economically, and several studies have shown that genus *Origanum* possessed the antimicrobial, antifungal, and insecticidal properties and antioxidant activities. In China, the whole plant of *O. vulgare* is a common Chinese herbal medicine in Chinese folk and was listed in Chinese Pharmacopoeia (1977 edition). It has the function of clearing away heat and reducing swelling and mainly used for sunstroke, cold, headache, acute enteritis, abdominal pain, and diarrhea. It is also used as a spice, condiment, and ornament.

Researches on genus *Origanum* are mainly carried out in Egypt, Tunisia, Turkey, and so on. The chemical constituents of genus *Origanum* are mainly essential oils, with the effects of removing phlegm, resisting spasm, nourishing and strengthening body, relieving pain, and having antisepsis, antibacterial, antimildew, antioxidation, and anticytotoxin effects. The nonvolatile constituents of *Origanum* plants are seldom studied, which mainly contain flavonoids, triterpenes, and organic acids. Therefore, systematic studies of their chemical constituents and biological activities are of great significance to elucidate its medicinal value.

2. Chemical Constituents

The essential oils of genus *Origanum* contain many active constituents. They have a broad spectrum of antibacterial, antitumor, and immunomodulatory effects, but there are few studies on the nonvolatile constituents, including flavonoids, organic acids, terpenoids, and sterols. The main constituents of essential oils from genus *Origanum* in the world are listed in Table 1 and the nonvolatile constituents of genus *Origanum* in the world are listed in Table 2.

2.1. Main Constituents of Essential Oils of Genus Origanum. Plants of genus *Origanum* are rich in essential oils and the main constituents are terpenoids, which mainly include carvacrol, thymol, carbamene, and terpilenol (Figures 1–3). [2–8, 18–20].

Hatipi collected 12 plants of *O. vulgare* from different parts in Kosovo. The essential oils were extracted by steam distillation and the yield of essential oils was 0.41–0.82% of dry weight. The main constituents included sesquiterpenoids (6.1–37.06%), monoterpenes (1.73–35.18%), oxygenated monoterpene (6.88–36.06%), oxygenated sesquiterpenoids (2.49–43.44%), 1, 8-cineole (1.31–13.54%), caryophyllene oxide (0.18–38.05%), (*E*)-β-caryophyllene (0.48–14.0%), *p*-cymene (1.27–19.62%), α-terpineol (1.05–19.23%), and germacrene D (0.35–16.09%) [19].

The essential oils from the above ground parts of *O. heracleoticum* and *O. majorana* made up 1.8% and 0.4% of their total dry weight, respectively. 55 compounds were identified from the essential oils, among which 35 compounds were from *O. heracleoticum*, accounting for 97.8% of the total oils, and 20 compounds were from *O. majorana*, accounting for 98.0% of the total oils. Oxygenated monoterpenes (80.1%) were the main constituents of *O. heracleoticum* essential oils, while monoterpenes (54.0%) were mainly found in *O. majorana* essential oils. Carvacrol (77.8%), *p*-cymene (5.3%), γ-terpinene (4.9%), and caryophyllene (1.3%) were the main components in *O. heracleoticum* essential oils. In *O. majorana* essential oils, the main constituents included terpineol (29.6%), 2-carene (20.1%), camphene (13.4%), and α-pinene (7.9%) [8].

Huo found monoterpenes and bicyclic sesquiterpenes were the main constituents of the essential oils of *O. vulgare* L. through the analysis of GC-MS, and the mass fractions of these two kinds of components in the essential oils of *O. vulgare* L. were 69.31% and 20.25%, respectively [20].

Gong identified 65 chemical constituents from the essential oils of genus *Origanum* plants in 6 different habitats from China and Pakistan by GC-MS and found that the main constituents of essential oils in 6 different habitats were all oxygenated monoterpenes [2].

Essential oils of *O. onites* aerial parts were analyzed by GC-MS with hydrodistillation (HD) and microwave-assisted HD (MWHD) methods. Thirty-one compounds were identified from HD method and 52 compounds were identified from MWHD method. Among them, carvacrol (76.8% HD and 79.2% MWHD) and thymol (4.7% HD and 4.4% MWHD) were the main constituents of these two essential oils [4]. Farhat found essential oils from the leaves of *O. syriacum* in Syria were mainly carvacrol (78.4%) and thymol (17.9%) analyzed by SPME GC/MS [7].

Shafaghat obtained 23 compounds from the essential oils of flowers, leaves, and stems of *O. vulgare* growing in northwest Iran by GC-MS, about 96.3% (19 compounds) of the flower oil, 92.8% (11 compounds) of the leaf oil, and 95.2% (12 compounds) of the stem oil. The dominant compounds in the flower, leaf, and stem oils were sesquiterpene (53.6%, 50.7%, and 70.4%, respectively) and linalyl acetate, sabinene, γ-terpinene and ocimene were the main constituents of the oil of the aerial parts of *O. vulgare* [6].

Aligiannis identified 48 compounds from the essential oils of *O. scabrum* and *O. microphyllum*, accounting for 98.59% and 98.66% of the total oils, respectively. Carvacrol, terpilenol, linalool, sabinene, and terpinene are the main constituents [5].

Spyridopoulou identified 64 compounds from essential oils of *O. onites*. The most abundant chemical constituent in essential oils is carvacrol (47.99%), which is consistent with those reported in literatures that the content of carvacrol in essential oils was between 50% and 85%. Other main constituents were identified as terp-1-in-4-ol (6.79%), sabinene hydrate (6.14%), γ-terpinene (5.20%), *p*-cymene (3.85%), and α-terpineol (3.76%) [3].

In conclusion, 92 compounds were found in essential oils to date, including monoterpenes (**1**–**49**), sesquiterpenoids (**50**–**69**), and other derivatives (**70**–**92**). Moreover, the chemical constituents of essential oils varied greatly with species in the genus *Origanum* and can be roughly divided into two categories: one is rich in carvacrol, thymol, cymene, and terpinene and the other is rich in coriandrol, germacrene D, and other ingredients. When the chemical constituents of essential oils in a certain plant were rich in the first group, then the compounds of the second group were few, and vice versa. Meanwhile, essential oils have many pharmacological activities. Therefore, understanding of their chemical compositions of essential oils thoroughly is more helpful to elucidate their material basis.

2.2. Nonessential Constituents of Genus Origanum

2.2.1. Flavonoids. 23 flavonoids (**93**–**115**) (Figure 4) were isolated from genus *Origanum* [9–14]. Compounds **93**–**107** belong to flavonoids, **108**–**111** belong to flavonols, and **112**–**115** belong to flavanone and their glycosides.

2.2.2. Organic Acids. 20 organic acid compounds (**116-135**) (Figure 5) were isolated from genus *Origanum* [9–16], mainly including phenols, cinnamic acids, and salvianolic acids.

2.2.3. Terpenes and Sterols. The terpenoids oleanolic acid (**136**), arbutin (**137**) [13], sterol stigmasterol (**138**) [11], β-sitosterol (**139**), and daucosterol (**140**) were isolated from genus *Origanum* (Figure 6) [15].

Table 1: The main constituents of essential oils from genus *Origanum* in the world.

Compound	Name	Source	Parts	Producing area	References
		Monoterpenes (**1–51**)			
1	Myrcene	*O. vulgare*	The whole plants	Anhui, China	[2]
2	Nerol	*O. onites*	Leaves, flowers	Athens, Greece	[3]
3	Geraniol	*O. vulgare*	The whole plants	Xinjiang, China	[2]
4	β-Citronellal	*O. onites*	Aerial parts	Izmir, Turkey	[4]
5	Acetic acid, geraniol ester	*O. vulgare*	The whole plants	Kunlun Mountain	[2]
6	Citronellol acetate	*O. vulgare*	The whole plants	Kunlun Mountain	[2]
7	Ocimene	*O. microphyllum*	Aerial parts	Crete	[5]
8	Citral	*O. onites*	Leaves, flowers	Athens, Greece	[3]
9	Citronellol	*O. vulgare*	The whole plants	Henan, China	[2]
10	Citronellyl formate	*O. vulgare*	The whole plants	Pakistan	[2]
11	Hydroxycitronellal	*O. vulgare SSP.*	Flowers, leaves, stems	Astara, Iran	[6]
12	Neryl acetate	*O. onites*	Leaves, flowers	Athens, Greece	[3]
13	Linalool	*O. microphyllum*	Aerial parts	Crete	[5]
14	Linalyl acetate	*O. onites.*	Leaves, flowers	Athens, Greece	[3]
15	Epoxy linalool	*O. onites*	Leaves, flowers	Athens, Greece	[3]
16	α-Terpinene	*O. microphyllum*	Aerial parts	Crete	[5]
17	γ-Terpinene	*O. syriacum*	Leaves	Arabsalim, Lebanon	[7]
18	α-Phellandrene	*O. onites*	Leaves, flowers	Athens, Greece	[3]
19	Terpinolene	*O. microphyllum*	Aerial parts	Crete	[5]
20	β-Phellandrene	*O. scabrum*	Aerial parts	Peloponissos	[5]
21	Limonene	*O. heracleoticum*	Dried aerial parts	Salerno, Montecorice	[8]
22	Cymene	*O. vulgare SSP.*	Flowers, leaves, stems	Astara, Iran	[6]
23	Piperitol	*O. onites*	Leaves, flowers	Athens, Greece	[3]
24	Thymol	*O. scabrum*	Aerial parts	Peloponissos	[5]
25	p-Cymen-2-ol	*O. vulgare*	The whole plants	Pakistan	[2]
26	Terpinen-4-ol	*O. scabrum*	Aerial parts	Peloponissos	[5]
27	α-Terpineol	*O. microphyllum*	Aerial parts	Crete	[5]
28	p-Cymen-8-ol	*O. onites*	Aerial parts	Izmir, Turkey	[4]
29	trans-Dihydrocarvone	*O. heracleoticum*	Aerial parts	Salerno, Montecorice	[8]
30	Carvone	*O. onites*	Aerial parts	Izmir, Turkey	[4]
31	Isopiperitenone	*O. onites*	Leaves, flowers	Athens, Greece	[3]
32	Thymol methyl ether	*O. heracleoticum*	Dried aerial parts	Salerno, Montecorice	[8]
33	Carvacrol methyl ether	*O. onites*	Leaves, flowers	Athens, Greece	[3]
34	Benzene, 1-methoxy-4-methyl-2-(1-methylethyl)	*O. vulgare*	The whole plants	Pakistan	[2]
35	Thymol acetate	*O. vulgare*	The whole plants	Anhui, China	[2]
36	Carvacrol acetate	*O. vulgare*	The whole plants	Anhui, China	[2]
37	α-Campholenal	*O. vulgare SSP.*	Flowers, leaves, stems	Astara, Iran	[6]
38	Sabinene	*O. microphyllum*	Aerial parts	Crete	[5]
39	Thujene	*O. heracleoticum*	Dried aerial parts	Salerno, Montecorice	[8]
40	Thujanol	*O. onites*	Leaves, flowers	Athens, Greece	[3]
41	Thujone	*O. onites*	Aerial parts	Izmir, Turkey	[4]
42	Sabinene hydrate	*O. scabrum*	Aerial parts	Peloponissos	[5]
43	α-3-Carene	*O. scabrum*	Aerial parts	Peloponissos	[5]
44	Pinocarvone	*O. vulgare SSP.*	Flowers, leaves, stems	Astara, Iran	[6]
45	α-Pinene	*O. vulgare SSP.*	Flowers, leaves, stems	Astara, Iran	[6]
46	β-Pinene	*O. scabrum*	Aerial parts	Peloponissos	[5]
47	α-trans-bergamotene	*O. vulgare*	The whole plants	Anhui, China	[2]
48	Camphene	*O. microphyllum*	Aerial parts	Crete	[5]

Table 1: Continued.

Compound	Name	Source	Parts	Producing area	References
49	Borneol	*O. vulgare SSP.*	Flowers, leaves, stems	Astara, Iran	[6]
50	(Z)-β-Farnesene	*O. vulgare*	The whole plants	Anhui, China	[2]
51	(E, E)-α-Farnesene	*O. vulgare*	The whole plants	Xinjiang, China	[2]
	Sesquiterpenoids (**52–69**)				
52	Germacrene D	*O. onites*	Leaves, flowers	Athens, Greece	[3]
53	β-Sesquiphellandrene	*O. vulgare*	Leaves, flowers	Athens, Greece	[3]
54	β-Bisabolene	*O. onites*	Aerial parts	Izmir, Turkey	[4]
55	β-Bisabolene	*O. scabrum*	Aerial parts	Peloponissos	[5]
56	Germacrene B	*O. vulgare*	The whole plants	Xinjiang, China	[2]
57	Humulene	*O. microphyllum*	Aerial parts	Crete	[5]
58	γ-Muurolene	*O. vulgare*	The whole plants	Henan, China	[2]
59	γ-Cadinene	*O. onites*	Leaves, flowers	Athens, Greece	[3]
60	Cubenol	*O. vulgare*	The whole plants	Xinjiang, China	[2]
61	Cadinol	*O. onites*	Leaves, flowers	Athens, Greece	[3]
62	Limonene	*O. heracleoticum*	Dried aerial parts	Salerno, Montecorice	[8]
63	α-Bulnesene	*O. vulgare*	The whole plants	Anhui, China	[2]
64	Caryophyllene	*O. heracleoticum*	Dried aerial parts	Salerno, Montecorice	[8]
65	Caryophyllene oxide	*O. scabrum*	Aerial parts	Peloponissos	[5]
66	Spathulenol	*O. vulgare SSP.*	Flowers, leaves, stems	Astara, Iran	[6]
67	Aromadendrene	*O. onites*	Leaves, flowers	Athens, Greece	[3]
68	Thujopsene	*O. vulgare SSP.*	Flowers, leaves, stems	Astara, Iran	[6]
69	Copaene	*O. vulgare*	The whole plants	Henan, China	[2]
	Others (**70–92**)				
70	Octen-3-ol	*O. scabrum*	Aerial parts	Peloponissos	[5]
71	3-Octanone	*O. scabrum*	Aerial parts	Peloponissos	[5]
72	3-Octanol	*O. vulgare*	The whole plants	Henan, China	[2]
73	Methyl 2-methylbutyrate	*O. onites*	Leaves, flowers	Athens, Greece	[3]
74	Isoamyl acetate	*O. onites*	Leaves, flowers	Athens, Greece	[3]
75	Cis-rose oxide	*O. vulgare*	The whole plants	Xinjiang, China	[2]
76	Phenylacetaldehyde	*O. microphyllum*	Aerial parts	Crete	[5]
77	Eugenol	*O. heracleoticum*	Dried aerial parts	Salerno, Montecorice	[8]
78	Camphor	*O. onites*	Leaves, flowers	Athens, Greece	[3]
79	p-Methylbenzaldehyde	*O. vulgare SSP.*	Flowers, leaves, stems	Astara, Iran	[6]
80	Acetovanillone	*O. heracleoticum*	Dried aerial parts	Salerno, Montecorice	[8]
81	Eugenol methyl ether	*O. vulgare*	The whole plants	Anhui, China	[2]
82	Isoeugenol methyl ether	*O. vulgare*	The whole plants	Anhui, China	[2]
83	Elemicin	*O. vulgare*	The whole plants	Anhui, China	[2]
84	Myristicin	*O. vulgare*	The whole plants	Anhui, China	[2]
85	Apiol	*O. vulgare*	The whole plants	Anhui, China	[2]
86	Dill apiol	*O. vulgare*	The whole plants	Anhui, China	[2]
87	Cis-asarone	*O. vulgare*	The whole plants	Anhui, China	[2]
88	Asarone	*O. vulgare*	The whole plants	Anhui, China	[2]
89	5-Methylfurfural	*O. vulgare SSP.*	Flowers, leaves, stems	Astara, Iran	[6]
90	1, 5, 5, 8-Tetramethyl-12-oxabicyclo [9.1.0] dodeca-3, 7-diene	*O. vulgare*	The whole plants	Xinjiang, China	[2]
91	Indole	*O. onites*	Leaves, flowers	Athens, Greece	[3]
92	5-Phenylisoquinoline	*O. vulgare SSP.*	Flowers, leaves, stems	Astara, Iran	[6]

Table 2: Nonvolatile constituents of genus *Origanum* in the world.

Compound	Name	Source	Parts	Producing area	References
		Flavonoids (**93–115**)			
93	Luteolin	*O. vulgare*	Dried aerial parts	Taiwan, China	[9]
94	Apigenin	*O. vulgare*	Dried aerial parts	Taiwan, China	[9]
95	Luteolin7-O-β-D-glucopyranoside	*O. vulgare*	Dried aerial parts	Taiwan, China	[9]
96	Luteolin7-O-β-D-glucuronide	*O. vulgare*	Dried aerial parts	Taiwan, China	[9]
97	Luteolin7-O-β-D-xylopyranoside	*O. vulgare*	Dried aerial parts	Taiwan, China	[9]
98	Apigenin7-O-β-D-glucuronide	*O. vulgare*	Dried aerial parts	Taiwan, China	[9]
99	Apigenin7-O-β-D-(6″-methyl) glucuronide	*O. vulgare*	Dried aerial parts	Taiwan, China	[9]
100	5, 6, 3′-Trihydroxy-7, 8, 4′-trimethoxyflavone	*O. majorana*	Dried aerial parts	Tokat, Turkey	[10]
101	5, 6, 4′-Trihydroxyl-7, 8-dimethoxylflavone	*O. x intercedens*	—	Greece	[11]
102	5, 6, 4′-Trihydroxyl-7, 3′-dimethoxylflavone	*O. x intercedens*	—	Greece	[11]
103	5, 6, 4′-Trihydroxyl-7, 8, 3′-trimethoxylflavone	*O. x intercedens*	—	Greece	[11]
104	6, 7, 4′-Trihydroxyflavone	*O. vulgare*	The whole plants	Guangdong, China	[12]
105	Tilianin	*O. vulgare*	The whole plants	—	[13]
106	5, 4′-Dihydroxyl-6, 7-dimethoxylflavone	*O. x intercedens*	—	Greece	[11]
107	5, 4′-Dihydroxyl-6, 7-dimethoxylflavone	*O. x intercedens*	—	Greece	[11]
108	Kaempferol	*O. vulgare*	—	—	[14]
109	Quercetin	*O. vulgare*	—	—	[14]
110	Morin	*O. vulgare.*	—	—	[14]
111	Galangin	*O. vulgare*	—	—	[14]
112	Naringin	*O. vulgare*	—	—	[14]
113	Hesperetin	*O. vulgare*	Dried aerial parts	—	[10]
114	Didymin	*O. vulgare*	The whole plants	Guangdong, China	[12]
115	Sagittatoside A	*O. vulgare*	The whole plants	—	[13]
		Organic acids (**116–135**)			
116	p-Dihydroxybenzene	*O. majorana*	Dried aerial parts	Tokat, Turkey	[10]
117	O-Dihydroxybenzene	*O. vulgare*	Dried aerial parts	Hubei, China	[15]
118	1, 2, 4-Trihydroxyphenol	*O. vulgare*	The whole plants	Guangdong, China	[12]
119	4-Methyl-5-isopropyl catechol	*O. vulgare*	Dried aerial parts	Hubei, China	[15]
120	Cinnamic acid	*O. vulgare*	—	—	[14]
121	2-Hydroxycinnamic acid	*O. vulgare*	—	Greece	[11]
122	4-Hydroxycinnamic acid	*O. dictamnus*	—	Greece	[11]
123	Caffeic acid	*O. vulgare*	—	—	[14]
124	Ferulic acid	*O. dictamnus*	—	Greece	[11]
125	Chlorogenic acid	*O. vulgare*	—	—	[14]
126	Rosmarinic acid	*O. vulgare*	The whole plants	Hubei, China	[16]
127	p-Hydroxybenzoic acid	*O. vulgare*	—	—	[14]
128	Protocatechuic acid	*O. vulgare*	The whole plants	Hubei, China	[16]
129	Hydroxy-3-methoxybenzoic acid	*O. vulgare*	The whole plants	Hubei, China	[16]
130	Hydroxy-4-methoxybenzoic acid	*O. vulgare*	The whole plants	Hubei, China	[16]
131	Syringic acid	*O. vulgare*	—	—	[14]
132	Salvianolic acid A	*O. vulgare*	Dried aerial parts	Taiwan, China	[10]
133	Salvianolic acid C	*O. vulgare*	Dried aerial parts	Taiwan, China	[10]
134	Lithospermic acid	*O. vulgare*	Dried aerial parts	Taiwan, China	[10]
135	Succinic acid	*O. vulgare*	Dried aerial parts	Hubei, China	[15]
		Steroids and terpenes (**136–140**)			
136	Oleanolic acid	*O. vulgare*	The whole plants	—	[13]
137	Arbutin	*O. vulgare*	The whole plants	—	[13]
138	Stigmasterol	*O. minutiflorum*	—	—	[11]
139	β-Sitosterol	*O. vulgare*	Dried aerial parts	Hubei, China	[15]
140	Daucosterol	*O. vulgare*	Dried aerial parts	Hubei, China	[15]
		Others (**141–148**)			
141	Origalignanol	*O. vulgare*	Dried aerial parts	Taiwan, China	[9]
142	Origanol A	*O. vulgare*	The air-dried leaves	Ooty, India	[17]
143	Origanol B	*O. vulgare*	The air-dried leaves	Ooty, India	[17]
144	Ethyl rosmarinate	*O. vulgare*	Dried aerial parts	Hubei, China	[15]
145	N-Butyl rosmarinate	*O. vulgare*	Dried aerial parts	Hubei, China	[15]
146	p-Hydroxy benzaldehyde	*O. vulgare*	Dried aerial parts	Hubei, China	[15]
147	Dihydrodehydrodiconiferyl alcohol	*O. vulgare*	Dried aerial parts	Hubei, China	[15]
148	Caffeic acid ethyl ester	*O. vulgare*	Dried aerial parts	Hubei, China	[15]

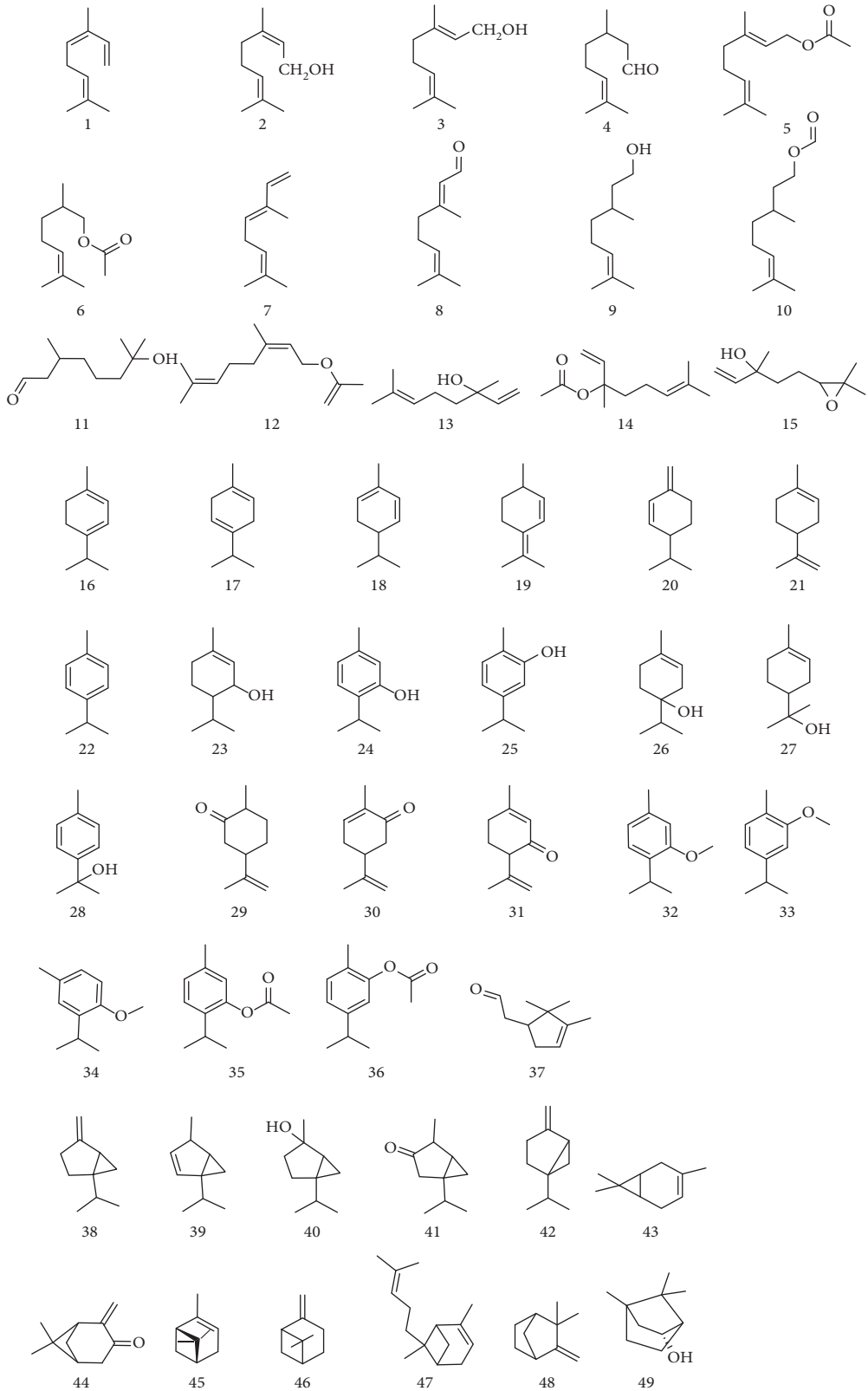

Figure 1: Monoterpenes of essential oils from genus *Origanum* in the world.

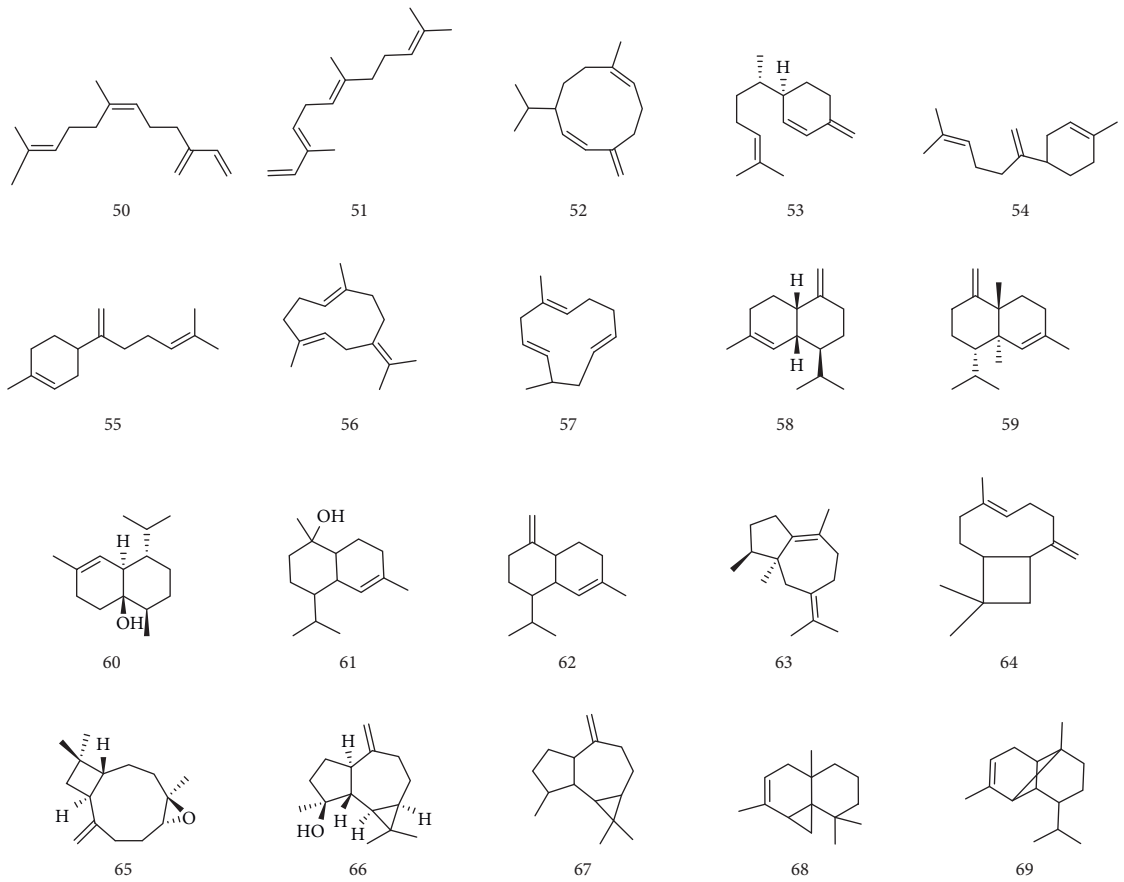

Figure 2: Sesquiterpenoids of essential oils isolated from genus *Origanum* in the world.

2.2.4. Others. Origalignanol was isolated from *O. vulgare* by Lin (**141**) [9]. Origanol A (**142**) and origanol B (**143**) were isolated from *O. vulgare* by Gottumukkala [17]. Sun isolated ethyl rosmarinate (**144**), *N*-butyl rosmarinate (**145**), *p*-hydroxybenzaldehyde (**146**), dihydrodehydrodiconiferyl alcohol (**147**), and caffeic acid ethyl ester (**148**) from *O. vulgare* L. (Figure 7) [15].

3. Biological Effects

The researches on the biological effects of genus *Origanum* are mainly focused on its essential oils, which have a wide range of biological effects, including antibacterial, antioxidant, anticancer, and anti-inflammatory effects and immune regulation.

3.1. Antibacterial Effect. Essential oils from genus *Origanum* had a strong antibacterial and bactericidal effect, which is related to its phenols' constituents. Phenols act on the cell membrane of bacteria to make their proteins denaturation and change the permeability of cell membrane, or destroy protein synthesis by reacting with phospholipids in cell membranes and finally inhibiting the growth of microbial cells [21, 22].

The antibacterial activities of *O. dictamnus* essential oils against *Salmonella enteritis*, *S. typhimurium*, *Escherichia coli*, *Listeria monocytogenes*, *Staphylococcus epidermis,* and *S. aureus* were determined by disk diffusion method. The results showed that bacteriostatic effect on *S. aureus* was the strongest and on *S. typhimurium* was the weakest [23].

Laghmouchi determined the minimum inhibitory concentration (MIC: 0.06–0.25% (v/v)) and the minimum bactericidal concentration (MBC: 0.12–0.5% (v/v)) of essential oils from *O. compactum* against *E. coli*, *B. subtilis*, *S. aureus*, and *L. innocua* by the microdilution method. And thymol and carvacrol in essential oils played the key role in antibacterial activity through penetrating and depolarizing the plasma membrane. Meanwhile, *p*-cymene in essential oils could enhance the anti-*S. aureus* effect by promoting the transport of carvacrol in the plasma membrane and entering the lipid bilayer of *Staphylococcus aureus* [24].

The antibacterial activity of *O. acutidens* essential oils and its methanol extract against four fish pathogens, *S. aureus*, *L. garvieae*, *Yersinia ruckeri*, and *Aeromonas hydrophila,* were determined by disk diffusion assay. The results indicate that the methanol extract and the essential oils of *O. acutidens* may be valuable as potential antibacterial agents against the major fish pathogens [25].

Souza reported that essential oils from *O. vulgare* could block the production of enterotoxin of *S. aureus*. When the concentration reached 0.15 or 0.3 μL/mL, the growth of bacteria was significantly inhibited. When the concentration reached 0.6 or 1.2 μL/mL, the permeability of the cell membrane was changed and the cytoplasm was lost. These

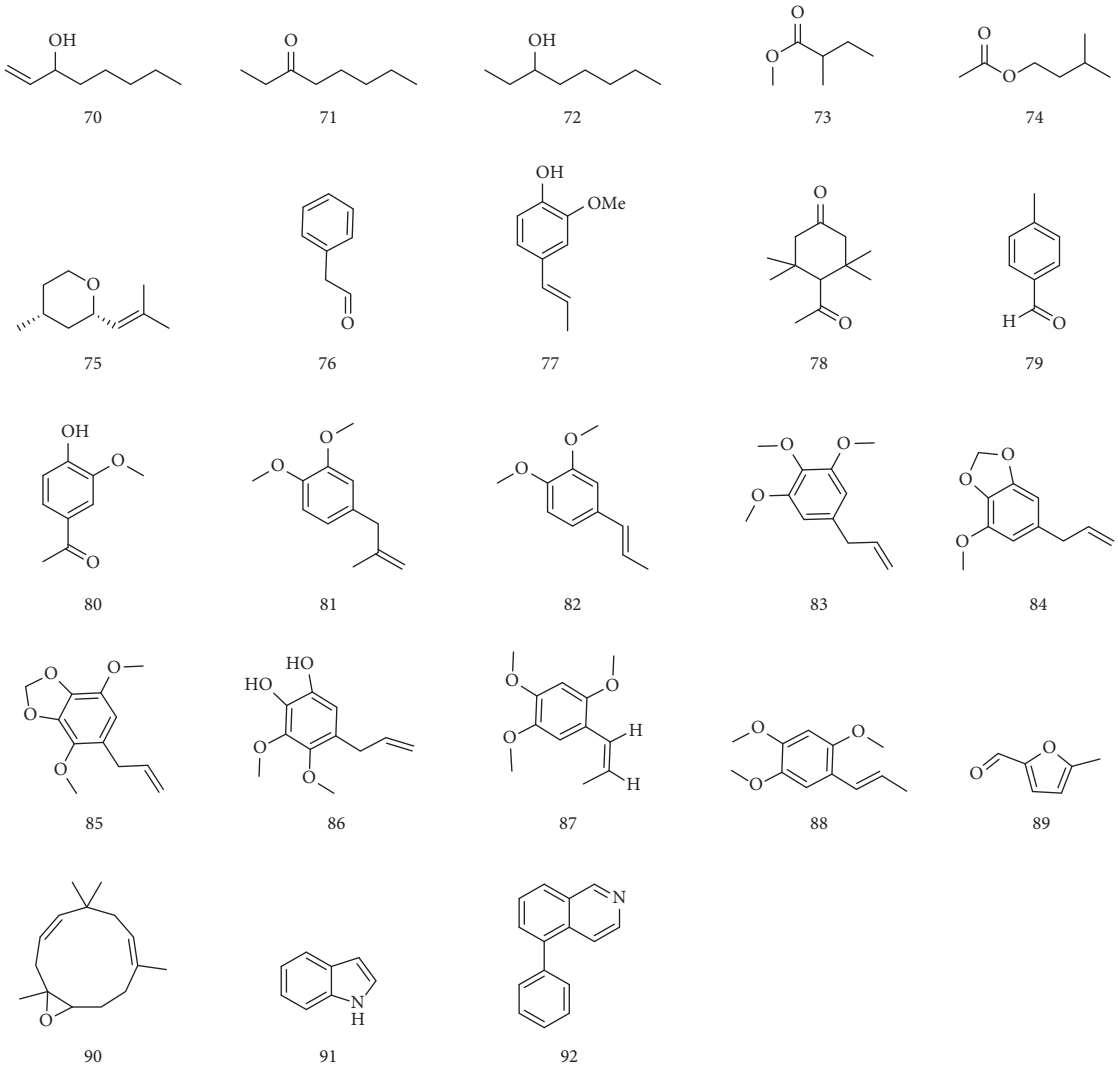

Figure 3: Other constituents of essential oils isolated from genus *Origanum* in the world.

suggested that essential oils from *O. vulgare* may prevent some of the symptoms caused by *S. aureus* enterotoxin [26].

Si studied the antibacterial effects of oregano essential oils (OEO) combined with antibiotics against extended-spectrum beta-lactamase (ESBL-) producing *E. coli* by two-fold dilution method. The results indicated that multiple drug-resistant *E. coli* was very sensitive to OEO essential oils and polymycin. The antibacterial effects of OEO in combination with kanamycin were independent against *E. coli*. The antibacterial effects of OEO in combination with fluoroquinolones, doxycycline, lincomycin, and maquindox florfenicol displayed synergism against *E. coli*. The antibacterial effects of OEO combined with amoxicillin, polymycin, and lincomycin showed an additive effect against *E. coli*. Thus, in clinical application, the dosage of chemical antibiotics can be reduced to lessen the adverse reactions of antibiotics [27].

3.2. Antioxidant Effect. Genus *Origanum* oils had a strong antioxidant effect and could protect cells from oxidative stress. Anastasia proved that *O. dubium* extract had strong antioxidant activity, antilipid peroxidation, and inhibitory activity of lipoxygenase by measuring the interaction between *O. dubium* extractive and 1, 1-diphenylphenylhydrazine (DPPH) radical [28].

Mechergui used the DPPH radical scavenging assay to determine the antioxidant activity of three essential oils of *O. vulgare* subsp. *glandulosum* (Desf.) from Tunisia. The results showed that the antioxidant activity of essential oils was mainly due to the presence of thymol and carvacrol and the presence of *p*-terpene. And antioxidant activity increased with the increase of total phenol content in essential oils [29].

O. majorana essential oils were found to be an effective antioxidant *in vitro* and exhibited concentration-dependent inhibitory effects on DPPH, hydroxyl radical, hydrogen peroxide, reducing power, and lipid peroxidation. The IC_{50} values were 58.67, 67.11, 91.25, 78.67, and 68.75 mg/mL respectively, while the IC_{50} values of standard antioxidants were 23.95, 44.97, 51.30, 42.22, and 52.72 mg/mL, respectively [30].

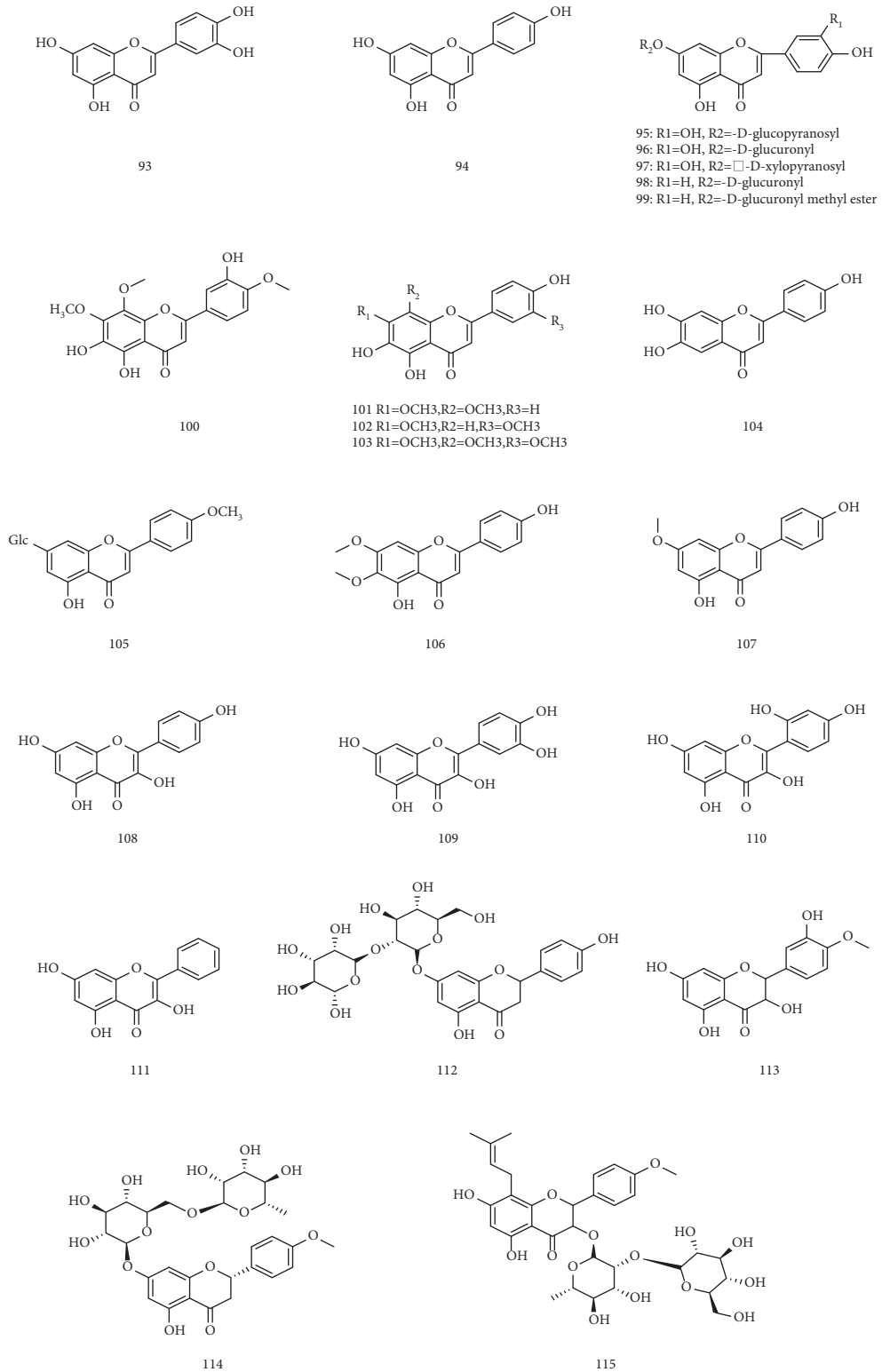

Figure 4: Flavonoids of nonvolatile constituents isolated from genus *Origanum* in the world.

Yao et al. found that adding proper amount of OEO to the diet could increase the total antioxidant level in the serum of weaned piglets, increase the activity of GSH-PX and SOD, reduce the content of lipid peroxide MDA, and enhance the antioxidant performance of the body [31]. Botsoglou found that adding 200 mg/kg of *O. vulgare* essential oils into the diet of rabbits could effectively delay the oxidation of fat, and its antioxidant capacity is equivalent to 200 mg/kg of α-tocopherol acetate [32]. Wang found that adding proper amount of OEO in rabbit feed could improve the activity of antioxidant enzymes in liver and serum [33]. Spiridon studied the antioxidant effect of essential oils *in*

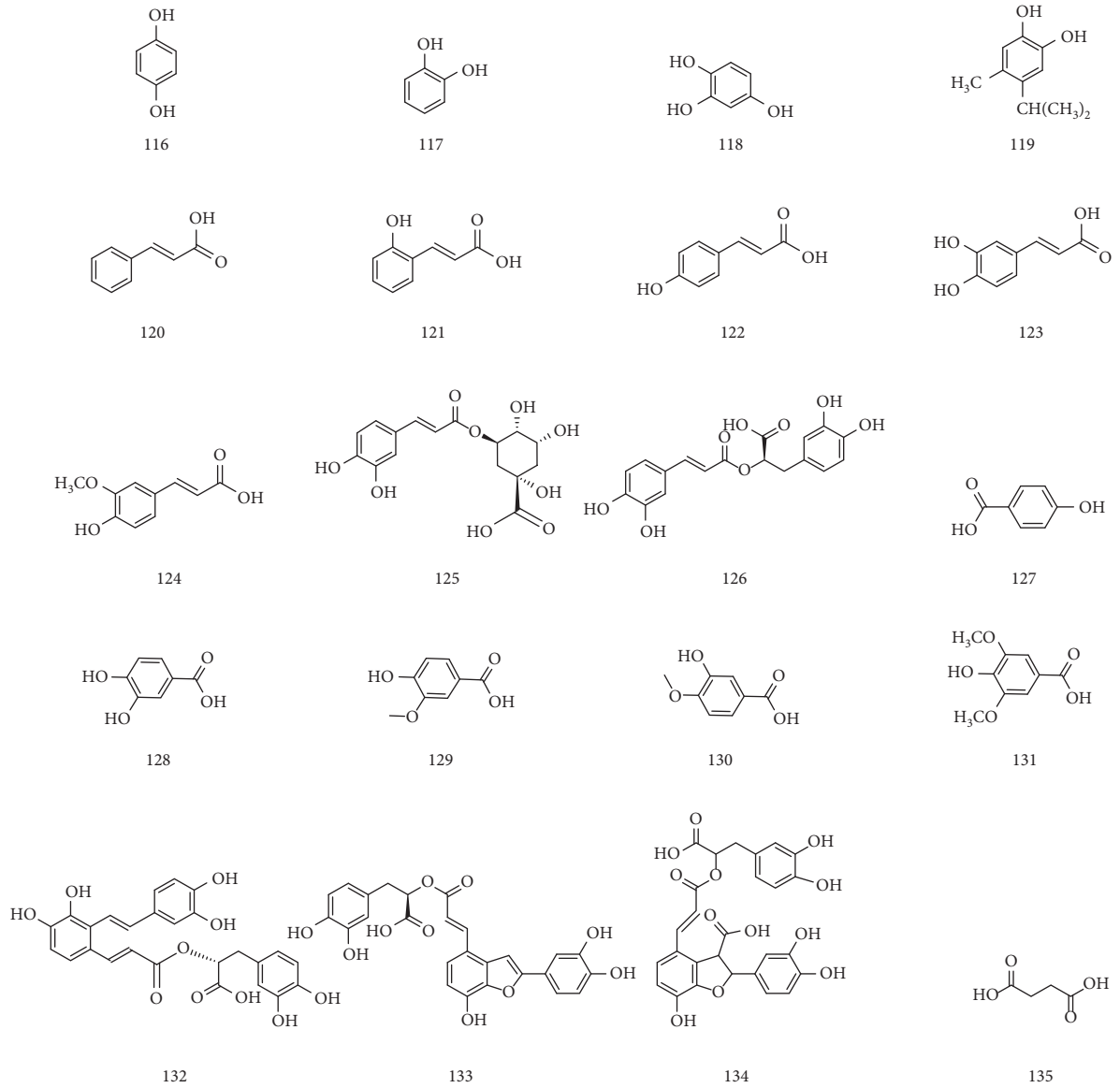

Figure 5: Organic acids of nonvolatile constituents isolated from genus *Origanum* in the world.

vitro from *O. vulgare* and found that the addition of its essential oils to edible sesame oils could prevent the oxidation of grease and maintain the stability of grease which showed that it had a good antioxidant effect [34].

3.3. Anticancer Effect. Dhaheri demonstrated that *O. majorana* significantly inhibited the migration and invasion of the MDA-MB-231 cells by wound-healing assays. MMPs are known to play an important role in breast cancer cell invasion and metastasis. The protein level of MMP-2 and MMP-9 was found to be significantly reduced after *O. majorana* essential oils (OME) treated MDA-MB-231 cells. Meanwhile, *O. majorana* could decrease adhesion of MBAMB-231 to HUVEC, and the level of ICAM-1 protein decreased in concentration-dependent manner in OME-treated MDA-MB-231 cells. In addition, the inhibitory effect of OME on the growth and metastasis of chicken blastoma further confirmed its antibreast cancer activity in vitro [35].

O. onites essential oils (OOEO) exhibited a dose-dependent antiproliferative activity against four types of human cancer cells: melanoma cells (A375), breast cancer cells (MCF-7), hepatocellular carcinoma cells (HepG2), and colon cancer cells (HT-29) lines with IC_{50} values of 8.90 ± 0.70, 10.0 ± 1.7, 23.0 ± 4.2 and 0.35 ± 0.2 g/mL, respectively. Among the cell lines studied, colon cancer cells were the most sensitive to OOEO's antiproliferative activity. Moreover, when administered orally, OOEO inhibited the growth of colon carcinoma tumors in mice [3].

OEO could reduce cell density, slow cell growth, shrinking, fragmentation, and floating. MTT method was used to detect HepG2, human cervical cancer cell line (JTC-26) and lung cancer cell line A549 treated with OEO. It was found that the cells treated with OEO show obvious inhibition of cell growth. Bliss method calculated that the IC_{50} values of OEO against hepatocellular carcinoma cells HepG2, human cervical cancer cell line JTC-26, and lung

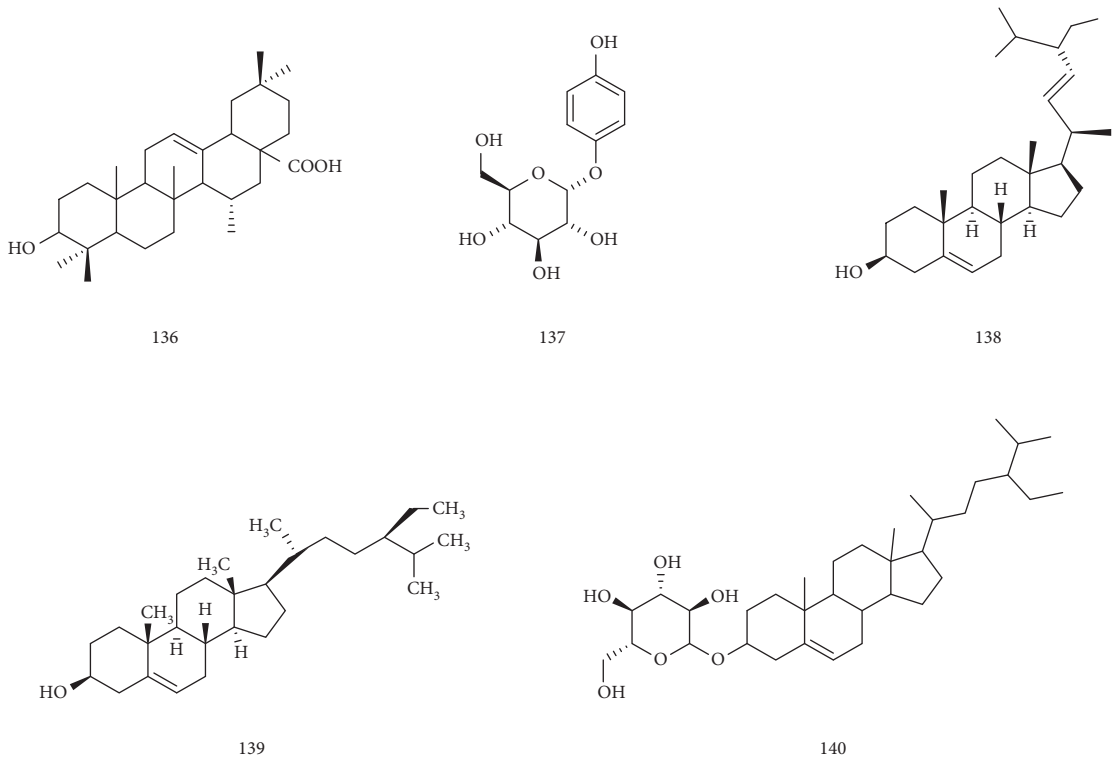

136 137 138

139 140

Figure 6: Steroids and terpenes of nonvolatile constituents isolated from genus *Origanum* in the world.

cancer A549 were 0.118, 0.118, and 0.059 mg/mL, respectively [36].

Sankar reported the cytotoxic effects of green silver nanoparticles synthesized by reducing 1 mM silver nitrate solution from *O. vulgare* water extract on human lung cancer A549 cells for the first time. Silver nanoparticles (500 g/mL) significantly inhibited cell growth, and the inhibition rate was up to 85%, which may be due to the presence of carvacrol, terpinenes, thymol, sabinene, linalool, terpinolene, quercetin, and apigenin in *O. vulgare* [37]. In addition, Jelnar found that in the essential oils of genus *Origanum*, there is a substance called trans-sabinene hydrate, which could play the role of antiproliferation of breast cancer cell line [38].

3.4. Anti-Inflammatory Effect. *O. vulgare* water extract intervenes with the RAW264.7 macrophage inflammatory model which was induced by LPS, TNF-α, and MCP-1 (monocyte chemotactic protein 1). PGE2, NO, and IL-6 were detected by ELISA. mRNA expression levels of TNF-α, IL-6, and MPC-1 (CC chemokine ligand 2) were detected by q-PCR. *O. vulgare* water extract had a good inhibitory effect on LPS-induced RAW264.7 macrophage inflammation by the detection of ELISA and mRNA expression levels. It could reduce the production of cytokines such as PGE2, IL-6, TNF-α, and MCP-1 in cells, as well as the expression levels of IL-6, TNF-α, and MCP-1 mRNA. These effects may be the mechanism of the anti-inflammatory activity of *O. vulgare* water extract [39].

Ocaña-Fuentes found that carvacrol and thymol from *O. vulgare* essential oils could reduce the synthesis of proinflammatory tumor necrosis factor, β-IL and synthesis of IL-6 cytokines, and increase the synthesis of anti-inflammatory IL-10. This indicated that some chemical components of *O. vulgare* essential oils have a strong anti-inflammatory effect on human THP-1 cells [40].

The effects of iNOS protein and COX-2 expression of rosmarinic acid, ursolic acid, and oleanolic acid from Oregano were observed by Nitrite Assay and western blotting. The reduced expression of iNOS protein by these compounds was consistent with reductions on the nitrite production assay, and these three compounds also suppressed COX-2 protein expression on western blotting, showing comparable anti-inflammatory activities contrasting to indomethacin, a recognized COX-2 inhibitor [41].

In addition, it had been reported that the methanol extract of *O. vulgare* can inhibit the secretion of COX-2 and have anti-inflammatory activity in human epithelial cancer cells. Methanol extract treatment specifically attenuated the proinflammatory response mediated by T helper 17 cells and enhanced anti-inflammatory T helper 2 and T regulatory cells through the impact on specific signalling pathways and transcription factors [42]. Yoshino et al. found that oregano extract exhibited anti-inflammatory activities in mouse models of stress-induced gastritis and contact hypersensitivity [43].

3.5. Immune Regulation. Both high and low doses of essential oils of *O. vulgare* had significant inhibitory effects on ear skin delayed hypersensitivity (DTH) induced by 2, 4-dinitrochlorobenzene through foot pad reaction and ear swelling test of mice. The determination of serum hemolysin and the spectrophotometric determination of spleen cell-

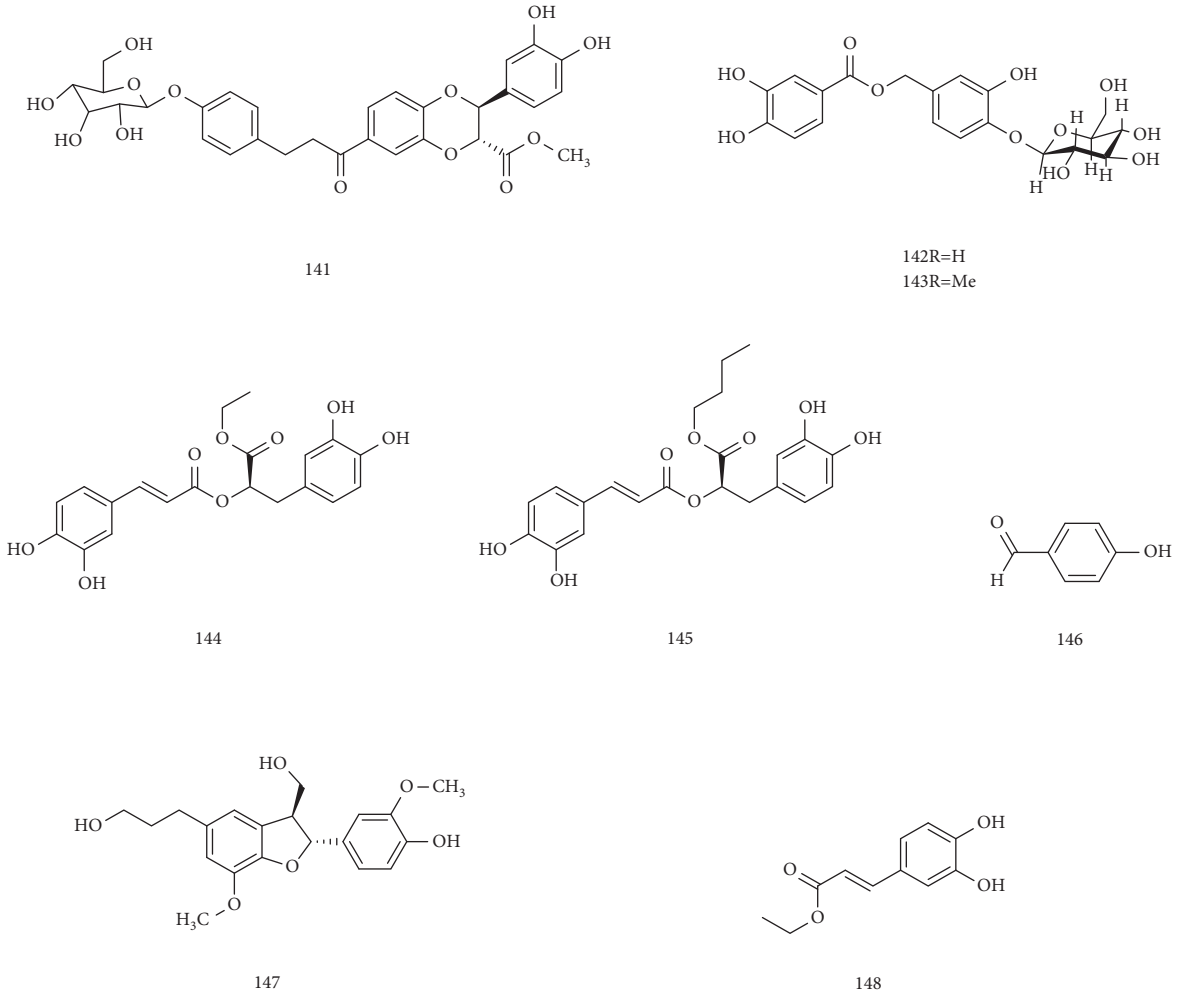

Figure 7: Other nonvolatile constituents isolated from the genus *Origanum* in the world.

mediated erythrocyte hemolysis showed that the high dose of essential oils could significantly inhibit the specific humoral immune function of mice. However, the low dose (50 mg/kg/d × 7 d) of essential oils had a very obvious promoting effect on the specific humoral immune function of mice. Moreover, the thymus and spleen of mice were significantly shrunk by a high dose of essential oils, but the spleen of mice was significantly enhanced by the low dose, which suggested that the essential oils of *O. vulgare* could affect the humoral and cellular immune function of mice [44].

Wang added OEO to broilers, and the results showed that at 42 days of age, the activity of acid α-naphthyl acetate esterase in T lymphocyte and the T lymphocyte conversion rate in the 100 mg/kg OEO group increased by 16.56% and 13.90%, respectively, compared with the control group ($P < 0.05$), which significantly enhanced the cellular immunity of broilers [45]. Malayoğlu added 500 mg/kg of *O. vulgare* essential oils to the diet of broilers and found a significant increase of IgG in the blood of broilers compared with the control group [46]. Hashemipour et al. indicated that long-term addition of carvacrol and thymol, the main components of OEO, could enhance cellular and humoral immunity of broilers [47].

3.6. Hypoglycemic Effect. *O. vulgare* leaves extract could inhibit gluconeogenesis, reduce lipid synthesis, and alleviate oxidative damage to reduce blood sugar. The *O. vulgare* extracts collected in October could effectively inhibit α-glucosidase, promote glucose absorption, reduce glycosylation levels, alleviate the oxidative damage caused by the overexpression of cytochrome P4502E1 (CYP2E1) in E47 cells, repair the activity of lactate dehydrogenase (LDH) in damaged cells, and reduce oxidative stress level caused by oxygen free radicals (ROS). The mechanism may be related to the reduction of the promoter activity of phosphoenolpyruvate kinase (PEPCK), the key factor of gluconeogenesis in HepG2 cells, and the expression of its mRNA and protein. It decreased the promoter activity of cholesterol regulating protein element (SREBP-1c), a key factor in lipid synthesis, and the expression of its mRNA and protein. It could also inhibit the expression of CYP2E1 mRNA and protein in E47 cells and increase the expression of glucose transporter 2 (GLUT2) mRNA and protein. Therefore, phenols and flavonoids may be the main active components in *O. vulgare* [48].

The water extract and methanol extract of *O vulgare* were used in C57BL/6 mice with multiple low-dose streptozotocin-induced diabetes, respectively. Water extract had no

effect on the induction of diabetes. Methanol extract could reduce the incidence of diabetes and maintain normal insulin secretion. Methanol extract prevented apoptosis of β cells by blocking caspase 3 *in vitro*, which may be relevant to rosmarinic acid, the dominant compound in methanol extract [42].

Vanadate was used as reference drug, and the hypoglycemic effect of *O. vulgare* was tested in normal and streptozotocin (STZ) induced diabetic rats. The results showed that *O. vulgare* leaves water extract had significant hypoglycemic effect on STZ diabetic rats. The low dose of *O. vulgare* water extract (20 mg/kg) for 2 weeks was enough to normalize blood glucose levels in severely diabetic rats with fasting blood glucose of more than 20 mM. Furthermore, *O. vulgare* leaves extract had no effect on basal plasma insulin concentration of normal and diabetic rats. This indicate that *O. vulgare* extract could inhibit glucose production in the liver, but not related to insulin secretion by islet cells [49].

3.7. Growth-Promoting Effect. The unique aroma of *O. vulgare* essential oils could stimulate the appetite of animals, stimulate the receptors of digestive tract, activate the activity of digestive enzymes, and promote the absorption of nutrients in the feed. The main chemical constituents of *O. vulgare* were thymol and carvol, which could enhance the barrier function of the intestinal tract and reduce the infection rate of pathogenic microorganisms to epithelial cells. In addition, the unique bactericidal and bacteriostatic effects of *O. vulgare* essential oils inhibit the growth of harmful bacteria in the intestinal tract of animals, maintain the balance of intestinal flora, and improve the absorption capacity of animals to nutrients, thereby improving the utilization rate of feed and ultimately promoting the growth of animals [13].

A comparative study on adding OEO and virginiamycin to chicken feed showed that the activity of intestinal protease in the group with the addition of OEO was 50% higher than that in the group with the addition of virginiamycin. The feed conversion rate of the OEO group was better than that of the virginiamycin group [50].

3.8. Liver Protection Effect. Ali found that *O. vulgare* leaf extract not only led to a significant decrease in serum ALT, AST, and ALP but also prevented liver damage [51].

3.9. Antispasmodic Effect. Different gastrointestinal smooth muscles were cultured to study the antispasmodic action of *O. compactum in vitro*. The results showed that aqueous extract of *O. compactum* powder could inhibit the effects of acetylcholine, histamine, serotonin, $BaCl_2$, 1, 1-dimethyl-4-phenylpiperazinium iodide, and nicotine responses to the guinea pig ileum and also block contractions elicited by electrical coaxial stimulation. Thymol and carvacrol were the active components of antispasmodic effect, which could block the release of intracellular bound Ca^{2+} and prevent the extracellular Ca^{2+} influx into smooth muscle cells [52].

3.10. Insecticidal Effect. El-Akhal found *O. majorana* essential oils could kill Culex pipiens larvae with LC_{50} 258.71 mg/L, which showed that *O. majorana* essential oils were an important natural insecticide [53].

Víctor tested the inhibitory activity of *O. compactum* essential oils to parasitic nematode Anisakis simplex and found that *O. compactum* essential oils showed a dose-dependent larvicidal activity at 24 and 48 h after treatments. All larvae were killed at doses of 1 μL/mL after 24 h. The effects of carvacrol and thymol on the larvae were similar to those of the oils. However, carvacrol exhibited a stronger activity than *O. compactum* and thymol, indicating that carvacrol might be responsible for the larvicidal effects [54].

3.11. Enzyme Inhibition. Goun discovered that aristolochia acid I and aristolochia acid II in *O. vulgare* could strongly inhibit thrombin activity [55]. Victor found *O. compactum* essential oils, carvacrol, and thymol had inhibitory effects on acetylcholinesterase [54]. The inhibitory activity of tyrosinase was detected by mushroom tyrosinase with arbutin as a positive control. The values for tyrosinase inhibitory activity of *O. vulgare* essential oils, ethanol extract, and arbutin were calculated to be $6.5 \pm 0.2\%$, $26.5 \pm 0.3\%$, and $50.0 \pm 0.1\%$, respectively. Both *O. vulgare* essential oils and ethanol extract had certain inhibitory effects on tyrosinase activity [56]. The pharmacological activities of *Origanum* plants are listed in Table 3.

4. Summary and Prospects

In summary, the essential oils of genus *Origanum* are the research focus and the components were mainly analyzed by GC-MS. The results showed that essential oils' compositions and content depend on the different parts of the plants and the origin of the plants. The main chemical components of essential oils are terpenoids and they have many pharmacological activities such as antibacterial, antioxidant, anticancer, anti-inflammatory, immune regulative, hypoglycemic, and growth promoting.

The essential oils of genus *Origanum* can be developed as a natural food additive because of its strong antibacterial and bactericidal effects. It also can be used as a natural growth promoter and insecticide. However, the anticancer and antioxidation studies of essential oils in *Origanum* plants are mainly conducted *in vitro* experiments. It can be further studied *in vivo* and the mechanism can be discussed. At present, the studies on the activities of *Origanum* plants are mainly focused on the extract of essential oil. In the future, the research can be transferred to the biological activity of monomer compounds of essential oil in *Origanum* plants.

In addition, the researches for nonvolatile constituents and their pharmacological activities are few. Therefore, the research on nonvolatile constituents of genus *Origanum* also

Table 3: Pharmacological activities of *Origanum* plants.

Type of the activities	Subjects	Activities	Supplement	References
Antibacterial effect	*O. dictamnus* essential oils	Against *salmonella enteritis*, *Salmonella typhimurium*, *Escherichia coli*, *Listeria monocytogenes*, *Staphylococcus epidermis,* and *Staphylococcus aureus.*	The inhibitory zone diameters of the six colonies were 25 ± 0.5 mm, 20 ± 0.7 mm, 30 ± 1.0 mm, 25 ± 0.5 mm, 25 ± 0.5 mm, 34 ± 0.5 mm, respectively.	[23]
	O. compactum essential oils	Against *Escherichia coli*, *Bacillus subtilis*, *Staphylococcus aureus*, and *Listeria innocua.*	The minimum inhibitory concentration (MIC: 0.06–0.25% (v/v)) and the minimum bactericidal concentration (MBC: 0.12–0.5% (v/v)).	[24]
	Methanol extract and *O. acutidens* essential oils	Obviously inhibit *Staphylococcus aureus*, *Lactococcus garvieae*, *Yersinia ruckeri*, and *Aeromonas hydrophila.*	The mean inhibitory zones of methanol extract and *O. acutidens* essential oils on the bacterial strains were 28.0 ± 1.2 mm and 36.7 ± 0.7 mm.	[25]
	O. vulgare L. essential oils	Inhibit *Staphylococcus aureus.*	When the concentration reached 0.15 or 0.3 μL/mL, the growth of bacteria was significantly inhibited.	[26]
	OEO	The antibacterial effects of OEO in combination with fluoroquinolones, doxycycline, lincomycin, and maquindox florfenicol displayed synergism against *Escherichia coli*. The antibacterial effects of OEO combined with amoxicillin, polymycin, and lincomycin showed an additive effect against *Escherichia coli.*	—	[27]
Antioxidant effect	*O. dubium* extract	Antioxidant activity, antilipid peroxidation, and inhibitory activity of lipoxygenase.	—	[28]
	O. vulgare L. subsp. *glandulosum* (Desf.) essential oils	Scavenge the DPPH radicals.	The IC_{50} values of three kinds of essential oils ranged from 59 to 80 mg/L.	[29]
	O. majorana essential oils	Exhibited concentration-dependent inhibitory effects on DPPH, hydroxyl radical, hydrogen peroxide, reducing power, and lipid peroxidation.	IC_{50} values of 58.67, 67.11, 91.25, 78.67, and 68.75 mg/mL, respectively.	[30]
	O. vulgare L. essential oils	Increase the total antioxidant level in the serum of weaned piglets, increase the activity of GSH-PX and SOD, reduce the content of lipid peroxide MDA, and enhance the antioxidant performance of the body.	—	[31]
	OEO	Effectively delay the oxidation of fat.	Adding 200 mg/kg of *O. vulgare* L. essential oils into the diet of rabbits.	[32]
	OEO	Improve the activity of antioxidant enzymes in liver and serum of rabbit.	—	[33]
	O. vulgare essential oils	The addition of its essential oils to edible sesame oils could prevent the oxidation of grease and maintain the stability of grease.	—	[34]

Table 3: Continued.

Type of the activities	Subjects	Activities	Supplement	References
Anti-cancer effect	*O. majorana* essential oils	Significantly inhibited the migration and invasion of the MDA-MB-231 cells.	Suppress the phosphorylation of IκB, downregulate the nuclear level of NFκB, and reduce nitric oxide (NO) production in MDA-MB-231 cells.	[35]
	O. onites essential oils (OOEO)	Exhibit a dose-dependent antiproliferative activity against four types of human cancer cells: melanoma cells (A375), breast cancer cells (MCF-7), hepatocellular carcinoma cells (HepG2), and colon cancer cells (HT-29) lines.	The antiproliferative effect (lowest IC_{50} value for 72 h) was observed in the HT-29 ($0.35 \pm 0.2\,\mu$g/mL) followed by A375 ($8.90 \pm 0.7\,\mu$g/mL), MCF-7 ($10.0 \pm 1.7\,\mu$g/mL), and HepG2 ($23.0 \pm 4.2\,\mu$g/mL).	[3]
	OEO	Inhibit liver cancer HepG2, son of man cervical cancer JTC-26, and lung cancer A549 growth.	The IC_{50} values of OEO against liver cancer HepG2, son of man cervical cancer JTC-26, and lung cancer A549 were 0.118, 0.118, and 0.059 mg/mL, respectively.	[36]
	O. vulgare water extract	Green silver nanoparticles synthesized by reducing 1 mM silver nitrate solution from *O. vulgare* water extract (500 g/mL) significantly inhibited human lung cancer A549 cells growth.	The green synthesized silver nanoparticles against human lung cancer A549 cell line (LD 50–100 μg/ml).	[37]
	Trans-sabinene hydrate from genus *Origanum* essential oils	Antiproliferation of breast cancer cell line.	—	[38]
Anti-inflammatory effect	*O. vulgare* L. water extract	Have a good inhibitory effect on LPS-induced RAW264.7 macrophage inflammatory.	Reduce the production of cytokines such as PGE2, IL-6, TNF-α, and MCP-1 in cells, as well as the expression levels of IL-6, TNF-α, and MCP-1 mRNA.	[39]
	O. vulgare essential oils	*O. vulgare* essential oils have a strong anti-inflammatory effect on human THP-1 cells.	Carvacrol and thymol from *O. vulgare* essential oils could reduce the synthesis of proinflammatory tumor necrosis factor, β-IL, and synthesis of IL-6 cytokines and increase the synthesis of anti-inflammatory IL-10.	[40]
	Rosmarinic acid, ursolic acid, and oleanolic acid from oregano	Exhibit comparable anti-inflammatory activities contrasting to indomethacin, a recognized COX-2 inhibitor.	Reduce expression of iNOS protein and suppress COX-2 protein expression.	[41]
	The methanol extract of *O. vulgare*	Inhibit the secretion of COX-2 and had anti-inflammatory activity in human epithelial cancer cells.	Methanol extract specifically attenuated the proinflammatory response mediated by T helper 17 cells and enhanced anti-inflammatory T helper 2 and T regulatory cells.	[42]
	Oregano extract	Exhibit anti-inflammatory activities in mouse models of stress-induced gastritis and contact hypersensitivity.	—	[43]

Table 3: Continued.

Type of the activities	Subjects	Activities	Supplement	References
Immune regulation	*O. vulgare* L. essential oils	Both the high dose of 100 mg/kg/d × 7 d and the low dose of 50 mg/kg/d × 7 d had obvious inhibitory effect on the specific cellular immune function of normal mice. The dose of 50 mg/kg/d × 7 d significantly promoted the humoral immunity of mice, and 100 mg/kg/d × 7 d significantly inhibited the humoral immunity of mice.	—	[44]
	OEO	Carvacrol and thymol of OEO could enhance cellular and humoral immunity of broilers.	—	[45]
Hypoglycemic effect	*O. vulgare* leaves extract	Significant hypoglycemic activity.	By inhibiting α-glucosidase activity, promoting glucose uptake, and inhibiting glycation.	[48]
	Methanol extract of *O. vulgare*	Methanol extract could reduce the incidence of diabetes and maintain normal insulin secretion.	Methanol extract prevented apoptosis of β cells *in vitro* by blocking caspase 3.	[42]
	O. vulgare leaves water extract	*O. vulgare* leaves water extract had significant hypoglycemic effect on STZ diabetic rats.	The low dose of *O. vulgare* water extract (20 mg/kg) for 2 weeks was enough to normalize blood glucose levels in severely diabetic rats with fasting blood glucose of more than 20 mM.	[49]
Growth-promoting effect	*O. vulgare* L. essential oils	Stimulate the appetite of animals, maintain the balance of intestinal flora, and improve the absorption capacity of animals to nutrients, promoting the growth of animals.	—	[13]
	OEO	Improve feed conversion rate.	—	[50]
Liver protection effect	Ethanol extract of *O. vulgare* leaves	The concentration of ethanol extract of *O. vulgare* leaves below 500 mg/kg had protective effect on paraquat-induced hepatotoxicity in rats.	—	[51]
Antispasmodic effect	Aqueous extract of *O. compactum* powder	Exhibit antispasmodic effect.	Aqueous extract of *O. compactum* powder inhibited the effects of acetylcholine, histamine, serotonin, $BaCl_2$, 1, 1-dimethyl-4-phenylpiperazinium iodide, and nicotine responses on the guinea pig ileum and also blocked the contractions elicited by electrical coaxial stimulation.	[52]
Insecticidal effect	The essential oil from the leaves of *O. majorana*	Exhibit significant *Culex pipiens*-larvicidal activity.	The LC_{50} and LC_{90} are 258.71 mg/L (lower limit-upper limit: 126.99–527.06 mg/L) and 580.49 mg/L and 580.49 mg/L (lower limit-upper limit:354.51–950.53 mg/L), respectively.	[53]
	O. compactum essential oils	Larvicidal activity of *O. compactum* essential oil against *Anisakis simplex* L3 larvae.	LD_{50} 0.429 mg/ml at 24 h and 0.344 mg/ml at 48 h. The mortality (%) after 24 and 48 h of treatment at 1 μl/ml was 100%.	[54]

Table 3: Continued.

Type of the activities	Subjects	Activities	Supplement	References
Enzyme inhibition	Aristolochia acid I and aristolochia acid II extracted from *O. vulgare* *O. compactum* essential oils, carvacrol and thymol from *O. compactum* essential oils	Inhibit thrombin activity.	—	[55]
		Inhibit acetylcholinesterase activity.	*O. compactum* essential oils (IC_{50} 0.124 mg/ml), carvacrol (IC_{50} 0.113 mg/ml), and thymol (IC_{50} 0.625 mg/ml).	[54]
	O. vulgare essential oils, ethanol extract	Inhibit tyrosinase activity.	The values for tyrosinase inhibitory activity of *O. vulgare* ethanol extract, essential oil, and arbutin (positive control) were calculated to be $6.5 \pm 0.2\%$, $26.5 \pm 0.3\%$ and $50.0 \pm 0.1\%$, respectively.	[56]

can be strengthened and its application prospect can be explored so as to make better use of the resources of this plant.

Conflicts of Interest

All authors declare that they have no conflicts of interest.

Authors' Contributions

Li Zhou and Fatma Al-Zahra K. K. Attia performed literature collection and writing and original draft preparation. Lijun Meng and Sitan Chen analyzed and summarized data. Wenyi Kang and Zhenhua Liu critically reviewed the manuscript. Zhenhua Liu, Changyang Ma, and Lijun Liu supervised project administration. Wenyi Kang provided resources, funding, and reviewed the manuscript. All the authors contributed to the article and approved the submitted version.

Acknowledgments

This work was supported by the Key Project in Science and Technology Agency of Henan Province (192102110214 and 202102110149) and Precision Nutrition and Health Food, Department of Science and Technology of Henan Province (CXJD2021006).

References

[1] J. J. Li and R. T. Li, "Research status of *Origanum vulgare* L," *Chinese Journal of Spectroscopy Laboratory*, vol. 30, no. 1, pp. 171–176, 2013.

[2] H. Y. Gong, W. H. Liu, G. Y. Lv, and X. Zhou, "Analysis of essential oils of *Origanum vulgare* from six production areas of China and Pakistan," *Revista Brasileira de Farmacognosia*, vol. 24, no. 1, pp. 25–32, 2014.

[3] K. Spyridopoulou, E. Fitsiou, E. Bouloukosta, A. Tiptiri, and K. Chlichlia, "Extraction, chemical composition, and anticancer potential of *Origanum onites* L. essential oils," *Molecules*, vol. 24, no. 14, 2019.

[4] A. Ayhan, T. Nurhayat, T. Erno et al., "Characterization of volatile constituents from *Origanum onites* and their antifungal and antibacterial activity," *Journal of AOAC International*, vol. 96, no. 6, pp. 1200–1208, 2013.

[5] N. Aligiannis, E. Kalpoutzakis, S. Mitaku, and I. B. Chinou, "Composition and antimicrobial activity of the essential oils of two Origanum species," *Journal of Agricultural and Food Chemistry*, vol. 49, no. 9, pp. 4168–4170, 2001.

[6] A. Shafaghat, "Antibacterial activity and GC/MS analysis of the essential oils from flower, leaf and stem of *Origanum vulgare* ssp. viride growing wild in North-west Iran," *Natural Product Communications*, vol. 6, no. 9, pp. 1351-1352, 2011.

[7] M. Farhat, J. Tóth, B. É. Héthelyi, S. Szarka, and S. Czigle, "Analysis of the essential oil compounds of origanum syriacum L," *Acta Facultatis Pharmaceuticae Universitatis Comenianae*, vol. 59, no. 2, pp. 6–14, 2012.

[8] T. D. Pepa, H. S. Elshafie, R. Capasso et al., "Antimicrobial and phytotoxic activity of *Origanum heracleoticum* and *O. majorana* essential oils growing in cilento (Southern Italy)," *Molecules*, vol. 24, no. 14, 2019.

[9] Y.-L. Lin, C.-N. Wang, Y.-J. Shiao, T.-Y. Liu, and W.-Y. Wang, "Benzolignanoid and polyphenols from Origanum vulgare," *Journal of the Chinese Chemical Society*, vol. 50, no. 5, pp. 1079–1083, 2003.

[10] R. Erenler, O. Sen, H. Aksit et al., "Isolation and identification of chemical constituents from *Origanum majorana* and investigation of antiproliferative and antioxidant activities," *Journal of the Science of Food and Agriculture*, vol. 96, no. 3, pp. 822–836, 2016.

[11] H. B. Hu, "Studies on chemical constituents and bacteriostatic activities of *Origanum vulgare* Linn," Master's Thesis, Northwest Normal University, Lanzhou, China, 2005.

[12] Y. S. Guo, G. C. Wang, C. H. Wang, X. J. Huang, Y. L. Li, and W. C. Ye, "Chemical constituents of *Origanum vulgare*," *Chinese Pharmaceutical Journal*, vol. 47, no. 14, pp. 1109–1113, 2012.

[13] R. Wu, Q. Ye, N. Y. Chen, and G. Zhang, "Study on the chemical constituents of *Origanum vulgare* L," *Natural Product Research and Development*, vol. 6, pp. 13–16, 2000.

[14] J. F. Zan, "The pharmaceutical researcher on the kuanxin soft capsule," Master's Thesis, Hubei College of Chinese Medicine, Wuhan, China, 2005.

[15] L. J. Sun, H. B. Liu, W. Q. Fan, H. L. Xu, and Y. W. Liu, "Chemical constituents of *Origanum vulgare* (I)," *Chinese herbal medicine*, vol. 12, pp. 1782–1785, 2007.

[16] G. Liu, X. Meng, and N. Chen, "Study on the chemical constituents of *Origanum vulgare*," *Journal of Chinese Medicinal Materials*, vol. 9, pp. 640-641, 2002.

[17] G. Rao, T. Mukhopadhyay, T. Annamalai, N. Radhakrishnan, and M. Sahoo, "Chemical constituents and biological studies of *Origanum vulgare* linn," *Pharmacognosy Research*, vol. 3, no. 2, pp. 143–145, 2011.

[18] B. Zhu, X. W. Cheng, and Y. X. Liu, "Advances in the chemical constituents, pharmacological activities and extraction methods of *Origanum*," *Journal of Chinese Medicinal Materials*, vol. 8, pp. 1038–1041, 2007.

[19] M. Hatipi, V. Papajani, S. Cavar, and R. Koliqi, "Analysis of volatile compounds of *Origanum vulgare* L. growing wild in kosovo," *Journal of Essential Oil Bearing Plants*, vol. 17, no. 1, pp. 148–157, 2014.

[20] W. Z. Huo, S. J. Wei, X. J. Yuan, X. B. Suo, and X. Y. Li, "Analysis of constituents in volatile oil from herba artemisiae capillariae and *origanum vulgare* L. by GC-MS," *Journal of Guangdong Pharmaceutical College*, vol. 26, no. 5, pp. 492–496, 2010.

[21] L. L. Liu and K. X. Tian, "Study and application of oil *origanum*," *Feed review*, vol. 7, pp. 9–11, 2005.

[22] R. Dai, Y. Y. Ma, L. X. Gao, Y. T. Gao, and Z. L. Gu, "Working mechanism and appication of Origanum vulgare oil," *Feed China*, vol. 8, pp. 44–47, 2016.

[23] G. Mitropoulou, E. Fitsiou, E. Stavropoulou et al., "Composition, antimicrobial, antioxidant, and antiproliferative activity of *Origanum dictamnus* (dittany) essential oils," *Microbial Ecology in Health and Disease*, vol. 26, no. 1, 2015.

[24] Y. Laghmouchi, O. Belmehdi, N. S. Senhaji, and J. Abrini, "Chemical composition and antibacterial activity of *Origanum compactum* Benth. essential oils from different areas at northern Morocco," *South African Journal of Botany*, vol. 115, pp. 120–125, 2018.

[25] A. K. Gulec, P. Erecevit, E. Yuce, A. Arslan, E. Bagci, and S. Kirbag, "Antimicrobial activity of the methanol extracts and essential oil with the composition of endemic *Origanum acutidens* (lamiaceae)," *Journal of Essential Oil Bearing Plants*, vol. 17, no. 2, pp. 353–358, 2014.

[26] D. S. E. Leite, D. B. J. Carneiro, D. O. C. E. Vasconcelos, and D. C. M. Lúcia, "Influence of *Origanum vulgare* L. essential oils on enterotoxin production, membrane permeability and surface characteristics of *Staphylococcus aureus*," *International Journal of Food Microbiology*, vol. 137, no. 2-3, pp. 308–311, 2010.

[27] H. B. Si, J. Q. Hu, Z. C. Liu, and Z. L. Zeng, "Antibacterial effect of oregano essential oils alone and in combination with antibiotics against extended-spectrum beta-lactamase-producing *Escherichia coli*," *FEMS Immunology and Medical Microbiology*, vol. 53, no. 2, 2008.

[28] A. Karioti, T. Milošević-Ifantis, N. Pachopos, N. Niryiannaki, D. Hadjipavlou-Litina, and H. Skaltsa, "Antioxidant, anti-inflammatory potential and chemical constituents of *Origanum dubium Boiss*. growing wild in Cyprus," *Journal of Enzyme Inhibition and Medicinal Chemistry*, vol. 30, no. 1, pp. 38–43, 2015.

[29] K. Mechergui, J. A. Coelho, M. C. Serra, S. B. Lamine, S. Boukhchina, and M. L. Khouja, "Essential oils of *Origanum vulgare* L. subsp. glandulosum (Desf.) ietswaart from Tunisia: chemical composition and antioxidant activity," *Journal of the Science of Food and Agriculture*, vol. 90, no. 10, pp. 1745–1749, 2010.

[30] A. T. H. Mossa and G. Nawwar, "Free radical scavenging and antiacetylcholinesterase activities of *Origanum majorana* L. essential oil," *Human & Experimental Toxicology*, vol. 30, no. 10, pp. 1501–1513, 2011.

[31] J. Yao, H. X. Xu, and W. Q. Xu, "The effect of *Origanum vulgare* on the growth performance and serum oxidation-antioxidation function of weaned piglets," *Feed China*, vol. 3, pp. 49–51, 2017.

[32] N. A. Botsoglou, P. Florou-Paneri, E. Christaki, I. Giannenas, and A. B. Spais, "Performance of rabbits and oxidative stability of muscle tissues as affected by dietary supplementation with Oregano essential oil," *Archives of Animal Nutrition*, vol. 58, no. 3, pp. 209–218, 2004.

[33] D. D. Wang, X. D. Dai, H. L. Ren, Z. Q. Wu, and Y. F. Lü, "Effect of dietary supplementation with *origanum* oil on growth performance,antioxidant indexes of meat rabbit," *Feed Industry*, vol. 34, no. 1, pp. 53–55, 2013.

[34] S. Kintzios, K. Papageorgiou, I. Yiakoumettis, D. Baričevič, and A. Kušar, "Evaluation of the antioxidants activities of four Slovene medicinal plant species by traditional and novel biosensory assays," *Journal of Pharmaceutical and Biomedical Analysis*, vol. 53, no. 3, pp. 773–776, 2010.

[35] Y. A. Dhaheri, S. Attoub, K. Arafat, A. Q. Synan, and V. Jean, "Anti-metastatic and anti-tumor growth effects of *Origanum majorana* on highly metastatic human breast cancer cells: inhibition of NFκB signaling and reduction of nitric oxide production," *PLoS One*, vol. 8, no. 7, 2013.

[36] Y. Wang, L. Wang, L. Li, J. X. Lu, S. X. Ma, and G. Chen, "Anti-tumor activity of *Origanum* oil *in vitro*," *Chinese Journal of Microecology*, vol. 22, no. 12, pp. 1101-1102, 2010.

[37] R. Sankar, A. Karthik, A. Prabu, S. Karthik, K. S. Shivashangari, and V. Ravikumar, "*Origanum vulgare* mediated biosynthesis of silver nanoparticles for its antibacterial and anticancer activity," *Colloids and Surfaces B: Biointerfaces*, vol. 108, pp. 80–84, 2013.

[38] J. Z. Al-Kalaldeh, R. Abu-Dahab, and F. U. Afifi, "Volatile oils composition and antiproliferative activity of Laurus nobilis, *Origanum syriacum*, *Origanum vulgare*, and Salvia triloba against human breast adenocarcinoma cells," *Nutrition Research*, vol. 30, no. 4, pp. 271–278, 2010.

[39] Z. Ismayil, "Study on antioxidation and anti-inflammatory effect of Origanum vulgare L." Master's Thesis, Xinjiang Medical University, Urumqi, China, 2018.

[40] A. Ocaña-Fuentes, E. Arranz-Gutiérrez, F. J. Señorans, and G. Reglero, "Supercritical fluid extraction of oregano (Origanum vulgare) essentials oils: anti-inflammatory properties based on cytokine response on THP-1 macrophages," *Food and Chemical Toxicology*, vol. 48, no. 6, pp. 1568–1575, 2010.

[41] D. Shen, M.-H. Pan, Q.-L. Wu, C. H. Park, and H. R. Juliani, "LC-MS method for the simultaneous quantitation of the anti-inflammatory constituents in oregano (*origanum* species)," *Journal of Agricultural and Food Chemistry*, vol. 58, no. 12, pp. 7119–7125, 2010.

[42] V. Milica, N. Ivana, K. Vassiliki G, T. Saksida, and P. Charisiadis, "Methanolic extract of *Origanum vulgare* ameliorates type 1 diabetes through antioxidant, anti-inflammatory and anti-apoptotic activity," *British Journal of Nutrition*, vol. 113, no. 5, pp. 770–782, 2015.

[43] K. Yoshino, N. Higashi, and K. Koga, "Antioxidant and antiinflammatory activities of oregano extract," *Journal of Health Science*, vol. 52, no. 2, pp. 169–173, 2006.

[44] Q. H. Lin, C. F. Zhang, and Y. W. Liu, "Effects of volatile oil of *Origanum vulgare* L. on specific immunological functions in mice," *Chinese Journal of Applied and Environmental Biology*, vol. 3, no. 4, pp. 389–391, 1996.

[45] Q. M. Wang, "The effect of volatile oil of *origanum vulgare* L. on the growth performance and cellular immune function

of broiler chicken," *Animal husbandry and feed science*, vol. 29, no. 3, pp. 13–16, 2008.

[46] H. B. Malayoğlu, S. Baysal, Z. Misirlioğlu, M. Polat, H. Yilmaz, and N. Turan, "Effects of *O. vulgare* L. essential oils with or without feed enzymes on growth performance, digestive enzyme, nutrient digestibility, lipid metabolism and immune response of broilsers fed on wheat-soybean meal diets," *British Poultry Science*, vol. 51, no. 1, pp. 67–80, 2010.

[47] H. Hashemipour, H. Kermanshahi, A. Golian, and T. Veldkamp, "Effect of thymol and carvacrol feed supplementation on performance, antioxidant enzyme activities, fatty acid composition, digestive enzyme activities, and immune response in broiler chickens," *Poultry Science*, vol. 92, no. 8, pp. 2059–2069, 2013.

[48] P. P. Zhang, *Research on Hypoglycemic Activity and Mechanism of Origanum Vulgare L.Leaf Extract*, Hubei University, Wuhan, China, 2018.

[49] A. Lemhadri, N. A. Zeggwagh, M. Maghrani, H. Jouad, and M. Eddouks, "Anti-hyperglycaemic activity of the aqueous extract of *Origanum vulgare* growing wild in Tafilalet region," *Journal of Ethnopharmacology*, vol. 92, no. 2-3, pp. 251–256, 2004.

[50] Y. M. Guo, J. L. Ding, Y. Q. Zhu, and Y. P. Xun, "The study on the effect of "Sudafei-500" on the growth performance of broiler chicken," *China Feed*, vol. 5, pp. 16-17, 1994.

[51] S.-R. Ali, H. Esfandiar, and A. S. Asadollah, "Protective and anti-inflammatory effects of hydroalcoholic leaf extract of *Origanum vulgare* on oxidative stress, TNF-α gene expression and liver histological changes in paraquat-induced hepatotoxicity in rats," *Archives Internationales de Physiologie*, vol. 125, no. 1, pp. 56–63, 2018.

[52] C. van den Broucke and J. Lemli, "Antispasmodic activity of *Origanum compactum*," *Planta Medica*, vol. 38, no. 4, pp. 317–331, 1980.

[53] F. El-Akhal, A. E. O. Lalami, Y. E. Zoubi, H. Greche, and R. Guemmouh, "Chemical composition and larvicidal activity of essential oil of *Origanum majorana* (Lamiaceae) cultivated in Morocco against *Culex pipiens* (Diptera: Culicidae)," *Asian Pacific Journal of Tropical Biomedicine*, vol. 4, no. 9, pp. 746–750, 2014.

[54] V. López, M. Cascella, G. Benelli, F. Maggi, and C. Gómez-Rincón, "Green drugs in the fight against anisakis simplex-larvicidal activity and acetylcholinesterase inhibition of Origanum compactum essential oil," *Parasitology Research*, vol. 117, no. 3, pp. 861–867, 2018.

[55] E. Goun, G. Cunningham, S. Solodnikov, O. Krasnykch, and H. Miles, "Antithrombin activity of some constituents from *Origanum vulgare*," *Fitoterapia*, vol. 73, no. 7-8, pp. 692–694, 2002.

[56] A. Moghrovyan, N. Sahakyan, A. Babayan, N. Chichoyan, M. Petrosyan, and A. Trchounian, "Essential oil and ethanol extract of oregano (origanum vulgare L.) from Armenian flora as a natural source of terpenes, flavonoids and other phytochemicals with antiradical, antioxidant, metal chelating, tyrosinase inhibitory and antibacterial activity," *Current Pharmaceutical Design*, vol. 25, no. 16, pp. 1809–1816, 2019.

Hindawi
Journal of Food Quality
Volume 2021, Article ID 2870969, 10 pages
https://doi.org/10.1155/2021/2870969

Review Article

Potential Effects of Dietary Isoflavones on Drug-Induced Liver Injury

Liangliang Yao,[1] **Muhammad Farrukh Nisar**,[2,3] **Tingdong Yan**,[4] **and Chunpeng (Craig) Wan**[2]

[1]*Affiliated Hospital of Jiangxi University of Traditional Chinese Medicine, Nanchang, Jiangxi 330006, China*
[2]*Jiangxi Key Laboratory for Postharvest Technology and Nondestructive Testing of Fruits & Vegetables, College of Agronomy, Jiangxi Agricultural University, Nanchang 330045, China*
[3]*Department of Physiology and Biochemistry, Cholistan University of Veterinary and Animal Sciences (CUVAS), Bahawalpur 63100, Pakistan*
[4]*School of Pharmacy, Nantong University, Nantong 226019, China*

Correspondence should be addressed to Tingdong Yan; yantdntu2018@163.com and Chunpeng (Craig) Wan; chunpengwan@jxau.edu.cn

Received 16 July 2021; Accepted 23 August 2021; Published 30 August 2021

Academic Editor: Shengbao Cai

Numerous prescribed drugs and herbal and dietary supplements have been reported to cause drug-induced acute liver injury, which is a frequent cause of acute liver failure (ALF). It is a tremendous challenge with ever-increasing drug application in the medication system for huge populations. Drug-induced acute liver injury can lead to diverse pathologies similar to acute and chronic hepatitis, acute liver failure, biliary obstruction, fatty liver disease, and so on. Recently, extensive work demonstrated that isoflavones play an essential and protecting role in drug-induced liver injury (DILI). The isoflavones mediated hepatoprotection by modulating specific genes linked with control of cellular redox homeostasis and inflammatory responses. Isoflavones upregulate oxidative stress-responsive nuclear factor erythroid 2-like 2 (Nrf2), downregulate inflammatory nuclear factor-κB (NF-κB) signaling pathways, and modulate a balance between cell survival and death. Moreover, isoflavones actively inhibit the expression of cytochromes P450 (CYPs) enzyme during drug metabolism. Moreover, isoflavones are also linked with farnesoid X receptor (FXR) activation and signal transducer and activator of transcription factor 3 (STAT3) phosphorylation in hepatoprotection DILI. *In vivo* and *in vitro* studies clearly stated that isoflavones bear strong antioxidant potential and promising agents for hepatotoxicity prevention and stressed their potential role as therapeutic supplements in DILI. The current review will elaborate on isoflavones' preventive and therapeutic potential concisely and highlight various molecular targets to exert a protective effect on DILI.

1. Introduction

Drug-induced liver injury (DILI) is a highly recognized issue that leads to withdrawal of the drugs from the market due to its prognosis with significant adverse effects such as asymptomatic transaminitis, acute and chronic hepatitis, cholestasis, and even death. It is caused not only by prescribed medicines such as nonsteroidal anti-inflammatory drugs (NSAIDs), anti-infective drugs, and anticancer drugs but also by herbal and dietary supplements (HDS) [1, 2], particularly acetaminophen (APAP), which is a crucial cause of acute liver failure (ALF) [3].

Acute DILI takes about three months to develop. The type of injured target cells set helps to classify acute DILI into three types using $R = (\text{ALT patient/ULN})/(\text{ALP patient/ULN})$. These types include (1) hepatocellular type: ALT ≥ 3 ULN and $R \geq 5$, (2) cholestatic type: ALP ≥ 2 ULN and $R \leq 2$, and (3) hepatocellular-cholestatic mixed type: ALT ≥ 3 ULN, ALP ≥ 2 ULN, and $2 < R < 5$ [1]. DILI is the frequent cause of ALF and accounts for 20–40% of all instances of fulminant

hepatic failure throughout the United States and Europe [4, 5]. The incidence of DILI is as low as 1 in 10,000 to 100,000 [6]. It is difficult to find any particular drug ascribed to hepatic injury. Recent studies indicated the involvement and association of multiple factors in developing DILI. These DILI inducing factors include various environmental factors [1], genetic background [7], drug types [8], age [9], gender [10], pregnancy [11], and underlying liver diseases [12, 13].

The in-time diagnosis of DILI is a big challenge. The viral diseases (hepatitis A, B, C, and E virus, cytomegalovirus, and Epstein-Barr virus), autoimmune (antinuclear antibody and antismooth muscle antibody), and metabolic (Wilson's disease and α1-antitrypsin deficiency) disorders mostly mimic any form of acute hepatocellular DILI [14]. Therefore, it is necessary to exclude other liver diseases before clinical diagnosis and treatment of DILI. The frequently used tool for DILI diagnosis is the Roussel Uclaf causality assessment method (RUCAM) [15], which remains highly rational, comprehensive, and convenient. To date, the severity of acute DILI can be classified into five grades, namely, grade 0–5, where 0 is no liver injury, 1 is mild liver injury, 2 is moderate liver injury, 3 is severe liver injury, 4 is acute liver failure, and 5 is lethal [16].

Different people who are exposed to certain potential hepatotoxic drugs may react differently. The tolerators or nonsusceptible will not have the clinical manifestation of DILI. Mild and transient liver injury can recover naturally after withdrawal of the toxic drug. In certain serve liver injury cases, timely clinical salvage is also needed. Isoflavones are polyphenolic compounds having strong bioactivities primarily found in fruits, flowers, and vegetables. Moreover, isoflavones have been reported to possess estrogen-like effects and hence often called phytoestrogens [17]. The isoflavones have drawn much attention and are considered promising molecules to cure cancer, liver injury, neurodegenerative diseases, osteogenic issues, cardiovascular diseases, and hematotoxicity problems [18–20]. Common isoflavones (biochanin A, formononetin, and genistin) are often found as glycosides are also recognized as mild antioxidants, whereas gut flora help convert these glycosides into aglycones [21]. The isoflavones found in soy are reported to replenish the progress of acetaminophen-mediated hepatotoxicity *in vivo* by ameliorating the glutathione levels [22]. The isoflavones protect against fatty liver disease (FLD) through multiple cellular pathways involving the β-oxidation of fatty acid, biosynthesis of lipids, and modulation of reactive oxygen species (ROS). Moreover, aldose reductase (AR)/polyol pathway leads to the development of FLD by modulating the production of fructose in liver, peroxisome proliferator-activated receptor PPAR-α protein, cytochrome P450 (CYP)2E1 expression, and inflammatory factors expressed by certain endotoxins released by the gut flora. The isoflavones have been reported as potent AR inhibitors and hence reduce the onset of FLD [23]. The presence of complex compounds such as biochanin A, calycosin, daidzein, genistein, kakkalide, and tectorigenin in isoflavones made it a vital plant compound bearing various pharmacological properties. Herein, we will elaborate on the updated pharmacological activities of those isoflavones being applied in DILI.

2. Pathophysiology of DILI

The nature of DILI is highly complex pathogenesis work in a sequence of effects or simultaneous effects through series of mechanisms along with numerous risk factors, which has not been yet fully explained yet. During drug metabolism, drugs arrive in liver cells via blood circulation, and hence initial drug transport into the hepatocytes begun via influx transporters [24]. The drug in the form of the parent drug is metabolized by phase I and II drug-metabolizing enzymes (DMEs) and products of many reactive metabolites [25]. Phase I metabolism mainly includes cytochrome P450-1 and P450-2 (CYP1 and CYP2) and flavin-containing monooxygenases (FMO) [26]. Human cytochrome P450 2E1 (CYP2E1) metabolizes various drugs, including antitubercular compounds, alcohol, and anesthetics [27]. The mutation in phase I DME genes is a common factor causing the quick incidences of adverse drug reactions (ADRs), which altered the activity of proteins during drug metabolism to induce liver injury [28]. The parent drug, reactive metabolites, and heavier products will then discharge into the bile by efflux transporters [24]. Through phase II DMEs, reactive metabolites with a heavy side chain will be deactivated as toxic compounds [25]. The action of phase II DMEs is to replace the reactive aldehyde and alcohol functional groups with more significant but less reactive functional groups. Conjugated metabolites can be produced and lead the drug to get out in excretion and toxicity via the efflux transporters. In the meantime, conjugated metabolites can also create specific protein adducts that participate in reactive oxygen species- (ROS-) mediated oxidation to damage the cells. While both phases I and II DMEs can clear the parent drug and drugs metabolic products, the phase II metabolized drugs are the most stable and common form of the drug metabolism, with a general tendency to cause cholestasis and DILI during the clearance [29].

3. Potential Damage and Mechanism in DILI

3.1. DILI and Reactive Metabolites. During phase I reactions, biotransformation of the parent drug involves necessary steps to complete the subsequent phases of detoxification, which altered the compound highly hydrophilic. The parent drug turned to reactive metabolites in phase I metabolism by adding certain functional groups such as hydroxyl, carboxyl, amino, or thiol groups [25]. These functional groups are said to be highly reactive with proteins compared to the parent drug. ROS and reactive nitrogen species (RNS) that create these reactive metabolites are produced by the interaction of drugs with the proteins and lipid at cellular membranes through oxidative stress [30, 31]. Moreover, they can disrupt the cellular redox homeostasis that leads to lymphocyte-signaled apoptosis [31].

Furthermore, it can also lead to the development of inflammations by releasing proinflammatory cytokines [32]. In addition, the upregulation of AMP-activated protein kinase (AMPK) and the overexpression of Forkhead box O 1 (FoxO1), which was inhibited by drugs, can increase the

synthesis of triglycerides (TG). Fatty acid biosynthesis aids in the occurrence of hepatic steatosis, hepatic fibrosis, and even hepatocellular carcinoma [33].

3.2. DILI Induces Mitochondrial Hazards. Mitochondria are cellular energy suppliers, if damaged, resulting in apoptosis and/or hepatic necrosis, even leading to the activation of the apoptotic signaling pathway if the mitochondrial damage exceeds a specific limit [34]. Excessive ROS are produced during the process of DILI. The interaction between ROS and the hepatic mitochondrial membranes is a vital factor of oxidative stress. For example, D-galactosamine/lipopolysaccharide (D-GalN/LPS), a high production level of MDA and an end-product of lipid hydroperoxide (LPO), may lead to decreased membrane fluidity and hence induce severe mitochondrial membranes damage [35]. Few studies have shown that the ethanol treatment can enhance the release of cytochrome C and apoptosis-inducing factor (AIF), restricted to the mitochondria but released into the cytosol [36]. Cytochrome C can trigger caspase-3 activation, which results in apoptosis. At the same time, proapoptotic protein AIF is independent of the caspase pathway and directly induces apoptosis of hepatocytes [31].

Moreover, mitochondrial permeability transition pore (MPTP) plays a significant role in maintaining mitochondrial physiology. In acute severe hemorrhagic shock, ROS sharply increased, leading to the opening of mitochondrial permeability transition pore (MPTP), resulting in the imbalance of H^+ on the inner mitochondrial membrane, destroying membrane proteins, inhibiting ATP synthesis, and causing mitochondrial swelling [37]. All these may exacerbate necrosis or apoptotic cascades, leading to rapid cell death [24, 38].

3.3. DILI Regulates Hepatic Transporters. Drug transporter proteins are crucial factors in clearing reactive metabolites in the liver, intestine, kidney, and brain [39]. According to the mechanism of action and location on the hepatocyte cell membrane, hepatic transporter proteins can be classified into the solute carrier (SLC) and the ATP-binding cassette (ABC) transporter family. Generally, SLC proteins are influx transporters, which bring drugs from the plasma into the cell [25, 40], while ABC transporters are efflux transporters, transforming metabolized drugs from the cytoplasm to the cell's exterior in the bile [41].

The transporter protein families in the hepatocytes include organic anion transporting polypeptides (OATPs), organic cation transporters (OCTs), multidrug-resistant proteins (MDRs), bile salt export pump (BSEP), breast cancer resistant proteins (BCRP), and multidrug resistance-associated proteins (MRPs) [41, 42]. It has been found that OATP1B and sodium-dependent taurocholate cotransporter (NTCP) significantly affect drug transport of all the influx transporters [39, 43], while ABC transport protein (ABCC2-4) is essential for liver cells to clear the chemicals and biliary excretion. The drugs induced mutations in ABC transporters cannot metabolize drugs to remain inside the hepatocytes and cause impaired canalicular bile flow. This situation generally appears as cholestasis and fatty liver disease [44]. Widely, inhibition of BSEP leads to the accumulation of toxic bile salts in hepatocytes, which are correlated with the incidence of cholestatic liver disease [41]. Therefore, drugs, such as troglitazone, ketoconazole, nefazodone, and lapatinib [45], which express inhibitory effects on BSEP, can have hepatotoxic potential [46]. Furthermore, age and race play an important role in the morbidity of ADRs from variations in the expression of transporter genes, leading to decreased expression of these functional transporters [47].

3.4. DILI Modulates Immunological Response. The immune response is also indispensable in DILI. Long-term drug exposure may cause inflammations in a healthy liver, drug-induced autoimmune hepatitis (DIAIH), or acute liver toxicity [48, 49]. In the adaptive immune response, the drug and its metabolites act as haptens that bind to liver protein cytochrome p450. The drug-protein adduct is then processed by an antigen-presenting cell (APC), while antigen associates with major histocompatibility complex (MHC) class II molecules. After that, CD4 T-cell is activated, resulting in adaptive immune response, which then triggers CD8 cytotoxic T-cell activation, leading to FasL, TNF-α, and other proteins that mediate cell death [50].

The nuclear factor kappa-light-chain enhancer of activated B cells (NF-κB) is a dimer protein, which plays an essential role in releasing inflammatory cytokines. It is generally composed of two functional subunits (P65 and P50) that bind to its natural inhibiting factor, IκB, preventing NF-particles from entering the nucleus and targeting downstream associated genes. Toll-like receptor 4 (TLR4)/myeloid differentiation factor 88 (MyD88) receptor receives the irritant cytokines, activates the mitogen-activated protein kinases (MPAK) signaling pathway to induce inflammation, and has three subunits (p38, JNK, and ERK) [51]. The activation of the NF-κB signaling pathway can increase the risk of inflammation and cell damage. High-mobility group protein box 1 (HMGB1) is reported to play an essential role in sepsis, and it can activate innate immune cells that result in antigen-presenting cells [52, 53]. Many studies reported that SRT1720 reduces the release of inflammatory cytokines (TNF-α and IL-6) and hence blocks the inflammatory reactions. Additionally, immune-based DILI can also connect with gender, age, race, and current immune state [54].

4. Health Benefits of Isoflavones

4.1. As Antioxidants. Oxidative stress, caused by imbalanced cellular ROS levels, is a critical phenomenon in chronic diseases, cardiopathy, and hepatotoxicity. Many studies showed that soybean isoflavones (daidzein and genistein) and red clover isoflavones (biochanin A) potentially protect from DILI [55–57]. Isoflavones play an essential role as dietary antioxidants by scavenging free radicals and deactivating detoxifying enzymes [57, 58]. Recently, it has been showing that germinated and fermented soybean extracts (GFSE) effectively inhibit the expression of NADPH oxidase

4 (Nox4), which is responsible for the synthesis of ROS [57–59]. Reduced metabolic activation of drugs by monooxygenase (P450 2E1) system depresses the initial formation of ROS and some intermediate toxic products, resulting in reduced lipid peroxidation [60, 61]. These isoflavones treatments were found to increase the mRNA and protein expression level of CYP2E1 and regulate the JNK/CYP7A1 signaling pathway [62, 63]. In addition to CYP450, the inhibition of phase II detoxifying enzymes, such as UDP-glucuronyltransferase (UGTs), can also have a resistance to oxidative stress [64].

Recently, huge reports highlighted the antioxidant defenses of isoflavones, including both the nonenzymatic (mainly GSH) and enzymatic antioxidant defenses (SOD, CAT, GSP, GST, and GR) [58, 60, 65, 66]. Nevertheless, this way has not already been confirmed in the antioxidant protection after GalN administration [67]. Formononetin (FMN) is one of the significant isoflavonoid constituents from red clover, and it showed that the pretreatment of FMN significantly enhanced Nrf2 protein expression, stimulated mRNA expression of antioxidant enzymes, and restored GSH level and cell viability upon APAP exposure [68]. Nrf2 regulates and induces its downstream heme oxygenase 1 (HO-1) enzyme, which is reported to have antioxidant activity. Biochanin A upregulated the expression of Nrf2 and HO-1 in a dose-dependent manner and helped resist LPS/D-GalN-induced acute liver injury [69].

The dose and route of isoflavones have different effects on resisting oxidative stress. It has been suggested that the efficacy of a high dose of biochanin A (BCA) is lower than a medium dose of BCA, and it is metabolized initially into genistein. Nevertheless, excessive BCA, which was metabolized into genistein and daidzein, could be the primary reason for the high dose of BCA, while BCA is lower than the medium dose of BCA [57]. Many phytochemicals, such as kakkalide, make contact with intestinal microflora and change it into irisolidone in the alimentary tract. The reports showed that irisolidone was intraperitoneally administered to mice or kakkalide was orally administered to mice. Both exhibited potent hepatoprotective activity. Nevertheless, intraperitoneally administration of kakkalide did not exhibit hepatoprotective activity [70–72].

4.2. Antiapoptosis. Recent studies have shown that high ROS concentrations may contribute to apoptotic cell death and DNA damage. Some studies indicated that puerarin (PR) could inhibit apoptosis due to the suppression of caspase-3 activity and alteration of Bcl-2/Bax ratio, which can alleviate raised lead-induced hepatic dysfunction and histopathologic changes rat liver [73]. Further, a downregulation in Bcl-2 and an upregulation in Bax induced by 7,12-dimethylbenz [α]-anthracene (DMBA) treatment were also decreased by daidzein [74]. Genistein treatment, on the other hand, also downregulates Bcl-2 levels [75]. Meanwhile, the metabolite tectorigenin from *Puerariae Flos* (isoflavones tectorigenin and tectoridin) prevents liver injury because of its inhibited ion of β-glucuronidase and apoptosis rather than its antioxidant activity [76, 77]. In addition, overexpression of GSK-3β activates caspase series to activate apoptosis, but puerarin (PR) may inhibit the GSK-3β-induced apoptosis by attenuating inflammatory responses via regulating the GSK-3β/NF-κB pathway [78].

4.3. Anti-Inflammatory and Antifibrosis Effects. With alcohol becoming popular in social life, inflammation is relatively easy to find in most clinical cases, especially alcohol-induced liver damage. The inflammatory responses are mainly linked with the activation of TNF-α mediators and the production of IL-1α, IL-6, and released hepatic stellate cells (HSC) following activation to recruit cytokine-mediated immunological attack/lesions.

It is further revealed that isoflavones play an essential role in removing inflammation-related issues. A study found that puerarin (PR) treatment significantly downregulated TLR4 and p38 phosphorylation levels in mouse livers to inhibit Ni-induced oxidative stress and inflammatory responses. However, p38 also can regulate inflammatory response by activating cAMP response element-binding protein (CREB). The TLR4/p38/CREB pathway plays a crucial role in activating transcription factor NF-kB, which plays a fundamental role in regulating gene expression of inflammatory mediators such as PGE2, COX-2, IL-6, and IL-8, by activating NF-kB and MAP Kinases [79]. NLRP3 inflammasome is responsible for the processing and secretion of the mature IL-1α. The BCA inhibits thioredoxin-interacting protein (TXNIP) expression and the interaction between NLRP3 and TXNIP induced by GalN/LPS, which may be due to the reduced expression of TXNIP [69].

Most of the studies showed a strong relationship between the inflammatory processes and fibrosis. Alcoholic liver disease (ALD) can cause a high death rate, which leaded liver fibrosis, cirrhosis1, and hepatocellular carcinoma [80]. Acetaldehyde, the primary metabolic product of alcohol, activates hepatic stellate cells (HSCs) that play a vital role in liver fibrosis. Herbal medicines have been regarded as new and promising drugs to resist liver fibrosis. It is confirmed that isoflavones (genistein) significantly decreased the extraordinarily high level of TGF-1α and Smad 3, which is the activator of HSCs [75]. Tyrosine kinase, one of the factors of HSC activation, is a crucial factor in the proliferation and activation of HSCs. Another study showed that genistein can prevent the activation and proliferation of HSC by inhibiting tyrosine kinase from reducing acute and chronic inflammation and liver fibrosis [61, 65]. Meanwhile, a study shows that ethyl acetate fraction (Beac) from *Butea monosperma* bark can inhibit thioacetamide-induced liver cancer and fibrosis via suppression of PI3K/Akt/mTOR pathway [81].

4.4. Antihematotoxicity. Hematotoxicity referred to the influence of drugs on the formation and function of blood, including the inhibition of red and blood cells, platelet count, and hematopoietic function of bone marrow cells. It is illuminated that daidzein pretreatment in rats had a potential beneficial effect on the hematopoietic system by elevating RBCs, Hb levels, and PCV and increasing platelet count against cisplatin-induced hematotoxicity markers.

Table 1: Hepatoprotective effects of isoflavone and extracts.

Isoflavone and extracts	Drugs	Injury	Mechanism	Refs
Biochanin A	Arsenic	Hepato/hematotoxicity	Increasing free radical scavenging properties	[57]
	CCl4	Acute liver injury	Increasing antioxidant	[60]
	LSP/D-GalN	Acute liver injury	Activation of the Nrf2 pathway	[69]
Formononetin	APAP	Hepatotoxicity	Enhancing Nrf2 activity	[68]
	TAA	Oxidative stress	Reducing ROS and expression of CYP2E1	[62]
Calycosin	APAP	NASH	Activating FXR	[85]
	HFD	NAFLD	Activating FXR	[86]
	CCl4	Acute liver injury	Activating FXR/increasing expressions of STAT3, Bcl-xl, and SOCS3	[87]
	LSP/D-GalN	Hepatic failure	Suppressing production of TNF-α; increasing caspase-3 activity	[56]
Daidzein	D-GalN	Liver injury	Activating PG-liposome-based system	[67]
	DMBA	Liver oxidative injury	Activation of antioxidant enzymes and Bcl-2; upregulation of caspase-3 and Bax	[74]
Puerarin	Cisplatin	Hepato/hematotoxicity	Increasing free radical scavenging properties; reducing bone marrow suppression	[82]
	CCl4	Liver oxidative injury/ hyperlipidaemia	Inhibiting JNK/c-Jun/CYP7A1 pathway/ROS generation	[63]
	Alcohol	Acute liver injury	Decreasing activity of oxidant enzyme (MDA)/increasing activity of antioxidant enzymes (SOD and GPX)	[66]
	Lead	Liver oxidative injury/ hyperlipidaemia	Reducing ROS production/hepatic metabolism genes expression; increasing activation of antioxidant enzymes	[73]
	Alcohol	Chronic liver injury	Inhibiting GSK-3β/NF-κB pathway	[78]
	Nickel	Liver oxidative stress/ immunotoxicity	Inhibiting TLR4/p38/CREB pathway	[79]
	TAA	Liver inflammatory/ fibrosis	Inhibiting tyrosine kinase/activation of HSC	[61]
Genistein	APAP	Liver injury	Increasing expression of UGTs; inhibiting CYP2E1	[64]
	Alcohol	Hepatic injury/fibrosis	Increasing activities of ADH and ALDH; downregulating expression of TIMP-1, MMP-2, and Bcl-2	[75]
	Endotoxin	Shock/MODS	Decreasing expression of iNOS and COX-2 protein; attenuating the vascular hyporeactivity to NA; inhibiting the activity of protein tyrosine kinase	[84]
	Fructose	NAFLD	Activating AMPK and suppressing SREBP-1 cleavage processing and de novo lipogenesis in hepatocytes	[88]
Kakkalide	Ethanol	Hepatic injury	Orally administered kakkalide and intraperitoneally administered irisolidone have the protective effect; kakkalide can be metabolized to form the bioactive irisolidone by intestinal microflora	[71, 72]
Tectorigenin	TBHQ	Apoptosis in liver injury	Inhibiting β-glucuronidase activity	[77]
	Ethanol	Liver steatosis	Increasing expression of PPAR-α; ameliorating mitochondrial function	[89]
Flemingia macrophylla	CCl4	Acute hepatotoxicity	Inhibiting ROS generation; preventing lipid peroxidation; strengthening antioxidant systems	[58]
Fraxin isolated from *Acer tegmentosum*	CCl4	Acute hepatotoxicity	Lowering AST and ALT	[91]
GFSE	TBHQ	Hepatotoxicity	Downregulating NOX4; upregulating the mRNA levels of antioxidant enzymes	[59]
Butea monosperma	TAA	Liver injury	Deregulation of PI3K/Akt/mTOR signaling	[81]

AST: aspartate aminotransferase; ALT: alanine aminotransferase; ADH: alcohol dehydrogenase; ALDH: aldehyde dehydrogenase; APAP: acetaminophen; CCl4: carbon-tetrachloride; CYP2E1: cytochromeP450, family 2, subfamily E, polypeptide1; COX: cyclooxygenase; DMBA: 7,12-dimethylbenz[a]-anthracene; FXR: farnesoid X receptor; GFSE: germinated and fermented soybean extract; GSK-3β/NF-κB pathway: glycogen synthase kinase-3β/nuclear factor kappa-B pathway; HFD: high-fat diet; iNOS: inducible nitric oxide synthase; JNK/c-Jun/CYP7A1 pathway: c-Jun NH2-terminal kinase/c-Jun protein/cholesterol 7a-hydroxylase pathway; LSP/D-GalN: lipopolysaccharide/D-galactosamine; LPO: lipid peroxides; MMP-2: matrix metalloproteinases; MODS: multiple organ dysfunction syndrome; NASH: nonalcoholic steatohepatitis; NAFLD: nonalcoholic fatty liver disease; NOX4: nicotinamide adenine dinucleotide phosphate oxidase 4; PI3K/Akt/mTOR: phosphatidylinositol 3-kinase/Akt/mammalian; SOCS3: suppressor of cytokine signaling 3; STAT3: signal transducer and activator of transcription 3; TAA: thioacetamide; TLR4/p38/CREB pathway: Toll-like receptor 4/cAMP response element-binding protein; TIMP-1: tissue inhibitors of metalloproteinases; TBHQ: tert-butyl hyperoxide.

Therein, enhancement of erythrocyte count by daidzein may be linked to either stimulation of erythropoiesis or prevention of bone marrow cell inhibition or decreasing cholesterol effects [82, 83]. In addition, the antihematotoxicity protective effect of isoflavones can also be related to the dose administered. Fine shreds of evidence claimed that only low-dose BCA had a significant ameliorative effect on arsenic-induced hematopoietic, especially the RBC indices [57].

4.5. Anticirculatory Failure and Organ Dysfunction Effects. The progression of anticirculatory failure (shock) to multiple organ dysfunction syndromes (MODS) is related to increased mortality. With the increasing number of organ failures, mortality is also progressively increased. The endotoxic shock in rats was regarded as the anticirculatory failure model. Different kinds of isoflavones have different effects on these models. It was found that genistein attenuated the vascular hyperactivity to noradrenaline (NA), but it did not reduce the hypotension elicited by LPS. Daidzein did not revive the circulatory failures caused by LPS. Additionally, both tyrphostin and genistein improve the liver and pancreatic injuries, hypoglycemia, and lactic acidosis caused by LPS, while daidzein did not prevent organ dysfunction or LPS-mediated lactic acidosis. Genistein reduced the high level of LPS-induced TNF-α and suppressed the expression of iNOS and COX-2 proteins and activity in the lung, but not daidzein [84]. Thus, genistein can be regarded as a novel and effective drug to improve LPS-induced circulatory failures.

4.6. Antisteatohepatitis. The risk of steatohepatitis has a rapid increase over the last decade because of the bountiful lifestyles and poor eating habits. Nonalcoholic steatohepatitis (NASH) and alcoholic steatohepatitis are two widespread types of steatohepatitis in clinic cases. NASH, being the frequent form of chronic liver disease, may be induced from nutritional (high-fat diet and high fructose diet), genetic, and immunologic factors, which cause disorders in lipid metabolism and hepatic fibrosis. It is further reported that calycosin is a main active component isolated from *Radix Astragali* and has strong anti-NASH activity. Calycosin treatment has significantly changed the liver histopathology, hepatocytes apoptosis, liver bile acid overload, and hepatocyte mitosis by inhibiting triglycerides (TG) synthesis, increasing fatty acid β-oxidation, and inhibiting HSCs activation, which helps prevent triglyceride accumulation and fibrosis [85]. It has been shown that calycosin that prevents HFD-induced NAFLD may be attributed to farnesoid X receptor (FXR-α and NR1H4) activation that modulates lipid metabolism and restoration of glucose homeostasis [86].

Furthermore, few studies reported that the protective effects of calycosin are in association with FXR activation and STAT3 phosphorylation. The phosphorylated STAT3 can activate the expressions of Bcl-xl and suppressor of cytokine signaling 3 (SOCS3), which can reduce NASH by preventing liver apoptosis and hemorrhagic necrosis [87]. In addition, it was also found that the treatment of sophoricoside, an isoflavone glycoside (genistein-4′-O-β-D-glucopyranoside), decreased the hepatic cholesterol and triglyceride levels and serum low-density lipoprotein-cholesterol (LDL) and apolipoprotein-B levels and elevated the serum high-density lipoprotein-cholesterol (HDL) and apolipoprotein-A1 levels [88]. Alcoholic steatosis may progress to hepatitis and fibrosis, which eventually leads to liver cirrhosis. Tectoridin, an isoflavone glycoside from the flower of *Pueraria lobata*, protected against ethanol-induced liver steatosis mainly through decreasing the expression of PPARα and its downstream target genes and ameliorating mitochondrial functions [89].

4.7. Antihyperlipidemia. Puerarin is a potent isoflavone, which seems to be a potential hepatoprotective drug used to inhibit hyperlipidemia, which can decrease serum cholesterol, triglycerides (TG), and LDL and increase HDL level. Hepatic HMGR and hepatic CYP7A1 are peroxisomal enzymes sequentially used in rate-limiting steps during cholesterol biosynthesis and the biosynthesis of bile acids formation. It has been shown that puerarin remarkably inhibited hyperlipidemia by influencing the expression of hepatic lipid biosynthesis and metabolic-related genes, including cholesterol 7α-hydroxylase (CYP7A1), HMGR, and low-density lipoprotein receptors (LDL-R) in the liver of lead treated rats [90]. Moreover, puerarin could also inhibit hyperlipidemia by regulating the JNK/CYP7A1 signaling pathways [63].

5. Conclusions

With the improvement of living standards and lifestyles, diseases, especially chronic conditions, have increased rapidly. Among various reasons, mainly lousy eating habits and DILI have become the common pathogenic factors. Therefore, specific therapeutic methods have been eagerly sought by many researchers. Recently, the traditional medicinal herbs got the attention. In current essays, puerarin, calycosin, and red clover contain isoflavones that have substantial effects on improving liver injury and circulatory system diseases. All the studies are summarized to elucidate the roles of isoflavones (Table 1) reported in the last decade and we hope it can offer help and convenience in the process of searching for drug treatments.

Abbreviations

ALF: Acute liver failure
AIF: Apoptosis-inducing factor
APAP: Acetaminophen
AMPK: AMP-activated protein kinase
ADRs: Adverse drug reactions
ABC: ATP-binding cassette
APC: Antigen-presenting cell
BSEP: The bile salt export pump
BCRP: Breast cancer resistant proteins
BCA: Biochanin A
CYPs: Cytochromes P450

CYP2E1: Human cytochrome P450 2E1
CYP1 and CYP2: Cytochromes P450 1 and P450 2
CYP7A1: Cholesterol 7a-hydroxylase
CREB: CAMP response element-binding protein
D-GalN/LPS: D-Galactosamine/lipopolysaccharide
DILI: Drug-induced liver injury
DMEs: Drug-metabolizing enzymes
DIAIH: Drug-induced autoimmune hepatitis
FoxO1: Forkhead box O 1
FXR: Farnesoid X receptor
FMN: Formononetin
FMO: Flavin-containing monooxygenases
GFSE: Germinated and fermented soybean extracts
HDS: Herbal and dietary supplements
HO-1: Heme oxygenase 1
HSC: Hepatic stellate cells
HDL: High-density lipoprotein-cholesterol
HMGB1: High-mobility group protein box 1
LPO: Lipid hydroperoxide
LDL: Low-density lipoprotein-cholesterol
LDL-R: Low-density lipoprotein receptors
MDA: Malondialdehyde
MPTP: Mitochondrial permeability transition pore
MDRs: Multidrug-resistant proteins
MyD88: Myeloid differentiation factor 88
MPAK: Mitogen-activated protein kinases
MRPs: Multidrug resistance-associated proteins
MHC: Major histocompatibility complex
MODS: Multiple organ dysfunction syndrome
NTCP: Sodium-dependent taurocholate cotransporter
NA: Noradrenaline
NASH: Nonalcoholic steatohepatitis
Nrf2: Nuclear factor erythroid 2-related factor 2
NF-κB: Nuclear factor kappa-light-chain-enhancer of activated B cells
NSAIDs: Nonsteroidal anti-inflammatory drugs
OATPs: Organic anion transporting polypeptides
OCTs: Organic cation transporters
PR: Puerarin
RUCAM: Roussel Uclaf causality assessment method
ROS: Reactive oxygen species
RNS: Reactive nitrogen species
STAT3: Signal transducer and activator of transcription factor 3
SLC: Solute carrier
SOCS3: Suppressor of cytokine signaling 3
TG: Triglycerides
TXNIP: Thioredoxin-interacting protein
TLR4: Toll-like receptor 4
UGTs: UDP-glucuronyltransferase.

Data Availability

All the data used to support the findings of this study are included in the paper.

Conflicts of Interest

The authors declare no conflicts of interest.

Acknowledgments

This research was funded by the Science and Technology project from Jiangxi Education Department (GJJ180694; 2017JZZDXK004; 20185321).

References

[1] N. P. Chalasani, P. H. Hayashi, H. L. Bonkovsky, V. J. Navarro, W. M. Lee, and R. J. Fontana, "ACG clinical guideline: the diagnosis and management of idiosyncratic drug-induced liver injury," *American Journal of Gastroenterology*, vol. 109, no. 7, pp. 950–966, 2014.

[2] E. S. Björnsson, O. M. Bergmann, H. K. Björnsson, R. B. Kvaran, and S. Olafsson, "Incidence, presentation, and outcomes in patients with drug-induced liver injury in the general population of Iceland," *Gastroenterology*, vol. 144, no. 7, pp. 1419–1425, 2013.

[3] M. W. Russo, J. A. Galanko, R. Shrestha, M. W. Fried, and P. Watkins, "Liver transplantation for acute liver failure from drug induced liver injury in the United States," *Liver Transplantation*, vol. 10, no. 8, pp. 1018–1023, 2004.

[4] H. Ye, L. J. Nelson, M. G. d. Moral, E. Martínez-Naves, and F. J. Cubero, "Dissecting the molecular pathophysiology of drug-induced liver injury," *World Journal of Gastroenterology*, vol. 24, no. 13, pp. 1373–1385, 2018.

[5] M. D. Aleo, Y. Luo, R. Swiss, P. D. Bonin, D. M. Potter, and Y. Will, "Human drug-induced liver injury severity is highly associated with dual inhibition of liver mitochondrial function and bile salt export pump," *Hepatology*, vol. 60, no. 3, pp. 1015–1022, 2014.

[6] D. Larrey, "Epidemiology and individual susceptibility to adverse drug reactions affecting the liver," *Seminars in Liver Disease*, vol. 22, no. 2, pp. 145–156, 2002.

[7] L. Dara, Z.-X. Liu, and N. Kaplowitz, "Mechanisms of adaptation and progression in idiosyncratic drug induced liver injury, clinical implications," *Liver International*, vol. 36, no. 2, pp. 158–165, 2016.

[8] E. Pukenyte, F. X. Lescure, D. Rey et al., "Incidence of and risk factors for severe liver toxicity in HIV-infected patients on anti-tuberculosis treatment," *International Journal of Tuberculosis & Lung Disease: The Official Journal of the International Union Against Tuberculosis and Lung Disease*, vol. 11, pp. 78–84, 2007.

[9] J. H. Hoofnagle and V. J. Navarro, "Drug-induced liver injury: Icelandic lessons," *Gastroenterology*, vol. 144, no. 7, pp. 1335-1336, 2013.

[10] F. J. de Abajo, D. Montero, M. Madurga, and L. A. G. Rodriguez, "Acute and clinically relevant drug-induced liver injury: a population based case-control study," *British Journal of Clinical Pharmacology*, vol. 58, no. 1, pp. 71–80, 2004.

[11] F. Azizi and A. Amouzegar, "Management of hyperthyroidism during pregnancy and lactation," *European Journal of Endocrinology*, vol. 164, no. 6, pp. 871–876, 2011.

[12] T. J. Davern, N. Chalasani, R. J. Fontana et al., "Acute hepatitis E infection accounts for some cases of suspected drug-

induced liver injury," *Gastroenterology*, vol. 141, no. 5, pp. 1665–1672, 2011.

[13] N. Kamar, C. Garrouste, E. B. Haagsma et al., "Factors associated with chronic hepatitis in patients with hepatitis E virus infection who have received solid organ transplants," *Gastroenterology*, vol. 140, no. 5, pp. 1481–1489, 2011.

[14] T. Alempijevic, S. Zec, and T. Milosavljevic, "Drug-induced liver injury: do we know everything?" *World Journal of Hepatology*, vol. 9, no. 10, pp. 491–502, 2017.

[15] G. Danan and R. Teschke, "RUCAM in drug and herb induced liver injury: the update," *International Journal of Molecular Sciences*, vol. 17, 2015.

[16] V. Usachov, T. J. Urban, T. J. Urban et al., "Prevalence of genetic variants of keratins 8 and 18 in patients with drug-induced liver injury," *BMC Medicine*, vol. 13, no. 1, p. 196, 2015.

[17] W. Oleszek, "Preface dietary phytochemicals and human health," *Phytochemistry Reviews*, vol. 1, no. 2, pp. 163–166, 2002.

[18] A. Aras, M. Guven, T. Akman et al., "Neuroprotective effects of daidzein on focal cerebral ischemia injury in rats," *Neural Regeneration Research*, vol. 10, no. 1, pp. 146–152, 2015.

[19] Y. B. Ye, A. L. Chen, W. Lu et al., "Daidzein and genistein fail to improve glycemic control and insulin sensitivity in Chinese women with impaired glucose regulation: a double-blind, randomized, placebo-controlled trial," *Molecular Nutrition & Food Research*, vol. 59, no. 2, pp. 240–249, 2015.

[20] J.-M. Guo, B.-X. Xiao, D.-J. Dai, Q. Liu, and H.-H. Ma, "Effects of daidzein on estrogen-receptor-positive and negative pancreatic cancer cellsin vitro," *World Journal of Gastroenterology*, vol. 10, no. 6, pp. 860–863, 2004.

[21] G. Bultosa, "Functional foods: overview," *Reference Module in Food Science*, Elsevier, Berlin, Germany, 2016.

[22] Y.-T. Liu, Y.-H. Chen, N. Uramaru et al., "Soy isoflavones reduce acetaminophen-induced liver injury by inhibiting cytochrome P-450-mediated bioactivation and glutathione depletion and increasing urinary drug excretion in rats," *Journal of Functional Foods*, vol. 26, pp. 135–143, 2016.

[23] L.-X. Qiu and T. Chen, "Novel insights into the mechanisms whereby isoflavones protect against fatty liver disease," *World Journal of Gastroenterology*, vol. 21, no. 4, pp. 1099–1107, 2015.

[24] A. Schlessinger, M. A. Welch, H. van Vlijmen, K. Korzekwa, P. W. Swaan, and P. Matsson, "Molecular modeling of drug-transporter interactions-an international transporter consortium perspective," *Clinical Pharmacology & Therapeutics*, vol. 104, no. 5, pp. 818–835, 2018.

[25] V. Arya and J. J. Kiser, "Role of transporters in drug development," *The Journal of Clinical Pharmacology*, vol. 56, pp. S7–S10, 2016.

[26] M.-Y. Lee and J. S. Dordick, "High-throughput human metabolism and toxicity analysis," *Current Opinion in Biotechnology*, vol. 17, no. 6, pp. 619–627, 2006.

[27] C. Matthias, U. Bockmühl, V. Jahnke et al., "Polymorphism in cytochrome P450 CYP2D6, CYP1A1, CYP2E1 and glutathione S-transferase, GSTM1, GSTM3, GSTT1 and susceptibility to tobacco-related cancers," *Pharmacogenetics*, vol. 8, no. 2, pp. 91–100, 1998.

[28] S. Crettol, N. Petrovic, and M. Murray, "Pharmacogenetics of phase I and phase II drug metabolism," *Current Pharmaceutical Design*, vol. 16, no. 2, pp. 204–219, 2010.

[29] T. H. Rushmore and A. N. Tony Kong, "Pharmacogenomics, regulation and signaling pathways of phase I and II drug metabolizing enzymes," *Current Drug Metabolism*, vol. 3, no. 5, pp. 481–490, 2002.

[30] Q. Cheng, Y.-W. Li, C.-F. Yang et al., "Methyl ferulic acid attenuates ethanol-induced hepatic steatosis by regulating AMPK and FoxO1 pathways in rats and L-02 cells," *Chemico-Biological Interactions*, vol. 291, pp. 180–189, 2018.

[31] A. F. M. Ismail, A. A. M. Salem, and M. M. T. Eassawy, "Hepatoprotective effect of grape seed oil against carbon tetrachloride induced oxidative stress in liver of γ-irradiated rat," *Journal of Photochemistry and Photobiology B: Biology*, vol. 160, pp. 1–10, 2016.

[32] D. Yang, X. Tan, Z. Lv et al., "Regulation of Sirt1/Nrf2/TNF-α signaling pathway by luteolin is critical to attenuate acute mercuric chloride exposure induced hepatotoxicity," *Scientific Reports*, vol. 6, no. 1, p. 37157, 2016.

[33] J. H. Pan, Y. Lim, J. H. Kim et al., "Root bark of ulmus davidiana var: japonica restrains acute alcohol-induced hepatic steatosis onset in mice by inhibiting ROS accumulation," *PLoS One*, vol. 12, no. 11, Article ID e0188381, 2017.

[34] M. Chen, A. Suzuki, J. Borlak, R. J. Andrade, and M. I. Lucena, "Drug-induced liver injury: interactions between drug properties and host factors," *Journal of Hepatology*, vol. 63, no. 2, pp. 503–514, 2015.

[35] J. Zhang, L. Xu, L. Zhang, Z. Ying, W. Su, and T. Wang, "Curcumin attenuates D-galactosamine/lipopolysaccharide-induced liver injury and mitochondrial dysfunction in mice," *Journal of Nutrition*, vol. 144, no. 8, pp. 1211–1218, 2014.

[36] X. Tian, Y. Hu, M. Li et al., "Carnosic acid attenuates acute ethanol-induced liver injury via a SIRT1/p66Shc-mediated mitochondrial pathway," *Canadian Journal of Physiology and Pharmacology*, vol. 94, no. 4, pp. 416–425, 2016.

[37] P. Li, X. Wang, M. Zhao, R. Song, and K.-S. Zhao, "Polydatin protects hepatocytes against mitochondrial injury in acute severe hemorrhagic shock via SIRT1-SOD2pathway," *Expert Opinion on Therapeutic Targets*, vol. 19, no. 7, pp. 997–1010, 2015.

[38] P. Guo, H. Pi, S. Xu et al., "Melatonin improves mitochondrial function by promoting MT1/SIRT1/PGC-1 alpha-dependent mitochondrial biogenesis in cadmium-induced hepatotoxicity in vitro," *Toxicological Sciences*, vol. 142, no. 1, pp. 182–195, 2014.

[39] B. Stieger, "The role of the sodium-taurocholate cotransporting polypeptide (NTCP) and of the bile salt export pump (BSEP) in physiology and pathophysiology of bile formation," *Handbook of Experimental Pharmacology*, vol. 201, pp. 205–259, 2011.

[40] L. Chedik, A. Bruyere, and O. Fardel, "Interactions of organophosphorus pesticides with solute carrier (SLC) drug transporters," *Xenobiotica*, vol. 49, no. 3, pp. 363–374, 2019.

[41] S. Dawson, S. Stahl, N. Paul, J. Barber, and J. G. Kenna, "In vitro inhibition of the bile salt export pump correlates with risk of cholestatic drug-induced liver injury in humans," *Drug Metabolism and Disposition*, vol. 40, no. 1, pp. 130–138, 2012.

[42] J. H. Chang, E. Plise, J. Cheong, Q. Ho, and M. Lin, "Evaluating the in vitro inhibition of UGT1A1, OATP1B1, OATP1B3, MRP2, and BSEP in predicting drug-induced hyperbilirubinemia," *Molecular Pharmaceutics*, vol. 10, no. 8, pp. 3067–3075, 2013.

[43] M.-K. Choi, H. J. Shin, Y.-L. Choi, J.-W. Deng, J.-G. Shin, and I.-S. Song, "Differential effect of genetic variants of Na+-taurocholate co-transporting polypeptide (NTCP) and organic anion-transporting polypeptide 1B1 (OATP1B1) on the uptake of HMG-CoA reductase inhibitors," *Xenobiotica*, vol. 41, no. 1, pp. 24–34, 2011.

[44] E. Kis, E. Ioja, Z. Rajnai et al., "BSEP inhibition—in vitro screens to assess cholestatic potential of drugs," *Toxicology in Vitro*, vol. 26, no. 8, pp. 1294–1299, 2012.

[45] R. E. Morgan, M. Trauner, C. J. van Staden et al., "Interference with bile salt export pump function is a susceptibility factor for human liver injury in drug development," *Toxicological Sciences*, vol. 118, no. 2, pp. 485–500, 2010.

[46] E. Ulzurrun, C. Stephens, E. Crespo et al., "Role of chemical structures and the 1331T > C bile salt export pump polymorphism in idiosyncratic drug-induced liver injury," *Liver International*, vol. 33, no. 9, pp. 1378–1385, 2013.

[47] C. M. Hunt, N. A. Yuen, H. A. Stirnadel-Farrant, and A. Suzuki, "Age-related differences in reporting of drug-associated liver injury: data-mining of WHO safety report database," *Regulatory Toxicology and Pharmacology*, vol. 70, no. 2, pp. 519–526, 2014.

[48] Z. Wu, M. Han, T. Chen, W. Yan, and Q. Ning, "Acute liver failure: mechanisms of immune-mediated liver injury," *Liver International*, vol. 30, no. 6, pp. 782–794, 2010.

[49] E. Björnsson, J. Talwalkar, S. Treeprasertsuk et al., "Drug-induced autoimmune hepatitis: clinical characteristics and prognosis," *Hepatology*, vol. 51, no. 6, pp. 2040–2048, 2010.

[50] M. Chakraborty, A. M. Fullerton, K. Semple et al., "Drug-induced allergic hepatitis develops in mice when myeloid-derived suppressor cells are depleted prior to halothane treatment," *Hepatology*, vol. 62, no. 2, pp. 546–557, 2015.

[51] W. Zhang, L. Yin, X. Tao et al., "Dioscin alleviates dimethylnitrosamine-induced acute liver injury through regulating apoptosis, oxidative stress and inflammation," *Environmental Toxicology and Pharmacology*, vol. 45, pp. 193–201, 2016.

[52] J. Xie, J. Wan, R. Jiang, H. Lu, X. Peng, and L. Zhang, "Upregulation of Sirt1 in carbon-tetrachloride-induced acute liver injury," *Drug and Chemical Toxicology*, vol. 36, no. 3, pp. 277–283, 2013.

[53] W. Xu, Y. Lu, J. Yao et al., "Novel role of resveratrol," *Shock*, vol. 42, no. 5, pp. 440–447, 2014.

[54] J. Li, X. Zhu, F. Liu et al., "Cytokine and autoantibody patterns in acute liver failure," *Journal of Immunotoxicology*, vol. 7, no. 3, pp. 157–164, 2010.

[55] B. Y. Chang, D.-S. Lee, J.-K. Lee, Y.-C. Kim, H.-K. Cho, and S. Y. Kim, "Protective activity of kudzu (*Pueraria thunbergiana*) vine on chemically-induced hepatotoxicity: in vitro and in vivo studies," *BMC Complementary and Alternative Medicine*, vol. 16, no. 1, p. 39, 2016.

[56] S.-H. Kim, J.-H. Heo, Y. S. Kim, S. S. Kang, J. S. Choi, and S.-M. Lee, "Protective effect of daidzin against d -galactosamine and lipopolysaccharide-induced hepatic failure in mice," *Phytotherapy Research*, vol. 23, no. 5, pp. 701–706, 2009.

[57] A. M. Jalaludeen, W. T. Ha, R. Lee et al., "Biochanin A ameliorates arsenic-induced hepato- and hematotoxicity in rats," *Molecules*, vol. 21, p. 69, 2016.

[58] P.-C. Hsieh, Y.-L. Ho, G.-J. Huang et al., "Hepatoprotective effect of the aqueous extract of flemingia macrophylla on carbon tetrachloride-induced acute hepatotoxicity in rats through anti-oxidative activities," *The American Journal of Chinese Medicine*, vol. 39, no. 2, pp. 349–365, 2011.

[59] E. Y. Kim, K.-B. Hong, H. J. Suh, and H.-S. Choi, "Protective effects of germinated and fermented soybean extract against tert-butyl hydroperoxide-induced hepatotoxicity in HepG2 cells and in rats," *Food & Function*, vol. 6, no. 11, pp. 3512–3521, 2015.

[60] R. M. Breikaa, M. M. Algandaby, E. El-Demerdash, and A. B. Abdel-Naim, "Biochanin A protects against acute carbon tetrachloride-induced hepatotoxicity in rats," *Bioscience, Biotechnology, and Biochemistry*, vol. 77, no. 5, pp. 909–916, 2013.

[61] D. O. Saleh, G. A. R. Abdel Jaleel, S. A. El-Awdan, F. Oraby, and M. Badawi, "Thioacetamide-induced liver injury: protective role of genistein," *Canadian Journal of Physiology and Pharmacology*, vol. 92, no. 11, pp. 965–973, 2014.

[62] L. Jian, L. Xin, M. Yufang, and H. Yifan, "Protective effect of calycosin-7-O-beta-D-glucopyranoside against oxidative stress of BRL-3A cells induced by thioacetamide," *Pharmacognosy Magazine*, vol. 11, pp. 524–532, 2015.

[63] J.-Q. Ma, J. Ding, H. Zhao, and C.-M. Liu, "Puerarin attenuates carbon tetrachloride-induced liver oxidative stress and hyperlipidaemia in mouse by JNK/c-Jun/CYP7A1 pathway," *Basic and Clinical Pharmacology and Toxicology*, vol. 115, no. 5, pp. 389–395, 2014.

[64] Y.-J. Fan, Y. Rong, P.-F. Li et al., "Genistein protection against acetaminophen-induced liver injury via its potential impact on the activation of UDP-glucuronosyltransferase and antioxidant enzymes," *Food and Chemical Toxicology*, vol. 55, pp. 172–181, 2013.

[65] N. Kuzu, K. Metin, A. F. Dagli et al., "Protective role of genistein in acute liver damage induced by carbon tetrachloride," *Mediators of Inflammation*, vol. 2007, Article ID 36381, 6 pages, 2007.

[66] M. Zhao, Y.-Q. Du, L. Yuan, and N.-N. Wang, "Protective effect of puerarin on acute alcoholic liver injury," *The American Journal of Chinese Medicine*, vol. 38, no. 2, pp. 241–249, 2010.

[67] M. C. Y. Wong, B. Portmann, R. Sherwood et al., "The cytoprotective effect of α-tocopherol and daidzein against d-galactosamine-induced oxidative damage in the rat liver," *Metabolism*, vol. 56, no. 7, pp. 865–875, 2007.

[68] F. Jin, C. Wan, W. Li et al., "Formononetin protects against acetaminophen-induced hepatotoxicity through enhanced NRF2 activity," *PLoS One*, vol. 12, no. 2, Article ID e0170900, 2017.

[69] X. Liu, T. Wang, X. Liu et al., "Biochanin A protects lipopolysaccharide/D-galactosamine-induced acute liver injury in mice by activating the Nrf2 pathway and inhibiting NLRP3 inflammasome activation," *International Immunopharmacology*, vol. 38, pp. 324–331, 2016.

[70] H.-U. Lee, E.-A. Bae, and D.-H. Kim, "Hepatoprotective effects of irisolidone on tert-butyl hyperoxide-induced liver injury," *Biological and Pharmaceutical Bulletin*, vol. 28, no. 3, pp. 531–533, 2005.

[71] T. Yamazaki, Y. Nakajima, Y. Niho et al., "Pharmacological studies on puerariae flos III: protective effects of kakkalide on ethanol-induced lethality and acute hepatic injury in mice," *Journal of Pharmacy and Pharmacology*, vol. 49, pp. 831–833, 1997.

[72] Y.-O. Han, M. J. Han, S.-H. Park, and D.-H. Kim, "Protective effects of kakkalide from flos puerariae on ethanol-induced lethality and hepatic injury are dependent on its biotransformation by human intestinal microflora," *Journal of Pharmacological Sciences*, vol. 93, no. 3, pp. 331–336, 2003.

[73] C.-M. Liu, J.-Q. Ma, and Y.-Z. Sun, "Puerarin protects the rat liver against oxidative stress-mediated DNA damage and apoptosis induced by lead," *Experimental & Toxicologic Pathology*, vol. 64, no. 6, pp. 575–582, 2012.

[74] E. J. Choi and G. H. Kim, "Hepatoprotective effects of daidzein against 7, 12-dimetylbenz[a]anthracene-induced oxidative stress in mice," *International Journal of Molecular Medicine*, vol. 23, pp. 659–664, 2009.

[75] Q. Huang, R. Huang, S. Zhang et al., "Protective effect of genistein isolated from hydrocotyle sibthorpioides on hepatic injury and fibrosis induced by chronic alcohol in rats," *Toxicology Letters*, vol. 217, no. 2, pp. 102–110, 2013.

[76] H.-U. Lee, E.-A. Bae, and D.-H. Kim, "Hepatoprotective effect of tectoridin and tectorigenin on tert-butyl hyperoxide-induced liver injury," *Journal of Pharmacological Sciences*, vol. 97, no. 4, pp. 541–544, 2005.

[77] H.-W. Lee, M.-K. Choo, E.-A. Bae, and D.-H. Kim, "β-Glucuronidase inhibitor tectorigenin isolated from the flower of *Pueraria thunbergiana* protects carbon tetrachloride-induced liver injury," *Liver International*, vol. 23, no. 4, pp. 221–226, 2003.

[78] R. Li, T. Liang, Q. He et al., "Puerarin, isolated from kudzu root (willd.), attenuates hepatocellular cytotoxicity and regulates the GSK-3β/NF-κB pathway for exerting the hepatoprotection against chronic alcohol-induced liver injury in rats," *International Immunopharmacology*, vol. 17, no. 1, pp. 71–78, 2013.

[79] C.-M. Liu, J.-Q. Ma, S.-S. Liu, Z.-J. Feng, and A.-M. Wang, "Puerarin protects mouse liver against nickel-induced oxidative stress and inflammation associated with the TLR4/p38/CREB pathway," *Chemico-Biological Interactions*, vol. 243, pp. 29–34, 2016.

[80] H. Kawaratani, T. Tsujimoto, T. Kitazawa, H. Yoshiji, M. Uemura, and H. Fukui, "Therapeutic effects of cytokine modulator Y-40138 in the rat alcoholic liver disease model," *Journal of Gastroenterology and Hepatology*, vol. 26, no. 4, pp. 775–783, 2011.

[81] V. Kaur, M. Kumar, P. Kaur, S. Kaur, A. P. Singh, and S. Kaur, "Hepatoprotective activity of butea monosperma bark against thioacetamide-induced liver injury in rats," *Biomedicine & Pharmacotherapy*, vol. 89, pp. 332–341, 2017.

[82] S. Karale and J. V. Kamath, "Effect of daidzein on cisplatin-induced hematotoxicity and hepatotoxicity in experimental rats," *Indian Journal of Pharmacology*, vol. 49, pp. 49–54, 2017.

[83] A. Y. Nasr, "Protective effect of aged garlic extract against the oxidative stress induced by cisplatin on blood cells parameters and hepatic antioxidant enzymes in rats," *Toxicology Reports*, vol. 1, pp. 682–691, 2014.

[84] H. Ruetten and C. Thiemermann, "Effects of tyrphostins and genistein on the circulatory failure and organ dysfunction caused by endotoxin in the rat: a possible role for protein tyrosine kinase," *British Journal of Pharmacology*, vol. 122, no. 1, pp. 59–70, 1997.

[85] X. Duan, Q. Meng, C. Wang et al., "Calycosin attenuates triglyceride accumulation and hepatic fibrosis in murine model of non-alcoholic steatohepatitis via activating farnesoid X receptor," *Phytomedicine*, vol. 25, pp. 83–92, 2017.

[86] X. Duan, Q. Meng, C. Wang et al., "Effects of calycosin against high-fat diet-induced nonalcoholic fatty liver disease in mice," *Journal of Gastroenterology and Hepatology*, vol. 33, no. 2, pp. 533–542, 2018.

[87] X. Chen, Q. Meng, C. Wang et al., "Protective effects of calycosin against CCl4-induced liver injury with activation of FXR and STAT3 in mice," *Pharmaceutical Research*, vol. 32, no. 2, pp. 538–548, 2015.

[88] W. Li and Y. Lu, "Hepatoprotective effects of sophoricoside against fructose-induced liver injury via regulating lipid metabolism, oxidation, and inflammation in mice," *Journal of Food Science*, vol. 83, no. 2, pp. 552–558, 2018.

[89] Y. Xiong, Y. Yang, J. Yang et al., "Tectoridin, an isoflavone glycoside from the flower of *Pueraria lobata*, prevents acute ethanol-induced liver steatosis in mice," *Toxicology*, vol. 276, no. 1, pp. 64–72, 2010.

[90] Y. P. Hwang, C. Y. Choi, Y. C. Chung, S. S. Jeon, and H. G. Jeong, "Protective effects of puerarin on carbon tetrachloride-induced hepatotoxicity," *Archives of Pharmacal Research*, vol. 30, no. 10, pp. 1309–1317, 2007.

[91] B. Chang, Y. Jung, C.-S. Yoon et al., "Fraxin prevents chemically induced hepatotoxicity by reducing oxidative stress," *Molecules*, vol. 22, no. 4, p. 587, 2017.

Hindawi
Journal of Food Quality
Volume 2021, Article ID 9943537, 10 pages
https://doi.org/10.1155/2021/9943537

Research Article

Inhibitory Effects of Myricetrin and Dihydromyricetin toward α-Glucosidase and Pancreatic Lipase with Molecular Docking Analyses and Their Interaction

Siyuan Mi,[1,2] Jia Liu,[3] Xiaojing Liu,[1] Yishan Fu,[1] Junjie Yi,[1] and Shengbao Cai[1]

[1]*Faculty of Agriculture and Food, Yunnan Institute of Food Safety, Kunming University of Science and Technology, Kunming 650500, Yunnan Province, China*
[2]*Zhongshan School of Medicine, Sun Yat-sen University, Guangzhou 510000, Guangdong Province, China*
[3]*Beijing Key Laboratory of the Innovative Development of Functional Staple and the Nutritional Intervention for Chronic Disease, China National Research Institute of Food and Fermentation Industries Co. Ltd., Beijing 100015, China*

Correspondence should be addressed to Junjie Yi; junjieyi@kust.edu.cn and Shengbao Cai; caikmust2013@kmust.edu.cn

Received 22 March 2021; Revised 24 May 2021; Accepted 17 July 2021; Published 27 July 2021

Academic Editor: Antoni Szumny

The aim of the current study was to evaluate the interaction effects of myricetrin and dihydromyricetin in inhibiting α-glucosidase and pancreatic lipase at different combination ratios and concentrations and to illuminate the underlying mechanisms of their inhibitions by molecular docking analyses. Results showed that both phenolic compounds possessed good inhibitory effects toward two enzymes in a dose-dependent manner. Myricetrin demonstrated a stronger inhibition against α-glucosidase (IC_{50}, 41.14 ± 2.52 and more than 200 μg/mL, respectively), while dihydromyricetin had a better pancreatic lipase inhibition (IC_{50}, 244.96 ± 4.24 and 373.26 ± 21.36 μg/mL, respectively). Different interaction types were observed when myricetrin and dihydromyricetin inhibited α-glucosidase and pancreatic lipase in combination, which were closely related to the combination ratio and concentration. For α-glucosidase inhibition, synergistic effects were observed at relative low concentrations when the combination ratio of myricetrin to dihydromyricetin was set as 1 : 2, while strong synergistic effects existed at relative high concentrations for pancreatic lipase inhibition. In other combination ratios (1 : 1 or 2 : 1), additive and/or antagonistic effects occurred. Molecular docking analyses showed that myricetrin formed nine hydrogen bonds with α-glucosidase, while only three hydrogen bonds were formed between dihydromyricetin and α-glucosidase. However, these two phenolic compounds had similar hydrogen bonds and hydrophobic interactions with pancreatic lipase. The present study suggested that myricetrin and dihydromyricetin or food materials rich in these two phenolic compounds could be exploited as α-glucosidase and/or pancreatic lipase inhibitors to deal with health problems caused by excessive energy intake, and the combination ratio and concentration of these two phenolic compounds should be considered when producing new functional foods.

1. Introduction

Along with the improvement of living standards and the enrichment of material conditions, the diet pattern with high sugar and high fat has become more common, coupled with the sedentary lifestyle with little exercise, resulting in a serious excess of energy intake and thereby leading to the prevalence of many chronic diseases, such as obesity, diabetes, fatty liver, and cardiovascular disease [1, 2]. These chronic diseases have caused heavy burden to the medical system all over the world. Therefore, how to effectively deal with these chronic diseases has become an urgent problem to be solved, which is also a hot and difficult research topic in many disciplines. Dietary intervention to reduce the risk of these chronic diseases is considered to be an effective approach [2–4]. Therefore, many food and nutrition scientists have put a lot of substantial efforts to prevent these chronic diseases.

Carbohydrates and fats in food are the main contributors to the body's energy intake, and therefore reducing

carbohydrate and/or fat intake is considered an effective way to suppress energy intake [5–7]. In the digestive system, carbohydrates and fats need to be digested before they can be absorbed. As for carbohydrates, α-glucosidase is one of the main enzymes for their digestion, and therefore, inhibiting α-glucosidase can not only reduce energy intake derived from carbohydrate but also effectively control postprandial blood glucose of diabetic patients [8, 9]. And for fats in food, pancreatic lipase is the main digestive enzyme, and thus, inhibiting pancreatic lipase is considered an effective method to reduce fat absorption [10, 11]. Clinically, acarbose and orlistat are inhibitors of α-glucosidase and pancreatic lipase, respectively. Although these clinical drugs are effective, they all have serious side effects. A large number of previous studies have found that many secondary metabolites of edible plants, especially phenolic compounds, have good inhibitory effects toward α-glucosidase and/or pancreatic lipase [6, 7, 10, 12, 13].

Phenolic compounds in plants are generally polyphenols, which contain multiple hydroxyl groups on the benzene ring. A certain edible plant commonly contains a variety of phenolic substances, and these phenolics often interact with each other when they exert their biological activities, such as synergistic or antagonistic effects [6, 10]. Our previous study about the different phenolic extracts from palm fruits inhibiting pancreatic lipase and α-glucosidase found that the main phenolics catechin and caffeic acid display complex interactions ranging from antagonistic effect to synergistic effect [6]. Moreover, a previous study also found that myricetrin and dihydromyricetin were the most predominant components of vine tea [14], and it is reported that vine tea has a good inhibitory effect toward pancreatic lipase or α-glucosidase [15, 16]. However, it is not clear how these two predominant phytochemical compounds interact with each other in inhibiting pancreatic lipase and/or α-glucosidase. In addition, the investigation of the underlying mechanism about their enzyme inhibition is also scarce. Therefore, in the present work, the interaction effects of myricetrin and dihydromyricetin in inhibiting pancreatic lipase and α-glucosidase were evaluated and the underlying mechanisms were illuminated by molecular docking analyses.

2. Materials and Methods

2.1. Materials and Chemical Reagent. Porcine pancreatic lipase (EC: 3.1.1.3, 127 U/mg), α-glucosidase of *Saccharomyces cerevisiae* (EC: 3.2.1.20; ≥10 units/mg protein Type I, lyophilized powder), *p*-nitrophenyl laurate, and *p*-nitrophenyl-α-D-glucopyranoside (*p*NPG, purity ≥ 99.0%) were obtained from Sigma (Sigma-Aldrich, Shanghai, China). The standards of myricetrin and dihydromyricetin (purity ≥98.0%) were purchased from Chengdu Must Bio-Technology Co., Ltd. (Chengdu, Sichuan, China). Other reagents used were of analytical grade.

2.2. α-Glucosidase Inhibition Assay. The inhibitory effects of myricetrin and dihydromyricetin toward α-glucosidase were measured according to the published method [13,17] with minor modifications. The concentrations of α-glucosidase solution and *p*NPG (the substrate) in the present study were 2.0 U/mL and 5.0 mM, respectively. Myricetrin and dihydromyricetin were dissolved in dimethyl sulfoxide (DMSO) as stock solution and then diluted with the reaction buffer solution (PBS, pH 6.8) to the appropriate concentration (finally DMSO <0.5%). A SpectraMax M5 microplate reader (Molecular Device, Sunnyvale, CA, USA) was used to measure the absorbance of each sample at 405 nm, and the inhibitory ratio of each sample was calculated by the following formula: Inhibitory ratio (%) = (1 − OD of sample/OD of control) × 100%.

2.3. Pancreatic Lipase Inhibition Assay. The inhibitory effects of these two phenolic standards toward pancreatic lipase were measured according to the method reported earlier [13,17] with some modifications. The concentration of porcine pancreatic lipase solution in the current study was 5 mg/mL. The sample was dissolved in DMSO and then diluted with the reaction buffer (Tris-HCl buffer, pH 8.0, finally DMSO <0.5%). The absorbance (OD value) at 400 nm was measured using a SpectraMax M5 microplate reader. The inhibition ratio of pancreatic lipase activity was determined as follows: Inhibitory ratio (%) = (1 − OD of sample/OD of control) × 100%.

2.4. Interaction of Myricetrin and Dihydromyricetin in α-Glucosidase and Pancreatic Lipase Inhibition. CalcuSyn software (Biosoft, Ferguson, MO, USA) was applied to analyze the interaction type of myricetrin and dihydromyricetin in α-glucosidase and pancreatic lipase inhibition. The dose ratios between myricetrin and dihydromyricetin were set as 1 : 1, 1 : 2, and 2 : 1, respectively. The tested method of inhibitory activity was completely consistent with the above corresponding method.

2.5. Molecular Docking. In order to illuminate the underlying mechanisms of these two phenolic compounds inhibiting lipase and α-glucosidase, molecular docking analyses of myricetrin and dihydromyricetin with lipase and glycosidase, respectively, were performed by using SYBYL-X 2.1.1 software (Tripos, Inc., St. Louis, MO, USA), and Surflex-Dock Geom was applied as the docking mode. The 3D structure of myricetrin and dihydromyricetin were downloaded from the NCBI database (http://www.ncbi.nlm.nih.gov/pccompound), and the 3D structure of lipase (PDB Code: 1ETH) were obtained from the RCSB protein database (http://www.rcsb.org/pdb/home.do). Since the crystal structure of α-glucosidase derived from *S. cerevisiae* was not available yet and the sequence of isomaltase derived from *S. cerevisiae* is very similar to that of α-glucosidase from the

same source, isomaltase (PDB Code: 3A4A) was used for molecular docking analysis in the present work, which was consistent with the previous publication [18]. The high-precision mode (SFXC) was used for docking assay. Before docking, 1ETH and 3A4A were optimized to remove water molecules, metal ions, and their own ligands, and then the protein was hydrogenated and charged. *C*-scores and *T*-scores were used as indicators for identifying the optimal analytical result.

2.6. Statistical Analysis. Data in the current work are presented as mean values ($n = 3$) ± standard deviation (SD) and analyzed by one-way ANOVA. Tukey's procedure was applied to determine the significance of the differences ($p < 0.05$). All analyses were performed by using Origin 8.5 software (OriginLab, Northampton, MA, USA).

3. Results and Discussion

3.1. α-Glucosidase Inhibition of Myricetrin and Dihydromyricetin. In the gastrointestinal tract, α-glucosidase is one of the most vital carbohydrate digestive enzymes. Inhibiting α-glucosidase activity has been regarded as an effective way to control postprandial blood glucose in diabetic patients [9], which is also the action mechanism of the clinical drug acarbose. In this study, the α-glucosidase inhibition results of myricetrin and dihydromyricetin are presented in Figure 1. Both myricetrin and dihydromyricetin displayed good inhibitory effects toward α-glucosidase in a dose-dependent manner at concentrations ranging from 25 μg/mL to 125 μg/mL. Compared with dihydromyricetin, myricetrin possessed a much stronger inhibition toward α-glucosidase at all tested concentrations ($p < 0.05$). At the lowest tested concentration (25 μg/mL), the inhibitory ratio of myricetrin was about 9 times as much as that of dihydromyricetin. When tested at 125 μg/mL, the inhibitory ratio of myricetrin was approximately 90%, while the inhibitory ratio of dihydromyricetin was no more than 30%. The IC_{50} values of myricetrin and dihydromyricetin were 41.14 ± 2.52 μg/mL and more than 200 μg/mL, respectively. The difference between these two phenolic compounds in the inhibitory capacity toward α-glucosidase may be mainly caused by their structural differences. A previous study also reported that flavonoids with different structures displayed great differences in the α-glucosidase inhibition [19]. Moreover, dietary phenolic compounds could cooperate with acarbose to inhibit α-glucosidase activity [20]. In the current study, the IC_{50} value of acarbose was 0.56 ± 0.08 μg/mL.

3.2. Pancreatic Lipase Inhibition of Myricetrin and Dihydromyricetin. In the intestinal tract, pancreatic lipase is one of the key enzymes responsible for fat digestion, and inhibition of this enzyme can effectively reduce fat absorption, thereby preventing obesity and other related health problems [10, 13]. As shown in Figure 2, both myricetrin and dihydromyricetin displayed good inhibitory effects toward pancreatic lipase in a dose-dependent response. Unlike the

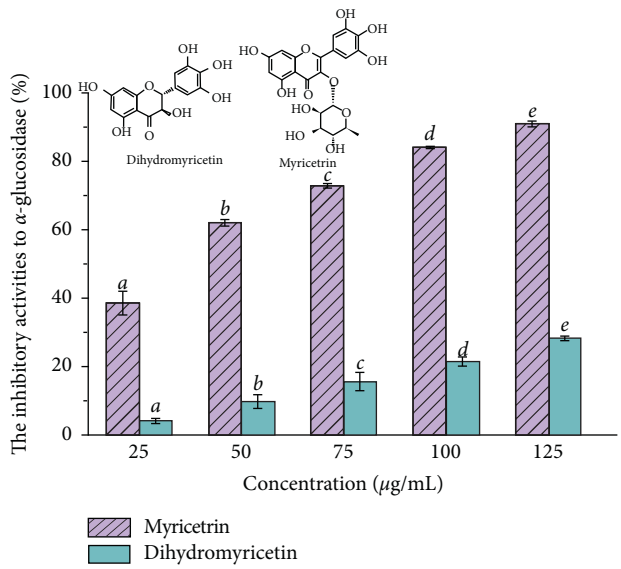

Figure 1: Inhibition effect of myricetrin and dihydromyricetin toward α-glucosidase. All values are expressed as mean ± SD ($n = 3$). Different letters indicate significant differences at $p < 0.05$.

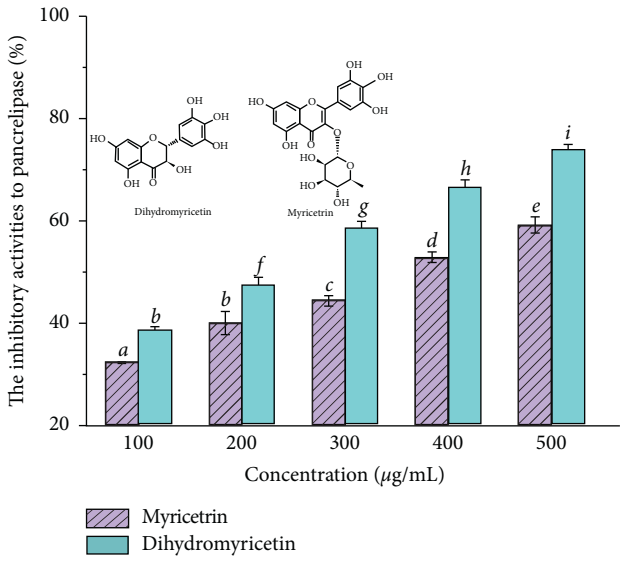

Figure 2: Inhibition effect of myricetrin and dihydromyricetin against pancreatic lipase. All values are expressed as mean ± SD ($n = 3$). Different letters indicate significant differences at $p < 0.05$.

phenomenon observed in the α-glucosidase inhibition, dihydromyricetin showed better inhibitory effects toward pancreatic lipase than myricetrin at all tested concentrations ranging from 100 μg/mL to 500 μg/mL ($p < 0.05$). In the present work, the IC_{50} values of myricetrin and dihydromyricetin were 373.26 ± 21.36 μg/mL and 244.96 ± 4.24 μg/mL, respectively. When the concentration was 100 μg/mL, the inhibition ratios were approximately 31% and 38% for myricetrin and dihydromyricetin, respectively, and the inhibition ratios increased to 84% and 92%, respectively, when the concentration was 500 μg/mL. As aforementioned in α-glucosidase inhibition, the inhibitory capacities of phenolic compounds toward a certain

enzyme may be closely dependent on their chemical structures. A previous study about the lipase inhibition of different tea polyphenols also found that the inhibitory capacities varied with the polyphenolic structures, and the structure-activity relationship was further analyzed by 3D-QSAR models [21].

3.3. Interaction of Myricetrin and Dihydromyricetin on Inhibition of α-Glucosidase and Pancreatic Lipase. Some previous reports have confirmed that phenolic compounds may interact with each other when inhibiting lipase or α-glycosidase, such as antagonistic effect, additive effect, or synergistic effect [6, 10]. Moreover, the type of interaction commonly depended on the concentration and proportion of phenolic substances [6]. In this study, the interactions of myricetrin and dihydromyricetin in inhibiting pancreatic lipase and α-glucosidase were determined by CalcuSyn software with three different combination ratios (1 : 1, 1 : 2, and 2 : 1), and results are summarized in Tables 1 and 2, respectively.

Table 1 presents the interaction types of myricetrin and dihydromyricetin on α-glucosidase inhibition at three different ratios. When the ratio was set at 1 : 1, the inhibitory capacities increased from 12.80 ± 1.53% to 76.68 ± 0.62% and CI values gradually decreased from 1.313 to 0.958 with the concentration of myricetrin increasing from 12.5 to 62.5 μg/mL, suggesting that the interaction type between myricetrin and dihydromyricetin changed from antagonistic (low concentration) to additive effect (high concentration). When the ratio of myricetrin to dihydromyricetin was set as 1 : 2, the inhibitory ratio was 16.80 ± 2.19% at the myricetrin concentration of 8.3 μg/mL and then increased by more than 3 times when the concentration of myricetrin was 41.6 μg/mL. The CI values increased from 0.821 to 0.929, indicating that the interaction type changed from synergistic effect to additive effect. However, when myricetrin and dihydromyricetin were combined at a ratio of 2 : 1, the CI values increased from 0.577 to 1.130, indicating that the interaction effect of these two phenolic compounds was synergistic effect at the low concentration but changed to antagonistic effect at the high concentration. It is worth noting that the combination of myricetrin and dihydromyricetin at a ratio of 2 : 1 showed stronger inhibitory effects toward α-glucosidase when compared with the combination at ratio of 1 : 1 or 1 : 2, especially at a relative low concentration. This phenomenon may be due to the much stronger α-glucosidase inhibitory effect of myricetrin. Similar phenomena were observed by some previous studies [6, 10]. For example, a previous study also found that different flavonoids isolated from *Moringa oleifera* leaf showed synergistic inhibition on α-glucosidase activity [22].

The interaction results of myricetrin and dihydromyricetin on pancreatic lipase are presented in Table 2. When myricetrin and dihydromyricetin were combined at the ratio of 1 : 1, the CI value decreased with the increasing concentration. An antagonistic effect was observed at the concentrations of 50 and 100 μg/mL, and an additive effect was observed at the concentrations of 150 and 200 μg/mL, while a synergistic effect was observed at the concentration of 250 μg/mL. When the ratio of myricetrin to dihydromyricetin was set as 1 : 2, the interaction type was additive at the myricetrin concentration of 33.3 μg/mL, while the interaction type was always synergistic at other tested concentrations according to the CI values. However, when the combined ratio was set as 2 : 1, CI values were always more than 1.10 at all tested concentrations, indicating that the antagonistic effect always existed at this combination ratio. Among these three combination doses, the ratio of myricetrin to dihydromyricetin at 1 : 2 possessed the strongest inhibitory effect toward pancreatic lipase, which was consistent with the stronger inhibitory capacity of dihydromyricetin. The current result was similar to the previous finding [10]. Cai et al. also found that the binary combination of caffeic acid, ferulic acid, and *p*-coumaric acid also exhibited synergistic effects in inhibiting pancreatic lipase only at relative higher concentrations [10]. Moreover, a previous study found that a phenolic compound kaempferol could exhibit synergistic effects with orlistat to inhibit lipase [11].

3.4. Molecular Docking Results of α-Glucosidase and Pancreatic Lipase. The enzyme inhibitory mechanisms of myricetrin and dihydromyricetin on α-glucosidase and pancreatic lipase were illuminated by the molecular docking method with the computational modeling software SYBYL-X 2.1.1, and the hydrophobic interactions were analyzed by Ligplot+ software. The related parameters of the docking scores, hydrogen bond parameters, and hydrophobic effects of these standards with α-glucosidase or pancreatic lipase are summarized in Tables 3 and 4, respectively. The parameters in Tables 3 and 4 displayed the detailed information of the receptor-ligand interactions, including reliability, charge, van der Waals force, hydrogen bond, lipophilic, and so on. Among these parameters, *C*-scores and *T*-scores are the most vital parameters, which reflect the reliability of docking results and binding affinity ability between receptor and ligand, respectively.

The docking results of myricetrin and dihydromyricetin with α-glucosidase are summarized in Table 3 and Figure 3. *C*-score values of myricetrin and dihydromyricetin were four, indicating that the docking results of these two phenolic compounds with α-glucosidase were credible. *T*-score values of myricetrin and dihydromyricetin were 4.1619 and 4.6978, respectively, suggesting that dihydromyricetin may bind more tightly to α-glucosidase than myricetrin. For myricetrin, it formed nine hydrogen bonds with seven amino acid residues, and the longest and shortest hydrogen bonds were 2.542 Å (formed with Asp352) and 1.666 Å (formed with Tyr158), respectively. However, dihydromyricetin just formed three hydrogen bonds with three amino acid residues, and the longest and shortest hydrogen bonds were 2.144 Å (formed with Gln353) and 1.908 Å (formed with Asp215), respectively. A previous study has pointed out that the number and distance of hydrogen bonds played important roles for inhibitors to inhibit enzyme activity [7]. In the present work, although the average distance of hydrogen bonds of these two phenolic

Table 1: Interaction between myricetrin and dihydromyricetin on α-glucosidase inhibition.

Ratio	Myricetrin Tested concentration (μg/mL)	Dihydromyricetin Tested concentration (μg/mL)	α-Glucosidase inhibition (%)	CI[a]	Fa[b] (%)	CI for Fa	Myricetrin Calculated concentration (μg/mL)	Dihydromyricetin Calculated concentration (μg/mL)
1 : 1	12.5	12.5	12.80 ± 1.53	1.313	25.0	1.236	19.58	19.58
	25.0	25.0	33.40 ± 1.51	1.225	50.0	1.101	34.45	34.45
	37.5	37.5	52.48 ± 1.94	1.127	75.0	0.983	60.61	60.61
	50.0	50.0	68.42 ± 1.44	0.992	90.0	0.880	106.64	106.64
	62.5	62.5	76.68 ± 0.62	0.958	—	—	—	—
1 : 2	8.3	16.7	16.80 ± 2.19	0.821	25.0	0.825	11.47	22.94
	16.7	33.3	37.34 ± 2.27	0.831	50.0	0.875	24.38	48.76
	25.0	50.0	52.10 ± 2.54	0.851	75.0	0.932	51.84	103.68
	33.3	66.7	60.54 ± 2.01	0.913	90.0	0.996	110.22	220.44
	41.6	83.4	68.07 ± 2.67	0.929	—	—	—	—
2 : 1	16.7	8.3	44.26 ± 3.36	0.577	25.0	0.438	7.46	3.73
	33.3	16.7	54.62 ± 1.10	0.892	50.0	0.727	24.22	12.11
	50.0	25.0	62.19 ± 1.03	1.107	75.0	1.207	78.66	39.33
	66.7	33.3	72.47 ± 1.17	1.109	90.0	2.007	255.28	127.64
	83.3	41.7	78.61 ± 3.92	1.130	—	—	—	—

[a]CI, combination index. CI ≤ 0.90, 0.90 < CI < 1.10, and CI ≥ 1.10 indicate synergistic, additive, and antagonistic effects, respectively; [b]Fa, fraction affected by the combination dose of myricetrin and dihydromyricetin.

Table 2: Interaction between myricetrin and dihydromyricetin on pancreatic lipase inhibition.

Ratio	Myricetrin Tested concentration (μg/mL)	Dihydromyricetin Tested concentration (μg/mL)	Pancreatic lipase inhibition (%)	CI[a]	Fa[b] (%)	CI for Fa	Myricetrin Calculated concentration (μg/mL)	Dihydromyricetin Calculated concentration (μg/mL)
1 : 1	50.0	50.0	28.33 ± 1.69	1.294	25.0	1.426	44.39	44.39
	100.0	100.0	42.39 ± 2.24	1.188	50.0	1.044	128.35	128.35
	150.0	150.0	52.76 ± 0.52	1.064	75.0	0.801	371.17	371.17
	200.0	200.0	60.61 ± 2.82	0.962	85.0	0.700	686.34	686.34
	250.0	250.0	68.32 ± 0.65	0.800	—	—	—	—
1 : 2	33.3	66.6	31.25 ± 2.41	1.034	25.0	1.247	26.52	53.03
	66.7	133.4	47.02 ± 0.53	0.858	50.0	0.778	70.68	141.37
	100.0	200.0	58.40 ± 0.63	0.711	75.0	0.511	188.41	376.83
	133.3	266.6	65.73 ± 1.65	0.636	85.0	0.410	332.36	664.71
	166.7	333.4	74.46 ± 0.41	0.469	—	—	—	—
2 : 1	66.7	33.3	29.50 ± 1.04	1.552	25.0	1.547	62.67	31.33
	133.3	66.7	38.70 ± 1.34	1.447	50.0	1.388	207.40	103.70
	200.0	100.0	46.78 ± 2.09	1.423	75.0	1.291	686.42	343.21
	266.7	133.3	55.93 ± 1.14	1.352	85.0	1.253	1372.44	686.22
	333.3	66.7	60.92 ± 1.23	1.331	—	—	—	—

[a]CI, combination index. CI ≤ 0.90, 0.90 < CI < 1.10, and CI ≥ 1.10 indicate synergistic, additive, and antagonistic effects, respectively; [b]Fa, fraction affected by the combination dose of myricetrin and dihydromyricetin.

compounds were similar, myricetrin formed far more hydrogen bonds than dihydromyricetin, which may explain why myricetrin showed much stronger α-glucosidase inhibition than dihydromyricetin (Figure 1). Both phenolic compounds formed a hydrogen bond with Gln353, suggesting that Gln353 may be one of the amino acid residues that affect α-glucosidase to exert its catalytic reaction. A previous study have reported that phloretin may inhibit α-glucosidase by forming hydrogen bonds with five amino acid residues of α-glucosidase, namely Asp69, Asp215, Arg442, Gln353, and Asn350 [23]. Moreover, it is found that gallocatechin gallate can form a hydrogen bond with Arg315 to exert their inhibitory effect on α-glucosidase [24]. In the present work, myricetrin was also found to form hydrogen bonds with Asp69, Arg315, and Gln353, and dihydromyricetin was observed to form hydrogen bonds with Asp215, Asn350, and Gln353. Besides hydrogen bonds, these two phenolic compounds were also found to form hydrophobic interactions with several amino acid residuals of α-glucosidase (Table 3, Figures 3(d) and 3(h)). Many previous studies have pointed out that the hydrophobic interaction may play a critical role in the enzymatic inhibition of some inhibitors [25, 26].

As for the molecular docking analysis of pancreatic lipase (Table 4 and Figure 4), the *C*-scores of the myricetrin and dihydromyricetin were 5 and 4, respectively, indicating that the docking results were reliable. And the *T*-scores of myricetrin and dihydromyricetin were 3.7803 and 3.8534,

Table 3: Docking parameters, hydrogen bonds, and hydrophobic interactions observed between flavonoids and α-glucosidase from molecular docking simulation analysis.

	Myricetrin	Dihydromyricetin
C-score	4	4
T-score	4.1619	4.6978
PMF-score	−192.4817	−126.1538
CHEM-score	−32.1584	−23.1931
G-score	−306.987	−162.9552
D-sore	−212.4343	−165.0354
Number of hydrogen interactions	9	3
Amino acid residues involved in hydrogen bonds	Arg315, Gln353, Asp352, Arg213, Asp69, Tyr158, Asn415	Asp215, Asn350, Gln353
H-bond donor	Arg315, Gln353, Asn415, Arg213, Asp69	Asn350, Gln353
H-bond receptor	Asp352, Tyr158	Asp215
Average distance (Å)	2.1720	2.0623
Number of hydrophobic interactions	9	10
Amino acid residues involved in hydrophobic interactions	Asp307, Arg315, Phe159, Tyr158, Glu411, Phe178, Tyr72, Arg442, Phe303	Phe303, Gln353, Asp215, Tyr158, Phe178, Glu277, His112, Tyr72, Val216, Asp352

Table 4: Docking parameters, hydrogen bonds, and hydrophobic interactions observed between flavonoids and pancreatic lipase from molecular docking simulation analysis.

	Myricetrin	Dihydromyricetin
C-score	5	4
T-score	3.7803	3.9067
PMF-score	−105.3467	−79.0799
CHEM-score	−26.5111	−24.1416
G-score	−231.122	−171.9494
D-sore	−164.596	−131.2446
Number of hydrogen interactions	3	3
Amino acid residues involved in hydrogen bonds	Gly77, Asp80, Phe216	Gly77, Asp80, Tyr115
H-bond donor	Gly77	Gly77
H-bond receptor	Asp80, Phe216	Asp80, Tyr115
Average distance (Å)	2.2590	2.3867
Number of hydrophobic interactions	10	10
Amino acid residues involved in hydrophobic interactions	Phe78, Ile79, Asp80, Tyr115, Ser153, Ala179, Pro181, Val260, Ala261, His264	Phe78, Asp80, Tyr115, Ser153, Ala179, Pro181, Phe216, Val260, Ala261, Leu265

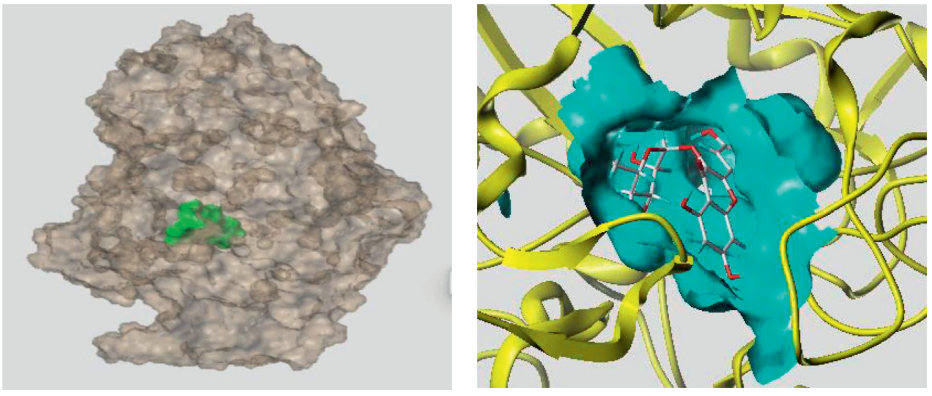

(a) (b)

Figure 3: Continued.

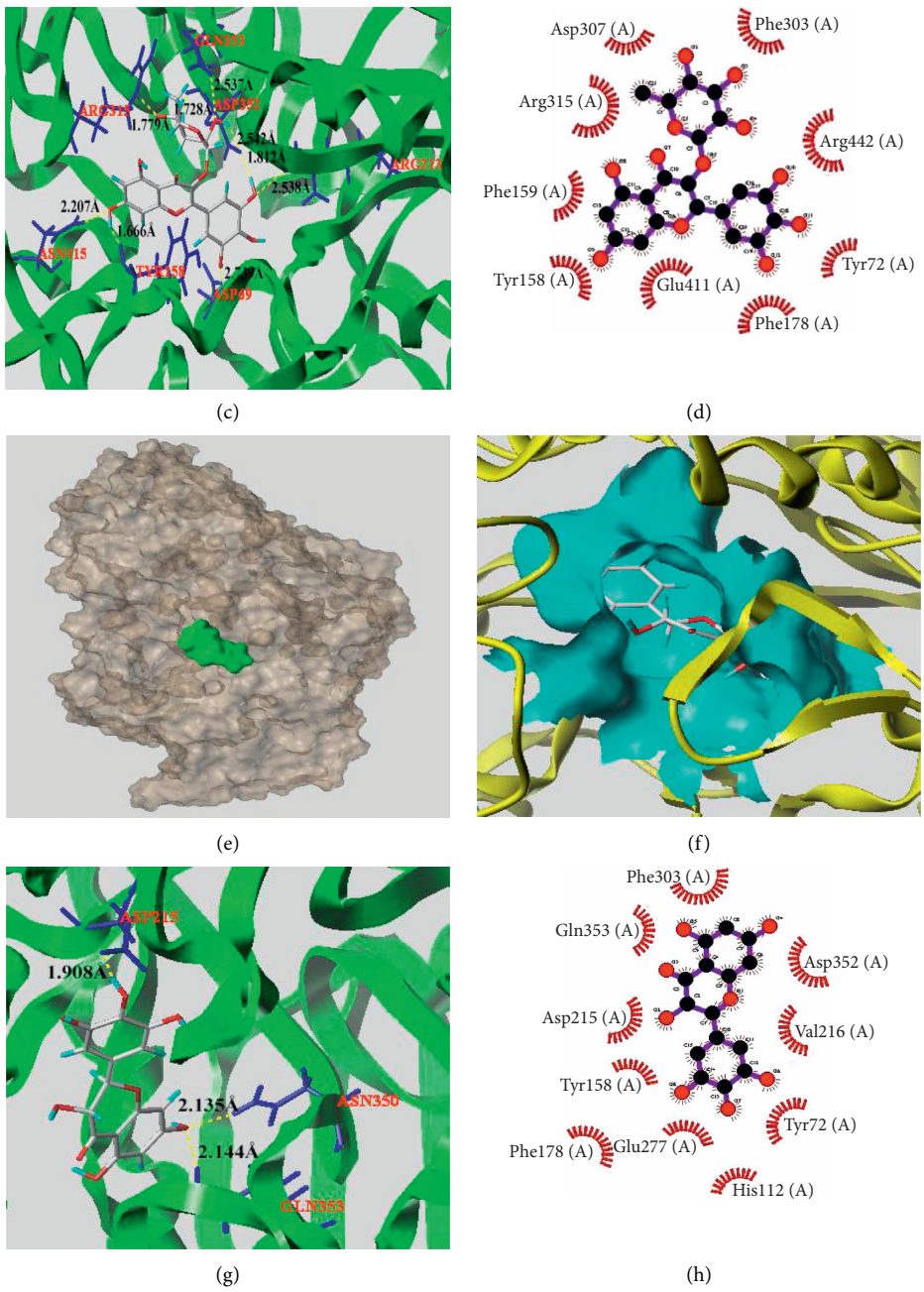

Figure 3: The molecule docking results of myricetrin (a–d) and dihydromyricetin (e–h) with α-glucosidase.

respectively, suggesting that these two phenolic compounds have a similar affinity with pancreatic lipase. As shown in Figure 4(c), myricetrin could form three hydrogen bonds with three amino acid residues, namely Gly77, Phe216, and Asp80, and the longest and shortest distances of hydrogen bonds were 2.360 Å (formed with Asp80) and 2.179 Å (formed with Gly77), respectively, with an average distance of 2.259 Å. Dihydromyricetin also formed three hydrogen bonds with three amino acid residues, namely Gly77, Tyr115, and Asp80, and the longest and shortest distances of hydrogen bonds were 2.396 Å (formed with Asp80) and 2.380 Å (formed with Gly77), respectively, with an average distance of 2.3867 Å. In addition, both of these phenolic compounds also formed ten hydrophobic interactions with ten amino acid residues of pancreatic lipase, and eight of the ten amino acid residues are the same. According to the docking result, it is reasonable to speculate that the difference in pancreatic lipase inhibitory activity between

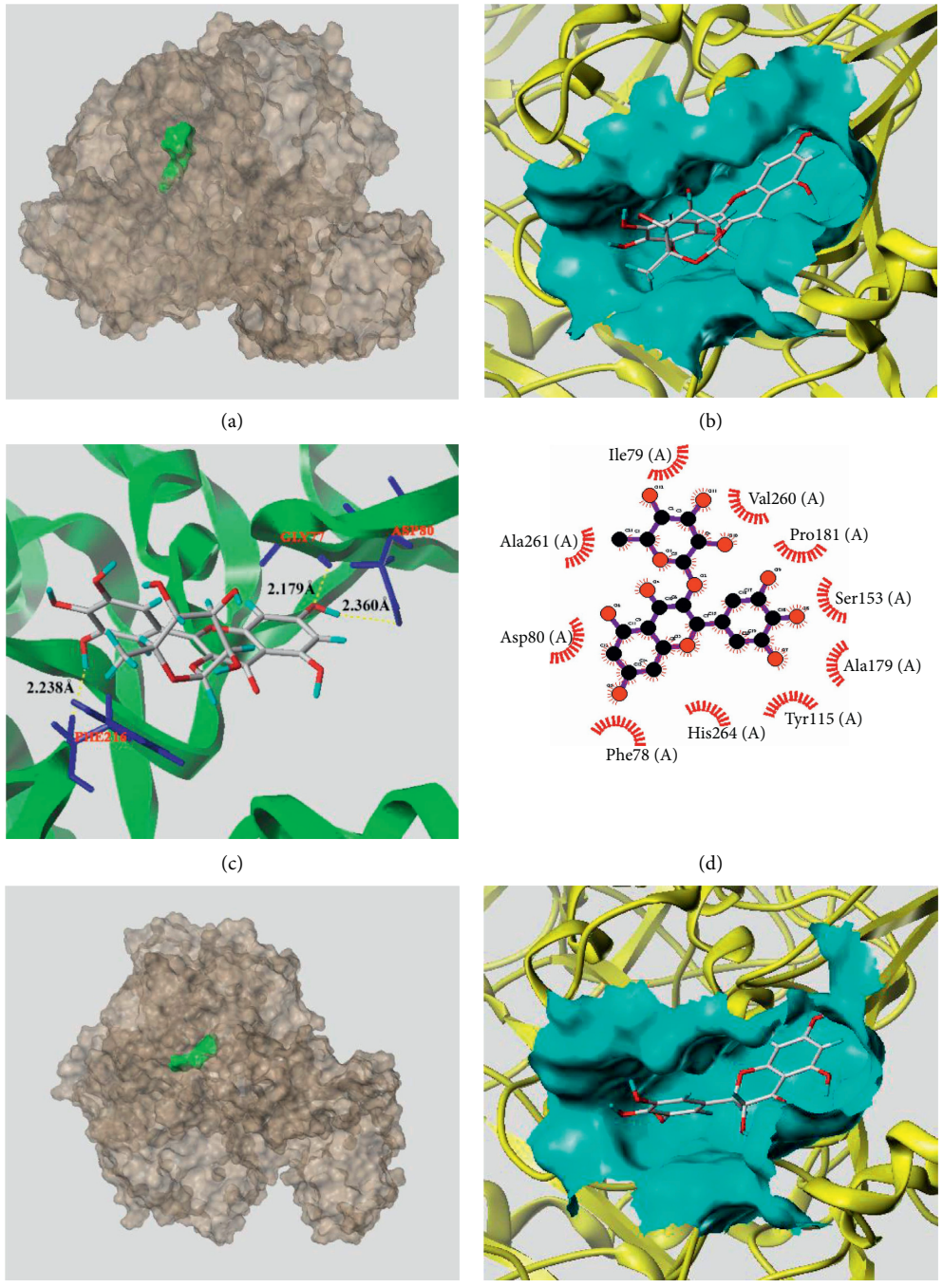

Figure 4: Continued.

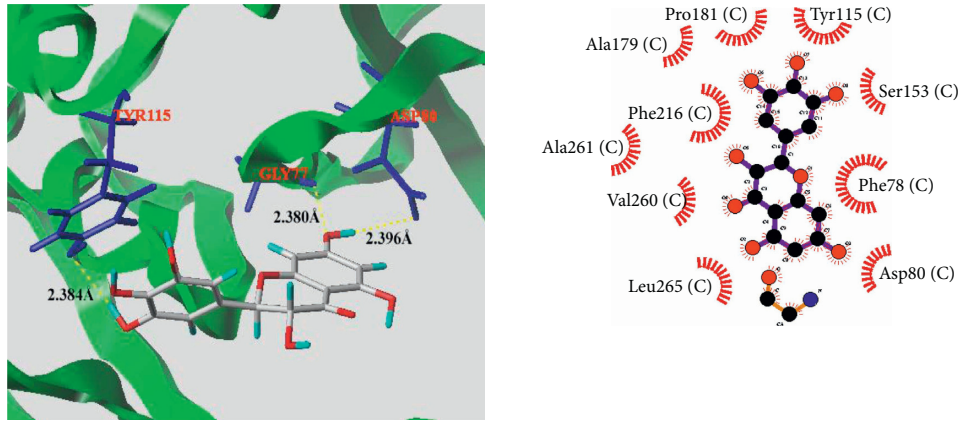

(g) (h)

Figure 4: The molecular docking results of myricetrin (a–d) and dihydromyricetin (e–h) with pancreatic lipase.

myricetrin and dihydromyricetin may be due to the slightly different amino acid residues they interacted with in hydrogen bonds and hydrophobic interactions.

4. Conclusions

In the current study, results showed that both myricetrin and dihydromyricetin exhibited good inhibitory effects toward α-glucosidase and pancreatic lipase in a dose-dependent manner. Myricetrin showed a much stronger α-glucosidase inhibitory effect than dihydromyricetin. However, dihydromyricetin had a better inhibitory activity against pancreatic lipase than myricetrin. Different interaction types existed when myricetrin and dihydromyricetin inhibited α-glucosidase and pancreatic lipase in combination, which were closely dependent on the combination ratio and concentration of these two phenolic compounds. For α-glucosidase inhibition, synergistic effects were observed at relative low concentrations when the combination ratio of myricetrin to dihydromyricetin was set as 1 : 2. However, for pancreatic lipase inhibition, strong synergistic effects were found at relative high concentrations when the combination ratio of myricetrin to dihydromyricetin was set as 1 : 2. In other combination ratios (1 : 1 or 2 : 1), additive and/or antagonistic effects were occurred. Molecular docking results indicated that forming more hydrogen bonds between myricetrin and α-glucosidase may be the reason that myricetrin had a stronger α-glucosidase inhibitory activity than dihydromyricetin. These two phenolic compounds had similar hydrogen bonds and hydrophobic interactions with pancreatic lipase only with a slight difference of interacted amino acid residues. The present study indicated that myricetrin and dihydromyricetin or food materials rich in these two phenolic compounds could be developed as α-glucosidase and/or pancreatic lipase inhibitors to deal with health issues caused by excessive energy intake, and the combination ratio and concentration of these two phenolic compounds should be taken into consideration when producing new functional foods.

Data Availability

All data included in this study are available upon request by contacting the corresponding author.

Conflicts of Interest

There are no conflicts of interest regarding the publication of this article.

Authors' Contributions

Siyuan Mi and Jia Liu contributed equally to this work.

Acknowledgments

This study was financially supported by the Applied Basic Research Project of Yunnan Province (Grant No. 2019FD051), Scientific Research Foundation of Education Department of Yunnan Province (Grant No. 2019J0047), and the Beijing Key Laboratory of the Innovative Development of Functional Staple and the Nutritional Intervention for Chronic Disease.

References

[1] T. Church and C. K. Martin, "The obesity epidemic: a consequence of reduced energy expenditure and the uncoupling of energy intake?" *Obesity*, vol. 26, no. 1, pp. 14–16, 2018.

[2] N. N. El-Agroudy, A. Kurzbach, R. N. Rodionov et al., "Are lifestyle therapies effective for NAFLD treatment?" *Trends in Endocrinology & Metabolism*, vol. 30, no. 10, pp. 701–709, 2019.

[3] S. A. Adefegha, "Functional foods and nutraceuticals as dietary intervention in chronic diseases; novel perspectives for health promotion and disease prevention," *Journal of Dietary Supplements*, vol. 15, no. 6, pp. 977–1009, 2018.

[4] D. Del Rio, A. Rodriguez-Mateos, J. P. E. Spencer, M. Tognolini, G. Borges, and A. Crozier, "Dietary (Poly) phenolics in human health: structures, bioavailability, and evidence of protective effects against chronic diseases,"

Antioxidants & Redox Signaling, vol. 18, no. 14, pp. 1818–1892, 2013.

[5] Y.-J. Kwon, H.-S. Lee, J.-W. Lee et al., "Association of carbohydrate and fat intake with metabolic syndrome," *Clinical Nutrition*, vol. 37, no. 2, pp. 746–751, 2018.

[6] Q. F. Zhou, J. X. Zhou, X. J. Liu et al., "Digestive enzyme inhibition of different phenolic fractions and main phenolic compounds of ultra-high-pressure-treated palm fruits: interaction and molecular docking analyses," *Journal of Food Quality*, vol. 2020, Article ID 8811597, 2020.

[7] Y. Zheng, J. Tian, W. Yang et al., "Inhibition mechanism of ferulic acid against α-amylase and α-glucosidase," *Food Chemistry*, vol. 317, Article ID 126346, 2020.

[8] U. Hossain, A. K. Das, S. Ghosh, and P. C. Sil, "An overview on the role of bioactive α-glucosidase inhibitors in ameliorating diabetic complications," *Food and Chemical Toxicology*, vol. 145, no. 2, Article ID 111738, 2020.

[9] C. Proença, D. Ribeiro, M. Freitas, and E. Fernandes, "Flavonoids as potential agents in the management of type 2 diabetes through the modulation of α-amylase and α-glucosidase activity: a review," *Critical Reviews in Food Science and Nutrition*, pp. 1–71, 2021.

[10] S. Cai, O. Wang, M. Wang et al., "In vitro inhibitory effect on pancreatic lipase activity of subfractions from ethanol extracts of fermented oats (*Avena sativa* L.) and synergistic effect of three phenolic acids," *Journal of Agricultural and Food Chemistry*, vol. 60, no. 29, pp. 7245–7251, 2012.

[11] S. Li, J. Pan, X. Hu, Y. Zhang, D. Gong, and G. Zhang, "Kaempferol inhibits the activity of pancreatic lipase and its synergistic effect with orlistat," *Journal of Functional Foods*, vol. 72, Article ID 104041, 2020.

[12] R. Huang, Y. Zhang, S. Shen et al., "Antioxidant and pancreatic lipase inhibitory effects of flavonoids from different citrus peel extracts: an in vitro study," *Food Chemistry*, vol. 326, Article ID 126785, 2020.

[13] M. J. Rahman, P. Ambigaipalan, and F. Shahidi, "Biological activities of camelina and sophia seeds phenolics: inhibition of LDL oxidation, DNA damage, and pancreatic lipase and α-glucosidase activities," *Journal of Food Science*, vol. 83, no. 3, pp. 237–245, 2018.

[14] J. Gao, B. Liu, Z. Ning, R. Zhao, A. Zhang, and Q. Wu, "Characterization and antioxidant activity of flavonoid-rich extracts from leaves of *Ampelopsis grossedentata*," *Journal of Food Biochemistry*, vol. 33, no. 6, pp. 808–820, 2009.

[15] Y. Chen, E. Wang, Z. Wei, Y. Zheng, R. Yan, and X. Ma, "Phytochemical analysis, cellular antioxidant and α-glucosidase inhibitory activities of various herb plant organs," *Industrial Crops and Products*, vol. 141, Article ID 111771, 2019.

[16] J. Chen, Y. Wu, J. Zou, and K. Gao, "α-Glucosidase inhibition and antihyperglycemic activity of flavonoids from *Ampelopsis grossedentata* and the flavonoid derivatives," *Bioorganic & Medicinal Chemistry*, vol. 24, no. 7, pp. 1488–1494, 2016.

[17] V. Spínola, E. J. Llorent-Martínez, and P. C. Castilho, "Inhibition of α-amylase, α-glucosidase and pancreatic lipase by phenolic compounds of *Rumex maderensis* (*Madeira sorrel*). Influence of simulated gastrointestinal digestion on hyperglycaemia-related damage linked with aldose reductase activity and protein glycation," *LWT*, vol. 118, Article ID 108727, 2020.

[18] Y. Jia, Y. Ma, G. Cheng, Y. Zhang, and S. Cai, "Comparative study of dietary flavonoids with different structures as α-glucosidase inhibitors and insulin sensitizers," *Journal of Agricultural and Food Chemistry*, vol. 67, no. 37, pp. 10521–10533, 2019.

[19] V. Kumar, S. Kumar, and P. Rani, "Pharmacophore modeling and 3D-QSAR studies on flavonoids as α-glucosidase inhibitors," *Der Pharma Chemica*, vol. 2, no. 3, pp. 324–335, 2010.

[20] J. Yang, X. Wang, C. Zhang et al., "Comparative study of inhibition mechanisms of structurally different flavonoid compounds on α-glucosidase and synergistic effect with acarbose," *Food Chemistry*, vol. 347, Article ID 129056, 2021.

[21] Y. F. Li, Y. Q. Chang, J. Deng et al., "Prediction and evaluation of the lipase inhibitory activities of tea polyphenols with 3D-QSAR models," *Scientific Reports*, vol. 6, no. 1, pp. 34387–34414, 2016.

[22] Y. S. Hamed, M. Abdin, A. M. Rayan, H. M. Saleem Akhtar, and X. Zeng, "Synergistic inhibition of isolated flavonoids from *Moringa oleifera* leaf on α-glucosidase activity," *LWT*, vol. 141, Article ID 111081, 2021.

[23] L. Han, C. Fang, R. Zhu, Q. Peng, D. Li, and M. Wang, "Inhibitory effect of phloretin on α-glucosidase: kinetics, interaction mechanism and molecular docking," *International Journal of Biological Macromolecules*, vol. 95, pp. 520–527, 2017.

[24] X. Wu, H. Ding, X. Hu et al., "Exploring inhibitory mechanism of gallocatechin gallate on a-amylase and a-glucosidase relevant to postprandial hyperglycemia," *Journal of Functional Foods*, vol. 48, pp. 200–209, 2018.

[25] M. Taha, F. Rahim, K. Zaman et al., "Synthesis, α-glycosidase inhibitory potential and molecular docking study of benzimidazole derivatives," *Bioorganic Chemistry*, vol. 95, Article ID 103555, 2020.

[26] H. Tang, F. Ma, D. Zhao, and Z. Xue, "Exploring the effect of salvianolic acid C on α-glucosidase: inhibition kinetics, interaction mechanism and molecular modelling methods," *Process Biochemistry*, vol. 78, pp. 178–188, 2019.

Hindawi
Journal of Food Quality
Volume 2021, Article ID 9478133, 12 pages
https://doi.org/10.1155/2021/9478133

Research Article

Preparation of Heat-Sensitivity Proteins from Walnut Meal by Sweep Frequency Ultrasound-Assisted Alkali Extraction

Wenjuan Qu,[1] **Wei Fan**,[2] **Yiting Feng**,[2] **Yunliang Li**,[2] **Haile Ma**,[1] **and Zhongli Pan**[3]

[1]*Institute of Food Physical Processing, Jiangsu University, 301 Xuefu Road, Zhenjiang, Jiangsu 212013, China*
[2]*School of Food and Biological Engineering, Jiangsu University, 301 Xuefu Road, Zhenjiang, Jiangsu 212013, China*
[3]*Department of Biological and Agricultural Engineering, University of California,Davis, One Shield Avenue, Davis, CA 95616, USA*

Correspondence should be addressed to Wenjuan Qu; wqu@ujs.edu.cn

Received 27 May 2021; Accepted 25 June 2021; Published 9 July 2021

Academic Editor: Shengbao Cai

Sweep frequency ultrasound- (SFU-) assisted alkali extraction was conducted to increase the yield and content of heat-sensitive protein of walnut meal under a relatively mild condition. The physicochemical and structural characteristics of the proteins obtained by SFU-assisted alkali extraction and the conventional alkali extraction were compared. It was found that the optimal parameters for the SFU-assisted extraction were the solid-liquid ratio of 1 : 12, pH value of 9, initial temperature of 25°C, ultrasonic frequency of 28 kHz, sweep frequency amplitude of 1.5 kHz, sweep frequency cycle of 100 ms, duty ratio of 77%, and ultrasonic time of 90 min. Under this condition, a vast improvement in the walnut protein yield (34.9%) and the walnut protein content (9.8%) was observed. Such improvement was due to the structural changes of the sonicated protein; e.g., SFU decreased the intermolecular/intramolecular hydrogen bond force of proteins and, therefore, caused more order secondary structures and more loosen microstructures. This helped to improve the thermoplastic and solubility of the heat-sensitivity protein. Thus, SFU treatment could be an effective auxiliary technology in the alkali extraction of heat-sensitivity walnut protein. It might also be a promising technology for the extraction of heat-sensitivity protein from other agricultural by-products.

1. Introduction

The world production of walnut is large, increasing year by year. As a healthy foodstuff, walnuts have gradually aroused extensive attention. It was reported that regular consumption of walnuts could reduce the risk of coronary heart disease [1]. Meanwhile, walnuts can be utilized as ingredients for many foodstuffs such as bakery products to enhance the nutrition value and the sensory properties of the final product [2]. There are a great variety of nutrition ingredients in walnuts including protein, magnesium, copper, folic acid, potassium, fiber, and vitamin E [3].

The main by-product of the walnut oil extraction process is the defatted walnut meal. Most of the walnut meal is used as animal feed, fish meal, fertilizer, or directly discarded, which could result in a waste of resources [4, 5]. It was reported that walnut meal contains 52.5% protein [6, 7]. With the development of textured protein (such as extruded artificial meat), the demand for low-temperature extracted protein with good thermoplastic, solubility, and foaming properties has been increased. Thus, a walnut protein with a low degree of denaturation (good thermoplasticity) was of great value. However, the protein ingredient in a walnut meal has not been well used in food processing because of the limited information on its structural and functional properties [8]. The proteins' structural and functional properties correlate to their preparation method. There are many studies on the extraction and structure of plant proteins [9, 10], but the studies of walnut protein mainly focused on the long-time and high-concentration alkali-soluble extraction [11, 12]. Nevertheless, the functional investigation of protein by this method showed some loss of nutritional value, such as the degradation of protein, the potential toxicity, and the formation of lysinoalanine, due to

extreme alkaline conditions. Thus, there is a need to explore a green technology to replace alkali extraction.

Ultrasound-assisted extraction has been widely applied in food, chemical, and biological processes [13, 14]. Essentially, the ultrasonic treatment can further improve the alkali extraction process of protein by reducing the amount of alkali or increasing the yield [15]. Meanwhile, the heat-sensitive compound can be extracted with minimal damage and higher extraction yield through this extraction method [16]. Therefore, the combination of ultrasound and alkaline in the heat-sensitivity protein extraction process (extraction temperature is usually under 60°C) is feasible.

Compared to the conventional ultrasound with a fixed frequency, sweep frequency sonication could generate more cavitation, which could improve the protein gelling properties and protein enzymolysis efficiency [17, 18]. From the acoustic point of view, compared with the fixed frequency ultrasound, sweep frequency ultrasound can produce a more conducive sound field to improve the cavitation effect [19]. However, there is no research report on the extraction of walnut protein by sweep frequency ultrasound (SFU). Therefore, in this research, SFU-assisted extraction was introduced to walnut protein extraction in order to reduce the amount of alkali and improve the yield and content of protein under relatively mild conditions. Correspondingly, we studied the effects of SFU parameters (i.e., ultrasonic frequency, sweep frequency amplitude, sweep frequency cycle, duty ratio, solid-liquid ratio, pH, initial temperature, and ultrasonic time) on the extraction efficiency of walnut protein. Moreover, the changes in protein structure and thermal stability caused by SFU treatment were determined compared to the conventional alkali extraction. The mechanism of SFU-assisted extraction was investigated. This research provides a practical strategy and solid foundation for ultrasonic extraction of heat-sensitivity proteins from agricultural by-products.

2. Materials and Methods

2.1. Materials and Reagents. Walnut meal defatted under a low temperature (<60°C) was obtained from Xi'an Bodaver Biotechnology Co. Ltd (China). Sodium hydroxide (NaOH), hydrochloric acid (HCl), bovine serum albumin (BSA), Folin-phenol reagent, potassium bromide (KBr), and other chemical reagents were purchased from the Sinopharm Chemical Reagent Co. Ltd (China). All reagents used in the experiments were of analytical grade.

2.2. SFU-Assisted Alkali Extraction Process of Walnut Protein. The walnut meal was dissolved to a fixed solid-liquid ratio, and the pH was adjusted to a fixed initial pH by adding 4.0 mol/L NaOH. Then, the sample solution was poured into an ultrasonic bag, sealed, and submerged into the ultrasonic reactor of the SFU equipment with 9 L added water. The SFU equipment (Figure 1) was manufactured by Jiangsu University with upper and lower ultrasonic transducers (total ultrasonic power of 1200 W). The sample solution in the ultrasonic bag was treated under the ultrasonic power intensity of 133.3 W/L at a fixed initial temperature for a fixed ultrasonic time. After SFU extraction, the solution was centrifuged at 5,000 r/min for 15 min by a centrifuge (Feige licensing DL-5-B, Shanghai Anting Scientific Instrument Factory, China), and then, the solution was adjusted to pH 4.5 by using 1.0 mol/L HCl. After standing for 20 min, the solution was centrifuged again and washed until it was neutralized by distilled water. The wet protein precipitate was collected and freeze-dried by using a freeze dryer (FD-8, Beijing Boyikang Laboratory Instrument Co. Ltd, China).

2.3. Optimization of SFU-Assisted Alkali Extraction Parameters. The frequency of SFU treatment was fixed at the center frequency (f kHz) with a sweep frequency amplitude (δ kHz) of $f \pm \delta$ kHz. So, the upper limit of frequency was $f + \delta$ kHz and the lower limit was $f - \delta$ kHz. In this experiment, the ultrasonic working mode was optimized. The working mode parameters include the ultrasonic frequency ($f = 28$, 33, 40, 68 kHz), sweep frequency amplitude ($\delta = 0.0$, 0.5, 1.0, 1.5, 2.0 kHz), sweep frequency cycle (20, 100, 300, 600, and 1000 ms) referring to the time of one periodic fluctuation from $f - \delta$ kHz to $f + \delta$ kHz, and duty ratio (33%, 50%, 77%, and 90%) referring to the percentage of the ultrasonic running time over the total ultrasonic time. The other extraction parameters including solid-liquid ratio (1 : 9, 1 : 12, 1 : 15, 1 : 18, 1 : 21, w/v), initial pH value (7, 8, 9, 10, 11), initial temperature (15, 25, 35, 45, and 55°C), and ultrasonic time (5, 10, 18, 30, 60, 90, 120, and 150 min) were also considered and optimized. The content and yield of walnut protein were set as indices for the optimization of these parameters. Meanwhile, the conventional alkali extraction without ultrasound was conducted under the same conditions as optimal SFU extraction and was selected as the control.

2.4. Determination of Protein Yield and Protein Content. The protein powder was accurately weighed 5 g (m_1), mixed with distilled water until completely dissolved, and then the protein solution was fixed to 500 mL. Then, the protein solution was diluted 20 times, and the protein concentration was determined by the Folin-phenol method [20]. The protein concentration (c, mg/mL) was calculated by the BSA standard equation ($c = 2.094x + 0.60$, $R^2 = 0.997$) based on the absorbance (x). The content and yield of protein were, respectively, calculated using the following equations:

$$\text{protein content}\,(\%) = \frac{c \times v \times n}{m_1 \times 10}, \quad (1)$$

$$\text{protein yield}\,(\%) = \frac{c \times v \times n \times m}{m_1 \times M \times 10}, \quad (2)$$

where n is the dilution time (20); v is the volume of protein solution (500 mL); m_1 is the weight of weighted protein powder (5 g); m is the weight of collected all protein powder (g); M is the weight of input walnut meal (g).

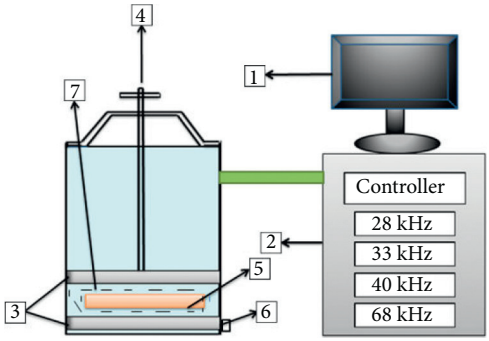

Figure 1: Sweep frequency ultrasound (SFU) equipment schematic diagram (1: computer control system; 2: ultrasonic controller; 3: upper and lower two ultrasonic transducers; 4: height adjusting screw; 5: sample solution in the ultrasonic bag; 6: water outlet; 7: added water).

2.5. Structural and Functional Analysis

2.5.1. Measurement of Fourier Transform-Infrared (FT-IR). The FT-IR spectra of the protein samples extracted with and without ultrasound were scanned by using a Fourier infrared spectrometer (Nicolet is50, Thermo Electron Corporation, America). According to the reported method [21], the ratio of sample to KBr was set at 1 : 100 (w/w). At room temperature ($25 \pm 1^{\circ}C$), the scanning wavenumber spectrum range was 4000~400 cm^{-1}, and the resolution was 4 cm^{-1}.

2.5.2. Measurement of Fluorescence. The fluorescence spectra of the protein samples extracted with and without ultrasound were scanned by using a fluorescence spectrophotometer (Cary Eclipse, Agilent Technologies Co. Ltd, China). Fluorescence was performed according to the method [21], and the method was slightly adjusted. The sample concentration of 0.05 mg/mL was used for determination. The emission spectrum detection was conducted at the excitation wavelength of 340 nm and the emission wavelength of 400~500 nm with a scanning speed of 600 nm/min and a slit width of 5 nm. The conditions of excitation spectrum scanning were as follows: emission wavelength was 430 nm, the excitation wavelength was 300~400 nm, and other conditions were the same as the conditions of emission spectrum scanning.

2.5.3. Measurement of Circular Dichroism (CD). The protein samples extracted with and without ultrasound at a concentration of 1.0 mg/mL were desalted by ultrafiltration (3 kDa) and then rehydrated to the original concentration. The solution was scanned by using a circular dichroism (CD) spectrometer (J-815, JASCO Corporation, Japan) in an N_2 charged environment. The parameters of CD were obtained based on the method reported by Hou et al. [22]. The scanning speed was 50 nm/min, the resolution was 0.1 nm, and the response time was 1 s. The generated data was used to calculate the content of the secondary structure by using analytical CDPro software (IBM Corporation, NY, USA).

2.5.4. Measurement of Scanning Electron Microscope (SEM). The microstructures of the protein samples extracted with and without ultrasound were studied by using a SEM device (S-3400N, HITACHI Corporation, Japan). The sample was glued on the sample table with the double-sided conductive adhesive, and gold was sprayed on the surface of the sample by an ion sputtering apparatus. The sample was placed under SEM (15 kV) to observe the microstructure.

2.5.5. Measurement of Thermal Stability. The thermal stability properties of the protein samples extracted with and without ultrasound were studied by using a synchronous thermal analyzer (STA449F3, NETZSCH Corporation, Germany). According to the reported method [23], the sample was heated from 25°C to 800°C. The heating rate was 10°C/min, and the nitrogen flow rate in the sample chamber was 70 mL/min.

2.6. Statistical Analysis. Each measurement was repeated three times. The data presented in this study was mean ± standard deviation. Results were statistically analyzed to identify differences by using one-way ANOVA and Duncan's test under the significance level of $p < 0.05$ using SPSS 19.0 software (IBM Corporation, NY, USA).

3. Results and Discussion

3.1. Optimization of SFU-Assisted Extraction Parameters

3.1.1. Ultrasonic Frequency. Frequency is an important factor in determining the ultrasonic field characteristics and also a key factor influencing cavitation [24]. The effects of ultrasonic frequency (28, 33, 40, and 68 kHz) on the yield and content of walnut protein were studied, and the data is shown in Figure 2(a). The results revealed that the protein yield and protein content fluctuated significantly with the change of ultrasonic frequencies ($p < 0.05$). The highest protein yield and protein content were observed at 28 kHz, and the lowest values were found at 33 kHz. This indicated that 28 kHz ultrasonic frequency was more conducive to protein extraction. The lowest value at 33 kHz was because of the resonance effect with the protein, which damaged the protein structure. Therefore, the content and yield of protein at 33 kHz were decreased significantly ($p < 0.05$). Raviyan et al. [25] also reported that when the conducted ultrasonic frequency *fa* was close to the resonance frequency *fr* of the system, the ultrasonochemical damage effect of the system reached the maximum. Similarly, Ren et al. [26] reported that 33 kHz ultrasound had the strongest protein damage effect. Apart from the resonant frequency of 33 kHz, the ultrasonic effect at other frequencies (28, 40, and 68 kHz) had a relatively high solubility promoting effect, showing a high protein yield. With the increase of ultrasonic frequency, the effect of protein solubilization became weaken. This may be because a higher frequency of ultrasound is easy to cause protein aggregation, which is not conducive to dissolution. Yang et al. [20] also reported that with the increase of ultrasonic frequency, the damaging effect was more strong.

Similarly, Wang et al. [19] reported that the degradation rate of phenolic acids was increased with the increase of ultrasonic frequency. These results are consistent with our findings where only an appropriate ultrasonic frequency away from the resonance frequency was beneficial to maintain a high dissolution of protein. Thus, the frequency selection of ultrasound treatment was essential for the extraction of protein. Overall, by full consideration of the protein extraction yield, the protein content, and the energy consumption of the ultrasound, it was appropriate to select 28 kHz in this study and applied to the following optimization.

3.1.2. Sweep Frequency Amplitude. The effects of amplitude (0.0, 0.5, 1.0, 1.5, and 2.0 kHz) on the yield and content of walnut protein were studied and the data is shown in Figure 2(b). As the sweep frequency amplitude changed, the protein yield significantly increased from 0.5 kHz to 1.5 kHz and then significantly declined from 1.5 kHz to 2.0 kHz ($p < 0.05$). The protein content showed the same tendency as the protein yield. At the sweep frequency amplitude of 1.5 kHz, both protein yield (14.7%) and protein content (34.7%) reached the highest. It was because, with the increasing sweep frequency amplitude, the ultrasonic cavitation effect gradually increased, and hence, the protein dissolution was accelerated. Wang et al. [19] also reported that sweep frequency ultrasound amplitude indeed affected the strength of cavitation. Therefore, the yield and content of protein were significantly increased by increasing sweep frequency amplitude. However, with the increased sweep frequency amplitude, the number of cavitation bubbles also increased. The destructive effect of ultrasound was more apparent due to the gradual approach of the ultrasonic frequency to the resonant frequency [27]. Thus, the yield and content of protein were decreased by excessive sweep frequency amplitude. Therefore, ultrasound with a moderate sweep frequency amplitude was conducive to accelerate protein dissolution. Furthermore, it was found that the yield and content of protein extracted by the sweep frequency ultrasound were significantly higher than those by the fixed frequency ultrasound (amplitude was 0.0 kHz). It was indicated that sweep frequency ultrasound was more advantageous to improving the effect of protein solubilization than fixed frequency ultrasound, which might be because the ultrasonic cavitation of the sweep frequency ultrasound was stronger than that produced by fixed frequency ultrasound [25]. Similarly, Ren et al. [26] reported that the effect of ultrasonic cavitation of the sweeping model was better than that of the fixed model. Wang et al. [19] also reported that the cavitation of FSFP (flat sweep frequency and pulsed) ultrasound was stronger than that of the fixed frequency ultrasound. Based on the above conclusions, the optimized sweep frequency amplitude of 1.5 kHz was selected and applied to the following optimization.

3.1.3. Sweep Frequency Cycle. The effects of the sweep frequency cycle (20, 100, 300, 600, and 1000 ms) on the yield and content of walnut protein were studied. As can be seen in Figure 2(c), the sweep frequency cycle of 100 ms had a significantly greater impact on the yield and content of protein than those of the other four sweep frequency cycles (20, 300, 600, and 1000 ms) ($p < 0.05$). This was ascribed to the strongest cavitation effect from the sweep frequency cycle of 100 ms. A shorter sweep cycle (<100 ms) means a faster change of sweep frequency, which produces a bigger vibration, weakens the cavitation effect, and therefore shows a lower yield and content of protein. With the increase of sweep frequency cycle (>100 ms), the protein yield and protein content decreased significantly. The lower yield and content of protein at 300~1000 ms might be due to the increased proportion of the resonance area caused by a slower frequency change and enhanced destroying effect of ultrasound. Wang et al. [19] also reported that either too short or too high sweep frequency cycle of ultrasound treatment could result in a large degradation rate of protein. Therefore, a moderate sweep frequency cycle was beneficial to maintain the high yield and content of protein. In this study, 100 ms was selected as the optimized sweep frequency cycle for the following optimization.

3.1.4. Duty Ratio. The effects of duty ratio (33%, 50%, 77%, and 90%) on the yield and content of walnut protein were studied, and the data is shown in Figure 2(d). With the increase in the duty ratio, the yield and content of protein increased significantly, reached the maximum at the duty ratio of 77%, and then significantly decreased ($p < 0.05$). The higher ultrasonic duty ratio represents the stronger cavitation. As the increasing ultrasonic duty ratio, stronger cavitation accelerated the protein dissolution. Lin et al. [28] also reported that the threshold of ultrasound cavitation was positively correlated with pulse duration. In addition, the mechanical shear of ultrasonic treatment at the high duty cycle could promote the disaggregation or dispersion of protein in the aqueous solution and lead to the increased extraction yield of protein [27]. However, a large number of cavitation bubbles generated by too high duty ratio also increased the scattering and refraction of ultrasonic wave, which could lead to the decrease of ultrasonic effect [19]; thus, a reduction was observed in the yield and content of protein at the duty ratio beyond 77%. The observations indicated that duty ratio significantly affected the extraction of protein. Based on the present results, either too low or too high ultrasonic duty ratio was not beneficial to maintain the high extraction performance. Therefore, a moderate ultrasonic duty ratio could be beneficial to maintain the high yield and content of protein. In this study, 77% was selected as the optimized duty ratio and applied to the following optimization.

3.1.5. Solid-Liquid Ratio. The effects of solid-liquid ratio (1 : 9, 1 : 12, 1 : 15, 1 : 18, and 1 : 21) on the yield and content of walnut protein were studied, and the data is shown in Figure 3(a). It showed that the yield of walnut protein increased slightly from 1 : 21 to 1 : 12 and then significantly decreased from 1 : 12 to 1 : 9 ($p < 0.05$). In the experimental range, the yield (11.1%) of walnut protein reached the

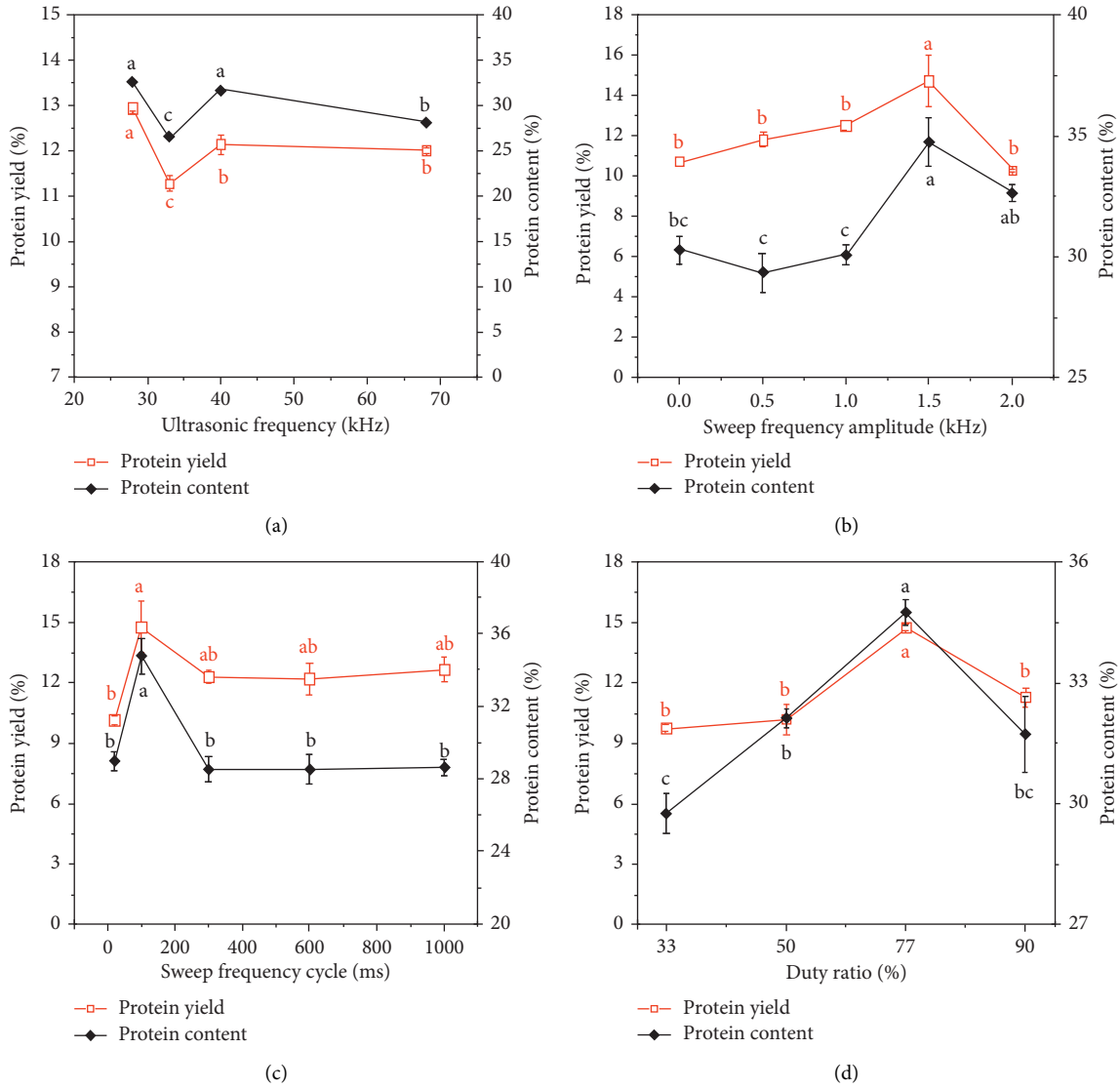

FIGURE 2: Effects of ultrasonic frequency (a), sweep frequency amplitude (b), sweep frequency cycle (c), and duty ratio (d) on the yield and content of walnut protein. The different superscript letters of data under the same line indicate that they are significantly different ($p < 0.05$).

highest at the solid-liquid ratio of 1 : 12. The lower yield at the solid-liquid ratio of 1 : 9 was due to a lower protein proportion in the amount of walnut meal added [29]. With the amount of walnut meal added to increase in a fixed volume of solution (from 1 : 21 to 1 : 12), the protein solubility and the protein yield gradually increased. When the soluble protein reached saturation in a fixed volume of solution, the protein concentration reached the highest at the solid-liquid ratio of 1 : 12 [30]. When the amount of walnut meal added continued to rise (from 1 : 12 to 1 : 9), the amount of soluble protein did not change, resulting in a lower proportion of protein in the amount of walnut meal added and so a decreasing protein yield. The trend of solid-liquid ratio on the protein content was the same as that on the protein yield. The highest protein content (32.6%) was obtained at the solid-liquid ratio of 1 : 12. The content of walnut protein in the extract increased first and then significantly decreased from 1 : 12 to 1 : 9 ($p < 0.05$). Xu et al. [31] also found that the content of soluble leaf protein increased as the ratio of solid to liquid increased, and when the ratio continued to rise, the content of soluble leaf protein decreased. Based on the present results, it was appropriate to select the solid-liquid ratio of 1 : 12 for the following optimization.

3.1.6. pH Value. The effects of pH value (7, 8, 9, 10, and 11) on the yield and content of walnut protein were studied, and the data is shown in Figure 3(b). It showed that the protein yield significantly increased with the increasing pH value ($p < 0.05$). The protein yield increased rapidly within the pH range of 7~9, and then, the growth rate became slow after pH 9. It was obvious that the alkaline environment had a significantly positive solubilization effect on the walnut protein. Stronger alkalinity means better solubility and a higher protein yield. This was because the high concentration of alkaline can result in the breakdown of the hydrogen bond of

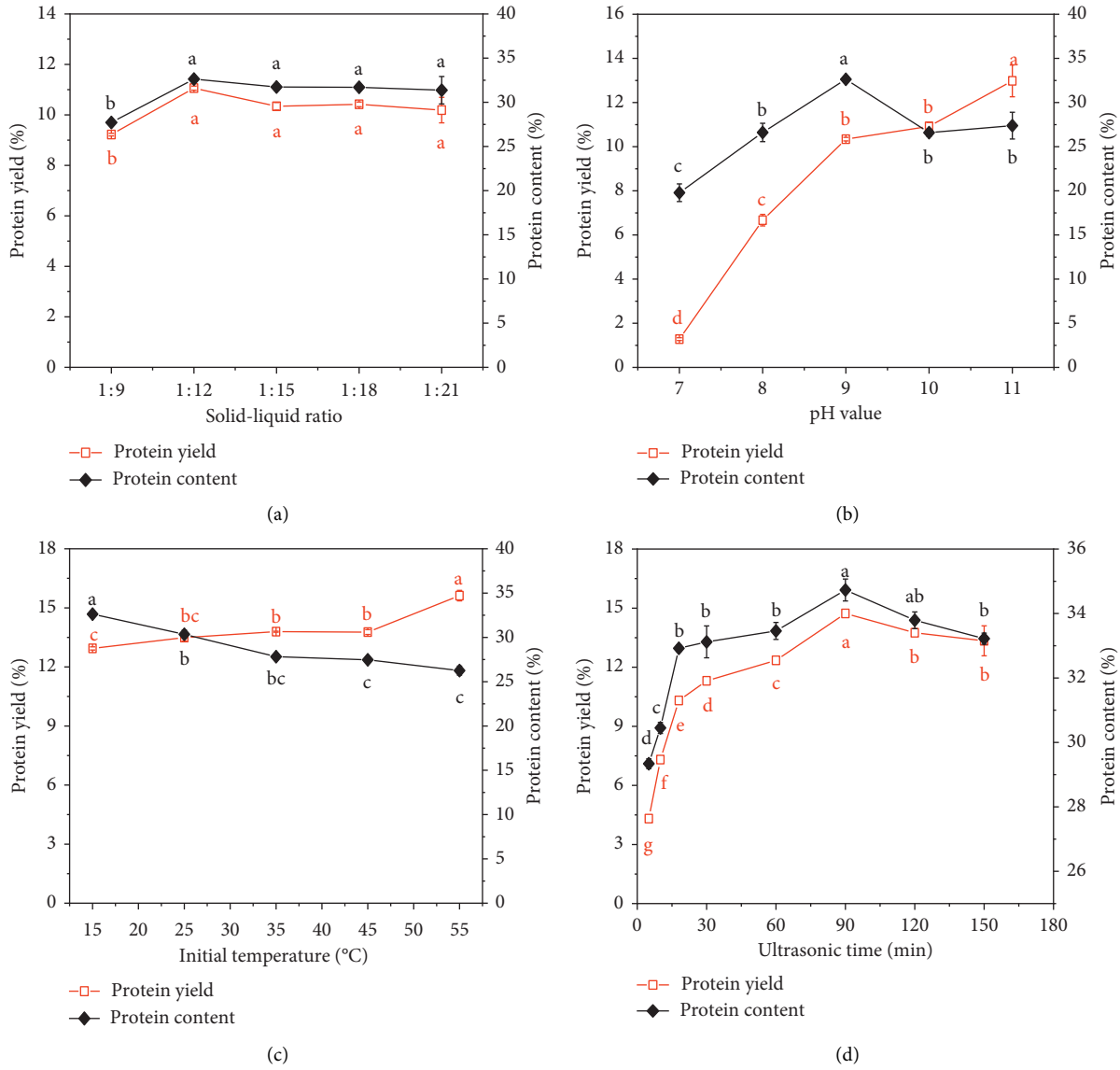

Figure 3: Effects of solid-liquid ratio (a), pH value (b), initial temperature (c), and ultrasonic time (d) on the yield and content of walnut protein. The different superscript letters of data under the same line indicate that they are significantly different ($p < 0.05$).

protein, and the protein-water interactions of protein molecules and its solubility could be enhanced by increasing the alkaline conditions. Guo et al. [32] used 0.1 mol/L NaOH solution for rice protein extraction and achieved a higher protein yield (55%). Lu et al. [33] used a 0.3 mol/L NaOH solution to extract protein from green tea and extracted a high content of protein (82%). Ding et al. [34] used one method based on alkaline extraction for extracting protein from *Camellia oleifera* seed meal and obtained a high protein yield of 57.8% at a high alkaline condition.

The content of walnut protein significantly increased from pH 7 to 9 and then significantly decreased after pH 9 ($p < 0.05$). Jain and Anal [35] reported a similar trend that protein content initially increased as pH increased. When the pH value was greater than 8, it was observed that the content followed a decreasing trend. The decreased protein content as pH increased may be due to a decrease in the proportion of the dissolved protein in the lye soluble substance as the pH continued to rise. It was reported that higher alkaline extraction can increase the brownish appearance and unpleasant bitterness [36]. In addition, exposing the protein to extreme alkaline conditions might cause the degradation of proteins and potential toxicity, such as the formation of lysinoalanine, resulting in the loss of nutritional value [37]. On the contrary, SFU-assisted alkali extraction can reduce the use of alkali and the production of harmful substances. By considering the protein content, protein yield, and product quality, pH 9 was more appropriate and applied to the following optimization.

3.1.7. Initial Temperature. The effects of initial temperature (15, 25, 35, 45, and 55°C) on the yield and content of walnut protein were studied, and the data is shown in Figure 3(c).

From the view of protein yield, it was in a slow rise phase from 15°C to 45°C and then significantly increased from 45°C to 55°C ($p < 0.05$). This was because the temperature had a positive effect on the dissolution and extraction of protein. Shewry and Miflin [38] found a similar phenomenon of the significant influence of temperature in the extraction of crude protein from *Termitomyces albuminosus*. With the increase in temperature, the ultrasonic cavitation effect also increased due to the decreasing of cavitation threshold caused by increased temperature except for the thermal effect. Because of the combination of temperature and ultrasound, the protein yield was increased significantly. However, the protein content decreased significantly with the increase in temperature ($p < 0.05$). This may be due to the decreasing proportion of the dissolved protein in the lye soluble substance. Moreover, it was reported that high temperature and high ultrasonic cavitation could change the structure of the protein and cause protein aggregation and degradation and thus affected the protein content. Consequently, the high ultrasonic temperature was not always recommended. Therefore, by full consideration of the yield and content, as well as the energy consumption of temperature, 25°C was chosen as the appropriate initial temperature and applied to the following optimization.

3.1.8. Ultrasonic Time. The effects of ultrasonic time (5, 10, 18, 30, 60, 90, 120, and 150 min) on the yield and content of walnut protein were studied. The results are plotted in Figure 3(d). With the prolongation of the ultrasonic time, the protein yield rapidly increased within 5~18 min, then slowly increased (18~90 min), and finally decreased (90~150 min). The protein yield reached the maximum (14.7%) at the ultrasonic time of 90 min. With the increased ultrasonic time, the cavitation effect correspondingly increased [39], which promoted the dissolution of protein in solution and eased the extraction. This led to an increase in protein yield. The decline of protein yield at later extraction time may be due to the stronger thermal effect produced by ultrasonic treatment for a longer ultrasonic time. With the temperature further increased, the decomposition or aggregation of protein occurred. Xu et al. [31] found a similar trend of soluble leaf protein yield that initially increased with ultrasonic time and then decreased. Similarly, Sun et al. [40] studied that the yield of polysaccharides from the fruit of *Camptotheca acuminata* was increased steadily and then decreased with the extended extraction time. The changing trend of protein content was the same as that of yield. The protein content reached the maximum (34.7%) at the ultrasonic time of 90 min. After the ultrasonic time of 90 min, the protein content slowly decreased, which was due to a relative decreasing proportion of the dissolved protein in the lye soluble substance caused by the decomposition of proteins. Therefore, the ultrasonic time of 90 min was chosen as the appropriate treatment time.

Through the screening of processing parameters, the SFU extraction condition of walnut protein was optimized. Under the solid-liquid ratio of 1 : 12, pH value of 9, the initial temperature of 25°C, ultrasonic frequency of 28 kHz, sweep frequency amplitude of 1.5 kHz, sweep frequency cycle of 100 ms, the duty ratio of 77%, and ultrasonic time of 90 min, the walnut protein yield (14.7%) and the walnut protein content (34.7%) were increased by 34.9% and 9.8%, compared to conventional alkali extraction (10.9% and 31.6%). Therefore, SFU treatment could be used as an effective auxiliary technology in the alkali extraction of heat-sensitivity walnut protein.

3.2. Structural Analysis

3.2.1. FT-IR Analysis. The functional groups of walnut proteins extracted with and without ultrasound were analyzed by FT-IR (Figure 4). It was reported that the peak at 1700~1600 cm^{-1} corresponds to amide I vibration, the peak at 1600~1500 cm^{-1} corresponds to amide II vibration, and the peak at 1046~1047 cm^{-1} corresponds to stretching vibration of C-N covalent bond [41]. The results showed that single alkali and SFU extracted proteins both had absorption peaks at 3419.8 and 3377.4 cm^{-1}, which corresponded to the O-H stretching vibration. Compared to the protein prepared by the single alkali extraction, the absorption peak of SFU-assisted extracted protein showed an obvious shift to lower wavenumber (3377.4 cm^{-1}). When the intermolecular or intramolecular hydrogen bonding is strengthened, the absorption peak will move to a high wavenumber [42]. This indicated that the intermolecular/intramolecular hydrogen bond force was decreased by ultrasonic treatment compared to the single alkali extraction method. Qu et al. [43] found the same phenomenon in the ultrasonic treatment of rapeseed protein isolate-dextran conjugates. The weakening of hydrogen bond force indicated that the protein structure is looser and more soluble in an aqueous solution, which helps to improve the protein solubility. Compared to the protein prepared by the single alkali extraction, the absorption peaks at other wavenumbers did not change significantly ($p > 0.05$). Based on the present results, it was concluded that ultrasound changed the protein structure and decreased the intermolecular/intramolecular hydrogen bond binding of the protein. These structural changes were more conducive to the improvement of protein solubility, which could well explain the increases in the protein yield and protein content during SFU extraction (described in Section 3.1).

3.2.2. Fluorescence Analysis. The tertiary structures of walnut proteins extracted with and without ultrasound were analyzed by fluorescence (Figure 5). The residues of aromatic amino acids such as Trp, Tyr, and Phe can be excited by excitation light to produce fluorescence [44], which can be used to characterize the conformational changes of the tertiary structure of proteins. In this study, the maximum fluorescence emission (Figure 5(a)) and fluorescence excitation peaks (Figure 5(b)) of proteins extracted without and with ultrasound were located at 430~432 nm and 340~341 nm, respectively. Despite no change in the peak position, the intensities of fluorescence emission and excitation of protein were significantly reduced by ultrasonic

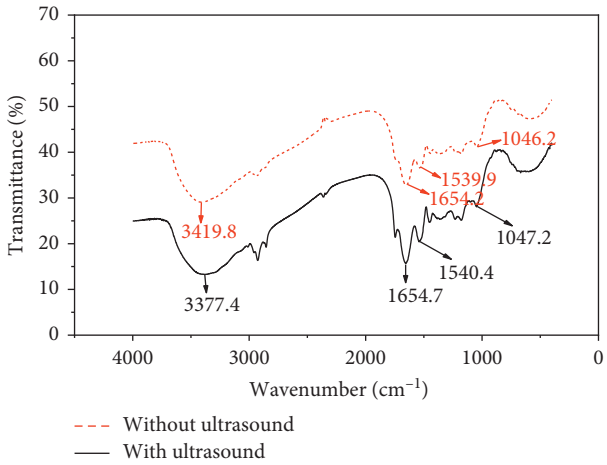

Figure 4: FT-IR spectra of walnut proteins extracted with and without ultrasound.

treatment. This phenomenon indicated that ultrasonic treatment changed the tertiary structure of protein and reduced the fluorescence intensity of the protein. The reason may be that ultrasonic cavitation reduced the amount of exposed chromophore, thus resulting in the decrease of protein fluorescence intensity [45]. Similarly, Zhang et al. [46] studied the influence of ultrasonic treatment on peanut protein isolate and found that sonication did not induce the shift of the wavelength of fluorescence emission peak but weakened the fluorescence intensity. In conclusion, the changes in fluorescence properties further proved that the SFU-assisted extraction altered the tertiary structure of proteins.

3.2.3. CD Analysis. CD is a rapid, simple, and accurate method for the detection of protein conformation. The CD spectrum can reflect the information of the secondary structure of proteins or polypeptide chains at the far UV range [47]. In the secondary structure, the α-helix and β-sheet represent the order state of protein molecules, while the β-turn and random coil reflect the looseness of protein molecules. The results in Figure 6 showed that the proteins extracted without and with ultrasound had obvious negative absorption peaks at 210 nm and 209 nm, respectively. According to the analysis of CDPro software, the secondary structure contents of walnut proteins were calculated, and the data is listed in Table 1. It can be seen that the β-sheet contents of walnut proteins extracted with and without ultrasound both were high (53.0%~54.4%), indicating that the structure of the walnut protein was stable. In addition, the contents of α-helix and random coil in the two samples changed significantly ($p > 0.05$), indicating that ultrasonic treatment had a significant effect on the secondary structure of the walnut protein. The content of α-helix of protein extracted with ultrasound significantly increased by 42.2% and the content of random coil significantly decreased by 16.7% ($p > 0.05$). The increase of α-helix and the decrease of random coil indicated that the molecular structure of sonicated walnut protein became more order. Jiang et al. [45] also observed small changes in the secondary structure of black soybean protein with ultrasound. Stathopulos et al. [48] reported an increase of β-sheet but a decrease in the protein aggregates following ultrasonic treatment. Vivian and Callis [49] found that there was an increase of α-helix but a reduction in β-sheet with whey protein concentrate after ultrasonic treatment. The contradictory results probably attributed to the difference in protein types and test conditions. Based on the present results, in addition to affecting the tertiary structure of the walnut protein by fluorescence spectroscopic analysis (described in Section 3.2.2), the secondary structure of the walnut protein was significantly affected by ultrasonic treatment and became more order.

3.2.4. SEM Analysis. The microstructures of walnut proteins extracted with and without ultrasound were analyzed by SEM (Figure 7). A significant difference was observed for the microstructures of the walnut proteins extracted without and with ultrasound. Figure 7(a) showed that the walnut protein without ultrasonic treatment was compact, presenting a relatively flat surface, while the microstructure of walnut protein with ultrasonic treatment shown in Figure 7(b) presented a loose structure, and the texture became porous and incompact. Qu et al. [43] also found that the surface structures of rapeseed protein isolate- (RPI-) dextran conjugates by ultrasonic treatment were more incompact and porous than RPI without ultrasound. Similarly, Zhao et al. [50] reported that the bulk density of the ultrasound-treated protein (loose structure) was smaller than that of the sample without ultrasound (compact structure), which helps to improve the solubility of the protein. It was concluded that ultrasonic treatment could improve the protein solubility by making the protein structure loose, which could well explain the increases in yield and content of protein during SFU-assisted extraction (described in Section 3.1).

3.3. Thermal Stability Analysis. Thermogravimetric analysis (TGA) can be used to analyze the pyrolysis rate of protein in different temperature environments [51]. Thermal stability properties were analyzed on walnut proteins extracted with and without ultrasound, and the results are shown in Figure 8. Regardless of the control or sonicated protein, the TGA (Figure 8(a)) and DTG curves (Figure 8(b)) showed that the two walnut proteins had a certain amount of weight loss in the first stage (0~150°C). The weight loss at this phase mainly was related to free water evaporation in protein structure. The weight loss rates of the two groups at this stage were similar, and they reached the maximum at 79°C. The second stage showed the rapid decomposition of protein (150~369°C). At about 150°C, the protein began to rapidly decompose, and most of the protein was rapidly decomposed by a high temperature at this stage [52]. The decomposition of protein was related to the noncovalent bonds including intermolecular and intramolecular hydrogen bonds, electrostatic interactions, and hydrophobic interactions. Except for noncovalent bonds, the covalent bonds in

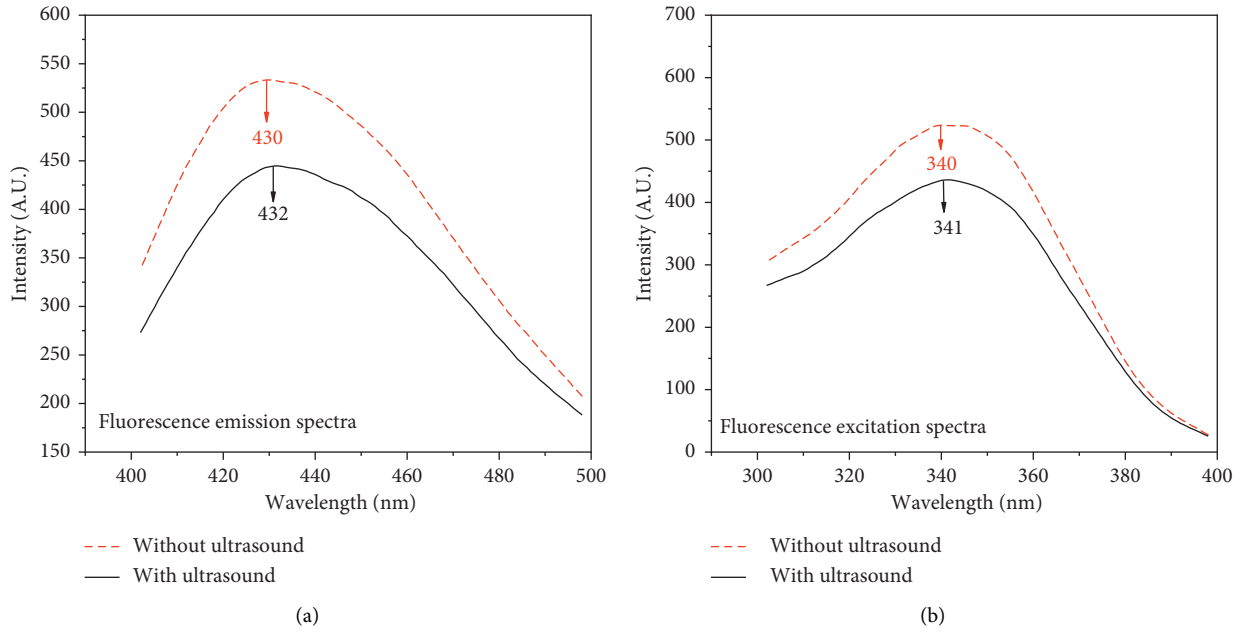

Figure 5: Fluorescence emission spectra (a) and excitation spectra (b) of walnut proteins extracted with and without ultrasound.

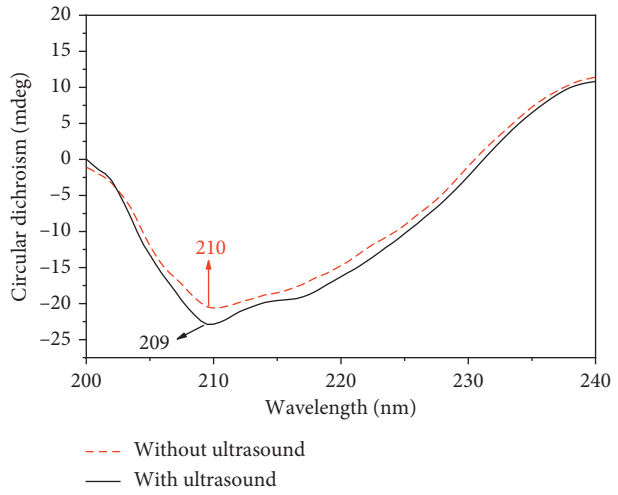

Figure 6: CD spectra of walnut proteins extracted with and without ultrasound.

Table 1: Secondary structures of walnut proteins extracted with and without ultrasound.

Sample	α-helix (%)	β-sheet (%)	β-turn (%)	Random coil (%)
Without ultrasound	4.5 ± 0.06^{b}	53.0 ± 0.23^{a}	18.6 ± 0.12^{a}	23.9 ± 0.28^{a}
With ultrasound	6.4 ± 0.04^{a} (↑42.2)*	54.4 ± 0.26^{a} (↑2.6)	19.3 ± 0.14^{a} (↑3.8)	19.9 ± 0.17^{b} (↓16.7)

The different superscript letters of data under the same column indicate that they are significantly different ($p < 0.05$). * The values in parenthesis are the change percentage points of secondary structure content in walnut protein with ultrasound compared to that without ultrasound.

the amino acid composition, such as C-N, C(O)-NH, and C(O)-NH_2, may be broken by a high temperature. The significant differences were observed in pyrolysis temperature between the walnut proteins extracted with ultrasound and without ultrasound. The maximum decomposition temperature of walnut protein extracted without ultrasound was 306°C, and the maximum decomposition rate was −0.369%/°C. However, the walnut protein extracted with ultrasound showed the lower decomposition rates at 319°C and 369°C, corresponding to the decomposition rates of −0.342%/°C and −0.336%/°C, respectively. This indicated that the SFU-assisted extraction obtained from walnut protein was more heat resistant. The third stage was the slower phase of mass loss in the range of 369~600°C. The loss of weight at this stage was due to the oxidative decomposition of small molecules. Combined with the structural

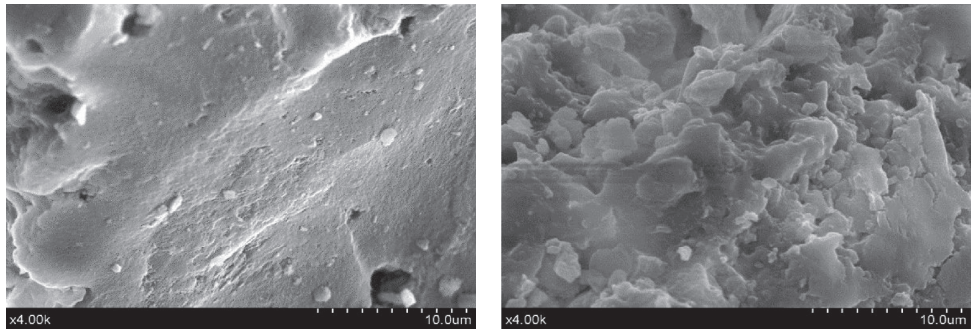

(a) (b)

Figure 7: SEM photos of walnut proteins extracted without ultrasound (a) and with ultrasound (b).

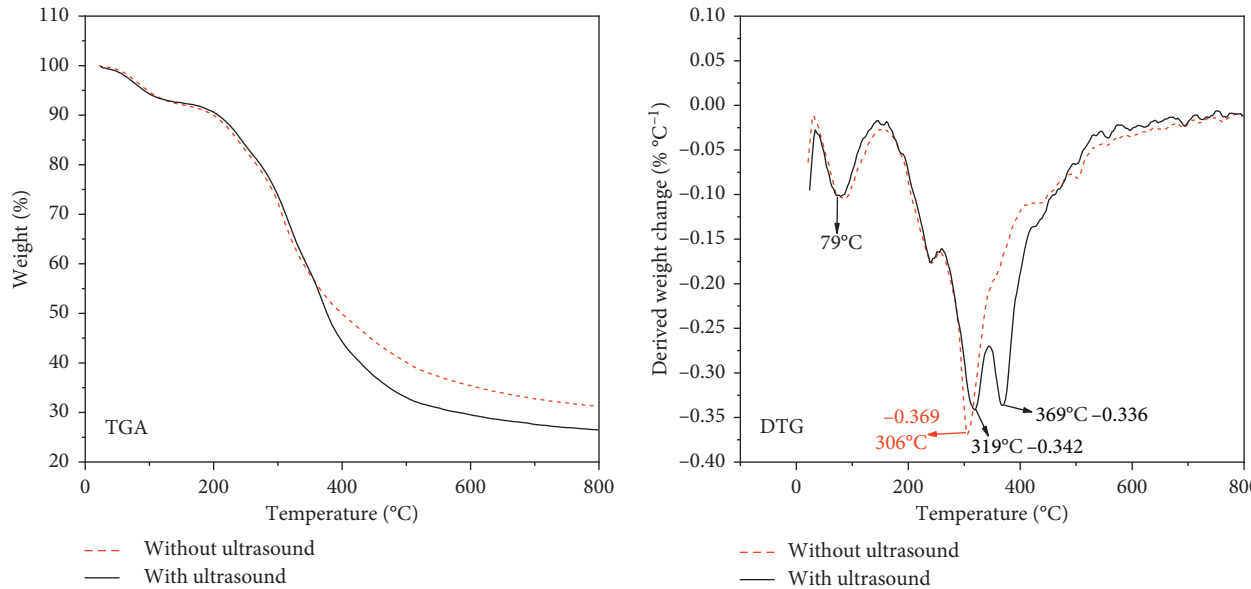

(a) (b)

Figure 8: Thermal stability TGA (a) and DTG (b) of walnut proteins extracted with and without ultrasound.

changes (described in Section 3.2), it was concluded that the thermal stability of heat-sensitivity walnut protein was increased by ultrasonic treatment.

4. Conclusions and Future Work

This study indicated that sweep frequency ultrasound (SFU) could be used as an effective auxiliary technology of alkali extraction of heat-sensitivity walnut protein to enhance its yield and content. Compared to the conventional alkali extraction (10.9% and 31.6%), SFU-assisted extraction significantly increased the yield and content of protein by 34.9% and 9.8%, respectively, at the optimum parameters as follows: solid-liquid ratio of 1 : 12, pH of 9, the initial temperature of 25°C, ultrasonic frequency of 28 kHz, sweep frequency amplitude of 1.5 kHz, sweep frequency cycle of 100 ms, duty ratio of 77%, and ultrasonic time of 90 min. This improvement was due to the structural changes of the sonicated protein including the decreased intermolecular/intramolecular hydrogen bond binding of protein, weakened fluorescence intensity, more order secondary structure, and more loosen microstructure, which could improve the thermoplastic and solubility of the heat-sensitivity walnut protein. Therefore, SFU treatment is an effective auxiliary technology in the alkali extraction of heat-sensitivity walnut protein. However, the biofunctions of the walnut meal protein were not investigated. Further studies on the functional characteristics of such high-valued protein will help to build the extraction criteria of the walnut meal. It will also facilitate the application of ultrasound in bioactive ingredients extraction from industrial and agricultural by-products.

Data Availability

The data supporting the results of this study are available within the paper or are available from the corresponding author upon reasonable request.

Conflicts of Interest

The authors declare that they have no conflicts of interest.

Acknowledgments

The authors wish to extend their appreciation to the National Natural Science Foundation-China (31872892), National Key Research and Development Program of China-Intergovernmental Key Program for International Science and Technology Innovation Cooperation (2017YFE0105300), and "Six Talents Peak" High-Level Talent Program of Jiangsu Province (NY-010).

References

[1] H. C. Huang, Z. F. Jiang, and H. J. Zhu, "The methods of protein conformation predicted by UV-circular dichroism," *Chemistry*, vol. 70, no. 7, pp. 501–506, 2007.

[2] X. N. Wang, L. J. Lin, and F. J. Wang, "Optimization of fermentation conditions for preparing walnut soy sauce," *Science and Technology of Food Industry*, vol. 35, no. 5, pp. 209–212, 2014.

[3] H. J. Xu, Y. B. Hao, J. X. Qi, G. S. Fan, and K. J. Wang, "Study on antioxidant activity and antihypertensive activity of enzymatic hydrolysis products of walnut protein," *Innovational Edition of Farm Products Processing*, vol. 10, pp. 38–42, 2009.

[4] X.-Y. Mao and Y.-F. Hua, "Chemical composition, molecular weight distribution, secondary structure and effect of NaCl on functional properties of walnut (*Juglans regia* L) protein isolates and concentrates," *Journal of Food Science and Technology*, vol. 51, no. 8, pp. 1473–1482, 2014.

[5] K. W. C. Szemilao and S. K. Sathe, "Walnuts (*Juglans regia* L): proximate composition, protein solubility, protein amino acid composition and protein in vitro digestibility," *Journal of the Science of Food & Agriculture*, vol. 80, pp. 1393–1401, 2000.

[6] R. Geng, W. Lu, and M. K. Wang, "The research status of walnut quality and process technology," *Farm Products Processing*, vol. 5, pp. 69–72, 2015.

[7] L. Jiang, H. D. Xu, Y. J. He, and Z. F. Hu, "Study on extraction of walnut cake protein and its functional," *Food Science and Technology*, vol. 4, pp. 237–240, 2007.

[8] S. Cofrades, A. Serrano, J. Ayo, J. Carballo, and F. Jiménez-Colmenero, "Characteristics of meat batters with added native and preheated defatted walnut," *Food Chemistry*, vol. 107, no. 4, pp. 1506–1514, 2008.

[9] R. Toews and N. Wang, "Physicochemical and functional properties of protein concentrates from pulses," *Food Research International*, vol. 52, no. 2, pp. 445–451, 2013.

[10] Q. Zhao, C. Selomulya, H. Xiong et al., "Comparison of functional and structural properties of native and industrial process-modified proteins from long-grain indica rice," *Journal of Cereal Science*, vol. 56, no. 3, pp. 568–575, 2012.

[11] F. Y. Fan, Y. P. Wang, Y. J. Ma, Y. C. Xu, and Y. J. Yang, "Study on protein extraction process from walnut," *Academic Periodical of Farm Products Processing*, vol. 5, pp. 13–15+19, 2010.

[12] N. Chen, H. Yang, Y. Sun, J. Niu, and S. Liu, "Purification and identification of antioxidant peptides from walnut (*Juglans regia* L.) protein hydrolysates," *Peptides*, vol. 38, no. 2, pp. 344–349, 2012.

[13] R. Velmurugan and K. Muthukumar, "Ultrasound-assisted alkaline pretreatment of sugarcane bagasse for fermentable sugar production: optimization through response surface methodology," *Bioresource Technology*, vol. 112, pp. 293–299, 2012.

[14] P. B. Subhedar and P. R. Gogate, "Alkaline and ultrasound assisted alkaline pretreatment for intensification of delignification process from sustainable raw-material," *Ultrasonics Sonochemistry*, vol. 21, no. 1, pp. 216–225, 2014.

[15] P. Filson and B. Dawsonandoh, "Sono-chemical preparation of cellulose nanocrystals from lignocellulose derived materials," *Bioresource Technology*, vol. 100, no. 7, pp. 2259–2264, 2009.

[16] A. Szydłowska-Czerniak, A. Tułodziecka, G. Karlovits, and E. Szlyk, "Optimisation of ultrasound-assisted extraction of natural antioxidants from mustard seed cultivars," *Journal of the Science of Food & Agriculture*, vol. 95, no. 7, pp. 1445–1453, 2015.

[17] W. Qu, H. Ma, J. Jia, R. He, L. Luo, and Z. Pan, "Enzymolysis kinetics and activities of ace inhibitory peptides from wheat germ protein prepared with SFP ultrasound-assisted processing," *Ultrasonics Sonochemistry*, vol. 19, no. 5, pp. 1021–1026, 2012.

[18] Y. Y. Wang, J. K. Yan, Y. H. Ding, M. T. Rashid, and H. L. Ma, "Effect of sweep frequency ultrasound and fixed frequency ultrasound thawing on gelling properties of myofibrillar protein from quick-frozen small yellow croaker and its possible mechanisms," *LWT-Food Science and Technology*, vol. 150, p. 111922, 2021.

[19] J. Wang, H. Ma, Z. Pan, and W. Qu, "Sonochemical effect of flat sweep frequency and pulsed ultrasound (FSFP) treatment on stability of phenolic acids in a model system," *Ultrasonics Sonochemistry*, vol. 39, pp. 707–715, 2017.

[20] H. Yang, W. Sheng, X. X. Zhang et al., "Effect of different ultrasonic treatment time on the physicochemical properties and structure of chicken blood plasma protein," *Jiangsu Agricultural Sciences*, vol. 47, no. 24, pp. 177–182, 2014.

[21] C. Yan and Z. Zhou, "Solubility and emulsifying properties of phosphorylated walnut protein isolate extracted by sodium trimetaphosphate," *LWT*, vol. 143, p. 111117, 2021.

[22] F. R. Hou, W. H. Ding, W. J. Qu et al., "Alkali solution extraction of rice residue protein isolates: influence of alkali concentration on protein functional, structural properties and lysinoalanine formation," *Food Chemistry*, vol. 218, pp. 207–215, 2018.

[23] W. Qu, X. Zhang, X. Han, Z. Wang, R. He, and H. Ma, "Structure and functional characteristics of rapeseed protein isolate-dextran conjugates," *Food Hydrocolloids*, vol. 82, pp. 329–337, 2018.

[24] L. Zhang, C. Zhou, B. Wang et al., "Study of ultrasonic cavitation during extraction of the peanut oil at varying frequencies," *Ultrasonics Sonochemistry*, vol. 37, pp. 106–113, 2017.

[25] P. Raviyan, Z. Zhang, and H. Feng, "Ultrasonication for tomato pectinmethylesterase inactivation: effect of cavitation intensity and temperature on inactivation," *Journal of Food Engineering*, vol. 70, no. 2, pp. 189–196, 2005.

[26] X. Ren, T. Hou, Q. Liang et al., "Effects of frequency ultrasound on the properties of zein-chitosan complex coacervation for resveratrol encapsulation," *Food Chemistry*, vol. 279, pp. 223–230, 2019.

[27] J.-K. Yan, Y.-Y. Wang, W.-Y. Qiu, Z.-B. Wang, and H. Ma, "Ultrasound synergized with three-phase partitioning for extraction and separation of *Corbicula fluminea* polysaccharides and possible relevant mechanisms," *Ultrasonics Sonochemistry*, vol. 40, pp. 128–134, 2018.

[28] Y. Lin, L. Lin, M. Cheng et al., "Effect of acoustic parameters on the cavitation behavior of SonoVue microbubbles induced by pulsed ultrasound," *Ultrasonics Sonochemistry*, vol. 35, pp. 176–184, 2017.

[29] S. L. Liu and B. Hu, "The study on the technology of preparation of walnut proteins," *Food Research and Development*, vol. 31, no. 10, pp. 107–110, 2010.

[30] S. Q. Jing, "Optimization of the preparation of walnut protein with ultrasonic-assisted extraction method," *Food Science and Technology*, vol. 37, no. 2, pp. 251–255, 2012.

[31] Y. Xu, Y. Li, T. Bao, X. Zheng, W. Chen, and J. Wang, "A recyclable protein resource derived from cauliflower by-products: potential biological activities of protein hydrolysates," *Food Chemistry*, vol. 221, pp. 114–122, 2017.

[32] R. R. Guo, S. Y. Pan, and K. X. Wang, "Comparing research on functionality of rice protein extracted by alkali and enzyme," *Food Science*, vol. 26, no. 3, pp. 173–177, 2005.

[33] C. Lu, S. K. Zhang, K. X. Zhu, B. Wang, and H. M. Zhou, "Extraction of tea protein using alkali extraction-acid precipitation method," *Modern Food Science and Technology*, vol. 27, no. 6, pp. 673–677, 2011.

[34] D. H. Ding, G. H. Peng, H. Xia, H. Wan, and D. P. He, "Orthogonal array design for extraction optimization of protein from camellia oleifera seed meal," *Food Science*, vol. 31, no. 8, pp. 102–105, 2010.

[35] S. Jain and A. K. Anal, "Optimization of extraction of functional protein hydrolysates from chicken egg shell membrane (ESM) by ultrasonic assisted extraction (UAE) and enzymatic hydrolysis," *LWT-Food Science and Technology*, vol. 69, pp. 295–302, 2016.

[36] H. Xi, Y. Liu, L. Guo, and R. Hu, "Effect of ultrasonic power on drying process and quality properties of far-infrared radiation drying on potato slices," *Food Science and Biotechnology*, vol. 29, no. 1, pp. 93–101, 2020.

[37] L. Xu and L. L. Diosady, "Removal of phenolic compounds in the production of high-quality canola protein isolates," *Food Research International*, vol. 35, no. 1, pp. 23–30, 2002.

[38] P. R. Shewry and B. J. Miflin, "Seed storage proteins of economically important cereals," *Advances in Cereal Science &Technology*, vol. 7, pp. 1–83, 1985.

[39] J. Liu, L. X. Li, H. X. Wei et al., "Optimization of ultrasonic-assisted extraction process of crude protein from *Termitomyces albuminosus* and its antioxidant activity," *Science and Technology of Food Industry*, vol. 40, no. 10, pp. 221–226, 2019.

[40] H. Sun, C. Li, Y. Ni et al., "Ultrasonic/microwave-assisted extraction of polysaccharides from *Camptotheca acuminata* fruits and its antitumor activity," *Carbohydrate Polymers*, vol. 206, pp. 557–564, 2019.

[41] Q. H. Zhang, X. Q. Huang, M. Y. Li, Y. X. Liu, and J. W. Zhang, "Study on secondary structure of meat protein by FTIR," *Food and Fermentation Industries*, vol. 41, no. 10, pp. 247–251, 2015.

[42] Y. Mine, "Effect of dry heat and mild alkaline treatment on functional properties of egg white proteins," *Journal of Agricultural and Food Chemistry*, vol. 45, no. 8, pp. 2924–2928, 1997.

[43] W. Qu, X. Zhang, W. Chen, Z. Wang, R. He, and H. Ma, "Effects of ultrasonic and graft treatments on grafting degree, structure, functionality, and digestibility of rapeseed protein isolate-dextran conjugates," *Ultrasonics Sonochemistry*, vol. 42, pp. 250–259, 2018.

[44] Y. X. Yin, B. Q. Xiang, and L. Tong, "The application of studying fluorescence spectroscopy on protein," *Experimental Technology and Management*, vol. 27, no. 2, pp. 33–40, 2010.

[45] L. Jiang, J. Wang, Y. Li et al., "Effects of ultrasound on the structure and physical properties of black bean protein isolates," *Food Research International*, vol. 62, pp. 595–601, 2014.

[46] Q.-T. Zhang, Z.-C. Tu, H. Xiao et al., "Influence of ultrasonic treatment on the structure and emulsifying properties of peanut protein isolate," *Food and Bioproducts Processing*, vol. 92, no. 1, pp. 30–37, 2014.

[47] X. C. Shen, H. Liang, X. W. He, and X. S. Wang, "Recent trends and spectroscopic methods for analysis of the protein conformation with circular dichroism," *Chinese Journal of Analytical Chemistry*, vol. 32, no. 3, pp. 388–394, 2004.

[48] P. B. Stathopulos, G. A. Scholz, Y. M. Hwang, J. Rumfeldt, and J. R. Lepock, "Sonication of proteins causes formation of aggregates that resemble amyloid," *Protein Science*, vol. 13, no. 11, pp. 3017–3027, 2010.

[49] J. T. Vivian and P. R. Callis, "Mechanisms of tryptophan fluorescence shifts in proteins," *Biophysical Journal*, vol. 80, no. 5, pp. 2093–2109, 2001.

[50] R. Z. Zhao, J. Jiang, J. W. Lin, and Y. F. Liu, "Influence of roast processing on secondary structure, surface hydrophobicity and emulsifying properties of walnut protein," *Science and Technology of Food Industry*, vol. 37, no. 16, pp. 157–166, 2016.

[51] Y. Feng, B. Xu, A. E. A. Yagoub et al., "Role of drying techniques on physical, rehydration, flavor, bioactive compounds and antioxidant characteristics of garlic," *Food Chemistry*, vol. 343, p. 128404, 2021.

[52] P. Liu, Z. Ji, and F. S. Chen, "Microwave and ultrasound-assisted conventional alkali extraction of wheat bran protein," *Journal of Qi Lu University of Technology*, vol. 32, no. 1, pp. 6–12, 2018.

Hindawi
Journal of Food Quality
Volume 2021, Article ID 3268149, 15 pages
https://doi.org/10.1155/2021/3268149

Research Article

Preparation Optimization, Characterization, and Antioxidant and Prebiotic Activities of Carboxymethylated Polysaccharides from Jujube

Runfang Feng,[1,2] **Jingjing Kou**,[1,3] **Shan Chen**,[1,3] **Na Wang**,[1,3] **Weiwei Wang**,[1,3] **Lili Wang**,[1,3] **Huiqiang Wang**,[4] **Christopher Ference**,[5] **Mengjun Liu**,[1,3] **Changwei Ao**,[1,2] **and Zhihui Zhao**[1,3]

[1]*Chinese Jujube Research Center, Hebei Agricultural University, Baoding, Hebei 071000, China*
[2]*College of Food Science and Technology, Hebei Agricultural University, Baoding, Hebei 071000, China*
[3]*College of Horticulture, Hebei Agricultural University, Baoding, Hebei 071000, China*
[4]*College of Mechanical and Electrical Engineering, Hebei Agricultural University, Baoding, Hebei 071000, China*
[5]*Department of Plant Pathology, University of Florida, 2550 Hull Road, Gainesville, FL 32611, USA*

Correspondence should be addressed to Changwei Ao; aocw@163.com and Zhihui Zhao; lyzhihuizhao@126.com

Received 11 May 2021; Revised 19 June 2021; Accepted 26 June 2021; Published 5 July 2021

Academic Editor: Shengbao Cai

In this study, jujube polysaccharides (JP) were extracted from *Jinsixiaozao*, and carboxymethylated jujube polysaccharides (CMJP) were prepared. The optimum carboxymethylation conditions optimized by Response Surface Methodology (RSM) were as follows: the reaction temperature was 60°C, the concentration of sodium hydroxide (NaOH) solution was 2.8 mol/L, and the content of chloroacetic acid was 2.12% with a degree of substitution (DS) of 0.2275 ± 0.0108. Physicochemical characterizations and *in vitro* antioxidant and prebiotic activities of JP and CMJP were evaluated. Compared with unmodified JP, water solubility and viscosity were improved in CMJP. Chemical analysis revealed that CMJP was composed of Rha: Ara: Xyl: Glc: Gal = 0.18 : 9.09 : 0.45 : 0.36 : 0.98 with a molecular weight of 3.04×10^5 Da. The signals of carboxymethyl were observed at 1600, 1420, and 1328 cm^{-1} in FT-IR. In addition, CMJP showed obviously strong hydroxyl radical scavenging ability compared with JP and also exhibited stronger abilities than JP on the proliferation growth of *Lactobacillus acidophilus*, *Lactobacillus plantarum*, and *Lactobacillus rhamnosus* strains. These results indicated that CMJP could be explored as a promising resource for the development of functional foods.

1. Introduction

Polysaccharides are complex biopolymers comprised of monosaccharides chains and widely distributed in plants, animals, and microorganisms. As one of the most important biopolymers existing in nature, polysaccharides play diverse and important roles in many biological processes [1]. In the past two decades, natural polysaccharides have attracted great attention particularly since they can be obtained in a reproducible way from the natural sources and usually considered to have low toxicity. Natural polysaccharides have been proved to possess antitumor, antioxidant, antimicrobial, antiviral, immunomodulatory, hypoglycemic, gastrointestinal-protective, and gut microbiota-modulating properties for health promotion [1, 2]. The biological activities of natural polysaccharide could be strongly affected by molecular modifications, such as sulfation [3], phosphorylation, carboxymethylation [4], and acetylation [5] due to the changing of their structural and conformational properties.

The application of natural polysaccharides as bioactive ingredients and food additives was limited by their complex structure and various bioactivities mechanism. Many natural polysaccharides lack useful bioactivities or exhibit weak biological activities and need to be further improved in a necessary

way [6]. Recently, a number of studies have reported that chemical modification brings an opportunity to enhance its biological characteristics by introducing the functional groups to polysaccharides [7]. Carboxymethylation, as a versatile modification method, has been found to have great influence on the physicochemical properties and biological activities of various polysaccharides. Xu et al. [8] found that the addition of carboxymethyl groups improved the relatively poor water solubility and *in vitro* antioxidant activities of *Ganoderma lucidum* polysaccharide. Zhu et al. [9] reported that carboxymethylated *Lycium barbarum* polysaccharide not only enhanced the intestinal microbiota but also boosted the beneficial bacteria levels for innate immune response modulation. Carboxymethylated polysaccharides from *Sargassum fusiforme* also had a much higher antioxidant and antimicrobial activities *in vitro* than the native ones [4].

Jujube (*Ziziphus jujuba* Mill.) belongs to the genus *Ziziphus* (Rhamnaceae family) and widely distributed in the subtropical regions especially in north China (Shandong, Hebei, and Henan Provinces) [7]. Jujube fruit is rich in nutrients and functional components such as polysaccharides, vitamin C, triterpenic acid, flavonoids, and cAMP [10]. Among the several bioactive compounds present in jujube, polysaccharides, one of the most important species with a large presence in amounts, have been identified to possess antioxidant capacities [11], immunomodulation properties [12], hepatoprotective activity [13], and antitumor benefits [14], thus gaining attention as a potential pharmacological and functional supplement. *Jinsixiaozao* is a traditional jujube variety, which is widely planted in Cangzhou City, Hebei Province. After drying, its polysaccharide content is significantly higher than other varieties. In our earlier studies, Zhao et al. [15] isolated two pectic polysaccharides from *Jinsixiaozao* polysaccharides, and one of the polysaccharides was demonstrated to possess immunological activities. Moreover, recent results have revealed that the water-soluble polysaccharides extracted and purified from *Jinsixiaozao* polysaccharides showed antioxidant and immunomodulation activities [16, 17]. Polysaccharides derived from *Jinchangzao* polysaccharides fruit represent enhanced immunomodulatory and anticoagulant activities after sulfated modification [3]. However, few researches have been carried out on the properties and the biological activities of modified especially carboxymethylated polysaccharides from *Jinsixiaozao* polysaccharides.

In order to further study and utilize the *Jinsixiaozao* polysaccharides, the aim of the present study was (i) to optimize the carboxymethylation conditions based on RSM; (ii) to analyze the preliminary physicochemical properties and structural characterizations of derivatives of carboxymethylated polysaccharides; and (iii) to evaluate the *in vitro* antioxidant and prebiotic activities and compare with the unmodified polysaccharides.

2. Materials and Methods

2.1. Materials and Reagents. The fruiting bodies of *Ziziphus jujuba cv. Jinsixiaozao* were collected from their original cultivation places located in Cangzhou, Hebei province, China, at optimum stage of maturity and identified by one of the authors (M. J., Liu, Chinese Jujube Research Center). Samples were preserved in a cooler box (0°C, 80–85% relative humidity) and transported to Chinese Jujube Research Center within 3 h. The fruit was then washed and dried to constant weight at 55°C through the processing line of the packaging plant. After that, kernels were removed, and fruit pulp was ground into fine powder using an electric mill (A-11 basic Analytical mill, IKA-Werke Staufen, Germany) and then stored in vacuum bags at room temperature (22 ± 1°C) for later use.

Chloroacetic acid and absolute ethyl alcohol were purchased from Sinopharm Chemical Reagent Co., Ltd. (Shanghai, China). 95% ethanol, trichloroacetic acid, concentrated hydrochloric acid (HCl), concentrated sulfuric acid, chloroacetic acid, sodium hydroxide (NaOH), disodium hydrogen phosphate, sodium dihydrogen phosphate, 1,1-diphenyl-2-picrylhydrazyl (DPPH), potassium sulfate, potassium ferricyanide, anhydrous iron chloride, salicylic acid, ferrous sulfate heptahydrate, hydrogen peroxide, chloroacetic acid, and vitamin C were purchased from Solarbio Science & Technology Co., Ltd. (Beijing, China). Dextrans with different molecular weight (T-10, T-40, T-70, T-100, and T-500) were purchased from Solarbio Science & Technology company (Shanghai, China). Monosaccharide standards including arabinose (Ara), rhamnose (Rha), xylose (Xyl), mannose (Man), glucose (Glc), and galactose (Gal) were obtained from Sigma Chemical Co. (St. Louis, MO, USA). All other chemicals and reagents were of analytical reagent grade. The ultrapure water was utilized from a Milli-Q water purification system (Millipore, Bedford, MA, USA).

Three bacterial strains, *Lactobacillus acidophilus* CGMCC 1.2919, *Lactobacillus plantarum* CGMCC 1.569, and *Lactobacillus rhamnosus* CGMCC 1.576 were obtained from the China General Microbiological Culture Collection Center (CGMCC). The strains were stored in MRS-G broth (2% glucose) containing 10% glycerol at −80°C until use. The bacteria were activated using MRS-G broth before use.

2.2. Preparation of JP and Its Carboxymethylated Derivatives

2.2.1. Preparation of JP. The crude *Jinsixiaozao* polysaccharide (JP) was obtained according to our earlier study [15]. Briefly, dried fruit powder (2500 g) was immerged and washed three times with 95% ethanol (1 : 10, *w*/*v*) at 80°C for 90 min each time to remove some soluble materials, including free sugars, lipids, and phenols. After that, the filtrated and dried residue was extracted in boiling water (1 : 20, *w*/*v*) at 100°C for three times (90 min each time). The supernatants were combined and concentrated by rotary evaporation (IKA-Werke-RV-10, Staufen, Germany) under reduced pressure and then mixed with absolute ethanol, stirred vigorously, and kept overnight at 4°C to precipitate polymers. The precipitate was collected by centrifugation (5000 rpm, 20 min), deproteinated following Sevag method [18], lyophilized using a freeze-dryer (Alpha-2, Christ, Germany), and weighed, and the extraction rate of crude JP is 5.66%.

2.2.2. Preparation of Carboxymethylated Derivative. The carboxymethylation of JP was performed based on the method described by Wang et al. [19] with modifications. A solution of JP (500 mg) in NaOH (1.0, 1.5, 2.0, 2.5, 3, and 3.5 mol/L, 100 mL) was vigorously stirred with a magnet stirrer for 60 min at room temperature (22 ± 1°C) until a homogeneous solution was obtained. Then different content of chloroacetic acid solution (1, 2, 3, 4, and 5%) was added and stirred at a certain temperature (40, 50, 60, 70, and 80°C) for 5 h. The reaction mixture was cooled to room temperature, adjusted to pH 7.0 with 0.5 mol/L glacial acetic acid, and dialyzed in dialysis bags (with a molecular weight cut-off of 8000–14,000 Da) for 72 h with distilled water and then freeze-dried to obtain carboxymethylated jujube polysaccharide (CMJP).

The influence of the concentration of NaOH solution, the content of chloroacetic acid, and the reaction temperature on the degree of substitution (DS) of CMJP was studied. Single-factor experiments showed that the optimal NaOH solution concentration, chloroacetic acid content, and reaction temperature were 2.5 mol/L, 2%, and 60°C, respectively. On the basis of single-factor test results, response surface methodology (RSM) was used to further optimize the preparation conditions of CMJP. Three-factor three-level, Box–Behnken factorial design (BBD) was used to evaluate the combined effect of three independent variables: NaOH solution concentration, chloroacetic acid content, and reaction temperature, coded as X_1, X_2, and X_3, respectively. The DS of CMJP was regarded as the response value, and 17 experiments were required, as shown in Table S1.

The adequacy and significance in the model was evaluated by analysis of variance (ANOVA) for each response. Design-Expert 11 software package (Trial Version, Stat-Ease Inc., Minneapolis, MN, USA) was used to analyze the experimental data.

2.2.3. Determination of Degree of Substitution (DS) of CMJP. According to the neutralisation titration method, 20 mg CMJP was dissolved in 20 mL NaOH (0.01 mol/L) and stirred thoroughly with a magnet stirrer for 60 min at 40°C. The solution was titrated with 0.1 mol/L HCl until the color of phenolphthalein disappeared. The DS was calculated as follows:

$$\mathrm{DS} = \frac{0.162A}{(1 - 0.058A)}, \tag{1}$$

$$A = \frac{\left[0.01V_1 - 0.1\left(V_2 - V_3\right)\right]}{W}, \tag{2}$$

where A was the amount of NaOH solution consumed per gram of sample (mol/g); V_1 and V_2 were the volume of NaOH and HCl consumed, respectively (mL); V_3 was the volume of HCl consumed by titrating the blank solution (mL); and W was the mass of the sample (gram).

2.3. Characterization of Carboxymethylated Derivatives

2.3.1. Water Solubility and Viscosity. For water solubility, 1 mL water was added to 100 mg samples and then shaken vigorously for 12 h until the sample was completely dissolved. The precipitate was dried at 55°C and weighed. The rheological properties of each sample were evaluated on a rotational rheometer (Anton Paar RheolabQC model) in three replicates. 10 mg/mL aqueous solution of JP and CMJP in distilled water was prepared. A shear rate sweep from 0.1 to 1000 s^{-1} was applied, and rheological data were collected at 25°C. The relationship between apparent viscosity and shear rate was modeled with a power law equation: $\eta_a = k\Upsilon^{(n-1)}$, where η_a is apparent viscosity (mPa s), Υ is shear rate (s^{-1}), k is consistency index (mPa), and n is the flow index (dimensionless).

2.3.2. Analysis of Chemical Compositions. The total sugar contents of JP and CMJP were determined by phenol-sulfuric acid method, using *D*-glucose as the standard. The content of uronic acid was estimated using *m*-hydroxybiphenyl method with galacturonic acid as the standard.

2.3.3. Determination of the Neutral Monosaccharide Composition. JP and CMJP samples (10 mg) were hydrolyzed with 2 mol/L trifluoroacetic acid (TFA, 4 mL) at 110°C for 6 h. The hydrolyzed samples and standard monosaccharides were acetylated by the addition of hydroxylamine hydrochloride, pyridine, and acetic anhydride. The acetylated polysaccharide was analyzed by gas chromatography (GC) on an Agilent model 7890A instrument, equipped with a TG-5MS capillary column (30 m × 0.25 mm × 0.25 μm) and a flame ionization detector (FID). The temperatures of the injector and the detector were 240°C and 260°C, respectively. The flow rate of carrier gas (high-purity nitrogen, 99.999%), air, and hydrogen were 20 mL/min, 400 mL/min, and 50 mL/min, respectively. The nitrogen gas pressure was adjusted to 8.79 psi at a constant linear velocity of 3 cm/s. The initial temperature was held at 140°C for 3 min and then increased at 10°C/min to the final temperature of 240°C and held for 11 min. The import of the sample into the column was accomplished using the split mode at a ratio of 20 : 1, and injection volume was 1 μL. The monosaccharide compositions were identified by comparing the retention time of standards and calculated by area normalization method using mass spectra of peaks on the chromatograms derived from the samples and the standard solution mix.

2.3.4. Molecular Weight (Mw) Determination. The Mw of JP and CMJP was measured using high-performance liquid chromatography (HPLC) which was undertaken on an Agilent 1200 Infinity Series LC system (Agilent Technologies, Germany) coupled with an ELSD-1260 (Agilent Technologies, UK) evaporative light detector. Samples were dissolved in ultrapure water (0.5 mg/mL), passed through a 0.22 μm filter, and applied to a gel-filtration chromatographic column of Shodex KS-805 (300 mm × 8.0 mm, Showa Denko K.K., Japan) at 35°C. Ultrapure water (pH 7.0) was used as the flow phase at a flow rate of 1 mL/min with an injection volume of 20 μL. The column was preliminary calibrated by standard dextrans (T-500, T-100, T-70, T-40, T-10, and glucose) with respective retention time and

molecular weights. Then, a standard curve was plotted, and the Mw of JP and CMJP was calculated based on the standard curve.

2.3.5. Fourier Transform Infrared Spectra (FT-IR) Analysis. The infrared spectra of JP and CMJP were measured by a FT-IR spectrophotometer (Spectrum 65, PerkinElmer, USA) using KBr compression method. One mg of JP or CMJP was ground with 200 mg of KBr powder (completely dried at 100°C) and pressed into a 1 mm agate mortar into a pellet with 1 mm thickness for a frequency resolution of 1 cm^{-1} and 32 scans between 400 and 4000 cm^{-1}.

2.3.6. UV-Vis Spectra. Ultraviolet spectra of JP and CMJP were obtained on TU-1810 ultraviolet spectrophotometer (Purkinje General Instrument Co., Ltd., Beijing, China). The scanning range was 190–900 nm at 1 nm intervals for each sample (0.1 mg/mL, w/v in distilled water).

2.3.7. Scanning Electron Microscope (SEM) and Energy-Dispersive X-Ray Spectroscopy (EDS) Analysis. Scanning electron micrographs of JP and CMJP were obtained with a TESCAN VEGA3 LMH scanning electron microscope (TESCAN Co., Brno, Czech Republic). Sample powders were placed on a specimen holder with the help of double-sided adhesive tapes and coated with a thin layer of gold powder. Each sample was observed with 5,000- and 10,000-fold magnification at an accelerating potential of 10 kV during micrography. Chemical analysis was performed using an energy-dispersive X-ray spectroscopy (EDS, Model TEAM, EDAX, USA) facility.

2.4. Antioxidant Activity

2.4.1. Scavenging Activity of DPPH Radical. The effect of scavenging DPPH radicals of JP and CMJP was determined by a reported method, with minor modification [20]. A polysaccharide solution (1, 2, 3, 4, and 5 mg/mL) was prepared by dissolving in distilled water. 2 mL DPPH solution (0.1 mmol in ethanol) was added to 0.5 mL of various concentrations of sample solutions with 1.5 mL distilled water. The mixture was shaken rigorously and incubated in the dark for 60 min at room temperature; the absorbance at 517 nm was measured using a spectrophotometer (TU-1810, Puxi General Instrument Co., Ltd., China). Vitamin C (0.1, 0.2, 0.5, 1, 2, 3, 4, and 5 mg/mL) was used as the positive control. DPPH radical scavenging activity of the sample was calculated as

$$\text{DPPH scavenging rate}\,(\%) = \left[1 - \frac{(A_s - A_c)}{A_b}\right] \times 100\%, \quad (3)$$

where A_b (blank) was the absorbance of the mixture of DPPH-ethanol solution without sample; A_c (control) was the absorbance of the mixture of ethanol and sample without DPPH; and A_s (sample) was the absorbance of the mixture of DPPH and sample.

2.4.2. Scavenging Activity of Hydroxyl radical ($HO^{\cdot}$). The hydroxyl radical scavenging abilities of JP and CMJP were evaluated according to the method of Duan et al. [21] with slight modifications. 2 mL polysaccharide solution (1, 2, 3, 4, and 5 mg/mL in distilled water) was mixed with salicylic acid (0.5 mL, 9 mmol in ethanol), $FeSO_4$ solution (0.5 mL, 9 mmol), H_2O_2 solution (0.5 mL, 8.8 mmol), and 6.5 mL distilled water. The resulting solution was shaken well and incubated in a water bath at 37°C for 30 min; the absorbance was determined at 510 nm. Vitamin C (0.1, 0.2, 0.5, 1, 2, 3, 4, and 5 mg/mL) was used as the positive control. The hydroxyl radical scavenging activity was calculated as

$$HO^{\cdot}\ \text{scavenging rate}\,(\%) = \left[1 - \frac{(A_s - A_c)}{A_b}\right] \times 100\%, \quad (4)$$

where A_b (blank) was the absorbance of distilled water, A_c (control) was the absorbance of distilled water replaced $FeSO_4$ solution, and A_s (sample) was the absorbance of sample.

2.4.3. Scavenging Activity of Superoxide Anion radical ($O_2^{\cdot -}$). The effect of scavenging $O_2^{\cdot -}$ of JP and CMJP was measured by the method of Liu and Huang [22] with minor modification. Different concentrations of polysaccharide solutions (0.03125, 0.0625, 0.125, 0.25, 0.5, 1, 2, and 4 mg/mL) were prepared by dissolving them in distilled water. 0.5 mL polysaccharide solution and 3 mL Tris-HCl buffer (50 mmol, pH 8.2) were mixed well and kept in a water bath at 30°C for 20 min; then 3 mL pyrogallol solution (7 mmol) was added and incubated for 4 min. 1 mL concentrated HCl was added to stop the reaction, and the absorbance was measured at 420 nm. Vitamin C (0.1, 0.2, 0.5, 1, 2, 3, 4, and 5 mg/mL) was used as positive control. The superoxide anion radical scavenging activity of the sample was calculated as

$$O_2^{\cdot -}\ \text{scavenging rate}\,(\%) = \left[1 - \frac{(A_s - A_c)}{A_b}\right] \times 100\%, \quad (5)$$

where A_b (blank) was the absorbance of the blank (without sample); A_c (control) was the absorbance of the sample without pyrogallol solution; and A_s (sample) was the absorbance in the presence of the sample.

2.4.4. Reducing Power Assay. The reducing power of JP and CMJP was quantified by the method described by Li et al. [16] with slight modification. 1 mL of different concentrations of polysaccharide solution (1, 2, 3, 4, and 5 mg/mL), 1 mL potassium ferricyanide solution (1%, w/v), and 1 mL phosphate buffer (0.2 mol, pH 6.6) were mixed, shaken rigorously, and incubated in a water bath at 50°C for 20 min. The reaction was terminated by 1 mL TCA solution (10%, w/v) and centrifuged at 4000 rpm for 10 min. 2 mL supernatant and 0.4 mL ferric chloride solution (0.1%, *w*/*v* in distilled water) were reacted at room temperature for 10 min. The

absorbance was measured at 700 nm. Vitamin C (0.1, 0.2, 0.5, 1, 2, 3, 4, and 5 mg/mL) was used as positive control. The increasing absorbance of the reaction mixture indicated the increasing reducing power of the sample.

2.5. Prebiotic Activity Analysis. The activated *Lactobacillus* strains incubated in MRS medium at 37°C incubator for 48 h. After centrifugation at 4°C, 5000 rpm for10 min, cells were collected and adjusted to 4×10^9 CFU/mL for preparation of the growth curve. Appropriate bacterial liquid was added to the MRS medium, incubated at 37°C for 48 h, and measured every 2 h at 600 nm with a spectrophotometer (TU-1810, Puxi General Instrument Co., Ltd., China). MRS broth with 2% (*w*/*v*) glucose (MRS-G, Beijing Solarbio Science & Technology Co., Ltd., Beijing, China) was used as the basal medium to investigate the prebiotic activity *in vitro* and to determine whether the polysaccharides (JP and CMJP) was potential substrate to support the growth of *L. acidophilus*, *L. plantarum*, and *L. rhamnosus*. JP and CMJP were filtered and sterilized and then added to the MRS-G broth to prepare polysaccharide solutions with different contents (0.5, 1.0, and 1.5%, *w*/*v*). The basal medium was used as a control. 2 μL of active lactic acid bacteria liquid (exponential phase) was added to the MRS-G broth medium and kept in a constant-temperature incubator at 37°C for 24 h, and the absorbance was measured every 6 h. The numbers of *Lactobacillus* strains in the samples were obtained by measuring their optical density values at 600 nm with a spectrophotometer.

2.6. Statistical Analysis. Each assay of all determinations was performed in triplicate and expressed as mean ± SD (standard deviation). One-way analysis of variance (ANOVA) followed by Duncan's multiple-range test was used for multiple comparisons by the SPSS 23.0 software package (Chicago, USA). $P < 0.05$ means significant difference while $P < 0.01$ means very significant difference. The results were performed with GraphPad Prism 7.0 (GraphPad Software, Inc., San Diego, CA).

3. Results and Discussion

3.1. Preparation of CMJP. As shown in Figure 1(a), when concentration of NaOH solution varied from 1 to 2.5 mol/L, the DS increased significantly and reached a maximum (0.2249) at 2.5 mol/L. Once alkalization has been achieved, further increasing the NaOH concentration from 2.5 to 3.5 mol/L encouraged side reactions [23]. Therefore, 2.5 mol/L was used as the optimal concentration condition for NaOH solution.

The DS of CMJP had been increasing when chloroacetic acid content increased from 1% to 2% as shown in Figure 1(b). The maximum DS (0.2133) of CMJP was observed when chloroacetic acid content was 2%. However, at chloroacetic acid concentration greater than 2%, NaOH was neutralized and further increasing the concentration of chloroacetic acid has no advantages on the modification of carboxymethylation. Therefore, 2% was used as the optimal condition for the chloroacetic acid content.

As shown in Figure 1(c), The DS of CMJP significantly increased from 0.1786 to 0.1891 as carboxymethylation temperature increased from 40 to 60°C. However, when carboxymethylation temperature is greater than 60°C, a significant decrease appeared which can speculate that excessively high temperature might reduce the stirring efficiency and the uniformity of the etherification reaction [24]. Therefore, 60°C was used as the optimal reaction temperature for the preparation of CMJP.

According to the single-parameter study, we adopted NaOH solution concentration of 2, 2.5, and 3 mol/L, chloroacetic acid content of 1%, 2%, and 3%, and extraction temperature of 50, 60, and 70°C for RSM experiments.

3.1.1. Model Fitting and Statistical Analysis. The variation of responses (DS of CMJP) at different experimental combinations was given in Table 1. By employing multiple regression analysis on the experimental data, the predicted response Y for the DS of CMJP can be obtained by the following second-order polynomial equation: $Y = -1.667 + 0.179X_1 + 0.273X_2 + 0.045X_3 - 0.001X_2X_3 - 0.027X_1^2 - 0.045X_2^2$, where X_1, X_2, and X_3 were the coded values of the test variables, concentration of NaOH solution (mol/L), content of chloroacetic acid (%), and the reaction temperature (°C), respectively.

The F-value and P-value were used to measure the significance of the coefficients of the model. The corresponding variables would be more significant if the absolute F-value becomes greater and the P-value becomes smaller [25]. F-test suggested that the model had a very high F-value ($F = 14.37$) and a very low P-value ($P = 0.001$), indicating that this model was highly significant. The lack-of-fit test measures the failure of the model to represent the data in the experimental domain at points which were not included in the regression [12]. F-value (1.34) and P-value (0.3808) of lack of fit implied that it was not significant relative to the pure error, which confirmed that the model equation was adequate for predicting the DS of CMJP under any combination of values of the variables. In addition, the determined coefficient of model ($R^2 = 0.9487$) indicated that the mode is applicable. The adjusted determination coefficient (adjusted $R^2 = 0.8826$) was also high, indicating a high degree of correlation between the experimental and predicted values [26]. At the same time, a low value 6.17% of coefficient of the variation (C.V.) clearly showed a very high degree of precision and a good deal of reliability of the experimental values.

The P-value was used as a tool to check the significance of each coefficient, which in turn may indicate the pattern of the interactions among the variables. The smaller the P-value was, the more significant the corresponding coefficient was [26]. As shown in Table 1, the linear coefficients (X_2) and quadratic term coefficients (X_2^2, X_3^2) were significant with very small P-values ($P < 0.05$ or $P < 0.01$), while the other term coefficients were not significant ($P > 0.05$). Meanwhile, the content of chloroacetic acid (X_2^2) was the most important

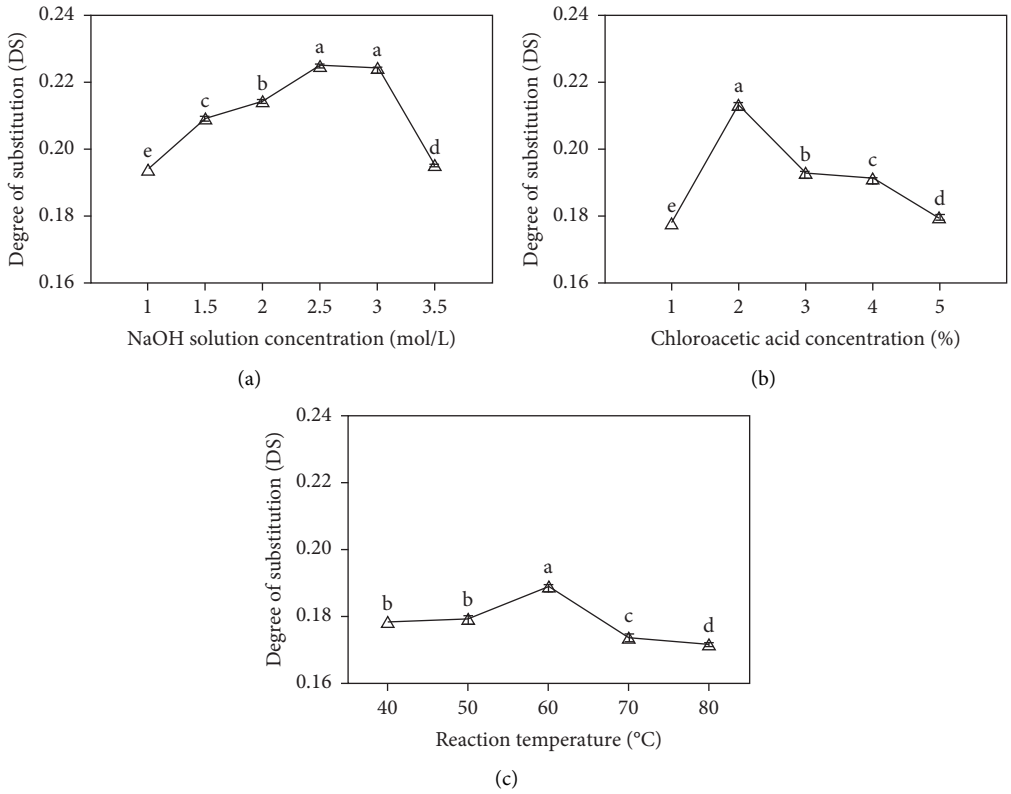

Figure 1: Effects of NaOH solution concentration (a), chloroacetic acid content (b), and reaction temperature (c) on the DS of CMJP. Data with different lowercase letters represent significant differences at $P < 0.05$.

Table 1: Analysis of variance (ANOVA) for response surface quadratic model for the optimization of carboxymethylation conditions.

Source	Sum of squares	Degree of freedom	Mean of squares	F-value	P-value	Significance
Model	0.0172	9	0.0019	14.37	0.0010	*
X_1	0.0005	1	0.0005	3.90	0.0888	ns
X_2	0.0010	1	0.0010	7.59	0.0283	*
X_3	0.0003	1	0.0003	1.89	0.2116	ns
X_1X_2	2.500E-09	1	2.500E-09	0.0000	0.9967	ns
X_1X_3	0.0000	1	0.0000	0.1519	0.7083	ns
X_2X_3	0.0007	1	0.0007	5.41	0.0530	ns
X_1^2	0.0002	1	0.0002	1.46	0.2655	ns
X_2^2	0.0087	1	0.0087	64.91	<0.0001	**
X_3^2	0.0048	1	0.0048	36.10	0.0005	*
Residual error	0.0009	7	0.0001			
Lack of fit	0.0005	3	0.0002	1.34	0.3808	ns
Pure error	0.0005	4	0.0001			
Total	0.0182	16				

$R^2 = 0.9487$. Adjusted $R^2 = 0.8826$. Predicted $R^2 = 0.5488$. C.V.% = 6.17. Adeq. precision = 12.3571. X_1: concentration of NaOH solution, X_2: content of chloroacetic acid solution, and X_3: reaction temperature. **Extremely significant difference ($P < 0.01$), *significant difference ($P < 0.05$), and ns: nonsignificant.

parameter affecting the degree of carboxymethyl substitution, followed by the concentration of NaOH solution and the reaction temperature.

3.1.2. Optimization of Preparation Conditions of CMJP. Three-dimensional (3D) response surface and two-dimensional (2D) contour plots (Figure 2) were obtained using Design-Expert 11 to study the effects of parameters and their interactions on the maximum response. Each figure showed the effects of two factors on the DS of CMJP, while the other one was kept at zero level. The interactions between the NaOH concentration and the other two parameters (X_1X_2 and X_1X_3) did not impact the DS of CMJP significantly. In Figure 2(e), when NaOH concentration (X_1) was fixed at 0 level, chloroacetic acid content (X_2) and reaction temperature (X_3) demonstrated comprehensive effects on the DS. The elliptical contour plot shown in Figure 2(f) indicated

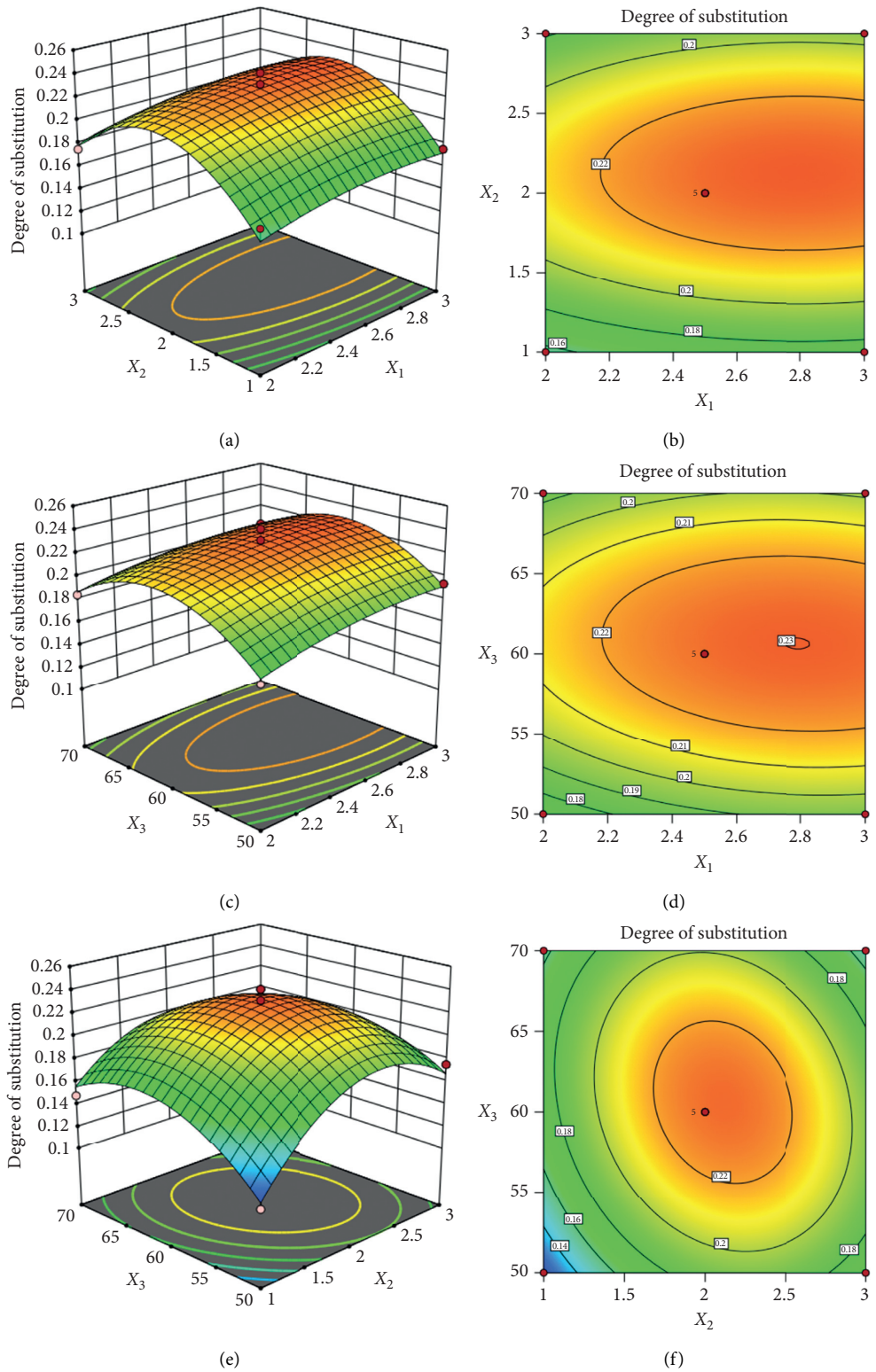

Figure 2: Response surface plots (a, c, e) and contour plots (b, d, f) showing the effect of NaOH concentration (mol/L, X_1), chloroacetic acid content (%, X_2), and reaction temperature (°C, X_3) on DS of CMJP.

that the mutual interactions between ratio of reaction temperature and chloroacetic acid content were significant.

According to software analysis, the optimal preparation conditions for CMJP were NaOH solution concentration of 2.79 mol/L, chloroacetic acid content of 2.12%, reaction temperature of 60.4°C, and DS of 0.2307. Three verification experiments were carried out in order to validate the adequacy of the model equation. Taking account of the

operating convenience, the optimal preparation parameters of CMJP were determined as follows: the concentration of NaOH solution was 2.8 mol/L, the content of chloroacetic acid was 2.12%, and the reaction temperature was 60.4°C. By these parameters, the DS of CMJP was 0.2275 ± 0.0108, which is close to the maximum predicted value, indicating an excellent fit with the mathematical model.

3.2. Characterization of Polysaccharides

3.2.1. Rheological Behavior of JP and CMJP. The rheological behavior in terms of dynamic viscosity and shear rate of JP and CMJP is shown in Figure 3. The shear stress-shear rate relationships showed nonlinear; flow curves of JP and CMJP demonstrate a non-Newtonian behavior because polysaccharides form an intertwined network structure in the aqueous phase [27]. With the increase in shear rate, apparent viscosity of JP and CMJP decreased continuously and showed a characteristic of pseudoplastic fluids. However, shear stress increased with the rise of shear rate. Compared with JP, it was found that carboxymethylation reduced apparent viscosity and shear stress of JP.

3.2.2. Composition of JP and CMJP. After carboxymethylation, water solubility improved in CMJP. The content of total carbohydrate in JP ($75.33 \pm 0.11\%$) was relatively higher than that in CMJP ($69.22 \pm 0.32\%$), indicating that JP may have been hydrolyzed during the carboxymethylation process (Table 2).

As in previous studies, the *Jinsixiaozao* polysaccharides were shown to be largely composed of rhamnose (Rha), arabinose (Ara), xylose (Xyl), mannose (Man), glucose (Glc), and galactose (Gal). However, the molar ratio was different, which may be related to different raw materials, purification processes, and detection methods [7]. In our study, both JP and CMJP were heteropolysaccharides. JP was mainly composed of Rha, Ara, Xyl, Man, Glc, and Gal in the molar ratios of 0.31 : 7.69 : 0.54 : 0.15 : 1.08 : 1 and CMJP was mainly composed of Rha, Ara, Xyl, Glc, and Gal, with a molar ratio of 0.18, 9.09, 0.45, 0.36, and 1, respectively. After carboxymethylation, the monosaccharide types have no significant changes expect Man (not detected in CMJP). Arabinose was also the major monosaccharide, but the CMJP had higher ratios of arabinose. Arabinose also was the main component monosaccharide in other jujube cultivars like "*Shaanbeitanzao*" [28], "*Huanghetanzao*" [13], and "*Muzao*" [14]. CMJP with high content of arabinose have good potential as antitumor [14], antioxidant, immunomodulation, and hepatoprotective agent [28]. For other monosaccharides, such as rhamnose, xylose, glucose, and galactose, the ratios were slightly decreased after modification. The result revealed that the carboxymethyl modification affects the physicochemical characteristics of JP but still retained the main component with almost the same monosaccharide types. The similar observations have been reported during the carboxymethylation of *Cyclocarya paliurus* polysaccharides [19].

3.2.3. Molecular Weight (Mw) Analysis. The weight-average molecular mass increased 10.62% from 2.75×10^5 Da (JP) to 3.04×10^5 Da (CMJP) after carboxymethylation. The raise might be owing to the incorporation of carboxymethyl-containing groups into the polymer structure during the carboxymethylation process. Wang et al. [29] also reported that the *Mw* of carboxymethylated polysaccharides extracted from *Poria cocos sclerotium* derivatives was higher than that of the natural polysaccharides.

3.2.4. FT-IR Spectrum Analysis. Figure 4 showed the FT-IR spectrum of JP and CMJP. In the range of 4000–400 cm^{-1}, the FT-IR spectra of JP and CMJP were similar. The strong and wide peak near 3420 cm^{-1} was caused by -OH stretching; the adsorption bands of 2927 cm^{-1} and 2370 cm^{-1} were related to the stretching angular vibration of C–H. These peaks can all be corresponding to the characteristic absorption peaks of polysaccharides [30]. Three new strong absorption peaks were observed near 1600 cm^{-1}, 1420 cm^{-1}, and 1328 cm^{-1} which were attributed to the symmetric scale absorption of -COO after carboxymethyl modification [31]. The new peak at 1600 cm^{-1} was attributed to the angular vibration of -COOH, while the absorption at wave number 1420 cm^{-1} corresponded to a vibrational absorption peak of C–H on the methyl linked to the carboxyl group. The stretching vibrational absorption of carbonyl at 1328 cm-1 was significantly enhanced, which indicated that the introduction of carboxymethyl (-OCH_2–COOH) is successful. That means the natural polysaccharide was carboxymethylated successfully without change of the molecular structure of JP. The fingerprint region between 800 and 1200 cm^{-1} is known in carbohydrate. The spectrum shows bands at 890 cm^{-1} may be assigned to the C_1–H deformation vibration of β-mannuronic acid residues. The band at 1012 cm^{-1} seems to be characteristic of uronic acid residues and bands at 1093 cm^{-1} may be assigned to the C-O stretching vibrations of pyranose rings [32, 33].

3.2.5. UV-Vis Spectra. The UV scanning analysis of crude jujube polysaccharide, JP, and CMJP was shown in Figure 5. Strong absorption peaks at 260 nm–280 nm of crude jujube polysaccharides indicated the presence of nucleic acids and protein [30]. No absorption peak was detected at 260 nm–280 nm, which means impurity was completely removed from both of JP and CMJP. There were no obvious differences between JP and CMJP from the spectrum.

3.2.6. SEM and EDS Analyses. Figures 6(a)–6(d) illustrated the scanning electron micrographs (SEM) of JP and CMJP at 5000x and 10,000x magnification. The morphology of CMJP showed significant variations in morphological properties compared with JP. JP occurred in a state of fibrous, layered, thin-sliced small particles, with a smooth surface. Single molecules and molecular groups linked together and formed polymers with a smooth fragmented appearance with various sizes. However, CMJP had a rough and uneven spherical shape with netted and loose porous structures,

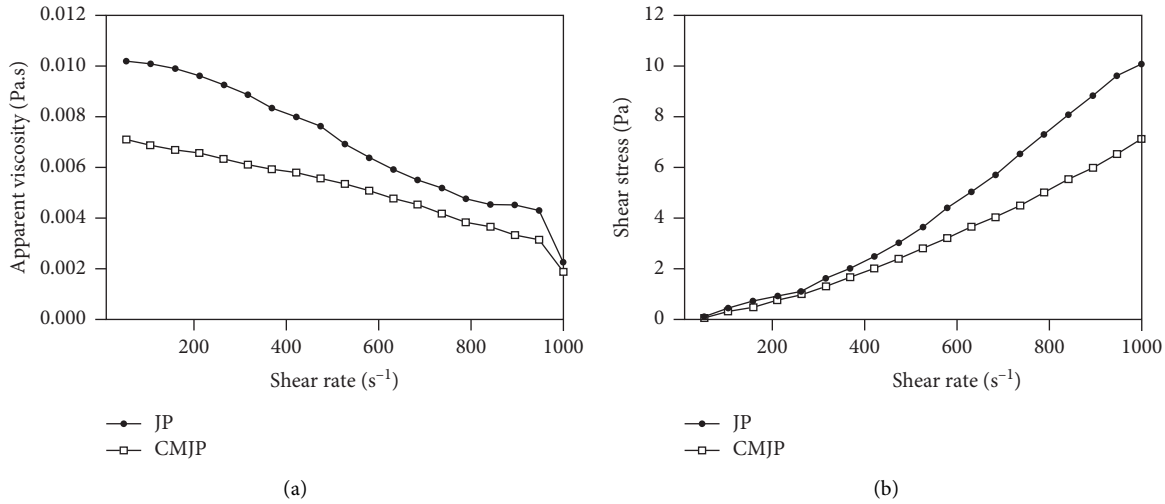

Figure 3: Effect of carboxymethylation modification on apparent viscosity (a) and shear stress (b) of JP and CMJP aqueous solution at 25°C.

Table 2: Water solubility, viscosity, and the chemical composition of polysaccharide from JP and CMJP.

Sample	Water solubility (mg/mL)	Total carbohydrate (%)	Uronic acid (%)	Monosaccharide composition (%)					
				Rhamnose	Arabinose	Xylose	Mannose	Glucose	Galactose
JP	50.8 ± 0.93	75.33 ± 0.11	39.35 ± 0.10	0.31	7.69	0.54	0.15	1.08	1
CMJP	85.1 ± 1.27	69.22 ± 0.32	40.38 ± 0.15	0.18	9.09	0.45	ND	0.36	0.98

Note. ND: not detected.

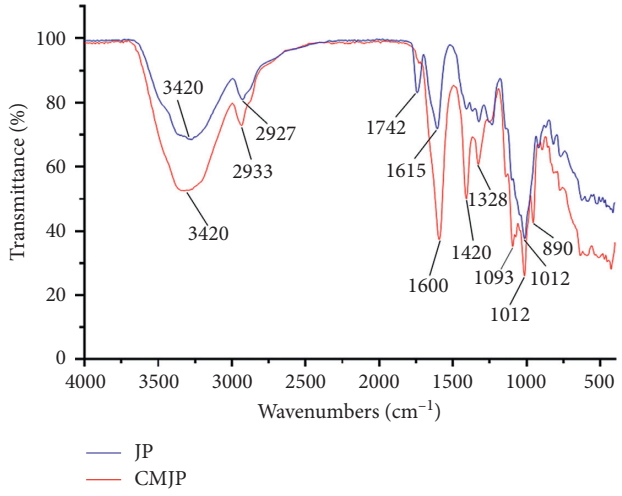

Figure 4: Fourier transform infrared spectra (FT-IR) of JP and CMJP.

which indicated there was no close binding, with repulsive forces between molecules and reduced intermolecular attraction. Li et al. [34] reported that the SEM of carboxymethylated corn bran polysaccharide exhibited a relatively rough appearance with some pores and featured large wrinkles on the surface, which was in accordance with our results.

The designated points in JP (Figure 6(e)) and CMJP (Figure 6(f)) were analyzed by EDS to further determine the elemental composition after carboxymethylation. JP mainly contain C and O elements while CMJP mainly contain C, O, and Na elements. The presence of Na in CMJP was due to the use of NaOH in carboxymethylation. Increasing of O/C ratio in CMJP was attributed to the introduction of -COOH.

3.3. In Vitro Antioxidant Activities of Polysaccharide. DPPH is a stable free radical which could be reduced on acceptance of hydrogen donated by the antioxidant and converted to DPPH-H (the nonradical from of DPPH) [35]. As shown in Figure 7(a), in the range of 0.1–5 mg/mL, the scavenging activities of the two polysaccharides were lower than vitamin C (IC_{50} = 0.28 mg/mL). The IC_{50} value of CMJP (1.87 mg/mL) for eliminating DPPH radicals was higher than JP (1.59 mg/mL). The carboxymethylated derivatives of *Ganoderma atrum* polysaccharide are weaker in scavenging DPPH free radicals than natural derivatives [36]. At the concentration of 5 mg/mL, JP (90.47 ± 0.04%) showed higher scavenging activity than CMJP (86.02 ± 0.85%). The scavenging capacity of DPPH radical was mainly ascribed to the electron donation power to the free radicals [37]. Carboxymethylation modification did not enhance the scavenging ability of DPPH radicals of polysaccharides; the same results were obtained on the carboxymethylation modification of *Ganoderma atrum* polysaccharide [36] and *Phellinus linteus* polysaccharide [38].

Hydroxyl radical is well known as a strong oxidant which can react with most of biomolecules in living cells and resulting in severe damage or cell death [35]. As shown in Figure 7(b), in the range of 1–5 mg/mL, the two polysaccharides have been found to possess the hydroxyl radical scavenging activity in a concentration-dependent manner

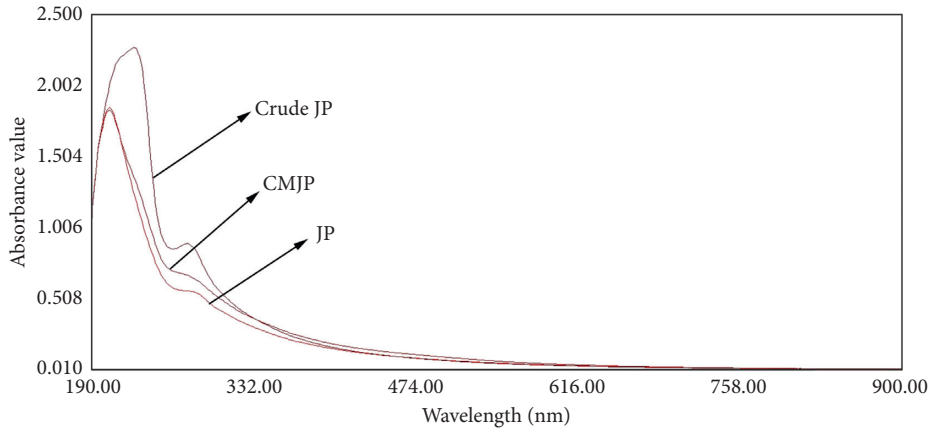

Figure 5: Ultraviolet and visible spectrophotometry (UV-Vis) spectra of crude JP, JP, and CMJP were recorded in the range of 190–900 nm.

lower than positive control (vitamin C, $IC_{50} = 0.32$ mg/mL). CMJP ($IC_{50} = 1.64$ mg/mL) showed significantly higher scavenging effect compared to JP ($IC_{50} = 2.46$ mg/mL, $P < 0.01$). These results indicated that the insertion of carboxymethyl has a noticeable effect on the scavenging abilities of hydroxyl radical. The scavenging rates of JP and CMJP were $37.34 \pm 0.68\%$ and $79.44 \pm 1.06\%$ while that of vitamin C was $99.24 \pm 0.14\%$ at the concentration of 5 mg/mL. CMJP has a strong hydroxyl radical scavenging ability and reached 80.05% of vitamin C, which indicated that CMJP could be explored as a potential antioxidant. The hydroxyl radical scavenging activity could be influenced by the donor of electron or hydrogen [39]. Xu et al. [8] reported that carboxymethylation modification significantly enhanced the hydroxyl radical scavenging ability of *Ganoderma lucidum* polysaccharides (83.7% at 5 mg/mL), which is in accordance with our results.

Superoxide radical is considered as an initial free radical, easily transformed from molecular oxygen and causes other cell damaging free radicals (H_2O_2, hydroxyl radicals) in living systems [40]. As shown in Figure 7(c), with an increase in concentration (1–5 mg/mL), the scavenging abilities of JP and CMJP were lower than that of vitamin C and that of CMJP was the weakest. The IC_{50} value of CMJP (2.59 mg/mL) for reducing superoxide radicals was higher than JP (1.77 mg/mL). According to reports, *Cyclocarya paliurus* polysaccharide also has a low scavenging effect on superoxide free radicals after carboxymethylation modification [19], which is consistent with the results of this study.

The electron-donating ability of antioxidants was measured using the potassium ferricyanide reduction method. As shown in Figure 7(d), in the range of 1–5 mg/mL, JP ($IC_{50} = 2.12$ mg/mL) and CMJP ($IC_{50} = 2.60$ mg/mL) showed a poor reducing ability compared with vitamin C ($IC_{50} = 0.18$ mg/mL). The reduction ability of JP was only $1.20 \pm 0.05\%$ at the concentration of 5 mg/mL, and the reduction ability of CMJP was significantly lower than JP ($0.94 \pm 0.01\%$). The reduction ability of JP could not be improved by carboxymethylation modification, and the same results were reported in cucumber polysaccharide [41].

In the present study, carboxymethylated modification could reduce DPPH radicals, superoxide radicals, and power but increase hydroxyl radical scavenging activity of *Jinsixiaozao* polysaccharides. Previous studies have suggested that the antioxidant activity may be related to monosaccharide composition, Mw, and structure of different kinds of polysaccharides [39, 42]. It was not a function of a single factor but a combination of several factors that might be responsible for the changes of antioxidant activities. The accurate clarification of mechanism underlying the antioxidant activity by JP and CMJP is still not fully understood, and the further in-depth works are in progress by our team.

3.4. Prebiotic Activities of JP and CMJP. Grow curves at pH 5.7 ± 0.2 of the three *Lactobacillus* strains were shown in Figure 8. The three *Lactobacillus* strains reached exponential growth phase after 4 h incubation. *L. acidophilus*, *L. plantarum*, and *L. rhamnosus* transitioned to stationary phase after 16 h, 16 h, and 18 h incubation, respectively. All of the three *Lactobacillus* strains reached stationary phase after 24 h incubation which were in accordance with the previous studies [43–45]. The effects of JP and CMJP on the proliferation of *L. acidophilus*, *L. plantarum*, and *L. rhamnosus* after 6 h, 10 h, 16 h, and 24 h incubation were shown in Figure 9. The populations of *Lactobacillus* strains raised with incubation time. Both of JP and CMJP were found to have a significant effect on the growth of probiotics, compared to control at all concentrations tested. For all tested times, it was observed that the growth of all tested *Lactobacillus* strains was remarkably higher on CMJP than JP, especially for *L. plantarum*. In addition, after 24 h incubation with the presence of increased concentration of CMJP as a carbon source, *L. plantarum* and *L. rhamnosus* showed an outstanding higher growth rate compared with CMJP that significantly increased the prebiotic activities of JP for all the *Lactobacillus* strains.

Wang et al. [46] reported that rapeseed polysaccharide with higher sugar content and lower *Mw* exert better proliferative effect on probiotic growth. However, our

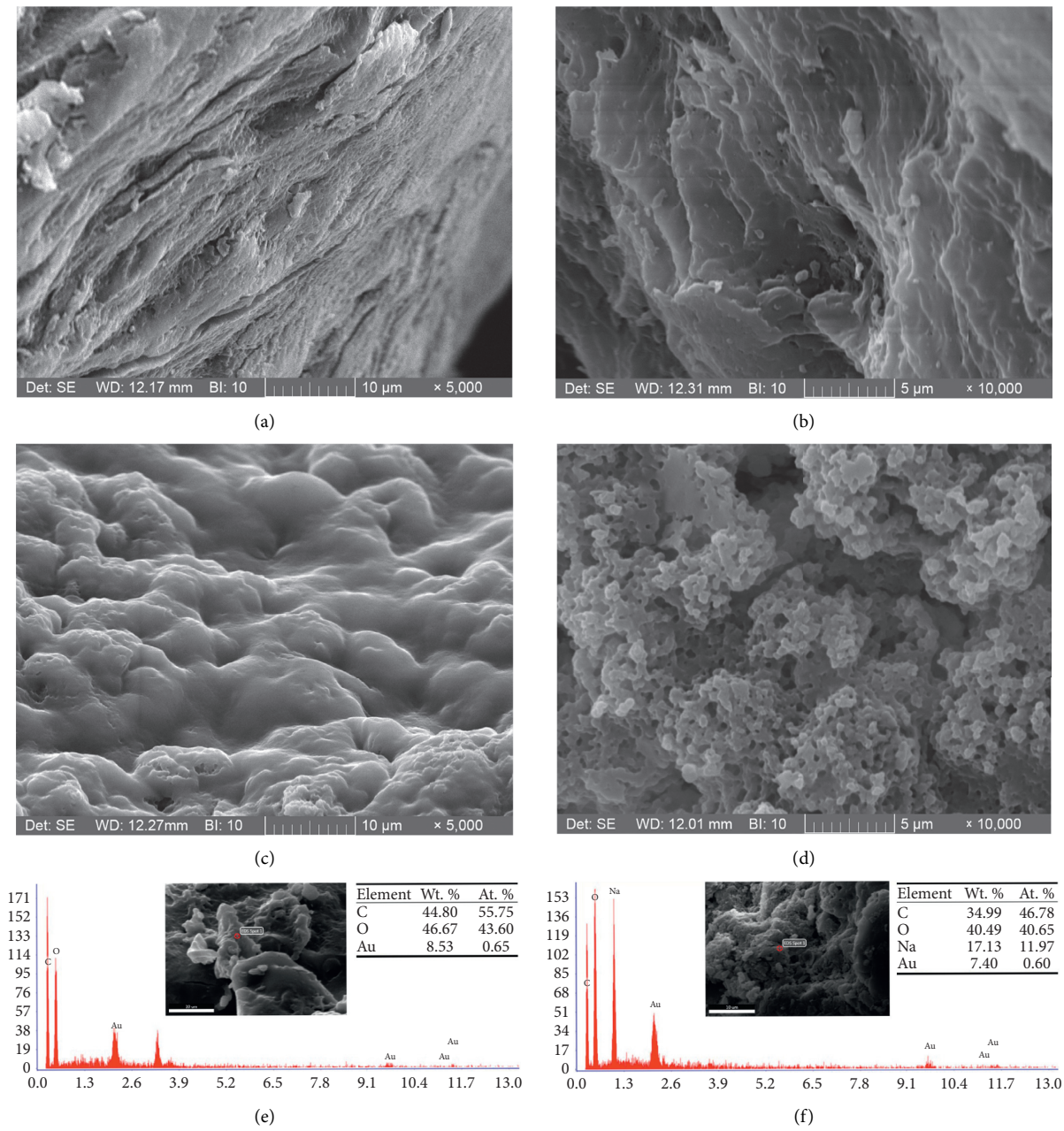

Figure 6: Scanning electron micrographs (SEM) and energy-dispersive X-ray spectroscopy (EDS) analysis of polysaccharide. (a) 5000x; (b) 10000x; (e) JP-point and carboxymethylated polysaccharide (c) 5000x; (d) 10000x; (f) CMJP-point from *Ziziphus Jujuba cv. Jinsixiaozao*.

analysis suggested that JP with higher sugar content and lower *Mw* showed weaker proliferative effect compared with CMJP. This could be due to the different physicochemical properties of different kinds of polysaccharides which need to be further investigated. Previous work also reported that more branch degree, good water solubility, and lower viscosity polysaccharides could more easily, rapidly, and completely be utilized by probiotics [46, 47]. CMJP had better prebiotic activity due to its significantly improved water solubility after the addition of carboxymethyl groups. In addition, previous studies have also shown that carbohydrates composed of arabinose, glucose, galactose, and xylose generally showed better prebiotic activities [47, 48]. JP and CMJP composed of the abovementioned monosaccharides, so both of them could promote the growth of probiotics. Besides, the different molar ratio of the monosaccharides in JP and CMJP might also attribute to their different prebiotic effects [46].

In this study, both of JP and CMJP possessed the potential as prebiotics and CMJP showed stronger prebiotic activities than JP. The mechanisms need to be disclosed, and future study will be continued to explore the *in vivo* prebiotic activities of JP and CMJP using animal model.

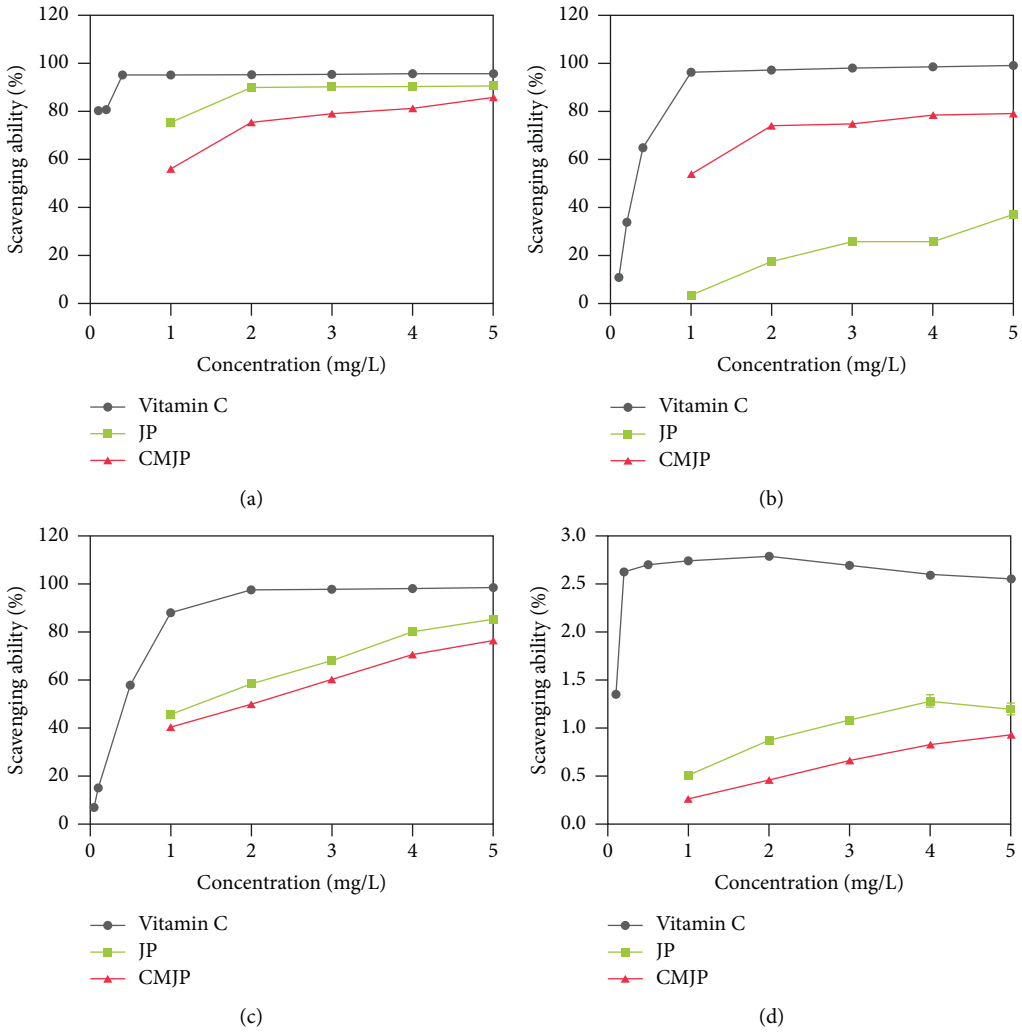

Figure 7: Scavenging effect of JP and CMJP on DPPH radicals (a), hydroxyl radicals (b), superoxide radicals (c), and reducing power (d) compared with that of vitamin C. Results were expressed as means ± SD of three parallel measurements.

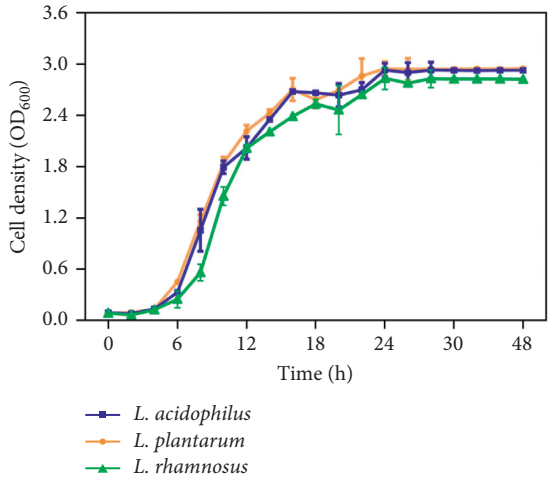

Figure 8: Growth curves of *L. acidophilus*, *L. plantarum*, and *L. rhamnosus* in MRS medium at 37°C (pH = 5.7 ± 0.2).

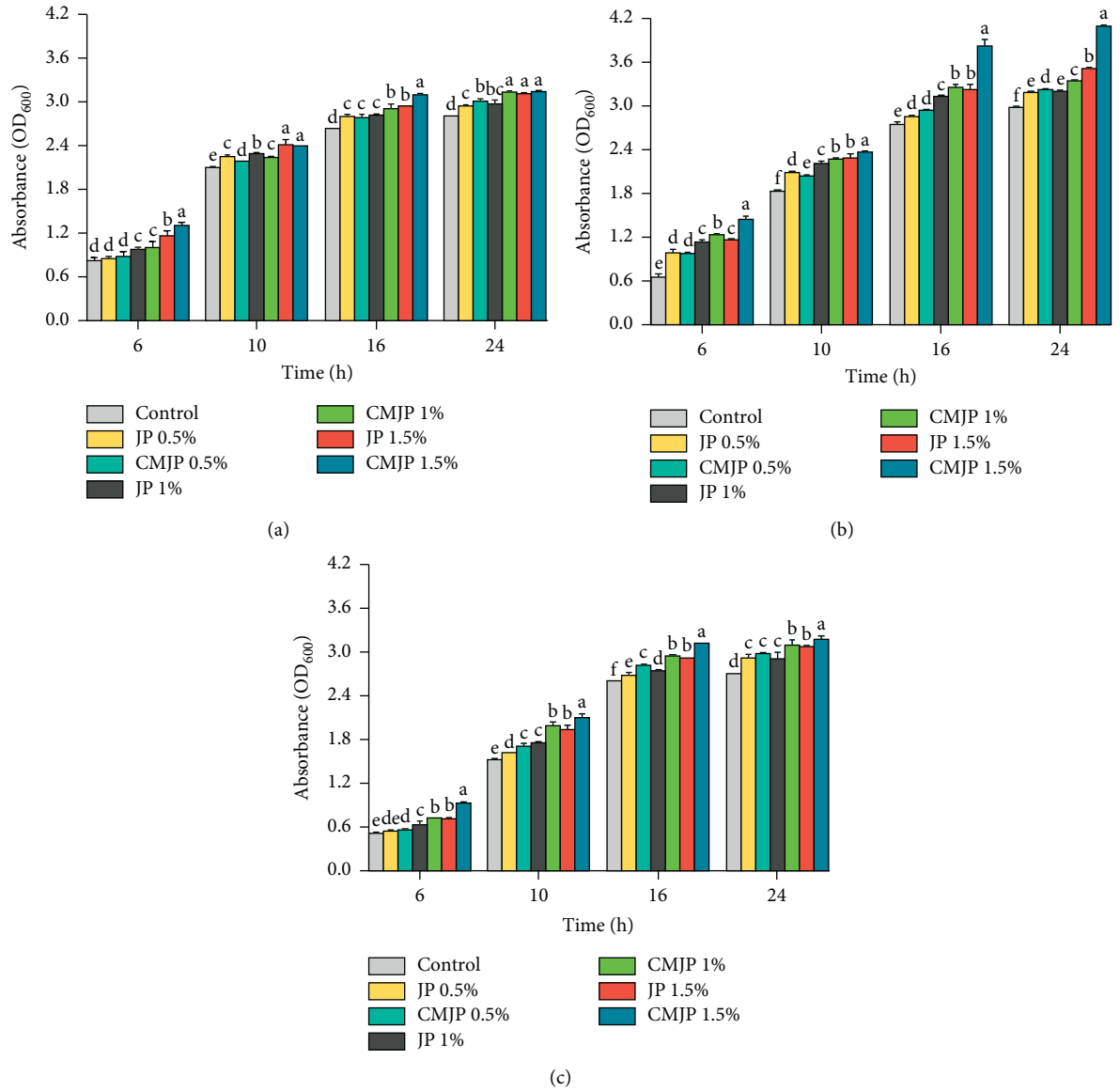

Figure 9: Effects of JP and CMJP on the proliferation of *Lactobacillus* strains after 6 h, 10 h, 16 h, and 24 h incubation. *L. acidophilus* (a), *L. plantarum* (b), and *L. rhamnosus* (c). Data with different lowercase letters represent significant differences at $P < 0.05$.

4. Conclusions

In this study, carboxymethylated *Jinsixiaozao* polysaccharides with high degree of substitution were successfully prepared. Compared with JP, introduction of carboxymethyl groups not only affected the physicochemical and structural characteristics, but promoted *in vitro* antioxidant and prebiotic activities. CMJP is a heteropolysaccharide, mainly composed of galacturonic acid, arabinose, and a small amount of rhamnose, xylose, glucose, and galactose. It exhibits higher water solubility, lower total carbohydrate content, and higher Mw. Both JP and CMJP are pseudoplastic fluids, and carboxymethylation modification can reduce the apparent viscosity and shear stress of jujube polysaccharides. FT-IR spectra showed that the carboxymethylation modification was successful, and the carboxymethylation modification can significantly enhance the hydroxyl radical scavenging activity of *Jinsixiaozao* polysaccharides. In addition, carboxymethylation can improve the proliferation of JP on *L. acidophilus*, *L. plantarum*, and *L. rhamnosus*. These results indicate that carboxymethylated jujube polysaccharide can be developed and utilized as a potential antioxidant and prebiotic. CMJP could be exploited as novel functional ingredient which is natural and safe. However, its application in functional foods or medicines needs to be combined with animal models to further study its safety *in vivo*.

Data Availability

The data used to support the study are included within the article. Raw data can be acquired from the corresponding author upon reasonable request (aocw@163.com and lyzhihuizhao@126.com).

Disclosure

Jingjing Kou is the co-first author.

Conflicts of Interest

The authors declare that there are no conflicts of interest regarding the publication of this paper.

Authors' Contributions

Runfang Feng and Jingjing Kou contributed equally to this work.

Acknowledgments

This research was financially supported by the Natural Science Foundation of Hebei Province (C2019204366) and the Key R&D Projects in Hebei Province (20327123D), Top Young Talents of Hebei Province.

Supplementary Materials

Table S1: Box–Behnken experimental design and the results for degree of substitution (DS) of CMJP polysaccharides ($n = 3$). (*Supplementary Materials*)

References

[1] J. Liu, S. Willför, and C. Xu, "A review of bioactive plant polysaccharides: biological activities, functionalization, and biomedical applications," *Bioactive Carbohydrates and Dietary Fibre*, vol. 5, no. 1, pp. 31–61, 2015.

[2] A. Zong, H. Cao, and F. Wang, "Anticancer polysaccharides from natural resources: a review of recent research," *Carbohydrate Polymers*, vol. 90, no. 4, pp. 1395–1410, 2012.

[3] Y. Cai, P. Chen, C. Wu, J. Duan, and H. Bai, "Sulfated modification and biological activities of polysaccharides derived from *Zizyphus jujuba cv. Jinchangzao*," *International Journal of Biological Macromolecules*, vol. 120, pp. 1149–1155, 2018.

[4] Y.-T. Li, B.-J. Chen, W.-D. Wu et al., "Antioxidant and antimicrobial evaluation of carboxymethylated and hydroxamated degraded polysaccharides from *Sargassum fusiforme*," *International Journal of Biological Macromolecules*, vol. 118, pp. 1550–1557, 2018.

[5] Y. Deng, M. Li, L.-X. Chen et al., "Chemical characterization and immunomodulatory activity of acetylated polysaccharides from *Dendrobium devonianum*," *Carbohydrate Polymers*, vol. 180, pp. 238–245, 2018.

[6] Z. Wang, J. Xie, M. Shen, S. Nie, and M. Xie, "Sulfated modification of polysaccharides: synthesis, characterization and bioactivities," *Trends in Food Science & Technology*, vol. 74, pp. 147–157, 2018.

[7] X. Ji, Q. Peng, Y. Yuan, J. Shen, X. Xie, and M. Wang, "Isolation, structures and bioactivities of the polysaccharides from jujube fruit (*Ziziphus jujuba* Mill.): a review," *Food Chemistry*, vol. 227, pp. 349–357, 2017.

[8] J. Xu, W. Liu, W. Yao, X. Pang, D. Yin, and X. Gao, "Carboxymethylation of a polysaccharide extracted from *Ganoderma lucidum* enhances its antioxidant activities *in vitro*," *Carbohydrate Polymers*, vol. 78, no. 2, pp. 227–234, 2009.

[9] W. Zhu, S. Zhou, J. Liu, R. J. C. McLean, and W. Chu, "Prebiotic, immuno-stimulating and gut microbiota-modulating effects of *Lycium barbarum* polysaccharide," *Biomedicine & Pharmacotherapy*, vol. 121, Article ID 109591, 2020.

[10] Q.-H. Gao, C.-S. Wu, and M. Wang, "The jujube (*Ziziphus jujuba* Mill.) fruit: a review of current knowledge of fruit composition and health benefits," *Journal of Agricultural and Food Chemistry*, vol. 61, no. 14, pp. 3351–3363, 2013.

[11] H. Rostami and S. M. T. Gharibzahedi, "Microwave-assisted extraction of jujube polysaccharide: optimization, purification and functional characterization," *Carbohydrate Polymers*, vol. 143, pp. 100–107, 2016.

[12] G. Cui, W. Zhang, Q. Wang et al., "Extraction optimization, characterization and immunity activity of polysaccharides from *Fructus Jujubae*," *Carbohydrate Polymers*, vol. 111, pp. 245–255, 2014.

[13] G. Liu, X. Liu, Y. Zhang et al., "Hepatoprotective effects of polysaccharides extracted from *Zizyphus jujube cv. Huanghetanzao*," *International Journal of Biological Macromolecules*, vol. 76, pp. 169–175, 2015.

[14] Y. Wang, X. Liu, J. Zhang et al., "Structural characterization and *in vitro* antitumor activity of polysaccharides from *Zizyphus jujuba cv. Muzao*," *RSC Advances*, vol. 5, no. 11, pp. 7860–7867, 2015.

[15] Z. Zhao, J. Li, X. Wu et al., "Structures and immunological activities of two pectic polysaccharides from the fruits of Ziziphus jujuba Mill. cv. Jinsixiaozao Hort," *Food Research International*, vol. 39, no. 8, pp. 917–923, 2006.

[16] J. Li, Y. Liu, L. Fan, L. Ai, and L. Shan, "Antioxidant activities of polysaccharides from the fruiting bodies of *Zizyphus Jujuba cv. Jinsixiaozao*," *Carbohydrate Polymers*, vol. 84, no. 1, pp. 390–394, 2011.

[17] J. Li, L. Shan, Y. Liu, L. Fan, and L. Ai, "Screening of a functional polysaccharide from *Zizyphus Jujuba cv. Jinsixiaozao* and its property," *International Journal of Biological Macromolecules*, vol. 49, no. 3, pp. 255–259, 2011.

[18] A. Staub, "Removeal of protein-Sevag method," *Methods Carbohydrate Chemistry*, vol. 5, pp. 5-6, 1965.

[19] Z.-J. Wang, J.-H. Xie, M.-Y. Shen et al., "Carboxymethylation of polysaccharide from *Cyclocarya paliurus* and their characterization and antioxidant properties evaluation," *Carbohydrate Polymers*, vol. 136, pp. 988–994, 2016.

[20] Y.-Y. Cao, Y.-H. Ji, A.-M. Liao et al., "Effects of sulfated, phosphorylated and carboxymethylated modifications on the antioxidant activities *in-vitro* of polysaccharides sequentially extracted from *Amana edulis*," *International Journal of Biological Macromolecules*, vol. 10, Article ID 10410, 2020.

[21] Z. Duan, W. Duan, F. Li, Y. Li, P. Luo, and H. Liu, "Effect of carboxymethylation on properties of fucoidan from *Laminaria japonica*: antioxidant activity and preservative effect on strawberry during cold storage," *Postharvest Biology and Technology*, vol. 151, pp. 127–133, 2019.

[22] Y. Liu and G. Huang, "The antioxidant activities of carboxymethylated cushaw polysaccharide," *International Journal of Biological Macromolecules*, vol. 121, pp. 666–670, 2019.

[23] Z. Wu, P. Zhou, J. Yang, and J. Li, "Determination of the optimal reaction conditions for the preparation of highly substituted carboxymethyl *Cassia tora* gum," *Carbohydrate Polymers*, vol. 157, pp. 527–532, 2017.

[24] G. Joshi, S. Naithani, V. K. Varshney, S. S. Bisht, V. Rana, and P. K. Gupta, "Synthesis and characterization of carboxymethyl cellulose from office waste paper: a greener approach towards waste management," *Waste Management*, vol. 38, pp. 33–40, 2015.

[25] W. Chen, W.-P. Wang, H.-S. Zhang, and Q. Huang, "Optimization of ultrasonic-assisted extraction of water-soluble polysaccharides from *Boletus edulis* mycelia using response surface methodology," *Carbohydrate Polymers*, vol. 87, no. 1, pp. 614–619, 2012.

[26] X. Guo, X. Zou, and M. Sun, "Optimization of extraction process by response surface methodology and preliminary characterization of polysaccharides from *Phellinus igniarius*," *Carbohydrate Polymers*, vol. 80, no. 2, pp. 344–349, 2010.

[27] F. Hentati, G. Pierre, A. V. Ursu et al., "Rheological investigations of water-soluble polysaccharides from the Tunisian brown seaweed *Cystoseira compressa*," *Food Hydrocolloids*, vol. 103, Article ID 105631, 2020.

[28] D. Wang, Y. Zhao, Y. Jiao, L. Yu, S. Yang, and X. Yang, "Antioxidative and hepatoprotective effects of the polysaccharides from *Zizyphus* jujube cv. Shaanbeitanzao," *Carbohydrate Polymers*, vol. 88, no. 4, pp. 1453–1459, 2012.

[29] Y. Wang, C. Zhong, J. Mao, M. Fan, and X. Wu, "Optimization of ultrasonic-assisted extraction process of *Poria cocos* polysaccharides by response surface methodology," *Carbohydrate Polymers*, vol. 77, pp. 713–717, 2009.

[30] X. Ji, F. Liu, Q. Peng, and M. Wang, "Purification, structural characterization, and hypolipidemic effects of a neutral polysaccharide from *Ziziphus Jujuba cv. Muzao*," *Food Chemistry*, vol. 245, pp. 1124–1130, 2018.

[31] L. Fan, L. Wang, S. Gao et al., "Synthesis, characterization and properties of carboxymethyl *kappa carrageenan*," *Carbohydrate Polymers*, vol. 86, no. 3, pp. 1167–1174, 2011.

[32] N. Chandía, B. Matsuhiro, and A. Vásquez, "Alginic acids in Lessonia trabeculata: characterization by formic acid hydrolysis and FT-IR spectroscopy," *Carbohydrate Polymers*, vol. 46, no. 1, pp. 81–87, 2001.

[33] N. P. Chandía, B. Matsuhiro, E. Mejías, and A. Moenne, "Alginic acids in Lessonia vadosa: partial hydrolysis and elicitor properties of the polymannuronic acid fraction," *Journal of Applied Phycology*, vol. 16, no. 2, pp. 127–133, 2004.

[34] J. Li, W. Shang, X. Si et al., "Carboxymethylation of corn bran polysaccharide and its bioactive property," *International Journal of Food Science & Technology*, vol. 52, no. 5, pp. 1176–1184, 2017.

[35] Z.-Y. Zhao, Q. Zhang, Y.-F. Li, L.-L. Dong, and S.-L. Liu, "Optimization of ultrasound extraction of *Alisma orientalis* polysaccharides by response surface methodology and their antioxidant activities," *Carbohydrate Polymers*, vol. 119, pp. 101–109, 2015.

[36] Y. Chen, H. Zhang, Y. Wang, S. Nie, C. Li, and M. Xie, "Acetylation and carboxymethylation of the polysaccharide from *Ganoderma atrum* and their antioxidant and immunomodulating activities," *Food Chemistry*, vol. 156, pp. 279–288, 2014.

[37] J.-H. Xie, M.-Y. Shen, M.-Y. Xie et al., "Ultrasonic-assisted extraction, antimicrobial and antioxidant activities of *Cyclocarya paliurus* (Batal.) *Iljinskaja* polysaccharides," *Carbohydrate Polymers*, vol. 89, no. 1, pp. 177–184, 2012.

[38] J.-Y. Shin, S. Lee, I. Y. Bae, S.-H. Yoo, and H. G. Lee, "Structural and biological study of Carboxymethylated Phellinus linteus Polysaccharides," *Journal of Agricultural and Food Chemistry*, vol. 55, no. 9, pp. 3368–3372, 2007.

[39] M.-J. Shi, X. Wei, J. Xu et al., "Carboxymethylated degraded polysaccharides from *Enteromorpha prolifera*: preparation and *in vitro* antioxidant activity," *Food Chemistry*, vol. 215, pp. 76–83, 2017.

[40] J. A. Vaz, L. Barros, A. Martins, C. Santos-Buelga, M. H. Vasconcelos, and I. C. F. R. Ferreira, "Chemical composition of wild edible mushrooms and antioxidant properties of their water soluble polysaccharidic and ethanolic fractions," *Food Chemistry*, vol. 126, no. 2, pp. 610–616, 2011.

[41] S. Chen, H. Huang, and G. Huang, "Extraction, derivatization and antioxidant activity of cucumber polysaccharide," *International Journal of Biological Macromolecules*, vol. 140, pp. 1047–1053, 2019.

[42] Y. Liu, G. Huang, and J. Hu, "Extraction, characterisation and antioxidant activity of polysaccharides from Chinese watermelon," *International Journal of Biological Macromolecules*, vol. 111, pp. 1304–1307, 2018.

[43] D. Olson and K. Aryana, "Effect of prebiotics on *Lactobacillus acidophilus* growth and resulting pH changes in skim milk and a model peptone system," *Journal of Microbial & Biochemical Technology*, vol. 4, pp. 121–125, 2012.

[44] Z. Matejčeková, D. Liptáková, S. Spodniaková, and Ľ. Valík, "Characterization of the growth of *Lactobacillus plantarum* in milk in dependence on temperature," *Acta Chimica Slovaca*, vol. 9, pp. 104–108, 2016.

[45] L. Cai, B. Chen, F. Yi, and S. Zou, "Optimization of extraction of polysaccharide from dandelion root by response surface methodology: structural characterization and antioxidant activity," *International Journal of Biological Macromolecules*, vol. 140, pp. 907–919, 2019.

[46] X. Wang, M. Huang, F. Yang et al., "Rapeseed polysaccharides as prebiotics on growth and acidifying activity of probiotics *in vitro*," *Carbohydrate Polymers*, vol. 125, pp. 232–240, 2015.

[47] S. He, X. Wang, Y. Zhang et al., "Isolation and prebiotic activity of water-soluble polysaccharides fractions from the bamboo shoots (*Phyllostachys praecox*)," *Carbohydrate Polymers*, vol. 151, pp. 295–304, 2016.

[48] F. Huang, H. Liu, R. Zhang et al., "Physicochemical properties and prebiotic activities of polysaccharides from longan pulp based on different extraction techniques," *Carbohydrate Polymers*, vol. 206, pp. 344–351, 2019.

Hindawi
Journal of Food Quality
Volume 2021, Article ID 3525667, 7 pages
https://doi.org/10.1155/2021/3525667

Research Article

Improving the Sense of Gain of Graduate Students in Food Science

Youling Wan and Zhiming Guo

School of Food and Biological Engineering, Jiangsu University, Zhenjiang 212013, China

Correspondence should be addressed to Youling Wan; wanyouling@ujs.edu.cn and Zhiming Guo; guozhiming@ujs.edu.cn

Received 21 May 2021; Accepted 10 June 2021; Published 14 June 2021

Academic Editor: Biao Yuan

Improvement of the sense of gain as an internal driving force is the key factor to improve the training quality of graduate students in food science. Utilizing Jiangsu University graduate students majoring in food science as research samples, this study analyzed the present situation of the "sense of gain" demand. We analyzed the reasonable appeals of graduate students during their study based on fully respecting and advocating students' right of speech, listened to their opinions and suggestions on higher education, analyzed the main contradictions, and further put forward a series of countermeasures. For improving the graduate students' sense of gain during the period of study, it is necessary to improve the training quality from the following five aspects: constructing high-quality courses, cultivating people's responsibilities, implementing "soft elimination" of training links, carrying out diversified extracurricular activities, and developing comprehensive quality. This research is significant in improving the training quality of food science graduate students.

1. Introduction

The postgraduate of food major is the new force of food science and technology innovation, representing the future and hope of food industry [1]. It is helpful to encourage postgraduate to devote themselves to food innovation with more enthusiasm and write a new chapter of food development. The word "sense of gain" was first put forward by General Secretary Xi Jinping at the 10th meeting of the Central Leading Group for Comprehensively Deepening Reform, and in the report of the 19th National Congress of the Communist Party of China, it was emphasized again to "ensure that all the people have a greater sense of gain in the joint construction and shared development" [2]. The group of postgraduate majoring in food science has both professional characteristics and commonalities among young people. On how to enrich and develop the "sense of acquisition" of postgraduate in school, the author combs many years of management and practical experience.

To enhance the learning enthusiasm of graduate students majoring in food and fully explore their technological innovation potential [3], Jiangsu University has launched a series of incentive policies. Why is the sense of acquisition of graduate students not strong? The reason is that the connotation of the sense of acquisition is not deeply understood, the demand of graduate students is not accurate, and the policy implementation process is lack of effective methods and countermeasures.

What is sense of acquisition? The academia has not formed a unified understanding. In ancient Chinese, "get" means "get," "get" means "accept," and "sense" means "reaction in consciousness, emotion, or psychological change caused by stimulation" [4]. Some popular concepts in foreign social governance, such as "well-being" and "subjective quality of life," are similar to "sense of acquisition" [5]. Jiang Yongmu and others believe that "sense of acquisition" refers to the positive psychological feelings of the people due to "acquisition" [6]. Wang Simin and others believe that "sense of acquisition" is not only material but also spiritual, both visible and invisible. The sense of acquisition refers to the satisfaction that can be maintained for a long time due to the acquisition of the material and spiritual level, which emphasizes a kind of real acquisition based on being for me [7]. By deeply grasping the connotation of sense of acquisition, we can have a definite aim in the implementation process of improving the sense of acquisition of food science postgraduates.

Maslow, an American social psychologist, once put forward the famous "hierarchy of needs theory," which divides people's needs into "physiological needs, security needs, belonging and love needs, respect needs, and self-realization needs" [8]. These five needs develop from low to high. The sense of acquisition is closely related to human needs at different levels, and it is the experience of satisfying individual needs. Because the needs have the characteristics of groups, the needs of different groups are not the same, even if same group at different times, the needs are not the same, so the sense of acquisition is also different. Happiness will not fall from the sky nor is it given by others, but it is obtained through active participation and hard struggle. Therefore, the promotion strategy of food science graduate students' sense of acquisition needs to be customized.

The core literacy of Chinese students' development points out that the core literacy of students' development refers to the necessary character and key ability that should be possessed and can meet the needs of lifelong and social development. It is comprehensively manifested in nine qualities: social responsibility, national identity, international understanding, humanistic background, scientific spirit, aesthetic taste, physical and mental health, learning to learn, practice, and innovation [9]. Some studies believe that students who have "sense of acquisition" are more likely to obtain positive learning experience, so "sense of acquisition" can often further promote the acquisition of new knowledge and form a virtuous circle [10]. Students' sense of acquisition lies in that they can get more knowledge and skills, give full play to their potential, respect and develop their personality, have good moral character and strong sense of social responsibility, have harmonious interpersonal relationship and healthy mind and personality, and have relatively high satisfaction with university education.

To fundamentally improve the sense of acquisition of graduate students, we should further improve the quality of education as the target and make efforts from the demand and supply sides of education [11]. On the one hand, it is necessary to deeply understand and accurately grasp the objective needs of graduate students in the new situation, listen to their opinions and suggestions on higher education, fully respect and advocate their right to speak, and meet their reasonable demands. On the other hand, we should improve the supply level of suppliers. If the school or college can update the education concept, innovate the education form, correctly understand the reasonable suggestions of students, integrate the demands of students into education, and understand the needs of students for a better life is one of the new situations of the current higher education, then the students' sense of acquisition will be further improved [8].

2. Materials and Methods

What are the main sources of postgraduates' sense of acquisition? As a university, how to improve graduate students' sense of acquisition during the semester? The school of food and biological engineering of Jiangsu University has carried out extensive questionnaires and personal interviews on this issue, which objectively reflects the current education needs of food postgraduates during the semester. This section showed the investigation and data analysis on "sense of acquisition" of graduate students majoring in food.

2.1. Questionnaire Survey

2.1.1. Sample Distribution. Questionnaire survey and interview were arranged from late November to early December every year. The design mainly considered that the new graduate students are familiar with the postgraduate study, and the fresh graduates have initially summarized their postgraduate work and thought about their career planning. The design of the questionnaire fully considered factors such as different sources of students, grade differences, academic performance, and gender ratio, which makes the sample survey more representative and typical. Food science and engineering discipline of Jiangsu University is one of the first batches of first-class key disciplines and advantageous disciplines in Jiangsu province. In this study, the samples of full-time graduate students studying in food science major degree of Jiangsu University are selected, and the sample selection is representative. At the beginning of three consecutive years, a total of 1300 questionnaires were distributed and 1197 were recovered, with a recovery rate of 92.1%. The basic characteristics of the survey sample are described in Table 1. The sample has a wide range of distribution, reasonable structure, and good representativeness.

2.1.2. Questionnaire Statistics

(1) Curriculum quality: in the evaluation of curriculum quality, 10 points were full, 11.4% of the students scored more than 9 points, 25.14% of the students scored 8-9 points, 37.11% of the students scored 7-8 points, 21.36% of the students scored 6-7 points, and 4.98% of the students scored below 6 points; 20.72% of the students thought that the quality of public courses was higher than that of professional courses, 66.72% of the students thought that the quality of public courses was similar to that of professional courses, and 12.55% of the students thought that the quality of public courses was similar to that of professional courses. The quality of public courses is lower than that of professional courses.

(2) Enterprise practice: 29.25% of doctoral students have enterprise practice experience, 28% of academic master students have enterprise practice experience, and 53.73% of professional degree master students have enterprise practice experience. Among those without enterprise practice experience, 31.91% of doctoral students are not willing to practice in enterprises, 63.76% of academic master students are not willing to practice in enterprises, and 46.99% of professional master students are not willing to practice in enterprises.

(3) Tutor satisfaction: 34.73% of the students were satisfied with the guidance of the current tutor, 43.32%

Table 1: Basic characteristics of the survey samples of graduate students majoring in food.

Variable name	Variable type	Number	Percent (%)
Gender	Male	461	38.51
	Female	736	61.49
Degree category	Academic doctoral students	229	19.13
	Academic postgraduates	444	37.09
	Master of professional degree	524	43.78
Graduate students in grade	First year doctor	59	4.93
	Second year doctor	53	4.43
	Third year doctor	48	4.01
	First year master	384	32.08
	Second year master	314	26.23
	Third year master	270	22.56
	Others	69	5.76

of the students were relatively satisfied or generally satisfied with the guidance of the current tutor, and 9.07% of the students were not satisfied with the guidance of the current tutor. Among the students who are not satisfied with the tutor's guidance, 26.90% of them can have in-depth communication with the tutor and receive the tutor's targeted guidance twice a month or more, 32.68% of them can have in-depth communication with the tutor and receive the tutor's targeted guidance once a month, and 40.42% of them can have in-depth communication with the tutor and receive the tutor's targeted guidance once a month or less.

(4) Employment pressure after graduation: 26.05% of the students thought that there was a huge contradiction between job hunting and graduation thesis, 63.39% thought that the contradiction between job hunting and graduation thesis could be adapted, and 10.56% thought that there was no contradiction between job hunting and graduation thesis.

(5) Campus cultural activities: 51.97% of the students want more recreational and sports activities for graduate students, 75.37% of the students want more scientific research activities for graduate students (subject competition, Sino-foreign exchange), 37.63% of the students want more salon activities for mental health counseling, 42.21% of the students want more salon activities for career planning, and 5.76% of the students do not care.

(6) Analysis of gender differences: in the sample of the survey, male students accounted for 38.51% and female students accounted for 61.49%, which was consistent with the proportion of male and female students in food science and engineering majors in China. Food industry was concerned with human nutrition and health and plays an important supporting role in improving people's living standards. Food majors need professional and technical talents with high engineering practice ability. Male students can play their advantages in mechanical design, engineering development, and structured scientific research. At the same time, food industry need to do food nutrition evaluation, configuration, and component analysis and detection, which can fully play the girls' meticulous and rigorous quality. By complementing each other, boys and girls contribute to food technology innovation together.

2.2. Personal Interview. According to the questions reflected in the questionnaire, some graduate students were randomly selected for one-to-one interview.

(1) Graduate students believe that the teacher's classroom content and scientific research is not closely related, lack of curriculum challenge, and students' sense of classroom acquisition is low; there are more theoretical courses, less practical courses, hope to strengthen the reform of curriculum teaching mode, add practical courses, and improve graduate students' enterprise cognition.

(2) The enterprise practice problems of professional degree master students are prominent, and they will face more unknown challenges when they join social practice. The students are not active and afraid of difficulties. The ability of graduate students to enter the enterprise has not been improved, but it affects the quality of graduation thesis, and the tutors are not at ease. The graduate students have not yet established a complete engineering thinking, and participating in the project will affect the R&D progress of the enterprise, and the enterprise is not willing to accept graduate practice.

(3) Graduate students reflect that the daily guidance of tutors is biased towards the dialogue between "boss" and "staff," tutors tend to pursue the quality of academic guidance, and the concern and effective communication for graduate students' personal growth are not enough. Students and tutors are just "fellow researchers" in scientific research, and it is difficult to form a close relationship similar to a partner.

(4) Most of the supervisors and postgraduates control the quality of their dissertations loosely first and then tightly. Three or four months after graduation, it is

difficult to give consideration to both job hunting and careful revision of dissertation, and the contradiction between teachers and students is easily intensified.

(5) Students' practical ability is weak in school, and the current education mechanism tends to theoretical learning, less experiential activities. It is hoped that more campus cultural practice activities will be beneficial to the improvement of comprehensive abilities, so that graduate students can participate in them personally, exercise their thinking in practical experience, strengthen their ability to distinguish right from wrong, firmly build the cornerstone of "Three Outlooks," and cultivate good moral quality [12].

3. Results and Discussion

According to the questionnaire survey and personal interview, graduate students are not "very satisfied" or "generally satisfied" in course teaching, enterprise practice, teacher-student relationship, dissertation, and campus cultural activities. Their sense of achievement needs to be further improved. Combining with the characteristics of food science discipline and the general needs of graduate students, Jiangsu University has tried to introduce a series of measures to improve the sense of gain of graduate students from five aspects during the study.

3.1. Cultivate Quality Courses without Breakpoints and Improve the Sense of Gain in Postgraduate Class. Give full play to the characteristics of food engineering in Jiangsu University, attach equal importance to both theory and practice in curriculum design, and establish a professional curriculum system [13]. The classroom teaching effect is evaluated comprehensively by the students' class participation and reflection degree, and the curriculum system is optimized. To improve the quality of postgraduate courses, it is possible to strengthen the integration and refinement of diversified teaching teams through individual tracking, highlight the individual design of courses, actively explore the case discussion and interactive classroom teaching modes that are flipped between teachers and students, and put more emphasis on the learning effect of course teaching evaluation. It is divided into four stages:

(1) For the teaching team applying for the construction of high-quality courses, the project defense will be carried out to mainly examine the teaching philosophy, teaching characteristics and construction objectives of the course leader, highlight the characteristics of the course, and the realization path of improving students' ability. After passing the defense, the teaching team will enter the cultivation period of the construction of high-quality courses.

(2) For selected high-quality courses, students will be given key marks when selecting courses, and guide students to participate in the evaluation of the teaching effect. In addition, the school follow-up the whole process and set up an expert group composed of the head of discipline, the school's leader in charge, and the graduate education supervisor, to select the part of the content to listen to the class and evaluate the teaching, to check whether the design of the classroom teaching is consistent with the defense concept, students' participation in the class, and the actual teaching effect.

(3) After the lecture, the expert group will meet and evaluate on the spot, work with the teachers to continuously optimize and improve the teaching, and put forward targeted suggestions, and in the later course teaching, according to the form of the student questionnaire to view the curriculum teaching mode before and after the reform of the comparative effect.

(4) The school and college will give policy rewards to the quality courses that have passed the acceptance inspection, for example, the teaching workload increases the performance coefficient, and the course acceptance inspection is a must for the evaluation of the professional title of teaching teachers. In addition, excellent courses can open demonstration classes in the whole school, accept most teachers and students' on-site observation, give teachers more peer recognition, and better play the role of demonstration radiation of the construction results of excellent courses.

After three years of cultivation and practice, the School of Food and Biological Engineering of Jiangsu University has achieved remarkable results. It has formed key postgraduate construction courses such as special subject of food science and technology, fundamentals of food nondestructive testing, and excellent postgraduate courses such as advanced biochemistry and modern microbiology. In addition, food nondestructive detection techniques, a postgraduate course for overseas study, was selected as an excellent course taught in English in Jiangsu Province.

3.2. Strengthen the Tutors' Moral Education and Enhance the Graduate Students' Sense of Achievement in Scientific Research. Tutors are the first responsible person for the cultivation of graduate students, the model for the practice of scientific research and academic ethics, and the guide for the growth of graduate students [14]. To strengthen the role of mentor, we can explore the following four aspects:

(1) Establish the "eight guides" duty evaluation mechanism. Build a test platform for tutors' moral education and take the evaluation results of graduate students' tutors as an important basis for their evaluation. By standardizing the relevant assessment work of graduate tutors and highlighting the "first evaluation standard" of teachers' ethics, we can further ensure that there is no blind spot in the effective implementation of the responsibilities of tutors' moral cultivation.

(2) Implement the old tutor annual training mechanism. It regularly organizes graduate supervisors to learn the relevant rules and regulations of the current state, province, and university through concentrated learning, expert reports, and group discussion, insists on repeated learning and multifacet learning, and carries out exchange of experience in postgraduate training. Establish the network question bank of "graduate tutor professional knowledge learning," implement tutor professional knowledge self-study on a regular basis, and effectively improve the tutor's guidance ability and guidance quality.

(3) Build an infiltrating teacher-student communication bridge to enhance the emotional communication between teachers and students. Set up graduate student information liaison in the mentor group, group liaison generally be held by a senior graduate student, effectively make up for the inadequacy of his fellow classmates' peer psychological support, a more accurate understanding of the junior graduate line information, become a mentor "right-hand man," alleviate the pressure of the teacher to students' psychological health education work, and form a good interactive mechanism between teachers and students.

(4) Set up advanced models and set up a mentor demonstration team. The construction standard of "Model Tutor Team" was issued, and columns were set up with the help of network media to publicize the characteristic practices of the demonstration team and establish the awareness of benchmarking. Give the outstanding mentor team a sense of honor and play the vanguard role of the outstanding team. Establish a dynamic assessment mechanism for demonstration teams. For the teams that have implemented it in place, award the enrollment quota; for the teams that do not meet the assessment standards, cancel the honorary title of demonstration.

3.3. Strictly Cultivate the Link of "Soft Elimination" to Improve the Sense of Gain of Postgraduates. Try to set up a collective thesis for master's degree and make clear the system of "10% delay passing" for the first time to ensure the degree thesis from the source to better quality assurance. With soft elimination as the incentive measure, the internal driving force of graduate students majoring in food has been improved, so that they can better complete their studies and make scientific and technological innovations. By doing what they have done, the sense of achievement and gain has been improved. The collective thesis proposal can play a good role in promoting the department, the supervisor, and the graduate students:

(1) The faculty level to promote college (discipline) strengthens the management of the dissertation work. The opening information is publicized in advance, and the graduate education supervisors of schools and colleges can participate in the on-the-spot inspection of the opening, collectively showing the scientific research progress, achievements, and level of all the same graduate students in the discipline, promoting the exchange of graduate students across research groups and research directions, and giving birth to scientific research inspiration.

(2) At the level of tutors, it encourages tutors to pay attention to students and strengthen guidance. Before the examination of the proposal, the proposal content must be examined by the tutor. When the supervisor determines the topic selection direction and research objectives, he is bound to discuss with the students for many times, including the scope and difficulty of the topic selection, research basis, research conditions, problems to be solved, technical route, and other aspects. Taking into account the existing basis and possible development level of the students, it is more conducive to the successful completion of the project.

(3) At the student level, it stimulates the graduate students to have more subjective initiative and sense of urgency, improves the students' attention to the dissertation, as well as their investment of time and energy in the dissertation, and fundamentally put an end to the past situation of "the tutor cannot find graduate students.

3.4. Create Diversified Extracurricular Activities to Enhance the Sense of Gain on the Campus of Graduate Students. Diversified extracurricular activities are a cup of tea for graduate students after scientific research and study, which can constantly relieve the boring pressure of the scientific research work and is a fertile soil for graduate students to improve their innovation and practice ability. The main after-school activities that we tried to carry out include the following:

(1) Strengthen the coordination and guidance of the discipline innovation forum and stimulate the enthusiasm of academic exchanges between teachers and students. Every year in November, Jiangsu University holds a forum for Chinese and foreign graduate students. Food science majors and life sciences, engineering disciplines, materials science, and other disciplines intersect. Ideas are generated through communication, and sparks are generated through collision. In 2020, it will host the Academic Innovation Forum of "Food Intelligent Testing and Processing" for Postgraduates in Jiangsu Province, break the intercollegiate barriers in food science discipline, encourage and guide cross-university academic exchanges, show themselves, build consensus, inspire, and promote each other. Through academic exchanges, the practical ability of graduate students can be improved to meet the needs of students' personalized development.

(2) To carry out the teachers and students joint brand of sport team, actively organize a variety of interesting and diverse activities between teachers and students, guide the graduate students and teachers out of the lab and out of the studio, fitness, compete, and promote the teachers and students and brand activities as a lubricant of the scientific research work, teachers and students to cooperate with team spirit, and improve the relationship between teachers and students. Creating a new model of education with warmth and feelings is more conducive to enhancing the cohesion of the scientific research community between teachers and students.

(3) The group organization is for graduate student's career planning, fire safety drill, psychological counseling salon second class activities, to create the "graduate student psychological group counseling room" and "graduate employment entrepreneurship training rooms". [15]. To provide graduate students salon and discussion, interview skills, and entrepreneurial skills, alleviate psychological pressure and regulate mood, effective support, and help graduate students devote themselves to scientific research.

4. Conclusion

To improve the sense of gain of food science graduate students during their study is to improve the quality of postgraduate training, not forget the original intention of benefiting the people and the country, and make more positive contributions to the development of China's food industry and to meet people's yearning for a better life. Under the background of the new era, we should not only have a clear understanding of the training objectives and requirements of talents in the new era from the perspective of social development but also affirm the dominant position of postgraduates from the perspective of "people-centered" and attach importance to improving the sense of gain of postgraduates from the perspective of training path. Through this survey, it is found that multidimensional information feedback channels are the most direct means to obtain the effectiveness of policy implementation. Subsequently, diversified student information feedback mechanisms will be established, such as network mailbox, WeChat public number, the graduate student class group interviews, and teacher-student cadre team liaison investigation, fully understand the graduate student to the curriculum, teacher and scientific research platform, management mechanism, and other aspects of evaluation and rationalization proposal, and real innovation thinking puzzles, for example, it is necessary to strengthen the construction of scientific research platform and faculty, increase the investment in education hardware, and strengthen the Sino-foreign cooperation in running double degrees, so as to form a collaborative education and promote the development of higher quality graduate education. To take multiple measures at the same time, keep pace with the times and improve the sense of gain of food science graduate students, with full enthusiasm into the field of food science and technology innovation.

Data Availability

The data used to support the findings of this study are available from the corresponding author upon request.

Conflicts of Interest

The authors declare that they have no conflicts of interest.

Acknowledgments

The authors acknowledge the financial support provided by the Research on the Teaching Reform of Postgraduate Education in Jiangsu Province, Research on the Planning and Development of Higher Education in Jiangsu University (G201912), Project of Evaluation Committee of Jiangsu Institute of Higher Education (2020-Y04), and Outstanding Young Teachers of Blue Project in Jiangsu Province.

References

[1] X. Cao and S. Li, "The connotation of the times of acquired sense and reference from foreign experiences," *People's Forum·Academic Frontier*, vol. 2, pp. 18–28, 2017.

[2] Z. Guo, X. Zou, S. Jiang, Q. Chen, and J. Zhao, "The construction of the physics course group of the food major for new engineering subjects supports the cultivation of engineering talents," *Food and Machinery*, vol. 34, no. 8, pp. 216–219, 2018.

[3] Y. He and F. Zuo, *Research on the Path of Improving College Students' Educational Acquisition in the New Era*, pp. 147–149, Beijing Education Beijing Education (Higher Education), Beijing, China, 2018.

[4] Y. Jiang and X. Zhang, "Sharing development and building a well-off society in an all-round way," *Journal of Ideological and Theoretical Education*, vol. 3, pp. 74–78, 2016.

[5] S. Ma and T. Zhang, "Research on the cultivation system of food professionals under the great discussion of educational thoughts," *Food Industry*, vol. 40, no. 3, pp. 235–237, 2019.

[6] X. Su, Q. Li, L. Miao, D. Qin, W. Wu, and C. Liu, "Exploration of the engineering ability training mechanism for food science and engineering students under the background of "new engineering"" *Food and Fermentation Industry*, vol. 46, no. 18, pp. 287–290, 2020.

[7] K. Wang and W. Chen, "A probe into the ways to improve the sense of educational acquisition of college students from the perspective of humanism," *Journal of Huainan Teachers College*, vol. 18, no. 5, pp. 132–134, 2016.

[8] S. Wang and J. Zhang: Let the people have more "sense of gain", https://epaper.gmw.cn/gmrb/html/2015-03/14/nw.D110000gmrb_20150314_1-05.htm 2015.

[9] L. Wei, "Research on the cultivation of innovation and entrepreneurship ability of food majors from the perspective of "craftsman spirit"" *Food Research and Development*, vol. 41, no. 12, p. 241, 2020.

[10] Q. Wei, L. Li, Y. Du et al., ""Platform-project-curriculum" interaction to promote the path exploration of students' innovation ability," *Food and Fermentation Industry*, vol. 46, no. 7, pp. 296–300, 2020.

[11] J. Wen, "Research on AIA three-dimensional degree of acquired sense of college students in the new era," *Journal of Guangzhou City Vocational College*, vol. 12, no. 1, pp. 97–100, 2018.

[12] J. Xi, "Decisive victory to build a moderately prosperous society in an all-round way, to win the great victory of socialism with Chinese characteristics in the new era-a report at the 19th National Congress of the Communist Party of China (excerpt)," *Heihe Academic Journal*, vol. 1, pp. 2–193, 2018.
[13] X. Yan, "Research on the sense of acquisition of contemporary college students," *Journal of Guangxi Youth Leaders College*, vol. 29, no. 3, pp. 18–22, 2019.
[14] X. Yang, "Cultivating newcomers of the era should pay attention to the issue of sense of gain," *Journal of the Party School of Shanxi Provincial Committee of the Communist Party of China*, vol. 41, no. 3, pp. 24–27, 2018.
[15] S. Yi, X. Li, H. Liu, Y. Ge, J. Li, and F. Bai, "Relying on the innovation and practice of the "four-dimensional drive" training model for food graduate students with first-class disciplines," *Food Industry*, vol. 41, no. 3, pp. 251–254, 2020.

Hindawi
Journal of Food Quality
Volume 2021, Article ID 5536148, 11 pages
https://doi.org/10.1155/2021/5536148

Research Article

Protease Hydrolysates Ameliorates Inflammation and Intestinal Flora Imbalance in DSS-Induced Colitis Mice

Lixia Zhao,[1] **Weijie Tian**,[1] **Wenjuan Qu**,[2] **Ting Li**,[1] **Junsong Zhu**,[1] **and Haile Ma**[2]

[1]*School of Food and Biological Engineering, Jiangsu University, Zhenjiang 212013, China*
[2]*Institute of Food Physical Processing, Jiangsu University, Zhenjiang 212013, China*

Correspondence should be addressed to Haile Ma; mhl@ujs.edu.cn

Received 27 February 2021; Revised 26 April 2021; Accepted 29 May 2021; Published 7 June 2021

Academic Editor: Shengbao Cai

Wheat germ and fish skin usually has not been completely utilized and sometimes may be discarded, thus causing a lot of waste. Here, we aim at exploring the therapeutic anti-inflammatory effects of protease hydrolysates of wheat germ and fish skin on the ulcerative colitis (UC) mice. In the current study, wheat germ protein hydrolysates (WGPH) and fish skin gelatin hydrolysates (FSGH) treated mice had a longer colon than the DSS-induced mice. Moreover, protease hydrolysates reversed DSS-induced gut dysbiosis. Protease hydrolysates were likely to shift the balance of the intestinal flora on inflammation. In summary, these findings suggested that protease hydrolysates might serve as a latent therapy for UC treatment.

1. Introduction

Ulcerative colitis (UC) is recognized as a type of chronic and recurrent inflammatory bowel disease (IBD) [1]. Unfortunately, UC patients often experienced abdominal pain and bloody diarrhea, and the course of the disease is quite long [2]. Additionally, the recurrence of UC is always along with grave complications and disappointing prognosis [3, 4]. Moreover, the incidence of UC has been rising year by year, particularly in the developed countries [5]. However, the etiology of UC is still unclear. Thus, it is emerging to find effective therapy for UC.

The continuous improvement in the understanding of UC has evidenced that heredity, environmental factors, dietary habits, immune factors, and gut microbiota are intently related to the occurrence of UC [6, 7]. Among them, the interaction between gut microbiota and the host immune system is considered as the major origin of colonic inflammation [8, 9]. Moreover, the amount of some ill bacteria (including *Bacteroides fragilis, Escherichia coli*, and *Helicobacter*) is flourishing in the UC patients' intestinal tract, which is markedly higher than that in healthy ones and is probably connected to the incidence of UC [10, 11]. On this basis, researchers have observed the correlation between UC and gut microbiota [12]. The ordinary gut microbiota composes the intestinal mucosal barrier of the human body and shields the intestines [13]. Once the intestinal flora is disturbed, it may cause inflammation of the colon [14].

The incidence of inflammation is increasing year by year, and the drugs for treating inflammation are always expensive along with side effects [15, 16]. Given the concerns about the side effects of long-term use of these drugs, food-based functional food as alternatives to anti-inflammatory drugs has become a research hotspot [17]. A number of studies have reported that some nutrients or food components exert beneficial effects on UC well beyond their conventional nutritional value [18]. Previous studies have shown that the wheat oligopeptides have a protective effect on DSS-induced colitis in mice [19, 20]. Vitexin and anapigenin-8-C-glucoside have been shown that they could possess the positive effects on human health as well as gut microbiota [21]. Corn proteolysis product has been proved to exert a good anti-inflammatory effect on trinitrobenzene sulfonic acid-induced colitis in rats [22]. Fish protein hydrolysates have multiple biological activities, containing antioxidative, anticancer, lipid homeostasis modulation, antihypertensive activities, anti-inflammatory, and neuroprotective effects which make them promising nutraceutical ingredients for application in food [23]. Moreover, oral

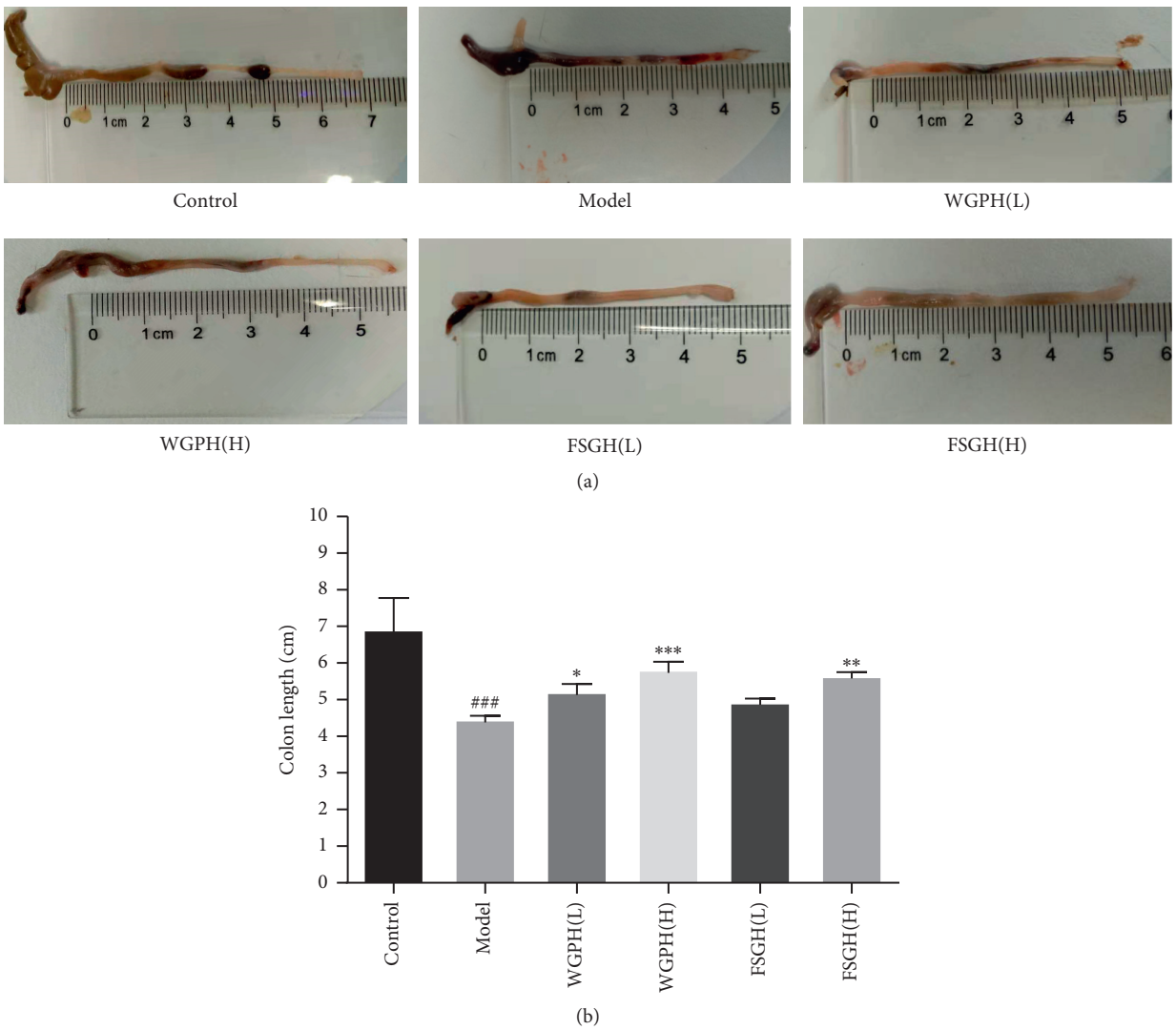

Figure 1: Protease hydrolysates could alleviate the symptoms of DSS-induced UC mice. (a) Protease hydrolysates validly improved the shorten of the colon tissue. (b) Quantitative results of colon length in different groups. $^{###}P < 0.001$ vs. control; $^{*}P < 0.05$, $^{**}P < 0.01$, and $^{***}P < 0.001$ vs. model.

bovine collagen peptides have also been proved to obsess the analgesic and anti-inflammatory effects on patients with arthritis [24].

However, the specific mechanism of the effects of WGPH and FSGH on colitis is still unclear. Therefore, the DSS-induced UC mouse model was utilized to detect the intervention of foodborne peptides on UC and observe the effects of peptides on the intestinal tract, which would provide new idea for the treatment of UC.

2. Materials and Methods

2.1. Protein Isolation Preparation. Wheat gluten protein peptide was extracted from our laboratory (Jiangsu Jiangda Wukesong Biotechnology Co., Ltd). Male c57 bl/6 mice, 6–8-week-old, weight 18~24 g, were selected and purchased from Jiangsu University Experimental Animal Center, license SCXK (Su) 2018–0012. Dextran sulfate sodium salt (DSS) salt buy in MP Biomedicals Company.

The raw wheat germ was obtained and cleaned to remove contaminants. N-hexane (1 : 8, w/w) was used to defat the wheat germ flour [25, 26], and the defatted wheat germ flour (DWGF) was scattered into the 1M NaCl solution (1 : 8, w/v) and stirred for 30 min at ambient temperature [27, 28]. Then, the pH was adjusted to 9.5. After stirring for 30 min, the suspension was centrifuged at 8,000 g for 20 min at 4°C. Then, the pH of the supernatant was adjusted to 4.0 and centrifuged again at 8,000 g for 20 min at 4–8°C. Finally, the precipitate was obtained [29, 30].

The skin of tilapia was homogenized with distilled water (1 : 20, w/v). Alcalase (7674 U/g protein) was added to the suspension, and the pH was adjusted to 9.0. Then, it was hydrolyzed for 4.92 h at 55°C. Afterwards, the reaction was terminated by heating the solution in a waterbath at 95°C for 20 min. The supernatant was

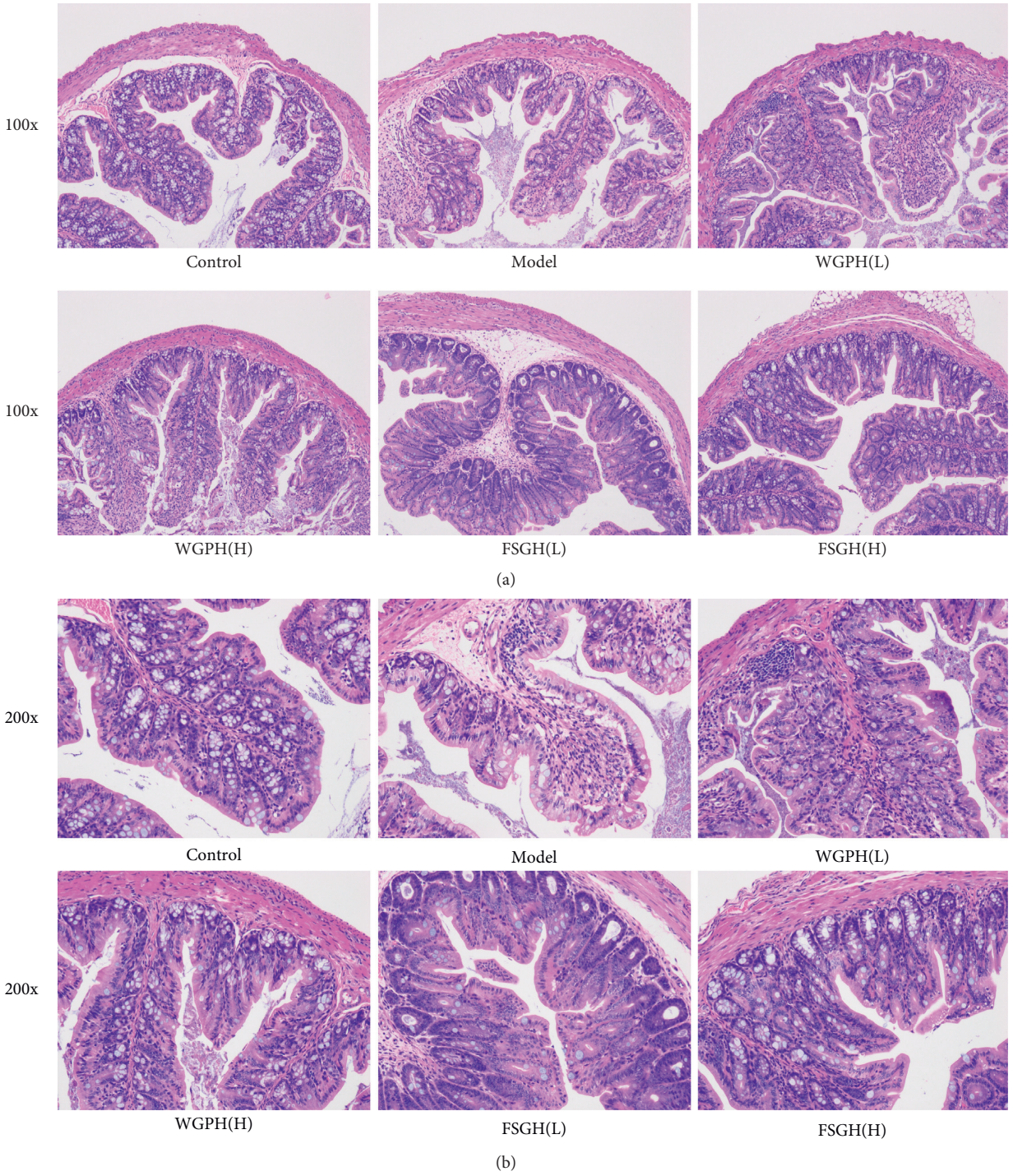

Figure 2: Histological observation and evaluation. (a) Representative photos of colonic segments (×100). (b) Representative photos of colonic segments (x200).

collected by centrifugation at 10,000 rpm for 15 min and then freeze-dried [31].

2.2. The Design of Experiments. Sixty male C57BL/6 mice (6–8-week-old) were obtained from Jiangsu University and housed at a constant temperature and humidity room. All mice were divided into 6 groups randomly with 10 mice each; they were the control group, DSS group, DSS + WGPH (300 mg/kg·d), DSS + WGPH (600 mg/kg·d), DSS + FSGH (300 mg/kg·d), and DSS + FSGH (600 mg/kg·d). We treated the mice in the control group with pure water, and 3% DSS solution was supplied to the other five groups to induce UC disease. The WGPH and FSGH were orally administrated once a day at the same time according to the abovementioned volume for 7 days. The control and DSS groups were given normal saline, and all

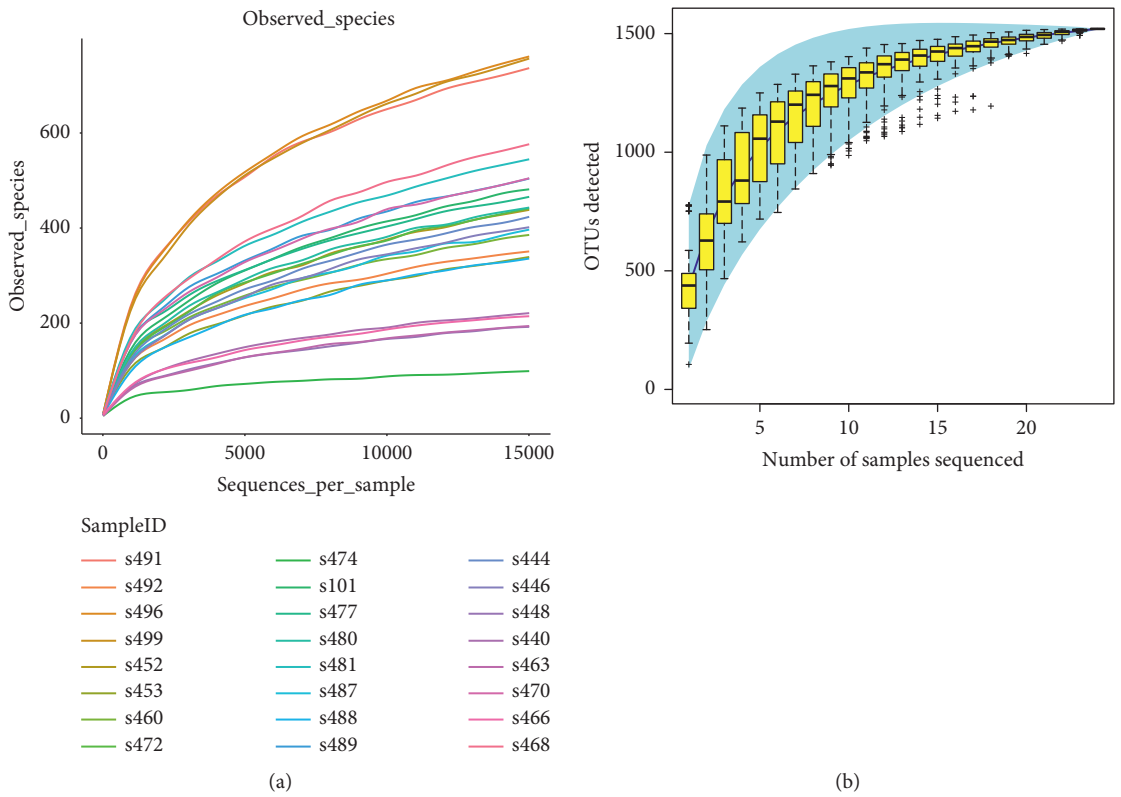

Figure 3: Rarefaction curves species (a) and accumulation curves (b) OTUs clustered at 97% sequence identity of all the samples.

the mice were endowed for cervical dislocation on the 15th day for anatomical sampling. All experiments were approved by the Institution Animal Care and Use Committee of Jiangsu University (UJS-IACUC-201920960) and met the guidelines of the National Institutes of Health Guide for the Care and Use of Laboratory Animals.

2.3. HE Assay. The mice' colon tissues were cut into 5 μm thick slices. After dewaxing and hydration, the slices were incubated in hematoxylin solution for about 3–5 min and later hatched in ethanol hydrochloric acid for 15 sec [32]. Subsequently, the sections were washed by PBS solution, and then, the sections were placed in eosin solution and incubated for about 2-3 min. Ultimately, the slices were dehydrated and transparent, and then, the staining results could be observed under a light microscope (Olympus, Tokyo, Japan) [33].

2.4. Gut Microbiota Analysis. For gut microbiota analysis, first, we collected the mice fecal samples and obtained the DNA of different groups through the Stool DNA Kit (Omega Bio-Tek, Inc., USA) according to the manufacturer protocols. Then, the spectrophotometer, as well as 1% agarose gel electrophoresis, was separately used for detecting the concentration and purity of microbial DNA. Next, the V3-V4 region of the bacteria 16S rRNA was enlarged, and two general primers 343F (TACGGRAGGCAGCAG) and 798R (AGGGTATCTAATCCT) were used through PCR assay. The conditions of PCR assay were listed as follows: primary denaturation at 94°C for 5 min; 32 cycles of 94°C for 30 sec, annealing at 55°C for 30 sec, and extension 72°C for 60 sec; and the final step was an extension at 72°C for 7 min. PCR amplification was carried out in a total volume of 25 μL reaction mixture including 3 μL BSA, 12.5 μL 2xTaq Plus Master Mix, 30 ng of template DNA and ddH_2O, and 1 μL of each primer. We collected and purified the PCR products via QIAquick Gel Extraction Kit (QIAGEN, Germany). After that, we prepared the amplicon pools for sequencing, size, and quantity of the amplicon library through the Agilent 2100 Bioanalyzer (Agilent, USA) as well as the Library Quantification Kit for Illumina, separately [12].

Next, the samples were then sequenced through the Illumina HiSeq platform following the manufacturer's instructions (LC-Bio). Flash was used to assign, truncate, and merge the paired-end reads. We assigned the sequences with ≥97% similarity to the same operational taxonomic units (OTUs) via VSEARCH (v2.3.4). After choosing the representative sequences for each OTU, the RDP (Ribosomal Database Project) classifier was then used to assign the taxonomic data. Then, we used the map software (V 7.310) to investigate the differences of the dominant species and utilized the QIIME (Version 1.8.0) to calculate all of the indices in our samples [34].

2.5. Statistical Analysis. SPSS (18.0 version, SPSS, Inc., USA) and GraphPad (6.0 version) were used to determine each group's statistic data. All data were presented as means ± SD.

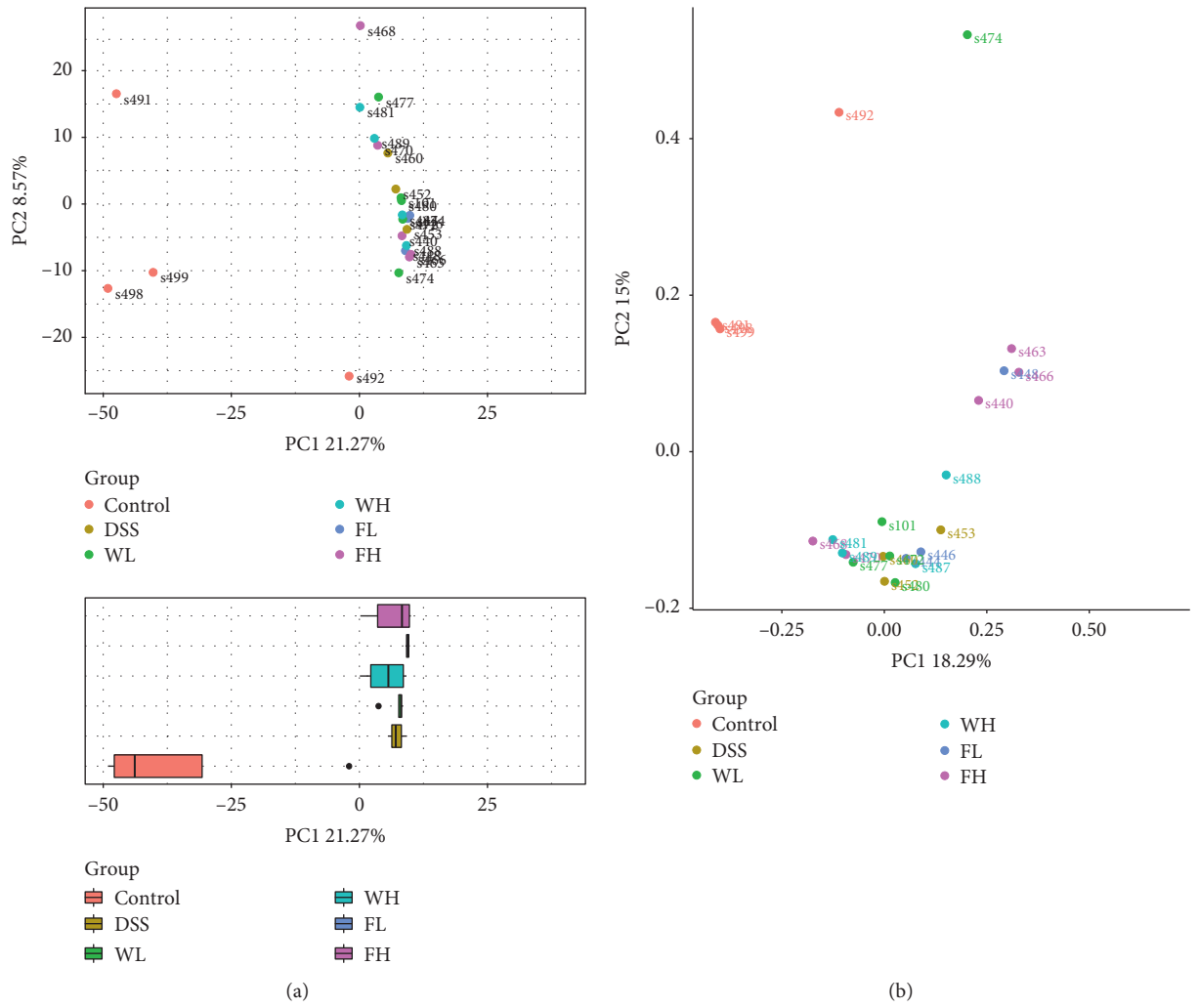

Figure 4: The variation of fecal microbiota based on 16S rRNA gene sequences among different treatment group samples including principal component analysis (PCA) (a) and principal coordinates analysis (PCoA) (b).

All experiments were independently implemented at least three times. Moreover, Student' *t*-test and one-way ANOVA were used to compare two groups or more than two groups. $^{*}P < 0.05$; $^{**}P < 0.01$; $^{***}P < 0.001$.

3. Results

3.1. Protease Hydrolysates Could Alleviate the Symptoms of DSS-Induced UC Mice. As shown in Figures 1(a) and 1(b), it could be seen that the colon length was markedly shortened in the model group, when comparing with control group. The colon length in the DSS + WGPH and DSS + FSGH groups was significantly longer than that in the DSS group. The colon length of the high-concentration group of DSS + WGPH was longer than that of the low-concentration group. Compared with the model group, the colon longer changes induced by different concentrations of WGPH in mice were alleviated to a certain extent, and the improvement effect of high-concentration (600 mg/kg·d) was better than that of low-concentration WGPH (300 mg/kg·d).

3.2. Histological Observation and Evaluation. As shown in Figures 2(a) and 2(b), the control group expressed normal colonic mucosal epithelium and H&E staining of the blank group showed normal colonic mucosal epithelium. On the contrary, the model group exhibited broad-scale glandular destruction and notably appeared inflammatory cell infiltration in the submucosa with the induce of DSS. What is more, compared with the model group, DSS + WGPH and DSS + FSGH groups both expressed a milder degree of congestion and edema.

3.3. Microbial Diversity Analysis

3.3.1. α-Diversity Analysis. As shown in Figure 3, the rarefaction curve (Figure 3(a)) and species accumulation curves (Figure 3(b)) evidenced that the curve of each treatment group tends to be flat, which indicated that the amount of sequencing data was reasonable and the sample depth was reliable. It has been showed that the sample size and the library volume we constructed were large enough to represent the vast majority of bacteria in the human intestinal

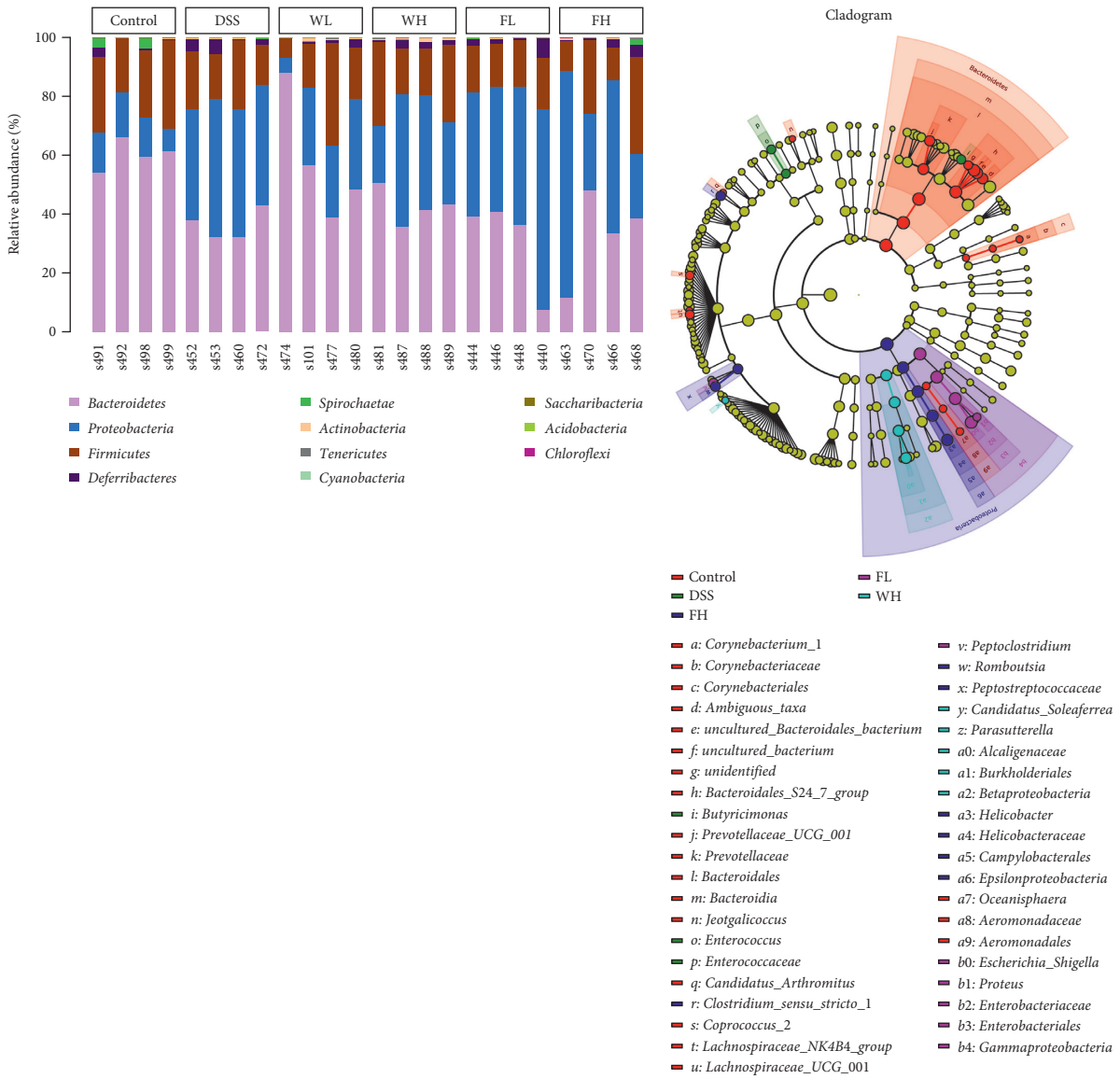

(a) (b)

Figure 5: Continued.

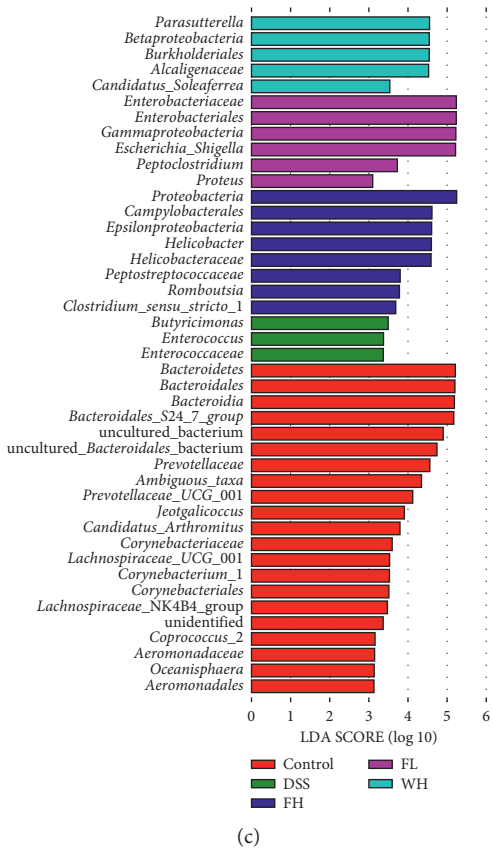

(c)

Figure 5: Structural comparison of fecal flora among different groups. (a) Bacterial taxonomic profling at the phylum level. (b) LEfSe analysis of fecal flora among different groups. (c) LEfSe analysis showing the distribution histogram of different groups in gut microbiota (LDA score > 4).

flora, and the species richness and library diversity were saturated.

3.3.2. β-Diversity Analysis. The results of principal component analysis (PCA) (Figure 4(a)) and principal coordinate analysis (PCoA) of weighted (Figure 4(b)) suggested no overlap between the control group and DSS model group, demonstrating that the number of differential OTUs was high. The samples of the WGPH high-dose administration group and FSGH high and low-dose administration groups were similar to those of the normal group.

3.3.3. Cluster Analysis. Metastatistical analysis illustrated that, at the phylum level, there were three phyla, containing *Bacteroidetes*, *Proteobacteria*, and *Firmicutes*, that displayed significant differences in the relative abundance between the control and model groups. Furthermore, these three phyla in the model group also displayed apparent differences in the relative abundance with the hydrolysates group (Figure 5(a)). In an in-deep step, to identify the fecal microbiota meaningful changes among the different groups, the relative abundance of 44 genera was presented by branch diagram via LEfSe analysis (Figures 5(b) and 5(c)). Clearly, different groups showed different genera levels. As shown in Figures 5(b) and 5(c), *Bacteroidales, Prevotellaceae, Ambiguous_taxa, Prevotellaceae_UCG_001, Corynebacteriaceae, Lachnospiraceae*, and *Aeromonadaceae* are the major components of the intestinal community of rats in the normal group. *Enterococcaceae, Butyricimonas,* and *Enterococcus* are the components of the intestinal community of rats in the model group. *Alcaligenaceae, Burkholderiales, Betaproteobacteria*, and *Parasutterella* were shown as the important parts of the high dose of the WGPH group and *Enterobacteriaceae, Gammaproteobacteria, Escherichia_Shigella, Proteobacteria, Campylobacterales*, and *Epsilonproteobacteria* are the principal parts of different dose of the FSGH group. To further identify the top 10 characteristic bacterial genera among the different groups, as shown in Figure 6, DSS increased the relative abundance of *Parasutterella, Allobaculum, Desulfovibrio, Lachnospiraceae,* and *Mucispirillum.* Meanwhile, DSS decreased the relative abundance of *Escherichia_Shigella, Bacteroides, Helicobacter, Parabacteroides,* and *Alloprevotella.* However, the abundances of the main bacterial genus could significantly be changed by WGPH and FSGH (Figure 6).

4. Discussion

Colitis, a type of inflammatory bowel disease, is recognized as one of the world's refractory diseases due to its unknown cause, difficulty in healing, and recurring attacks [1]. Its

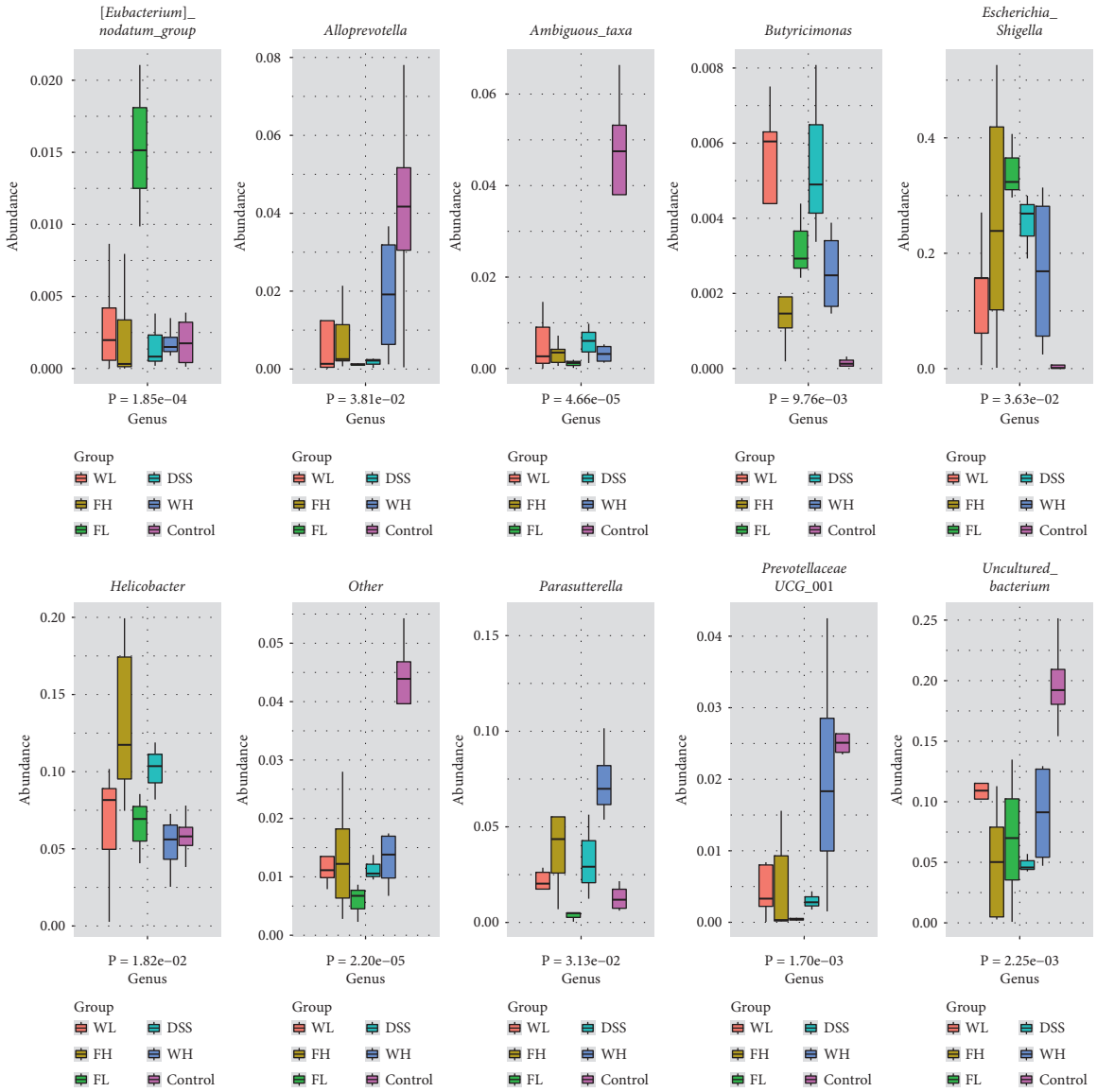

Figure 6: Boxplot analysis of relative abundance of the top 10 species among different groups at the genus level.

etiology may involve genetics, environment, diet, immunity, psychology, and many other aspects [6, 7]. The current treatments are mostly aminosalicylic acid drugs (such as sulfasalazine), adrenal glycosides, and immunosuppressants [35]. However, these treatments generally have large side effects and limited efficacy. Preventing and reducing the side effects of drugs for the treatment of inflammatory bowel disease [15, 16] and at the same time, developing new, safe, and effective drugs that interfere with inflammatory bowel disease has become one of the research hotspots in the global medical field [17]. Foodborne protease hydrolysates, as natural polymer compounds, have a wide range of sources [36]. They are safe and nontoxic and also have a wide range of functional activities such as antiangiogenesis, antioxidation, immune regulation, three high (high sugar, high fat, and high blood pressure), antiaging, anti-inflammatory, and so on [37, 38]. According to research reports at home and abroad, protease hydrolysates have received extensive attention in the treatment and improvement of inflammatory bowel disease [39].

DSS-induced UC in mice is one of the most mature methods at present [40]. The influencing factors of DSS modeling include molecular weight and concentration of DSS, research environment, mouse species, and administration time [41]. In our study, after 7 days of DSS intervention, the mice in the DSS group lost weight and shortened the length of colon. The colon length and histopathological score in the polypeptides group were much improved than that in the DSS-induced model group.

Gut microbiota is the most complex and the highest population of symbiotic microbial ecosystems in the human body. They are recognized as an essential factor in the body's health and homeostasis [13]. They have profound effects on human physiology and nutrition [42]. Besides, the changes in gut microbiota are likely to be related to intestinal diseases [14]. Studies based on 16S rRNA gene sequencing showed

that the two major categories of *Bacteroides* and *Firmicutes* are the main groups of intestinal microbes. The typical symptoms of UC are inflammation and ulcers in the rectum, colonic mucosa, and submucosa [43]. Gut microbiota is a key protective factor of the intestinal mucosa [44]. Previous studies have reported colonizing the fecal bacteria from healthy donors into patients with inflammatory bowel disease, which could significantly improve the symptoms of patients [45]. Previous studies expressed that microbial diversity research could reflect the abundance and diversity of microbial communities through a single-sample diversity analysis (alpha diversity), which included a series of statistical analysis indexes to estimate the species abundance and diversity of environmental communities [46, 47]. In our study, the results showed that the intestinal flora balance system of DSS-induced colitis mice was severely broken, and the intake of wheat germ protein hydrolysates (WGPH) from wheat as well as the fish skin gelatin hydrolysates (FSGH) from tilapia skin could alleviate the imbalance of flora and reduce the symptoms of inflammatory diseases. Based on 16S rRNA gene sequencing, the content samples of mice in the normal group, DSS-induced colitis mice group, and different dose of hydrolysates treatment groups were analyzed. After analyzing the α-diversity between different groups, the results evidenced that the sample size and the library volume we constructed were large enough to represent the vast majority of bacteria in the human intestinal flora, and the species richness and library diversity were saturated. PCoA analysis expressed that the distance between the control group and the DSS group was far from each other, indicating that there was a great difference in the composition of the flora between the two groups [48]. After giving different doses of hydrolysates from wheat and fish protein, each administration group deviated from the model group to a certain extent, indicating that each dose could improve the intestinal flora diversity of colitis rats to a certain extent, which was the same as the previous conclusion. The study also suggests that high-dose WGPH, as well as low and high-dose FSGH, could improve the structure of the intestinal flora of rats in the model group, which indicated better colitis improvement and relief effects.

According to the results of the phylum level, there were three phyla, containing *Bacteroidetes*, *Proteobacteria*, and *Firmicutes*, that displayed significant differences in the relative abundance between the control and model groups. Furthermore, these three phyla in the model group also displayed apparent differences in the relative abundance with the polypeptides group. Moreover, considering the results of the family level, after DSS modeling, in comparison to the control group, the bacteria in the intestines of DSS-induced mice had undergone tremendous. However, the intestinal flora of the polypeptides group was closer to that of the control group. Compared with the DSS-induced model group, *Parasutterella, Allobaculum, Desulfovibrio, Lachnospiraceae*, and *Mucispirillum* were significantly reduced in the blank and polypeptides groups, while the relative abundance of *Escherichia_Shigella, Bacteroides, Helicobacter, Parabacteroides*, and *Alloprevotella* increased ($P < 0.05$).

In summary, the oral administration of WGPH and FSGH exhibited therapeutic effects on DSS-induced UC in mice. The wheat germ protein hydrolysates and fish skin gelatin hydrolysates could be considered as a novel attractive intestinal microecological improver for UC treatment.

Data Availability

The data used to support the findings of this study are available from the corresponding author upon request.

Conflicts of Interest

The authors declare that they have no conflicts of interest.

Acknowledgments

The authors wish to extend their appreciation to the National Key Research and Development Program of China-Intergovernmental Key Program for International Science and Technology Innovation Cooperation (2017YFE0105300), National Natural Science Foundation of China (31872892), and "Six Talents Peak" High-level Talent Program of Jiangsu Province (NY-010). In addition, the authors would like to acknowledge the financial support from the project (2013AA102203), funded by National High-tech R&D Program of China (863 Program).

References

[1] I. Ordás, L. Eckmann, M. Talamini, D. C. Baumgart, and W. J. Sandborn, "Ulcerative colitis," *The Lancet*, vol. 380, no. 9853, pp. 1606–1619, 2012.

[2] M. Eisenstein, "Ulcerative colitis: towards remission," *Nature*, vol. 563, no. 7730, p. S33, 2018.

[3] D. Y. Jeong, S. Kim, M. J. Son et al., "Induction and maintenance treatment of inflammatory bowel disease: a comprehensive review," *Autoimmunity Reviews*, vol. 18, no. 5, pp. 439–454, 2019.

[4] D. K. Lei, J. E. Ollech, M. Andersen et al., "Long-duration oral vancomycin to treat clostridioides difficile in patients with inflammatory bowel disease is associated with a low rate of recurrence," *American Journal of Gastroenterology*, vol. 114, no. 12, pp. 1904–1908, 2019.

[5] N. A. Molodecky, I. S. Soon, D. M. Rabi et al., "Increasing incidence and prevalence of the inflammatory bowel diseases with time based on systematic review," *Gastroenterology*, vol. 142, no. 1, pp. 46–54, 2012.

[6] E. Cabré and E. Domenech, "Impact of environmental and dietary factors on the course of inflammatory bowel disease," *World Journal of Gastroenterology*, vol. 18, no. 29, pp. 3814–3822, 2012.

[7] F. Laudisi, C. Stolfi, and G. Monteleone, "Impact of food additives on gut homeostasis," *Nutrients*, vol. 11, p. 12, 2019.

[8] N. Shi, N. Li, X. Duan, and H. Niu, "Interaction between the gut microbiome and mucosal immune system," *Military Medical Research*, vol. 4, p. 14, 2017.

[9] M. G. Rooks and W. S. Garrett, "Gut microbiota metabolites and host immunity," *Nature Reviews Immunology*, vol. 16, no. 6, pp. 341–352, 2016.

[10] C. P. Kaur, J. Vadivelu, and S. Chandramathi, "Impact ofKlebsiella pneumoniaein lower gastrointestinal tract

diseases," *Journal of Digestive Diseases*, vol. 19, no. 5, pp. 262–271, 2018.

[11] S. Paramsothy, S. Nielsen, M. A. Kamm et al., "Specific bacteria and metabolites associated with response to fecal microbiota transplantation in patients with ulcerative colitis," *Gastroenterology*, vol. 156, no. 5, pp. 1440–1454, 2019.

[12] E. A. Franzosa, A. Sirota-Madi, J. Avila-Pacheco et al., "Gut microbiome structure and metabolic activity in inflammatory bowel disease," *Nature Microbiology*, vol. 4, no. 2, pp. 293–305, 2019.

[13] M. Serino, J. M. Fernández-Real, E. G. Fuentes et al., "The gut microbiota profile is associated with insulin action in humans," *Acta Diabetologica*, vol. 50, no. 5, pp. 753–761, 2013.

[14] H. Tilg, T. E. Adolph, R. R. Gerner, and A. R. Moschen, "The intestinal microbiota in colorectal cancer," *Cancer Cell*, vol. 33, no. 6, pp. 954–964, 2018.

[15] A. Tsoupras, R. Lordan, and I. Zabetakis, "Inflammation not cholesterol, is a cause of chronic disease," *Nutrients*, vol. 10, no. 5, p. 604, 2018.

[16] J. D. Sheppard, T. L. Comstock, and M. E. Cavet, "Impact of the topical ophthalmic corticosteroid loteprednol etabonate on intraocular pressure," *Advances in Therapy*, vol. 33, no. 4, pp. 532–552, 2016.

[17] M. Serafini and I. Peluso, "Functional foods for health: the interrelated antioxidant and anti-inflammatory role of fruits vegetables herbs spices and cocoa in humans," *Current Pharmaceutical Design*, vol. 22, no. 44, pp. 6701–6715, 2016.

[18] A. Levine, J. M. Rhodes, J. O. Lindsay et al., "Dietary guidance from the International Organization for the study of inflammatory bowel diseases," *Clinical Gastroenterology and Hepatology*, vol. 18, no. 6, pp. 1381–1392, 2020.

[19] S. Wada, K. Sato, R. Ohta et al., "Ingestion of low dose pyroglutamyl leucine improves dextran sulfate sodium-induced colitis and intestinal microbiota in mice," *Journal of Agricultural and Food Chemistry*, vol. 61, no. 37, pp. 8807–8813, 2013.

[20] K. Sato, Y. Egashira, S. Ono et al., "Identification of a hepatoprotective peptide in wheat gluten hydrolysate against D-galactosamine-induced acute hepatitis in rats," *Journal of Agricultural and Food Chemistry*, vol. 61, no. 26, pp. 6304–6310, 2013.

[21] Y. Peng, R. Gan, H. Li et al., "Absorption, metabolism, and bioactivity of vitexin: recent advances in understanding the efficacy of an important nutraceutical," *Critial Reviews in Food Science and Nutrition*, vol. 61, no. 6, pp. 1049–1064, 2020.

[22] M. Mochizuki, H. Shigemura, and N. Hasegawa, "Anti-inflammatory effect of enzymatic hydrolysate of corn gluten in an experimental model of colitis," *Journal of Pharmacy and Pharmacology*, vol. 62, no. 3, pp. 389–392, 2010.

[23] R. Gao, Q. Yu, Y. Shen et al., "Production, bioactive properties and potential applications of fish protein hydrolysates: developments and challenges," *Trends in Food Science & Technology*, vol. 110, no. 1, pp. 687–699, 2021.

[24] S. Kumar, F. Sugihara, K. Suzuki, N. Inoue, and S. Venkateswarathirukumara, "A double-blind, placebo-controlled, randomised, clinical study on the effectiveness of collagen peptide on osteoarthritis," *Journal of the Science of Food and Agriculture*, vol. 95, no. 4, pp. 702–707, 2015.

[25] X. Yang, C. Chi, X. Liu, Y. Zhang, H. Zhang, and H. Wang, "Understanding the structural and digestion changes of starch in heat-moisture treated polished rice grains with varying amylose content," *International Journal of Biological Macromolecules*, vol. 139, pp. 785–792, 2019.

[26] H. Wang, N. Xiao, X. Wang, X. Zhao, and H. Zhang, "Effect of pregelatinized starch on the characteristics, microstructures and quality attributes of glutinous rice flour and dumplings," *Food Chemistry*, vol. 283, pp. 248–256, 2019.

[27] B. Wang, Y. Li, H. Wang, X. Liu, Y. Zhang, and H. Zhang, "In-situ analysis of the water distribution and protein structure of dough during ultrasonic-assisted freezing based on miniature Raman spectroscopy," *Ultrasonics Sonochemistry*, vol. 67, p. 105149, 2020.

[28] Y. Zhang, B. Wang, W. Wang, H. Wang, X. Liu, and H. Zhang, "Study on the mechanism of ultrasonic treatment impact on the dough's fermentation capability," *Journal of Cereal Science*, vol. 100, Article ID 103191, 2021.

[29] X. Sun, S. Zhang, C. C. Udenigwe et al., "Wheat germ-derived peptides exert antiadhesive activity against *Helicobacter pylori*: insights into structural characteristics of identified peptides," *Journal of Agricultural and Food Chemistry*, vol. 68, no. 43, pp. 11954–11974, 2020.

[30] Z. Karami, S. H. Peighambardoust, J. Hesari, B. akbari-Adergani, and D. Andreu, "Identification and synthesis of multifunctional peptides from wheat germ hydrolysate fractions obtained by proteinase k digestion," *Journal of Food Biochemistry*, vol. 43, no. 4, p. e12800, 2019.

[31] C. H. Hsieh, T. Y. Wang, C. C. Hung, M. C. Chen, and K. C. Hsu, "Improvement of glycemic control in streptozotocin-induced diabetic rats by Atlantic salmon skin gelatin hydrolysate as the dipeptidyl-peptidase IV inhibitor," *Food & Function*, vol. 6, no. 6, pp. 1887–1892, 2015.

[32] W. Gao, C. Wang, L. Yu et al., "Chlorogenic acid attenuates dextran sodium sulfate-induced ulcerative colitis in mice through MAPK/ERK/JNK pathway," *BioMed Research International*, vol. 2019, Article ID 6769789, 13 pages, 2019.

[33] Y.-X. Yan, M.-J. Shao, Q. Qi et al., "Artemisinin analogue SM934 ameliorates DSS-induced mouse ulcerative colitis via suppressing neutrophils and macrophages," *Acta Pharmacologica Sinica*, vol. 39, no. 10, pp. 1633–1644, 2018.

[34] J. D. Forbes, C.-Y. Chen, N. C. Knox et al., "A comparative study of the gut microbiota in immune-mediated inflammatory diseases-does a common dysbiosis exist?" *Microbiome*, vol. 6, no. 1, p. 221, 2018.

[35] R. Ungaro, S. Mehandru, P. B. Allen, L. Peyrin-Biroulet, and J.-F. Colombel, "Ulcerative colitis," *The Lancet*, vol. 389, no. 10080, pp. 1756–1770, 2017.

[36] X. Ju, M. Zhu, J. Han, Z. Lu, H. Zhao, and X. Bie, "Combined effects and cross-interactions of different antibiotics and polypeptides in Salmonella bredeney," *Microbial Drug Resistance*, vol. 24, no. 10, pp. 1450–1459, 2018.

[37] Y.-S. Kim, T. Zerin, and H.-Y. Song, "Antioxidant action of ellagic acid ameliorates paraquat-induced A549 cytotoxicity," *Biological and Pharmaceutical Bulletin*, vol. 36, no. 4, pp. 609–615, 2013.

[38] S.-D. Chen, C.-L. Wu, W.-C. Hwang, and D.-I. Yang, "More insight into BDNF against neurodegeneration: anti-apoptosis anti-oxidation and suppression of autophagy," *International Journal of Molecular Sciences*, vol. 18, no. 3, p. 545, 2017.

[39] M. El-Salhy, T. Solomon, T. Hausken, O. H. Gilja, and J. G. Hatlebakk, "Gastrointestinal neuroendocrine peptides/amines in inflammatory bowel disease," *World Journal of Gastroenterology*, vol. 23, no. 28, pp. 5068–5085, 2017.

[40] H. Cao, J. Liu, P. Shen et al., "Protective effect of naringin on DSS-induced ulcerative colitis in mice," *Journal of Agricultural and Food Chemistry*, vol. 66, no. 50, pp. 13133–13140, 2018.

[41] S. Kitajima, M. Morimoto, and E. Sagara, "A model for dextran sodium sulfate (DSS)-induced mouse colitis: bacterial degradation of DSS does not occur after incubation with mouse cecal contents," *Experimental Animals*, vol. 51, no. 2, pp. 203–206, 2002.

[42] R. Hills Jr., B. Pontefract, H. Mishcon, C. Black, S. Sutton, and C. Theberge, "Gut microbiome: profound implications for diet and disease," *Nutrients*, vol. 11, no. 7, p. 1613, 2019.

[43] J. D. Feuerstein, A. C. Moss, and F. A. Farraye, "Ulcerative colitis," *Mayo Clinic Proceedings*, vol. 94, no. 7, pp. 1357–1373, 2019.

[44] T. Takiishi, C. I. M. Fenero, and N. O. S. Câmara, "Intestinal barrier and gut microbiota: shaping our immune responses throughout life," *Tissue Barriers*, vol. 5, no. 4, p. e1373208, 2017.

[45] A. R. Weingarden and B. P. Vaughn, "Intestinal microbiota fecal microbiota transplantation, and inflammatory bowel disease," *Gut Microbes*, vol. 8, no. 3, pp. 238–252, 2017.

[46] Y. Xia, X. Wen, B. Zhang, and Y. Yang, "Diversity and assembly patterns of activated sludge microbial communities: a review," *Biotechnology Advances*, vol. 36, no. 4, pp. 1038–1047, 2018.

[47] A. D. Willis, "Rarefaction alpha diversity, and statistics," *Frontiers in Microbiology*, vol. 10, p. 2407, 2019.

[48] G. Cao, K. Wang, Z. Li et al., "Bacillus amyloliquefaciens ameliorates dextran sulfate sodium-induced colitis by improving gut microbial dysbiosis in mice model," *Frontiers in Microbiology*, vol. 9, p. 3260, 2019.

Hindawi
Journal of Food Quality
Volume 2021, Article ID 5599219, 14 pages
https://doi.org/10.1155/2021/5599219

Research Article

Protective Effects of Almond Oil on Streptozotocin-Induced Diabetic Rats via Regulating Nrf2/HO-1 Pathway and Gut Microbiota

Rui Liu, Ying Shu, Wenhui Qi, Weili Rao, Zihan Fu, Zhenxiao Shi, and Zhisheng Zhang

College of Food Science and Technology, Hebei Agricultural University, Lekai South Avenue, Baoding, Hebei 071000, China

Correspondence should be addressed to Zhisheng Zhang; zhangzhisheng66@139.com

Received 27 January 2021; Revised 23 April 2021; Accepted 11 May 2021; Published 7 June 2021

Academic Editor: Biao Yuan

Almond oil has been used as a medicine substitution for its numerous health benefits. This study aimed to evaluate the effect of almond oil on streptozotocin- (STZ-) induced diabetic rats for 4 weeks. The results showed that the administration of almond oil could significantly increase body weight, attenuate abnormally elevated blood glucose, promote insulin secretion, and improve glucose tolerance. Almond oil treatment also suppressed oxidative stress, reduced inflammation reaction, improved liver and kidney function, upregulated the expressions of Nrf2, HO-1, and NQO1, while downregulating the expression of Keap1. Furthermore, almond oil reversed the gut microbiota change by STZ and regulated the gut microbiota associated with glucose metabolism. At the phylum level, the relative abundance of Firmicutes was decreased, while Bacteroidetes was increased by almond oil treatment. More importantly, the ratio of Firmicutes/Bacteroidetes was significantly increased. At the genus level, administration of almond oil increased the abundances of *Lactobacillus*, *Bacteroides*, and *Lachnospiraceae_NK4A136_group*, while decreased the abundances of *Ruminococcaceae_UCG*-014, *Clostridium_sensu_stricto*_1, and *Fusicatenibacter*. These results provided evidence for the regulating effect of almond oil on diabetic rats via the Nrf2/HO-1 pathway and gut microbiota.

1. Introduction

Diabetes is a chronic metabolic disease characterized by hyperglycemia that has been recognized as an increasing global health problem [1]. Genetics and environments are important factors in the pathogenesis of diabetes. In 2017, approximately 451 million adults lived with diabetes, and the number was estimated to rise to 693 million by 2045 throughout the world [2]. Chronic hyperglycemia causes oxidative stress and inflammation in the occurrence of diabetes. Besides, it is frequently associated with dysfunction and severe clinical complications, such as diabetic retinopathy [3], nephropathy [4], neuropathy [5], and peripheral artery disease, owing to the glucotoxicity effects [6, 7], which accelerate the mortality of diabetes. Therefore, controlling a high level of blood glucose and alleviating the generation of reactive oxygen species (ROS) are essential for controlling diabetes or ameliorating diabetic complications.

The nuclear factor erythroid 2-related factor 2 (Nrf2) is an intracellular transcription factor that could maintain cellular redox homeostasis and upregulate cytoprotective proteins, such as heme oxygenase 1 (HO-1) and NAD(P)H quinone oxidoreductase 1 (NQO1). Under normal conditions, the binding of Kelch-like ECH-associated protein 1 (Keap1) to Nrf2 could suppress the Keap1/Nrf2 pathway, which leads to the ubiquitination and degradation of cytoplasmic Nrf2 [8]. The deficiency of expression of Nrf2 could enhance the susceptibility to many oxidative stress-related pathologies [9]. Some agents could protect diabetes-related organs or cells from injuries by upregulating the expression of Nrf2 [10]. Nrf2 regulates the expressions of a series of antioxidant enzymes and is considered an effective target on oxidative stress-

related diseases [11]. Heme oxygenase-1 (HO-1) is a downstream cytokine of Nrf2, which exerts a vital function in maintaining the redox balance of cells [12]. The Nrf2/HO-1 pathway plays a critical role in regulating oxidative stress.

More importantly, the gut microbiota plays a critical role in host homeostasis, and the dysbiosis of the gut microbiota is strongly associated with the onset and progress of metabolic diseases, such as diabetes [13, 14]. A previous study found that commensal bacteria, such as *Lactobacillus plantarum*, can promote the transfer of insulin vesicles and insulin secretion by ligand binding with NOD1 in islet *ß* cells [15]. Furthermore, a decreased proportion of anaerobes, especially *Bacteroides*, can lead to hyperglycemia. The aberrant microbiota in STZ-induced diabetic rats and the upsurge of the Gram-negative bacteria could lead to inflammation and the development of a pathological microenvironment [16]. Lipopolysaccharide (LPS) as a gut-derived endotoxin might be crucially involved in chronic inflammation. Release of LPS by pathogenic bacteria in the intestine can enter the bloodstream and trigger low-level inflammation and oxidative damage in rats with high intestinal permeability. Reducing the levels of LPS-producing bacteria in diabetic rats might contribute to reducing systemic inflammation and promoting normal liver insulin signaling [17]. Therefore, regulation of the gut microflora may be beneficial for reversing the inflammatory and maintaining the balance of glucose metabolism. Diet is an important factor altering the composition and metabolism of the gut microbiota, especially the main dietary macronutrients whose amount, type, and balance greatly impact the large intestinal microbiota [18].

Some natural products isolated from plant sources had therapeutic and antioxidant properties and could be used as a form of supplement or replacement with antioxidant activity and fewer side effects, which should be searched for attenuating the risk of diabetes. Almond (*Prunus amygdalus*) is the most popular nuts and widely used as ingredients in some processed foods such as bakery and confectionery products. A previous study showed that the consumption of almonds could reduce the risk of chronic diseases and prevent colon cancer [19]. Besides, almond contains proteins, certain minerals, vitamins E and D, and about 50% oil. Almond oil has high amounts of monounsaturated fatty acids (MUFA), especially a rich concentration of oleic fatty acids [20], which could alleviate cellular apoptosis, oxidative stress, mitochondrial dysfunction, and inflammation in hepatocytes [21]. Almond oil has long been used as a medicine substitution [22] and has significant potential in biomedical and pharmacological studies. Previous studies illustrated that the consumption of almond oil could inhibit lipid peroxidation processes in CCl_4-induced hepatic damage rats and boost immunity [23, 24] due to its anti-inflammatory and antioxidant activity and free radical scavenging capacity. However, the gut microbiota changes in STZ-induced diabetes by the dietary supplement of almond oil were hardly reported.

Due to the excellent antioxidant activity of almond oil, we speculated the beneficial effect of almond oil on diabetes. Therefore, our present study aimed to investigate the effects of almond oil on diabetic rats induced by STZ via the regulation of oxidative stress and inflammatory response, Nrf2/HO-1 signaling pathway, and gut microbiota changes. The study would provide a beneficial suggestion for choosing a diet supplement.

2. Materials and Methods

2.1. Chemicals. The almond oil was kindly provided by Laiyuan Almond Processing Co., Ltd., in Hebei, China, in November 2019. The sunflower seed oil was purchased from a local grocery store in Baoding, Hebei, China, in November 2019, as the positive control. They were both stored at 4°C before use.

Streptozotocin (STZ) was purchased from Sigma-Aldrich Co. (St. Louis, MO, USA).

The biochemical kits of superoxide dismutase (SOD), catalase (CAT), malondialdehyde (MDA), alanine transaminase (ALT), aspartate transaminase (AST), creatinine (CRE), and blood urea nitrogen (BUN) were obtained from Jiancheng Bioengineering Research Institute (Nanjing, China). The enzyme-linked immunosorbent assay (ELISA) kits of inflammation indicators of tumor necrosis factor α (TNF-α) and interleukin 1β (IL-1β), insulin (INS), and advanced glycation end products (AGEs) were purchased from Boster Biological Technology Co., Ltd. (Wuhan, China).

2.2. Composition Analysis of Almond Oil. The composition analysis of almond oil was detailed in Table S1.

2.3. Animals and Experimental Treatment. Male Sprague Dawley rats (200~220 g) were purchased from Beijing HFK Bioscience Co., Ltd. The rats were kept under standardized conditions at a constant temperature of 23–25°C, and 50 ± 5% humidity with a 12 h light/dark cycle, and they had free access to standard diet and water for one week adjustment period. All experimental procedures and animal welfare were performed under a protocol that was approved by the Research Ethics Committee of the College of Food Science and Technology in Hebei Agricultural University.

After the adjustment period, the rats were weighed and randomly divided into six groups ($n = 10$): the control group (CON), the model control group (MC), the low dose of almond oil group (LAO), medium dose of almond oil group (MAO), high dose of almond oil group (HAO), and sunflower seed oil group (SSO). All rats were fasted for 12 h, and rats in MC, LAO, MAO, HAO, and SSO were intraperitoneally injected STZ with 60 mg/kg, which was dissolved in 0.l M citrate buffer (pH 4.2–4.5), while those in CON were intraperitoneally injected with the same dose of citrate buffer solution. Fasting blood glucose (FBG) was determined three days after the injection. The rats with levels of FBG >16.7 mmol/L were considered as diabetic rats for experiments.

Rats in LAO, MAO, and HAO were intragastrically administrated with almond oil at doses of 2, 4, and 8 g/kg b.w. and SSO administrated with sunflower seed oil at a dose of 4 g/kg b.w. for 4 continuous weeks, respectively, while rats in CON and MC were given at an equal volume of sterile water.

Body weights and FBG of all the rats were monitored weekly throughout the whole experimental period. At the

last week of the experiment, oral glucose tolerance test (OGTT) was determined. At the end of the experiment, the rats were deprived of food overnight and 10% chloralic hydras (6 ml/kg) was intraperitoneally injected for anesthesia. The blood samples were collected from the abdominal artery aorta of rats and separated by centrifugation at 3000 rpm for 15 min to obtain serum and then stored at −80°C for further assay. The liver samples were rinsed with saline and dried on filter paper, then quickly snap-frozen, and preserved at −80°C for Western blotting analysis.

The colon contents sample of each rat was collected at a sterile condition and preserved at −80°C for further microbiota analysis.

2.4. Measurement of Fasting Glucose and OGTT. FBG levels were measured from the tail vein of rats after overnight (12 h) fasting using a glucose meter. The OGTT was estimated at the last week after administration of AO or SSO. The blood glucose levels were estimated at 0, 30, 60, and 120 minutes after administration with glucose solution (2 g/kg BW). The area under the curve (AUC) during the OGTT was calculated by the trapezoid rule.

2.5. Biochemical Parameters Analysis. The enzyme activities of SOD, CAT, MDA, ALT, AST, CRE, and BUN in the serum were determined by biochemical kits; INS, TNF-α, IL-1β, and AGEs in the serum were quantified by ELISA kits strictly according to the instructions of instruments and reagents.

2.6. Western Blot Analysis. The expressions of Keap1, Nrf2, HO-1, and NQO1 protein in liver were determined by Western blotting. The liver samples were homogenized and lysed in lysis buffer containing a protease inhibitor on ice. The suspension was centrifuged at 10,000g for 10 min at 4°C and the supernatant was collected for Western blot assay. The total protein concentration was quantified using a BCA assay kit. Equal concentrations of protein samples were separated by 10% SDS-polyacrylamide gel electrophoresis (PAGE) and then transferred to the polyvinylidene fluoride membranes (PVDF). The membranes were blocked with 5% BSA in TBST buffer for 1 h and incubated in primary antibodies against Keap1, Nrf2 (1 : 1000), HO-1, NQO1 (1 : 10000), and β-actin (1 : 4000) at 4°C overnight. The membranes were washed 5 times in TBST and incubated with HRP-conjugated anti-rabbit or anti-mouse secondary antibodies at room temperature for 1 h. After washing 7 times with TBST, the protein bands were visualized by enhanced chemiluminescence reagent (Thermo, Rockford, USA). Finally, bands were analyzed using image analysis system (Bio-Rad, CA, USA).

2.7. Fecal DNA Extraction and Sequencing. According to the manufacturer's instructions, total DNA was extracted from colon contents using the TIANamp Stool DNA kit (Tiangen, Beijing, China). The bacterial 16S rRNA gene V3-V4 region was amplified with primers 338F (5′-ACTCCTACGGGAGGCAGCAG-3′) and 806R (5′-GGACTACHVGGGTWTCTAAT-3′). The PCR amplification program was performed as follows: initial denaturation at 95°C for 3 min, followed by 27 cycles PCR (95°C for 30 s, 55°C for 30 s, and 72°C for 30 s), finally 72°C for 10 min. The PCR product was extracted from 2% agarose gel, purified using AxyPrepDNA (Axygen Biosciences, Union City, CA, USA), quantified using Quantus™ Fluorometer (Promega, USA), and finally sequenced using Illumina MiSeq platform (Illumina San Diego, USA) at Majorbio Bio-Pharm Technology company (Shanghai, China).

Sequences with ≥97% similarity were assigned to the same operational taxonomic units (OTUs). The sequences were trimmed with UCHIME and annotated using RDP Classifier (http://rdp.cme.msu.edu/) based on the SILVA database (SSU123) at the threshold of 70%.

2.8. Statistical Analysis. Data were expressed as mean ± SD. Statistical analysis was performed using SPSS 17.0. Statistical significance between groups was analyzed using one-way analysis of variance (ANOVA) followed by Duncan's new multiple range test. P values <0.05 or P values <0.01 were considered statistically significant or statistically highly significant.

3. Results

3.1. Effect of Almond Oil on Body Weight in Diabetic Rats. The changes in body weight are presented in Figure 1. Body weight of the rats decreased significantly one week after the injection of STZ ($P < 0.01$). The body weight among diabetic groups had no significant differences during the first two weeks. However, treatment with almond oil could obviously reverse the reduction during 4-week administration. Compared with the MC group, the body weight of the MAO group was significantly increased at week 2 ($P < 0.05$); the three doses of almond oil and the SSO group significantly increased body weight ($P < 0.01$) at weeks 3 and 4. The results showed that different doses of almond oil could reduce the weight loss of diabetic rats.

3.2. Effect of Almond Oil on FBG, OGTT, and Insulin Levels in Diabetic Rats. Elevated FBG is one of the main characteristics of diabetes. The FBG was estimated every week. As shown in Figure 2(a), FBG of the MC group was significantly higher than the CON group after STZ induction ($P < 0.01$), which proved that the diabetes model had been established. Compared with the MC group, there was no significant difference in FBG in rats during the first two weeks' intervention. However, FBG of the LAO and HAO groups exhibited a significant descent tendency ($P < 0.05$) compared with the MC group at week 3, and FBG was decreased by 20.9% in the LAO group at the last week. The results suggested that AO could suppress the increase in FBG.

OGTT aims to measure the ability to tolerate glucose in rats. Results of OGTT among all groups are shown in Figure 2(b). The maximum blood glucose level occurred 30 minutes after the oral administration of glucose, and the MC group had a significantly lower level of glucose tolerance compared with the CON group ($P < 0.01$). The LAO group

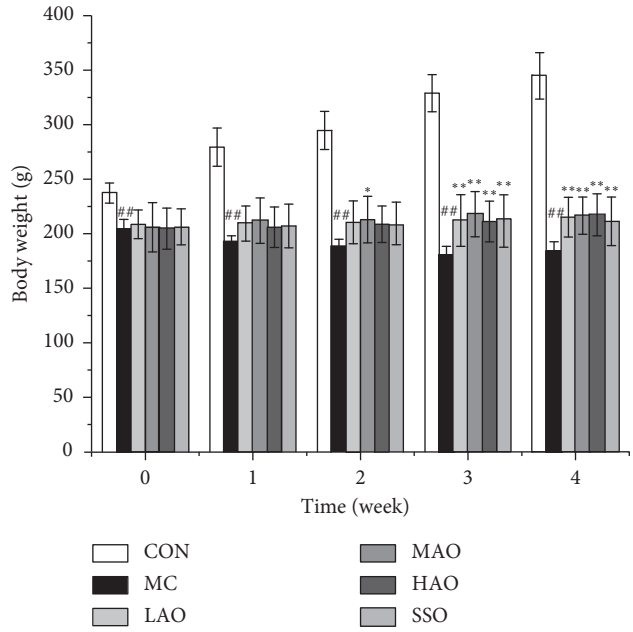

Figure 1: Effect of almond oil on body weight in STZ-induced diabetic rats. CON, control group; MC, model control group; LAO, low dose of almond oil-treated group; MAO, middle dose of almond oil-treated group; HAO, high dose of almond oil-treated group; SSO, sunflower seed oil-treated group. Data were expressed as means ± SD. The MC group compared with the CON group, $^{\#}P < 0.05$, $^{\#\#}P < 0.01$; the LAO, MAO, HAO, and SSO groups compared with the MC group, $^{*}P < 0.05$, $^{**}P < 0.01$.

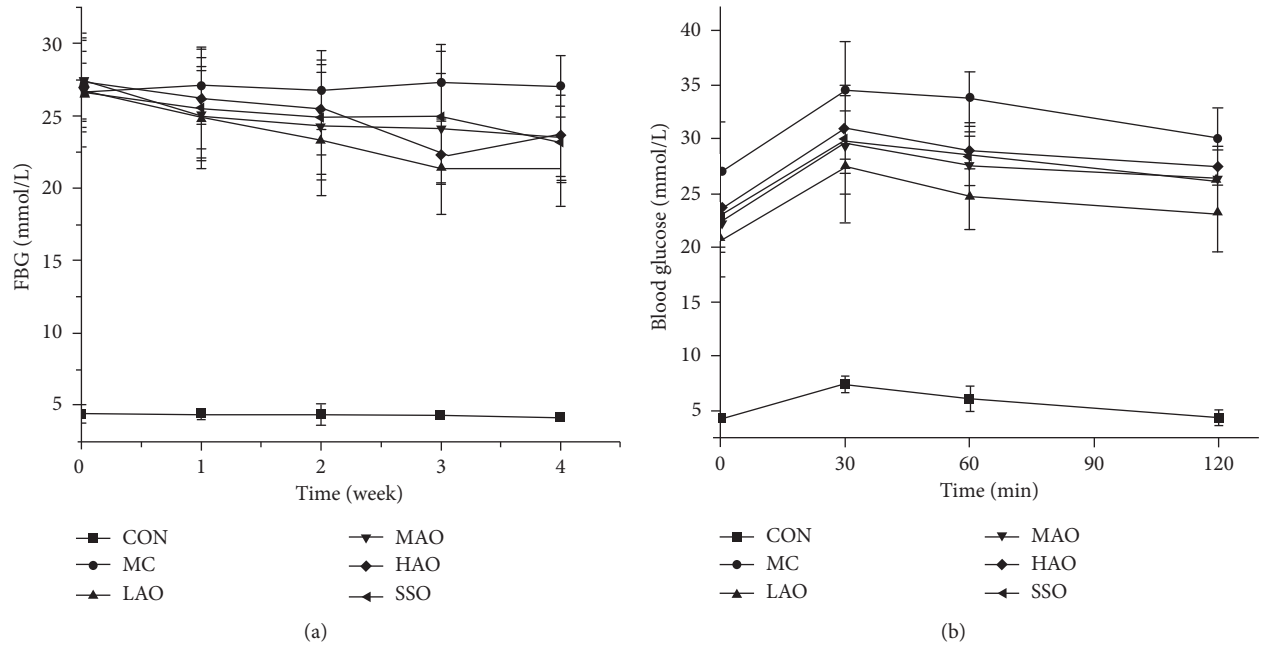

Figure 2: Continued.

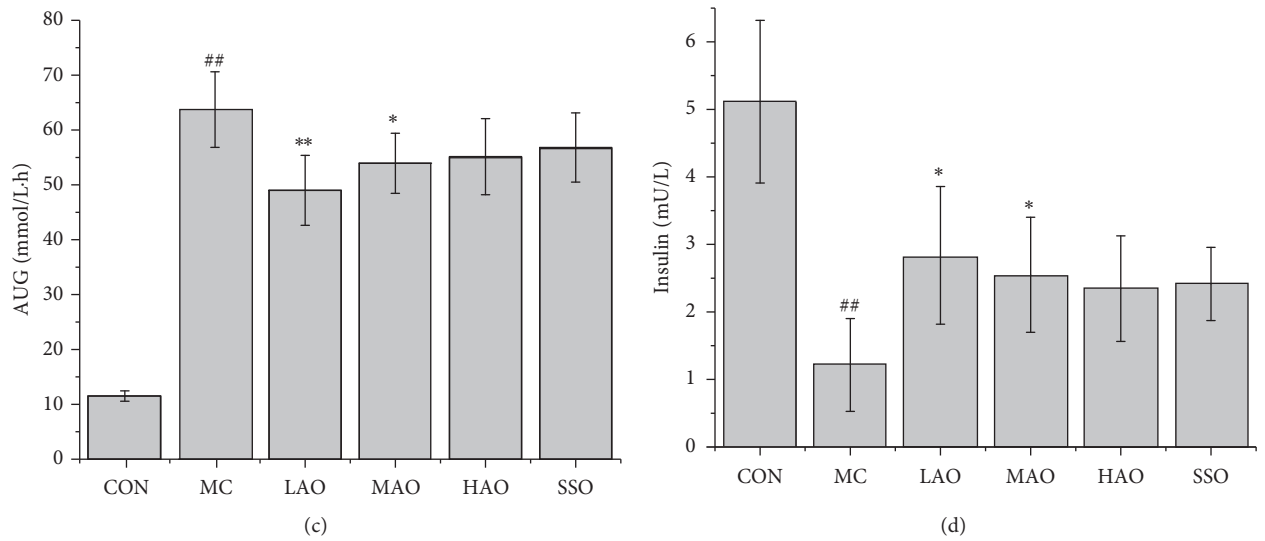

Figure 2: Effects of almond oil on the FBG, glucose tolerance, and insulin levels in STZ-induced rats. (a) Fasting blood glucose. (b) Glucose tolerance. (c) Area under the curve of blood glucose (AUC). (d) Serum insulin. Data were expressed as means ± SD. The MC group compared with the CON group, $^{\#}P < 0.01$, $^{\#\#}P < 0.01$; the LAO, MAO, HAO, and SSO groups compared with the MC group, $^{*}P < 0.05$, $^{**}P < 0.01$.

significantly suppressed the blood glucose elevation after gavaging glucose 30 minutes. At 60 minutes, significantly lower glucose levels were observed among almond oil groups and SSO group ($P < 0.05$). The glucose levels of LAO and MAO were significantly reduced at 120 minutes compared with the MC group ($P < 0.05$).

The AUC levels were presented in Figure 2(c). The MC group had a significantly higher level of glucose AUG compared with the CON group ($P < 0.01$). Significantly lower AUC levels were observed in LAO and MAO groups ($P < 0.01$, $P < 0.05$) compared with the MC group.

Based on the results of blood glucose, changes in insulin levels in serum were also detected. As shown in Figure 2(d), the insulin level was significantly reduced in STZ-induced rats compared with the CON group ($P < 0.01$); however, the amount of insulin released was significantly increased in the LAO and MAO groups ($P < 0.05$, $P < 0.05$). These results showed that the AO treatment could effectively maintain glucose homeostasis in STZ-induced rats.

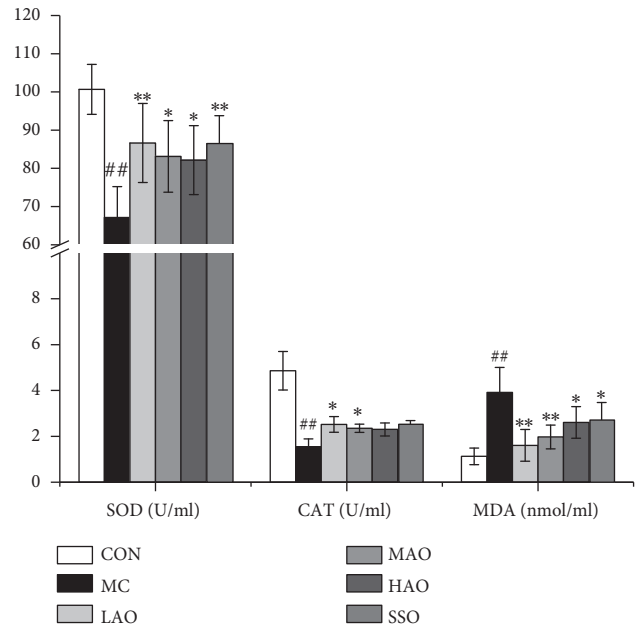

Figure 3: Effect of almond oil on serum oxidative status in STZ-induced rats. SOD, superoxide dismutase; CAT, catalase; MDA, malondialdehyde. Data were expressed as means ± SD. The MC group was compared with the CON group, $^{\#}P < 0.05$, $^{\#\#}P < 0.01$; the LAO, MAO, HAO, and SSO groups were compared with the MC group, $^{*}P < 0.05$, $^{**}P < 0.01$.

3.3. Effect of Almond Oil on the Oxidative and Inflammation-Related Factors in Diabetic Rats. The results of oxidative stress in the serum are shown in Figure 3. The STZ-induced rats had significantly lower SOD and CAT antioxidant enzymes activity and higher MDA level ($P < 0.01$), while almond oil administration could reverse the changes. Treatments with almond oil for four weeks and the activity levels of SOD in LAO, SSO ($P < 0.01$, $P < 0.01$), and MAO, HAO groups ($P < 0.05$, $P < 0.05$) were increased compared with MC group; levels of CAT in LAO and MAO groups were increased ($P < 0.05$, $P < 0.05$). MDA level in LAO and MAO groups ($P < 0.01$, $P < 0.01$) and HAO and SSO groups ($P < 0.05$, $P < 0.05$) were decreased compared with MC group. The results suggested that almond oil had the ability to suppress oxidative stress via increasing the activity of antioxidant enzymes and inhibiting lipid peroxidation in diabetic rats.

As shown in Figure 4, the levels of inflammatory factors were significantly elevated in the MC group compared with the CON group. TNF-α and IL-1β levels were significantly reduced in LAO, MAO, and HAO groups ($P < 0.01$,

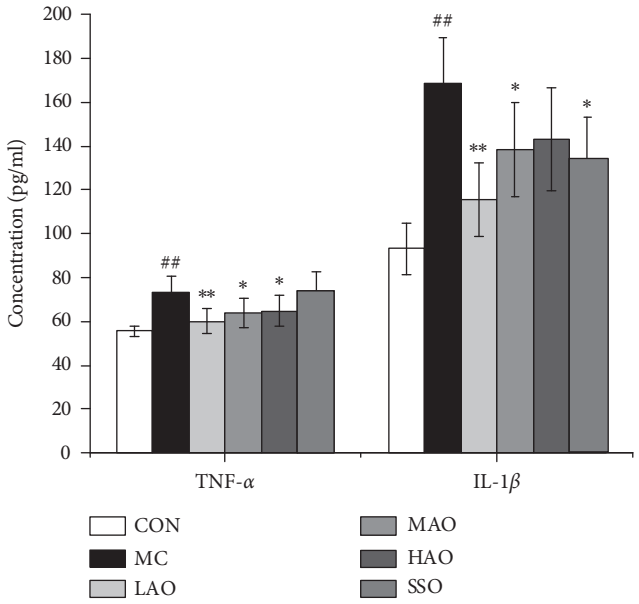

Figure 4: Effects of almond oil on serum TNF-α and IL-1β in STZ-induced rats. TNF-α, tumor necrosis factor-α; IL-1β, interleukin 1β. Data were expressed as means ± SD. The MC group was compared with the CON group, $^{\#}P < 0.05$, $^{\#\#}P < 0.01$; the LAO, MAO, HAO, and SSO groups were compared with the MC group, $^{*}P < 0.05$, $^{**}P < 0.01$.

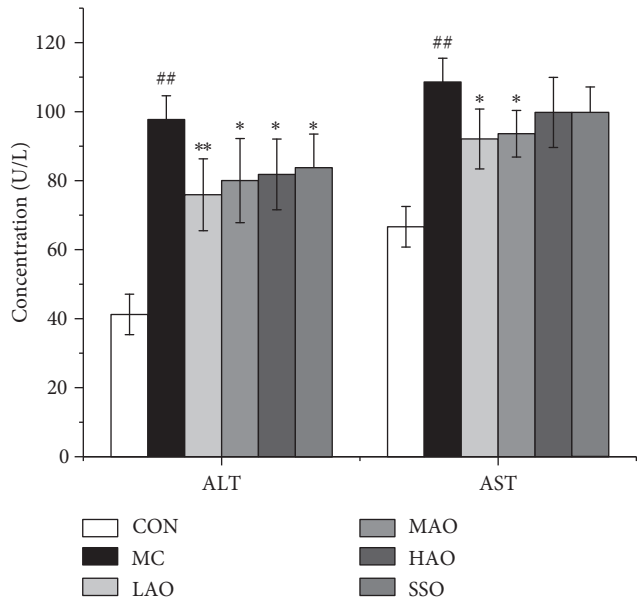

Figure 5: Effects of almond oil on serum ALT and AST in STZ-induced rats. ALT, alanine transaminase; AST, aspartate transaminase. Data were expressed as means ± SD. The MC group compared with the CON group, $^{\#}P < 0.05$, $^{\#\#}P < 0.01$; the LAO, MAO, HAO, and SSO groups compared with the MC group, $^{*}P < 0.05$, $^{**}P < 0.01$.

$P < 0.05$, $P < 0.05$) and LAO, MAO, and SSO groups ($P < 0.01$, $P < 0.05$, $P < 0.05$) compared with MC group, respectively.

3.4. Effect of Almond Oil on Biochemical Parameters in Diabetic Rats. As shown in Figure 5, the levels of ALT, AST, CRE, BUN, and AGEs were significantly increased ($P < 0.01$) after STZ-induced diabetes in rats compared with the CON group. The levels of serum ALT and AST are important indicators of liver damage. The three doses of AO and SSO treatment groups significantly decreased ALT levels compared with the MC group ($P < 0.01$, $P < 0.05$, $P < 0.05$, $P < 0.05$), and AST level was significantly reduced in LAO and MAO groups ($P < 0.05$, $P < 0.05$). BUN, CRE, and AGEs are also indicators of kidney damage. As shown in Figure 6, the levels of BUN, CRE, and AGEs in STZ-induced diabetic rats were significantly upregulated compared with the CON group ($P < 0.01$). Conversely, lower levels of BUN and CRE were observed in LAO and MAO groups ($P < 0.05$, $P < 0.05$) and LAO group ($P < 0.05$) compared to those of the MC group, respectively. AGEs level was significantly enhanced in all AO and SSO treatment groups ($P < 0.01$, $P < 0.05$, $P < 0.05$, $P < 0.05$). The results demonstrated that almond oil treatment could alleviate liver and kidney dysfunctions.

3.5. Effects of Almond Oil on Nrf2/HO-1 Pathway in Diabetic Rats. To determine whether almond oil affects the antioxidant ability in diabetes through the Nrf2/HO-1 pathway, the expressions of Keap1, Nrf2, HO-1, and NQO1 were measured by Western blot. As shown in Figure 7, compared with

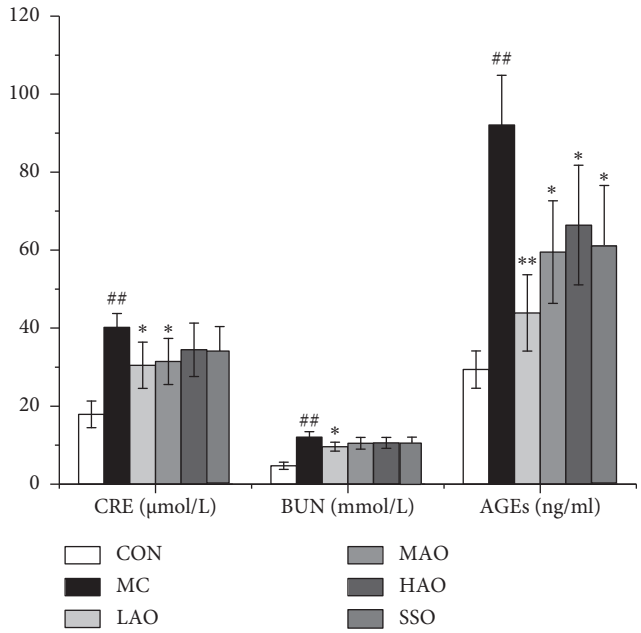

Figure 6: Effects of almond oil on serum CRE, BUN, and AGEs in STZ-induced rats. CRE, creatinine; BUN, blood urea nitrogen; AGEs, advanced glycation end products. Data were expressed as means ± SD. The MC group compared with the CON group, $^{\#}P < 0.05$, $^{\#\#}P < 0.01$; the LAO, MAO, HAO, and SSO groups compared with the MC group, $^{*}P < 0.05$, $^{**}P < 0.01$.

the CON group, the expressions of Nrf2 and HO-1 ($P < 0.01$, $P < 0.01$) were significantly downregulated while the expression of Keap1 ($P < 0.01$) was upregulated in STZ-induced rats, which showed that the Nrf2 antioxidant signaling

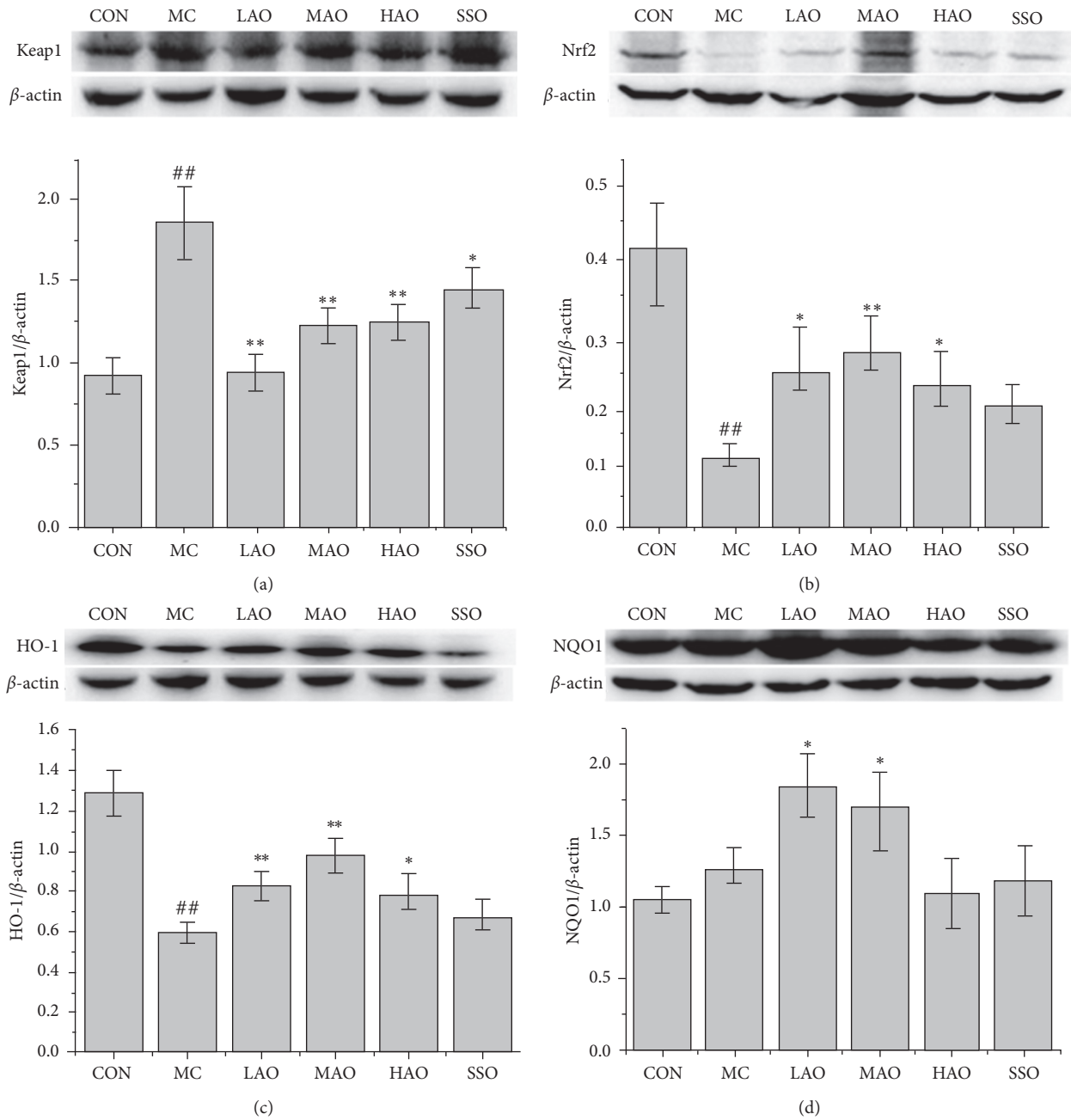

Figure 7: Effects of almond oil on Nrf2/HO-1 pathway in STZ-induced rats. Data are Western blotting results and gradation analysis of Keap1 (a), Nrf2 (b), HO-1 (c), and NQO1 (d). Data were expressed as means ± SD. The MC group compared with the CON group, $^{\#}P < 0.05$, $^{\#\#}P < 0.01$; the LAO, MAO, HAO, and SSO groups compared with the MC group, $^{*}P < 0.05$, $^{**}P < 0.01$.

pathway was impaired. Conversely, treatment with almond oil could reverse the changes compared with the MC group. Nrf2, HO-1, and NQO1 expressions were significantly upregulated in LAO, MAO, and HAO groups ($P < 0.05$, $P < 0.01$, $P < 0.05$), LAO, MAO, and HAO groups ($P < 0.01$, $P < 0.01$, $P < 0.05$), and LAO and MAO groups ($P < 0.05$, $P < 0.05$). Keap1 expression was significantly downregulated in LAO, MAO, HAO, and SSO groups ($P < 0.01$, $P < 0.01$, $P < 0.01$, $P < 0.05$). However, no significant changes in Nrf2, HO-1, or NQO1 expressions were observed between the SSO and MC groups. The results demonstrated that almond oil treatment could protect against oxidative-mediated injury by activating the Nrf2/HO-1 signaling pathway, which was correlated to its antioxidant effects.

3.6. Almond Oil Modified the Gut Microbiota Structure. The imbalance of interactions between host and gut microbiota could cause many important metabolic disorders, such as diabetes. In order to assess the effects of AO on the modulation of gut microbiota composition in diabetic rats, colon digesta samples were analyzed by 16S rDNA

sequencing. The effects of AO treatments on the changes of gut microbiota are shown in Figures 8–10.

The different microbial composition with overlaps was observed in the Venn diagram (Figure 8). Specifically, the CON group had 542 OTUs, MC group had 673 OTUs, SSO group had 584 OTUs, and the AO groups (LAO, MAO, and HAO) had 689, 648, and 518 OTUs, respectively. 331 OTUs were shared by these groups.

As shown in 1, compared with the CON group, Chao 1, Ace, and Shannon indices ($P < 0.01$, $P < 0.01$) were significantly increased, while Simpson index ($P < 0.01$) was decreased in STZ-induced rats.

In the beta diversity analysis, the principal coordinate analysis (PCoA) was used to reflect the compositional differences among groups. As shown in Figure 10, there was a clear separation of gut microbiota composition between the CON and MC groups, and the microbial composition in the almond oil treatment groups was more close to that in the CON group.

We analyzed the phylum and genus level characteristics further to explore the gut microbiota structure differences among groups. The relative abundance in the phylum level was shown in Figure 10(a). In the CON group, the dominant phyla were Firmicutes (60.74%) and Bacteroidetes (26.79%). Compared with the CON group, the abundance of Firmicutes increased to 72.57%, while the Bacteroidetes significantly decreased to 16.85% in the MC group ($P < 0.05$). However, the consumption of almond oil modified the gut microbiota. Specifically, the middle dose of almond oil decreased the abundance of Firmicutes to 62.87% and significantly increased Bacteroidetes to 21.89% ($P < 0.05$).

At the genus level, the microbiota of the MC group changed greatly compared to that of the normal rats (Figure 10(b)). The abundances of *Ruminococcaceae_UCG*-014, *Clostridium_sensu_stricto*_1, and *Fusicatenibacter* were increased, while *Lactobacillus*, *Bacteroides*, and *Lachnospiraceae_NK4A136_group* were decreased in the MC group compared with the CON group. Different doses of AO treatment can partially restore the microbiota change. The high dose of AO decreased *Ruminococcaceae_UCG*-014 ($P < 0.05$), the low dose of AO decreased *Clostridium_sensu_stricto*_1 and *Fusicatenibacter* ($P < 0.05$, $P < 0.05$), the high dose of AO increased *Lactobacillus* and *Lachnospiraceae_NK4A136_group* ($P < 0.05$, $P < 0.05$), and the middle dose of AO increased *Bacteroides* ($P < 0.05$).

3.7. Spearman's Correlation Analysis. Spearman's correlation analysis was used to further explore the relationship between gut microbiota and metabolic parameters (Figure 11). We analyzed the correlation between bacteria genus, FBG, insulin (INS), body weight (BW), SOD, CAT, MDA, TNF-α, IL-1β, Keap1, Nrf2, HO-1, and NQO1. The abundances of *Clostridium_sensu_stricto*_1 and *Fusicatenibacter* were positively correlated with FBG, MDA, TNF-α, IL-1β, and Keap1, while being negatively correlated with INS, BW, SOD, CAT, Nrf2, and HO-1. The abundance of *Ruminococcaceae_UCG*-014 was negatively correlated with BW, SOD, Nrf2, and HO-1. The abundance of *Lachnospiraceae_NK4A136_group* was positively correlated with SOD and Nrf2, while being negatively correlated with FBG. The abundance of *Bacteroides* was positively correlated with INS, SOD, CAT, Nrf2, and HO-1, while being negatively correlated with FBG and IL-1β. These bacteria genus changes were relevant to the regulations of glucose metabolism, oxidative stress, and inflammation. The result showed that almond oil treatment could recover some relevant dysbiosis of the gut microbiota and regulate the glucose metabolism and Nrf2/HO-1 pathway.

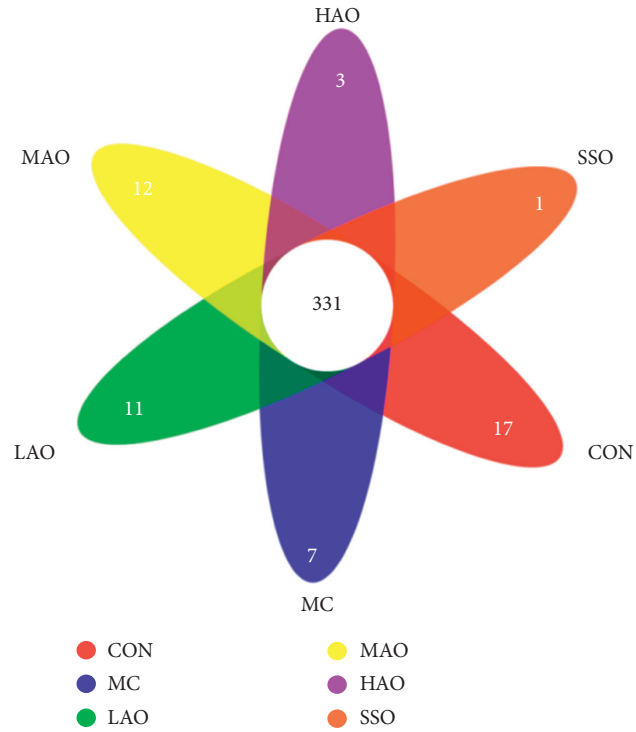

Figure 8: Venn diagrams of the OTUs between different groups.

4. Discussion

As a chronic metabolic disease, diabetes has proven to be a major threat to health risks. In recent years, the diet has been considered a crucial tool in the prevention and protection from disease and its complications, and dietary lipids have been regarded as one of the most necessary macronutrients for human health. Searching for dietary lipids with antidiabetic activity and few side effects has been essential to control the development of diabetes. In the present study, we exhibited that oral administration of almond oil for 4 weeks alleviated the symptoms of diabetes induced by STZ.

STZ is commonly used to induce experimental diabetes in rodents. STZ enters pancreatic β-cells through the GlUT2 glucose transporter [25] and induces the production of ROS, which rapidly and irreversibly destroys pancreatic β cells [26, 27]. As the characteristics of diabetes, polyphagia, polydipsia, hyperglycemia, and reduced BW were observed after STZ induction, which were demonstrated in previous research [28].

The main bioactive compound of almond oil is the oleic (n-9) fatty acids. Previous studies found that n-9 fatty acids could reduce the local inflammatory response [29]. Oleic

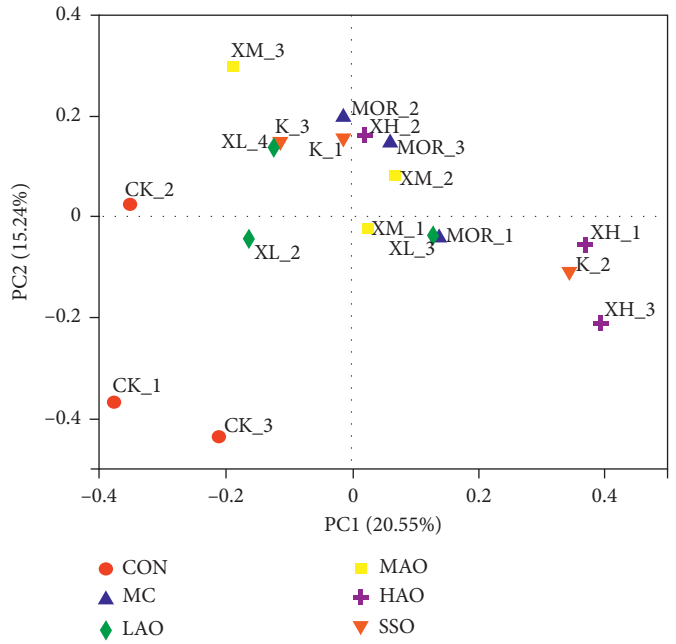

Figure 9: Principal coordinate analysis (PCoA) between different groups.

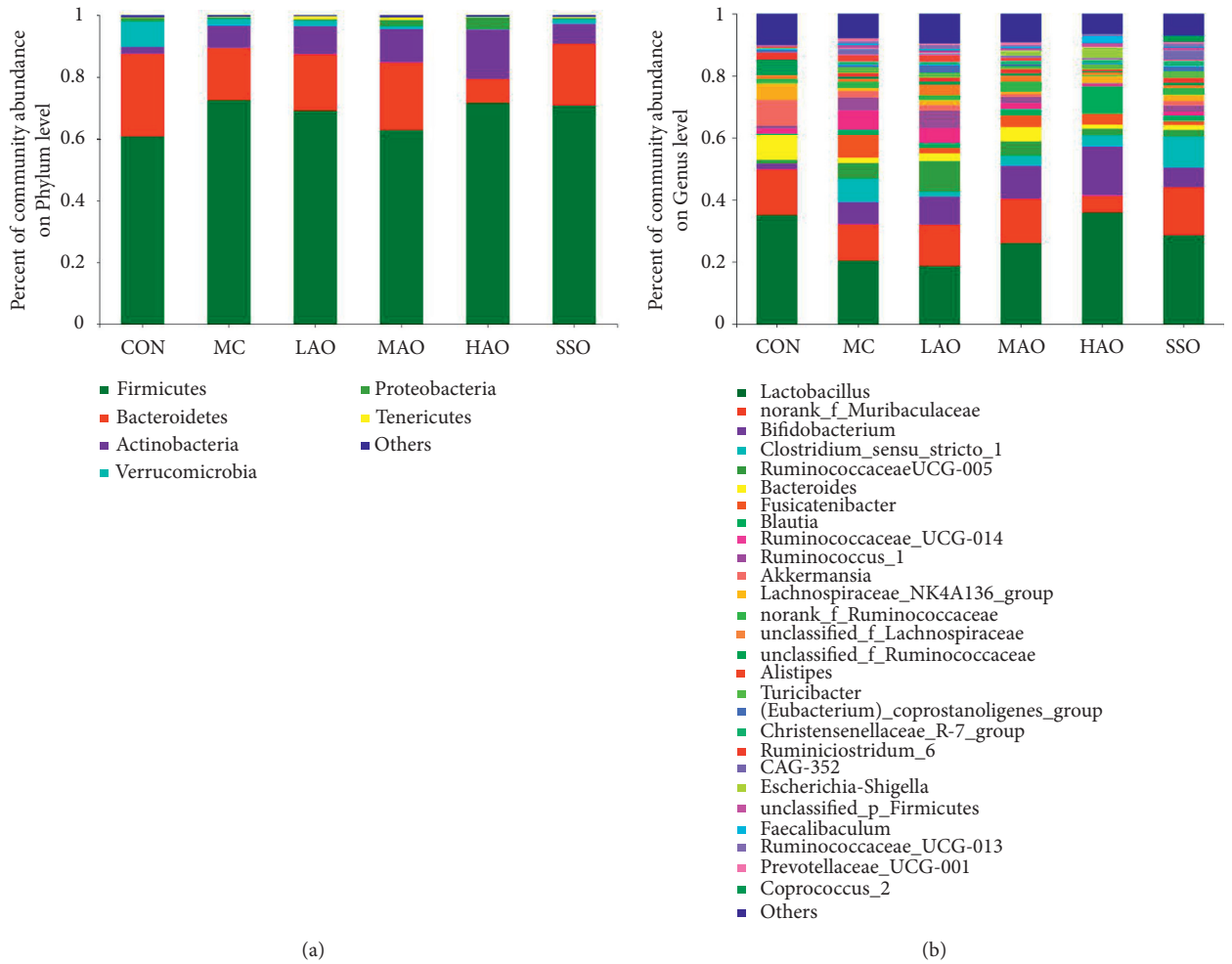

Figure 10: Modulation effect of almond oil on the gut microbiota in rats. (a) The effect of almond oil on microbial community structures at the phylum level. (b) The effect of almond oil on relative abundances at the genus level.

Table 1: Effects of almond oil on Alpha diversity.

Group	Community richness		Community diversity	
	Chao 1	Ace	Simpson	Shannon
CON	416.97 ± 44.77	419.59 ± 46.40	0.3175 ± 0.1282	2.6319 ± 0.3733
MC	541.84 ± 21.36$^{\#\#}$	533.70 ± 24.61$^{\#}$	0.0713 ± 0.0253$^{\#}$	3.7212 ± 0.2476$^{\#}$
LAO	475.53 ± 69.38	480.15 ± 77.50	0.0802 ± 0.0335	3.6362 ± 0.4064
MAO	428.57 ± 51.25**	424.33 ± 45.06**	0.1277 ± 0.0902	3.3834 ± 0.5983
HAO	395.07 ± 33.71**	394.07 ± 39.80**	0.1804 ± 0.1007	2.8502 ± 0.6498
SSO	480.08 ± 58.78	481.47 ± 55.62	0.1325 ± 0.1546	3.5032 ± 0.9386

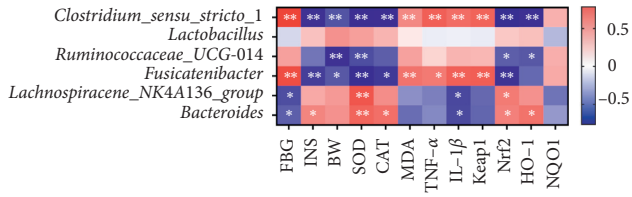

Figure 11: Significant correlation between the abundance of bacteria genus and metabolic parameters was selected using Spearman correlation analysis ($^{*}P < 0.05$, $^{**}P < 0.01$).

acid also has a cytoprotective effect for ß-cells, and dietary MUFAs have the potential to act as regulators of glucose homeostasis in either the inner-digestive or postabsorptive period [30]. Previous research demonstrated that oleic acid could suppress the deleterious effects of palmitic acid on the insulin signaling pathway [31]. In this study, we chose sunflower seed oil as the positive group. Sunflower seed oil is one of the most consumed dietary sources of polyunsaturated fatty acids and a kind of dietary lipids, which is widely used in the Chinese diet.

Chronic hyperglycemia leads to the excessive generation of ROS, such as hydrogen peroxide (H_2O_2), superoxide (O_2^-), hydroxyl (OH), or peroxyl (·OOH) radicals through glucose autoxidation [32]. Oxidative stress occurs as the excessive accumulation of ROS exceeding local antioxidant capacity, which may damage cellular organelles and causes an increase in lipid peroxidation [33]. More importantly, the oxidative status level, which plays a crucial role in the antioxidant system, was evaluated by measuring MDA, SOD, and CAT activities in our study. SOD is an essential endogenous antioxidant enzyme used to eliminate superoxide radicals and protect cells against the toxic byproducts of aerobics metabolism [34]. SOD could convert superoxide radicals to hydrogen peroxide (H_2O_2), which is decomposed into oxygen and water by catalase, and maintain the oxidation balance. Polyunsaturated fatty acids in the cell membrane were attacked by free radicals and formed MDA. MDA was formed by the attacking free radicals of polyunsaturated fatty acids in the cell membrane. As an oxidation end product and a biomarker of lipid peroxidation, MDA could indirectly reflect the extent of oxidative damage in the body [35]. The present study found that SOD and CAT activity were significantly decreased, and MDA content was increased in the MC group rats treated by STZ. In contrast, the results were reversed after almond oil treatment. Consistent results have proved that almond oil had an antioxidant modulating effect on rats with hepatic injury [24].

Oxidative stress has a crucial effect on the inflammatory reaction, which increases the excretion of inflammation-related cytokines [36]. TNF-α and IL-β are considered the central proinflammatory mediators for the inflammatory reaction, which are the major parts of the inflammatory process leading to ß-cell destruction and closely associated with the progression of diabetes [37]. TNF-α is a cytotoxin mainly produced by monocytes and macrophages and could induce the activation and accumulation of IL-1β, stimulating the immune disorder [38]. IL-1β affects the activation of nuclear factor kappa B (NF-κB), promoting the expression of several ß-cells genes [39]. The overproduction of IL-1β leads to the pathogenesis of inflammation and autoimmune diseases and correlates with the recruitment of immune cells and ß-cell damage in islets [40]. In our study, almond oil treatment significantly reduced the levels of TNF-α and IL-1β induced by STZ, suggesting that it had the potential effects of suppressing the expression of proinflammatory cytokines. However, no significant change of TNF-α was observed between the sunflower seed oil treatment group and the STZ-induced group. The sunflower seed oil contains about 67% linoleic acid (LA). LA is a direct precursor of the proinflammatory arachidonic acid (AA). AA can participate in cell signaling and trigger inflammation, which is linked to oxygen-free radical rise and results in more severe reactions in some tissues [41]. In contrast, the inflammatory markers of people with high MUFAs dietary habits have been considerably reduced, and oleic acid can reverse the inhibitory effect of TNF-α on insulin production, revealing that oleic acid has the potential therapeutic effect in an inflammatory context [42]. In summary, the anti-inflammatory effect of almond oil was better than sunflower seed oil according to the results of inflammatory factors due to its high content of oleic acid probably.

The chronic accumulation of circulating glucose might cause damage to the whole body blood vessels, which affected the functionality of some vital organs and increased the risk of various life-threatening health complications, such as chronic liver and kidney disease. ALT and AST activities may reflect the damage of hepatocytes and the markers of hepatocyte integrity. The contents of ALT and AST are low in the serum of normal rats but released into the blood due to the damage of hepatocytes or cell membrane permeability. In the present study, ALT and AST levels were increased in diabetes groups induced by STZ. Simultaneously, the administration of almond oil significantly reduced those levels, which was consistent with the result that treatment with almond oil suppressed the acute hepatic damage [23].

Hyperglycemia is characterized by the high content of glycated proteins and binding of monosaccharides to amino groups of proteins, leading to the formation of AGEs and changes in the structure and functions of proteins. Besides, glycated proteins can activate membrane receptors by glycation end products and induce intracellular oxidative stress and a proinflammatory status [43], consequently affecting kidney functions. CRE and BUN are also the biochemical markers of kidney functions. In the present study, the increased CRE, BUN, and AGEs levels in diabetic rats were reversed by almond oil treatment, which were consistent with the result that administration with almond oil changed the levels of CRE and BUN in rats exposed to a sublethal concentration of lead [44].

Nrf2/HO-1 is the main signaling pathway for antioxidative stress [12]. Under normal conditions, Nrf2 is bound by Keap1 in the cytoplasm and then degraded by the ubiquitination system. Under oxidative stress or inflammatory conditions, Nrf2 is released from Keap1 and translocated into the nucleus, where it combines with antioxidant response elements [10], upregulates the transcription of HO-1 and NQO1, and then participates in the antioxidation processes. HO-1 is a redox-sensitive inducible stress protein activated by Nrf2. HO-1 degrades heme into biliverdin, free iron, and carbon monoxide, which exerts a protective role by reducing oxidative injury and attenuating inflammatory response [45]. Our results found that the antioxidant mechanism of almond oil appeared to activate Nrf2 signaling pathway and upregulate the downstream of Nrf2. The consistent result also found that taurine could reduce the severity of oxidative stress by activating the antioxidative defense signaling pathway in diabetic rats [46]. The results also showed that the antioxidant ability of almond oil was better than sunflower seed oil.

Previous studies suggested that the blood glucose levels were also regulated in the intestine, which was a major organ involved in the glucose homeostasis, carbohydrate digestion, and secretion of glucose into the circulation, and the energy substrates can be used by intestinal colonized microbiota [4]. It indicated that gut microbiota has a protective effect on metabolism regulation and has a positive effect on glucose metabolism [47].

The Chao 1 and Ace indices were used to reflect the richness of the communities; the Simpson and Shannon indices were used to reflect the diversity of the communities. The richness and diversity of gut microbiota in STZ-induced rats were increased compared with the CON group, which were consistent with the previous report. The increase of gut microbiota diversity and richness could be associated with the development of disease [48].

Firmicutes and Bacteroidetes were the most abundant phyla in normal rats. The ratio of Firmicutes/Bacteroidetes was widely regarded as an indicator of gut microbiota dysbiosis in many metabolic diseases [49]. A decrease in Bacteroidetes has been associated with pathologies such as inflammatory bowel disease and diabetes [50]. A reduced relative abundance of Bacteroidetes and an increase in Firmicutes were observed in STZ-induced rats, resulting in an increased ratio of Firmicutes/Bacteroidetes, which were consistent with the previous study [4]. However, the ratio was downregulated upon treatment with almond oil.

Lactobacillus can promote glucose metabolism through directly consuming glucose in the host intestines [51]. *Lactobacillus* can inhibit the growth of acid-sensitive pathogenic bacteria by lowering the pH of the intestinal environment. It also competes with pathogens to protect the gut barrier and immune response of the host and improves intestinal oxidative stress in rats with liver damage [52]. In our study, the abundance of *Lactobacillus* was decreased in the MC group, while the change was reversed by oral administration of almond oil, which was in line with the previous report that dietary administration with pistachio nuts increased the abundance of *Lactobacillus* in diabetic rats [53]. Some bacteria in Ruminococcaceae are proinflammatory bacteria and associated with inflammatory bowel diseases [54]. The previous research analyzed the correlation between gut microbiota and blood glucose, and results showed that *Ruminococcaceae_UCG*-014 had a positive correlation with the occurrence and development of diabetes [55]. In this study, the abundance of *Ruminococcaceae_UCG*-014 was increased in the MC group, while the level of *Ruminococcaceae_UCG*-014 was decreased by almond oil. *Clostridium_sensu_stricto*_1 is considered as an LPS-producing pathogenic bacteria associated with intestinal inflammation and infection [56, 57]. High level of LPS accumulates in the intestine and participates in the inflammation of diabetics. Reducing the level of LPS-producing bacteria could reduce harmful substances from the intestines into the blood and inhibit the incidence of oxidative stress and inflammation [58]. *Clostridium_sensu_stricto*_1 and *Fusicatenibacter* were positively correlated with FBG levels. Our study also found that the abundance of *Clostridium_sensu_stricto*_1 and *Fusicatenibacter* was decreased by almond oil treatment compared to the MC group, which was in accordance with the report that propolis decreased the abundance of *Clostridium_sensu_stricto*_1 and *Fusicatenibacter* in diabetic rats [59]. *Lachnospiraceae_NK*4*A*136*_group* and *Bacteroides* are both short-chain fatty acids- (SCFA-) producing intestinal bacteria, which enhance the gut barrier function [60]. *Lachnospiraceae_NK*4*A*136*_group* inhabits the human gut and produces butyric acid that is considered as an intestinal barrier protector, which is associated with maintaining intestinal health [61]. *Bacteroides* is beneficial bacteria that plays an important role in glucose metabolism in the host [62]. The present study found that almond oil increased the abundances of *Lachnospiraceae_NK*4*A*136*_group* and *Bacteroides* compared with the MC group induced by STZ, which were consistent with the report that *Lycium barbarum* alleviated gut microbiota dysbiosis [63]. The results indicated that almond oil could reduce the relative abundance of proinflammatory bacteria and enhance the butyrate-producing bacteria, which alleviated abnormal glucose metabolism. Our results showed that the intake of low dose almond oil presented the best protective effect; however, the high dose almond oil presented a better impact on the antidysbiosis of gut microbiota. According to the correlation analysis, the abundance of *Clostridium_sensu_stricto*_1 and

Fusicatenibacter was positively correlated with oxidative stress and inflammatory response, while being negatively correlated with glucose metabolism and antioxidant enzymes activity. The abundance of these two genera was significantly reduced in the LAO group. The LAO group might regulate the main pathogenic bacteria to reduce the levels of oxidative stress and proinflammatory factors.

Our study suggested that almond oil administration for four weeks could positively regulate the gut microbiota of the host and inhibit the blood glucose elevation through increasing beneficial bacteria and reducing colonization of potentially pathogenic bacteria in metabolism pathways. Whether almond oil could increase the levels of SCFAs and maintain intestinal barrier function should be studied in further research.

5. Conclusions

In conclusion, almond oil alleviated the development of STZ-induced diabetes in rats.

The administration of almond oil significantly decreased the levels of FBG, promoted insulin secretion, increased BW and the ability to glucose tolerance, suppressed oxidative stress and inflammatory reaction, and improved liver and kidney function. The beneficial effect of almond oil appeared to be associated with activating Nrf2/HO-1 pathway against oxidative stress and regulating gut microbiota on glucose metabolism.

These results showed that the effect of almond oil on ameliorating diabetes is associated with its antioxidative and anti-inflammatory properties in STZ-induced diabetic rats, which indicated that replacing the common oil in the diet with almond oil may have a potential beneficial effect on diabetes, suggesting that almond oil could be used as an adjunct treatment strategy for diabetes.

Data Availability

The data used to support the findings of this study are available from the corresponding author upon request.

Ethical Approval

All the experimental procedures and animal welfare were in accordance with the related ethical regulation guidelines and approved by the Research Ethics Committee of the College of Food Science and Technology in Hebei Agricultural University (2017-006).

Conflicts of Interest

The authors declare that they have no conflicts of interest.

Acknowledgments

This work was supported by the Hebei Province Modern Agricultural Industrial Technology System Sheep Industry Innovation Team Special (No. HBCT2018140203); the Food Processing Discipline Group of Hebei Agricultural University (No. 2020-04); and the Research and Demonstration of the Key Technology of Using Nanocellulose Stabilized Pickering Emulsion Substitute Fat In Low-Fat Meat Products (No. 20327116D).

Supplementary Materials

The fatty acid composition analysis of almond oil was shown in Table S1 in the Supplementary Material. (*Supplementary Materials*)

References

[1] Y. Xu, L. M. Wang, and J. He, "Prevalence and control of diabetes in Chinese adults," *Jama*, vol. 310, no. 9, pp. 948–958, 2013.

[2] N. H. Cho, J. E. Shaw, S. Karuranga et al., "IDF Diabetes Atlas: global estimates of diabetes prevalence for 2017 and projections for 2045," *Diabetes Research and Clinical Practice*, vol. 138, pp. 271–281, 2018.

[3] J. Xie, W. Song, X. C. Liang et al., "Protective effect of quercetin on streptozotocin-induced diabetic peripheral neuropathy rats through modulating gut microbiota and reactive oxygen species level," *Biomedicine & Pharmacotherapy*, vol. 127, Article ID 110147, 2020.

[4] Y. Feng, H. Weng, L. Ling et al., "Modulating the gut microbiota and inflammation is involved in the effect of Bupleurum polysaccharides against diabetic nephropathy in mice," *International Journal of Biological Macromolecules*, vol. 132, pp. 1001–1011, 2019.

[5] M. Yang, Y. Chen, T. Zhao, and Z. J. Wang, "Effect of astaxanthin on metabolic cataract in rats with type 1 diabetes mellitus," *Experimental and Molecular Pathology*, vol. 113, Article ID 104372, 2020.

[6] A. Avogaro and G. P. Fadini, "The effects of dipeptidyl peptidase-4 inhibition on microvascular diabetes complications," *Diabetes Care*, vol. 37, no. 10, pp. 2884–2894, 2014.

[7] A. I. Vinik and E. J. Vinik, "Prevention of the complications of diabetes," *The American Journal of Managed Care*, vol. 9, no. 3, pp. 63–80, 2014.

[8] T. I. Adelusi, L. Du, M. Hao et al., "Keap1/Nrf2/ARE signaling unfolds therapeutic targets for redox imbalanced-mediated diseases and diabetic nephropathy," *Biomedicine & Pharmacotherapy*, vol. 123, Article ID 109732, 2020.

[9] H. Murata, H. Takamatsu, and S. Lie, "NRF2 regulates PINK1 expression under oxidative stress conditions," *PLoS One*, vol. 10, no. 11, Article ID 0142438, 2015.

[10] S. Y. Wang, P. Nie, X. D. Lu et al., "Nrf2 participates in the anti-apoptotic role of zinc in type 2 diabetic nephropathy through Wnt/beta-catenin signaling pathway," *The Journal of Nutritional Biochemistry*, vol. 84, Article ID 108451, 2020.

[11] X. Cheng, R. C. M. Siow, and G. E. Mann, "Impaired redox signaling and antioxidant gene expression in endothelial cells in diabetes: a role for mitochondria and the nuclear factor-E2-related factor 2-kelch-like ECH-associated protein 1 defense pathway," *Antioxidants & Redox Signaling*, vol. 14, no. 3, pp. 469–487, 2011.

[12] J. Ren, D. Su, L. X. Li et al., "Anti-inflammatory effects of Aureusidin in LPS-stimulated RAW264.7 macrophages via suppressing NF-kappaB and activating ROS- and MAPKs-dependent Nrf2/HO-1 signaling pathways," *Toxicology & Applied Pharmacology*, vol. 387, Article ID 114846, 2020.

[13] A. L. Wang, D. C. Cai, H. Zhang et al., "Using herbal medicine to target the "microbiota-metabolism-immunity" axis as

possible therapy for cardiovascular disease," *Pharmacological Research*, vol. 142, pp. 205–222, 2019.

[14] M. Knip and H. Siljander, "The role of the intestinal microbiota in type 1 diabetes mellitus," *Nature Reviews Endocrinology*, vol. 12, no. 3, pp. 154–167, 2016.

[15] Q. Zhang, Y. Pan, B. Zeng et al., "Intestinal lysozyme liberates Nod1 ligands from microbes to direct insulin trafficking in pancreatic beta cells," *Cell Research*, vol. 29, no. 7, pp. 516–532, 2019.

[16] R. Wirth, N. Bdi, G. Marti et al., "Regionally distinct alterations in the composition of the gut microbiota in rats with streptozotocin-induced diabetes," *PLoS One*, vol. 9, no. 12, Article ID 0110440, 2014.

[17] Y. Liu, C. Wang, J. Li et al., "Phellinus linteus polysaccharide extract improves insulin resistance by regulating gut microbiota composition," *The FASEB Journal*, vol. 34, no. 1, pp. 1065–1078, 2020.

[18] K. P. Scott, S. W. Gratz, P. O. Sheridan, H. J. Flint, and S. H. Duncan, "The influence of diet on the gut microbiota," *Pharmacological Research*, vol. 69, no. 1, pp. 52–60, 2013.

[19] S. S. K. Wijeratne, M. M. Abou-Zaid, and F. Shahidi, "Antioxidant polyphenols in almond and its coproducts," *Journal of Agricultural and Food Chemistry*, vol. 54, no. 2, pp. 312–318, 2006.

[20] C.-Y. Chen, K. Lapsley, and J. Blumberg, "A nutrition and health perspective on almonds," *Journal of the Science of Food and Agriculture*, vol. 86, no. 14, pp. 2245–2250, 2006.

[21] X. Chen, L. Li, X. Liu et al., "Oleic acid protects saturated fatty acid mediated lipotoxicity in hepatocytes and rat of non-alcoholic steatohepatitis," *Life Sciences*, vol. 203, pp. 291–304, 2018.

[22] Z. Ahmad, "The uses and properties of almond oil," *Complementary Therapies in Clinical Practice*, vol. 16, no. 1, pp. 10–12, 2010.

[23] X.-Y. Jia, Q.-A. Zhang, Z.-Q. Zhang et al., "Hepatoprotective effects of almond oil against carbon tetrachloride induced liver injury in rats," *Food Chemistry*, vol. 125, no. 2, pp. 673–678, 2011.

[24] L. R. D. O. Torres, F. C. D. Santana, F. L. Torres-Leal et al., "Pequi (Caryocar brasiliense Camb.) almond oil attenuates carbon tetrachloride-induced acute hepatic injury in rats: antioxidant and anti-inflammatory effects," *Food and Chemical Toxicology*, vol. 97, pp. 205–216, 2016.

[25] H. E. Eitah, Y. A. Maklad, N. F. Abdelkader, A. A. Gamal el Din, M. A. Badawi, and S. A. Kenawy, "Modulating impacts of quercetin/sitagliptin combination on streptozotocin-induced diabetes mellitus in rats," *Toxicology and Applied Pharmacology*, vol. 365, pp. 30–40, 2019.

[26] M. H. Jin, G. N. Shen, Y. H. Jin et al., "Peroxiredoxin I deficiency increases pancreatic β-cell apoptosis after streptozotocin stimulation via the AKT/GSK3β signaling pathway," *Molecular Medicine Reports*, vol. 22, no. 3, pp. 1831–1838, 2020.

[27] T. Szkudelski, "The mechanism of alloxan and streptozotocin action in Bcells of the rat pancrea," *Physiological Research*, vol. 50, no. 6, pp. 537–546, 2001.

[28] Y. Cheng, L. Sibusiso, L. Hou et al., "Sargassum fusiforme fucoidan modifies the gut microbiota during alleviation of streptozotocin-induced hyperglycemia in mice," *International Journal of Biological Macromolecules*, vol. 131, pp. 1162–1170, 2019.

[29] C. R. B. Cardoso, M. A. Souza, E. A. V. Ferro et al., "Influence of topical administration of n-3 and n-6 essential and n-9 nonessentia," *Wound Repair and Regeneration*, vol. 12, no. 2, pp. 235–243, 2004.

[30] S. López, B. Bermúdez, R. Abia, F. J. Muriana et al., "The influence of major dietary fatty acids on insulin secretion and action," *Current Opinion in Lipidology*, vol. 21, no. 1, pp. 15–20, 2010.

[31] V. Pardo, Á. González-Rodríguez, S. C. Kozma, and Á. M. Valverde, "Role of hepatocyte S6K1 in palmitic acid-induced endoplasmic reticulum stress, lipotoxicity, insulin resistance and in oleic acid-induced protection," *Food and Chemical Toxicology*, vol. 80, pp. 298–309, 2015.

[32] S. A. Sheweita, S. A. ElHady, and H. M. Hammoda, "Trigonella stellata reduced the deleterious effects of diabetes mellitus through alleviation of oxidative stress, antioxidant- and drug-metabolizing enzymes activities," *Journal of Ethnopharmacology*, vol. 256, Article ID 112821, 2020.

[33] A. G. Jagtap and P. B. Patil, "Antihyperglycemic activity and inhibition of advanced glycation end product formation by Cuminum cyminum in streptozotocin induced diabetic rats," *Food & Chemical Toxicology*, vol. 48, no. 8-9, pp. 2030–2036, 2010.

[34] B. Mansuroğlu, S. Derman, A. Yaba, and K. Kızılbey, "Protective effect of chemically modified SOD on lipid peroxidation and antioxidant status in diabetic rats," *International Journal of Biological Macromolecules*, vol. 72, pp. 79–87, 2015.

[35] S. Nabi, "Promotion of peroxidation and hydroperoxidation of lipids," *Toxic Effects of Mercury*, Springer, Berlin, Germany, 2014.

[36] G. R. Inmaculada, R. J. Cristina, D. S. Teresa et al., "Uric acid and anti-TNF antibody improve mitochondrial dysfunction in ob/ob mice," *Hepatology*, vol. 44, pp. 581–591, 2006.

[37] S. J. Burke, D. Lu, T. E. Sparer, M. D. Karlstad, and J. J. Collier, "Transcription of the gene encoding TNF-α is increased by IL-1β in rat and human islets and β-cell lines," *Molecular Immunology*, vol. 62, no. 1, pp. 54–62, 2014.

[38] C. Liu, X. Feng, Q. Li, Y. Wang, Q. Li, and M. Hua, "Adiponectin, TNF-α and inflammatory cytokines and risk of type 2 diabetes: a systematic review and meta-analysis," *Cytokine*, vol. 86, pp. 100–109, 2016.

[39] H. Heimberg, Y. Heremans, C. Jobin et al., "Inhibition of cytokine-induced NF-κB activation by adenovirus-mediated expression of a NF-κB super-repressor prevents β-cell apoptosis," *Diabetes*, vol. 50, no. 10, pp. 2219–2224, 2001.

[40] E. Brioudes, M. Alibashe-Ahmed, V. Lavallard, T. Berney, and D. Bosco, "Syndecan-4 is regulated by IL-1beta in beta-cells and human islets," *Molecular and Cellular Endocrinology*, vol. 510, Article ID 110815, 2020.

[41] A. Akrami, F. Nikaein, S. Babajafari, S. Faghih, and H. Yarmohammadi, "Comparison of the effects of flaxseed oil and sunflower seed oil consumption on serum glucose, lipid profile, blood pressure, and lipid peroxidation in patients with metabolic syndrome," *Journal of Clinical Lipidology*, vol. 12, no. 1, pp. 70–77, 2018.

[42] E. K. Vassiliou, A. Gonzalez, C. Garcia et al., "Oleic acid and peanut oil high in oleic acid reverse the inhibitory effect of insulin production of the inflammatory cytokine TNF-alpha both in vitro and in vivo systems," *Lipids in Health and Disease*, vol. 8, no. 25, pp. 1–10, 2009.

[43] C.-C. Chen, Y.-C. Lu, Y.-W. Chen et al., "Hemopexin is up-regulated in plasma from type 1 diabetes mellitus patients: role of glucose-induced ROS," *Journal of Proteomics*, vol. 75, no. 12, pp. 3760–3777, 2012.

[44] A. M. Al-Attar, "Therapeutic influences of almond oil on male rats exposed to a sublethal concentration of lead," *Saudi Journal of Biological Sciences*, vol. 27, no. 2, pp. 581–587, 2020.

[45] Y. Gao, J. T. Li, S. F. Chu et al., "Ginsenoside Rg1 protects mice against streptozotocin-induced type 1 diabetic by modulating the NLRP3 and Keap1/Nrf2/HO-1 pathways," *European Journal of Pharmacology*, vol. 866, Article ID 172801, 2020.

[46] C. A. Agca, M. Tuzcu, A. Hayirli, and K. Sahin, "Taurine ameliorates neuropathy via regulating NF-κB and Nrf2/HO-1 signaling cascades in diabetic rats," *Food and Chemical Toxicology*, vol. 71, pp. 116–121, 2014.

[47] H. Han, Y. Y. Li, J. Fang et al., "Gut microbiota and type 1 diabetes," *International Journal of Molecular Sciences*, vol. 19, no. 4, 2018.

[48] J. Z. Wu and L. J. Yan, "Streptozotocin-induced type 1 diabetes in rodents as a model for studying mitochondrial mechanisms of diabetic beta cell glucotoxicity," *Diabetes, Metabolic Syndrome and Obesity: Targets and Therapy*, vol. 8, pp. 181–188, 2015.

[49] M. Lyu, Y. F. Wang, G. W. Fan et al., "Balancing herbal medicine and functional food for prevention and treatment of cardiometabolic diseases through modulating gut microbiota," *Frontiers in Microbiology*, vol. 8, Article ID 02146, 2017.

[50] C. P. Tamboli, C. Neut, P. Desreumaux, and J. F. Colombel, "Dysbiosis in inflammatory bowel disease," *Gut*, vol. 53, no. 1, pp. 1–4, 2004.

[51] L. Wang, Q. Y. Shang, W. X. Guo et al., "Evaluation of the hypoglycemic effect of probiotics via directly consuming glucose in intestines of STZ-induced diabetic mice and glucose water-induced diabetic mice," *Journal of Functional Foods*, vol. 64, Article ID 103614, 2020.

[52] R. Zhao, Q. Hu, G. Ma et al., "Effects of flammulina velutipes polysaccharide on immune response and intestinal microbiota in mice," *Journal of Functional Foods*, vol. 56, pp. 255–264, 2019.

[53] A. E. Yanni, G. Mitropoulou, I. Prapa et al., "Functional modulation of gut microbiota in diabetic rats following dietary intervention with pistachio nuts (Pistacia vera L.)," *Metabolism Open*, vol. 7, Article ID 100040, 2020.

[54] D. N. Frank, A. L. Amand, R. A. Feldman, E. C. Boedeker, N. Harpaz, and N. R. Pace, "Molecular-phylogenetic characterization of microbial community imbalances in human inflammatory bowel diseases," *Proceedings of the National Academy of Sciences*, vol. 104, no. 34, pp. 13780–13785, 2007.

[55] Q. T. Ma, Y. Q. Li, J. K. Wang et al., "Investigation of gut microbiome changes in type 1 diabetic mellitus rats based on high-throughput sequencing," *Biomedecine & Pharmacotherapie*, vol. 124, Article ID 109873, 2020.

[56] W. T. Zhou, G. J. Chen, D. Chen, H. Ye, and X. X. Zeng, "The antidiabetic effect and potential mechanisms of natural polysaccharides based on the regulation of gut microbiota," *Journal of Functional Foods*, vol. 75, Article ID 104222, 2020.

[57] Y. Li, Q. Ma, J. Wang et al., "Relationship between hyperlipidemia and the gut microbiome of rats, characterized using high-throughput sequencing," *Journal of Traditional Chinese Medical Sciences*, vol. 7, no. 2, pp. 154–161, 2020.

[58] H. X. Cui, Y. N. Hu, J. W. Li, and K. Yuan, "Hypoglycemic mechanism of the berberine organic acid salt under the synergistic effect of intestinal flora and oxidative stress," *Oxidative Medicine and Cellular Longevity*, vol. 2018, Article ID 8930374, 13 pages, 2018.

[59] M. L. Xue, Y. Liu, H. W. Xu et al., "Propolis modulates the gut microbiota and improves the intestinal mucosal barrier function in diabetic rats," *Biomedicine & Pharmacotherapy*, vol. 118, Article ID 109393, 2019.

[60] Q. Z. Ding, B. W. Zhang, W. Zhang et al., "Liupao tea extract alleviates diabetes mellitus and modulates gut microbiota in rats induced by streptozotocin and high-fat, high-sugar diet," *Biomedicine & Pharmacotherapy*, vol. 118, Article ID 109262, 2019.

[61] S. Hu, J. Wang, J. Wang, H. Yang, X. Yan, and L. Su, "Fucoidan from acaudina molpadioides improves insulin resistance by altering gut microbiota dysfunction," *Journal of Functional Foods*, vol. 57, pp. 59–67, 2019.

[62] M. Gurung, Z. P. Li, H. You et al., "Role of gut microbiota in type 2 diabetes pathophysiology," *EBioMedicine*, vol. 51, Article ID 102590, 2020.

[63] B. Tian, M. Liu, W. An et al., "Lycium barbarum relieves gut microbiota dysbiosis and improves colonic barrier function in mice following antibiotic perturbation," *Journal of Functional Foods*, vol. 71, Article ID 103973, 2020.

Hindawi
Journal of Food Quality
Volume 2021, Article ID 6110743, 11 pages
https://doi.org/10.1155/2021/6110743

Research Article

ARTP Mutagenesis to Improve Mycelial Polysaccharide Production of *Grifola frondosa* Using a Mixture of Wheat Bran and Rice Bran as Substrate

Weimin Liu[1], **Weiwei Yang**[1], **Juan Wu**[1], **Yu Cheng**[1], **Zhencheng Wei**[2], **Tao Wang**[1], **Kwame Attafuah Ampofo**[1], **Haile Ma**[1], **Fengjie Cui**[1], **Xiaoming Yang**[1], **Jingkun Yan**[1], **Liuqing Yang**[3] **and Hao Zhang**[1]

[1]*School of Food and Biological Engineering, Jiangsu University, 301 Xuefu Road, Zhenjiang, Jiangsu 212013, China*
[2]*Sericulture and Agri-Food Research Institute, Guangdong Academy of Agricultural Sciences, Key Laboratory of Functional Foods, Ministry of Agricultural and Rural Affairs, Guangdong Key Laboratory of Agricultural Products Processing, No. 133 Dongguanzhuang Yiheng Road, Guangzhou, Guangdong 510610, China*
[3]*School of Pharmacy, Jiangsu University, 301 Xuefu Road, Zhenjiang, Jiangsu 212013, China*

Correspondence should be addressed to Weimin Liu; liuwmwu@ujs.edu.cn

Received 6 April 2021; Accepted 22 May 2021; Published 4 June 2021

Academic Editor: Biao Yuan

Mycelial polysaccharides from *Grifola frondosa* have shown potential for the prevention of chronic diseases. Atmospheric and room temperature plasma (ARTP) technology was used to enhance the ability of *G. frondosa* to efficiently utilize a mixture of rice bran and wheat bran in the production of mycelial polysaccharides. The ARTP-mutant *G. frondosa* GFA2 had an improved growth rate of 6.0 mm/d and polysaccharide yield of 2.65 g/L and showed stable genetic characteristics. Uniform design experiments showed that polysaccharide yield could be increased to 5.90 g/L using the optimized conditions of 10.0 g/L rice bran and 110.0 g/L wheat bran while omitting KH_2PO_4 and $MgSO_4{\cdot}7H_2O$. Gas chromatography demonstrated that GFA2 polysaccharides were composed of the monosaccharides rhamnose, arabinose, fucose, xylose, mannose, glucose, and galactose. This study provides an effective strategy for improving polysaccharide production in edible fungi while proposing the added-value utilization of rice and wheat brans.

1. Introduction

Grifola frondosa (*G. frondosa*) is a widely used medicinal and edible fungus in China, Japan, and Korea, having good texture, delicious taste, and excellent aroma [1]. Over the past three decades, many studies have shown that *G. frondosa*'s main functional components are polysaccharides. It has potential applications in the prevention of chronic diseases due to its antioxidative [2], immunoregulation [3, 4], antitumor [5, 6], antivirus [7], and blood glucose and lipid regulating bioactivities [8]. The polysaccharides from different sources and extraction processes might display different structures. It could result in the polysaccharides varying in the biological activities significantly. *G. frondosa* polysaccharides can be obtained from submerged culture broth or cultivated fruiting bodies. For example, the mycelial polysaccharides extracted by Zhao et al. from *G. frondosa* submerged culture could block EV71 virus replication and has certain antiviral activity [9]. Guo et al. extracted polysaccharides from *G. frondosa* fruiting body that could be used as a potential functional food component for the prevention and treatment of hyperglycemia and hyperlipidemia [10]. Generally, the cultivation of *G. frondosa* fruiting bodies takes several months using composts or lignocellulosic wastes such as straw or wood. Submerged culturing has the advantages of a shorter

cultivation period and consistent quality of the product. Moreover, agricultural by-products such as rice and wheat brans can be used as the substrate for this fungal fermentation.

Rice and wheat are the most important grains in China, with annual yields of 206 million and 100 million tons, respectively. After processing, 16 million tons of rice bran and 20 million tons of wheat bran are produced per year as primary by-products and are mainly used as feed, fermentation additives, or for extracting usable components. However, their overall utilization rate is below 20% [11, 12]. Rice bran contains carbohydrates (18–23%), proteins (16–20%), and other valuable components such as dietary fiber (20–35%) [13]. Wheat bran is rich in proteins (12–18%) and carbohydrates (45–65%). [14]. The proteins in rice and wheat brans have been thoroughly investigated [15, 16]. For example, rice bran protein extracted with alkali by Han et al. had a pepsin digestibility of 89.8%, while its true digestibility (94.8%) was significantly higher than soy protein, rice endosperm protein, and whey protein [17]. Recently, various studies have shown that rice and wheat brans can be used as carbon and nitrogen sources for microorganisms [18–20]. This increases the value of the bran and reduces wastage of agricultural resources.

G. frondosa strains show significant differences in their production of biomass, mycelial polysaccharides, and other metabolites. For instance, Quan et al. [21] screened a *G. frondosa* strain by the protoplast ultraviolet method and achieved a biomass yield of 11.5 g/L and intracellular polysaccharide yield of 0.78 g/L after 7 days of fermentation. Liu [22] used ultraviolet and microwave irradiation to obtain two *G. frondosa* mutants with improved fermentation performance using rice bran and wheat bran as substrates. However, *G. frondosa* strains with high fermentation performance using rice and wheat brans need to be continually improved. Recently, a new microbial mutation technique has been developed: atmospheric and room temperature plasma (ARTP) mutation. ARTP has proven to be a reliable and effective microbial breeding method with a high frequency of random mutations induced by reactive chemical species produced by the helium-based atmospheric and room temperature plasmas [23]. Compared to traditional mutation methods, ARTP can lead to the generation of multiple mutation mechanisms and types of genetic material. It has the advantages of high-throughput mutagenesis, high positive mutation rate, and good mutation stability [24]. Liu et al. [25] obtained a *Crypthecodinium cohnii* mutant (M7) with a volume yield of 1.02 g/L EPS and a biological yield of 0.39 g/g EPS, which are 33.9% and 85.4% higher than the native microalgae, respectively. The T31 mutant of *Candida tropicalis* yeast bred by ARTP showed a 22% increase in xylitol yield (0.61 g/g) [26]. Zhuang et al. [27] used the *Phaffia rhodozyma* mutant Y1 obtained by ARTP to hydrolyze bagasse for 96 h, achieving biomass and carotenoid concentrations of 12.65 g/L and 88.57 mg/L, respectively. There have been few reports on the use of ARTP to improve the fermentation performance of *G. frondosa*.

This study, therefore, focused on (i) using ARTP to produce a new *G. frondosa* mutant strain which could use rice and wheat brans to produce high-yield mycelial polysaccharides, (ii) optimizing the cultivation conditions to maximize production of mycelia and mycelial polysaccharides by this ARTP-mutated strain, and (iii) analyzing the components of the mycelial polysaccharides before and after mutation of *G. frondosa*.

2. Materials and Methods

2.1. Materials. Rice bran was purchased from Zhenjiang Sanshan Rice Factory Co., Ltd. and wheat bran from Zhenjiang Fuhua Flour Co., Ltd. (Zhenjiang, Jiangsu, China). The brans were hot-air-dried, ground to 60 mesh, and stored at 4°C for further investigation.

2.2. Fungal Strain and Media. G. frondosa ZJQYLIU2017 was isolated from *G. frondosa* fruiting body (Qinghui151, national certification of edible fungi variety for cultivation and food) from Qingyuan Scientific Research Center of Edible Fungi, Lishui, Zhejiang, China.

Culture media were prepared as follows: potato dextrose agar medium (PDA, g/L) contained potato 200, glucose 20, peptone 5, KH_2PO_4 1.5, $MgSO_4{\cdot}7H_2O$ 0.75, and agar 20; potato dextrose medium (PD, g/L) consisted of potato 200, glucose 20, peptone 5, KH_2PO_4 1.5, and $MgSO_4{\cdot}7H_2O$ 0.75; screening plate medium (g/L) contained rice bran 20, wheat bran 30, KH_2PO_4 1.5, $MgSO_4{\cdot}7H_2O$ 0.75, and agar 20; and screening fermentation medium (g/L) included rice bran 40, wheat bran 60, KH_2PO_4 1.5, and $MgSO_4{\cdot}7H_2O$ 0.75.

2.3. ARTP Mutagenesis. The parent strain *G. frondosa* ZJQYLIU2017 was incubated on PDA plates, brushed with 10 mL of sterile normal saline to produce a liquid suspension, then diluted for ARTP mutagenesis. With pure helium as the working gas, the parameters of the ARTP mutation instrument (ARTP-IIS; Wuxi Yuanqing Tianmu Biotechnology Co., Ltd., Jiangsu, China) were 120 W radio frequency power input, 10 L/min gas flow, and 2 mm irradiation distance [28]. Suspension samples (20 μL) were exposed to the ARTP plasma jet for 0 to 130 s, spread on screening media plates, and incubated for 15 days at 23°C, observing colony growth (Figure 1). Lethality was calculated under various treatment times according to the following equation:

$$\text{Lethality}\,(\%) = \frac{(\text{Control colonies} - \text{Survival colonies})}{\text{Control colonies} \times 100}. \quad (1)$$

Surviving ARTP-mutated strains were inoculated onto screening media to compare their colony morphologies and sizes. Eleven positive mutants with high growth rate were identified and transferred to screening medium plates to determine their growth rate. The mycelia were inoculated into PD medium to obtain a seed solution of *G. frondosa*. This seed solution was then inoculated (10% v/v) into fermentation media at 23°C and 150 rpm for 10 days. Samples of the fermentation broth were filtered and washed with distilled water through a 40-mesh filter to separate mycelia

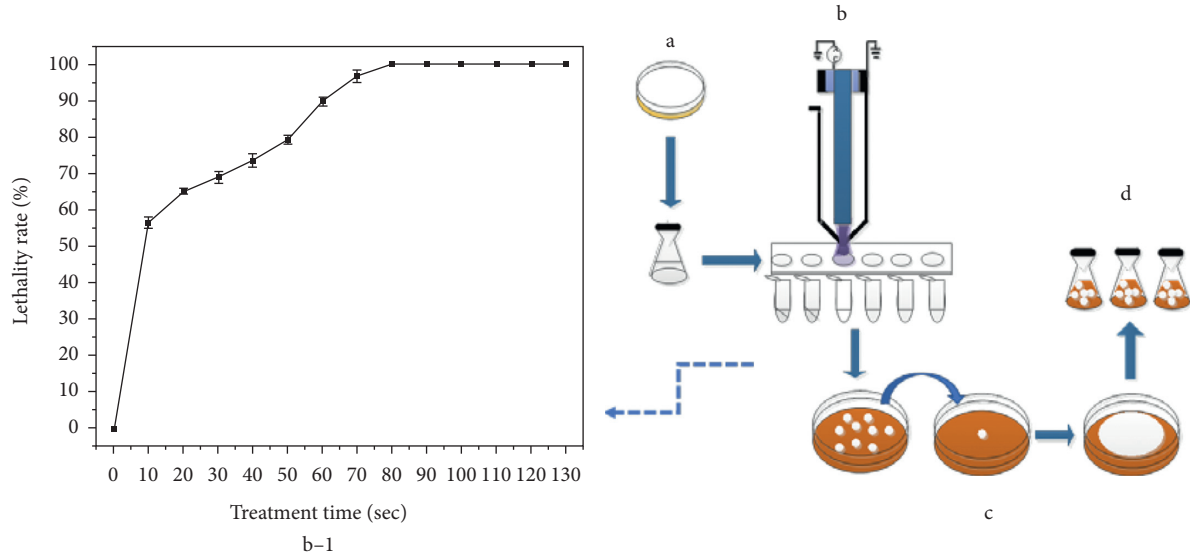

Figure 1: Flow chart of ARTP screening. (a) Cultivation of *G. frondosa*; (b) ARTP mutagenesis, and b–1: lethality of *G. frondosa* at different irradiation times; (c) positive mutants transfer to rice bran and wheat bran for growth tests, and (d) dominance mutants performance in rice bran and wheat bran submerged culture. The results were calculated from three independent tests.

and residues, then dried at 50°C, ground to a powder and extracted in 90°C water for 2 h at 1 : 30 (*w*/*v*) [29]. The concentration of mycelial polysaccharides was determined by the phenol-sulfuric acid method [30].

2.4. Preparation of Crude Polysaccharide Samples. Mycelial polysaccharides were precipitated by adding four volumes of 95% ethanol to the polysaccharide extract solution, protein was removed three times with Sevag reagent (4 : 1 chloroform: n-butyl alcohol), the solution was dialyzed against distilled water in a 3500 Da molecular weight cut-off dialysis bag for 72 h, and the retained crude *G. frondosa* polysaccharides were freeze-dried.

2.5. Strain Identification. The parent strain *G. frondosa* ZJQYLIU2017 and mutant strain *G. frondosa* JSULIUWANG2019 (GFA2) were sequenced by Sangon Biotech Co. (Shanghai, China) via PCR amplification using an ITS primer [31]. NCBI BLAST was used for homology comparison and phylogenetic analysis was performed using Mega 7.0 software to identify the mutant.

2.6. Optimization of Fermentation Medium for Mutant GFA2. One-factor-at-a-time experiments were carried out to investigate the influence of rice bran (10, 30, 50, 70, 90, and 110 g/100 L), wheat bran (10, 30, 50, 70, 90, and 110 g/L), KH_2PO_4 (0, 0.5, 1, 1.5, 2, and 2.5 g/L), and $MgSO_4{\cdot}7H_2O$ (0, 0.5, 1, 1.5, 2, and 2.5 g/L) on the *G. frondosa* mycelial biomass and polysaccharides. A seed solution of 10% (v/v) was inoculated into 100 mL fermentation media (250 mL flask) and cultured at 23°C and 150 rpm for 10 days.

The U_{11} (11^3) uniform experimental design allowed more factors and levels to be assessed in a limited number of experiments [32] and the regression equation enabled the selection of the optimum fermentation media composition based on the ratio of rice bran to wheat bran, KH_2PO_4, and $MgSO_4{\cdot}7H_2O$.

2.7. Monosaccharide Composition Analysis. Monosaccharide composition of the freeze-dried polysaccharides was determined by gas chromatography using an Agilent 7890A (DB-5MS quartz capillary column, 30 m × 0.25 mm × 0.25 μm) with flame ionization detector. The sample derivatization procedure was based on Yan et al. [33]. Briefly, 10 mg of polysaccharide was hydrolyzed with 5.0 mL TFA (2 M) at 110°C for 8 h. Hydroxylamine hydrochloride (10 mg) and pyridine (1 mL) were heated at 90°C for 30 min, then the hydrolysate was derivatized with 1 mL acetic anhydride at 90°C for 30 min. The detection conditions were as follows: column temperature started at 120°C, rose at 5°C/min to 200°C, then at 2°C/min to 215°C, and finally 20°C/min to 270°C; inlet and detector temperatures were 250°C; the split ratio was 30 : 1; flow rates of H_2, N_2 and air were 35, 30 and 350 mL/min, respectively.

2.8. Fourier Transform Infrared Spectroscopy. Fourier transform infrared (FT-IR) spectra were acquired using a Bruker Vector33 FT-IR spectrophotometer in the wavelength region 4000 to 400 cm^{-1} [34].

2.9. Statistical Analysis. All experiments were performed in triplicate and the results expressed as mean ± standard deviation. Correlation and regression analyses were performed using Origin 9.0. Student's *t*-test was used to determine significant differences between samples with $p < 0.05$ considered to indicate significance (SPSS 22.0; SPSS Inc., USA).

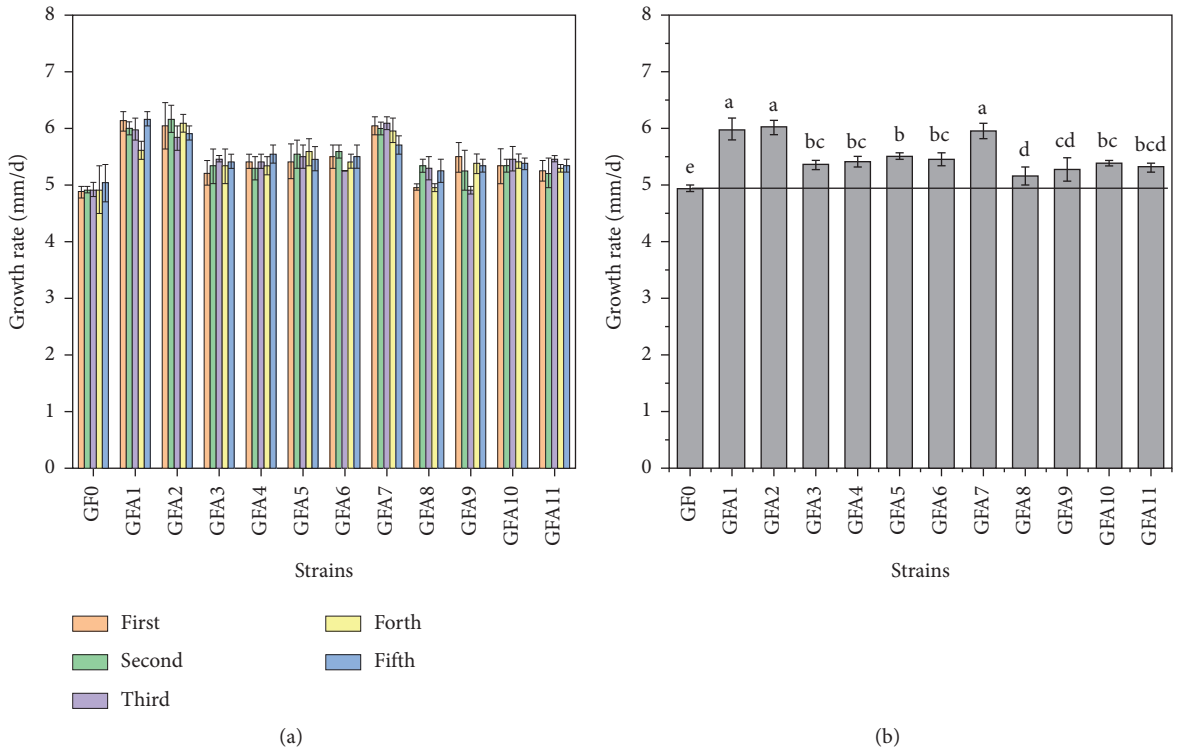

Figure 2: Growth rate of the parent strain (GF0) and mutants (GFA1–GFA11) of *G. frondosa* on screening media at 23°C. The growth rate in five generations (a). The average growth rate of five generations (b). Each data point is the mean of three replicate samples. (a), (b), (c), and so forth indicate significant difference at $p < 0.05$.

3. Results and Discussion

3.1. Mutation of G. frondosa by ARTP. ARTP breaks DNA strands and induces mutations using high purity helium gas in a high-frequency electrical field at atmospheric pressure and room temperature [27, 35]. Figure 1 shows the dose- and time-dependent lethality, based on equation (1), induced by ARTP mutagenesis of the parent *G. frondosa* strain (GF0). When GF0 was treated for 10 s, about 55% of cells were killed, indicating that many cells were sensitive to the treatment. The lethality reached 89.9% at 60 s and 96.9% at 70 s. Substantial DNA damage may cause cells to initiate their SOS emergency repair mechanism. This repair process can generate various types of mismatch site, significantly raising the mutation rate [36]. Longer treatment time increases the lethality, DNA damage, and mutation rate. The positive mutation rate was the highest when lethality was 90–95% [37], so 60 s was considered to be the optimum ARTP treatment time in this study.

3.2. Screening of Mutant Strains. As an effective method to generate mutant bacterial and fungal strains with improved properties such as tolerance to growth conditions and increased production of biomass, polysaccharides, enzymes, and other components [38], ARTP was adopted to produce an improved mutant strain of *G. frondosa*. After ARTP mutagenesis, the parent strain GF0 and 11 mutant strains (GFA1, GFA2, ..., GFA11) from large colonies were screened by culturing on screening media plates for five generations. The mycelial growth rates per generation of these 12 strains are shown in Figure 2(a). Figure 2(b) shows that the daily mycelial growth rate of GF0 was 4.93 ± 0.05 mm/d, while the mutants GFA1, GFA2, and GFA7 were 5.98 ± 0.19 mm/d, 6.00 ± 0.12 mm/d, and 5.96 ± 0.43 mm/d, which increases of 21.5%, 22.2%, and 21.1%, respectively. These mutant strains showed significant improvement in mycelia growth on rice and wheat brans media compared with GF0.

After five generations, GFA1, GFA2, and GFA7 were selected for fermentation performance testing (Figure 3). As shown in Figure 3(c), GFA1, GFA2, and GFA7 had average mycelial biomass yields of 21.81 ± 0.61 g/L, 22.26 ± 0.43 g/L, and 22.06 ± 0.23 g/L, respectively (GF0 was 20.02 ± 0.29 g/L). GFA2 had the highest mycelial polysaccharide concentration of 2.65 ± 0.02 g/L, with the parent strain GF0 having 2.43 ± 0.06 g/L. Thus, biomass and polysaccharide concentration increased by 11.2% and 9.2%, respectively, in GFA2. However, notwithstanding the increases shown in Figure 3(c), the weight-for-weight yields of polysaccharides from mutants GFA1, GFA2, and GFA7 were not significantly different from the parent strain GF0 in Figure 3(d), indicating that ARTP mutation could improve the ability to utilize wheat and rice brans, but not significantly change the synthesis of mycelial polysaccharides. Nevertheless, GFA2 was the most efficient strain to use with rice and wheat brans for *G. frondosa* polysaccharide production.

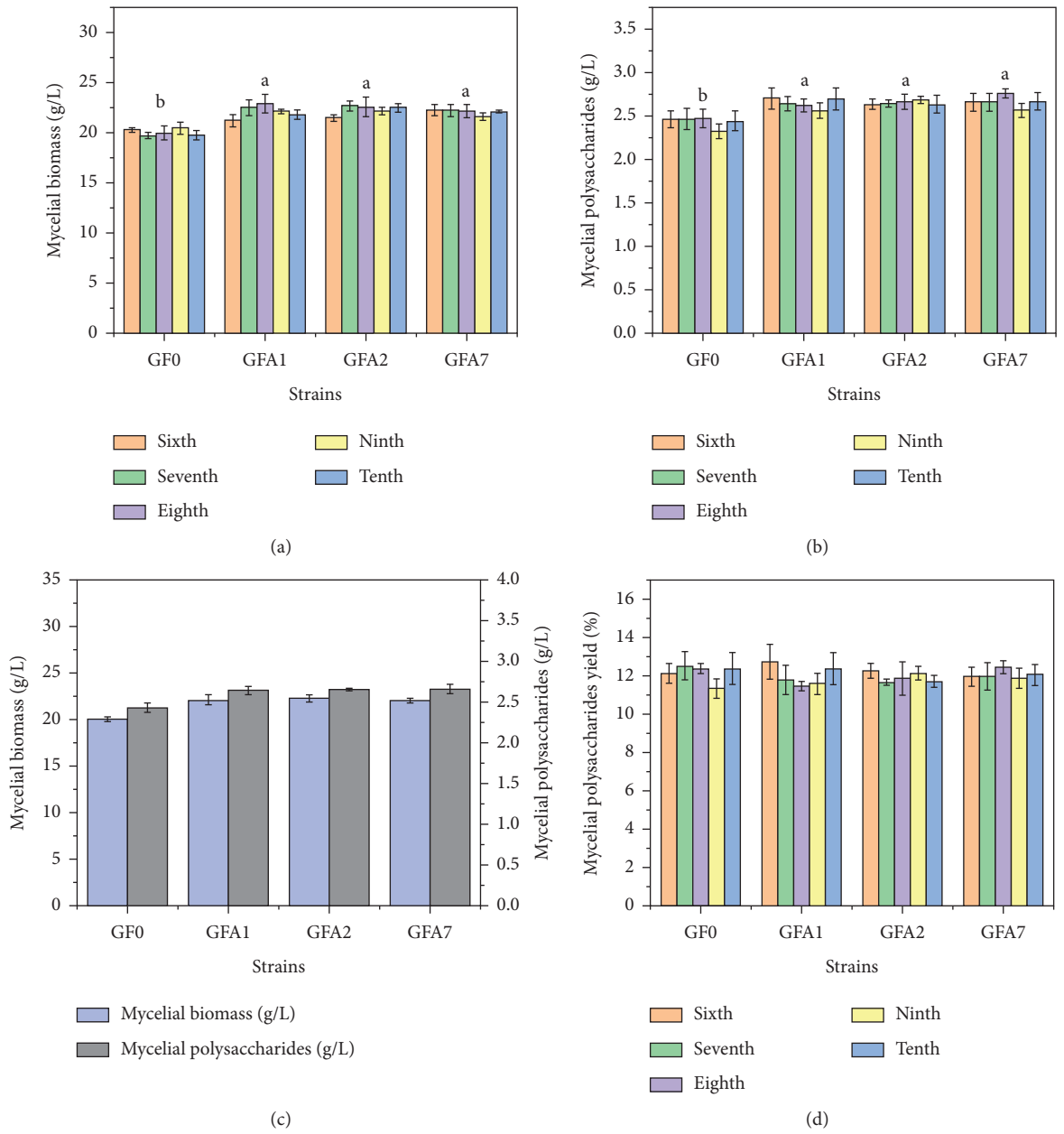

Figure 3: Five generations of fermentation of the parent strain and three mutant strains (GFA1, GFA2, GFA7) during bioconversion of wheat bran and rice bran at 23°C and 150 r/min. The mycelial biomass concentration in five generations (a), the mycelial polysaccharides concentration in five generations (b), the average mycelial biomass and mycelial polysaccharides of five generations (c), the weight-for-weight yields of mycelial polysaccharides (d). The mycelial biomass was calculated as the dry weight of mycelia. Each data point is the mean of three replicate samples. (a) and (b) indicate significant difference at $p < 0.05$ in average five generations.

The growth and fermentation performances of the mutant strains were investigated by culturing for ten generations, including five generations on screening plate media and five on screening fermentation media to measure fermentation performance. GFA1 had the lowest biomass production, 21.81 g/L (Figure 3), and the growth rate of GFA7 decreased significantly from 6.04 mm/d to 5.71 mm/d by the 5th generation ($p < 0.05$) (Figure 2), whereas GFA2 was genetically stable ($p > 0.05$) and its bran utilization rate was higher than the parent strain. Hence, GFA2 was selected as the preferred polysaccharide-producing strain for subsequent studies.

3.3. DNA Sequence Analysis of the GFA2. Partial sequencing of the internal transcribed spacers and the 5.8S gene of the parent *G. frondosa* strain ZJQYLIU2017 (NCBI accession no. MT830899) and mutant strain *G. frondosa* JSULIU-WANG19 (NCBI accession no. MT830900) were uploaded to the NCBI database. GFA2 (*G. frondosa* JSULIU-WANG19) was identified by partial sequence analysis and a neighbor-joining phylogenetic tree was constructed to compare strains. The phylogenetic tree (Figure 4) demonstrates the very close genetic relationship between GFA2 and the parent strain.

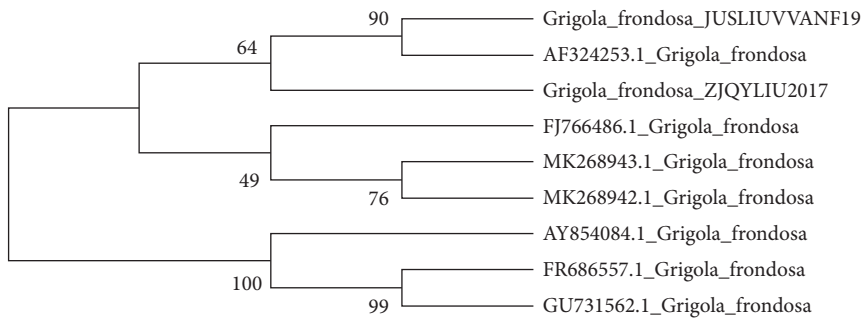

Figure 4: The phylogenetic tree based on gene sequence of GFA2.

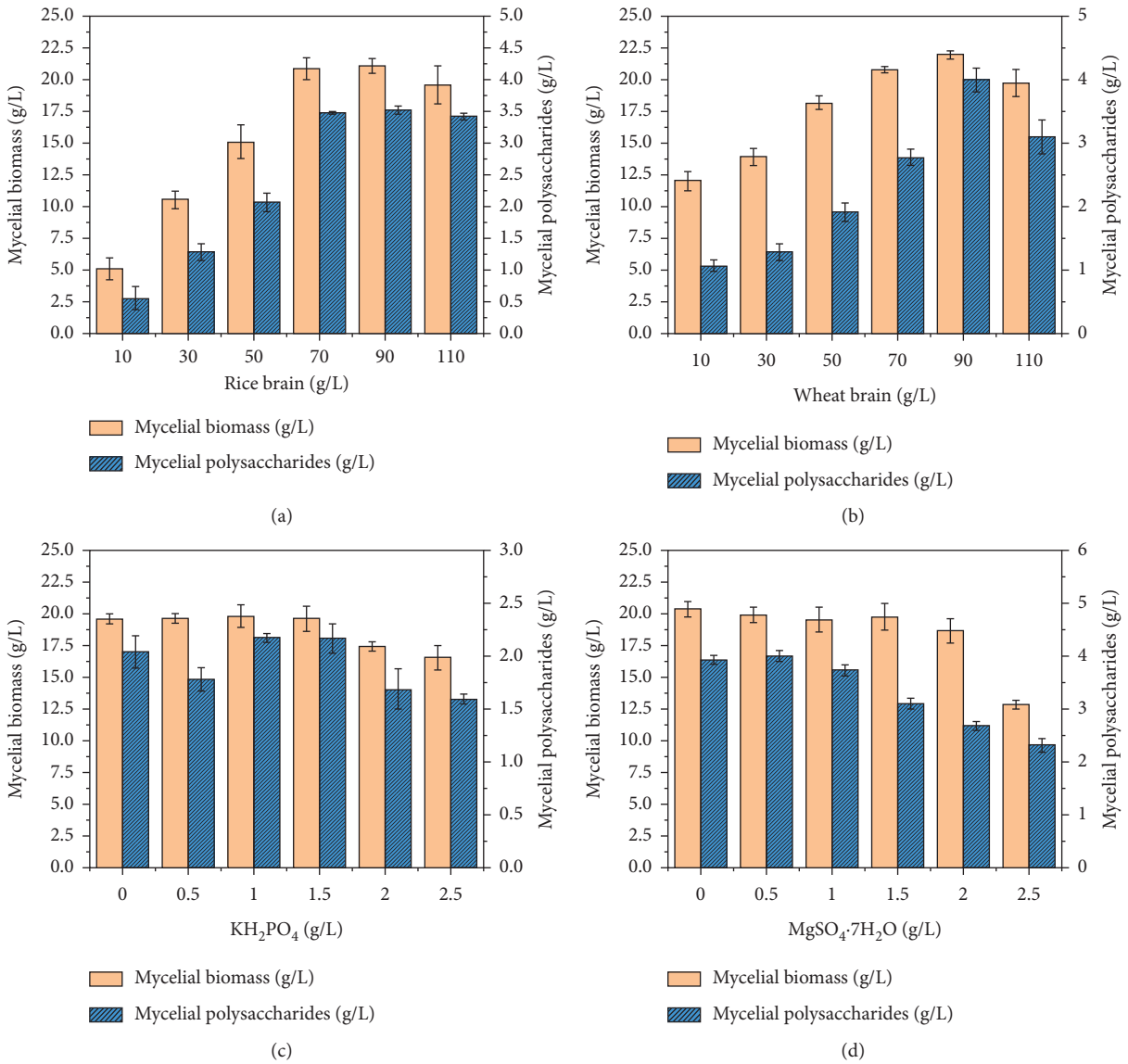

Figure 5: Effect of single factor on mycelial biomass and mycelial polysaccharides: effects of rice bran (a), effects of wheat bran (b), effects of KH_2PO_4 (c), and effects of $MgSO_4{\cdot}7H_2O$ (d).

3.4. Optimization of the GFA2 Fermentation Medium. Rice and wheat brans were the main carbon and nitrogen sources in the submerged fermentation media for the GFA2 strain. Figure 5(a) shows the influence of rice bran on the production of mycelial biomass and polysaccharide concentration. Biomass reached a maximum of 21.08 g/L when rice bran increased to 90 g/L but decreased to 19.58 g/L at higher bran concentrations. Mycelial polysaccharide

Table 1: Uniform design of $U_{11}(11^3)$ parameters and results for GFA2 fermentation optimization. Each data point is the mean of three replicate samples.

Runs	Factors			Biomass Y_1 (g/L)	Mycelial polysaccharides Y_2 (g/L)
	$^1x_1$	$^2x_2$	$^3x_3$		
1	2.2727	2	2.25	21.61 ± 0.57	3.38 ± 0.17
2	9.909	0.25	2	18.33 ± 0.44	2.39 ± 0.13
3	1.1818	0.5	0.5	18.38 ± 1.16	2.42 ± 0.09
4	6.6363	1.25	2.5	20.76 ± 0.35	2.15 ± 0.12
5	5.5454	0	1	17.15 ± 1.38	1.72 ± 0.20
6	8.8181	1	0	19.40 ± 1.11	1.98 ± 0.06
7	0.0909	1.5	1.25	17.71 ± 2.12	2.44 ± 0.13
8	11	1.75	0.75	22.76 ± 1.18	3.15 ± 0.15
9	3.3636	0.75	1.75	21.10 ± 1.42	2.25 ± 0.22
10	7.7272	2.5	1.5	18.58 ± 0.74	1.80 ± 0.13
11	4.4545	2.25	0.25	19.27 ± 0.91	2.09 ± 0.06

$^1x_1$: the ratio of rice bran to wheat bran (total amount of rice and wheat brans was 120 g/L). $^2x_2$: the concentration of KH_2PO_4. $^3x_3$: the concentration of $MgSO_4{\cdot}7H_2O$.

concentration rose from 0.55 ± 0.02 g/L (rice bran concentration 10 g/L) to a maximum of 3.51 ± 0.07 g/L (rice bran 90 g/L). Wheat bran from 10 to 70 g/L gave a relatively consistent yield of mycelial biomass (Figure 5(b)), which then peaked at 21.96 g/L with 90 g/L wheat bran (while polysaccharide concentration peaked at 4.00 ± 0.17 g/L). Low bran concentrations provided insufficient substrate, leading to a low yield of mycelia.

Appropriate concentrations of macromineral elements are essential for substrate utilization by fungi [39]. Concentrations of mycelial biomass and polysaccharides peaked at 19.83 ± 0.88 g/L and 2.18 ± 0.03 g/L, respectively, when KH_2PO_4 was 1.0 g/L (Figure 5(c)). Notably, as $MgSO_4{\cdot}7H_2O$ increased, biomass concentrations fell, in contrast to mycelial polysaccharide concentrations (Figure 5(d)) which reached 4.01 ± 0.10 g/L when $MgSO_4{\cdot}7H_2O$ was 0.5 g/L. K^+ and Mg^{2+} regulate cellular osmotic pressure and influence the metabolic processes of mycelial growth. Moreover, Mg^{2+}, as an enzyme cofactor, affects the activities of many intracellular and extracellular enzymes, thus impacting the synthesis of polysaccharides in mycelia and their ability to degrade substrates. In agreement with the current study, Mg^{2+} has been reported to increase the mycelial growth of *Ganoderma lucidum* cau5501 [40]. It is notable that high concentrations of KH_2PO_4 and $MgSO_4{\cdot}7H_2O$ suppressed mycelial growth and polysaccharide accumulation. Yuan et al. [41] also reported that when KH_2PO_4 exceeded its optimum concentration of 5.0 g/L, cell growth slowed, and inulinase activity was inhibited.

Table 2: ANOVA data of mycelial polysaccharides concentration in rice and wheat brans fermentation media for GFA2.

Factor	Coefficient estimate	Standard error	t value	p value
x_1	0.299	0.080	3.739	0.013
x_2	17.134	3.240	5.288	0.003
x_3	11570	3.157	3.665	0.015
x_1x_1	−0.023	0.008	−2.976	0.031
x_2x_2	−62.756	13.668	−4.591	0.006
x_3x_3	−44.624	13.226	−3.374	0.020

The results of uniform experiments on biomass and mycelial polysaccharides are shown in Table 1. SPSS was used to analyze the linear regression of rice: wheat bran ratio (x_1), KH_2PO_4 (x_2), and $MgSO_4{\cdot}7H_2O$ (x_3) against mycelial biomass (Y_1) and mycelial polysaccharides (Y_2):

$$Y_1 = 0.299x_1 + 17.134x_2 + 11.570x_3 - 0.023x_1^2 - 62.756x_2^2 - 44.624x_3^2. \quad (2)$$

The previous equation was the mycelial biomass model equation with the best degree of fit and strongest significance of regression equation and coefficient. The correlation coefficient ($R^2 = 0.990$) and high adjusted determination coefficient ($R^2_{adj} = 0.978$) show that this model is highly reliable (Table 2). Both coefficients are highly significant ($p < 0.01$). Equation (2) yields maximum mycelial biomass of 28.91 g/L when wheat bran is 16.0 g/L, rice bran is 104.0 g/L, KH_2PO_4 is 1.4 g/L, and $MgSO_4{\cdot}7H_2O$ is 1.3 g/L:

$$Y_2 = 602.174 - 131.163x_1 - 5394.101x_2 - 203.406x_3 + 10.571{x_1}^2 + 310.670x_1x_2 - 3556.507x_1x_3 + 19567.853{x_2}^2 - 13258.589x_2x_3 + 18948.745{x_3}^2. \quad (3)$$

The previous equation was the mycelial polysaccharide model equation with the best degree of fit and strongest significance of regression equation and coefficient. The correlation coefficient ($R^2 = 1.000$) and high adjusted determination coefficient ($R^2_{adj} = 1.000$) show that this model is extremely reliable ($p < 0.05$) and fits the experimental data

Table 3: ANOVA data of mycelial biomass in rice and wheat brans fermentation media for GFA2.

Factor	Coefficient estimate	Standard error	t value	p value
a	602.174	5.000	120.444	0.005
x_1	−131.163	1.279	−102.580	0.006
x_2	−5394.101	65.488	−82.368	0.008
x_3	−203.406	26.490	−7.679	0.082
x_1x_1	10.571	0.092	114.596	0.006
x_1x_2	310.670	3.964	78.382	0.008
x_1x_3	−356.507	3.769	−94.600	0.007
x_2x_2	19567.853	230.209	85.000	0.007
x_2x_3	−13258.589	171.039	−77.518	0.008
x_3x_3	18948.745	210.091	90.193	0.007

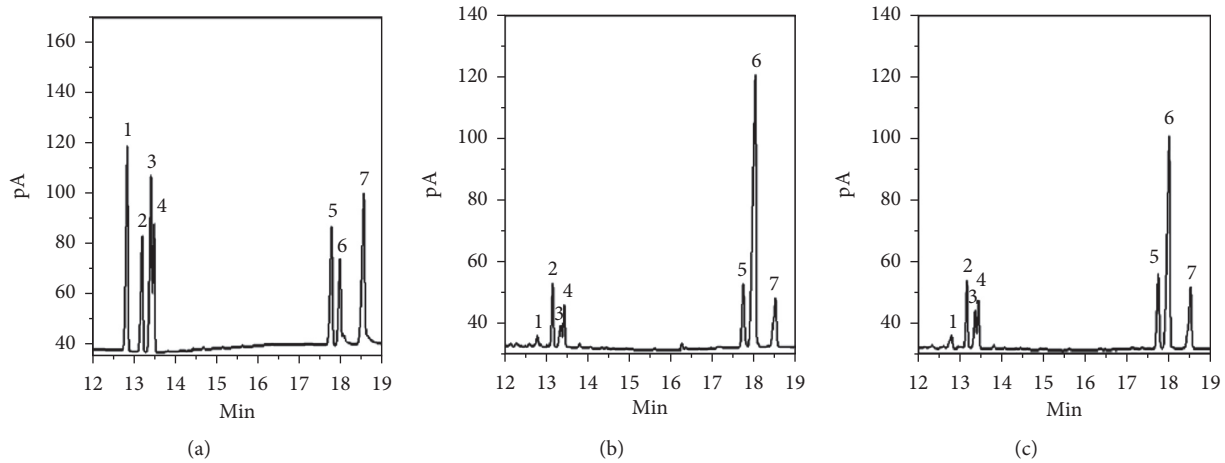

Figure 6: GC profiles of nitrile acetates of (a) monosaccharide standards, (b) the parent strain GF0 polysaccharides, (c) the mutant strain GFA2 polysaccharides. Peaks (Rt: min): 1, rhamnose; 2, arabinose; 3, fucose; 4, xylose; 5, mannose; 6, glucose; and 7, galactose.

very well (Table 3). Equation (3) yields a maximum mycelial polysaccharide concentration of 5.90 g/L when wheat bran is 110 g/L, rice bran is 10 g/L, and KH_2PO_4 and $MgSO_4{\cdot}7H_2O$ are zero. KH_2PO_4 and $MgSO_4{\cdot}7H_2O$ had no significant effect on mycelial polysaccharide concentration, so the addition of KH_2PO_4 and $MgSO_4{\cdot}7H_2O$ was optional within the experimental value range.

It must be pointed out that equations (2) and (3), which model the relationships between variables and criteria, were selected from many equations according to the principles of multiple regression modeling. This selection may differ between researchers, leading to differing interpretations of the data.

3.5. Monosaccharide Composition. After hydrolysis and derivatization, monosaccharide composition and molar ratios of the polysaccharides from GF0 and mutant GFA2 were determined by gas chromatography (Figure 6). The strains had the same monosaccharide composition (rhamnose, arabinose, fucose, xylose, mannose, glucose, and galactose) but in different molar ratios: 1.14 : 7.81 : 3.60 : 5.04 : 10.85 : 61.45 : 10.09 for GF0 polysaccharides and 1.65 : 9.73 : 6.24 : 6.75 : 13.71 : 48.04 : 13.89 for GFA2 polysaccharides. *G. frondosa* mycelial polysaccharides obtained by fermentation were heteropolysaccharides and glucose was the main monosaccharide.

3.6. FT-IR Analysis. The bonds and functional groups of the mutant and parent strain polysaccharides were analyzed by FT-IR spectroscopy (Figure 7). Stretching vibration of O-H caused a wide, strong band around 3397 cm^{-1}, while the weak band near 2927 cm^{-1} was ascribed to C-H stretching vibrations [42]. Absorption around 1654 cm^{-1} was associated with water [43]. The band in the polysaccharide fingerprint region 1400–1000 cm^{-1} was attributed to tensile vibrations of C-C, C=O, C-O-H, and C-O-C groups. The existence of these characteristic peaks confirmed this component as a polysaccharide. The peaks at approximately 1079 cm^{-1} and 1025 cm^{-1} were due to C-O-C glycosidic bond vibrations, which indicated the presence of pyranose monomers [44]. The small absorption peaks at 910 cm^{-1} and 844 cm^{-1} were assigned to β-glycosidic and α-glycosidic bonds in the polysaccharides [45]. The main absorption bands were similar in GF0 polysaccharides and GFA2 polysaccharides, indicating the same basic structures, with only a few differing peaks.

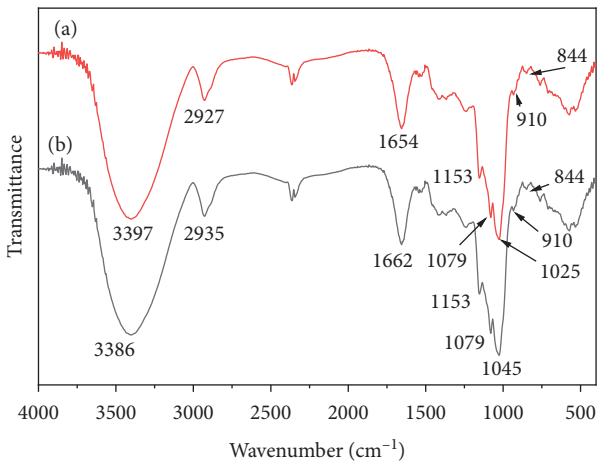

Figure 7: FT-IR spectra of (a) the parent strain GF0 polysaccharides and (b) the mutant strain GFA2 polysaccharides.

4. Conclusions

A mutant strain of *G. frondosa* (GFA2) exhibiting stable growth and fermentation performance was induced by ARTP and showed improved mycelial growth rate (6.0 mm/d) and polysaccharide production (2.65 g/L). Uniform design experiments optimized the culture conditions and maximized the mycelial biomass (28.91 g/L) and polysaccharide production (5.90 g/L). The mycelial polysaccharides from the parent and mutated strains had the same monosaccharide composition (rhamnose, arabinose, fucose, xylose, mannose, glucose, and galactose) at different molar ratios. Ongoing experiments are elucidating the detailed mechanisms of mycelial biomass and polysaccharide synthesis in *G. frondosa* by analyzing their related transcriptional reactions. The effects and mechanisms of *G. frondosa* polysaccharides in the prevention of chronic diseases are worthy of further study.

Data Availability

The data used to support the findings of this study are available from the corresponding author upon request.

Ethical Approval

This article does not contain any studies with human participants or animals performed by any of the authors.

Conflicts of Interest

All authors declare that they have no conflicts of interest.

Authors' Contributions

W. M. Liu conceived the study, participated in its design and coordination, and reviewed the manuscript. W. W. Yang analyzed results and drafted the manuscript. Y. Cheng and J. Wu revised the manuscript. T. Wang performed experiments and analyzed results. Z. C. Wei, H. L. Ma, L. Q. Yang, and F. J. Cui were responsible for the project. F. J. Cui, X. M. Yang, and J. K. Yan revised the manuscript. K. A. Ampofo and, Hao Zhang performed partial experiments. All authors read and approved the manuscript.

Acknowledgments

This work was supported by funding from China National Key R&D Projects (2017YFD0401105), National Natural Science Foundation of China (NSFC31101269 and NSFC31771961), Modern Agricultural Industry Technology System of Jiangsu Province (2017-2020), and Priority Academic Program Development of Jiangsu Higher Education Institutions (PAPD). The authors would like to express their gratitude to EditSprings (https://www.editsprings.com/) for the expert linguistic services provided.

References

[1] A. Klaus, M. Kozarski, J. Vunduk et al., "Biological potential of extracts of the wild edible Basidiomycete mushroom Grifola frondosa," *Food Research International*, vol. 67, pp. 272–283, 2015.

[2] G.-T. Chen, X.-M. Ma, S.-T. Liu, Y.-L. Liao, and G.-Q. Zhao, "Isolation, purification and antioxidant activities of polysaccharides from *Grifola frondosa*," *Carbohydrate Polymers*, vol. 89, no. 1, pp. 61–66, 2012.

[3] Q. Li, F. Zhang, G. Chen et al., "Purification, characterization and immunomodulatory activity of a novel polysaccharide from *Grifola frondosa*," *International Journal of Biological Macromolecules*, vol. 111, pp. 1293–1303, 2018.

[4] M. Meng, D. Cheng, L. Han, Y. Chen, and C. Wang, "Isolation, purification, structural analysis and immunostimulatory activity of water-soluble polysaccharides from *Grifola frondosa* fruiting body," *Carbohydrate Polymers*, vol. 157, pp. 1134–1143, 2017.

[5] J. Yu, H.-Y. Ji, C. Liu, and A.-J. Liu, "The structural characteristics of an acid-soluble polysaccharide from *Grifola frondosa* and its antitumor effects on H22-bearing mice," *International Journal of Biological Macromolecules*, vol. 158, pp. 1288–1298, 2020.

[6] H. Y. Ji, J. Yu, and A. J. Liu, "Structural characterization of a low molecular weight polysaccharide from *Grifola frondosa* and its antitumor activity in H22 tumor-bearing mice," *Journal of Functional Foods*, vol. 61, 2019.

[7] C.-Q. Gu, J.-W. Li, F. Chao, M. Jin, X.-W. Wang, and Z.-Q. Shen, "Isolation, identification and function of a novel anti-HSV-1 protein from *Grifola frondosa*," *Antiviral Research*, vol. 75, no. 3, pp. 250–257, 2007.

[8] Y. Chen, D. Liu, D. Wang et al., "Hypoglycemic activity and gut microbiota regulation of a novel polysaccharide from *Grifola frondosa* in type 2 diabetic mice," *Food and Chemical Toxicology*, vol. 126, pp. 295–302, 2019.

[9] C. Zhao, L. Gao, C. Wang, B. Liu, Y. Jin, and Z. Xing, "Structural characterization and antiviral activity of a novel heteropolysaccharide isolated from *Grifola frondosa* against enterovirus 71," *Carbohydrate Polymers*, vol. 144, pp. 382–389, 2016.

[10] W.-L. Guo, J.-C. Deng, Y.-Y. Pan et al., "Hypoglycemic and hypolipidemic activities of *Grifola frondosa* polysaccharides and their relationships with the modulation of intestinal microflora in diabetic mice induced by high-fat diet and streptozotocin," *International Journal of Biological Macromolecules*, vol. 153, pp. 1231–1240, 2020.

[11] E. Arte, C. G. Rizzello, M. Verni, E. Nordlund, K. Katina, and R. Coda, "Impact of enzymatic and microbial bioprocessing on protein modification and nutritional properties of wheat bran," *Journal of Agricultural and Food Chemistry*, vol. 63, no. 39, pp. 8685–8693, 2015.

[12] H. S. Kim, E. J. Lee, S.-T. Lim, and J.-A. Han, "Self-enhancement of GABA in rice bran using various stress treatments," *Food Chemistry*, vol. 172, pp. 657–662, 2015.

[13] L. X. Li, S. Li, X. F. Wang, and P. Huang, "Discussion on physicochemical properties and deep processing technology of wheat bran," *Food Process*, vol. 44, pp. 20–23, 2019.

[14] E. Arte, X. Huang, E. Nordlund, and K. Katina, "Biochemical characterization and technofunctional properties of bio-processed wheat bran protein isolates," *Food Chemistry*, vol. 289, pp. 103–111, 2019.

[15] E. P. Ryan, A. L. Heuberger, T. L. Weir, B. Barnett, C. D. Broeckling, and J. E. Prenni, "Rice bran fermented with *Saccharomyces boulardii* generates novel metabolite profiles with bioactivity," *Journal of Agricultural and Food Chemistry*, vol. 59, no. 5, pp. 1862–1870, 2011.

[16] H.-J. Zhang, H. Zhang, L. Wang, and X.-N. Guo, "Preparation and functional properties of rice bran proteins from heat-stabilized defatted rice bran," *Food Research International*, vol. 47, no. 2, pp. 359–363, 2012.

[17] S.-W. Han, K.-M. Chee, and S.-J. Cho, "Nutritional quality of rice bran protein in comparison to animal and vegetable protein," *Food Chemistry*, vol. 172, pp. 766–769, 2015.

[18] S. Nagar, A. Mittal, D. Kumar, L. Kumar, R. C. Kuhad, and V. K. Gupta, "Hyper production of alkali stable xylanase in lesser duration by *Bacillus pumilus* SV-85S using wheat bran under solid state fermentation," *New Biotechnology*, vol. 28, no. 6, pp. 581–587, 2011.

[19] H. Demir and C. Tari, "Bioconversion of wheat bran for polygalacturonase production by *Aspergillus sojae* in tray type solid-state fermentation," *International Biodeterioration & Biodegradation*, vol. 106, pp. 60–66, 2016.

[20] W. M. Liu and Z. W. Yu, "Study on the kinetic model of *Ganoderma lucidum* liquid fermentation in rice bran and wheat bran substrate," *Food Industry Science Technology*, vol. 41, no. 15, pp. 113–118, 2020.

[21] W. F. Quan, H. H. Zheng, and G. J. Liu, "Study on mutagenesis and breeding of high-yielding strains of *Grifola frondosa* polysaccharide," *Edible Fungus*, vol. 39, pp. 31–35, 2017.

[22] W. M. Liu, *Study on mutation of Grifola frondosa and liquid fermentation of new strain with rice bran and wheat bran added without or with selenium*, Doctoral Dissertation, Jiangsu University, Zhenjiang, China, 2015.

[23] Y. Lu, L. Wang, K. Ma et al., "Characteristics of hydrogen production of an *Enterobacter aerogenes* mutant generated by a new atmospheric and room temperature plasma (ARTP)," *Biochemical Engineering Journal*, vol. 55, no. 1, pp. 17–22, 2011.

[24] X. Zhang, X.-F. Zhang, H.-P. Li et al., "Atmospheric and room temperature plasma (ARTP) as a new powerful mutagenesis tool," *Applied Microbiology and Biotechnology*, vol. 98, no. 12, pp. 5387–5396, 2014.

[25] B. Liu, Z. Sun, X. Ma et al., "Mutation breeding of extracellular polysaccharide-producing microalga *Crypthecodinium cohnii* by a novel mutagenesis with atmospheric and room temperature plasma," *International Journal of Molecular Sciences*, vol. 16, no. 4, pp. 8201–8212, 2015.

[26] C. Zhang, J. Qin, Y. Dai, W. Mu, and T. Zhang, "Atmospheric and room temperature plasma (ARTP) mutagenesis enables xylitol over-production with yeast *Candida tropicalis*," *Journal of Biotechnology*, vol. 296, pp. 7–13, 2019.

[27] Y. Zhuang, G.-L. Jiang, and M.-J. Zhu, "Atmospheric and room temperature plasma mutagenesis and astaxanthin production from sugarcane bagasse hydrolysate by *Phaffia rhodozyma* mutant Y1," *Process Biochemistry*, vol. 91, pp. 330–338, 2020.

[28] L.-Y. Wang, Z.-L. Huang, G. Li et al., "Novel mutation breeding method for *Streptomyces* avermitilisusing an atmospheric pressure glow discharge plasma," *Journal of Applied Microbiology*, vol. 108, no. 3, pp. 851–858, 2010.

[29] X. Chen, H. Zhang, W. Du et al., "Comparison of different extraction methods for polysaccharides from *Crataegus pinnatifida* bunge," *International Journal of Biological Macromolecules*, vol. 150, pp. 1011–1019, 2020.

[30] M. Dubois, K. A. Gilles, J. K. Hamilton, P. A. Rebers, and F. Smith, "Colorimetric method for determination of sugars and related substances," *Analytical Chemistry*, vol. 28, no. 3, pp. 350–356, 1956.

[31] R. Kumari and K. Pramanik, "Improvement of multiple stress tolerance in yeast strain by sequential mutagenesis for enhanced bioethanol production," *Journal of Bioscience and Bioengineering*, vol. 114, no. 6, pp. 622–629, 2012.

[32] Y. Wang and K. Fang, "Uniform mixing design," *Science China*, vol. 26, pp. 1–10, 1996.

[33] J.-K. Yan, Z.-C. Ding, X. Gao et al., "Comparative study of physicochemical properties and bioactivity of *Hericium erinaceus* polysaccharides at different solvent extractions," *Carbohydrate Polymers*, vol. 193, pp. 373–382, 2018.

[34] X. D. Dong, Y. Y. Feng, Y. N. Liu et al., "A novel polysaccharide from *Castanea mollissima* blume: preparation, characteristics and antitumor activities *in vitro* and *in vivo*," *Carbohydrate Polymers*, vol. 240, 2020.

[35] R.-S. Zou, S. Li, L.-L. Zhang et al., "Mutagenesis of *Rhodobacter sphaeroides* using atmospheric and room temperature plasma treatment for efficient production of coenzyme Q10," *Journal of Bioscience and Bioengineering*, vol. 127, no. 6, pp. 698–702, 2019.

[36] C. Ottenheim, M. Nawrath, and J. C. Wu, "Microbial mutagenesis by atmospheric and room-temperature plasma (ARTP): the latest development," *Bioresources and Bioprocessing*, vol. 5, 2018.

[37] S. Cao, X. Zhou, W. Jin et al., "Improving of lipid productivity of the oleaginous microalgae *Chlorella pyrenoidosa* via atmospheric and room temperature plasma (ARTP)," *Bioresource Technology*, vol. 244, no. Pt 2, pp. 1400–1406, 2017.

[38] R. Xin, W. Xie, Z. Xu, H. Che, Z. Zheng, and X. Yang, "Efficient extraction of chitin from shrimp waste by mutagenized strain fermentation using atmospheric and room-temperature plasma," *International Journal of Biological Macromolecules*, vol. 155, pp. 1561–1568, 2020.

[39] S. Hafsa, B. Zainab, K. Aysha, A. Afsheen, and A. Shah, "Degradation of complex casein polymer: production and optimization of a novel serine metalloprotease from *Aspergillus niger* KIBGE-IB36," *Biocatalysis and Agricultural Biotechnology*, vol. 21, 2019.

[40] D. Deblina, S. Raja, and B. M. Ramananda, "Optimization of inulinase production by a newly isolated strain *Aspergillus flavus var. flavus* by solid state fermentation of *Saccharum arundinaceum*," *Biocatalysis and Agricultural Biotechnology*, vol. 22, 2019.

[41] B. Yuan, X. Chi, and R. Zhang, "Optimization of exopolysaccharides production from a novel strain of *Ganoderma*

lucidum cau5501 in submerged culture," *Brazilian Journal of Microbiology*, vol. 43, no. 2, pp. 490–497, 2012.

[42] J. Y. Gu, H. H. Zhang, J. X. Zhang et al., "Optimization, characterization, rheological study and immune activities of polysaccharide from *Sagittaria sagittifolia* L," *Carbohydrate Polymers*, vol. 246, 2020.

[43] J. Zhang, C. Wen, J. Gu, C. Ji, Y. Duan, and H. Zhang, "Effects of subcritical water extraction microenvironment on the structure and biological activities of polysaccharides from *Lentinus edodes*," *International Journal of Biological Macromolecules*, vol. 123, pp. 1002–1011, 2019.

[44] J. Y. Gu, H. H. Zhang, H. Yao, J. Zhou, Y. Q. Duan, and H. L. Ma, "Comparison of characterization, antioxidant and immunological activities of three polysaccharides from *Sagittaria sagittifolia* L," *Carbohydrate Polymers*, vol. 235, 2020.

[45] Y.-Q. Wang, J.-X. Huang, and W.-W. Zhou, "Isolation, characterization and cytoprotective effects against UV radiation of exopolysaccharide produced from *Paenibacillus polymyxa* PYQ1," *Journal of Bioscience and Bioengineering*, vol. 130, no. 3, pp. 283–289, 2020.

Hindawi
Journal of Food Quality
Volume 2021, Article ID 9914508, 7 pages
https://doi.org/10.1155/2021/9914508

Research Article

Chemical Constituents and Coagulation Activity of *Amygdalus persica* L. Flowers

Juanjuan Zhang,[1,2,3] **Zhenhua Yin**,[1,2,3] **Lin Chen**,[1,2,3] **Baocheng Yang**,[1,2,3] **Wei Zhang**,[1,2] **and Wenyi Kang**[1,2]

[1]*Henan Engineering Research Center for Comprehensive Utilization of Edible and Medicinal Plant Resources, Huanghe Science and Technology College, Zhengzhou 450063, China*
[2]*Zhengzhou Key Laboratory of Synthetic Biology of Natural Products, Huanghe Science and Technology College, Zhengzhou 450063, China*
[3]*Henan Joint International Research Laboratory of Drug Discovery of Small Molecules, Zhengzhou 450063, China*

Correspondence should be addressed to Wenyi Kang; kangweny@hotmail.com

Received 12 March 2021; Accepted 9 May 2021; Published 20 May 2021

Academic Editor: Quancai Sun

Amygdalus persica L., belongs to Rosaceae family, and its flowers are used as medicine and food. *n*-Butanol extract of *A. persica* flowers were isolated and purified with various column chromatographies, and the fourteen compounds, chlorogenic acid butyl ester (**1**), rutin (**2**), protocatechuic acid (**3**), caffeic acid (**4**), 5-O-coumarroylquinic acid methyl ester (**5**), kaempferol-3-O-neohesperidoside (**6**), quercetin-3-O-*β*-D-glucoside (**7**), 3,5-dicaffeoylquinic acid (**8**), quercetin-3-O-*α*-L-rhamnoside (**9**), 5-O-coumaroylquinic acid (**10**), kaempferol-3-O-*α*-L-rhamnoside (**11**), kaempferol-3-O-*β*-D-galactoside (**12**), D-glucitol (**13**), and multiflorin A (**14**), were identified by spectroscopic data and physical data. All the compounds except compound **2** were identified from *A. persica* flowers for the first time. The compounds were investigated for their coagulation activity by activated partial thromboplastin time (APTT), prothrombin time (PT), thrombin time (TT), and bibrinogen (FIB) *in vitro*. The results of coagulation activity showed that rutin (**2**), caffeic acid (**4**), kaempferol-3-O-neohesperidoside (**6**), kaempferol-3-O-*α*-L-rhamnoside (**11**), and kaempferol-3-O-*β*-D-galactoside (**12**) exhibited significant procoagulant activity, while chlorogenic acid butyl ester (**1**) possessed anticoagulant activity *in vitro*.

1. Introduction

Amygdalus persica L., belonging to Rosaceae, is an excellent plant resource that had the concomitant function of both medicine and foodstuff, and with relaxing bowel, diuresis, and reducing swelling effects [1]. *A. persica* flowers are widely used in traditional Chinese medicine and also used as a healthy food for beauty and constipation treatment, as well as wine and tea drinks [2, 3].

At present, there are few studies on chemical composition and pharmacological activity of *A. persica*, mainly focusing on the volatile constituents and extraction process of polyphenols. Yuan et al. studied the optimum ultrasonic-assisted extraction technology of polyphenols from *A. persica* with response surface methodology and found the polyphenols had certain scavenging effects on hydroxyl and DPPH radicals [4]. In addition, Zhang et al. found that the major volatile constituents of *A. persica* flowers were linolenic alcohol, *n*-hexadecanoic acid, cyclohexane, and octadecanoic acid [5]. Zeng et al. analyzed the conditions for purification of total flavonoids from *A. persica* by macroporous resin, with adsorption-desorption ratios as indexes, and optimum resin DM-28 was selected by static adsorption-desorption and dynamic adsorption-desorption ratio tests and also found that flavonoids had an obvious antioxidant activity. The IC_{50} values of DPPH and ABTS were 13.47 μg/mL and 32.16 μg/mL, respectively [6].

According to literature research, *A. persica* had the effect of promoting blood circulation and removing blood stasis [7]. In our previous research, we found that the constituents of ethyl acetate extract from *A. persica* flowers showed strong coagulation activity. In the light of previous research, the coagulation activities of *n*-butanol extract of *A. persica* were researched with coagulation parameters *in vitro*.

2. Methods

2.1. Materials and Reagents. Sodium chloride injection (1603311336) and breviscapine injection (20190813-1) were obtained from Kunming Longjin Pharmaceutical Co., Ltd. (Kunming, Yunnan, China). Yunnan Baiyao (ZJA1708) was obtained from Yunnan Baiyao Group Co., Ltd. (Kunming, Yunnan, China). PT (20191209M), APTT (20200319M), TT (20190821M), and FIB (20191120M) assay kits were purchased from Shenzhen Leidu Life Science Co., Ltd. (Guangdong, China). Sephadex LH-20 was purchased from Pharmacia (Burlington, MA, USA). NMR was recorded on a Bruker Avance AM-400 spectrometer. RAC-030 automatic blood coagulation analyzer was obtained from Shenzhen Leidu Life Science Co., Ltd. (Guangdong, China).

2.2. Plant Material. Amygdalus persica flowers were purchased from Anhui Pharmaceutical Zhiyuan Chinese Medicine Co., Ltd., Anhui, China. A voucher specimen (no. 201803027) was identified by Professor Changqin Li of Henan University and deposited in the Institute of Natural Medicine of Huanghe Science and Technology College.

2.3. Animals. Female Sprague Dawley (SD) rats (6–8 weeks, 200–250 g) were obtained from the Experimental Animal Center of Henan Province (Zhengzhou, Henan, China), and the animal certificate number was SCXK 2019-0004. The female SD rats were maintained at 25°C and 45–65% humidity, in a 12 h light/12 h dark cycle, and fed with standard rodent diet and water ad libitum.

2.4. Extraction and Isolation. The extraction work of air-dried *A. persica* flowers (2000 g) with petroleum ether, ethyl acetate, and *n*-butanol have been published in our previous research [8]. And, we get ether extract 28 g, ethyl acetate extract 93 g, and *n*-butanol extract 180 g.

The extracted method of *n*-butanol extract was similar to our previous research [9]. *n*-Butanol extract (180 g) was subjected to a silica gel H medium-pressure liquid chromatography and successively eluted with methylene chloride/methanol (from $v{:}v = 100{:}1\text{-}7{:}3$) to obtain eight fractions: Fr.1–Fr.8. Fr.2 (6.81 g) was applied to a silica gel H column chromatography and eluted with petroleum ether/methylene chloride ($v{:}v = 25{:}1\text{-}3{:}1$) and then separated with Sephadex LH-20 (petroleum ether/methylene chloride/methanol, $v{:}v{:}v = 9 : 9{:}2$) to obtain compound **1** (20.0 mg). Fr.3 (5.47 g) was subjected to a silica gel H column chromatography, eluted with methylene chloride/methanol ($v{:}v = 35{:}1\text{–}1{:}1$) to three fractions (Fr.3.1–Fr.3.3) based on TLC analyses. Fr.3.2 was separated on a silica gel H with methylene chloride/ethyl acetate ($v{:}v = 10 : 1$) and further separated with Sephadex LH-20 (methylene chloride/methanol, $v{:}v = 1 : 1$) to obtain compound **2** (21.0 mg). Fr.3.3 was separated with Sephadex LH-20 (methylene chloride/methanol, $v{:}v = 1 : 1$) and Sephadex LH-20 (methanol) to obtain compounds **3** (8.0 mg) and **4** (11.7 mg). Fr.4 (8.20 g) was separated on silica gel H with a stepwise-gradient of methylene chloride/ethyl acetate/methanol ($v{:}v{:}v = 40 : 1 : 1\text{-}5 : 1 : 1$) to yield 2 fractions: Fr.4.1~Fr.4.2. Fr.4.2 was separated on silica gel H with methylene chloride/methanol ($v{:}v = 15 : 1$) and Sephadex LH-20 (methylene chloride/methanol, $v{:}v = 1 : 1$) to give compounds **5** (15.7 mg) and **6** (10.3 mg). Fr.5 (6.40 g) was separated with silica gel column with methylene chloride/methanol ($v{:}v = 8 : 1$) and further with Sephadex LH-20 (methylene chloride/methanol = 1 : 1) to obtain compound **7** (10.5 mg). Fr.6 (11.95 g) was subjected to a silica gel H column chromatography, eluted with methylene chloride/methanol ($v{:}v = 20 : 1\text{-}1 : 1$) to three fractions (Fr.6.1–Fr.6.3) based on TLC analyses. Fr.6.1 was purified by silica gel column with methylene chloride/methanol ($v{:}v = 10 : 1\text{-}1 : 1$) and further with Sephadex LH-20 (methanol) to yield compounds **8** (11.2 mg) and **9** (7.5 mg). Fr.6.2 was purified by Sephadex LH-20 (methylene chloride/methanol, $v{:}v = 1 : 1$) to give compound **10** (5.6 mg). Fr.7 (10.07 g) was subjected to a silica gel H column chromatography, eluted with methylene chloride/ethyl acetate/methanol ($v{:}v{:}v = 35 : 20 : 1\text{-}2 : 1 : 1$) to four fractions (Fr.7.1–Fr.7.4) based on TLC analyses. Fr.7.2 was subjected to atmospheric pressure chromatographic column of silica gel H with methylene chloride/methanol ($v{:}v = 25 : 1\text{-}2 : 1$) and Sephadex LH-20 (methanol) to obtain compounds **11** (10.7 mg) and **12** (11.8 mg). Compound **13** (20.4 mg) was isolated by the same separation method from Fr.7.4. Fr.8 (7.26 g) was purified by silica gel column with methylene chloride/methanol ($v{:}v = 15 : 1\text{-}1 : 1$) and Sephadex LH-20 (methanol) to obtain compound **14** (18.6 mg).

2.5. Coagulation Time Assays In Vitro

2.5.1. Sample Preparation. In this test, blank solvent (ethyl alcohol: 1, 2-propylene glycol: normal saline = 1 : 1:3) was used as the negative control group, while breviscapine (8 mg) was prepared into 13.33 mg/mL solution with 600 μL blank solvent and Yunnan Baiyao (1 mg) was prepared into 40 mg/mL solution with 25 μL blank solvent and used as positive control groups. The compound (3 mg) was prepared into 3 mg/mL solution with 1000 μL blank solvent. The method was similar to our previous research [10, 11].

2.5.2. Collection of Blood Sample. Rats were anesthetized with chloral hydrate, and the blood was collected from abdominal aorta. Blood was placed in a disposable anticoagulant negative pressure vacuum tube, then mixed gently upside down, and centrifuged at 3,000 rpm at 5°C for 15 min, and the supernatant was taken for use.

2.5.3. APTT Assay. Add 25 μL sample and 50 μL plasma into the test cup, then put it into the coagulation apparatus, automatically add 25 μL APTT reagent, incubate for 5 min at 37°C, and then, add 50 μL $CaCl_2$. Clotting times were recorded as the value of APTT.

2.5.4. PT Assay. Add 25 μL sample and 50 μL plasma into the test cup, then put it into the coagulation apparatus, and automatically add 100 μL PT reagent. Clotting times were recorded as the value of PT.

2.5.5. TT Assay. Add 25 μL sample and 100 μL plasma into the test cup, then put it into the coagulation apparatus, and automatically add 100 μL TT reagent. Clotting times were recorded as the value of TT.

2.5.6. FIB Assay. Add 25 μL sample and 50 μL plasma into the test cup, then put it into the coagulation apparatus, and automatically add 100 μL FIB reagent. And, the content of FIB was recorded.

APTT, PT, TT, and FIB assays were conducted by using an automatic blood coagulation analyzer.

2.6. Statistical Analysis. The results were expressed as mean ± standard deviation (SD). Statistical analysis was performed using SPSS19.0 software, and comparison between any two groups was evaluated using one-way analysis of variance (one-way ANOVA). The difference between groups with $P < 0.05$ was regarded as statistically significant.

3. Results

3.1. Identification of the Compounds. By correlating melting points, ^{1}H-NMR, ^{13}C-NMR, and MS from the literature values, compounds **1**–**14** were identified as chlorogenic acid butyl ester (**1**) [12], rutin (**2**) [13], protocatechuic acid (**3**) [14], caffeic acid (**4**) [15], 5-O-coumaroylquinic acid methyl ester (**5**) [16], kaempferol-3-O-neohesperidoside (**6**) [17], quercetin-3-O-β-D-glucoside (**7**) [18], 3,5-dicaffeoylquinic acid (**8**) [19], quercetin-3-O-α-L-rhamnoside (**9**) [20], 5-O-coumaroylquinic acid (**10**) [16], kaempferol-3-O-α-L-rhamnoside (**11**) [21], kaempferol-3-O-β-D-galactoside (**12**) [22], D-glucitol (**13**) [23], multiflorin A (**14**) [24]. Flavonoids were the main components [25–27]. All the compounds except compound **2** were identified from *A. persica* flowers for the first time. The structures of compounds **1**–**14** are shown in Figure 1.

3.2. Effects on Plasma Coagulation Parameters In Vitro. The APTT, PT, TT, and FIB assays results of *A. persica* flowers are shown in Table 1 and Figure 2.

In APTT assay, compounds **2**, **4**, **6**, **8**, **12**, and **14** could remarkably shorten APTT ($P < 0.05$, $P < 0.01$, $P < 0.001$, respectively), while compound **1** could remarkably lengthen APTT ($P < 0.01$) compared with the blank group. In PT assay, all the compounds except compounds **1** and **10** could remarkably shorten PT ($P < 0.05$, $P < 0.01$, and $P < 0.001$, respectively), and compound **1** could remarkably lengthen PT ($P < 0.05$) compared with the blank group. Then, the shortening PT effects of compounds **4** and **7** were better than those of Yunnan Baiyao ($P < 0.05$ and $P < 0.01$, respectively), and compounds **5**, **6**, **11**, **12**, and **13** had no difference with Yunnan Baiyao ($P > 0.05$). In TT assay, compounds **5**, **6**, **7**, **9**, **10**, **11**, **12**, **13**, and **14** could remarkably shorten TT ($P < 0.05$, $P < 0.01$, and $P < 0.001$, respectively) compared with the blank group. And, the shortening TT effects of compounds **7**, **9**, **11**, and **12** were better than those of Yunnan Baiyao ($P < 0.05$, $P < 0.01$, and $P < 0.001$, respectively), and compounds **5** and **14** had no difference with Yunnan Baiyao ($P > 0.05$). In FIB assay, compound **11** could remarkably increase the content of FIB ($P < 0.01$) compared with the blank group, and the effect of compound **11** was better than that of Yunnan Baiyao ($P < 0.05$). While compounds **1**, **2**, **4**, **5**, **6**, **7**, **8**, **10**, **12**, and **13** could remarkably reduce the content of FIB ($P < 0.05$, $P < 0.01$, and $P < 0.001$, respectively), and the effects of compounds **1**, **2**, **4**, **5**, **10**, **12**, and **13** were better than those of breviscapine ($P < 0.05$, $P < 0.01$, and $P < 0.001$, respectively), and compounds **6** and **7** had no difference with the breviscapine ($P > 0.05$).

4. Discussion

Blood coagulation refers to the process in which blood changes from a flowing liquid state to a gel state that cannot flow. Its essence is the process of transforming soluble fibrinogen into insoluble fibrin in plasma. The key to this transformation is the occurrence of a series of complex enzymatic reactions, which require the participation of various coagulation factors [28]. According to the activation pathway of coagulation factor *X* and the different factors involved in coagulation, blood coagulation was divided into endogenous coagulation pathway, exogenous coagulation pathway, and common coagulation pathway [29].

The measurement of PT, APTT, TT, and FIB is an important index to judge the pathological changes of hemostasis and coagulation system, and it is the most commonly used and basic screening experiment of coagulation system in clinic. APTT mainly reflects the endogenous coagulation pathway and measures the time required for fibrinogen to transform into insoluble fibrin with the participation of Ca^{2+}. PT mainly reflects the exogenous coagulation pathway and the overall activity of coagulation factors I, II, V, VII, and X in plasma. TT mainly reflects the time required for fibrinogen to transform into insoluble fibrin eggs in the common pathway of coagulation [30, 31]. FIB reflects the content of fibrinogen, which is mainly synthesized by liver and is the substrate of thrombin. Peptide A and peptide B are hydrolyzed by thrombin, and finally, insoluble fibrin is formed [32].

In coagulation activity assay, compared with the blank group, chlorogenic acid butyl ester (**1**) could remarkably lengthen APTT and PT and reduce the content of FIB, which indicated the beneficial effect of it on endogenous and exogenous coagulation pathways, and hinder fibrin formation.

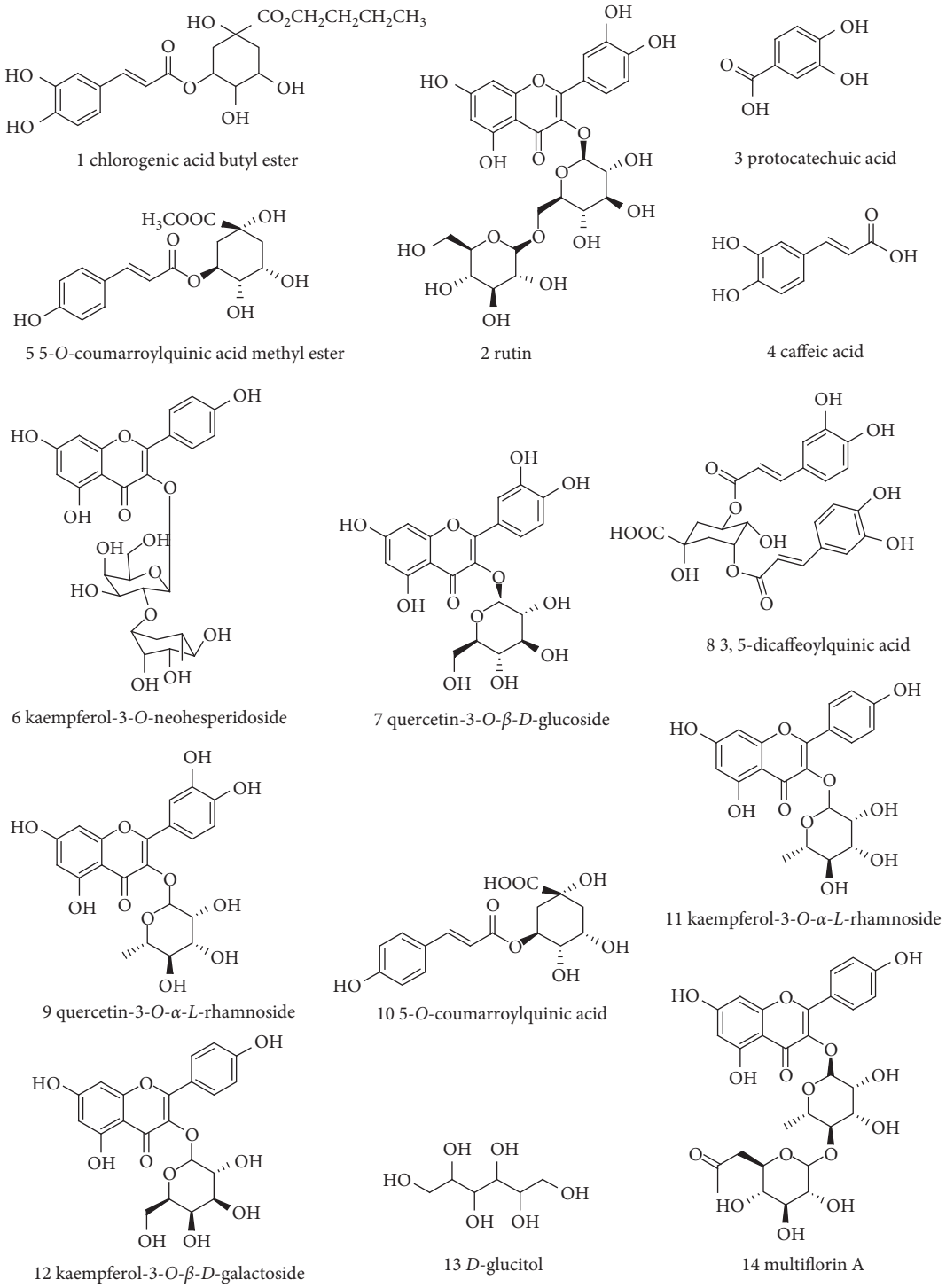

Figure 1: Chemical structures of compounds **1–14** isolated from *A. persica* flowers.

Rutin (**2**), caffeic acid (**4**), and 3,5-dicaffeoylquinic acid (**8**) could remarkably shorten APTT and PT and reduce the content of FIB, which indicated the beneficial effect of them on endogenous and exogenous coagulation pathways, and hinder fibrin formation. 5-O-coumaroylquinic acid methyl ester (**5**), quercetin-3-O-β-D-glucoside (**7**), and D-glucitol (**13**) could remarkably shorten PT and TT and reduce the content of FIB, which indicated the beneficial effect of them on exogenous coagulation pathways, and hinder fibrin formation. Kaempferol-3-O-neohesperidoside (**6**) and kaempferol-3-O-β-D-galactoside (**12**) could remarkably shorten APTT, PT, and TT and reduce the content of FIB, which indicated the beneficial effect of them on endogenous and exogenous coagulation pathways, and hinder fibrin formation. Quercetin-3-O-α-L-rhamnoside (**9**) could remarkably shorten PT and TT, which indicated the beneficial

Table 1: Effects of compounds on plasma coagulation parameters *in vitro*.

Groups	APTT(s)	PT(s)	TT(s)	FIB(g/L)
Blank group	15.65 ± 0.35	20.80 ± 0.14	82.05 ± 1.06	112.94 ± 0.72
Yunnan Baiyao	$10.40 \pm 0.85^{\#\#\#}$	$19.10 \pm 0.28^{\#\#\#}$	$76.75 \pm 0.63^{\#\#\#}$	$115.83 \pm 0.62^{\#\#}$
Breviscapine	$22.85 \pm 0.21^{\#\#\#}$	$22.65 \pm 0.49^{\#\#\#}$	$88.35 \pm 1.06^{\#\#\#}$	$108.30 \pm 0.81^{\#\#\#}$
Compound **1**	$16.50 \pm 0.14^{\#\#***}$	$21.05 \pm 0.50^{\#**}$	$82.30 \pm 4.67^{*}$	$106.65 \pm 0.47^{\#\#\#*}$
Compound **2**	$15.00 \pm 0.14^{\#\Delta\Delta\Delta}$	$19.95 \pm 0.35^{\#\#\Delta}$	80.25 ± 4.45	$104.81 \pm 0.92^{\#\#\#**}$
Compound **4**	$13.35 \pm 0.07^{\#\#\#\Delta\Delta}$	$17.70 \pm 0.71^{\#\#\#\Delta}$	80.40 ± 10.18	$104.81 \pm 1.02^{\#\#\#**}$
Compound **5**	$15.00 \pm 0.85^{\Delta\Delta\Delta}$	$19.20 \pm 0.57^{\#\#}$	$78.90 \pm 1.97^{\#}$	$106.25 \pm 0.90^{\#\#\#*}$
Compound **6**	$14.90 \pm 0.14^{\#\#\Delta\Delta\Delta}$	$18.65 \pm 0.50^{\#\#\#}$	$79.05 \pm 1.34^{\#\Delta}$	$108.49 \pm 0.67^{\#\#\#}$
Compound **7**	$15.35 \pm 0.21^{\Delta\Delta\Delta}$	$18.35 \pm 0.07^{\#\#\#\Delta\Delta}$	$74.95 \pm 0.35^{\#\#\#\Delta\Delta}$	$106.98 \pm 0.90^{\#\#\#}$
Compound **8**	$14.60 \pm 0.71^{\#\Delta\Delta\Delta}$	$19.60 \pm 0.00^{\#\#\#\Delta}$	82.70 ± 0.99	$110.43 \pm 1.09^{\#*}$
Compound **9**	$15.56 \pm 0.21^{\Delta\Delta\Delta}$	$20.15 \pm 0.07^{\#\#\#\Delta\Delta\Delta}$	$71.85 \pm 1.20^{\#\#\#\Delta\Delta\Delta}$	$113.27 \pm 1.23^{**}$
Compound **10**	$14.61 \pm 0.14^{\Delta\Delta\Delta}$	$20.60 \pm 0.14^{\Delta\Delta\Delta}$	$80.40 \pm 0.57^{\#\Delta\Delta\Delta}$	$103.41 \pm 0.67^{\#\#\#***}$
Compound **11**	$15.90 \pm 0.57^{***}$	$19.20 \pm 0.14^{\#\#\#}$	$69.45 \pm 4.03^{\#\#\Delta}$	$118.06 \pm 0.93^{\#\#\Delta}$
Compound **12**	$12.30 \pm 0.14^{\#\#\#\Delta\Delta}$	$19.05 \pm 0.21^{\#\#\#}$	$73.55 \pm 1.34^{\#\#\#\Delta\Delta}$	$105.16 \pm 0.63^{\#\#\#**}$
Compound **13**	$15.80 \pm 0.42^{***}$	$19.60 \pm 0.70^{\#}$	$74.00 \pm 3.39^{\#\#}$	$103.75 \pm 1.04^{\#\#\#**}$
Compound **14**	$14.75 \pm 0.49^{\#\Delta\Delta\Delta}$	20.00 ± 0.98	$76.4 \pm 0.85^{\#\#\#}$	$112.44 \pm 0.93^{**}$

Note. Data represent mean ± SD, $n = 4$. Compared with blank group, $^{\#}P < 0.05$, $^{\#\#}P < 0.01$, and $^{\#\#\#}P < 0.001$. Compared with Yunnan Baiyao, $^{\Delta}P < 0.05$, $^{\Delta\Delta}P < 0.01$, and $^{\Delta\Delta\Delta}P < 0.001$. Compared with breviscapine, $^{*}P < 0.05$, $^{**}P < 0.01$, and $^{***}P < 0.001$.

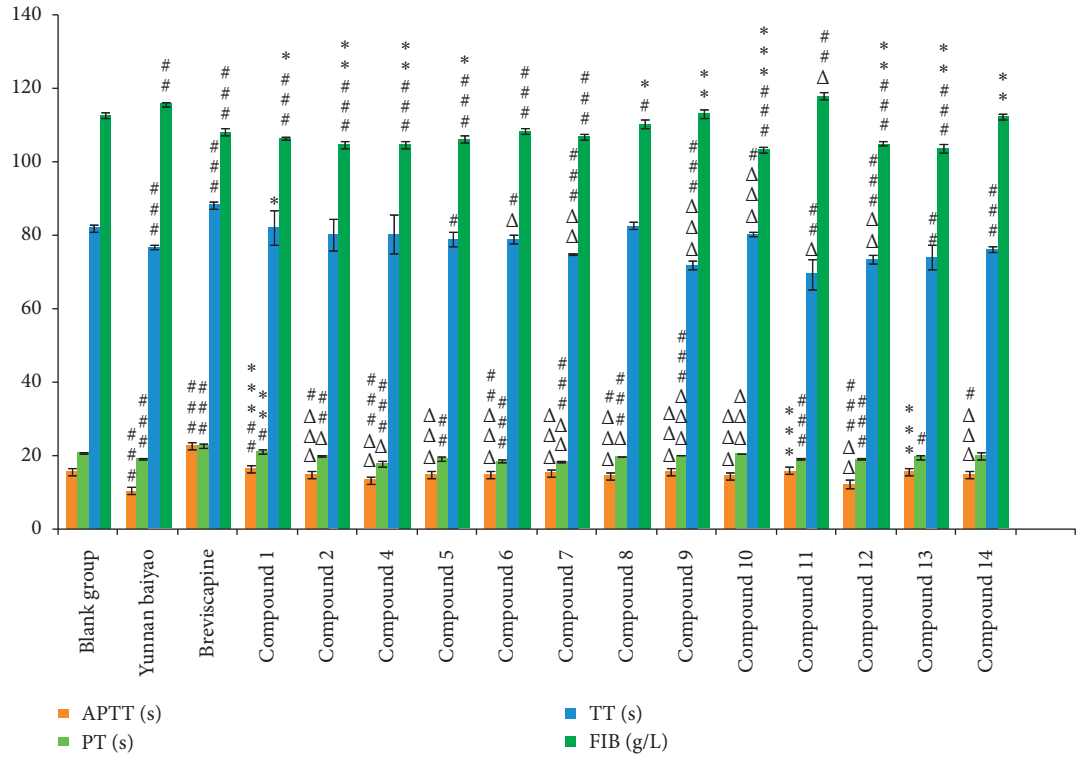

Figure 2: Effects of compounds from *A. persica* flowers on plasma coagulation parameters *in vitro* ($X \pm SD$, $(n = 4)$. Compared with blank group, $^{\#}P < 0.05$, $^{\#\#}P < 0.01$, and $^{\#\#\#}P < 0.001$. Compared with Yunnan Baiyao, $^{\Delta}P < 0.05$, $^{\Delta\Delta}P < 0.01$, and $^{\Delta\Delta\Delta}P < 0.001$. Compared with breviscapine, $^{*}P < 0.05$, $^{**}P < 0.01$, and $^{***}P < 0.001$.

effect of it on exogenous coagulation pathways. Kaempferol-3-O-α-L-rhamnoside (**11**) could remarkably shorten PT and TT and increase the content of FIB, which indicated the beneficial effect of it on exogenous coagulation pathways, and encourage fibrin formation. And, it was for the first time to investigate the coagulation activity of all the compounds except rutin (**2**), quercetin-3-O-β-D-glucoside (**7**) and kaempferol-3-O-α-L-rhamnoside (**11**).

5. Conclusions

In this study, fourteen compounds were isolated and identified from *n*-butanol extract of *A. persica* by various modern chromatographic methods. The coagulation activity assay of the compounds showed that rutin, caffeic acid, kaempferol-3-O-neohesperidoside, and kaempferol-3-O-β-D-galactoside possessed significant procoagulant activity

through endogenous and exogenous coagulation pathways, and kaempferol-3-O-α-L-rhamnoside possessed significant procoagulant activity through exogenous coagulation pathways, while chlorogenic acid butyl ester exerted good anticoagulant effects through endogenous and exogenous coagulation pathways *in vitro*.

Data Availability

The data used to support the findings of this study are included within the article.

Ethical Approval

All the animal procedures were approved by the Ethical Committee in accordance with "Institute Ethical Committee Guidelines" for Animal Experimentation and Care. Animals were housed in standard cages. The experiment was carried out according to the guidelines of the National Institutes of Health for Care and Use of Laboratory Animals and was approved by the Bioethics Committee of Henan University, Kaifeng, Henan, China.

Conflicts of Interest

The authors declare that there are no conflicts of interest regarding the publication of this paper.

Acknowledgments

This study received financial support from the Key Research Projects of Colleges and Universities in Henan Province (21B360006) and Special Fund Project of Zhengzhou Basic and Applied Basic Research (ZZSZX202003).

References

[1] Chinese Academy of Sciences, *China Flora Editorial Board," Flora of China*, Science Press, Beijing, China, 1986.

[2] L. Zhou, "The medicinal food therapy of *Peach blossom*," *Shandong Food Science and Technology*, vol. 11, no. 11, p. 24, 2004.

[3] X. C. Chen, "Peach blossom set each other off in red-peach blossom moisturizes the skin and beauty, into the medicine treatment disease has said," *Oriental Food Therapy Health Care*, vol. 4, no. 4, p. 39, 2004.

[4] J. M. Yuan, M. J. Geng, R. F. Yan, G. L. Guo, and D. P. Ren, "Optimization of ultrasonic-assisted extraction on polyphenols from *peach blossom* and antioxidant activity evaluation," *Food Science and Technology*, vol. 37, no. 12, pp. 179–183, 2012.

[5] J. J. Zhang, Z. H. Yin, L. Chen, Q. F. Guo, and W. Zhang, "Analysis of fat-soluble constituents from flowers of *Amygdalus persica* L," *Journal of Henan University (Medical Science)*, vol. 38, no. 2, pp. 158–160, 2019.

[6] Z. Zeng, H. G. Liu, and Y. P. Hong, "A study on purification of total flavonoids from *Prunus persica* by macroporous resin and their antioxidant activity," *Acta Agriculturae Universitatis Jiangxiensis*, vol. 39, no. 1, pp. 182–189, 2017.

[7] National Administration of Traditional Chinese Medicine, *Chinese Materia Medica*, Shanghai Science Technology Press, Shanghai, China, 1999.

[8] J. J. Zhang, W. Zhang, Z. H. Yin, B. C. Yang, and W. Y. Kang, "Chemical constituents and coagulation activity of *Amygdalus persica* L. flowers," *Natural Product Communications*, vol. 16, no. 4, pp. 1–5, 2021.

[9] J. Zhang, L. Zhou, L. Cui, Z. Liu, J. Wei, and W. Kang, "Antioxidant and α-glucosidase inhibitiory activity of *Cercis chinensis* flowers," *Food Science and Human Wellness*, vol. 9, no. 4, pp. 313–319, 2020.

[10] L. L. Cui, M. Y. Hu, and P. R. Cao, "Chemical constituents and coagulation activity of *Syringa oblata* Lind flowers," *BMC Chemistry*, vol. 13, no. 1, p. 108, 2019.

[11] J. Zhang, W. Zhang, Z. Yin, C. Li, and W. Kang, "Procoagulant constituents from *Cordyceps militaris*," *Food Science and Human Wellness*, vol. 7, no. 4, pp. 282–286, 2018.

[12] J. Q. Wang, Y. Liu, and Y. F. Yang, "Anti-oxidant chemical constituents from *Patrinia villosa*," *Chinese Traditional and Herbal Drugs*, vol. 50, no. 21, pp. 5206–5211, 2019.

[13] X. J. Wang, X. Luo, and J. M. Zhou, "Chemical constituents from rhizomes of *Rhodiola wallichiana* var. cholaensis and their protective effects on myocardium," *Chinese Traditional and Herbal Drugs*, vol. 47, no. 16, pp. 2822–2826, 2016.

[14] Y. Luo, H. Y. Shen, and M. Zhang, "Chemical constituents from the dregs of *Brucea javanica*," *Journal of Tropical and Subtropical Botany*, vol. 27, no. 3, pp. 294–298, 2019.

[15] M. J. Hu, Y. Tang, Z. Z. Feng, Z. B. Wu, and M. Bolati, "Chemical constituents from *Nardostachys chinensis*," *Chinese Traditional Patent Medicine*, vol. 41, no. 7, pp. 1597–1601, 2019.

[16] C. Wan, T. Yuan, A. L. Cirello, and N. P. Seeram, "Antioxidant and α-glucosidase inhibitory phenolics isolated from highbush blueberry flowers," *Food Chemistry*, vol. 135, no. 3, pp. 1929–1937, 2012.

[17] Y. Chen, F. T. Li, and W. W. Tao, "Chemical constituents of *typhae Pollen*," *Natural Product Research and Development*, vol. 27, no. 9, pp. 1558–1563, 2015.

[18] X. Y. Wang, "Chemical constituents from *Lobelia chinensis*," *Chinese Traditional Patent Medicine*, vol. 42, no. 12, pp. 3208–3210, 2020.

[19] S. Y. Li, L. Teng, and Y. J. Zhan, "Chemical constituents and simultaneous determination of three compounds from *Lonicera alberti* caulis," *Chinese Jounrnal of Experimental Traditional Medical Formulae*, vol. 23, no. 19, pp. 94–99, 2017.

[20] X. Tao, D. Pan, N. Xu, X. Y. Liu, and H. R. Zhang, "Chemical constituents from *Polygonum lapathifolium*," *Chinese Traditional Patent Medicine*, vol. 40, no. 4, pp. 866–870, 2018.

[21] L. R. Li, L. P. Wu, and C. R. Li, "Study on the chemical constituents of the branches and leaves of *Juniperus formosana*," *West China Journal of Pharmaceutical Sciences*, vol. 34, no. 1, pp. 5–9, 2019.

[22] J. Zhou, C. J. Li, and F. Y. Chen, "Flavonoids from the aerial parts of *Lespedeza cuneata*," *Acta Pharmaceutica Sinica*, vol. 54, no. 11, pp. 2055–2058, 2019.

[23] J. J. Xiang, Q. J. Li, and Y. Yang, "Immunological activity and chemical constituents of fermentation product in *Cynanchum auriculatum* Royle ex Wight," *Chinese Pharmaceutical Journal*, vol. 55, no. 7, pp. 498–503, 2020.

[24] Q. H. Zhang, S. L. Huang, and X. J. Wang, "Studies on the sapogenins and prosapogenins in *Aidsilla pusilla* A. DC," *China Journal of Chinese Materia Medica*, vol. 18, no. 9, pp. 548-549, 1993.

[25] X. Sun, Z. Xu, Y. Wang, and N. Liu, "Protective effects of blueberry anthocyanin extracts on hippocampal neuron damage induced by extremely low-frequency electromagnetic

field," *Food Science and Human Wellness*, vol. 9, no. 3, pp. 264–271, 2020.

[26] R. Gao, Q. Yu, Y. Shen et al., "Production, bioactive properties, and potential applications of fish protein hydrolysates: developments and challenges," *Trends in Food Science & Technology*, vol. 110, pp. 687–699, 2021.

[27] Z. Chen, J. Lin, and N. X. Gao, "Blueberry malvidin-3-galactoside modulated gut microbial dysbiosis and microbial TCA cycle KEGG pathway disrupted in a liver cancer model induced by HepG2 cells," *Food Science and Human Wellness*, vol. 9, no. 3, pp. 245–255, 2020.

[28] N. E. Núñez-Navarro, F. M. Santana, L. P. Parra, and F. C. Zacconi, "Surfing the blood coagulation cascade: insight into the vital factor Xa," *Current Medicinal Chemistry*, vol. 26, no. 17, pp. 3175–3200, 2019.

[29] S. A. Yang, N. K. Im, and I. S. Lee, "Effects of methanolic extract from *Salvia miltiorrhiza* Bunge on in vitro antithrombotic and antioxidative activities," *Korean J Food Sci Technol*, vol. 39, no. 1, pp. 83–87, 2007.

[30] W. Cai, L. Xie, Y. Chen, and H. Zhang, "Purification, characterization and anticoagulant activity of the polysaccharides from green tea," *Carbohydrate Polymers*, vol. 92, no. 2, pp. 1086–1090, 2013.

[31] N. He, P. Wang, Y. Niu, J. Chen, C. Li, and W.-y. Kang, "Evaluation antithrombotic activity and action mechanism of myricitrin," *Industrial Crops and Products*, vol. 129, pp. 536–541, 2019.

[32] L. Cui, M. Xing, L. Xu et al., "Antithrombotic components of *Malus halliana* Koehne flowers," *Food and Chemical Toxicology*, vol. 119, pp. 326–333, 2018.

Hindawi
Journal of Food Quality
Volume 2021, Article ID 8394152, 14 pages
https://doi.org/10.1155/2021/8394152

Research Article

The Preparation and Identification of Characteristic Flavour Compounds of Maillard Reaction Products of Protein Hydrolysate from Grass Carp (*Ctenopharyngodon idella*) Bone

Yunliang Li,[1] **Xiaojing Wang**,[1] **Xue Yang**,[2] **Siyu Ruan**,[1] **Anqi Zhou**,[1] **Shanfeng Huang**,[1] **and Haile Ma**[1]

[1]*Key Laboratory of Food Processing in Jiangsu Province of China, School of Food and Biological Engineering, Jiangsu University, 301 Xuefu Road, Zhenjiang, Jiangsu 212013, China*
[2]*Department of Basic Medicine, Chengde Medical University, Anyuan Road, Chengde, Hebei 067000, China*

Correspondence should be addressed to Yunliang Li; liyunliang@ujs.edu.cn and Xue Yang; yangxue19891012@163.com

Received 7 April 2021; Accepted 27 April 2021; Published 7 May 2021

Academic Editor: Shengbao Cai

This study aims at preparing the Maillard reaction products of protein hydrolysate from grass carp (*Ctenopharyngodon idella*) bone and identifying its characteristic flavour compounds. Meanwhile, bioactivities and amino acids composition of hydrolysates and its Maillard reaction products were compared with the thermal degradation reaction as one positive control. Single factor experiment was applied to optimize the enzymolysis parameters of grass carp bone protein using flavourzyme, under which the highest degree of hydrolysis (40.1%) was obtained. According to the response surface methodology, the top predicted value (70.45%) of degree of graft of Maillard reaction was obtained with initial pH of 7.07, temperature of 118.33°C, and time of 1.75 h. Moreover, the results of Maillard reaction products illustrated a significant increase in DPPH radical scavenging activity ($p < 0.05$) compared to that of hydrolysate and its thermal degradation products, which was accompanied by the decreased ACE inhibitory activity. Besides, the umami-sweet taste amino acid ratio in free amino acids of Maillard reaction products climbed considerably compared to those of hydrolysate and its thermal degradation products, which proved that Maillard reaction is an effective way to improve the flavour taste of protein hydrolysate. The GC-MS results showed that 37, 40, and 62 kinds of volatile compounds were detected in hydrolysate, thermal degradation products, and Maillard reaction products, respectively. The Maillard reaction products contained more flavour volatile compounds of aldehydes, alcohol, ketone, pyrazine, and other compounds that contribute to pleasant aromas. These results suggested that the grass carp bone protein hydrolysate after Maillard reaction could potentially have a wide range of applications as antioxidant and flavour substances.

1. Introduction

As a traditional freshwater fish, grass carp (*Ctenopharyngodon idellus*) is one of the major freshwater-cultured fishes [1]. Its production comprises up to 35~40% (3.7 million tons annually) of the total freshwater fish species [2] and it is widely popular with consumers for its palatability, nutritional characteristic, and low price [1, 3]. Therefore, it would not be a surprise that there are various categories of intensive processing products for grass carp in contemporary society, such as fish ball, fish noodle, and fish tofu. With the rapid growth of the fish products industry, the amount of fish bones rich in nutrition, such as protein, fat, and minerals, also increases proportionately. However, in most circumstances, these high-quality resources of nutrition are merely used as animal feed additives and fertilizer or buried directly, which is regarded to be a waste. Therefore, it is of great urgency to develop value-added products from grass carp bone.

The application of enzymolysis technology has attracted considerable interest in the conversion of underutilized resource into a more marketable and functional form, which can promote the physicochemical, functional, and sensory properties of the native protein [4]. Researches showed that

the grass carp proteins were mainly used to prepare bioactive peptide and functional material in secondary processing [5, 6]. For example, the research of Li et al. [7] revealed that the grass carp protein hydrolysate displayed high antioxidant activities. What is more, Wang et al. [8] claimed that grass carp peptides associated with NO regulation and the rennin-angiotensin system present to have antihypertensive effect. In other researches, fish protein hydrolysate was proved to be of use for flavour enhancer for direct human consumption for the material composition of free amino acids, smaller peptides, salt, and many savory compounds [9]. However, the study of protein hydrolysate from grass carp bone on food flavour agents has not been fully investigated.

The flavour of protein hydrolysate is related to the type of protease and enzymatic condition, among which bitter taste is the major problem affecting the sensory acceptability of protein hydrolysate. Some methods exist to limit the formation of bitter compounds during hydrolysis, such as controlling degree of hydrolysis (DH), choosing some specific enzymes, and masking by cyclodextrin [10]. The choice of protease affects the functional and flavour characteristics of protein hydrolysate. Flavourzyme is one commonly used protease in various commercial proteases to produce low-bitter flavour peptide compounds. It is endo- and exopeptidase enzymes mixture, which can effectively minimize the bitterness produced by the previous hydrolysis in the hydrolyzed peptide product [11]. It can hydrolyze proteins and produce more flavour peptides as well as amino acids for the product, which is more suitable for the hydrolysis of seafood. Also, recent studies show that a higher DH is more conducive to the formation of flavour amino acids and potential flavouring material [11, 12]. Therefore, it is an effective method to produce hydrolysate using flavourzyme under longer enzymatic time from grass carp bone protein (GCBP).

Besides, the Maillard reaction has also been reported to be an effective method to improve the functional properties of protein hydrolysate [13], masks the initial fish off-flavours, and improves the odour characteristics of hydrolysates [14]. Other researches regard that the peptides with smaller molecular weight showed a higher reaction degree to produce more characteristic flavour compounds through Maillard reaction [15]. According to these researches, it can be concluded that enzymolysis of protein and Maillard reaction of protein hydrolysate were two effective methods for preparing flavour compounds. However, which one is beneficial for making full use of grass carp bone is still uncertain.

Therefore, the objective of this study was to demonstrate the use of by-products of the fish industry (fish bone) for the generation of bioactive substances and fish flavour compounds. The content includes the three following contents: (1) to optimize enzymatic parameters of GCBP and Maillard reaction conditions of GCBP hydrolysate, (2) to investigate the bioactivities of GCBP hydrolysate and its Maillard reaction products with the thermal degradation reaction as one positive control, and (3) to analyze and compare the flavour components of the GCBP hydrolysate and its Maillard reaction products with the thermal degradation reaction as one positive control. It is also hoped that the results of the present research will be of great value to the application of grass carp bone and even other fish bones.

2. Materials and Methods

2.1. Materials. Grass carp (*Ctenopharyngodon idella*) bone was provided by a fish market of Zhenjiang, Jiangsu, China. Flavourzyme (activity of 2.44×10^4 U/mg) was purchased from Novozymes Co. Ltd. (China). Angiotensin-I-converting enzyme (ACE) was extracted from the pig lung according to the reported method (Maruyama et al., 1999). N-[3-(2-Furyl)-acryloyl]-L-phenylalanyl-glycyl-glycine (FA PGG), 1,1-Diphenyl-2-picrylhydrazyl (DPPH), and 4-(2-Hydroxyethyl)piperazine-1-ethanesulfonic acid (HEPES) were purchased from Sigma-Aldrich Corp. (USA). All the other chemicals and solvents used in the experiment were of analytical grade.

2.2. Extraction of Fish Bone Protein. In this study, alkali extraction combined with high-temperature treatment was applied to improve protein purity. Briefly, the fresh fish bone with a few of meat (byproduct of fish balls) was washed by using running water and then chopped into pieces (~0.3 cm) homogenized with water (w/v, 1 : 4.5) and the mixture was adjusted to pH 9.0 by adding 2 mol/L NaOH. Afterwards, the mixture was placed in high-pressure cooking machine at 120°C for 60 min. The homogenate was cooled to room temperature and centrifuged for 20 min at 5,000 r/min. The insoluble pellets and grease suspensions were discarded. Soluble protein in the supernatant was frozen-dried to prepare fish bone protein powder. The protein content of the fish bone powder was assayed by the Kjeldahl method (AOAC 991.20) and the value was 92.38% (dry weight).

2.3. Screening of Enzymolysis Conditions of Fish Bone Protein. In order to optimize enzymolysis conditions of fish bone protein for the maximum DH, single factor experimental design was employed. The fish bone powder was mixed with distilled water and then the mixture was hydrolyzed with flavourzyme according to the enzymatic conditions defined by the experimental design with DH as an index. The single factor experiment was conducted under the following conditions: substrate concentration of 20, 30, 40, 50, and 60 g/L; pH value of 6, 6.5, 7, 7.5, and 8; temperature of 40, 45, 50, 55, and 60°C; enzyme-to-substrate ratio of 5%, 5.5%, 6%, 6.5%, 7%, and 7.5%; and enzymolysis time of 5, 6, 7, 8, and 9 h. The reaction was terminated by boiled water bath for 15 min to inactivate the enzyme. Then the sample was centrifuged for 15 min at 4000 r/min after cooling to the room temperature (25 ± 1°C). The supernatant of protein hydrolysate was used for further analysis. All reactions were operated in triplicate.

2.4. Determination of Degree of Hydrolysis. DH is defined as the percentage of the number of peptide bonds broken to the

total number of bonds per unit weight, which was calculated from the ratio of α-amino nitrogen to total nitrogen. The amino nitrogen content was determined by a formaldehyde titration method [16]. An equal amount of distilled water was added to 10 mL supernatant of protein hydrolysate (Section 2.3) and the mixture was adjusted to pH 7.0 using 0.1 mol/L NaOH. Then 10 mL of 38% (v/v) formaldehyde solution was added to the mixture and titration was continued to the end point at pH 9.5 with 0.2 mol/L standard NaOH solution. The total nitrogen content was determined by Kjeldahl method (AOAC 991.20). Tests were conducted in triplicate.

2.5. Optimization of Maillard Reaction Condition. Based on the optimal protein enzymolysis condition (Section 2.3), the supernatant of the grass carp bone protein hydrolysate was prepared for Maillard reaction. According to our previous experiment results, the supernatant of protein hydrolysate was mixed with glucose of 4% (w/v), glycine-arginine (ratio of 1 : 1) mixture of 3% (w/v), vitamin C of 0.15% (w/v), and vitamin B_1 of 0.05% (w/v). Then the sample (protein concentration of 1 mg/mL) was put in sealed tube and heated for 1 h at 120°C in oil bath. The mixture was immediately cooled in ice bath for 30 min to terminate Maillard reaction. Then Maillard reaction products (MRP) were kept at −20°C for further analysis.

The initial pH (X_1), reaction temperature (X_2), and reaction time (X_3) were found to have significant influences on Maillard reaction by one-way analysis of variance. In order to optimize the reaction parameters, Box-Behnken design was selected and used to encode the test factors. The actual and coded values for the independent variables are shown in Table 1. The factors with the same coded levels (−1, 0, 1) and corresponding actual values were as follows: initial pH of 6, 7, and 8; reaction temperature of 90, 110, and 130°C; and reaction time of 1, 2, and 3 h. The degree of graft (DG) was an index to evaluate Maillard reaction and it was set as the response (Y). Each run was conducted in triplicate. The quadratic equation was the same as that of equation (2).

The complete quadratic equation reflecting the effect of the three independent variables on the DG was shown as follows:

$$Y = \beta_0 + \sum_{i=1}^{3} \beta_i X_i + \sum_{i=1}^{3} \beta_{ii} X_i^2 + \sum_{i=1}^{3} \sum_{j=i+1}^{3} \beta_{ij} X_i X_j, \quad (1)$$

where Y is the response variable; β_0 is a constant; β_i, β_{ii}, and β_{ij} are the regression coefficients for intercept, linearity, square, and interaction, respectively; X_i and X_j are the different independent variables ($i \neq j$). To deduce the quadratic equation (1), seventeen factorial points and five replicates of the center points were designed by the Box-Behnken design (Table 1).

In order to evaluate the effects of Maillard reaction, thermal degradation reaction of protein hydrolysate was employed to be a positive control. After hydrolysis of fish bone protein, the protein hydrolysate was directly heated for 1 h at 120°C in oil bath without adding glucose, glycine-arginine mixture, vitamin C, and vitamin B_1 under the optimal conditions of Maillard reaction, including temperature, pH, and time. Then the mixture was immediately cooled in ice bath for 30 min to terminate the heat reaction. The thermal degradation products (TDP) were stored at −20°C for further analysis. All trials were performed in triplicate.

2.6. Determination of the DG. The DG value was determined by o-phthaldialdehyde method [17] with light modifications. The preparation method of o-phthaldialdehyde reagent was as follows: 40 mg of o-phthaldialdehyde was dissolved in 1.0 mL of methanol, 25 mL sodium tetraborate (0.1 mol/L), 2.5 mL sodium dodecyl sulfate (20%, w/w), and 100 μL of β-mercaptoethanol. Then the mixture was diluted to a final volume of 50 mL with distilled water, after which two hundred microliter sample solution (protein concentration of 1 mg/mL) was added to 4 mL o-phthaldialdehyde reagent. The solution was mixed briefly and incubated for 2 min at 37°C. The absorbance was read at 340 nm using a spectrophotometer (Unic 7200, Unocal Corporation, Shanghai, China). Tests were performed in triplicate, and DG was calculated according to the following formula:

$$\mathrm{DG}\,(\%) = \frac{A_0 - A_1}{A_0} \times 100\%, \quad (2)$$

where A_0 was the absorbance of the supernatant of protein hydrolysate at 340 nm; A_1 was the absorbance of mixture after Maillard reaction at 340 nm.

2.7. DPPH Radical Scavenging Activity and ACE Inhibitory Activity Assays. The DPPH radical scavenging activity was measured by the method of Nasrollahzadeh et al. [18] with some modifications. 2 mL of DPPH solution (0.1 mol/L, dissolved in methanol) was added to 2 mL of sample (protein concentration of 1 mg/mL). Then the mixture was kept in the dark for 20 min at 37°C, followed by the centrifugation for 10 min at 4000 r/min and the measurement of the absorbance at 517 nm using spectrophotometer (Unic 7200, Unocal Corporation, Shanghai, China). The blank and control were prepared with the distilled water instead of samples and methanol instead of DPPH solution, respectively. All reactions were operated in triplicate. The DPPH radical scavenging activity was calculated by the following formula:

$$\text{DPPH radical scavenging rate}\,(\%) = \left(1 - \frac{A_1 - A_2}{A_0}\right) \times 100\%, \quad (3)$$

where A_0 is the absorbance of the blank (methanol instead of the sample), A_1 is the absorbance of sample, and A_2 is the background absorbance (methanol instead of DPPH).

The ACE activity was measured following the method of Zhou et al. [19] with some modifications. The samples were diluted 100 times with a HEPES buffer (80 mmol/L, pH 8.3, 300 mmol/L NaCl). The reaction mixture contained 50 μL ACE, 100 μL sample, and 50 μL FAPGG (1.0 mmol/L). The control was prepared with HEPES buffer instead of samples. After being incubated for 30 min at 37°C, the mixture was

Table 1: Box-Behnken design and results of Maillard reaction of protein hydrolysate from grass carp bone.

Level	X_1	X_2	X_3		Y
1	−1 (6)	−1 (90)	0 (2)		36.52
2	1 (8)	−1 (90)	0 (2)		41.33
3	−1 (6)	1 (130)	0 (2)		50.08
4	1 (8)	1 (130)	0 (2)		53.89
5	−1 (6)	0 (110)	−1 (1)		47.62
6	1 (8)	0 (110)	−1 (1)		53.14
7	−1 (6)	0 (110)	1 (3)		39.17
8	1 (8)	0 (110)	1 (3)		39.82
9	0 (7)	−1 (90)	−1 (1)		56.33
10	0 (7)	1 (130)	−1 (1)		60.31
11	0 (7)	−1 (90)	1 (3)		42.24
12	0 (7)	1 (130)	1 (3)		59.30
13	0 (7)	0 (110)	0 (2)		66.04
14	0 (7)	0 (110)	0 (2)		68.17
15	0 (7)	0 (110)	0 (2)		69.42
16	0 (7)	0 (110)	0 (2)		67.36
17	0 (7)	0 (110)	0 (2)		64.88
$R^2 = 0.9891$					
Term	Sum of squares	Df	Mean square	F-value	p value
Model	2013.44	9	223.72	70.68	<0.0001
X_1	916.04	1	916.04	289.41	<0.0001
X_2	108.89	1	108.89	34.40	0.0006
X_3	6.29	1	6.29	1.99	0.2014
X_1X_2	0.25	1	0.25	0.079	0.7868
X_1X_3	5.93	1	5.93	1.87	0.2134
X_2X_3	42.77	1	42.77	13.51	0.0079
X_1X_1	1033.00	1	1033.00	326.36	<0.0001
X_2X_2	154.41	1	154.41	48.78	0.0002
X_3X_3	181.93	1	181.93	57.48	0.0001
Residual	22.16	7	3.17		
Lack of fit	9.54	3	3.18	1.01	0.4763
Pure error	12.62	4	3.15		
Sum	2035.59	16			

measured in the absorption at 340 nm. The ACE inhibitory activity was calculated using the following formula:

$$\text{ACE inhibitory activity}\,(\%) = 1 - \frac{A_{s0} - A_{s30}}{A_{b0} - A_{b30}} \times 100\%, \tag{4}$$

where A_{s0} and A_{s30} represent the absorption of sample at 0 min and 30 min. A_{b0} and A_{b30} represent the absorption of blank at 0 min and 30 min.

2.8. Determination of Amino Acids Composition. The total amino acids profile of grass carp bone protein hydrolysates (GCBPH), thermal degradation products (TDP), and Maillard reaction products (MRP) was determined using an amino acid analyzer (S433D, Sykam, German) after hydrolyzing under vacuum with 6 mol/L HCl at 110°C for 24 h in the presence of 1% phenol (*v*/*v*). The free amino acid (FAA) profile was measured directly by the analyzer. The peptide-bound amino acid was calculated by subtracting FAA from total amino acid (TAA) [20]. The results were expressed as mg/g dry weight of products.

2.9. Determination of Volatile Compounds by Dynamic Headspace Gas Chromatography-Mass Spectrometry. The volatile compounds in GCBPH, TDP, and MRP were detected using HP6890/5973 dynamic headspace gas chromatography-mass spectrometry (DHS GC-MS) (Agilent Technologies (China) Co., Ltd.) [21] with some modifications. Each sample was prepared from 4 mL of samples (GCBPH, TDP, and MRP) and 1.0 g of NaCl in a 15 mL vial for the headspace technique. During the headspace collection procedure, samples were magnetically stirred at 600 r/m and equilibrated for 40 min at 60°C after purging the nitrogen. The separation of volatile compounds was achieved on a DB-WAX capillary column (60 mm × 0.25 mm × 0.25 μm). Helium was used as carrier gas at a flow rate of 0.8 mL/min. Oven initial temperature was set at 120°C for 4 min and then programmed to 90°C by a temperature ramp of 5°C/min and lastly increased to 210°C at 10°C/min with a final isothermal period of 10 min. The inlet and interface temperature were both kept at 250°C. A mass spectrometer scanned from 33 to 450 u. The ion source was set at 200°C and spectra were obtained by electron impact (70 eV).

In this experiment, the compound standards of C_7~C_{30} were selected for qualitative analysis and 2,4,6-trimethy lpyridine (chromatographic purity) was used as internal standard for quantitative analysis. The results were expressed as the relative area percentages being indices of the mass percentages of the compounds.

2.10. Statistical Analysis. The data were expressed as means ± standard differences. Results were statistically analyzed to identify differences by using one-way ANOVA and the Duncan test under the significance level of $p < 0.05$ using SPSS 19.0 software (IBM Corporation, NY, USA). Design expert 8.0.5b (Trial Version, State-Ease, Inc., Minneapolis, MN, USA) software package was used to analyze the experimental data of Box-Behnken design.

3. Results

3.1. Single Factor Experimental Results of Enzymolysis of Grass Carp Bone Protein. In order to determine the optimal levels of each variable of enzymolysis conditions for maximum DH, single factor experimental design was employed. Figures 1(a)–1(e) show the DH of grass carp bone protein at different substrate concentration (20~60 g/L), pH value (6.0~8.0), temperature (40~60°C), enzyme-to-substrate ratio (5.5~7.5%), and enzymolysis time (5~9 h). When screening the first parameter (substrate concentration), other parameters were set as follows: pH value of 7.0, temperature of 50°C, enzyme-to-substrate ratio of 6.5%, and enzymolysis time of 5 h. The following parameters were optimized using the best condition selected previously.

The effects of substrate concentration on the DH of grass carp bone protein are shown in Figure 1(a). As reflected in the results, DH and the substrate concentration showed a reversed trend and those of 20 g/L (with the DH value of 21.55%) and 30 g/L (with the value of 20.99%) had no significant difference. To obtain more hydrolysates, 30 g/L was selected to optimize the following enzymatic parameters. As shown in Figure 1(b), the results showed that different pH values influenced ($p < 0.05$) the DH of grass carp bone protein to a great extent and the highest DH (23.54%) was obtained when the pH was 7.5, which was selected to optimize the following enzymatic parameters. Similar to that of pH value, the DH of grass carp bone protein significantly ($p < 0.05$) increased and then decreased with the elevated enzymatic temperature (Figure 1(c)). At the temperature of 50°C, the highest DH of 23.54% was obtained. The DH increased significantly ($p < 0.05$) with the increase in enzyme-to-substrate ratio and that of 7.0% and 7.5% had no significant difference ($p > 0.05$) (Figure 1(d)). In order to reduce the cost, enzyme-to-substrate ratio of 7.0% was used to optimize the following parameter. As for enzymatic time, the DH of grass carp bone protein increased gradually with its extension. However, the data of 8 h had no significant effect ($p > 0.05$) compared to that of 9 h. Therefore, enzymatic time of 8 h was selected.

Enzymatic parameters afforded by this study produced different influence on the DH of grass carp bone protein. The optimal enzymatic conditions were as follows: substrate concentration of 30 g/L, pH value of 7.5, enzymatic temperature of 50°C, enzyme-to-substrate ratio of 7.0%, and enzymatic time of 8 h. Under these conditions, the DH of grass carp bone protein reached the highest value of 40.1%.

3.2. Response Surface Results of Maillard Reaction of Grass Carp Bone Protein Hydrolysates (GCBPH). In order to determine the optimal levels of each variable of Maillard reaction conditions for maximum DG, Box-Behnken design was employed to determine their optimal levels. The design matrix and the DG of the Maillard reaction are shown in Table 1. Multiple regression analysis was used to analyze the data and thus a quadratic polynomial equation was derived from regression analysis as follows:

$$\begin{aligned} Y = &- 936.65 + 224.94X_1 + 3.39X_2 + 12.22X_3 - 0.013X_1X_2 \\ &- 1.22X_1X_3 + 0.16X_2X_3 - 15.66X_1X_1 - 0.015X_2X_2 \\ &- 6.57X_3X_3. \end{aligned} \tag{5}$$

The analysis of variance, goodness of fit, and the adequacy of the regression model are summarized in Table 1. The statistical significance of equation (5) was checked by F-test, and the results of analysis of variance indicated that the F-value of 70.68 ($p < 0.0001$) implied that the model was statistically highly significant. The F-value and p value of the lack of fit were 1.01 and 0.4763, respectively. This illustrated that the lack of fit was not significant, which confirmed the goodness of fit and hence suitability of the regression model for predicting the DG of Maillard reaction of GCBPH under any combination of values of the independent variables. The coefficient of multiple determinations (R^2 of 0.9891) revealed that 98.91% of the variation in the DG was due to the independent variables and only 1.09% of the total variation was not explained by the model. Table 1 also demonstrates that the independent variables (X_1, X_2) exerted significant effects on DG within a 95% confidence interval ($p < 0.05$). The quadratic terms (X_1X_1, X_2X_2, and X_3X_3) as well as the interaction terms (X_2X_3) were also significant. Parity plot (Figure 2) showed an acceptable level of agreement. The strong correlation between the actual and the predicted results confirmed that the response model was accurate to reflect the expected optimization. All these results confirmed the predictability of the model for DG of Maillard reaction of GCBPH.

The response surface and contour plots drawn by the Box-Behnken design are shown in Figure 3, which provided a method to visualize the mutual effects of test variables at different levels and the reciprocal interactions between the test variables on the DG. The mutual interactions of initial pH (x_1) and reaction temperature (x_2) are illustrated in Figures 3(a) and 3(b). The pattern of Figure 3(a), which witnessed a slow rise in DG at first, unexpectedly declined with the continuing increase of pH. Effects of initial pH (x_1) and reaction time (x_3) are illustrated in Figures 3(c) and 3(d), which showed that, with the prolonging of reaction time, the DG changed in a certain range. What is more, the effects of reaction temperature (x_2) and time (x_3) are illustrated in Figures 3(e) and 3(f).

According to the results in Figure 3 and Table 1, the response surface had both the highest point and the contour of the response surface within the experimental range of the independent variables. According to the established mathematical response surface design method, the optimum conditions of Maillard reaction derived from interactions of

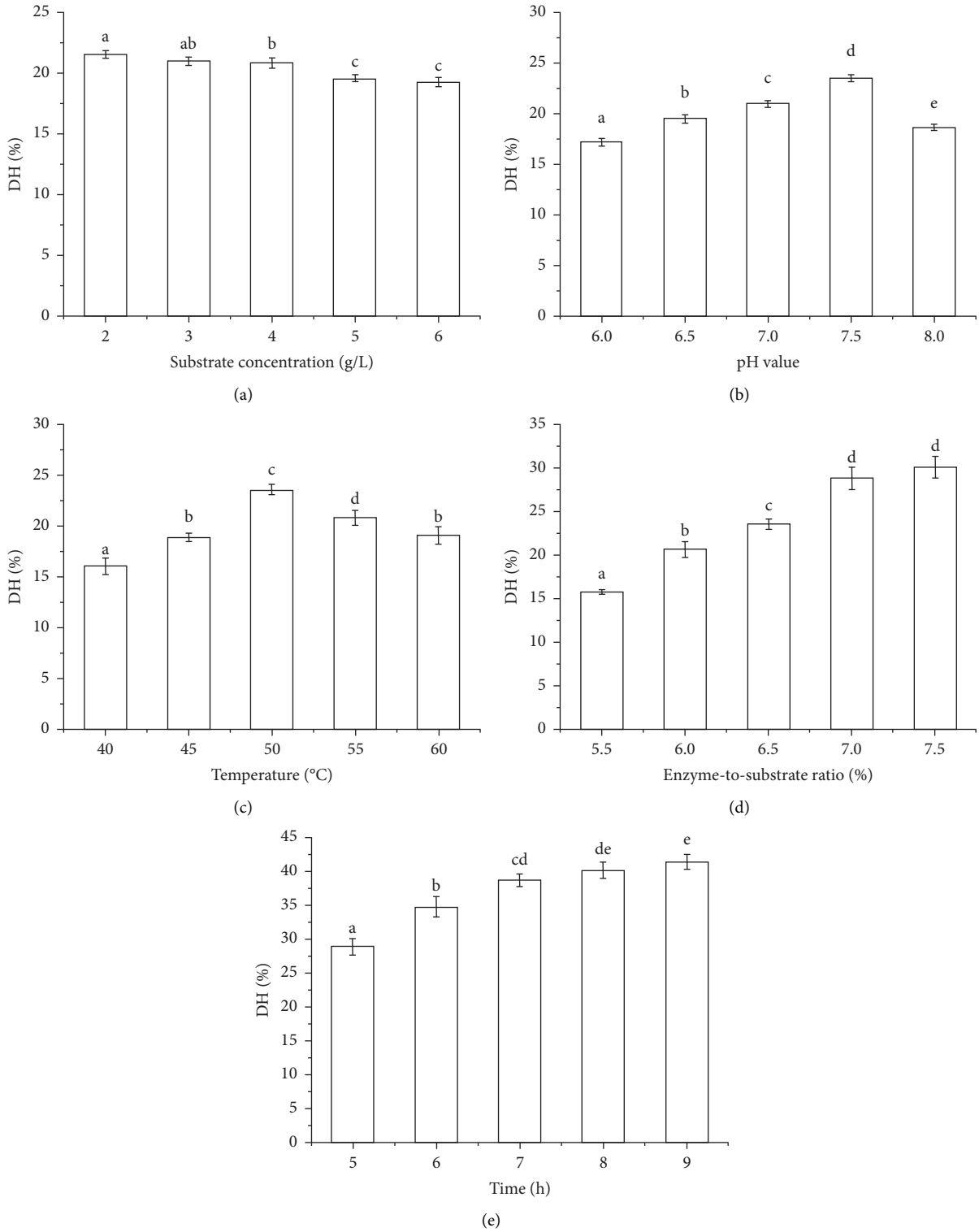

Figure 1: Single factor experimental results of enzymolysis conditions: (a) substrate concentration, (b) pH value, (c) temperature, (d) enzyme-to-substrate ratio, and (e) time. Means with different superscripts are significantly different ($p < 0.05$).

the three independent variables were initial pH of 7.07, the temperature of 118.33°C, and the time of 1.75 h. To confirm the validity of the model, three assays were performed under the optimum conditions and the average data of three tests notified that the DG was 69.05%, which was closely associated with the predicted value (70.45%) calculated by equation (5). The strong correlation between the actual and the predicted results confirmed that the response model was accurate to reflect the expected optimization of Maillard reaction.

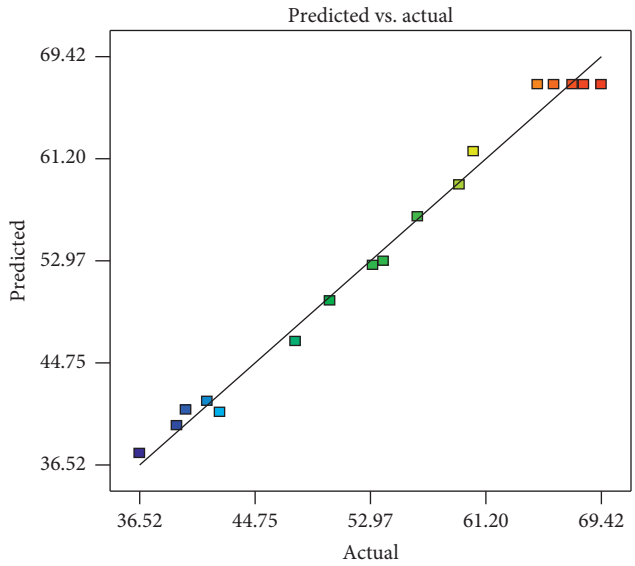

Figure 2: Relationship between the observed and predicted values of the degree of graft (Parity plot).

3.3. Biological Activity. Figure 4 shows the DPPH radical scavenging rate and ACE inhibitory rate of different products. The DPPH radical scavenging rate of MRP increased significantly ($p < 0.05$) compared to that of GCBPH and TDP. These results were in consistency with the literatures [18, 22]. The reason why the antioxidant activity of MRP rose markedly may be due to the generation of increased antioxidant products during Maillard reaction rather than the thermal degradation reaction of protein hydrolysate.

The ACE inhibitory rate of MRP had no significant difference ($p > 0.05$) compared to that of GCBPH. However, the ACE inhibitory rate of TDP (with its value of 39.67%) decreased by 8.9% in contrast to that of GCBPH, which indicated that thermal degradation methods reduced the ACE inhibitory activity of protein hydrolysate significantly ($p < 0.05$). The reason might be that thermal treatment degraded some of the active proteins or peptides into inactive fragment. Furthermore, Maillard reaction could generate more compounds and substances with strong ACE inhibitory activities, which resulted in no difference of ACE inhibitory activity between MRP and GCBPH.

3.4. Amino Acid Composition. The selectivity and specificity of flavourzyme to hydrolyze the fish bone protein resulted in a considerable amount of peptide and amino acids production. Amino acids were highly correlated with taste characteristics in foods peptides and related to some mechanisms of functionality, such as umami taste or umami-enhancing properties [23, 24]. The flavour peptides were a group of peptides related to the feelings of taste and smell, which would be of varying structures and length and possess unique taste properties [25]. In order to evaluate the flavour compounds of different treatment methods on the fish bone, the amino acid compositions of GCBPH, TDP, and MRP were analyzed.

The results of total amino acid and free amino acid are shown in Table 2. In GCBPH, the contents of TAA and FAA were 566.15 and 210.32 mg/g, respectively, which suggested that the ratio of FAA to TAA was 37.15%, of which the umami-sweet taste amino acids much lower than individual thresholds expected for Glu, Asp, and Arg accounted for 35.47% of FAA. In TDP, the total amino acid content (505.33 mg/g) was lower than that of GCBPH, which might result from the generation of new compound during thermal treatment. However, the FAA content and its ratio to TAA and the ratio of umami-sweet taste amino acids to FAA did not change significantly ($p > 0.05$). This might be attributed to the crack of some of the amino acids existent in peptide into free amino acid during the high-temperature treatment. In MRP, the FAA proportion of TAA slumped to 31.82% after the Maillard reaction of hydrolysate, which proved that more FAA engaged in the Maillard reaction, compared to the amino acids present in the peptide form. Among all the FAA, Lys (9.51 mg/g), Arg (11.49 mg/g), and Leu (14.25 mg/g) presented dominant position in Maillard reaction, which decreased by 15.14, 6.16, and 13.94 mg/mL compared to that of GCBPH, respectively. This indicated that Lys, Arg, and Leu of FAA probably were main free amino acids involved in the Maillard reaction. In addition, umami-sweet taste amino acids of FAA were of 41.32%, which increased significantly ($p < 0.05$) compared to those of GCBPH. These results showed that simple heating hydrolysis did not affect the ratios of FAA and umami-sweet taste amino acids. The decreased ratio of FAA to TAA and increased ratio of umami-sweet taste amino acids to FAA were ascribed to the Maillard reaction rather than the heat treatment during reaction processing.

3.5. Volatile Compounds. The flavourzyme hydrolysis is valuable due to the large number of natural fragrances and volatile compounds produced in the hydrolysis. The role of flavourzyme is to increase the concentrations of most of the volatile compounds that are predominantly chemical families in the hydrolysate [26]. Also, Maillard reaction can modify the odour of protein hydrolysate [14]. Accordingly, the volatile compounds of GCBPH, TDP, and MRP were detected and quantified using the DHS-GC-MS technique.

Table 3 declares the total detected individual volatile compounds with 37 flavour compounds of GCBPH, which were categorized into seven groups, namely, aldehydes, alcohol, ketone, hydrocarbon, furans, phenol, and esters, where each was composed of 9, 8, 3, 5, 5, 4, and 3 individuals, respectively. Aldehydes, indicated as final oxidation products of ω-3 fatty acids for seafood and marine raw materials, were important aroma compounds in food stuffs [27]. Results illustrated that pentanal, hexanal, heptanal, and 2-hexenal with low threshold values were the major volatiles in hydrolysate which mainly associated with tallow aroma. Moreover, hexanal was the aldehyde with the highest relative content of 5.21%, which could be resulting from a degradation process of preformed volatiles, such as 2-octenal [28]. The 2-Methyl-butanal and 3-Methyl-butanal, representing 1.56% and 2.68% of the total volatile compounds, have been

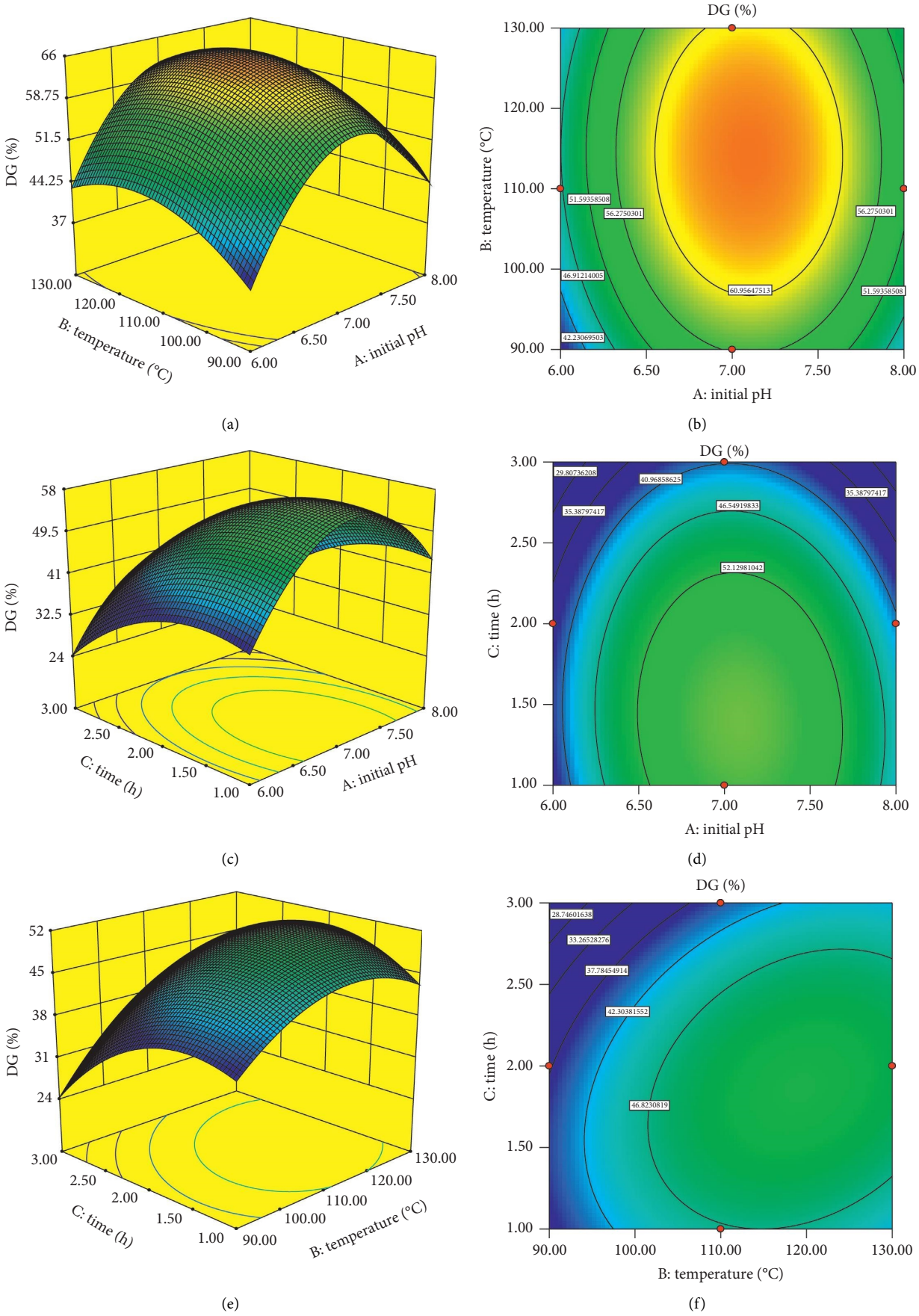

FIGURE 3: Response surface plots (a, c, and e) and contour plots (b, d, and f) for the interactive effects of initial pH (x_1), temperature (x_2), and time (x_3) on the DG of the Maillard reaction.

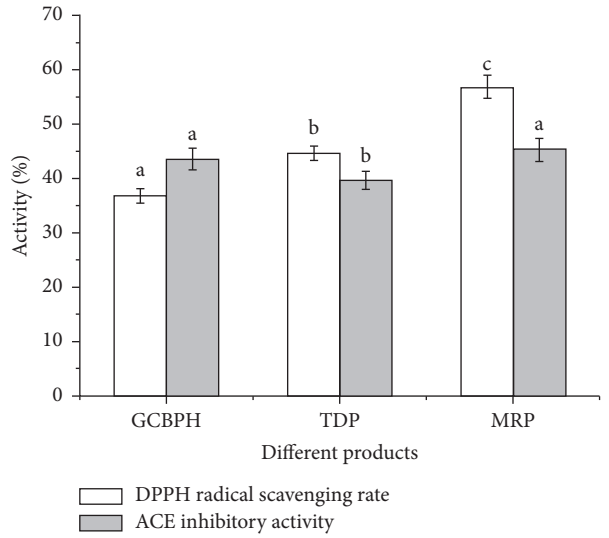

Figure 4: The DPPH radical scavenging rate and ACE inhibitory activity of GCBPH, TDP, and MRP. Means with different superscripts are significantly different ($p < 0.05$).

Table 2: Amino acid composition of GCBPH, TDP, and MRP.

AA	Taste threshold	TAA (mg/g)			FAA (mg/g)		
		GCBPH	TDP	MRP	GCBPH	TDP	MRP
Pro	300	87.65	84.18	68.17	6.38	5.95	2.87
Trp	—	67.58	58.5	37.65	11.77	14.37	4.94
Leu	90	38.35	32.94	22.65	28.19	24.28	14.25
Val	150	17.97	11.7	8.55	12.04	6.63	5.62
Ile	380	17.86	11.88	6.2	11.65	8.8	6.25
Phe	150	18.52	17.23	13.16	13.54	14.13	6.38
Met	30	14.87	12.75	9.57	9.05	9.48	6.58
His	20	15.69	14.78	12.49	3.85	4.5	2.17
Glu	5	64.51	59.45	33.84	12.18	13.12	5.85
Asp	3	41.69	39.37	24.63	13.24	12.45	8.57
Arg	10	34.16	28.38	21.29	17.65	14.83	11.49
Ala	60	23.97	23.64	12.47	9.85	9.39	5.52
Gly	110	28.48	24.17	19.5	5.83	6.22	3.45
Thr	260	17.41	16.23	9.34	9.85	8.73	5.21
Ser	150	9.2	8.64	5.62	6.01	6.08	4.87
Cys	—	8.74	5.35	2.65	2.85	2.57	1.25
Lys	50	42.85	40.79	24.69	24.65	23.62	9.51
Tyr	—	16.65	15.35	9.49	11.74	11.46	4.02
Total		566.15	505.33	341.96	210.32	196.61	108.8
FAA ratio					37.15	38.91	31.82
USAA		219.42	199.88	126.69	74.61	70.82	44.96
USAA ratio		38.76	39.55	37.05	35.47	36.02	41.32

TAA represents total amino acids; FAA represents free amino acids; USAA represents umami-sweet taste amino acids, including Glu, Asp, Arg, Ala, Gly, Thr, and Ser.

identified as spoilage index. Benzaldehyde, with a relative content of 1.26%, characterized by sweet and oily flavour, was reported in meat, bone meal, and sukiyaki flavour [29]. In alcohol, the 1-Octen-3-ol, identified and characterized as lipid oxidation product in fish oil, was an important flavour contributor due to its low odour threshold [28, 30]. So far, 1-Octen-3-ol as a predominant alcohol of hydrolysate (with relative amount of 4.10%) revealed a pungent, soil, and fruit odour. It has been mentioned as the most distinct volatile characterizing fresh sardine and other fatty fish aromas [31]. Compared to short straight chain alcohols, long straight chain alcohols like 1-pentanol, 1-hexanol, and heptanol, as well as branched-chain alcohols like 1-Penten-3-ol and (Z)-2-Octen-1-ol, contributed aroma to the products with relatively lower threshold value [32]. The 2,4-Di-tert-butylphenol was found to be the most abundant volatile (17.10%) in the hydrolysate, which revealed a fermented sausage odour and contributed to antibiofilm activity [33]. Furans,

Table 3: Volatile Compounds identified in GCBPH, TDP, and MRP by DHS GC-MS.

	Compound	Rta	Percentage of total area (%)		
			GCBPH	TDP	MRP
	Aldehydes				
1	2-Methyl-propanal	6.91			0.27
2	Butanal	7.92			0.14
3	2-Methyl-butanal	8.69	1.56	2.12	1.86
4	3-Methyl-butanal	8.69	2.68	2.31	2.25
5	Pentanal	10.21	1.68	1.44	0.72
6	2-Butenal	11.81		0.18	0.21
7	Hexanal	12.71	5.21	7.84	6.05
8	(E)-2-Pentenal	13.13			0.19
9	Heptanal	14.96		0.33	0.33
10	2-Hexenal	15.8		1.05	0.86
11	(Z)-2-Heptenal	17.77		2.27	2.41
12	2-Methyl-2-heptenal	18.27			0.43
13	Nonanal	18.82	0.75	1.08	1.06
14	(E, E)-2,4-Hexadienal	19.08			0.21
15	(E, E)-2,4-Heptadienal	19.95			1.95
16	3-(Methylthio)-propanal	19.84	0.57	1.23	1.08
17	Furfural	19.89	0.75	0.42	
18	Benzaldehyde	20.91	1.26	1.71	1.56
19	(E,Z)-2,6-Nonadienal	21.64			0.83
20	(E,E)-2,4-Nonadienal	23.11			0.59
21	4-Ethyl-benzaldehyde	23.3	0.41	0.48	0.77
22	(E,E)-2,4-Decadienal	24.41			1.85
23	α-Ethylidene-benzeneacetaldehyde	26.08			0.42
	Subtotal		14.87	22.46	26.04
24	*Alcohol*				
25	(E)-2-Pentenol	13.92	1.22	0.10	
26	1-Penten-3-ol	14.55	3.25	2.89	2.18
27	1-Pentanol	16.31	2.70	3.04	2.35
28	1-Hexanol	18.05	2.45	2.24	1.95
29	1-Octen-3-ol	19.46	4.10	4.43	3.49
30	Heptanol	19.59	2.11	1.71	1.52
31	2-Ethyl-1-hexanol	20.06	0.69	1.06	0.78
32	1-Octanol	20.99			0.88
33	(Z)-2-Octen-1-ol	21.75	0.83	1.29	0.71
34	6-Undecanol	22.4			2.45
35	Benzyl alcohol	25.12			0.39
	Subtotal		17.35	16.77	16.70
	Ketone				
36	2-Heptanone	15.04			1.09
37	3-Octen-2-one	19.12	0.89		
38	2-Ethylidenecyclohexanone	19.37	1.44		
39	3,5-Octadien-2-one	21.46	7.67	4.88	1.51
40	1H-Inden-1-one	24.4			0.73
41	2-Ethyl-cyclopentanone	28.47		1.56	1.95
	Subtotal		10.00	6.44	5.29
	Hydrocarbon				
42	Hexamethyl-cyclotrisiloxane	7.33	0.37	2.72	1.43
43	Octamethyl-cyclotetrasiloxane	10.07	8.64	7.17	5.90
44	p-Xylene	14.05			0.77
45	D-Limonene	15.09			0.46
46	Tetradecane	18.69	0.34		
47	1,3-Cyclooctadiene	22.6	5.80	2.71	
48	Hexamethyl-cyclotrisiloxane	23.42	0.34		
49	2,6-Dimethyl-2,4,6-octatriene	24.53			1.67
	Subtotal		15.48	12.60	10.23
	Furans				
50	2-Ethyl-furan	9.53	3.87	3.34	2.69

Table 3: Continued.

	Compound	Rta	Percentage of total area (%)		
			GCBPH	TDP	MRP
51	2-Pentyl-furan	15.88	3.43	2.97	1.91
52	(E)-2-(1-Pentenyl)-furan	17.04	1.76		
53	cis-2-(2-Pentenyl)furan	17.18	4.20	3.39	1.64
54	2-Methyl-furan	20.16			0.98
55	(E)-2-(1-Pentenyl)-furan	25.51	0.65	1.59	4.99
	Subtotal		13.90	11.29	12.20
	Phenol				
56	4-Ethyl-phenol	15.53	0.49		
57	2-Ethyl-phenol	15.65			1.04
58	4-(1-Methylpropyl)-phenol	25.03	1.54		
59	2,6-Bis(1,1-Dimethylethyl)-4-(1-oxopropyl)phenol	25.43	1.85		0.34
60	2,4-Di-tert-butylphenol	32.37	17.10	9.74	1.96
	Subtotal		20.98	9.74	3.34
	Esters				
61	Pentyl ester	20		1.05	1.11
62	Dioctyl phthalate	20.99	2.64	1.79	
63	Benzyl benzoate	24.89	3.25	2.86	
64	Bis(2-Ethylhexyl)ester	27.27			0.61
65	Butylisohexylester	29.28		1.71	2.29
66	Methyl palmitate	30.44	1.52	0.56	
	Subtotal		7.41	7.97	4.01
	Pyrazine				
67	Methyl-pyrazine	16.83		5.33	4.12
68	2,6-Dimethyl-pyrazine	17.86			0.93
69	3-Ethyl- 2,5-Dimethyl-pyrazine	19.75			1.85
70	2,5-Dimethyl-3-Propyl-pyrazine	20.7			0.87
71	2-Butyl-3,5-Dimethyl-pyrazine	22.53			2.87
	Subtotal			5.33	10.63
	Others				
72	Butanamide	13.52			3.22
73	1,3-Diazine	15.72			0.81
74	2-Chloro-4-(4-Methoxyphenyl)-6-(4-Nitrophenyl)pyrimidine	16.56		4.73	3.32
75	4-Methylthiazole	22.26		1.31	1.87
76	2-Methylpiperidine	28.47		1.36	2.35
	Subtotal			7.40	11.56
	Total		100	100	100

providing green bean and butter flavours, could be generated from sugar caramelization and carbohydrate degradation [28] and had been identified in fish oil and fish sauce [30, 34]. Esters were identified in contributing to pleasant seafood aromas in general [31].

During the thermal degradation process, the flavour compounds of sample were 40 kinds, with eleven new substances added in aldehydes, pyrazine, and other categories, and eight substances disappeared in ketone, hydrocarbon, furans, and phenol. In addition to taste-eliciting compounds such as peptides and amino acids, aroma compounds were generated by Maillard browning reaction, Strecker degradation, and so forth [35]. The volatile compounds identified in the MRP with 62 kinds are presented in Table 3, which included 22 aldehydes, 10 alcohol, 4 ketone, 5 hydrocarbon, 5 furans, 3 phenol, 3 esters, 5 pyrazine, and 5 others. The volatile aldehydes class contributed the major volatiles in the MRP, which were of relative higher amounts 26.04%, which were much higher than those of GCBPH. Straight and branched-chain aldehydes generally provided herbaceous, grassy, and pungent aromas, while unsaturated aldehydes were linked with vegetal and fishy notes and each of these compounds possesses its own specific odours. For instance, 2-Methyl-Propanal (value of 0.27%) gave a pungent smell and fishy and grassy aroma was provided by hexanal (value of 6.05%). Moreover, 2-Methyl-butanal (value of 1.86%) and 3-Methyl-butanal (value of 2.25%) produced nutty odours. Furthermore, unsaturated n-2-alkenals, such as (Z)-2-Heptenal, (E, E)-2,4-Heptadienal, and (E, E)-2,4-Decadienal, might play a more important role in the formation of species-specific flavour [36]. The volatile ketones were most likely the products of lipid and/or amino acid degradation. Only four ketone compounds were detected in the MRP samples, which may contribute to the cheesy odour of MRP with relative lower total amount. All of these factors contributed to the overall aroma of the MRP. The pyrazines, furans, and esters were the most desirable compounds in food products to enhance the aroma of the products. Compared with volatile components in GCBPH, the compounds in MRP increased from 8 to 13 kinds. The

relative content of pyrazine in the volatile components was 10.63%. Pyrazine, due to its large size and low taste threshold, was considered to be a significant volatile flavour in many heat-processed products and gave a pleasant nutty and baking flavour. The 4-Methylthiazole in the sulfur-containing compound accounted for 1.87% of the total amount, which was regarded as a perfume intermediate that might come into being during the process of Maillard reaction consisting of amino acids and sugars or compounds containing carbonyl groups. Compared to that of GCBPH and TDP, MRP contained more kinds of flavour volatile compounds of aldehydes, alcohol, ketone, pyrazine, and others. Maillard reaction was then indicated to be capable of perfecting the flavour and aroma of the hydrolysate from grass carp protein.

4. Discussion

In this paper, the fish bone of common species of fish, grass carp, was used as a sample to investigate its high value utilization using different methods. The preparation of bioactive peptide and flavour compounds by enzymatic method was an effective method to make full use of protein resources. However, it still has a relatively low biological activity and low content of flavour compounds. Many researches showed that Maillard reaction not only can increase the bioactivities but also can improve the flavour of protein hydrolysate [15, 22]. As a consequence, the Maillard reaction of hydrolysate from grass carp bone protein was used for preparation of bioactive compounds and identification of characteristic flavour compounds using thermal degradation method as the positive control. Compared with the thermal degradation methods, Maillard reaction probably generated more compounds and substances with higher DPPH radical scavenging activity and ACE inhibitory activities. However, thermal degradation methods significantly reduced the ACE inhibitory activity of protein hydrolysate in contrast to those of GCBPH and MRP. The reason might be that thermal treatment degraded some of the active proteins or peptides into inactive fragment.

The flavour and taste quality of foods are the most important factors affecting consumers' choice and acceptance. In terms of aquatic products, the flavour, as the main factor, determines its quality to a great extent. These flavours include not only the soft and pleasant smell but also the unpleasant odour. In the products related to protease hydrolysis, some peptides with sensory properties, such as sweet peptides, bitter peptides, acid peptides, salty peptides, and flavour-enhancing peptides, play a vital role in improving sensory characteristics and flavour enhancement of hydrolysates. Therefore, the proportion of umami-sweet taste amino acids in free amino acids directly affects the flavour and quality of hydrolysates. In this experiment, Maillard reaction can lead to the increase of the umami-sweet taste amino acids ratio in free amino acids and improve the flavour by increasing the volatile compounds. It indicated that Maillard reaction was an effective way to process fish bone, which provided a new direction for the application of fish bone.

In conclusion, compared to grass carp bone protein hydrolysate and its thermal degradation products, Maillard reaction significantly increased the DPPH radical scavenging activity of hydrolysate and the proportion and variety of umami-sweet taste amino acid in total free amino acids of grass carp protein hydrolysate. These findings suggested that fish bone protein hydrolysate could be effectively prepared by enzymolysis and Maillard reaction could improve its utilization by increasing antioxidant activity and flavours.

Data Availability

The data supporting the results of this study are available within the paper or are available from the corresponding author upon reasonable request.

Conflicts of Interest

The authors declare that they have no conflicts of interest.

Acknowledgments

The authors would like to acknowledge the National Natural Science Foundation of China (no. 31701538), Youth Science Fund Project of Natural Science Foundation of Hebei Province (no. C2019406071), the Natural Science Foundation of the Jiangsu Higher Education Institutions of China (17KJB550001), and Program Sponsored for Scientific Innovation Research of College Graduate in Jiangsu Province, China (KYCX18_2279).

References

[1] H. Zhan, X. Liu, S. Jia, and Y. Luo, "Antimicrobial effects of cinnamon bark oil on microbial composition and quality of grass carp (*Ctenopharyngodon idellus*) fillets during chilled storage," *Food Control*, vol. 82, pp. 316–324, 2017.

[2] J. Xiao and L. Niu, "Antilisterial and antioxidant activities of neutrase-treated grass carp proteins and their effects on the storage and quality properties of fresh noodle," *Journal of Food Processing and Preservation*, vol. 40, no. 6, pp. 1421–1428, 2016.

[3] D. Yu, Q. Jiang, Y. Xu, and W. Xia, "The shelf life extension of refrigerated grass carp (*Ctenopharyngodon idellus*) fillets by chitosan coating combined with glycerol monolaurate," *International Journal of Biological Macromolecules*, vol. 101, pp. 448–454, 2017.

[4] H. G. Kristinsson and B. A. Rasco, "Biochemical and functional properties of Atlantic salmon (*Salmo salar*) muscle proteins hydrolyzed with various alkaline proteases," *Journal of Agricultural and Food Chemistry*, vol. 48, no. 3, pp. 657–666, 2000.

[5] J. Ren, M. Zhao, J. Shi et al., "Optimization of antioxidant peptide production from grass carp sarcoplasmic protein using response surface methodology," *LWT—Food Science and Technology*, vol. 41, no. 9, pp. 1624–1632, 2008.

[6] J. Wasswa, J. Tang, X. Gu, and X. Yuan, "Influence of the extent of enzymatic hydrolysis on the functional properties of protein hydrolysate from grass carp (*Ctenopharyngodon idella*) skin," *Food Chemistry*, vol. 104, no. 4, pp. 1698–1704, 2007.

[7] X. Li, Y. Luo, H. Shen, and J. You, "Antioxidant activities and functional properties of grass carp (*Ctenopharyngodon idellus*)

protein hydrolysates," *Journal of the Science of Food and Agriculture*, vol. 92, no. 2, pp. 292–298, 2012.

[8] S. Wang, L.-M. Lin, Y.-N. Wu et al., "Angiotensin I converting enzyme (ACE) inhibitory activity and antihypertensive effects of grass carp peptides," *Food Science and Biotechnology*, vol. 23, no. 5, pp. 1661–1666, 2014.

[9] X. Guo, X. Han, Y. He, H. Du, and Z. Tan, "Optimization of enzymatic hydrolysis for preparation of shrimp flavor precursor using response surface methodology," *Journal of Food Quality*, vol. 37, no. 4, pp. 229–236, 2014.

[10] H. Hu, B. Li, and X. Zhao, "Enzymatic hydrolysis of defatted mackerel protein with low bitter taste," *Journal of Ocean University of China*, vol. 10, pp. 85–92, 2011.

[11] R. Liyt, E. Daukšas, E. Falch, I. Storr, and T. Rustad, "Characteristics of protein fractions generated from hydrolysed cod (*Gadus morhua*) by-products," *Process Biochemistry*, vol. 40, pp. 2021–2033, 2005.

[12] X. M. Feng, X. H. Yang, W. C. Xie et al., "Optimization of enzymatic hydrolysis of white shrimp (*Penaeus vannamei*) head Using response surface methodology," *Food Science*, vol. 30, pp. 66–70, 2009.

[13] Y. Li, F. Zhong, W. Ji, W. Yokoyama, C. F. Shoemaker, and S. Zhu, "Functional properties of Maillard reaction products of rice protein hydrolysates with mono-, oligo- and polysaccharides," *Food Hydrocolloids*, vol. 30, pp. 53–60, 2013.

[14] C. Kouakou, J.-P. Bergé, R. Baron, L. Lethuaut, C. Prost, and C. Mireille, "Odor modification in salmon hydrolysates using the Maillard reaction," *Journal of Aquatic Food Product Technology*, vol. 23, pp. 453–467, 2014.

[15] G. Su, Z. Lin, C. Cui, Y. Bao, J. Ren, and M. Zhao, "Characterization of antioxidant activity and volatile compounds of Maillard reaction products derived from different peptide fractions of peanut hydrolysate," *Food Research International*, vol. 44, pp. 3250–3258, 2011.

[16] S. Nilsang, S. Lertsiri, M. Suphantharika, and A. Assavanig, "Optimization of enzymatic hydrolysis of fish soluble concentrate by commercial proteases," *Journal of Food Engineering*, vol. 70, pp. 571–578, 2005.

[17] J. J. Guan, A. Y. Qiu, X. Y. Liu, Y. F. Hua, and Y. H. Ma, "Microwave improvement of soy protein isolate-saccharide graft reactions," *Food Chemistry*, vol. 97, pp. 577–585, 2006.

[18] F. Nasrollahzadeh, M. Varidi, A. Koocheki, and F. Hadizadeh, "Effect of microwave and conventional heating on structural, functional and antioxidant properties of bovine serum albumin-maltodextrin conjugates through Maillard reaction," *Food Research International*, vol. 100, pp. 289–297, 2017.

[19] C. Zhou, H. Ma, Q. Ding et al., "Ultrasonic pretreatment of corn gluten meal proteins and neutrase: effect on protein conformation and preparation of ACE (angiotensin converting enzyme) inhibitory peptides," *Food and Bioproducts Processing*, vol. 91, pp. 665–671, 2013.

[20] M. R. Rhyu and E. Y. Kim, "Umami taste characteristics of water extract of Doenjang, a Korean soybean paste: low-molecular acidic peptides may be a possible clue to the taste," *Food Chemistry*, vol. 127, pp. 1210–1215, 2011.

[21] V. Kachrimanidou, N. Kopsahelis, A. Chatzifragkou, S. Papanikolaou, and A. A. Koutinas, "Utilisation of by-products from sunflower-based biodiesel production processes for the production of fermentation feedstock," *Waste and Biomass Valorization*, vol. 4, pp. 529–537, 2013.

[22] M. Yu, S. He, M. Tang, Z. Zhang, Y. Zhu, and H. Sun, "Antioxidant activity and sensory characteristics of Maillard reaction products derived from different peptide fractions of soybean meal hydrolysate," *Food Chemistry*, vol. 243, pp. 249–257, 2018.

[23] Y. Yamasaki and K. Maekawa, "A peptide with delicious taste," *Agricultural and Biological Chemistry*, vol. 42, pp. 1761–1765, 1978.

[24] M. Behrens, W. Meyerhof, C. Hellfritsch, and T. Hofmann, "Sweet and umami taste: natural products, their chemosensory targets, and beyond," *Angewandte Chemie International Edtion (in English)*, vol. 50, pp. 2220–2242, 2011.

[25] Z. Yu, H. Jiang, R. Guo et al., "Taste, umami-enhance effect and amino acid sequence of peptides separated from silkworm pupa hydrolysate," *Food Research International*, vol. 108, pp. 144–150, 2018.

[26] X. B. Dong, L. Xia, C. H. Zhang et al., "Development of a novel method for hot-pressure extraction of protein from chicken bone and the effect of enzymatic hydrolysis on the extracts," *Food Chemistry*, vol. 157, pp. 339–346, 2014.

[27] W. Kolanowski, D. Jaworska, and J. Weissbrodt, "Importance of instrumental and sensory analysis in the assessment of oxidative deterioration of omega-3 long-chain polyunsaturated fatty acid-rich foods," *Journal of the Science of Food & Agriculture*, vol. 87, pp. 181–191, 2010.

[28] J. Iglesias, I. Medina, F. Bianchi, M. Careri, A. Mangia, and M. Musci, "Study of the volatile compounds useful for the characterisation of fresh and frozen-thawed cultured gilthead sea bream fish by solid-phase microextraction gas chromatography-mass spectrometry," *Food Chemistry*, vol. 115, pp. 1473–1478, 2009.

[29] C. Sonklin, N. Laohakunjit, and O. Kerdchoechuen, "Physicochemical and flavor characteristics of flavoring agent from mungbean protein hydrolyzed by bromelain," *Journal of Agricultural and Food Chemistry*, vol. 59, pp. 8475–8483, 2011.

[30] K. Hartvigsen, P. Lund, L. F. Hansen, and G. H. Holmer, "Dynamic headspace gas chromatography/mass spectrometry characterization of volatiles produced in fish oil enriched mayonnaise during storage," *Journal of Agricultural and Food Chemistry*, vol. 48, pp. 4858–4867, 2000.

[31] K. Grigorakis, I. Giogios, A. Vasilaki, and I. Nengas, "Effect of the fish oil, oxidation status and of heat treatment temperature on the volatile compounds of the produced fish feeds," *Animal Feed Science & Technology*, vol. 158, pp. 73–84, 2010.

[32] A. Giri, K. Osako, and T. Ohshima, "Identification and characterisation of headspace volatiles of fish miso, a Japanese fish meat based fermented paste, with special emphasis on effect of fish species and meat washing," *Food Chemistry*, vol. 120, pp. 621–631, 2010.

[33] S. Kalaichelvan, N. Sundaraganesan, O. Dereli, and U. Sayin, "Experimental, theoretical calculations of the vibrational spectra and conformational analysis of 2,4-di-tert-butylphenol," *Spectrochimica Acta Part A Molecular and Biomolecular Spectroscopy*, vol. 85, pp. 198–209, 2012.

[34] J. S. Elmore, M. M. Campo, M. Enser, and D. S. Mottram, "Effect of lipid composition on meat-like model systems containing cysteine, ribose, and polyunsaturated fatty acids," *Journal of Agricultural and Food Chemistry*, vol. 50, pp. 1126–1132, 2002.

[35] M. X. Zhang, X. C. Wang, Y. Liu, X. L. Xu, and G. H. Zhou, "Isolation and identification of flavour peptides from Puffer fish (*Takifugu obscurus*) muscle using an electronic tongue and MALDI-TOF/TOF MS/MS," *Food Chemistry*, vol. 135, pp. 1463–1470, 2012.

[36] X. Shi, X. Zhang, S. Song, C. Tan, C. Jia, and S. Xia, "Identification of characteristic flavour precursors from enzymatic hydrolysis-mild thermal oxidation tallow by descriptive sensory analysis and gas chromatography-olfactometry and partial least squares regression," *Journal of Chromatography B-Analytical Technologies in the Biomedical and Life Sciences*, vol. 913-914, pp. 69–76, 2013.

Hindawi
Journal of Food Quality
Volume 2021, Article ID 9975586, 9 pages
https://doi.org/10.1155/2021/9975586

Research Article

Evaluating the Effects of MKAVCFSL Derived from Bighead Carp (*Hypophthalmichthys nobilis*) Flesh on Antioxidant Activity in Caco-2 Cells *In Vitro*

Chi Zhang, Yinxiao Zhang, Shaoqi Xia, Shuya Zhu, He Li, and Xinqi Liu

Beijing Advanced Innovation Center for Food Nutrition and Human Health, Beijing Engineering and Technology Research Center of Food Additives, National Soybean Processing Industry Technology Innovation Center, School of Food and Health, Beijing Technology and Business University, Beijing 100048, China

Correspondence should be addressed to Xinqi Liu; liuxinqi@btbu.edu.cn

Received 31 March 2021; Accepted 23 April 2021; Published 4 May 2021

Academic Editor: Shengbao Cai

The effect of an antioxidative peptide Met-Lys-Ala-Val-Cys-Phe-Ser-Leu (MKAVCFSL) on oxidative stress in Caco-2 cell lines was investigated. Caco-2 cells exposed to excess oxidative stress could be restored when pretreated with the peptide. Reactive oxygen species (ROS) and malondialdehyde (MDA) within the cells could be scavenged by MKAVCFSL. The peptide could also enhance the activity of glutathione peroxidase (GPx), glutathione reductase (GR), and superoxide dismutase (SOD), while catalase (CAT) activity did not show a significant difference between treatment and control samples. Meanwhile, it was observed that peptide treatment increased the concentration of glutathione (GSH). Yet the content of glutathione disulfide (GSSG) was hardly affected. The stability of MKAVCFSL was also assessed and an intact peptide was observed after simulated gastrointestinal digestion. Part of the peptide was hydrolyzed into fragments including MKA, FSL, AVCFSL, and MKAVCF. This study demonstrated that MKAVCFSL derived from bighead carp hydrolysates could ameliorate oxidative stress to protect the Caco-2 cells.

1. Introduction

Oxidative stress is defined as the potential biological damage caused by free radicals [1]; it demonstrates an excessive production of ROS that cannot be counteracted by the action of antioxidative protection systems of the cells. The imbalance between the oxidant species such as hydrogen peroxide (H_2O_2), superoxide (O_2–•), singlet oxygen (1/2 O_2), and the hydroxyl radical (•OH) was mainly produced from the mitochondrion. The oxidant species may trigger specific factors responsible for oxidative damage in the cells including cellular proteins, membrane lipids, nucleic acids, and eventually cell death. This damage has a correlation with several pathologies like cardiovascular, cancer, diabetes, and inflammatory diseases [2].

All cells possess elaborate antioxidant systems constitutive of interacting various weight components. Among them, SOD, GPx, and CAT play a significant role in scavenging ROS. Increased oxidative stress associated with the disease is often related to a depletion in enzymatic and nonenzymatic antioxidants [3], which reduced the ability to protect against excess ROS exposure. Therefore, extra antioxidants are supposed to be utilized as direct scavengers of free radicals, as inhibitors of lipid peroxidation, and so on [4]. Therefore, researchers' interest in the identification, characterization, and application of antioxidants has increased to protect organisms from oxidative stress. Natural sources have been specifically considered because they appear to be safer for consumers than synthetic antioxidants, such as butylated hydroxytoluene (BHT), which have shown to be carcinogenic [5]. Food-derived antioxidant peptides have been purified from many protein hydrolysates such as sardinelle (*Sardinella aurita*) [6], chickpea (*Cicer arietinum* L.) protein [7], blue mussel (*Mytilus edulis*) protein [8], and

barley glutelin [9]. Yet, antioxidant peptide identified from freshwater fish was limited.

In our previous study, we identified an antioxidant peptide MKAVCFSL from flesh hydrolysate of bighead carp (*Hypophthalmichthys nobilis*), which had effective DPPH radical scavenging activity, ferrous ions (Fe^{2+}) chelating activity, and reducing power [10]. However, there is a lack of research on the evaluation of antioxidant activity at the cellular level. In this study, the protective role of this antioxidant peptide against H_2O_2-induced oxidative stress was further evaluated in Caco-2 cell lines since the intestinal epithelium is the interface between the organism and its luminal environment, which is prone to suffer oxidative stress [11]. Contents of cellular ROS and MDA were assessed to study the antioxidant capacity at the cellular level. The enzyme activities, including SOD, GPx, GR, and CAT, and cellular antioxidant GSH were investigated to evaluate whether this peptide also initiated the cellular antioxidant system to protect Caco-2 cells against H_2O_2-mediated cell death. Besides, simulated gastrointestinal digestion was performed to evaluate the stability of the peptide before *in vivo* experiments.

2. Materials and Methods

2.1. Materials. Caco-2 cells were purchased from American Type Culture Collection (ATCC, Manassas, VA, USA). Dulbecco's modified Eagle's medium (DMEM) was the product of Hyclone (Logan, UT). Fetal bovine serum (FBS) was purchased from Gibco (New York, NY, USA). The flasks for growing cells were acquired from Corning Costar (New York, NY, USA). MKAVCFSL was synthesized by Jietai Synpeptide Co., Ltd. (Shanghai, China). H_2O_2 and all other chemicals were purchased from China National Medicines Corporation Ltd. (Shanghai, China). Bicinchoninic acid (BCA) protein was from Solarbio (Beijing, China). Catalase, SOD, cellular GPx, GR, and GSH/GSSG assay kits were purchased from Beyotime Institute of Biotechnology (Jiangsu, China).

2.2. Simulated Gastrointestinal Digestion. In vitro pepsin-pancreatin-simulated digestion was performed according to the method described by Samaranayaka with slight modifications [12]. The peptide MKAVCFSL (50 μg/mL) was initially dissolved in distilled water, and the pH was adjusted to 2.0 using 5 M HCl. Pepsin was mixed with the peptide in a ratio of 1 : 100 w/w of the substrate, and the mixture was incubated at 37°C for 1 h. After that, the pH was adjusted to 5.3 using saturated $NaHCO_2$ solution and was further augmented to 7.5 with 5 M NaOH. Subsequently, pancreatin (enzyme : substrate ratio, 1 : 50 w/w) was added to the mixture, which was incubated again at the temperature of 37°C for 2 h. Aliquots of the digested samples were collected at 1 h, 2 h, and 3 h. The enzymatic reaction was terminated by immerging the samples in a 95°C water bath for 10 min and cooling the samples to room temperature on ice. The digested samples were used to evaluate the stability utilizing LC-MS/MS analysis.

2.3. Determination of Amino Acid Sequence by LC-MS/MS. After simulated gastrointestinal digestion, the molecular mass and peptide sequencing analysis was performed using a Thermo Q-Exactive high-resolution mass spectrometer (Thermo Scientific, Waltham, MA, USA) in positive ion mode with a capillary temperature of 320°C and a 2 kV spray voltage applied to the emitter. The following electrospray ionization (ESI) conditions were utilized for MS analysis: a high resolution (70,000 FWHM) MS full scan (m/z 300–2000 Da) was performed to select the 10 most intense ions prior to MS/MS analysis using 10 eV energy collisional dissociation.

2.4. Induction of Oxidative Stress. The Caco-2 cells' cultivation was conducted at the concentration of 3.2×10^5 cells/mL in 24-well culture plates for 3 days and the fresh medium was replaced daily. Prior to oxidative induction, Caco-2 cells were incubated with antioxidant peptide for 24 h and then washed twice with phosphate-buffered saline (PBS), pH 7.2. After that, the cells were incubated for 2 h with 1 mM H_2O_2 to induce oxidative stress. The cells were treated as follows: medium treatment without H_2O_2 and peptide (control 1: C1), H_2O_2 treated only (control 2: C2), peptide treated only (sample 1: S1), and medium treatment with H_2O_2 and peptide (sample 2: S2). The cells were then lysed with cell lysis buffer (Beyotime, Jiangsu, China) and centrifuged at 10,000 g and 4°C for 10 min. The supernatant was collected and stored at −80°C until further experiment. The cell lysate protein concentration was measured using the Bicinchoninic Acid (BCA) Protein Assay Kit (Solarbio, Beijing, China).

2.5. Cytotoxicity Assay. Cell Counting Kit-8 (CCK-8) from Solarbio (Beijing, China) was used to measure the cytotoxicity of MKAVCFSL in Caco-2 cells. The peptide was dissolved in DMEM and then diluted in a culture medium and added to the cultures 24 h after cell seeding. Cells were treated as the method of 2.2, after which 10 μL of CCK-8 was added to each well, and the plates were further incubated for 4 h. Thereafter, the absorbance was read using a microplate reader (Bio-Tek, Synergy HT, USA) with 450 nm. The viability of cells was expressed as a percentage of the viability of cells in C1 treatment.

2.6. Determination of Intracellular ROS. The intracellular ROS contents inside the Caco-2 cells were measured according to the instruction of the ROS Assay Kit. Cells were seeded in 96-well plates at a concentration of 2.5×10^5 cells/mL. Cultured cells were treated as the method of 2.4. After incubation, 10 μM DCFH-DA was added to the wells and then incubated at 37°C and 5% CO_2 for 20 min, and cells were then washed with DMEM without FBS for three times. Fluorescence readings were taken at excitation and emission wavelengths of 488 and 525 nm using a Multi-Detection Microplate Reader (Bio-Tek, Synergy HT, USA), respectively. Cellular ROS levels were expressed as fluorescence intensity.

2.7. Measurement of Lipid Peroxidation. The cellular MDA content was evaluated to investigate the level of lipid peroxidation under oxidative stress according to the method of the MDA Assay Kit (Solarbio, Beijing). 100 μL cell lysate supernatant was mixed with 200 μL MDA working solution and heated at 100°C for 30 min. After cooling the mixture to room temperature, samples were centrifuged at 10,000 g for 10 min. The absorbance at 532 nm and 600 nm was measured in a 96-well plate, respectively. The results of the MDA assay were expressed as nanomoles of MDA per milligram of protein.

2.8. Effect of MKAVCFSL on Endogenous Antioxidant Defence Systems in Caco-2 Cells under Oxidative Stress

2.8.1. Measurement of GSH and GSSG Concentration. Cellular GSH and GSSG were evaluated according to the direction of GSH and GSSG Assay Kit. Cell lysate supernatants were obtained by being rapidly freeze-thawed twice with liquid nitrogen and 37°C water baths and then centrifuged at 10,000 g for 10 min at 4°C. 10 μL total GSH and GSSG standards were mixed with 150 μL of 100 mM PBS containing 4 mM EDTA, 0.2 mM NADPH, 0.5 mM DTNB, and 100 units/mL glutathione reductase in a 96-well plate, respectively. Sample supernatants and supernatants which eliminated reduced GSH were mixed with the same PBS as well. The mixture was incubated for 5 min at room temperature and 0.5 mg/mL NADPH was added to each corresponding well. The absorbance was read at 412 nm. The concentration of total glutathione and GSSG in the cell lysate was calculated using a standard curve and GSH concentration was calculated from total glutathione contents deducted GSSG contents.

2.8.2. Glutathione Peroxidase (GPx) Activity. GPx was assessed according to the procedure of the Cellular Glutathione Peroxidase Assay Kit. Briefly, 10 μL cell lysate was mixed with 175 μL 100 mM potassium phosphate buffer (pH 7.0) containing 1 mM EDTA and 11 μL of GR solution which contains 30 mM NADPH, 84 mM GSH, and 1 μL 5 U/μL GR. 4 μL 15 mM H2O2 was added to the solution mixture. The absorbance was monitored at 340 nm every 2 min for 10 min. The activity of GPx within the cell was calculated using a standard curve and expressed as milliunit of GPx per milligram of protein. One unit of activity was expressed as the conversion of 1 mM/min NADPH to NADP+.

2.8.3. Glutathione Reductase (GR) Activity. GR activity was determined using the method described by the Glutathione Reductase Assay Kit. In brief, 20 μL cell lysate was added to 100 mM PBS (0.85 mL, pH 7.5) containing 1 mM EDTA and 2.32 mM GSSG. NADPH (2 mM, 10 μL) was mixed with the solution and the absorbance of 340 nm was read every 1 min for 5 min at 25°C using a Multi-Detection Microplate Reader (Bio-Tek, Synergy HT, USA). Changes in the rate of absorbance were converted into units of GR per milligram of protein using a molar extinction coefficient of 6.22 mM^{-1} cm^{-1}. One unit of activity was defined as the reduction of 1 μmol/min GSSG.

2.8.4. Superoxide Dismutase Assay. SOD activity was investigated utilizing a Total Superoxide Dismutase Assay Kit according to the manufacture's instruction. The water-soluble tetrazolium-8 (WST-8) method, which is more stable and sensitive, is currently used in the determination of SOD activity. Absorbance was determined at 450 nm. Results were expressed as units milligram of protein where protein content was determined by the BCA method. One unit of SOD is defined as the quantity of the enzyme in 20 μL of the sample solution that inhibits the reduction reaction of WST-8 with superoxide anion by 50%.

2.8.5. Catalase Assay. In order to measure the level of catalase in Caco-2 cell lysate, the Catalase Activity Assay Colorimetric Kit was used according to the manufacturer's instructions. Absorbance was measured at 520 nm and results were expressed as units milligram of protein. One unit of catalase is defined as the amount of the enzyme that can catalyze 1 μmol H_2O_2 within 1 minute under the condition of pH7.

2.9. Statistical Analysis. Statistical analysis was performed with SPSS software, version 20 (SPSS Inc., Chicago, IL, USA), using one-way ANOVA followed by Duncan's multiple range test. Differences were considered at a significance level of $p < 0.05$.

3. Results and Discussion

3.1. Evaluating the Stability of MKAVCFSL after Simulated Gastrointestinal Digestion. To investigate the stability of the peptide, LC-MS/MS was performed to identify the variation of MKAVCFSL. According to the RP-HPLC chromatogram in Figure 1, undigested MKAVCFSL was eluted at 33–35 min. After pepsin-pancreatin digestion, several new peaks appeared such as fractions from 28.44 min, 30.13 min, and 37.55 min besides the MKAVCFSL peak. LC-MS/MS confirmed that new fragments MKA, FSL, AVCFSL, MKAVCF were released from MKAVCFSL after simulated gastrointestinal digestion. The majority of the peptide remained stable according to LC-MS/MS, which indicated the peptide had the ability to resist pepsin-pancreatin digestion. These results suggested MKAVCFSL was highly likely to successfully pass through the digestive tract and reach intestine to exert antioxidant activity pepsin-pancreatin.

3.2. Analysis of Effects of MKAVCFSL on Cellular Viability, ROS, and MDA. Our previous study has confirmed that the MKAVCFSL peptide showed effective antioxidant activity such as DPPH scavenging activity, reducing power, and ferrous ions (Fe^{2+}) chelating activity [10]. Therefore, we highlighted if the antioxidant peptide could express good antioxidant activity at the cellular level. In our current study,

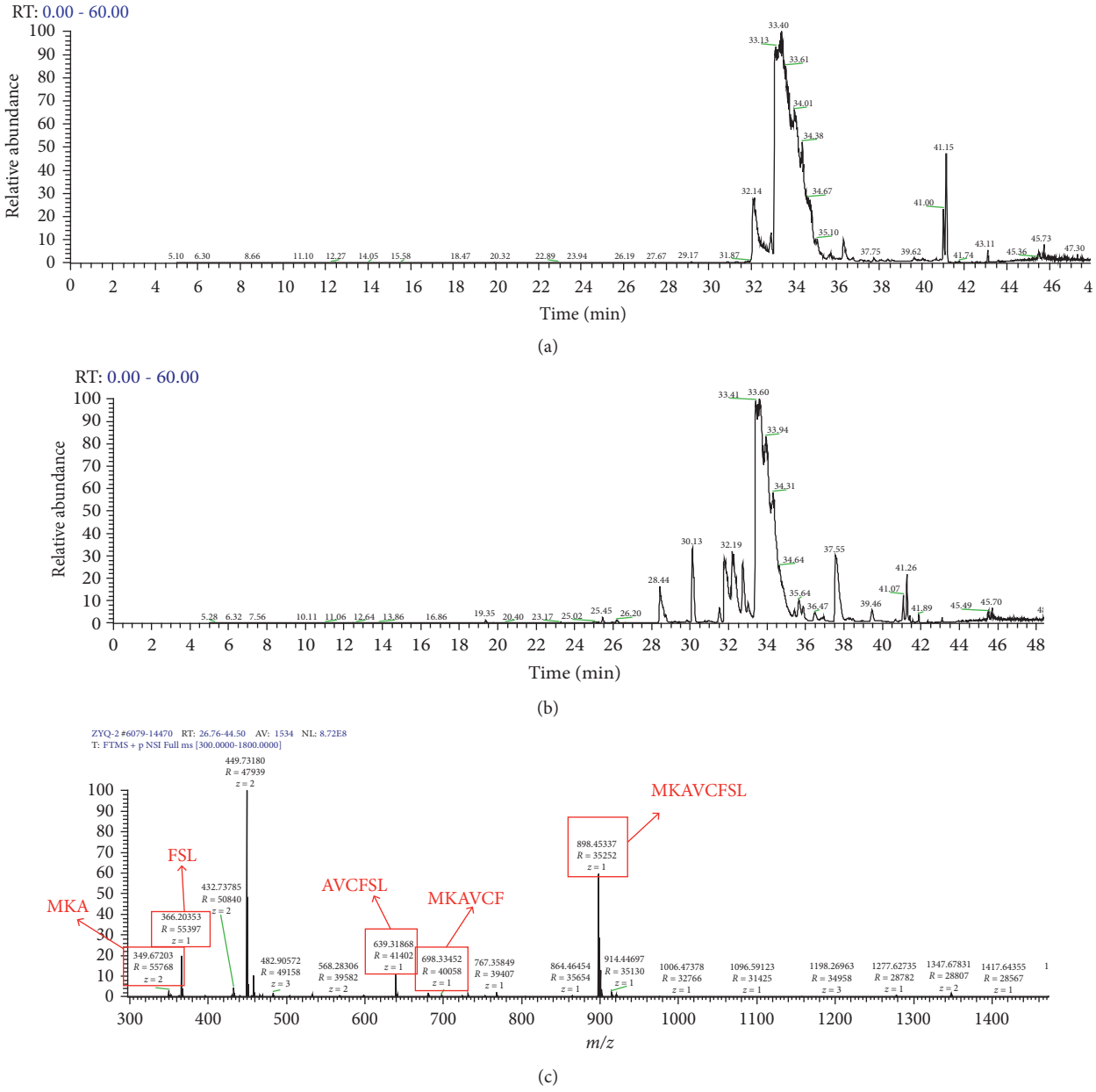

Figure 1: RP-HPLC and LC-MS/MS analysis of MKAVCFSL after simulated gastrointestinal digestion. (a) RP-HPLC chromatogram of undigested MKAVCFSL. (b) RP-HPLC chromatogram of MKAVCFSL after pepsin-pancreatin digestion. (c) LC-MS/MS identification of pepsin-precretin digested peptide.

Caco-2 cells were induced by 1 mM H_2O_2 which was excessive and impaired the cell viability detected by cytotoxicity assay (data not shown). Figure 2 has shown that when cells are treated with H_2O_2, the cell activity was inhibited significantly compared with C1 samples suggesting that the cells' ability to adapt to the addition of H_2O_2 in the media has been conquered. However, cell protection was achieved when cells were pretreated with 50 μg/mL MKAVCFSL (determined by cytotoxicity assay, data not shown) for 24 h since cell viability recovered from $(72.06 \pm 0.68)\%$ to $(89.18 \pm 3.54)\%$. It was interesting that the viability of cells with peptide treated alone could also be improved. Thus, the concentration of ROS and MDA, which were biomarkers of oxidative stress in Caco-2 cells, was measured to investigate whether this phenomenon was associated with the peptide antioxidant activity or not. Figure 3 exhibited that intracellular ROS level expressed as fluorescence intensity has been increased after H_2O_2 treatment. While being pretreated with the peptide, ROS decreased to the untreated level. Meanwhile, peptide alone hardly influenced the ROS concentration, which indicated that the protective effect of the cells after H_2O_2 stimulation was related to antioxidant activity. MDA which was produced from lipid peroxidation could also further confirm the conclusion we have made. When Caco-2 cells were treated with 1 mM H_2O_2 for 2 hours, an almost 3-fold increase in lipid peroxidation

products was observed (from (0.40 ± 0.08) nmol/mg protein to (1.15 ± 0.08) nmol/mg protein) compared with the C1 sample. However, peptide significantly inhibited the formation of MDA to a concentration of (0.77 ± 0.06) nmol/mg protein in stressed cells (S2 sample) when compared with C2 sample. These results were in accordance with those observed with peptides isolated from Hoki fish on human embryonic lung fibroblasts [13] and silver carp peptides in human intestinal epithelial Caco-2 cells [14]. Besides antioxidant peptides, the antioxidant effect of other food compositions was also highlighted such as ascorbic acid, tocopherols, arotenoids, and other varieties of polyphenols and flavonoids [15]. However, the study on food-derived antioxidant peptides that was evaluated at the cellular level was still limited. The results for the protective effect of MKAVCFSL in Caco-2 cells completed the non-cellular antioxidant activity that we reported previously.

3.3. Analysis of Antioxidant Enzymes Activity Pretreated with MKAVCFSL. To investigate if the antioxidant peptide could also affect the internal antioxidant system of Caco-2 cells, various antioxidant enzymes including SOD, CAT, GPx, and GR as well as the endogenous antioxidant GSH were determined. SOD could contribute to converting superoxide to hydrogen peroxide, which is then decomposed by CAT or GPx into H_2O [16]. Deleterious actions of H_2O_2 on Caco-2 cells were observed since SOD activity was inhibited for about 2-folds compared with C1. The reduction in SOD activity is deemed to be caused by an interaction between H_2O_2 and a copper moiety within the SOD molecule. Hydroxyl and copper-bound radicals could be produced during the process, which oxidized histidine residues resulting in the denaturation of the SOD protein [17, 18]. When preincubated with peptide for 24 h, SOD activity showed no significant difference in S2 compared with C2 treatment, which suggested that peptide had the ability to protect the SOD from the H_2O_2 toxicity. It is deduced that the SOD-protecting effects of MKAVCFSL may be due to their possible chelation of surplus copper ions in the SOD complex preventing the metal from reacting with H_2O_2. H_2O_2 stimulation, on the contrary, increased the catalase activities from (0.33 ± 0.06) units $min^{-1} mg^{-1}$ protein to (0.55 ± 0.04) units $min^{-1} mg^{-1}$ protein compared to the untreated baseline cells (Figure 4(b)). Catalase, as a primary defense enzyme against oxidative stress from exogenous, is a porphyrin-containing enzyme which catalyzes the decomposition of hydrogen peroxide to water and oxygen [19]. Therefore, it is reasonable that the activity of catalase increased to scavenging excessive H_2O_2. On the contrary, Shi et al. [20] have reported that CAT activity decreased after treated by 1 mM H_2O_2 because it is a high dose for CAT to completely decompose H_2O_2 into H_2O [21]. The addition of the peptide had no significant effect ($p < 0.05$) on the CAT activity of normal cells and H_2O_2-challenged cells. These results were similar to O'Sullivan et al. [22] and Kim et al. [23].

GPx also plays a critical role in protecting the cells from oxidative stress damage induced by a high concentration of H_2O_2 [21, 24]. GPx utilizes GSH to degrade H_2O_2 into H_2O and converts GSH into GSSG. GR catalyzes the decrease of GSSG to the GSH in its sulfhydryl form. Therefore, GSH can regenerate through the cyclic action between GPx and GR [25]. In normal cells without H_2O_2 stimulation, peptides did not enhance GPx and GR activity significantly (Figure 4). After the addition of MKAVCFSL, the activity of GPx, GR in the cells H_2O_2 treatment were increased with presented in Figures 4(c) and 4(d). This indicated that the peptide could not enhance the GPx and GR activity directly. The protective effect was involved in the removal of oxidative factors that occurred in the cellular metabolic environment. Mammalian GPx1-4 are selenoproteins with selenocysteine (Sec) in the catalytic center, of which GPx2 is mainly expressed in the intestinal epithelium [26]. The presence of Sec as the catalytic moiety of GPx was suggested to guarantee a fast reaction with the hydroperoxide and fast reducibility by GSH [27]. The selenol (-SeH) in SecGPxs reacts in form of a selenolate with H_2O_2 to selenenic acid (-SeOH) which is reduced back to -SeH by two GSH forming GSSG and H_2O [28, 29]. Thus, MKAVCFSL might protect Sec in GPx from being attacked by H_2O_2. GR contains highly conserved domains, one of which can bind reduced nicotinamide adenine dinucleotide phosphate (NADPH) sustaining reduced GSH in cells. The antioxidant activity of MKAVCFSL may decrease the NAPDH converting into $NADP^+$ contributing to the GR activity. Some studies have also verified the impact of oligopeptide and polyphenols on antioxidant enzyme activities in cells. It is demonstrated that the egg-derived peptide elevated GR, GST, and CAT enzymatic activity in human intestinal cells [30]. Other researchers have demonstrated phenolic compounds from olive oil significantly enhanced GR and GP activities in macrophages and verified that the impact of flavonoids on antioxidant protein expression was gene-specific in Caco-2 cells [31, 32].

3.4. Analysis of Cellular Antioxidants GSH. GSH is a tripeptide consisting of glutamine, cysteine, and glycine and is a key component in the nonenzymatic antioxidant mechanism of cells [33]. The present study has found that GSH level was significantly decreased in the cells treated with 1 mM H_2O_2 only (Figure 5) compared to untreated cells. However, pretreatment of peptide supplementation for 24 h before the addition of H_2O_2 restored GSH levels significantly. Meanwhile, MKAVCFSL alone could also elevate the GSH concentration in the cells. While GSSG, the oxidized state of glutathione, was not significantly influenced by the peptide without H_2O_2 stimulation. H_2O_2 alone augmented the concentration of GSSG from (3.06 ± 0.41) μM to (4.92 ± 0.63) μM compared to the C1 sample. Nevertheless, decreased GSSG concentration was observed in the S2 sample. Increased GSH concentration was unexpectedly in S1 since the activity of GPx and GR was not significantly different from untreated samples (C1). We inferred that the peptides may have a positive effect on GSH synthesis. Increased GSSG in C2 samples was also interesting because GPx and GR activity were both inhibited by excessive H_2O_2.

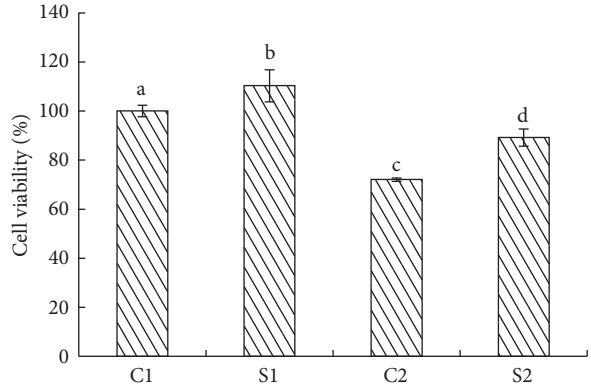

Figure 2: Viability of Caco-2 cells after different treatment as follows: medium treatment without H_2O_2 and peptide (control 1: C1), H_2O_2 treated only (control 2: C2), peptide treated only (sample 1: S1), and medium treatment with H_2O_2 and peptide (sample 2: S2). The viability of cells was expressed as a percentage of the viability of cells in C1 treatment. Results were the means ± SD from three independent experiments. Different small letters indicated significant differences between groups ($p < 0.05$).

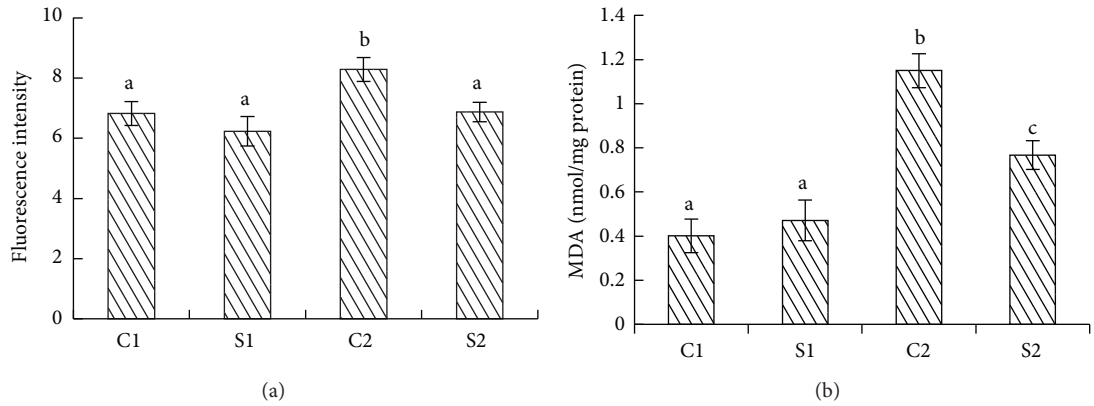

Figure 3: Effects of MKAVCFSL on (a) intracellular ROS level and (b) MDA concentration C1: control 1, medium treatment without H_2O_2 and peptide; S1: sample 1, peptide treated only; C2: control 2, H_2O_2 treated only; S2: sample 2, medium treatment with H_2O_2 and peptide. ROS level was expressed as fluorescence intensity. Results are the means ± SD from three independent experiments. Different small letters indicate significant differences between groups ($p < 0.05$).

It could be speculated that the GPx showed effectively antioxidant activity to dispose oxidant stress initially. Thus, plenty of GSH was converted into GSSH. Besides, the toxicity of H_2O_2 decreased GR activity, which also prohibited the GSSH from reducing back to GSH, thus bringing about the accumulation of GSSH. The decreased GSSH in S2 was in accordance with the restored activity of GR, which could catalyze GSSG to form GSH at high efficiency to promote GSH level in the cells. MKAVCFSL had the potential for normal activity and functionality in the H_2O_2 model system to allow cells to maintain a balanced redox. These results validate the MKAVCFSL could protect the cells from oxidative stress damage.

Generally, MKAVCFSL enhanced GPx activity for subsequent lipid hydroperoxide and ROS induced detoxification using GSH and increased GR activity to regenerate GSH from GSSG. It also contributed to SOD activity without the addition of H_2O_2, but CAT was not influenced. The synergistic actions of cellular antioxidants, antioxidant enzymes, and the peptide efficiently ameliorated the damage of oxidative stress. The protective effect of MKAVCFSL against H_2O_2-induced injury may be due to two reasons correlated to its amino acids composition. On one hand, a peptide having radical scavenging activity can suppress free radical-mediated oxidation [34]. As a previous study earlier, MKAVCFSL contains more aromatic and hydrophobic amino acids and exhibited higher radical scavenging activity, which may be responsible for its protection [20]. In particular, phenylalanine and methionine residues in peptides and proteins were regarded as free radical scavengers *in vivo* [35]. On the other, some studies have exhibited that some peptides can prevent oxidative stress through reducing antioxidant enzyme capacity [30, 34], which concurred with our results. Indeed, the cellular regulation of the antioxidant system is complicated and involves intricate signaling networks which is not fully understood. Besides, different signaling networks enhance the complexity and increase difficulties to understand redox control and related processes. Although the novel peptide was proved to have effective antioxidant activity, it is necessary to conduct a profound investigation on the relationship between oxidative stress and the antioxidant activity *in vivo*.

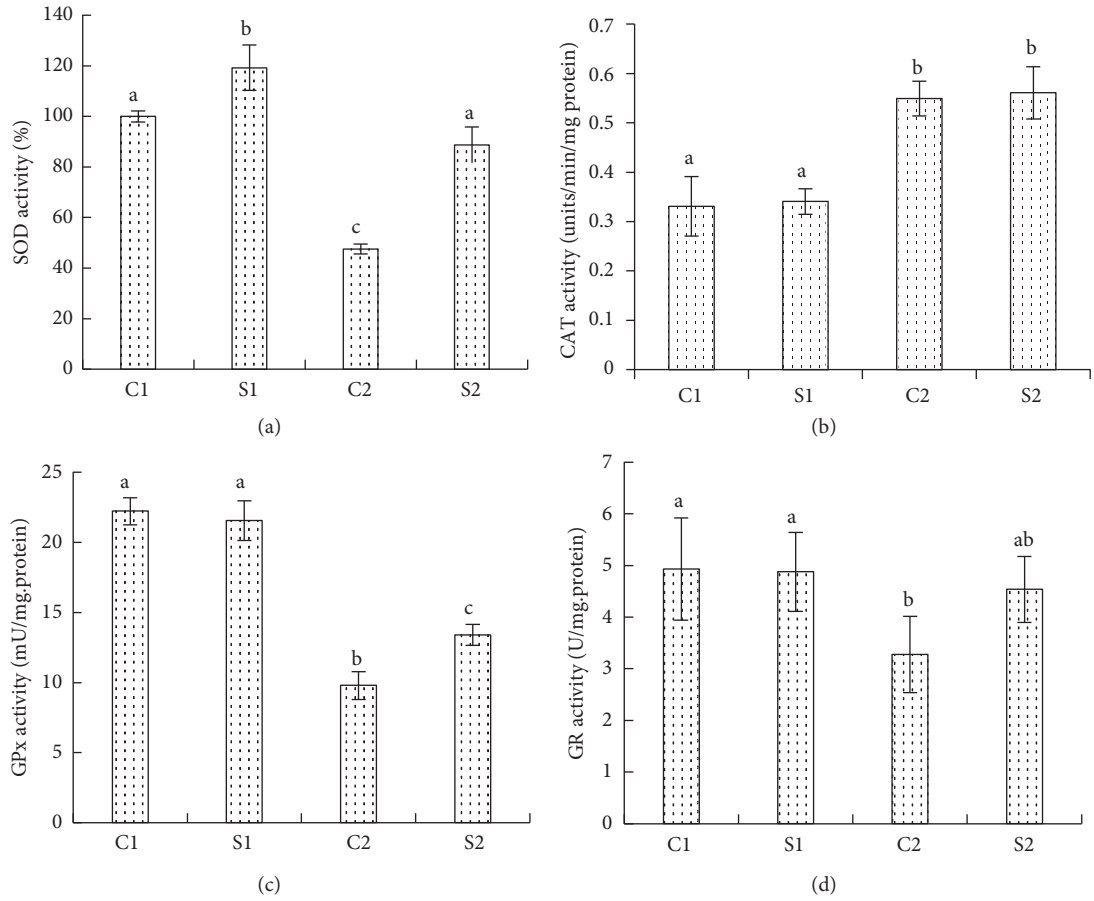

Figure 4: Effects of MKAVCFSL on the cellular antioxidant enzyme. (a) SOD activity, (b) CAT activity, (c) GPx activity, and (d) GR activity. C1: control 1, medium treatment without H_2O_2 and peptide; S1: sample 1, peptide treated only; C2: control 2, H_2O_2 treated only; S2: sample 2, medium treatment with H_2O_2 and peptide. Results are the means ± SD from three independent experiments. Different small letters indicate significant differences between groups ($p < 0.05$).

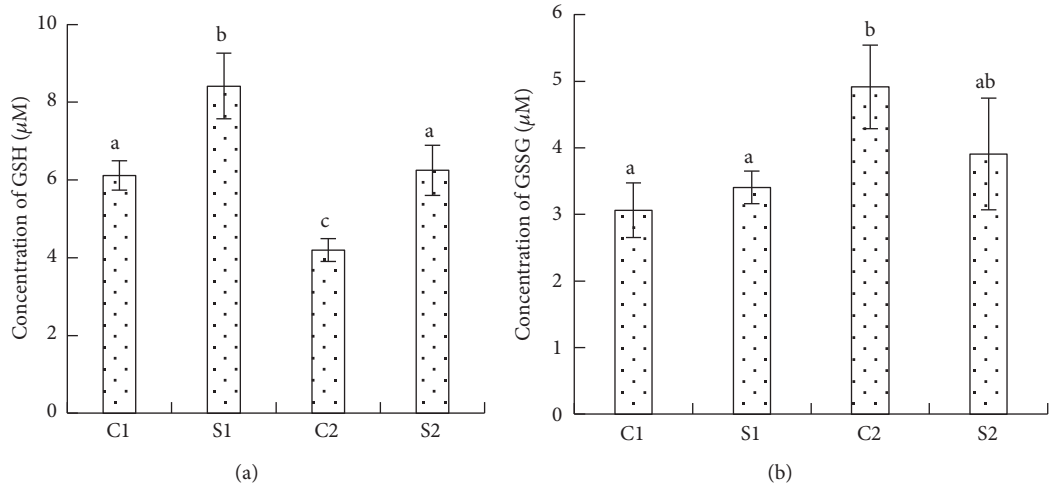

Figure 5: Effects of MKAVCFSL on the cellular GSH and GSSG. (a) GSH concentration. (b) GSSG concentration. C1: control 1, medium treatment without H_2O_2 and peptide; S1: sample 1, peptide treated only; C2: control 2, H_2O_2 treated only; S2: sample 2, medium treatment with H_2O_2 and peptide. Results are the means ± SD from three independent experiments. Different small letters indicate significant differences between groups ($p < 0.05$).

4. Conclusion

This study demonstrated that MKAVCFSL derived from bighead carp protein hydrolysates can remain stable through simulated gastrointestinal digestion, although part of the peptides were degraded into smaller fragments. The peptide could effectively scavenge ROS and MDA within the Caco-2 cells. Meanwhile, after being pretreated with the peptide, upregulation of the activity of several cellular antioxidant enzymes was observed including GPx, GR, and SOD in H_2O_2-induced Caco-2 cells. However, CAT was not influenced significantly. In addition, the concentration of endogenous antioxidant GSH was also increased, led by MKAVCFSL. In summary, this octapeptide displayed protective effects in Caco-2 cells and may be a potential protective agent or food additives against oxidative stress.

Data Availability

The data used to support the findings of this study are included within the article.

Conflicts of Interest

The authors declare that they have no conflicts of interest.

Acknowledgments

This work was supported by the National Key Research and Development Program of China (2019YFC1606200, 2016YFD0400401).

References

[1] P. Kovacic and J. D. Jacintho, "Mechanisms of carcinogenesis focus on oxidative stress and electron transfer," *Current Medicinal Chemistry*, vol. 8, no. 7, pp. 773–796, 2001.

[2] A. M. Pisoschi and A. Pop, "The role of antioxidants in the chemistry of oxidative stress: a review," *European Journal of Medicinal Chemistry*, vol. 97, pp. 55–74, 2015.

[3] I. Dalle-Donne, R. Rossi, R. Colombo, D. Giustarini, and A. Milzani, "Biomarkers of oxidative damage in human disease," *Clinical Chemistry*, vol. 52, no. 4, pp. 601–623, 2006.

[4] Y. Zhang, G. Sun, M. Yang et al., "Chronic accumulation of cadmium and its effects on antioxidant enzymes and malondialdehyde in Oxya chinensis (Orthoptera: Acridoidea)," *Ecotoxicology and Environmental Safety*, vol. 74, no. 5, pp. 1355–1362, 2011.

[5] J. Pokorný, "Are natural antioxidants better - and safer - than synthetic antioxidants?" *European Journal of Lipid Science and Technology*, vol. 109, no. 6, pp. 629–642, 2007.

[6] A. Bougatef, N. Nedjar-Arroume, L. Manni et al., "Purification and identification of novel antioxidant peptides from enzymatic hydrolysates of sardinelle (*Sardinella aurita*) by-products proteins," *Food Chemistry*, vol. 118, no. 3, pp. 559–565, 2010.

[7] T. Zhang, Y. Li, M. Miao, and B. Jiang, "Purification and characterisation of a new antioxidant peptide from chickpea (*Cicer arietium* L.) protein hydrolysates," *Food Chemistry*, vol. 128, no. 1, pp. 28–33, 2011.

[8] B. Wang, L. Li, C.-F. Chi, J.-H. Ma, H.-Y. Luo, and Y.-F. Xu, "Purification and characterisation of a novel antioxidant peptide derived from blue mussel (*Mytilus edulis*) protein hydrolysate," *Food Chemistry*, vol. 138, no. 2-3, pp. 1713–1719, 2013.

[9] Y. Xia, F. Bamdad, M. Gänzle, and L. Chen, "Fractionation and characterization of antioxidant peptides derived from barley glutelin by enzymatic hydrolysis," *Food Chemistry*, vol. 134, no. 3, pp. 1509–1518, 2012.

[10] C. Zhang, Y. Zhang, Z. Wang, S. Chen, and Y. Luo, "Production and identification of antioxidant and angiotensin-converting enzyme inhibition and dipeptidyl peptidase IV inhibitory peptides from bighead carp (*Hypophthalmichthys nobilis*) muscle hydrolysate," *Journal of Functional Foods*, vol. 35, pp. 224–235, 2017.

[11] M. L. Circu and T. Y. Aw, "Intestinal redox biology and oxidative stress," *Seminars in Cell & Developmental Biology*, vol. 23, no. 7, pp. 729–737, 2012.

[12] A. G. P. Samaranayaka, D. D. Kitts, and E. C. Y. Li-Chan, "Antioxidative and angiotensin-I-converting enzyme inhibitory potential of a Pacific Hake (*Merluccius productus*) fish protein hydrolysate subjected to simulated gastrointestinal digestion and Caco-2 Cell permeation," *Journal of Agricultural and Food Chemistry*, vol. 58, no. 3, pp. 1535–1542, 2010.

[13] S.-Y. Kim, J.-Y. Je, and S.-K. Kim, "Purification and characterization of antioxidant peptide from hoki (*Johnius belengerii*) frame protein by gastrointestinal digestion," *The Journal of Nutritional Biochemistry*, vol. 18, no. 1, pp. 31–38, 2007.

[14] Z. Saiyi, M. Changwei, Y. C. Lin, and L. Yongkang, "Antioxidant properties of peptide fractions from silver carp (*Hypophthalmichthys molitrix*) processing by-product protein hydrolysates evaluated by electron spin resonance spectrometry," *Food Chemistry*, vol. 126, pp. 1636–1642, 2011.

[15] M. Serafini, R. Bellocco, A. Wolk, and A. M. Ekström, "Total antioxidant potential of fruit and vegetables and risk of gastric cancer," *Gastroenterology*, vol. 123, no. 4, pp. 985–991, 2002.

[16] T. Finkel and N. J. Holbrook, "Oxidants, oxidative stress and the biology of ageing," *Nature*, vol. 408, no. 6809, pp. 239–247, 2000.

[17] R. C. Bray, S. A. Cockle, E. M. Fielden, P. B. Roberts, G. Rotilio, and L. Calabrese, "Reduction and inactivation of superoxide dismutase by hydrogen peroxide," *Biochemical Journal*, vol. 139, no. 1, pp. 43–48, 1974.

[18] O. I. Aruoma, "Free radicals, oxidative stress, and antioxidants in human health and disease," *Journal of the American Oil Chemists' Society*, vol. 75, no. 2, pp. 199–212, 1998.

[19] E. K. Hodgson and I. Fridovich, "The Interaction of bovine erythrocyte superoxide dismutase with hydrogen peroxide. Inactivation of the enzyme," *Biochemistry*, vol. 14, no. 24, pp. 5294–5299, 1975.

[20] Y. Shi, J. Kovacs-Nolan, B. Jiang, R. Tsao, and Y. Mine, "Antioxidant activity of enzymatic hydrolysates from eggshell membrane proteins and its protective capacity in human intestinal epithelial Caco-2 cells," *Journal of Functional Foods*, vol. 10, pp. 35–45, 2014.

[21] H. Masaki, Y. Okano, and H. Sakurai, "Differential role of catalase and glutathione peroxidase in cultured human fibroblasts under exposure of H 2 O 2 or ultraviolet B light," *Archives of Dermatological Research*, vol. 290, no. 3, pp. 113–118, 1998.

[22] A. M. O'Sullivan, Y. C. O'Callaghan, M. N. O'Grady et al., "*In vitro* and cellular antioxidant activities of seaweed extracts prepared from five brown seaweeds harvested in spring from the west coast of Ireland," *Food Chem*, vol. 126, pp. 1064–1070, 2011.

[23] L. Kim, Y. Kim, O. Kwon, and J. Y. Kim, "Antioxidant activities of ethanolic and acidic ethanolic extracts of astringent persimmon in H_2O_2-stimulated Caco-2 human colonic epithelial cells," *Food Science and Biotechnology*, vol. 26, no. 4, pp. 1085–1091, 2017.

[24] S. S. K. Wijeratne, S. L. Cuppett, and V. Schlegel, "Hydrogen peroxide induced oxidative stress damage and antioxidant enzyme response in Caco-2 human colon cells," *Journal of Agricultural and Food Chemistry*, vol. 53, no. 22, pp. 8768–8774, 2005.

[25] A. Meister, "Glutathione metabolism and its selective modification," *Journal of Biological Chemistry*, vol. 263, no. 33, pp. 17205–17208, 1988.

[26] F. F. Chu, J. H. Doroshow, and R. S. Esworthy, "Expression, characterization, and tissue distribution of a new cellular selenium-dependent glutathione peroxidase, GSHPx-GI," *Journal of Biological Chemistry*, vol. 268, no. 4, pp. 2571–2576, 1993.

[27] L. Flohé and M. Maiorino, "Glutathione peroxidases," *Biochimica et Biophysica Acta*, vol. 1830, pp. 399–404, 2013.

[28] S. Toppo, L. Flohé, F. Ursini, S. Vanin, and M. Maiorino, "Catalytic mechanisms and specificities of glutathione peroxidases: variations of a basic scheme," *Biochimica et Biophysica Acta (BBA)—General Subjects*, vol. 1790, no. 11, pp. 1486–1500, 2009.

[29] L. Flohé, S. Toppo, G. Cozza, and F. Ursini, "A comparison of thiol peroxidase mechanisms," *Antioxidants and Redox Signaling*, vol. 15, no. 3, pp. 763–780, 2011.

[30] S. Katayama, S.-i. Ishikawa, M. Z. Fan, and Y. Mine, "Oligophosphopeptides derived from egg yolk phosvitin upregulate γ-glutamylcysteine synthetase and antioxidant enzymes against oxidative stress in caco-2 cells," *Journal of Agricultural and Food Chemistry*, vol. 55, no. 8, pp. 2829–2835, 2007.

[31] R. Masella, R. Varì, M. D'Archivio et al., "Extra virgin olive oil biophenols inhibit cell-mediated oxidation of LDL by increasing the mRNA transcription of glutathione-related enzymes," *The Journal of Nutrition*, vol. 134, no. 4, pp. 785–791, 2004.

[32] S. Kameoka, P. Leavitt, C. Chang, and S.-M. Kuo, "Expression of antioxidant proteins in human intestinal Caco-2 cells treated with dietary flavonoids," *Cancer Letters*, vol. 146, no. 2, pp. 161–167, 1999.

[33] M. F. Knapen, P. L. Zusterzeel, W. H. Peters, and E. A. Steegers, "Glutathione and glutathione-related enzymes in reproduction," *European Journal of Obstetrics & Gynecology and Reproductive Biology*, vol. 82, no. 2, pp. 171–184, 1999.

[34] E. R. Stadtman and R. L. Levine, "Free radical-mediated oxidation of free amino acids and amino acid residues in proteins," *Amino Acids*, vol. 25, no. 3-4, pp. 207–218, 2003.

[35] Y. Guo, T. Zhang, B. Jiang, M. Miao, and W. Mu, "The effects of an antioxidative pentapeptide derived from chickpea protein hydrolysates on oxidative stress in Caco-2 and HT-29 cell lines," *Journal of Functional Foods*, vol. 7, pp. 719–726, 2014.

Hindawi
Journal of Food Quality
Volume 2021, Article ID 5523356, 9 pages
https://doi.org/10.1155/2021/5523356

Research Article

Influence of Lactic Acid Bacteria Fermentation on Physicochemical Properties and Antioxidant Activity of Chickpea Yam Milk

Xue Zhang,[1,2] Shuai Zhang,[1] Bijun Xie,[1] and Zhida Sun [1]

[1]*College of Food Science and Technology, Huazhong Agricultural University, Wuhan, Hubei 430070, China*
[2]*College of Food Engineering, Henan University of Animal Husbandry and Economy, Zhengzhou, Henan 450011, China*

Correspondence should be addressed to Zhida Sun; sunzhidawh@163.com

Received 28 February 2021; Revised 10 April 2021; Accepted 15 April 2021; Published 27 April 2021

Academic Editor: Shengbao Cai

This study aimed to evaluate the influence of lactic acid bacteria fermentation on the physicochemical properties and antioxidant activity of chickpea yam milk. Four groups of chickpea milk were prepared through fermentation with lactic acid bacteria for quality and functionality improvement. Results indicate that the polysaccharide content of four samples declines during the fermentation process, and their infrared spectrums are similar with a slight difference in the transmittances of some characteristic bands. The sodium dodecyl sulfate-polyacrylamide gel electrophoresis (SDS-PAGE) profiles of four samples with 24 h fermentation showed a band disappearance in the range of 94.3 KDa and generation of many small-molecule peptides, revealing the protein degradation during fermentation. The moderate enzymatic hydrolysis had no adverse effect on the texture and color of the samples. A substantial increase in DPPH, ABTS radical scavenging rates, and FRAP value was observed after 12 h fermentation, especially the CPBY sample. The present results indicate that lactic acid bacteria fermentation can be used to improve the physicochemical properties of samples and enhance their antioxidant activity.

1. Introduction

With increasing concern for health (lactose intolerance and animal milk allergies), environment protection, and sustainability, the interest and demand for plant-based milk are growing [1]. Plant-derived milk is made from legumes, cereals, or edible plant seeds [2, 3]. Applying lactic acid bacteria fermentation to plant-based milk is a subtrend of innovative plant-derived products. This process provides a natural method to increase the safety, nutrition, and shelf life of plant-derived products. The biological activities of plant-based products can be improved by fermentation because microbial proteases promote protein degradation and generate bioactive peptides during fermentation. Researchers demonstrated that lactic acid bacteria possess the ability to hydrolyze proteins [4]. Studies have proven that the concentrations of bioactive components, such as small-size peptides and free amino acids, are improved by fermentation [5]. Thus, the microbial modification of lactic acid bacteria fermented beans is an effective method to increase their antioxidant and/or other biological activities.

In recent years, relevant studies have been conducted on the process optimization and antioxidant properties of plant-based fermented milk. Traditional fermented soybean products have been increasingly recognized to have powerful antioxidant effects. Soymilk fermented with *Lactobacillus paracasei* KUMB B005 has a credible antioxidative potential [6]. The contents of antioxidant compounds in fermented soymilk are closely related to reducing power and antiradical ability. A previous study reported that the antioxidant capacity is highly correlated with proteolytic activity [7]. Glucosidase produced by lactobacilli in the fermentation process can hydrolyze soybean isoflavone from glycoside to aglycone, causing them to exhibit strong biological activity [8]. Fermented soymilk can enrich B group vitamins, promote gut health, and enrich anticancer effect [9].

Chickpea (*Cicer arietinum* L.) is the third most important pulse crop in production, next to dry beans and field peas [10]. Compared with other legumes, chickpea is a good source of protein and carbohydrates, accounting for approximately 80% of the total dry seed mass [11]. Chickpea is also rich in minerals, dietary fiber, and vitamins [12]. The demand for chickpea milk as a good substitute for soymilk is increasing due to its nonallergenic and nutritional value [13, 14]. Yam, a famous food material, has a sweet taste and contains a variety of substances with antioxidant activity, which is good for the spleen. A previous study found that Chinese yam extract induces an improvement in digestive capability and affects the conversion of some intestinal flora to beneficial gut bacteria [15]. Therefore, adding yam to chickpea fermented milk may help to improve the flavor, function, and nutrition of chickpea fermented milk. Previous studies illustrated the effect of fermentation technology on the quality of chickpea milk [14, 16]. However, whether the physicochemical properties and antioxidant activity of chickpea yam milk can be positively influenced by lactic acid bacteria fermentation remains unknown. Therefore, this study aimed to evaluate the influence of lactic acid bacteria fermentation on the physicochemical characteristics and antioxidant activity of chickpea yam milk before and after fermentation. The findings are expected to provide theoretical support for developing new products of yam and chickpea milk.

2. Materials and Methods

2.1. Raw Materials and Chemicals. Untoasted chickpeas (Desi), yam, and sugar were purchased from a local supermarket (Zhengzhou, China). Papain (10^4 U/g) was purchased from Nanning Pangbo Biological Engineering Co., Ltd. (Nanning, China). Cellulase was purchased from Ningxia Heshibi Biotechnology Co., Ltd. (Ningxia, China). *Lacticaseibacillus rhamnosus* CICC 20257 was purchased from the China Center of Industrial Culture Collection (Beijing, China). Chemicals required for the analysis including 2,2′-azinobis-3-ethylbenzthiazoline-6-sulphonate ($ABTS^+$) and 1,1-diphenyl-2-picrylhydrazyl (DPPH) were purchased from Sigma Chemical Co. (St. Louis, USA). All other chemicals used were of analytical grade and obtained from Sinopharm Chemical Reagent Co., Ltd. (Shanghai, China).

2.2. Preparation of Fermented Chickpea Yam Milk. Chinese yam was pulverized into powder on a 200-mesh sieve and was mixed with deionized water (ratio 2 : 7 w/v). The yam milk was heated at 100°C for 2 min to inactivate the enzyme.

Fermented chickpea milk was prepared as follows: whole chickpeas were washed and soaked for 12 h in distilled water. A total of 200 g of swollen chickpeas was ground in 1.6 L water (ratio 1 : 8 w/v). The slurry was cooked at 85°C for 15 min and then filtered with double-layer gauze to separate insoluble residues. The filtrate was transferred into glass bottles and sterilized at 100°C for 15 min. After being cooled to room temperature, chickpea milk was evenly divided into four groups. The first group consisted of chickpea milk and water at a ratio of 8 : 3 without adding enzyme and denoted as CP. The second group was made by mixing chickpea milk and water at a ratio of 8 : 3 with addition of 80 U papain per chickpea protein gram and denoted as CPB. This group was kept at 50°C for 30 min and then boiled to inactivate the enzyme. The third group was prepared by mixing chickpea milk and yam milk at a ratio of 8 : 3 without adding enzyme and marked as CPY. The fourth group was made by mixing chickpea milk and yam milk at a ratio of 8 : 3 with addition of 80 U papain per chickpea protein gram and marked as CPBY. This group was kept at 50°C for 30 min and then boiled to inactivate the enzyme. All samples were added with sucrose (previously sterilized by filtration) with a final concentration of 5% (v/v) and then stored at 4°C.

Lacticaseibacillus rhamnosus CICC 20257 was used as a starter for the production of fermented chickpea milk. The microorganism was propagated (1%, v/v) twice in MRS broth [17] and incubated at 37°C for 24 h without stirring in microaerophilic condition.

Four hundred milliliters of each chickpea milk sample was inoculated with 2% (v/v) (more than 1×10^8 cfu/mL) of an active culture of *Lacticaseibacillus rhamnosus* CICC 20257, and the mixture was allowed to ferment at 37°C for 24 h. The sample was aseptically collected at 0, 3, 6, 9, 12, and 24 h, immediately cooled on ice, and stored at 4°C until analysis.

2.3. Measurements of Polysaccharides from Chickpea Samples before and after Fermentation

2.3.1. Extraction of Polysaccharides. The extraction of polysaccharides was determined in accordance with the previous method [18] with some modifications. Samples (20 mL) of 0, 3, 6, 9, 12, and 24 h were mixed with deionized water at a ratio of 1 : 10. The pH of the mixture was adjusted to 5.0 by adding sodium acetate-acetic acid buffer, and then 1% cellulase was added. Subsequently, polysaccharide was extracted by ultrasonic method (300 W) at 50°C for 30 min. The slurry was filtered through vacuum filtration after the extraction. The filtrate was stirred with medium-speed magnetic for 10 min and then centrifuged at 6,000 g for 10 min to remove the protein. The supernatant was collected and was mixed with 95% ethanol at a ratio of 1 : 3 for 12 h at 4°C until white precipitation appeared. The residue was washed with 85% ethanol twice and dried at 60°C for 2 h after centrifugation. The content of polysaccharides was determined by the phenol-sulfuric acid method.

2.3.2. FTIR Spectra Interpretation. Dry polysaccharide (approximately 2 mg/sample) from fermented samples of 0, 12, and 24 h was mixed with 100 mg of KBr. The spectrum was collected with a Fourier transform infrared spectroscopy (FTIR) spectrometer (iS™10 FTIR Persee, Beijing, China) at 4 cm^{-1} resolution for 32 scans in the range of 4,000–400 cm^{-1}.

2.4. Measurements of SDS-PAGE. In accordance with the modified method [19], sodium dodecyl sulfate-polyacrylamide gel electrophoresis (SDS-PAGE) was conducted to characterize the changes in protein during the fermentation process. The samples (20 μL/sample) collected at 0 and 24 h were mixed with loading buffer (20 μL) at 1 : 1 ratio. The mixture was boiled at 100°C for 5 min to induce protein denaturation, kept in an ice bath for 3 min, and centrifuged at 6,000 g for 5 min. A 10 μL aliquot of each supernatant solution was loaded on a 10% polyacrylamide gel (Bio-Rad Laboratories, Hercules, CA, USA). At a constant voltage of 110 V, the gels were run on a Bio-Rad Mini-Protean system (Bio-Rad) for 3 h. The proteins were then stained with Coomassie Blue R-250 for 30 min and destained for 24 h until the bands were clear. The gels were scanned (Tanon-2500; Bio-Tanon, Shanghai, China) at a resolution of 500 dpi.

2.5. Physical Properties of the Fermented Chickpea Milk

2.5.1. Texture Profile Analysis (TPA). The TPA of each sample was determined by CT3 (Brookfield Engineering Laboratories, Inc., USA). The intermediate layer of each sample was selected for texture analysis. The hardness (g), consistency (g·s), viscosity index (g·s), and cohesion (g) of the samples were measured with a cylindrical TA4/1000 probe under 1 mm/s test speed, 0.5 mm/s pretest speed, 1 mm/s posttest speed, 30% compressed strain, and 5 s compression interval.

The color of each fermented sample for 24 h was determined with a Konica Minolta CR-400 spectrophotometer (Konica Minolta Holdings Inc., Japan). The fermented sample was filled in a glass cuvette, and the CIELAB tristimulus color values of lightness/darkness (L^*), redness/greenness (a^*), and yellowness/blueness (b^*) were measured at 25°C.

2.6. Determination of Antioxidant Capacity

2.6.1. DPPH Radical Scavenging Assay. The fermented samples were analyzed for the scavenging effect on DPPH radical as described by Soison et al. [20] with minor modification. Each sample (1 mL) of 0, 3, 6, 9, 12, and 24 h was mixed with 3 mL of 0.2 mmol/L DPPH ethanol solution. The absorbance of the reaction mixture was measured at 517 nm after reaction in darkness at room temperature for 30 min. The blank control consisted of 95% ethanol and DPPH ethanol solution. The DPPH free radical scavenging rate (%) of each sample was calculated in accordance with the following equation:

$$\text{DPPH scavenging rate } (\%) = \left[\frac{(A_0 - A_s)}{A_0}\right] \times 100\%, \quad (1)$$

where A_0 is the absorbance of the blank and A_s is the absorbance of the samples.

2.6.2. Determination of Ferric Reducing Antioxidant Power (FRAP). The FRAP antioxidant capacity of fermented samples was determined in accordance with the method of Oyaizu [21] and Marazza [22] with some modifications. An aliquot (2.0 mL) of the fermented sample was mixed with 2.0 mL of pH 6.6 phosphate buffer (0.2 M) and 2.0 mL of 1% potassium ferricyanide. The mixture was incubated at 50°C for 20 min, and then 10% trichloroacetic acid (2.0 mL) was added. The mixture was centrifuged at 6,000 g at 4°C for 10 min. The supernatant was mixed with 0.1% ferric chloride (1.0 mL) and deionized water (5.0 mL). The absorbance was measured at 700 nm after 10 min.

2.6.3. ABTS Radical Scavenging Assay. ABTS radical scavenging activity was determined, as described by Raquel [23] with some modifications. $ABTS^+$ (7 mmol/L) and potassium persulfate (140 mmol/L) were prepared separately. Under the dark condition, 1.76 mL potassium persulfate solution and 100 mL $ABTS^+$ were mixed evenly and reacted overnight. The prepared liquor with 95% ethanol was diluted. The absorbance at 734 nm is 0.700 ± 0.02. Subsequently, 1.0 mL of the sample solution was mixed with 3 mL of ABTS radical solution, and the absorbance was recorded at 734 nm.

2.7. Statistical Analysis. Each experiment was conducted thrice, and results are presented as the mean values ($n = 3$) ± standard deviation (SD). Differences among different groups were analyzed by using analysis of variance and Duncan's multiple range test. Differences were considered significant at $p < 0.05$ level.

3. Results and Discussion

3.1. Polysaccharide Contents of Different Samples during Fermentation. As presented in Figure 1, the polysaccharide contents of samples in the four groups declined gradually from 0 h to 12 h. This phenomenon was because the polysaccharide molecules were hydrolyzed by lactic acid bacteria to provide a carbon source for their proliferation during the fermentation process. Therefore, the polysaccharide content gradually decreased, which was consistent with Hong's report [24].

As shown in Figure 1, the chickpea yam fermented milk without hydrolyzed enzyme in the four samples had higher polysaccharide content than those of enzymatically fermented chickpea yam milk. This condition was due to the enzymatic hydrolysis of polysaccharide molecules, resulting in a decrease in its content. The content of polysaccharides in fermented milk with yam addition was high. This condition was because the total polysaccharide content was increased by polysaccharide contained in yam itself.

3.2. FTIR Analysis. The FTIR spectra of fermented samples at 0, 12, and 24 h are presented in Figure 2. Results showed that the bands at 1019 and 1153 cm^{-1} of four samples fermented for 0 h indicated the O–H absorption peak and the C–O bending vibration, which were the characteristic bands of polysaccharides. Similar results were obtained by Yan [25]. The absorption peak at 1641 cm^{-1} indicated the

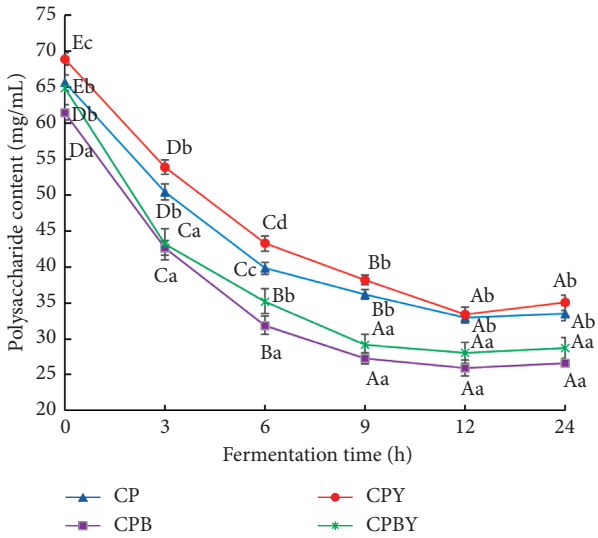

Figure 1: Polysaccharide contents of four samples at different fermentation times. All the values are expressed as mean ± SD ($n = 3$). Means with different uppercase letters indicate significant differences of the same sample at the different fermentation time ($p < 0.05$). Means with different lowercase letters indicate a significant difference of four group samples at the same fermentation time ($p < 0.05$). CP: chickpea fermentation milk; CPB: chickpea fermentation milk with enzyme hydrolysis; CPY: chickpea yam fermentation milk; CPBY: chickpea yam fermentation milk with enzyme hydrolysis.

stretching of carbonyl (C=O) [26]. The weak band at 2902 cm^{-1} was attributed to the stretching vibration of methylene (–CH), and the hydroxyl group was identified by the broad band at 3423 cm^{-1}.

Compared with the samples at 0 h, the four samples fermented for 12 h had the band at 485 cm^{-1}, indicating the deformation vibration of C–C–C. The band at 1019 and 1041 cm^{-1} indicated the stretching vibration of C–O. The former was the ether group (C–O–C) of the pyran ring, whereas the latter was C–O–H [25]. The peaks near 1078 cm^{-1} were ascribed to the ether group, the peak at 1651 cm^{-1} was the carboxyl group, and the band at 2923 cm^{-1} indicated the stretching vibration of saturated C–H. The hydroxyl absorption peak was at 3427 cm^{-1}, and the antioxidant activity of polysaccharides was connected with the number of hydroxyl groups [27].

Compared with the samples at 0 h, the four samples fermented for 24 h contained the peaks at 436 cm the^{-1}, indicating the deformation vibration of C–C–C. The band at 759 cm^{-1} was ascribed to degraded D-glucose of the polysaccharides in four samples during fermentation, which was consistent with Hong's results [24]. The two absorption peaks observed in the spectra at 929 and 1022 cm^{-1} were the C–O stretching vibration, indicating a β-pyranose ring structure. The region around 1154–1079 cm^{-1} can be used to infer the position of the ether groups in polysaccharides [28]. The peak near 1660–1206 cm^{-1} was assigned to the carboxyl group, and the peak at 2924 cm^{-1} was ascribed to the alkyl group. The peak located at 3404 $cm^{-1}$was the O–H stretching vibration in the associated state. However, all the four samples had characteristic bands of polysaccharides, which were β-pyranose ring structures.

As shown in Figure 2, the infrared spectrum characteristics of the four samples CP, CPB, CPY, and CPBY fermented at 0, 12, and 24 h were similar. However, the transmittance of some specific wavelength characteristic bands was different.

3.3. Effect of Fermentation on Protein Subunit Composition. SDS-PAGE (Figure 3) of four samples reflected the effect of fermentation treatment on the composition of chickpea milk protein subunits. 7S protein and 11S protein are the main components of chickpea storage proteins. The 7S protein contained three subunits: α, α', and β. The 11S protein was divided into acidic subunit A and basic subunit B. The 94.3 KDa subunit band of the CPBY sample at 0 h disappeared, and the four groups of samples at 0 h demonstrated an intensification of bands in the range of 20.1–14.3 KDa by comparing Figures 3(a) and 3(b) of the SDS-PAGE profiles of protein. The SDS-PAGE profiles of the CPB sample treated with papain at 0 h illustrated the lightening of 7Sα' band.

In accordance with Figure 3(b), the SDS-PAGE profiles of four samples fermented for 24 h showed a band disappearance in the range of 94.3 KDa and the lightening of bands in the range of 44.3–94.3. The bands in the range of 29.0–44.3 KDa of the CPB sample fermented for 24 h lightened. The bands in the range of 44.3–94.3 KDa of the CP, CPY, and CPBY fermented for 24 h lightened, and more small-molecule protein peptides were generated. In particular, the SDS-PAGE profiles of four samples showed an intensification of bands in the range of 29.0–20.1 KDa. These proteins were identical to the polypeptide chains A and B of the 11S protein [29]. The extracellular enzymes produced by lactic acid bacteria fermentation had certain hydrolysis power. The result indicated that the 11S protein of chickpea milk was less prone to hydrolysis than the 7S protein.

3.4. Physical Characteristics of the Samples. The physical characteristics of fermented samples were the vital aspect influencing customers' assessment on the quality of fermented chickpea milk. As shown in Table 1, a difference was observed in terms of firmness among the four samples, revealing that CP > CPY > CPB > CPBY. Some previous reports found correlations between the structure of chickpea globulin and the gel structure, where chickpea globulin was relatively compact and had weak flexibility, thereby forming a hard and brittle gel structure [30]. Therefore, the firmness of the CP sample was the highest. The firmness of CPB and CPBY samples after enzymatic hydrolysis and yam milk addition decreased, and the consistency increased. In accordance with the viscosity index, the viscosity of the CP sample was low ($p < 0.05$), and no significant difference was found in the viscosity of CPB, CPY, and CPBY samples ($p > 0.05$). The cohesion of the four samples was not significantly different ($p > 0.05$). The addition of yam milk and protease promoted the proliferation of lactic acid bacteria in

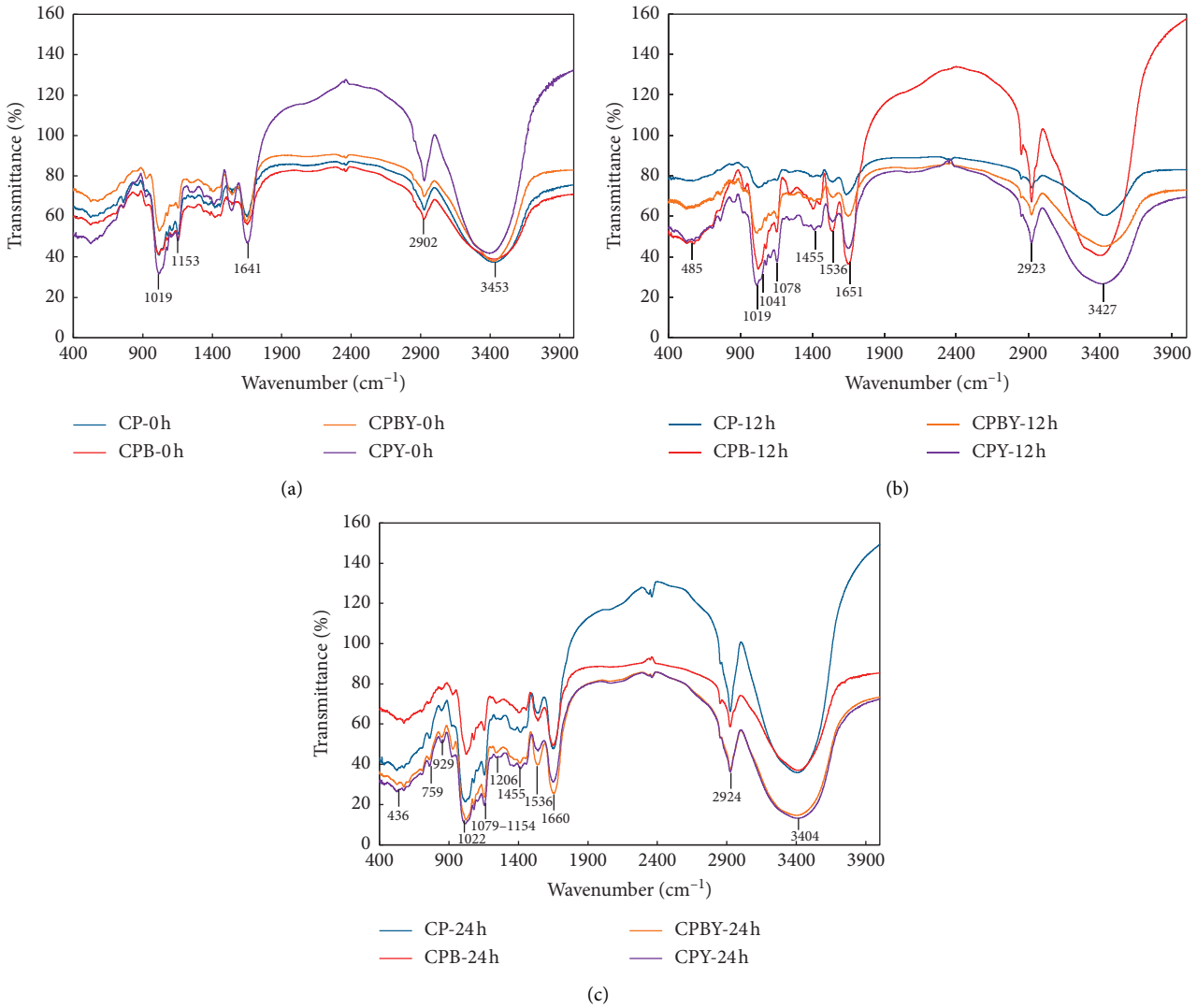

Figure 2: FTIR spectrum analysis of polysaccharides of four samples at 0 h (a), 12 h (b), and 24 h (c). CP, chickpea fermentation milk; CPB, chickpea fermentation milk with enzyme hydrolysis; CPY, chickpea yam fermentation milk; CPBY, chickpea yam fermentation milk with enzyme hydrolysis.

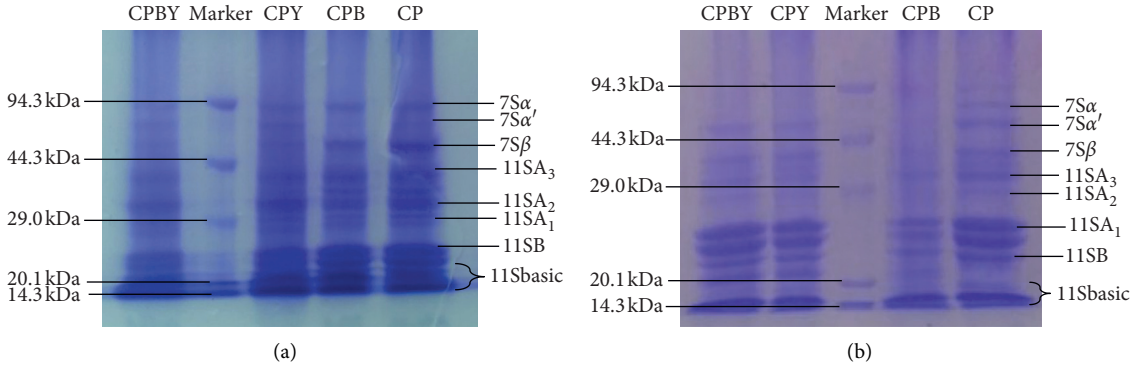

Figure 3: SDS-PAGE diagram of four samples at 0 h (a) and 24 h (b). CP, chickpea fermentation milk; CPB, chickpea fermentation milk with enzyme hydrolysis; CPY, chickpea yam fermentation milk; CPBY, chickpea yam fermentation milk with enzyme hydrolysis.

Table 1: The TPA of four samples of fermented milk.

Samples	Firmness (g)	Consistency (g·s)	Cohesion	Viscosity index (g·s)
CP	28.34 ± 0.06^{c}	425.01 ± 1.89^{a}	0.52 ± 0.05^{a}	19.41 ± 0.47^{a}
CPB	27.13 ± 0.02^{b}	457.32 ± 4.13^{b}	0.53 ± 0.07^{a}	21.6 ± 1.35^{b}
CPY	27.58 ± 0.03^{b}	461.86 ± 2.37^{b}	0.55 ± 0.08^{a}	21.8 ± 0.26^{b}
CPBY	26.67 ± 0.01^{a}	488.49 ± 3.52^{c}	0.56 ± 0.03^{a}	22.35 ± 0.71^{b}

All the values are expressed as mean ± SD ($n = 3$). Different superscript lowercase letters in the same column indicate significant differences ($p < 0.05$). CP, chickpea fermentation milk; CPB, chickpea fermentation milk with enzyme hydrolysis; CPY, chickpea yam fermentation milk; CPBY, chickpea yam fermentation milk with enzyme hydrolysis.

fermented chickpea milk to produce hydrolase for degrading polysaccharides in fermented milk. This condition affected its viscosity [7] and resulted in delicate and smooth fermented chickpea milk.

As an important visual indicator, color plays a key role in influencing consumers' impression on the quality of plant-based fermented milk products. The results in Table 2 revealed that some color variation trends of fermented chickpea milk samples can be concluded after fermentation for 24 h. Among the four samples, the L^* of CPY was the highest (86.90), and the L^* of CP was the lowest (83.05) ($p < 0.05$). The a^* values of CPB and CPBY samples with enzymatic hydrolysis decreased (a^* was −3.26 and −3.23, respectively). This condition represented that the fermented chickpea milk seemed to be brighter and greener after enzymatic hydrolysis. Previous studies on soy yogurt with enzymatic hydrolysis reported similar results [31]. The b^* value of the CPBY sample was the lowest (9.08). However, a small difference was observed in the CPY sample (9.12). A significant difference was observed for yellowness (b^*) between the CPB and CPY samples ($p < 0.05$). On the whole, moderate enzymatic hydrolysis had no adverse effect on the color of the sample, and the L^* of the sample with yam milk addition becomes bright. Hence, enzymatic hydrolysis and yam milk addition can be used for the processing of fermented chickpea milk.

Table 2: The color features of four samples of fermented milk.

Samples	Color characteristic value		
	L^*	a^*	b^*
CP	83.05 ± 0.08^{a}	-2.81 ± 0.05^{a}	10.63 ± 0.12^{b}
CPB	85.36 ± 0.12^{b}	-3.26 ± 0.18^{b}	10.27 ± 0.07^{b}
CPY	86.90 ± 0.26^{c}	-2.72 ± 0.03^{a}	9.12 ± 0.35^{a}
CPBY	86.52 ± 0.53^{c}	-3.23 ± 0.06^{b}	9.08 ± 0.16^{a}

All the values are expressed as mean ± SD ($n = 3$). Different superscript lowercase letters in the same column indicate significant differences ($p < 0.05$). CP, chickpea fermentation milk; CPB, chickpea fermentation milk with enzyme hydrolysis; CPY, chickpea yam fermentation milk; CPBY, chickpea yam fermentation milk with enzyme hydrolysis.

3.5. Analysis of Antioxidant Activity

3.5.1. DPPH Radical Scavenging Rate Analysis. As a classic method for evaluating the free radical scavenging activity, the DPPH radical scavenging has been widely adopted [32]. As shown in Figure 4, in the fermentation progress, The DPPH radical scavenging rate of the four samples increased with the extension of fermentation time, and the increase in DPPH radical scavenging rates decreased after 12 h. As shown in Figure 4, some differences in DPPH were observed after 24 h fermentation among the four samples. A significant increase ($p < 0.05$) in DPPH radical scavenging rates was observed in the CPBY sample with enzymatic hydrolysis and yam milk addition (reaching 73.6%), followed by CPY. The CP sample had the lowest DPPH radical scavenging rate. The results of DPPH radical scavenging activity clearly revealed that enzymatic hydrolysis and yam milk addition facilitated to enhance the antioxidant activity of the CPBY sample. This condition was because the polyphenols and other active ingredients contained in yam were released during the fermentation process. This condition can be helpful to increase the antioxidant capacity of chickpea milk. This finding was consistent with the study of Lee [33].

3.5.2. Analysis of ABTS Free Radical Scavenging Ability. As shown in Figure 5, the change trend of the ABTS radical scavenging rate was similar to that of the DPPH radical scavenging rate. Compared with the counterpart of samples at 0 h, the ABTS radical scavenging rates of all samples gradually increased during 24 h fermentation and reached the highest at 12 h. Among the four samples, the ABTS radical scavenging rate of the CPB sample with enzymatic hydrolysis was higher than that of the CP sample without enzymolysis. This finding indicated that small-molecule peptides may be released in chickpea milk during proteolysis. This condition can be helpful to enhance its antioxidant capability. The CPBY sample with yam milk addition had the highest ABTS radical scavenging rate after 12 h fermentation, reaching 73.89% ($p < 0.05$). It can be speculated that the polysaccharide of yam and protein of chickpea emerged as the polysaccharide-protein conjugate, which contained crevasses, and hydrophobic cavities increased the antioxidant activities [34].

3.5.3. FRAP Antioxidant Capacity Analysis. As shown in Figure 6, a significant increase in FRAP antioxidant capacity of four samples was observed in the chickpea milk during 24 h fermentation ($p < 0.05$). However, the FRAP antioxidant capacity increased slightly after fermentation for 12 h. The order of the FRAP antioxidant capacity of four samples was CPBY > CPY > CPB > CP. The CPBY sample with enzymatic hydrolysis had the highest FRAP antioxidant capacity after 24 h fermentation, reaching 398.86 mmol Trolox/mL.

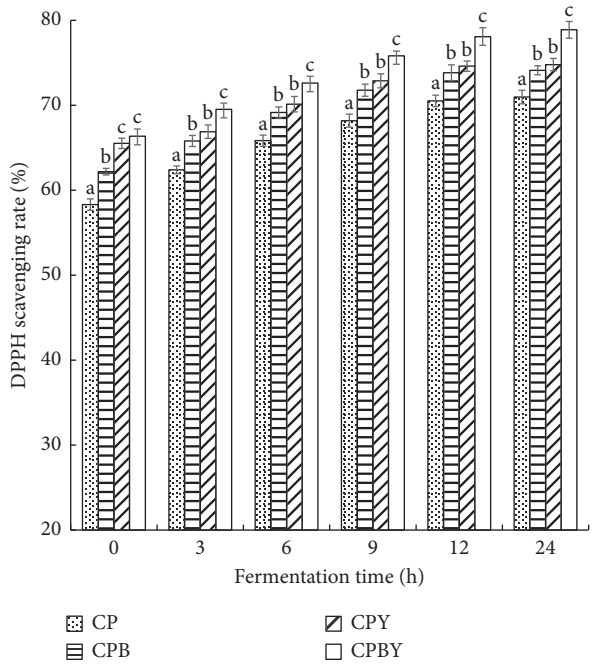

Figure 4: DPPH free radical scavenging rate of four samples at different fermentation times. All the values are expressed as mean ± SD ($n = 3$). Means with different lowercase letters indicate a significant difference of four group samples at the same fermentation time ($p < 0.05$). CP, chickpea fermentation milk; CPB, chickpea fermentation milk with enzyme hydrolysis; CPY, chickpea yam fermentation milk; CPBY, chickpea yam fermentation milk with enzyme hydrolysis.

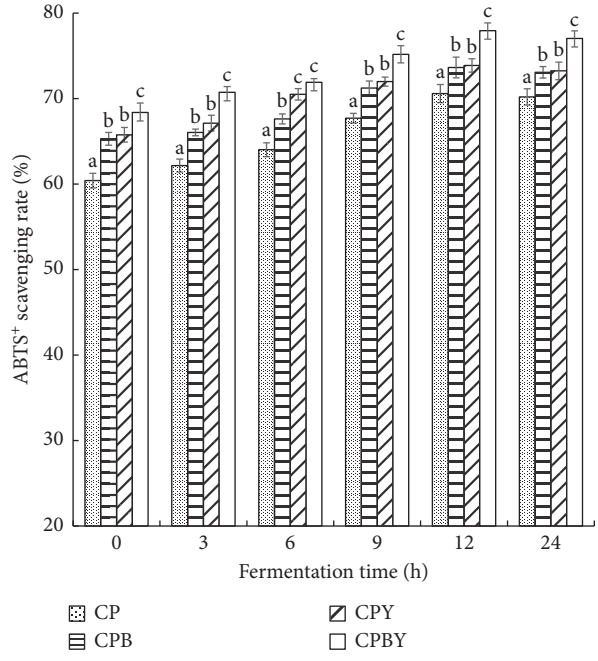

Figure 5: ABTS + free radical scavenging rate of four samples at different fermentation times. All the values are expressed as mean ± SD ($n = 3$). Means with different lowercase letters indicate a significant difference of four group samples at the same fermentation time ($p < 0.05$). CP, chickpea fermentation milk; CPB, chickpea fermentation milk with enzyme hydrolysis; CPY, chickpea yam fermentation milk; CPBY, chickpea yam fermentation milk with enzyme hydrolysis.

We hypothesized that the enhancement of the antioxidant capacity of chickpea fermented milk might be related to the change in bioactive ingredients, such as polysaccharides, or the conversion of bioactive compounds, such as protein, during the fermentation process. As mentioned above, the changes in polypeptide content caused by protease hydrolysis during fermentation lead to the release of antioxidant materials. The research of Sung-Mee Lim et al. [35] showed

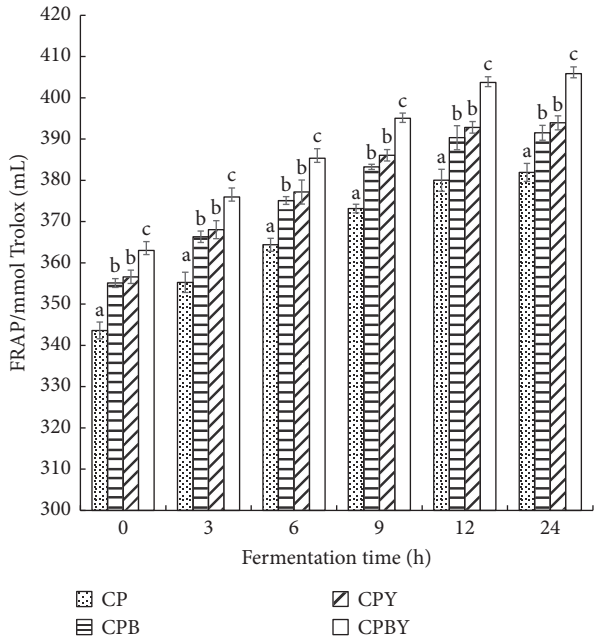

Figure 6: FRAP antioxidant capacity of four samples at different fermentation times. All the values are expressed as mean ± SD ($n = 3$). Means with different lowercase letters indicate a significant difference of four group samples at the same fermentation time ($p < 0.05$). CP, chickpea fermentation milk; CPB, chickpea fermentation milk with enzyme hydrolysis; CPY, chickpea yam fermentation milk; CPBY, chickpea yam fermentation milk with enzyme hydrolysis.

that the proteins and peptides in chickpea milk are positively correlated with free radical scavenging activity. Studies showed that the biologically active peptides released through the fermentation process can increase the antioxidant activity [20]. In this study, the enhancement of antioxidant capacity was related to the changes in biologically active compounds, such as proteins. Moreover, the antioxidant capacity was highly correlated with proteolytic activity. External factors such as enzymatic hydrolysis can hydrolyze proteins and produce some hydrophobic amino acids. The antioxidant capacity depended on peptides, amino acids, and other bioactive substances in chickpea milk, such as polysaccharides and polyphenols. This finding implied that lactic acid bacteria fermentation had obvious effects on the antioxidant bioactivity of chickpea milk. This condition was probably attributed to the alteration of its physicochemical characteristics.

4. Conclusion

In this study, four groups of chickpea milk were prepared through fermentation with lactic acid bacteria for quality and function improvement. The results indicated that the polysaccharide content of four samples declined during the 24 h fermentation process. The infrared spectrums were similar, but the transmittances of some characteristic bands were different. The SDS-PAGE profiles of four samples fermented for 24 h showed a band disappearance in the range of 94.3 KDa and generation of more small-molecule peptides, revealing the protein degradation during fermentation. The moderate enzymatic hydrolysis had no adverse effect on the texture and color of the samples. A significant increase in DPPH, ABTS radical scavenging rate, and FRAP value was observed in the 0–12 h fermentation, especially the CPBY sample, reaching 73.60%, 73.89%, and 398.86 mmol Trolox/mL, respectively. Accordingly, lactic acid bacteria fermentation can be developed to improve the physicochemical properties of chickpea milk and enhance its antioxidant activity.

Data Availability

The data used to support the findings of this study are available from the corresponding author upon request.

Conflicts of Interest

The authors declare that have no conflicts of interest.

Acknowledgments

This work was supported by Henan Provincial Key Scientific and Technological Research Projects of China (212102110343). The authors thank Baoying Wang for supporting FTIR determination and Zhen Zhang for performing SDS-PAGE.

References

[1] S. Sethi, S. K. Tyagi, and R. K. Anurag, "Plant-based milk alternatives an emerging segment of functional beverages: a review," *Journal of Food Science and Technology*, vol. 53, no. 9, pp. 3408–3423, 2016.

[2] C. Cortés, M. J. Esteve, A. Frıgola, and F. Torregrosa, "Quality characteristics of horchata (a Spanish vegetable beverage) treated with pulsed electric fields during shelf-life," *Food Chemistry*, vol. 91, no. 2, pp. 319–325, 2015.

[3] H. Kim, H. Kim, J. Bang, Y. Kim, L. R. Beuchat, and J.-H. Ryu, "Reduction of Bacillus cereus spores in sikhye, a traditional Korean rice beverage, by modified tyndallization processes with and without carbon dioxide injection," *Letters in Applied Microbiology*, vol. 55, no. 3, pp. 218–223, 2012.

[4] J. W. Hou, R. C. Yu, and C. C. Chou, "During fermentation with Bifidobacterial," *Changes in Some Components of Soymilk, Food Research International*, vol. 33, no. 5, pp. 393–397, 2000.

[5] S. Sanjukta and A. K. Rai, "Production of bioactive peptides during soybean fermentation and their potential health benefits," *Trends in Food Science & Technology*, vol. 50, no. 4, pp. 1–10, 2016.

[6] R. V. Usha and B. V. Pradeep, "Antioxidant properties of soy milk fermented with Lactobacillus paracasei KUMBB005," *International Journal of Pharmaceutical Sciences Review and Research*, vol. 30, no. 01, pp. 39–42, 2015.

[7] J. Gou, D. A. Hoang, T. Salmon et al., "Effect of grape juice press fractioning on polysaccharide and oligosaccharide compositions of Pinot meunier and Chardonnay Champagne base wines," *Food Chemistry*, vol. 232, pp. 49–59, 2017.

[8] K.-I. Chen, M.-H. Erh, N.-W. Su, W.-H. Liu, C.-C. Chou, and K.-C. Cheng, "Soyfoods and soybean products: from

traditional use to modern applications," *Applied Microbiology and Biotechnology*, vol. 96, no. 1, pp. 9–22, 2012.

[9] Y.-Y. Zhu, K. Thakur, J.-Y. Feng et al., "B-vitamin enriched fermented soymilk: a novel strategy for soy-based functional foods development," *Trends in Food Science & Technology*, vol. 105, pp. 43–55, 2020.

[10] S. Lev-Yadun, A. Gopher, and S. Abbo, "The cradle of agriculture," *Science*, vol. 288, pp. 1062-1063, 2000.

[11] R. N. Chibbar, P. Ambigaipalan, and R. Hoover, "REVIEW: molecular diversity in pulse seed starch and complex carbohydrates and its role in human nutrition and health," *Cereal Chemistry*, vol. 87, no. 4, pp. 342–352, 2010.

[12] J. A. Wood and M. A. Grusak, "Nutritional value of chickpea," in *Chickpea Breeding and Management*, S. S. Yadav, R. Redden, W. Chen, and B. Sharma, Eds., pp. 101–142, CAB International, Wallingford, UK, 2007.

[13] A. K. Jukanti, P. M. Gaur, C. L. L. Gowda, and R. N. Chibbar, "Nutritional quality and health benefits of chickpea (Cicer arietinumL.): a review," *British Journal of Nutrition*, vol. 108, no. S1, pp. S11–S26, 2012.

[14] S. Wang, V. Chelikani, and L. Serventi, "Evaluation of chickpea as alternative to soy in plant-based beverages, fresh and fermented," *Lwt*, vol. 97, no. 07, pp. 570–572, 2018.

[15] J. R. Jeon, J. S. Lee, C. H. Lee, J. Y. Kim, S. D. Kim, and D. H. Nam, "Effect of ethanol extract of dried Chinese yam (Dioscorea batatas) flour containing dioscin on gastrointestinal function in rat model," *Archives of Pharmacal Research*, vol. 29, no. 5, pp. 348–353, 2006.

[16] R. Luana and E. Rodrigues de Alencar, "Development of novel plant-based milk based on chickpea and coconut," *LWT-food Science and Technology*, vol. 128, pp. 96–106, 2020.

[17] J. C. De Man, M. Rogosa, and M. E. Sharpe, "A medium for the cultivation of lactobacilli," *Journal of Applied Bacteriology*, vol. 23, no. 1, pp. 130–135, 1960.

[18] W. Yang, Y. Wang, X. Li, and P. Yu, "Purification and structural characterization of Chinese yam polysaccharide and its activities," *Carbohydrate Polymers*, vol. 117, no. 6, pp. 1021–1027, 2015.

[19] P. Meinlschmidt, E. Ueberham, J. Lehmann, U. Schweiggert-Weisz, and P. Eisner, "Immunoreactivity, sensory and physicochemical properties of fermented soy protein isolate," *Food Chemistry*, vol. 205, pp. 229–238, 2016.

[20] S. Bisri, J. Kamolwan, J. Anuvat et al., "Physico-functional and antioxidant properties of purple-flesh sweet potato flours as affected by extrusion and drum-drying treatments," *International Journal of Food Science and Technology*, vol. 49, pp. 2067–2075, 2014.

[21] Z. C. olod, "Trifolium species-derived substances and extracts–biological activity and prospects for medicinal applications," *Journal of Ethnopharmacology*, vol. 143, pp. 14–23, 2012.

[22] J. A. Marazza, M. A. Nazareno, G. S. de Giori, and M. S. Garro, "Enhancement of the antioxidant capacity of soymilk by fermentation with *Lactobacillus rhamnosus*," *Journal of Functional Foods*, vol. 4, no. 3, pp. 594–601, 2012.

[23] R. Lucas-González, M. Viuda-Martos, J. A. Pérez Álvarez, J. Fernández-López, and J. Fernández-López, "Changes in bioaccessibility, polyphenol profile and antioxidant potential of flours obtained from persimmon fruit (*Diospyros kaki*) co-products during in vitro gastrointestinal digestion," *Food Chemistry*, vol. 256, no. 8, pp. 252–258, 2018.

[24] Y. R. Hong, *Research on the Physicochemical Property and Biological Activity of Polysaccharides from Longan Pulp Fermentation by Lactic Acid Bacteria*, South China Normal University, Guangzhou, China, 2018.

[25] Y. Yan, X. Li, M. Wan et al., "Effect of extraction methods on property and bioactivity of water-soluble polysaccharides from Amomum villosum," *Carbohydrate Polymers*, vol. 117, pp. 632–635, 2015.

[26] X. Guo, Z. Wang, F. Pi, R. Pan, Z. Zhao, and S. Yu, "Sequential extraction and physicochemical characterization of polysaccharides from chicory (*Cichorium intybus*) root pulp," *Food Hydrocolloids*, vol. 77, pp. 277–285, 2018.

[27] Y. Yuan, C. Li, Q. Zheng et al., "Effect of simulated gastrointestinal digestion on the antioxidant activity, in vitro molecular weight and microstructure of polysaccharides from a tropical sea cucumber (*Holothuria leucospilota*)," *Food Hydrocolloids*, vol. 89, no. 4, pp. 735–741, 2018.

[28] H. Li, X. Wang, Q. Xiong, Y. Yu, and L. Peng, "Sulfated modification, characterization, and potential bioactivities of polysaccharide from the fruiting bodies of Russula virescens," *International Journal of Biological Macromolecules*, vol. 154, pp. 1438–1447, 2020.

[29] F. Vairinhos and D. R. Murray, "Changes in polypeptide composition during seed development in chickpea, cicer arietinum L," *Zeitschrift für Pflanzenphysiologie*, vol. 106, no. 5, pp. 447–452, 1982.

[30] T. Zhang, "Preparation and functional properties of chickpea isolates," PHD Dissertation, Jiangnan University, Wuxi, China, 2005.

[31] Q. Yu, *Study on the Effect of Enzymatic Action on the Quality of Soybean Yogurt*, Master Dissertation, South China University of Technology, Guangzhou, China, 2015.

[32] M. K. Patel, B. Tanna, A. Mishra, and B. Jha, "Physicochemical characterization, antioxidant and anti-proliferative activities of a polysaccharide extracted from psyllium (P. ovata) leaves," *International Journal of Biological Macromolecules*, vol. 118, pp. 976–987, 2018.

[33] J.-G. Lee, "Antioxidant activities and monacolin K production on solid-state fermentation of diverse yam by Aspergillus species strain," *The Korean Journal of Microbiology*, vol. 50, no. 1, pp. 53–59, 2014.

[34] A.-L. Lee, Y.-P. Yu, J.-F. Hsieh, M.-I. Kuo, Y.-S. Ma, and C.-P. Lu, "Effect of germination on composition profiling and antioxidant activity of the polysaccharide-protein conjugate in black soybean [Glycine max (L.) Merr.]," *International Journal of Biological Macromolecules*, vol. 113, pp. 601–606, 2018.

[35] M. L. Sung, "Microbiological, physicochemical and antioxidant properties of plain yogurt and soy yogurt," *Korean Journal of Microbiology*, vol. 49, no. 4, pp. 403–414, 2013.

Hindawi
Journal of Food Quality
Volume 2021, Article ID 5523965, 9 pages
https://doi.org/10.1155/2021/5523965

Research Article

The Effect of Luteolin and Luteoloside on the Secondary Structure of Lysozyme

Yu Wu,[1] Lijian Cui,[2] Lingling Qu,[1] Rong Wang,[1] Ning Chen,[1] Yun Huang,[1] Yan Zhang,[1,3] and Pin Lv[1]

[1]*Hebei Medical University, Shijiazhuang 050017, Hebei, China*
[2]*Experiment Center, Hebei University of Chinese Medicine, Shijiazhuang 050020, Hebei, China*
[3]*Hebei Food Inspection and Research Institute, Hebei Food Safety Key Laboratory, Shijiazhuang 050227, Hebei, China*

Correspondence should be addressed to Yun Huang; 17400921@hebmu.edu.cn, Yan Zhang; snowwinglv@126.com, and Pin Lv; lvpinzy@163.com

Received 20 January 2021; Revised 25 March 2021; Accepted 3 April 2021; Published 23 April 2021

Academic Editor: Biao Yuan

The changes of lysozyme conformation in the absence and presence of luteolin and luteoloside were investigated by spectral analysis including fluorescence, UV, CD, Raman, and ATR-FTIR, and the biological activity of lysozyme was investigated by lysozyme assay kit. The results showed that the microenvironment hydrophobicity of lysozyme increased and peptide extension decreased with the addition of luteolin or luteoloside. The α-helix of lysozyme might be influenced by luteolin or luteoloside, and its relative content had a significant difference after adding luteolin or luteoloside by the ATR-FTIR method, which was reconfirmed by CD and Raman spectra. The lysozyme activity changed obviously after adding luteolin or luteoloside. All of the conclusions above indicated the active site of lysozyme in the α-helix might be influenced by luteolin and luteoloside.

1. Introduction

Lysozyme (LYSO), also called muramidase, killing or inhibiting the bacteria with little drug resistance, is an important immune factor widely existing in many tissues of the human body [1, 2]. It can lyse cell walls of bacteria [3], without degradation to the cells in the human body. As early as 2010, the National Health Commission of P. R. China issued a document allowing lysozyme to be used as a food additive. In addition, lysozyme is clinically available to promote the repair of injured tissues, to correct the degree of immune activation, and to reduce the acute inflammatory reaction, especially in burn wound infection and herpes treatment [4]. Lysozyme has a globular fold divided into two domains, whose native conformation displays four α-helix structures and a three-strand antiparallel β-sheet [5] which consist of 129 amino acid residues, including six Trp residues, three of which (Trp 62, Trp 63, and Trp 108) locate in the active pocket of the helices domain of lysozyme [6]. Therefore, it is very meaningful to research the change of helices domain structure which is closely associated with the activity of lysozyme. Flavonoids exhibit a wide range of physiological activity [7, 8], which have specific nutritional and medicinal values with antioxidant, antiviral, and antibacterial activities, such as luteolin and its glycoside (luteoloside, luteolin-7-O-glucoside) (Figure 1) widely distributed in vegetables, fruits, and some food-medicine herbs including pepper, chrysanthemum indicum, honeysuckle, and perilla, approved by the National Ministry of Health. Although lysozyme, luteolin, or luteoloside has many biological activities with little drug resistance, the biological activity of them used alone is limited. Our previous studies [9] have shown that some flavonoids can form noncovalent complexes with lysozyme, so it is very necessary to explore whether this combination would have any influence on the structure-activity of lysozyme.

The synchronous fluorescence spectrum is used to research the information about the microenvironment in the vicinity of the chromophores, which has several advantages including high sensitivity, simplicity, and reducing the influence of spectral overlap and diffused light [10]. The shift of the maximum emission wavelength can prove the change of

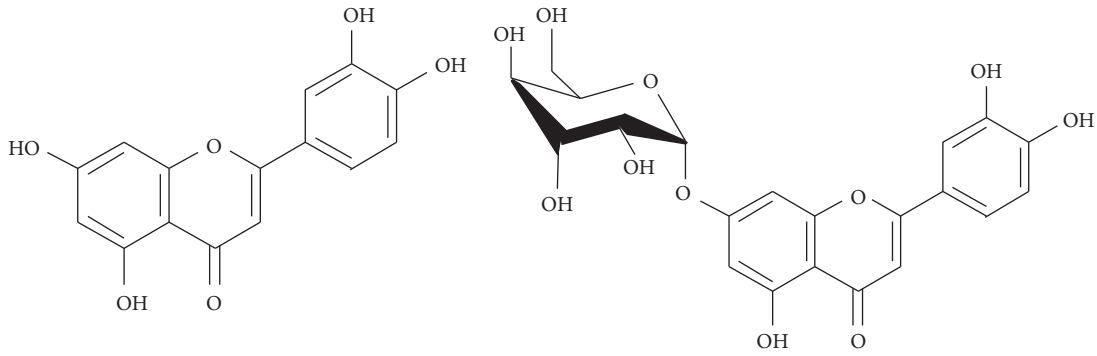

Figure 1: Structures of luteolin (a) and luteoloside (b).

amino residues microenvironment polarity of lysozyme in the absence and presence of luteolin or luteoloside, which is related to the lysozyme conformation [11].

UV absorption spectrum shows the characteristic peaks of the peptide bond, tryptophan residues, and tyrosine residues at about 210 and 280 nm [12].

Circular dichroism (CD) spectrum [13], Raman spectrum [14], and Fourier transform infrared reflection (FTIR) [15, 16] spectrum belong to molecular vibration spectra, which are usually used to investigate the secondary structure change of protein. The different types of secondary structure contained in protein produce the characteristic CD spectra in the far UV [17], primarily from 190 to 230 nm, in which two negative peaks at about 220 nm and 208 nm caused by a negative Cotton effect are the main characteristic peaks of π-$\pi*$ and n-$\pi*$ transitions of peptide bonds in lysozyme α-helix. In Raman and infrared spectra, we primarily focus on the amide I (1700–1600 cm^{-1}) and the amide III (1220–1330 cm^{-1}) bands, which are sensitive to the secondary structure of protein, caused by C=O stretching, C-N stretching, and N-H in-plane bending vibration [18]. Raman spectrum is important to study protein molecular structure, which overcomes water peak interference and weak signal of some chromophores [19]. The ranges of 1650–1660 cm^{-1} and 1260–1300 cm^{-1} are suitable for the analysis of lysozyme α-helix [20], for which the shift and intensities of peaks are sensitive. The change of α-helix structure of lysozyme can be further inferred by combining with FTIR spectra and then speculating the change of its active site.

FTIR with the attenuated total reflection (ATR) attachment can provide the important structures' information of lysozyme solution. The absorption bands observed in the amide I region correspond to α-helix (1642–1660 cm^{-1}), β-sheet (1613–1637 cm^{-1} and 1682–1689 cm^{-1}), β-turn (1662–1700 cm^{-1}), and disordered (1637–1645 cm^{-1}) structures [21]. In cooperation with the information from CD and Raman, comparing the changes of lysozyme secondary structure relative contents in the absence and presence of luteolin and luteoloside by ATR-FTIR can infer the change of lysozyme active site.

The structure of lysozyme is related to the biological activity and its change may influence the lysozyme biological function. There are many methods [22–24] to detect lysozyme activity, including turbidimetry, colorimetry, and agar plate method, among which turbidimetry is the most widely used in the detection with rapidness high reliability, and simple operation. As a classical method, turbidimetry is also popularized by Pharmacopoeia Commission of PRC. To confirm whether the lysozyme activity was influenced by flavonoids, we did the lysozyme activity test with the lysozyme assay kit.

Our previous studies have indicated that when small molecule compounds combined with lysozyme, lysozyme usually increased their biological activities, such as lysozyme enhancing the antibacterial activity of baicalin, baicalein, and scutellarin and increasing the cytotoxicity of caffeine to HepG2 cells. But the influence of the combination on the biological activity of lysozyme is still unclear. This paper focuses on the study of the nonspecific binding of luteolin or luteoloside to lysozyme to evaluating their application from the perspective of lysozyme activity, which might provide important theoretical research for the attempt of combined utilization between lysozyme and luteolin or luteoloside in the field of food and health.

2. Materials and Methods

2.1. Materials and Spectral Equipment. Lysozyme was purchased from China Pharmaceutical Group Chemical Reagent Co., Ltd. Luteolin and luteoloside were from the National Institute for the Control of Pharmaceutical and Bioproducts (China). Lysozyme assay kit (30 T/28S) was bought from the Nanjing Jiancheng Bioengineering Institute.

All spectra were mainly measured on F-380 spectrofluorometer (China), TU-1901 UV-Vis spectrophotometer (Purkinje general, China), MOS-450 spectropolarimeter (Bio-Logic, French), DXR SmartRaman Spectrometer (Thermo, Germany), and FTIR-8400S spectrophotometer (Shimadzu, Japan) with the ATR attachment (PIKE, USA).

2.2. Procedures and Methods. Appropriate amounts of lysozyme were dissolved in Tris-HCl buffer solution to 1.0×10^{-2} mmol/L as lysozyme stock solution. Luteolin or luteoloside solutions were dissolved with 50% methanol-

Tris-HCl buffer solution to 1.0 mmol/L as stock solution. All the stock solutions were diluted to the lower concentrations for actual use with Tris-HCl buffer solution.

2.2.1. Fluorescence Spectrum Analysis. A 2.0 mL solution containing 1.0 μmol/L lysozyme, was titrated by successive additions of 1.0 mmol/L luteolin or luteoloside. The final concentration of luteolin or luteoloside was 6.0 μmol/L at an increment of 1.0 μmol/L.

Fluorescence spectra were recorded in the range of 290–350 nm with an excitation wavelength of 280 nm. The synchronous fluorescence spectra were obtained by scanning the excitation and emission monochromator simultaneously. The wavelength interval was set at 60 nm. Both excitation and emission bandwidths were adjusted at 5 nm.

2.2.2. UV Spectrum Analysis. A 2.0 mL solution, containing 1.0 μmol/L lysozyme, was titrated by successive additions of 1.0 mmol/L luteolin or luteoloside. The final concentration of luteolin or luteoloside was 1.0 μmol/L.

UV spectra of lysozyme, luteolin, luteoloside, luteolin-lysozyme, and luteoloside-lysozyme were recorded in the range of 200–400 nm. The UV differential spectrum of LYSO is obtained by subtracting the spectrum of luteolin or luteoloside solution from that of LYSO in the presence of luteolin or luteoloside.

2.2.3. CD Spectrum Analysis. Mos-450 + SMF-300 spectrometer was used to scan between 185 and 250 nm. The optical length of the sample cell was 1 mm, scan speed 100 nm/min, and resolution 0.1 nm. Each sample was measured three times. The final concentration of lysozyme was 1.0×10^{-2} mmol/L in the presence or absence of 3.0×10^{-1} mmol/L luteolin or luteoloside.

2.2.4. Raman Spectrum Analysis. Raman spectrum of lysozyme solution containing 200 μL lysozyme stock solution (1.0×10^{-2} mmol/L) and 220 μL Tris-HCl buffer solution was recorded in the range of 1200–1800 cm^{-1}. Another solution, containing 400 μL Tris-HCl and 20 μL luteolin or luteoloside stock solution, was used for the determination of flavonoid Raman spectrum. The last solution, containing 200 μL lysozyme stock solution, 200 μL Tris-HCl, and 20 μL luteolin or luteoloside stock solution, was used for the determination of lysozyme-flavonoid Raman spectrum. All the above measurements were carried out at room temperature with 200 scanning times. The interference of the background solvent should be deducted before the sample is determined. Spectra processing procedures were followed: spectra of Tris-HCl buffer solution and lysozyme solution were collected first, and then the spectrum of Tris-HCl buffer solution was subtracted from that of lysozyme solution to obtain the differential spectrum of lysozyme. We used the same technique to obtain the differential spectrum of lysozyme after binding with luteolin (or luteoloside) by lysozyme-luteolin (or luteoloside) minus luteolin (or luteoloside).

2.2.5. ATR-FTIR Spectrum Analysis. FTIR absorption spectra were taken by the ATR-FTIR method with the resolution of 4 cm^{-1} and 30 scans. The solutions used for the determination of the infrared spectrum were prepared in the same way as Raman spectrum analysis. The spectrum was measured without pressure and the IR beam was directly onto the crystal and the internal reflectance created the evanescent wave getting through the sample [25]. Spectra processing procedures were similar to those of Raman spectrum analysis.

The FTIR differential spectra were first to be baseline correction and then were smoothed with the five-point Savitzky–Golay smooth function through the Origin 9.0. The second-derivative spectra were assigned to the different types of lysozyme secondary structures. Fourier self-deconvolution with the secondary derivative was used to estimate the number, position, and width of bands from 1700 to 1600 cm^{-1} in the amide I region [26].

2.2.6. Lysozyme Activity Assay. The lysozyme assay kit was applied to measure the lysozyme activity. The content of the active lysozyme was calculated according to the assay kit instructions. Put 0.2 mL distilled water and 2.0 mL bacterial working solution into the control tube. 0.2 mL 2.5 μg/mL standard lysozyme working solution and 2.0 mL bacteria working solution were added into the standard tube. The sample lysozyme solutions contained 1.0×10^{-2} mmol/L lysozyme with 0, 1×10^{-2}, 2×10^{-2}, 3×10^{-2}, 4×10^{-2}, and 5×10^{-2} mmol/L luteolin or luteoloside. 0.2 mL sample solution and 2.0 mL bacteria working solution were put into the sample tube. The above tubes were placed in 37°C water bath for 15 minutes and then put in the ice water bath for 3 minutes. We transferred them in a cuvette with 1 cm light path and measured the T_{15} values at 530 nm by using the UV-Vis measurement which was adjusted 100% transmittancy with the distilled water and then calculated the contents of active lysozyme by the equation followed.

Active lysozyme = $(UT_{15}–OT_{15}) \times$ lysozyme standard concentration (2.5 μg/mL) $\times$ dilution ratio of sample/$(ST_{15}–OT_{15})$, in which UT_{15} was the transmittancy of sample tube after 15-minute water bath, OT_{15} was that of control group, and ST15 standard tube. The activity of standard lysozyme is regarded as 1.

2.2.7. Data Analysis. The data were processed in SPSS 13.0, which performed the independent-samples t-test to compare the difference. If P values < 0.05, it was considered to have significant differences.

3. Results and Discussion

The spectra of proteins are closely related to the microenvironments of luminescent amino acid residues. When proteins combine with endogenous or exogenous substances, they usually show changes in spectral behaviors. Therefore, spectrometry is commonly used to study the interaction between proteins and small molecules.

3.1. Fluorescence Spectra of Luteolin-Lysozyme System and Luteoloside-lysozyme System. Trp 62 and Trp 108, located at the substrate binding sites, are the main fluorophores in LYSO, whose maximum emission wavelength is closely associated with the microenvironment [27]. The synchronous spectra give the characteristic information of Trp residues when $\Delta\lambda$ was set at 60 nm. The maximum emission wavelength of Trp residues did blue shifts, indicating the microenvironment hydrophobicity increased and the spread of peptide strands decreased [28]. The fluorescence intensities of lysozyme decreased to 396 regularly with the increasing concentration of luteolin (a2 in Figure 2), and 385 with luteoloside (b2 in Figure 2). Meanwhile, from the synchronous fluorescence spectra of LYSO-luteolin (a1 in Figure 2) and LYSO-luteoloside (b1 in Figure 2) when $\Delta\lambda = 60$ nm, luteolin made the emission peak blue-shift 4 nm from 286 nm to 282 nm and luteoloside did 2 nm from 285 to 283 nm. Both luteolin and luteoloside could increase hydrophobicity and decrease the polarity of the microenvironment around Trp, but luteolin had more influence on the microenvironment with a more obvious blue shift than luteoloside did. In addition, the lysozyme activity might be influenced, because the Trp residues located in the active site of lysozyme.

3.2. UV Spectra. The difference of peak intensities and shifts in the UV differential spectra of luteolin (or luteoloside)-LYSO-luteolin (or luteoloside), UV absorption spectrum of LYSO, and those of luteolin (or luteoloside)-LYSO system at about 210 nm and 280 nm suggested the complex formation between luteolin (or luteoloside) and lysozyme.

The addition of luteolin or luteoloside made the absorption peaks of LYSO increase in the luteolin (or luteoloside)-LYSO system (Figure 3), which has two main peaks [29] (208 and 278 nm) in its absorption spectrum, showing that the peak intensity at 208 increased slightly without shift and the peak at 278 nm increased 18% with blue shift 3 nm or 8 nm in the presence of luteolin or luteoloside. Compared with absorption spectra of LYSO, the peak intensity at 208 nm in UV differential spectra decreased 6% or 8% without shift and the peak at 278 nm decreased slightly without shift or decreased 25% with blue shift 2 nm.

3.3. Lysozyme Secondary Structure Change. The active site of lysozyme is mainly in the helices region, so we further focus on studying the change of lysozyme α-helix. The spectroscopic methods have shown that lysozyme conformation changed with the addition of luteolin or luteoloside. The hydroxyl group on the benzene ring of flavonoid might combine with -NH-CO- in lysozyme to change the stretching vibration of C=O, and the hydrogen on the hydroxyl group of benzene ring might form a hydrogen bond with C-N in lysozyme, changing the stretching vibration of C-N, which increased lysozyme microenvironment hydrophobicity and made the peptide chain structure more compact. Those would influence the secondary structure of the enzyme and change the spectra characteristics.

3.3.1. Circular Dichroism Spectra. The two negative peaks near 208 and 222 nm are the main characteristic peaks corresponding to the α-helix structure of protein [17]. The CD spectra of lysozyme in the absence of luteolin or luteoloside (Figure 4) exhibited two negative peaks at 209 and 222 nm, which was the characteristic peaks of pure lysozyme α-helix. Although the two negative peaks were at 212 and 220 nm or 214 and 222 nm (Figure 4(B) and Figure 4(C)), after adding luteolin or luteoloside, the CD spectra of lysozyme in the absence and presence of luteolin or luteoloside were similar in shape, suggesting the structure of lysozyme was also α-helical predominantly. In terms of significant changes in intensity and position, we inferred the lysozyme α-helix was influenced by the luteolin and luteoloside. Besides that, the two negative peaks intensities of lysozyme increased, indicating the increase of α-helix content in lysozyme [30].

The obvious difference in the CD spectra, when luteolin or luteoloside was added into the lysozyme solution, reconfirmed the interaction between lysozyme and luteolin or luteoloside causing the changes in lysozyme α-helix.

3.3.2. Raman Spectra. The three peaks [31] at 1653, 1296, and 1277 cm^{-1} in amide I band and amide III band are the main characteristic peaks of lysozyme α-helix in Raman spectra. A, B, and C in Figure 5 exhibited the intensities and shifts of three characteristic peaks of lysozyme α-helix changed after luteolin or luteoloside added, although the Raman spectra of lysozyme in the absence and presence of luteolin or luteoloside were similar in shape, from which we inferred the lysozyme α-helix was influenced by luteolin or luteoloside.

3.3.3. ATR-FTIR Spectra. According to the above spectra, the lysozyme α-helix structure might be influenced after adding luteolin and luteoloside. To further study the changes of lysozyme α-helix relative content, the ATR-FTIR method was used to confirm the conjectures of CD and Raman spectra.

The absorption bands observed in the amide I region correspond to α-helix (1642–1660 cm^{-1}), β-sheet (1613–1637 cm^{-1} and 1682–1689 cm^{-1}), β-turn (1662–1700 cm^{-1}), and disordered (1637–1645 cm^{-1}) structures [21].

The relative contents of lysozyme secondary structure in the absence and presence of luteolin and luteoloside are shown in Table 1. The correlative differential spectra and Gaussian fitting plots of lysozyme, (luteolin-LYSO)-luteolin, (luteoloside-LYSO)-luteoloside are shown in Figure 6, respectively.

The relative contents of lysozyme secondary structure were changed after adding luteolin and luteoloside. From Table 1, the average relative contents of lysozyme α-helix in the presence of luteolin and luteoloside significantly increased by 43% and 30% with β-sheet decreasing by 19% and 14%, respectively, indicating the interaction between lysozyme and luteolin or luteoloside induced conformational compactness of lysozyme

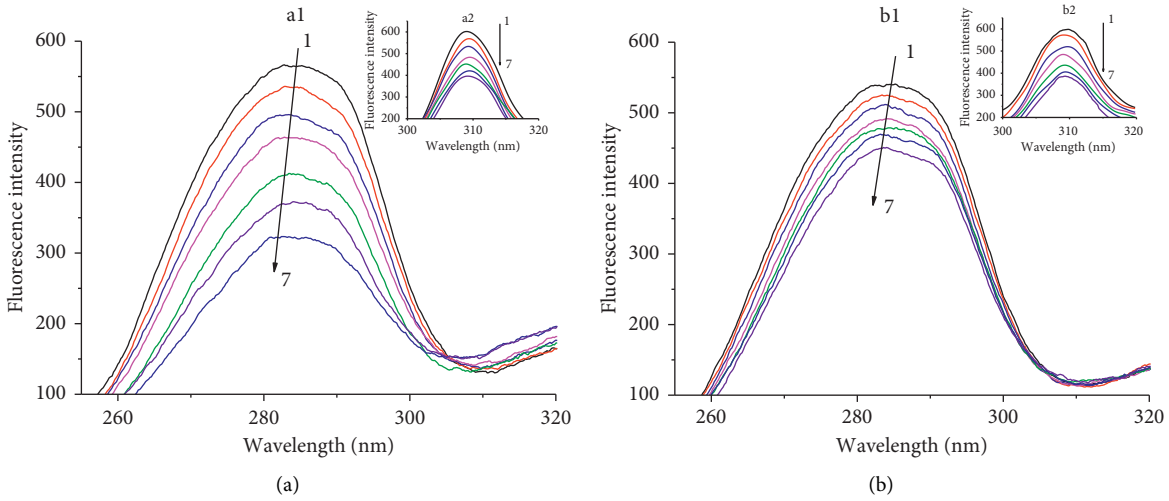

FIGURE 2: Synchronous fluorescence spectra of luteolin-LYSO (a1) and luteoloside-LYSO (b1) and fluorescence quenching spectra of luteolin-LYSO (a2) and luteoloside-LYSO(b2), when $\Delta\lambda = 60$ nm, $T = 298$ K. From curve $1 \longrightarrow 7$, $C_{(\mathrm{LYSO})} = 1.0\,\mu$mol/L, $C_{(\mathrm{luteolin})} = C_{(\mathrm{luteoloside})} = 0$, 1.0, 2.0, 3.0, 4.0, 5.0, and 6.0 μmol/L, respectively.

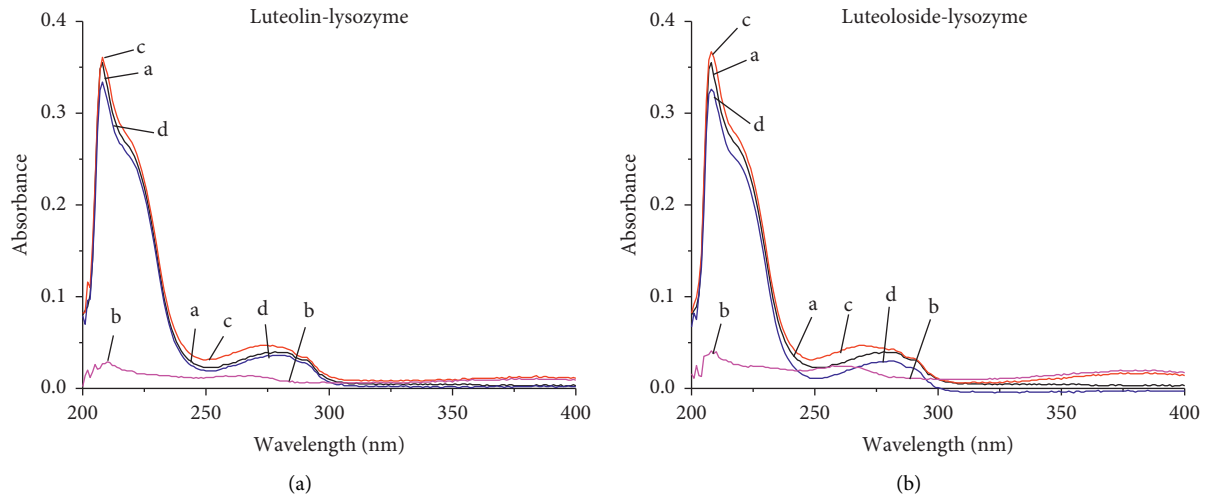

FIGURE 3: The absorption spectra of LYSO, luteolin (or luteoloside), and luteolin (or luteoloside)-LYSO system. (a) LYSO, (b) luteolin (or luteoloside), (c) luteolin (or luteoloside)-LYSO, and (d) luteolin (or luteoloside)-LYSO-luteolin (or luteoloside); $C_{(\mathrm{LYSO})} = C_{(\mathrm{luteolin})} = C_{(\mathrm{luteoloside})} = 1.0\,\mu$mol/L.

peptides to increase hydrophobicity of microenvironment, which were coincident with the conclusions of synchronous fluorescence spectra.

Luteoloside had less effect on the lysozyme helices structure than that of luteolin did; maybe a molecule of glucose on the 7-hydroxyl group of luteoloside impeded the binding of luteoloside to lysozyme, suggesting the lysozyme secondary structure was influenced by the steric hindrance.

There was a significant difference in the lysozyme α-helix relative contents after luteolin or luteoloside was added with P values less than 0.05, which indicated the active site of lysozyme and the biological function of lysozyme might be affected.

3.4. Lysozyme Activity. The change of lysozyme α-helix relative content might cause the change of lysozyme active site, and assay kit was used to evaluate the activities of lysozyme in the absence and presence of luteolin and luteoloside. The lysozyme activity plots (Figure 7) were obtained. The lysozyme activity decreased obviously with the addition of luteolin and luteoloside. The change of lysozyme activity in the presence of luteolin was more obvious than that of luteoloside, suggesting the steric hindrance might also affect the lysozyme activity. The results indicated the changes of lysozyme helices structure were closely related to the changes of the activity.

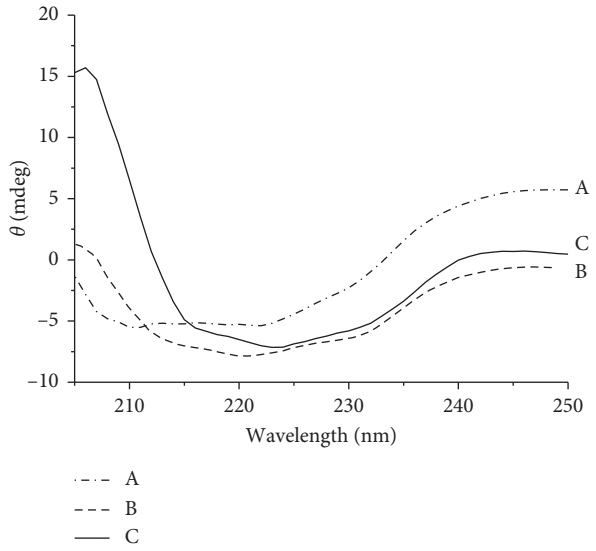

Figure 4: The CD spectra of (A) lysozyme, (B) lysozyme-luteolin, and (C) lysozyme-luteoloside. $C_{(LYSO)} = 1 \times 10^{-2}$ mmol/L, $C_{(luteolin)} = C_{(luteoloside)} = 3 \times 10^{-1}$ mmol/L.

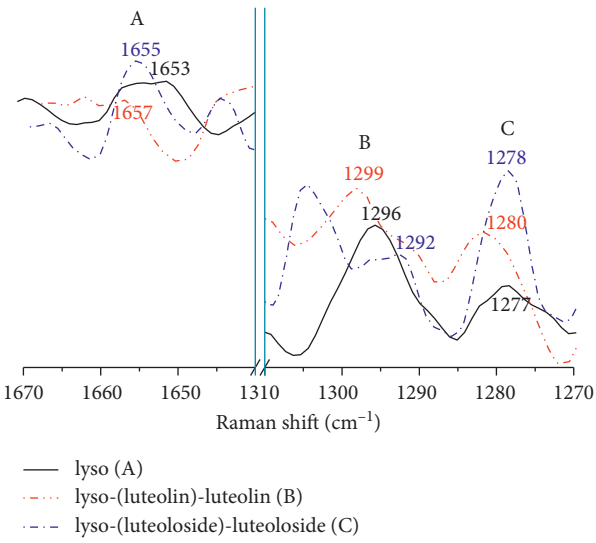

Figure 5: Raman spectra of LYSO (A), (luteolin-LYSO)-luteolin, (B) and (luteoloside-LYSO)-luteoloside (C). $C_{(LYSO)} = 1 \times 10^{-2}$ mmol/L, $C_{(Luteolin)} = C_{(Luteoloside)} = 5 \times 10^{-2}$ mmol/L.

Table 1: The relative contents of lysozyme secondary structure ($n = 3$).

	α-Helix	β-Sheet	Disordered	β-Turn
LYSO	22.63 ± 1.561	32.54 ± 1.056	11.69 ± 1.299	33.13 ± 0.933
(Luteolin-LYSO)-luteolin	32.47 ± 1.726*	26.33 ± 2.718*	11.08 ± 1.500	30.12 ± 1.218*
(Luteoloside-LYSO)-luteoloside	29.33 ± 0.709*	27.80 ± 3.300	9.54 ± 0.228	33.32 ± 3.993

*$P < 0.05$ compared with lysozyme system.

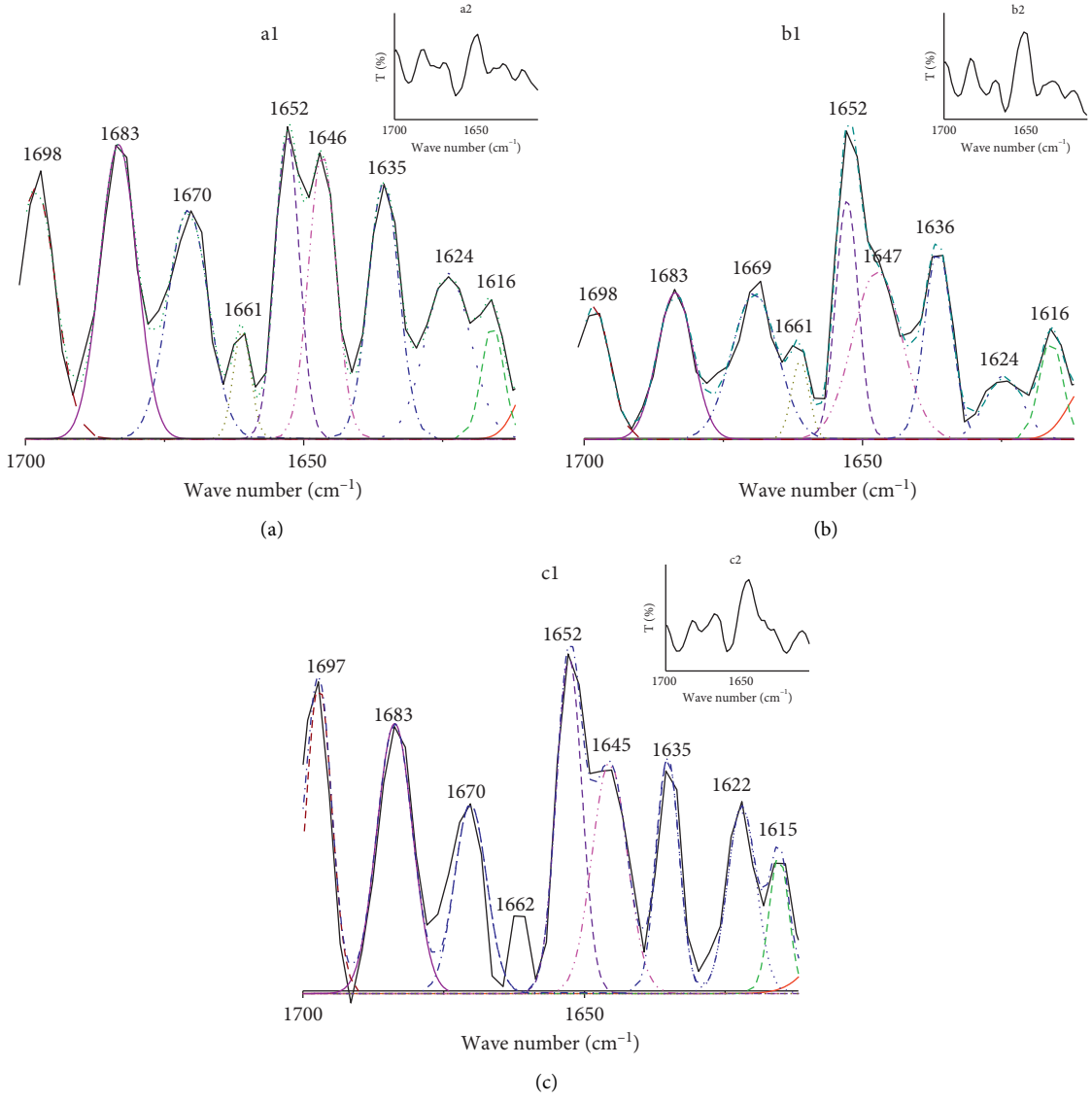

Figure 6: ATR-FTIR curve-fitting spectra of LYSO (a1), (luteolin-LYSO)-luteolin (b1) and (luteoloside-LYSO)-luteoloside (c1), and differential spectra of LYSO (a2), (luteolin-LYSO)-luteolin (b2), and (luteoloside-LYSO)-luteoloside (c2), when $T = 298$K. $C_{(\mathrm{LYSO})} = 1 \times 10^{-2}$ mmol/L, $C_{(\mathrm{luteolin})} = C_{(\mathrm{luteoloside})} = 5 \times 10^{-2}$ mmol/L, respectively.

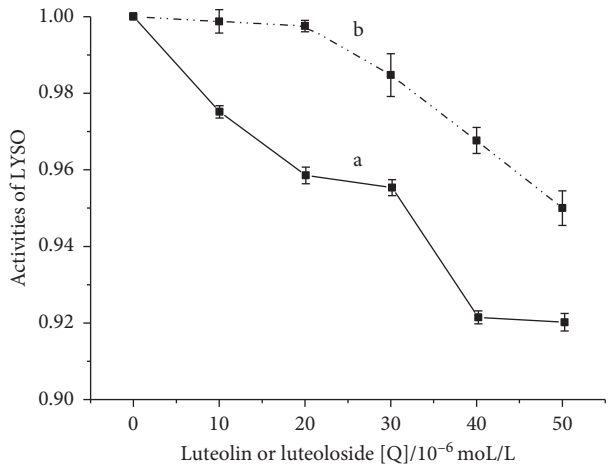

Figure 7: The activities of LYSO at different concentrations of luteolin or luteoloside. (a) luteolin-LYSO and (b) luteoloside-LYSO.

4. Conclusions

Fluorescence and UV spectra analyses proved that luteolin and luteoloside could combine with lysozyme. According to the ATR-FTIR method, the lysozyme α-helix relative content had a significant difference in the absence and presence of luteolin and luteoloside, which confirmed the conjectures of fluorescence spectra, CD spectra, and Raman spectra. Lysozyme activity experiment indicated the activities of lysozyme relating to α-helix structure and the more the α-helix changed, the more the biological activity was affected. The results might provide important theoretical research for the attempt of combined utilization between lysozyme and luteolin or luteoloside in the field of food and health.

Data Availability

The data used to support the findings of this study are included within the article.

Disclosure

Lijian Cui is the co-first author.

Conflicts of Interest

The authors declare that they have no conflicts of interest.

Authors' Contributions

Yu Wu and Lijian Cui contributed equally to this work.

Acknowledgments

This work was supported by the National Key Research Project of China (2019YFC1606400), National Key Research Project of Hebei Province (20375502D), Natural Science Foundation of Hebei Province (H2017206281, H2019206535, H2020206003), High-Level Talent Funding Project of Hebei Province (A201905006), Science and Technology Research Project of Hebei Province (QN2018058), and Fund of National R&D Center for Edible Fungus Processing Technology, Henan University (20200109).

References

[1] T. Wu, Q. Jiang, D. Wu et al., "What is new in lysozyme research and its application in food industry? a review," *Food Chemistry*, vol. 274, pp. 698–709, 2019.

[2] S. A. Hu and A. K. Criss, "From bacterial killing to immune modulation: recent insights into the functions of lysozyme," *PLoS Pathogens*, vol. 13, no. 9, Article ID e1006512, 2017.

[3] Y. Kawai, K. Mickiewicz, and J. Errington, "Lysozyme counteracts β-lactam antibiotics by promoting the emergence of L-form bacteria," *Cell*, vol. 172, no. 5, pp. 1038–1049, 2018.

[4] Y. Yang, Y. Sun, N. Zhang et al., "The up-regulation of two identified wound healing specific proteins-HSP70 and lysozyme in regenerated *Eisenia fetida* through transcriptome analysis," *Journal of Ethnopharmacology*, vol. 237, pp. 64–73, 2019.

[5] R. M. Li, D. T. Ali, R. G. Mohammad, and B. M. Ahmad, "Structural-functional integrity of lysozyme in imidazolium based surface active ionic liquids," *International Journal of Biological Macromolecules*, vol. 156, pp. 271–279, 2020.

[6] S. Das, Z. Hazarika, S. Sarmah et al., "Exploring the interaction of bioactive kaempferol with serum albumin, lysozyme and hemoglobin: a biophysical investigation using multispectroscopic, docking and molecular dynamics simulation studies," *Journal of Photochemistry and Photobiology B: Biology*, vol. 205, Article ID 111825, 2020.

[7] S. Baruah, L. Perez De Souza, M. Benina, and A. R. Fernie, "The style and substance of plant flavonoid decoration; towards defining both structure and function," *Phytochemistry*, vol. 174, Article ID 112347, 2020.

[8] S. Wang, L. Fu, Y. Wu, H. Xiao, J. Wang, and G. Sun, "Influence of luteolin on the apoptosis of esophageal cancer Eca109 cells and its mechanism of action," *Food Science and Human Wellness*, vol. 8, no. 2, pp. 189–194, 2019.

[9] Y. Huang, L.-J. Cui, J.-M. Wang et al., "Comparative studies on interactions of baicalein, baicalin and scutellarin with lysozyme," *European Journal of Medicinal Chemistry*, vol. 46, no. 12, pp. 6039–6045, 2011.

[10] A. Huo, "Analysis of various solid samples by synchronous fluorescence spectroscopy and related methods: a review," *Talanta*, vol. 216, Article ID 120944, 2020.

[11] K. Wang, D.-W. Sun, H. Pu, and Q. Wei, "Principles and applications of spectroscopic techniques for evaluating food protein conformational changes: a review," *Trends in Food Science & Technology*, vol. 67, pp. 0924–2244, 2017.

[12] L. Dimitrova-Paternoga, P. K. A. Jagtap, P.-C. Chen, and J. Hennig, "Integrative structural biology of protein-RNA complexes," *Structure*, vol. 28, no. 1, pp. 6–28, 2020.

[13] S. M. Kelly, T. J. Jess, and N. C. Price, "How to study proteins by circular dichroism," *Biochimica et Biophysica Acta (BBA)-Proteins and Proteomics*, vol. 1751, no. 2, pp. 119–139, 2005.

[14] C. M. Laurent, J. M. Dyke, R. B. Cook, G. Dyke, and R. de Kat, "Spectroscopy on the wing: investigating possible differences in protein secondary structures in feather shafts of birds using Raman spectroscopy," *Journal of Structural Biology*, vol. 211, no. 1, Article ID 107529, 2020.

[15] G. Bellocco, "FTIR, ESI-MS, VT-NMR and SANS study of trehalose thermal stabilization of lysozyme," *International Journal of Biological Macromolecules: Structure, Function and Interactions*, vol. 63, pp. 225–232, 2014.

[16] H. Tiernan, B. Byrne, and S. G. Kazarian, "ATR-FTIR spectroscopy and spectroscopic imaging for the analysis of biopharmaceuticals," *Spectrochimica Acta Part A: Molecular and Biomolecular Spectroscopy*, vol. 241, Article ID 118636, 2020.

[17] D. M. Rogers, S. B. Jasim, N. T. Dyer, F. Auvray, and M. Réfrégiers, "Electronic circular dichroism spectroscopy of proteins," *Chem*, vol. 5, no. 11, pp. 2751–2774, 2019.

[18] M. Hirst, C. Hao, Z. Qing et al., "Protective characterization of low dose sodium nitrite on yak meat myoglobin in a hydroxy radical oxidation environment: Fourier transform Infrared spectroscopy and laser Micro-Raman spectroscopy," *Academic Press*, vol. 116, Article ID 108556, 2019.

[19] Z. Q. Wen, "Raman spectroscopy of protein pharmaceuticals," *Journal of Pharmaceutical Sciences*, vol. 96, no. 11, pp. 2861–2878, 2007.

[20] Z. Ming, N. Yingqun, A. Paul, and D. Gerard, "Application of Raman spectroscopy and chemometric techniques to assess sensory characteristics of young dairy bull beef," *Food Research International*, vol. 107, pp. 27–40, 2018.

[21] L. Sheng, J. Wang, M. Huang, Q. Xu, and M. Ma, "The changes of secondary structures and properties of lysozyme along with the egg storage," *International Journal of Biological Macromolecules*, vol. 92, pp. 600–606, 2016.

[22] B. Mandal, S. Mondal, A. Pan, S. P. Moulik, and S. Ghosh, "Physicochemical study of the interaction of lysozyme with surface active ionic liquid 1-butyl-3-methylimidazolium octylsulfate [BMIM] [OS] in aqueous and buffer media," *Colloids and Surfaces A: Physicochemical and Engineering Aspects*, vol. 484, pp. 0927–7757, 2015.

[23] R. K. Mishra, A. Hayat, G. K. Mishra, G. Catanante, V. Sharma, and J. L. Marty, "A novel colorimetric competitive aptamer assay for lysozyme detection based on superparamagnetic nanobeads," *Talanta*, vol. 165, pp. 436–441, 2016.

[24] S. Yvon, L. Schwebel, L. Belahcen et al., "of thermized donkey milk with lysozyme activity on altered gut barrier in mice exposed to water-avoidance stress," *Journal of Dairy Science*, vol. 102, no. 9, pp. 7697–7706, 2019.

[25] T. G. Haimoud-Lekhal and J. Popp, "Electric field standing wave effects in internal reflection and ATR spectroscopy," *Spectrochimica Acta Part A: Molecular and Biomolecular Spectroscopy*, vol. 191, pp. 165–171, 2018.

[26] G. Güler, M. M. Vorob'ev, V. Vogel, and W. Mäntele, "Proteolytically-induced changes of secondary structural protein conformation of bovine serum albumin monitored by Fourier transform infrared (FT-IR) and UV-circular dichroism spectroscopy," *Spectrochimica Acta Part A: Molecular and Biomolecular Spectroscopy*, vol. 161, pp. 8–18, 2016.

[27] A. Fl, B. Mm, A. Jr et al., "Photo-oxidation of lysozyme triggered by riboflavin is O_2-dependent, occurs via mixed type 1 and type 2 pathways, and results in inactivation, site-specific damage and intra- and inter-molecular crosslinks," *Free Radical Biology and Medicine*, vol. 152, pp. 61–73, 2020.

[28] D. Juretić, Y. Sonavane, N. Ilić et al., "Designed peptide with a flexible central motif from ranatuerins adapts its conformation to bacterial membranes," *Biochimica et Biophysica Acta-Biomembranes*, vol. 1860, no. 12, pp. 2655–2668, 2018.

[29] N. Zoranić, D. D. Mulmi, and M. L. Nakarmi, "Optical transitions in lysozyme mediated zinc oxide nanoparticles probed by deep UV photoluminescence," *Optik*, vol. 202, Article ID 163622, 2020.

[30] J. M. Khan, A. Ahmed, S. Farah et al., "Millimolar concentration of sodium dodecyl sulfate inhibit thermal aggregation in hen egg white lysozyme via increased α-helicity," *Colloids and Surfaces A: Physicochemical and Engineering Aspects*, vol. 572, pp. 167–173, 2019.

[31] X. Hussain, L. Yang, Y. Li, E. C. Cheshari, and X. Li, "The integration of molecular imprinting and surface-enhanced Raman scattering for highly sensitive detection of lysozyme biomarker aided by density functional theory," *Spectrochimica Acta Part A: Molecular and Biomolecular Spectroscopy*, vol. 228, Article ID 117764, 2020.

Hindawi
Journal of Food Quality
Volume 2021, Article ID 5580772, 10 pages
https://doi.org/10.1155/2021/5580772

Research Article

Secoisolariciresinol Diglucoside Regulates Adipose Tissue Metabolic Disorder in Obese Mice Induced by a Western Diet

Shan Dong,[1] **Wenliang Bai**,[1] **Jiaping Chen**,[1] **Li Zhang**,[2] **Wanli Sheng**,[3] **and Ronghu Feng**[1]

[1]*Shenzhen Academy of Metrology and Quality Inspection, National Nutrition Food Testing Center, Shenzhen 518055, China*
[2]*College of Food Science and Engineering, Northwest A&F University, Yangling 712100, China*
[3]*Technical Center of Hohhot Customs District, Huhehaote 010000, China*

Correspondence should be addressed to Shan Dong; 2810558181@qq.com

Received 5 February 2021; Revised 17 March 2021; Accepted 24 March 2021; Published 2 April 2021

Academic Editor: quancai sun

Secoisolariciresinol diglucoside (SDG) is the main component of flax lignans. Current studies have reported a positive effect of SDG on obesity and metabolic diseases. SDG has strong blood fat- and blood sugar-lowering, anti-inflammatory, and antioxidant effects and prevents heart disease and other chronic diseases. In this study, we explored the effects of SDG on Western diet-induced obesity and lipid metabolic disorder. Supplementing Western diet-induced obese mice with 40 mg kg^1 d^1, SDG for 12 weeks significantly reduced body and tissue weights. Increased adiponectin levels and decreased serum leptin and resistin levels were observed in obese mice orally administered SDG. Proliferation of adipose tissue was observed by hematoxylin and eosin staining, and cell size was quantitatively analyzed. As a result, SDG inhibited the proliferation of adipose tissue. In addition, SDG suppressed the mRNA expression of lipid synthetic genes and upregulated the mRNA expression of lipolytic genes. Overall, these results indicate that SDG inhibits obesity induced by a Western diet and regulates adipose tissue metabolic disorder. These results provide a theoretical basis for further study on the regulation of obesity and lipid metabolic disorder caused by SDG.

1. Introduction

Obesity is a chronic state of excessive accumulation of body fat. A positive correlation has been reported between obesity and metabolic diseases, including diabetes, hypertension, and hyperlipidemia [1]. An imbalance in the amount of energy consumed and expended is the main cause of obesity [2]. When caloric intake exceeds the amount expended, adipocyte hypertrophy and mature hyperplastic adipocytes are produced, resulting in increased fat mass [3]. The diet has gradually shifted to a Western diet high in sugar and fat, which has led to a rapid rise in the incidence of obesity [4]. Therefore, obesity has become a global health problem that cannot be ignored [5].

Obesity is characterized by excessive adipose tissue accumulation, triglyceride accumulation, and prominent adipocyte hypertrophy, resulting in disrupted adipose tissue homeostasis and adipocyte cell death, which are important in lipid metabolic disorder [6]. Lipid metabolic disorder refers to the imbalance between anabolism and catabolism of lipids, which causes the accumulation of lipids in various tissues, thus affecting metabolic balance [7]. Adipose tissue increases in mass and quantity in obesity with a significant variation in its metabolic and immunological profile. This variation leads to lytic death of adipocytes and triggers the release of free fatty acids and several metabolites, thus transforming the immune repertoire into a proinflammatory state. This results in abnormal cytokine secretion, which promotes heterotopic fat accumulation and low-grade inflammation, ultimately exacerbating liver steatosis and insulin resistance [8–10]. In addition, upregulation of several inflammatory genes in immune cells drives the inflammatory response in adipose tissue, leading to insulin resistance and glucose intolerance [11]. Therefore, variations in metabolism and inflammation in adipose tissue destroy physiological homeostasis in tissues and systems by directly impacting the development of obesity and the initiation and

progression of cancer and metabolic syndrome and creating a positive feedback loop between them [12].

Adipokines are biologically active cytokines secreted by adipocytes that play important regulatory roles in insulin resistance, inflammatory response, and glucose and lipid metabolism [13]. Adiponectin is an important adipokine that increases insulin sensitivity, promotes healthy expansion of adipose tissue, and improves ectopic fat deposition [14]. Studies have shown that human and rodent serum levels of adiponectin decrease in insulin resistance and type 2 diabetes or obesity, and that increased levels of adiponectin inhibit the accumulation of hepatic lipids in obese animals induced by a high-fat diet [15]. Leptin, or antiobesity factor, is an appetite-related adipose factor that affects lipid metabolism by regulating food intake through the hypothalamus [16, 17]. Leptin receptors are widely expressed in many tissues and the level of circulation is proportional to the amount of fat. It has been reported that leptin reduces fat production and increases triglyceride hydrolysis and fatty acid oxidation [18].

tIn recent years, the antiobesity function of natural products has been gradually explored and studied. Among them, researchers pay more attention on polyphenols, which are derived from natural plants such as fruits and vegetables [19, 20]. Studies showed that polyphenols such as quercetin, curcumin, and resveratrol exerted beneficial effects on lipid and energy metabolism and potential body weight change [21–23]. Quercetin is the most abundant of flavonoids which is found naturally in vegetables, fruits, and tea [24]. Animal studies showed that quercetin can protect mice or rats from high-fat diet-induced body weight gain and adipose tissue accumulation [25, 26]. In another study, quercetin (10 mg/kg of body weight) improved the inflammatory status of visceral adipose tissue by suppressing the expression of TNF-α and enhancing the levels of adiponectin, which indicates the recovery of the functions of the adipose tissue, in obese Zucker rats, a genetically obese rat model [27]. Curcumin is derived from the spice turmeric which is the most bioactive polyphenol. Curcumin exerts several biological functions including antioxidation, anti-inflammation, and antiangiogenesis in different organs including adipose tissue [28]. Curcumin showed beneficial effects on energy metabolism and body weight reduction. Two weeks of high dietary curcumin supplementation feeding in rats reduced epididymal adipose tissue and increased fatty acid β-oxidation, indicating the increase of energy expenditure after curcumin treatment [29]. Resveratrol is a polyphenolic compound, which showed beneficial effects in preventing the development of many diseases including obesity and diabetes [30–32]. Dietary treatment of rodents with resveratrol protected mice against HFD-induced body weight gain and obesity by increasing energy expenditure which was partly mediated by stimulating intracellular mitochondrial functions in adipose tissue and by the suppression of fatty acid synthesis [33–35].

Secoisolariciresinol diglucoside (SDG) is the main form of flax lignan in flaxseed, which has beneficial effects in diseases, such as diabetes, hypertension, cardiovascular disease, and obesity [36]. The structure of SDG is shown in Figure 1. Studies have shown that SDG reduces liver and serum lipid levels, inhibits excess accumulation of visceral lipids, and improves glucose tolerance, insulin resistance, and liver steatosis in obese mice [37–40]. These reports have demonstrated that SDG effectively improves obesity. However, few reports are available on the SDG mechanism of regulating lipid metabolic disorder. Therefore, in this study, adipose tissue was targeted to explore the regulatory effects of SDG on lipid metabolic disorder in Western diet-induced obese mice, and the related mechanisms were explored.

2. Materials and Methods

2.1. Animal Experiments. Male C57BL/6J mice (age 8 weeks) were purchased from Xian Jiaotong University (Xi 'an, Shaanxi, China) and raised in a standard environment (12 h/12 h light/dark cycle, temperature $25 \pm 2^{\circ}$C, humidity $50 \pm 5\%$), and were given free access to feed and drinking water. All animal experiments followed the Guidelines for the Protection and Use of Experimental Animals (8th Edition) and the Laboratory Animal Management Measures of Northwest A&F University. This animal protocol was approved by the Animal Ethics Committee of Xian Jiaotong University. AIN-93M standard feed used in the experiment (LAD3001M, calorie value 3.6 kcal/g) and the 45% high-fat feed (TP230100, calorie value 4.5 kcal/g) were purchased from Nantong Troffer Feed Technology Co., Ltd. (Nantong, Jiangsu, China). SDG (>95%) was purchased from Chengdu Biopurify Phytochemicals Ltd. (Chengdu, China). Fructose (99%) was purchased from Sigma-Aldrich (St. Louis, MO, USA). The mice were randomly divided into four groups (10/group) and fed a different diet for 12 weeks: control (standard diet, AIN-93M, containing 3.6 kcal/g; Trophic Animal Feed High-Tech Co., Ltd., Nantong, China; drinking purified water), control + SDG (40 mg $kg^{-1}d^{-1}$ SDG, mixed with the AIN-93M diet; drinking purified water), HFFD (45% kcal from fat, TP230100, containing 4.5 kcal/g and 10% fructose in drinking water), and the HFFD + SDG groups (40 mg $kg^{-1}d^{-1}$ SDG, mixed with the TP230100 diet and 10% fructose in drinking water). The feed composition is shown in Tables 1 and 2, respectively.

2.2. Hematoxylin-Eosin Staining. The white adipose tissue was fixed in 4% formalin, paraffin-embedded, and cut into 5-μm thick slices, respectively, in xylene I and II, dewaxed for 10 min, and then run through in gradient ethanol series (100% I and II, 90% I and II, 80%, 70%) and rinsed in double distilled water for 5 min. After rinsing with PBS (3 times, 5 min each), hematoxylin stain was used for 3 min, and 1% acetic acid differentiation solution was used to separate the color for 15 s. After rinsing with running water, the sections were placed in 1% dilute ammonia for 5–10 s and then dyed with eosin solution for 3 min. They were dehydrated through a gradient ethanol series (70%, 80%, 90%, and 100%) for 1 min each treated with xylene and observed under an optical microscope.

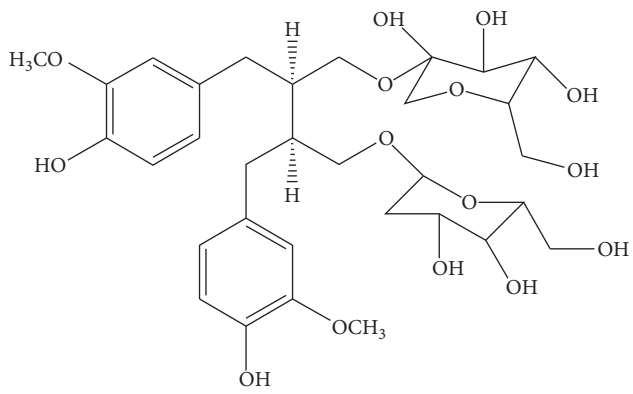

Figure 1: Structure of SDG.

Table 1: Composition of nutrients of standard diet.

Nutrients	Content
Corn starch	465.7
Maltodextrin	155
Sucrose	100
Soybean oil	40
Mineral mix, M1021	35
Casein	140
TBHQ	0.036
Choline chloride	2.5
Cellulose	50
Vitamin mix, V1010	10
L-Cystine	1.8
Total	1000

Table 2: Composition of nutrients of high-fat diet.

Nutrients	Content
Corn starch	132
Maltodextrin	125
Choline bitartrate	3
Sucrose	202
Soybean oil	30
Lard	196
Mineral mix, M1021	61
TBHQ	0.045
Casein	175
Vitamin mix, V1010	12
Cellulose	62
L-Cystine	2
Total	1000

2.3. Serum Adipokines. After the mice were sacrificed, eyeball blood was extracted, plasma was separated, and the plasma levels of adiponectin, leptin, and resistin were detected according to the manufacturer's instructions for the enzyme-linked immunosorbent assay kit.

2.4. Quantitative Real-Time PCR Analysis. Total RNA was extracted from mouse adipose tissue with TRIZOL according to the manufacturer's instructions (TransGen Biotech, Beijing, China) quantified with a nucleic acid quantifier (OD260/280) and diluted to a uniform concentration. The samples were reverse-transcribed to cDNA according to the HiFiScript gDNA Removal RT MasterMix instructions. Reverse transcriptional products were treated according to the manufacturer's method described in the SYBR kit. mRNA expression of the treated samples was detected. The relative expression of genes was calculated with the $2^{-\triangle\triangle Ct}$ method using GAPDH as the internal reference. The primer sequences are shown in Table 3.

2.5. Statistical Analysis. Data are expressed as mean ± standard error. Significant differences between the groups were determined by two-way analysis of variance followed by Tukey's test. The statistical analysis was performed with GraphPad Prism 6 software (GraphPad Software Inc., La Jolla, CA, USA). A p value <0.05 was considered significant.

3. Results and Discussion

3.1. SDG Inhibits Weight Gain in HFFD-Fed Mice. The mice were divided into four groups during the 12-week diet intervention: control (normal diet), HFFD (high-fat and fructose diet), SDG (SDG mixed with the normal diet), and HFFD + SDG (SDG mixed with high-fat and fructose diet) groups. As shown in Figure 2(b), mice in the HFFD group increased their body weight by 9.7% compared to that in the control group ($p < 0.05$), which lasted until week 12 (21.9%, $p < 0.01$). The SDG treatment significantly suppressed weight gain in the obese mice from week 7 (9.3%, $p < 0.05$) to week 12 (13.3%, $p < 0.01$; Figure 2(b)). The progression of obesity is related to the ratio of tissue weight to body weight. The percentage of tissue weight in the mice was analyzed after sacrifice, and the results showed that the liver and adipose tissue ratio increased in the HFFD group compared with the control group ($p < 0.05$), while the percentage decreased significantly in response to the SDG supplement ($p < 0.05$; Figure 2(c)).

3.2. SDG Regulates Serum Adipokines in Obese Mice Induced by a Western Diet. Adipokines are closely related to the pathogenesis of obesity. Leptin promotes food intake, thereby regulating the energy and weight balance of the body. The serum leptin content in the HFFD group increased significantly ($p < 0.01$) compared to that in the control group, and SDG notably reduced this trend ($p < 0.01$; Figure 3(a)). High resistin levels reduce insulin sensitivity. Our results show that the HFFD group presented a significantly higher serum resistin level compared with that in the control group. However, the SDG treatment reversed this effect ($p < 0.01$; Figure 3(c)). Similarly, adiponectin levels also reflect the state of insulin resistance in the body. Figure 3(b) shows that the adiponectin level in the HFFD group decreased significantly compared with that in the control group ($p < 0.01$), and administration of SDG reversed this trend ($p < 0.01$).

Table 3: Primer sequences for RT-PCR (all primers are mouse primers).

	Forward primers	Reverse primers
Srebp1c	AAGCAAATCACTGAAGGACCTGG	AAAGACAAGGGGCTACTCTGGGAG
Fasn	AGGTGGTGATAGCCGGTATGT	TGGGTAATCCATAGAGCCCAG
PpARγ	TGCTGTTATGGGTGAAACTCTG	CTGTGTCAACCATGGTAATTTCTT
Acaca	CCGATTCATAATTGGGTCTGTGT	CCATCCTGTAAGCCAGAGATCC
PpARα	ACAGGAGAGCAGGGATTTGC	TACCTACGCTCAGCCCTCTT
Pgc1α	GAAAGGGCCAAACAGAGAGA	GTAAATCACACGGCGCTCTT
GAPDH	TGGAGAAACCTGCCAAGTATGA	TGGAAGAATGGGAGTTGCTGT

3.3. SDG Alleviates Adipose Tissue Hyperplasia Induced by a Western Diet in Obese Mice. Obesity is associated with excessive accumulation of lipids in tissues, which leads to increased adipose tissue, an increase in the number of adipose cells, and expansion in particle size and area. To investigate the effect of SDG on the proliferation of adipose tissue in HFFD-induced obese mice, the morphology of epididymal white adipose tissue (eWAT), subcutaneous white adipose tissue (iWAT), and brown adipose tissue (BAT) was observed by hematoxylin and eosin (H&E) staining, and the area of adipose tissue cells was quantitatively analyzed (Figure 4). The adipose tissue cells in the HFFD group were dilatated, and the dilatation was significantly inhibited by SDG (Figure 4(a)). The analysis of adipocyte area further confirmed this effect. The mean adipocyte area of eWAT, iWAT, and BAT cells in the HFFD group increased compared to that in the control group ($p < 0.01$), but this increase was suppressed after SDG was administered ($p < 0.01$; Figure 4). In addition, supplementing with SDG had no effect on morphology or cell area of adipose tissue in normal mice. These results indicate that oral administration of SDG inhibits the accumulation of lipids in adipose tissue of HFFD-induced obese mice.

3.4. SDG Regulates Lipid Metabolic Genes in White Adipose Tissue of Obese Mice Induced by a Western Diet. To investigate the mechanism of SDG regulating lipid metabolic homeostasis in adipose tissue, the mRNA expression of genes involved in lipogenesis and lipolysis in eWAT was evaluated by real-time polymerase chain reaction analysis. As shown in Figure 5, the expression of genes associated with lipogenesis, such as Srebp1c, Fasn, Ppar, and Acaca, in mice of the HFFD group were significantly upregulated ($p < 0.05$; Figures 5(a)–5(d)), and the expression levels of Ppar and Pgc1 were downregulated ($p < 0.05$; Figures 5(e) and 5(f)). SDG reversed this tendency. These results suggest that SDG improves lipid metabolic disorder in HFFD-induced obese mice by regulating the mRNA expression levels of lipid-related genes.

3.5. Discussion. The results of this study show that SDG significantly improved obesity and regulated the lipid metabolic disorder induced by a Western diet: SDG suppressed body weight gain and tissue weight in obese mice; SDG regulated the energy and body weight balance by regulating serum adipokines; SDG reduced the proliferation of adipose tissue cells in mice and inhibited excessive accumulation of lipids; SDG improved the lipid metabolic disorder caused by obesity by promoting the expression of lipolytic genes and inhibiting the expression of lipogenic genes.

Flaxseed is the mature seed of flax, which is rich in fat, protein, and dietary fiber, as well as other bioactive components, such as alpha-linolenic acid, lignans, and vitamins. Flaxseed is a dietary source containing high-value functional components, mainly used to produce and process edible vegetable oil seeds [41, 42]. A number of studies have shown that flaxseed has strong blood fat- and blood sugar-lowering, anti-inflammatory, and antioxidant effects and prevents heart disease and other chronic diseases [43, 44]. Flaxseed lignan is an important bioactive ingredient of flaxseed. Its main form is SDG. Dietary intake of SDG has positive effects on a variety of diseases, including cancers, cardiovascular diseases, diabetes, obesity, and metabolic syndrome [36]. Fukumitsu et al. reported that adding 0.1% or 0.5% SDG to a high-fat diet significantly reduces liver triglycerides, total cholesterol levels, and serum insulin and leptin levels in C57BL/6 mice, indicating that SDG improves diet-induced obesity and insulin resistance [45]. In a clinical study, Zhang et al. reported that a daily supplement of 600 mg SDG for 8 weeks in patients with hypercholesterolemia reduces plasma total cholesterol, low-density lipoprotein cholesterol, and fasting blood glucose levels [46]. Kang et al. reported that supplementation with SDG (50 mg/kg/d) inhibits fat formation in obese mice induced by a high-fat diet by reducing Ppar protein expression [47]. Pan et al. further demonstrated the beneficial effects of SDG in a randomized, double-blind trial of 68 patients with type 2 diabetes who were given 360 mg of SDG daily for 12 weeks. The results showed that indicators related to insulin resistance, type 2 diabetes, and inflammation, such as C-reactive protein, improved [48]. Based on these results, the dosage of SDG (40 mg/kg/d) used in this study was safe and effective. The body and tissue weights of obese mice induced by a Western diet were significantly inhibited in response to this SDG dose for 12 weeks, which improved obesity induced by the Western diet (Figures 2(b) and 2(c)).

As a chronic metabolic disease, obesity causes hypertension, diabetes, hyperlipidemia, coronary heart disease, and other diseases, which seriously threaten human health. According to the World Health Organization, the number of obese people worldwide increased nearly threefold between 1975 and 2016. By 2018, the number of obese people worldwide was still on the rise, reaching 672 million [4, 5]. At present, the main cause of obesity is the change in the

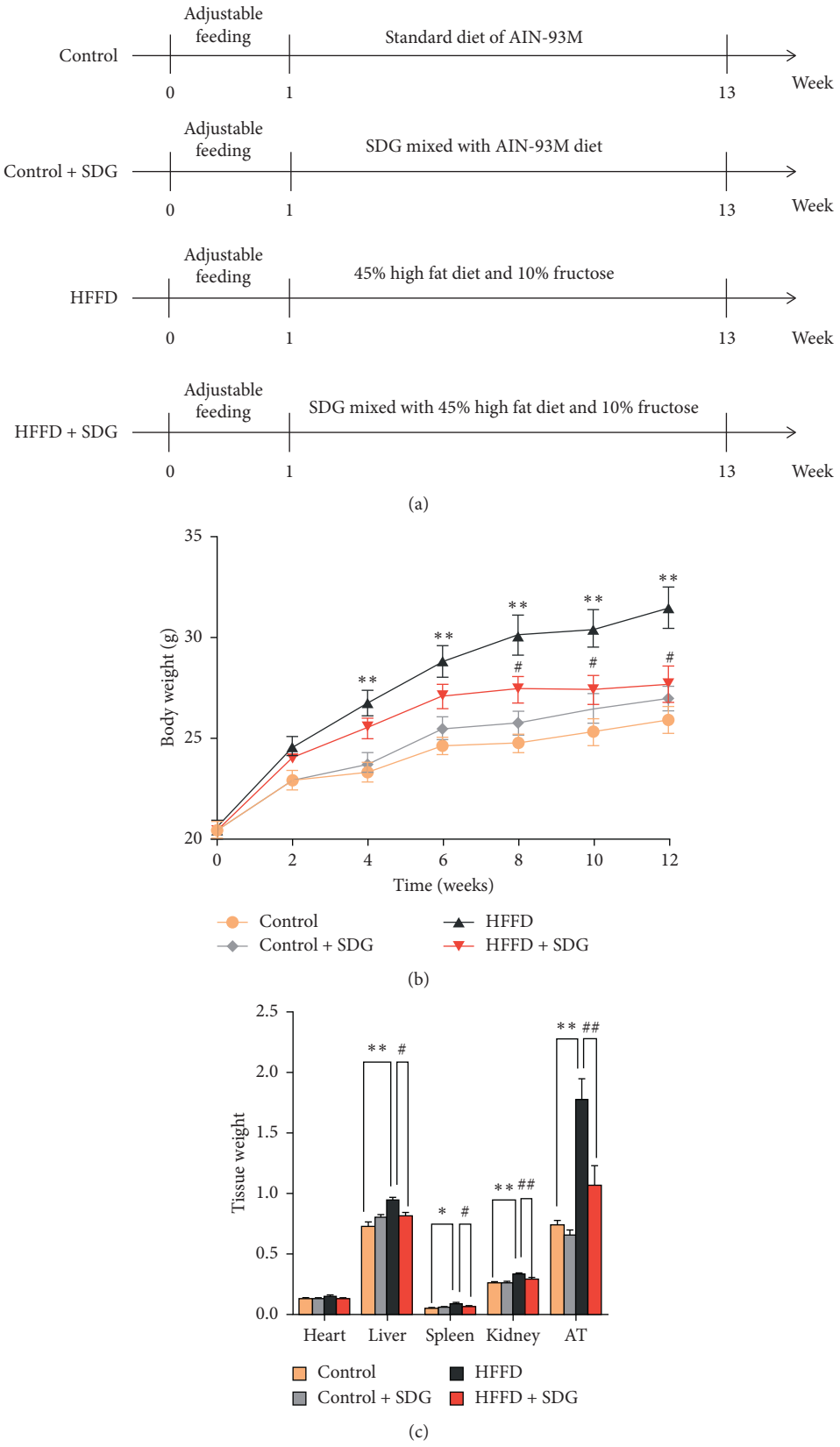

FIGURE 2: SDG inhibits weight gain in HFFD-fed mice. (a) Test design and groups; (b) trends in body weight during feeding and (c) tissue weight to body weight ratio (heart, liver, spleen, kidney, adipose tissue (AT)). Data are represented as mean ± SEM, $n = 10$ biologically independent animals. $^{*}p < 0.05$, $^{**}p < 0.01$ versus the control group; $^{\#}p < 0.05$, $^{\#\#}p < 0.01$ versus the HFFD group.

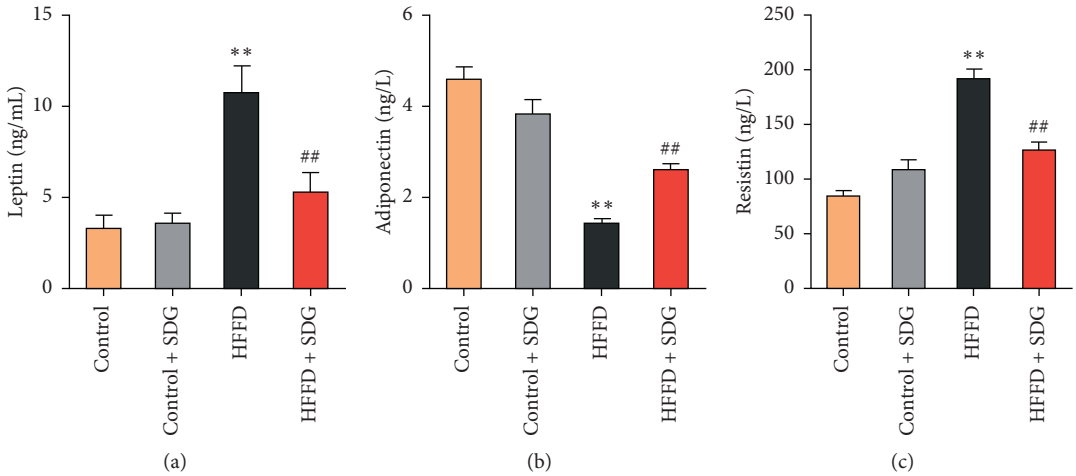

Figure 3: SDG regulates serum adipokines in obese mice induced by a Western diet. (a) Leptin; (b) adiponectin, and (c) resistin. Data are represented as mean ± SEM, $n = 10$ biologically independent animals. $^{*}p < 0.05$, $^{**}p < 0.01$ versus the control group; $^{\#}p < 0.05$, $^{\#\#}p < 0.01$ versus the HFFD group.

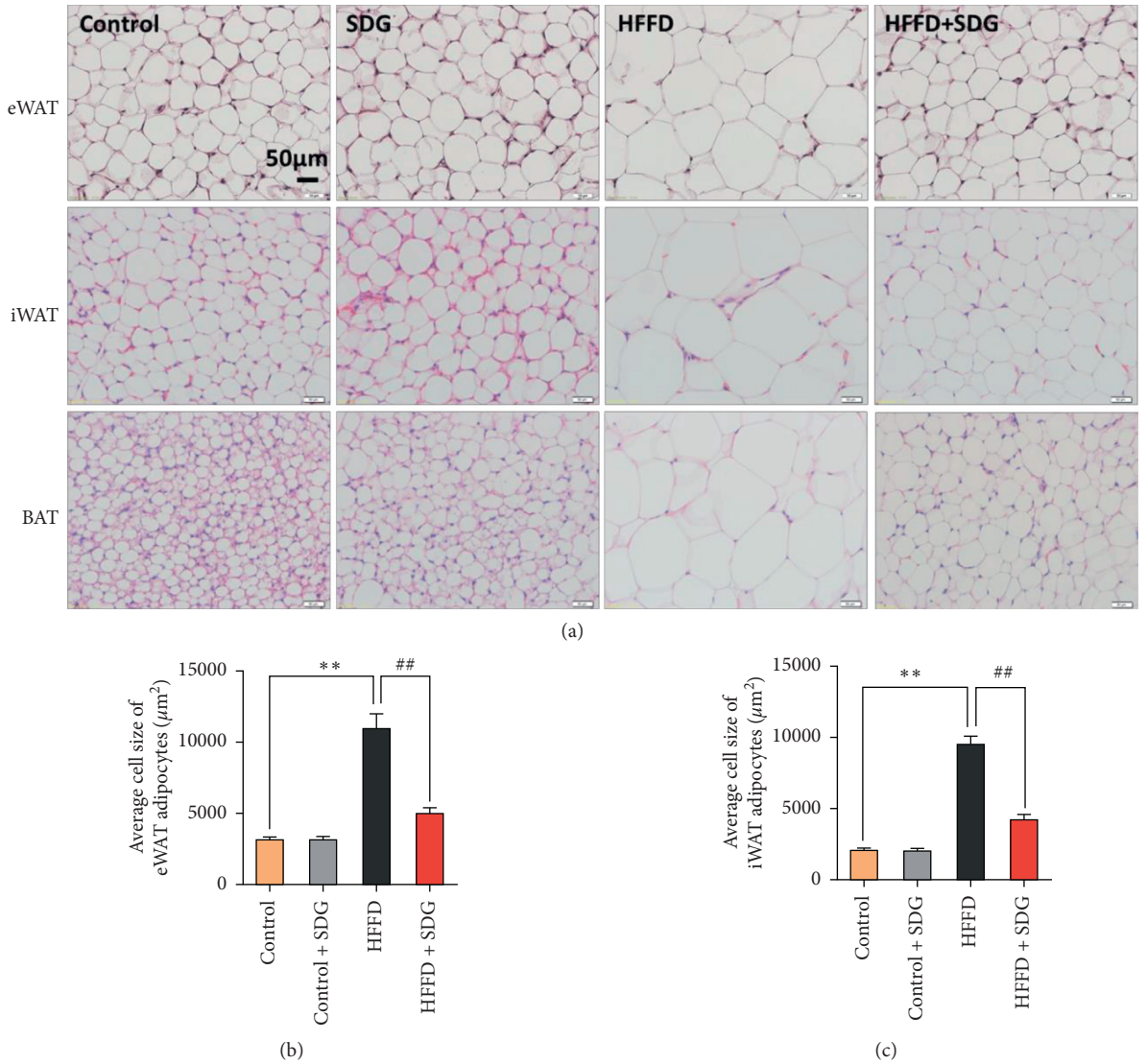

Figure 4: Continued.

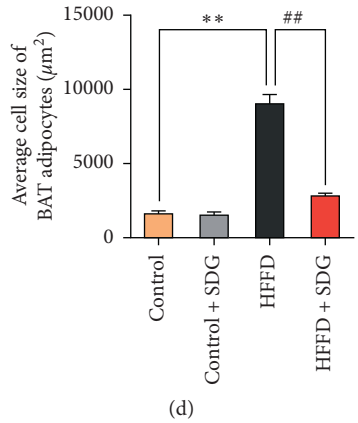

Figure 4: SDG alleviates adipose tissue hyperplasia induced by a Western diet in obese mice. (a) H&E staining (×200); (b) average area of white adipose tissue cells in the epididymis; (c) average area of subcutaneous white adipose tissue cells; and (d) average area of brown adipose tissue cells. Data are represented as mean ± SEM, $n = 10$ biologically independent animals. $^{*}p < 0.05$, $^{**}p < 0.01$ versus the control group; $^{\#}p < 0.05$, $^{\#\#}p < 0.01$ versus the HFFD group.

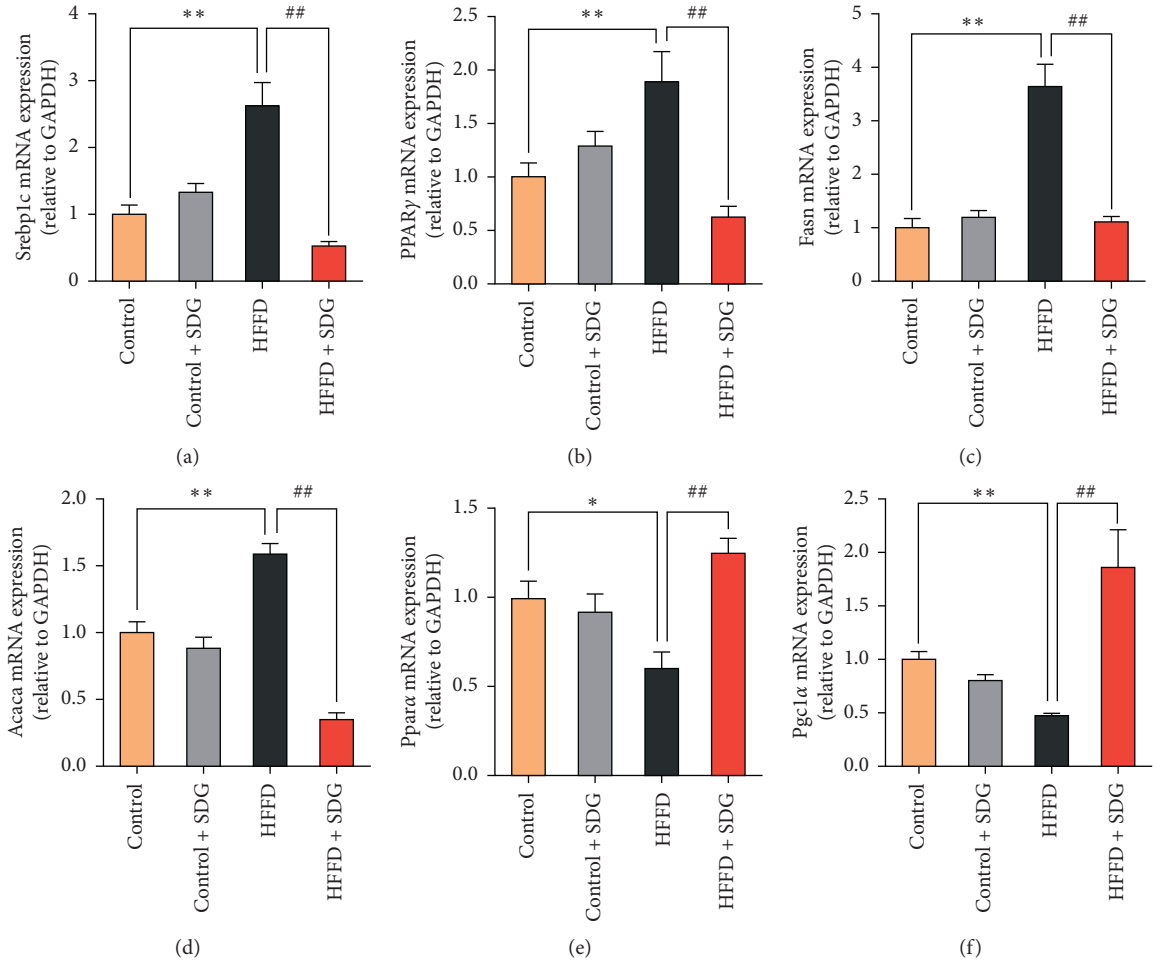

Figure 5: SDG regulates lipid metabolic genes in white adipose tissue of obese mice induced by a Western diet. (a) Srebp1c mRNA level; (b) PPARγ mRNA level; (c) Fasn mRNA level; (d) Acaca mRNA level; (e) Pparα mRNA level; and (f) Pgc1 mRNA level. Data are represented as mean ± SEM, $n = 10$ biologically independent animals. $^{*}p < 0.05$, $^{**}p < 0.01$ versus the control group; $^{\#}p < 0.05$, $^{\#\#}p < 0.01$ versus the HFFD group.

dietary pattern. A Western diet with high sugar and fat has gradually become popular. People take in more energy than the body needs, which leads to obesity. One of the metabolic diseases closely associated with obesity is diabetes. Obese adults increased their risk of developing diabetes by about one-tenth between 1960 and 2000 [49]. The most common form of diabetes is type 2 diabetes (T2DM). T2DM is often accompanied by insufficient insulin secretion or insulin resistance, while obesity leads to the deposition of ectopic fat and the proliferation of adipose tissue cells, which causes insulin resistance. Adipose tissue participates in the circulation of fatty acids by regulating lipid metabolism. Fatty acids are usually derived from dietary fat and endogenous neonatal fats. When glycogen storage is saturated, ingesting glucose produces endogenous neonatal fat and promotes continuous triglyceride output and storage in adipose tissue [50–52]. In addition, obesity leads to excessive activation of lipolysis in adipose tissue, stimulating the release of fatty acids and leading to abnormal secretion of adipogenic factors, thus promoting the accumulation of ectopic fat and mild inflammation and aggravating insulin resistance [10].

Adipokines play important regulatory roles in insulin resistance, inflammatory response, and glucose and lipid metabolism [13]. Adiponectin is triggered to reduce fat by AMP protein kinase (AMPK) and through the higher peroxisome proliferator-activated receptor-alpha to increase the oxidation of fatty acids [53]. In addition, adiponectin also inhibits the expression of sterol reactive element binding protein 1C by inducing the LKB-AMPK pathway, thus downregulating the expression of downstream genes involved in fat generation and cholesterol synthesis [54]. As an appetite-related adipose factor, leptin regulates food intake through the hypothalamus, which affects energy metabolism and body weight [16, 17]. Leptin receptors are expressed in a variety of tissues, and their circulating level is proportional to the amount of fat. Studies have shown that leptin reduces the production of fat, increases the hydrolysis of triglycerides, and increases the oxidation of fatty acids [18]. Leptin also promotes the breakdown of fat in adipose tissue by increasing sympathetic nerve signaling [55]. Based on these studies, serum levels of adiponectin, leptin, and resistin were measured, and serum leptin and resistin levels increased significantly ($p < 0.01$), whereas adiponectin levels decreased significantly under the Western diet ($p < 0.01$). The level of adiponectin increased significantly ($p < 0.01$) after supplementation with desensitizers, and the levels of leptin and resistin decreased significantly ($p < 0.01$; Figures 3(a)–3(c)).

Abnormal secretion of adipokines damages the storage of lipids in adipose tissue, leading to the heterotopic deposition of lipids, eventually inducing a series of chronic metabolic diseases [8, 9]. In this study, we observed proliferation of histopathological areas of eWAT, white fat in the groin, and brown fat by H&E staining and quantitatively analyzed the mean area of the three kinds of tissue cells. The results show that the cell area of the three types of adipocytes increased significantly under the Western diet ($p < 0.01$), and proliferation of the three types of adipocytes was significantly inhibited after administration of SDG ($p < 0.01$; Figures 4(a)–4(c)).

Although the positive effects of SDG in improving obesity and regulating lipid metabolic disorder have been clearly reported, few reports are available on the molecular mechanisms [37–39]. In this experiment, gene expression related to lipid synthesis and lipid oxidative decomposition was analyzed, and SDG significantly inhibited the mRNA expression of lipogenic genes, such as Srebp1c, Fasn, Ppar, and Acaca ($p < 0.01$; Figures 5(a)–5(d)), and promoted mRNA expression of lipolytic genes, such as Pparα and Pgc1α ($p < 0.01$; Figures 5(e) and 5(f)). These results indicate that SDG regulates obesity and lipid metabolic disorder caused by a Western diet by regulating the expression of genes related to fat synthesis and decomposition. However, the further mechanism of action remains to be further studied.

In summary, SDG effectively inhibited weight gain, regulated the secretion of adipogenic factors, and suppressed the synthesis and accumulation of fat by regulating the expression of lipid synthesis and decomposition-related genes, which improved the obesity caused by a Western diet.

4. Conclusion

In this study, SDG effectively alleviated obesity and regulated lipid metabolic disorder. Improved obesity in response to SDG was preliminarily determined by suppression of body and tissue weight gains. Adipose tissue hyperplasia was further observed by H&E staining and adipocyte area was quantified, leading us to conclude that SDG inhibited hyperplasia of adipose tissue. In addition, SDG regulated the secretion of adipokines to achieve a balanced state. SDG inhibited the expression of lipogenic genes and promoted the expression of lipolytic genes.

Data Availability

Data were analyzed or generated during the study. The authors have conducted a lot of experiments where the data come from. The data used to support the findings of this study are available from the corresponding author upon request.

Conflicts of Interest

The authors declare no conflicts of interest.

Authors' Contributions

Shan Dong designed the study and developed methodology; Shan Dong, Wanli Sheng, and Ronghu Feng conducted the experiments; Wenliang Bai and Ronghu Feng did statistical analysis; Li Zhang edited the article.

Acknowledgments

This research was funded by Science, Technology and Innovation Commission of Shenzhen Municipality (grant number JCYJ20180306172311983).

References

[1] S. Roossner, "Obesity: the disease of the twenty-first century," *International Journal of Obesity*, vol. 4, no. S4, pp. S2–S4, 2002.

[2] R. S. Cassani, P. G. Fassini, J. H. Silvah, C. M. Lima, and J. S. Marchini, "Impact of weight loss diet associated with flaxseed on inflammatory markers in men with cardiovascular risk factors: a clinical study," *Journal of Nutrition*, vol. 15, no. 1, p. 59, 2015.

[3] C. M. Steppan, S. T. Bailey, S. Bhat et al., "The hormone resistin links obesity to diabetes," *Nature*, vol. 409, no. 6818, pp. 307–312, 2001.

[4] Y. S. Mi, G. Y. Qi, Y. Gao et al., "EGCG ameliorates insulin resistance and mitochondrial dysfunction in hepg2 cells: involvement of bmal1," *Molecular Nutrition & Food Research*, vol. 61, no. 12, Article ID 1700440, 2017.

[5] M. Blüher, "Obesity: global epidemiology and pathogenesis," *Nature Reviews Endocrinology*, vol. 15, no. 5, pp. 288–298, 2019.

[6] G. S. Hotamisligil, P. Arner, J. F. Caro, R. L. Atkinson, and B. M. Spiegelman, "Increased adipose tissue expression of tumor necrosis factor-alpha in human obesity and insulin resistance," *Journal of Clinical Investigation*, vol. 95, no. 5, pp. 2409–2415, 1995.

[7] D. M. Muoio and C. B. Newgard, "Obesity-related derangements in metabolic Regulation," *Annual Review of Biochemistry*, vol. 75, pp. 367–401, 2006.

[8] G. D. Pergola and F. Silvestris, "Obesity as a major risk factor for cancer," *Journal of Obesity*, vol. 2013, Article ID 291546, 11 pages, 2013.

[9] L. R. Howe, K. Subbaramaiah, C. A. Hudis, and A. J. Dannenberg, "Molecular pathways: adipose inflammation as a mediator of obesity-associated cancer," *Clinical Cancer Research*, vol. 19, no. 22, pp. 6074–6083, 2013.

[10] B. Kálmán and R. Michael, "Energy metabolism of white adipose tissue and insulin resistance in humans," *European Journal of Clinical Investigation*, vol. 48, no. 11, Article ID e13017, 2018.

[11] J. M. Olefsky and C. K. Glass, "Macrophages, inflammation, and insulin resistance," *Annual Review of Physiology*, vol. 72, no. 1, pp. 219–246, 2010.

[12] G. S. Heyn, L. H. Corrêa, and K. G. Magalhães, "The impact of adipose tissue–derived miRNAs in metabolic syndrome, obesity, and cancer," *Frontiers in Endocrinology*, vol. 11, Article ID 563816, 2020.

[13] N. Hosogai, A. Fukuhara, K. Oshima et al., "Adipose tissue hypoxia in obesity and its impact on adipocytokine dysregulation," *Diabetes*, vol. 56, no. 4, pp. 901–911, 2007.

[14] A. H. Berg, T. P. Combs, X. Du, M. Brownlee, and P. E. Scherer, "The adipocyte-secreted protein Acrp30 enhances hepatic insulin action," *Nature Medicine*, vol. 7, no. 8, pp. 947–953, 2001.

[15] P. E. Scherer, "Adipose tissue: from lipid storage compartment to endocrine organ," *Diabetes*, vol. 55, no. 6, pp. 1537–1545, 2006.

[16] J. M. Friedman and J. L. Halaas, "Leptin and the regulation of body weight in mammals," *Nature*, vol. 395, no. 6704, pp. 763–770, 1998.

[17] J. M. Montez, A. Soukas, E. Asilmaz, and G. F. Fayzikhodjaeva, "Acute leptin deficiency, leptin resistance, and the physiologic response to leptin withdrawal," *Proceedings of the National Academy of Sciences of the United States of America*, vol. 102, no. 7, pp. 2532–2542, 2005.

[18] W. N. William Jr., R. B. Ceddia, and R. Curi, "Leptin controls the fate of fatty acids in isolated rat white adipocytes," *Journal of Endocrinology*, vol. 175, no. 3, pp. 735–744, 2002.

[19] C. Rice-Evans, "Plant polyphenols: free radical scavengers or chain-breaking antioxidants?" *Biochemical Society Symposia*, vol. 61, pp. 103–116, 1995.

[20] J. Avila, J. R. García, G. Aguilar, and L. Rosa, "The antidiabetic mechanisms ofpolyphenols related to increased glucagon-like peptide-1 (GLP1) and insulinsignaling," *Molecules*, vol. 22, no. 6, p. 903, 2017.

[21] S. S. Deshpande, S. K. Sathe, and D. K. Salunkhe, "Chemistry and safety of plant polyphenols," *Advances in Experimental Medicine and Biology*, vol. 177, pp. 457–495, 1984.

[22] L. Vámos-Vigyázó, "Polyphenol oxidase and peroxidase in fruits and vegetables," *Critical Reviews in Food Science and Nutrition*, vol. 15, no. 1, pp. 49–127, 1981.

[23] E. Haslam, T. Lilley, Y. Cai, R. Martin, and D. Mangnolato, "Traditional herbal medicines—the role of polyphenols," *Planta Medica*, vol. 55, no. 1, pp. 1–8, 1989.

[24] R. J. Nijveldt, E. van Nood, D. E. van Hoorn, P. G. Boelens, K. van Norren, and P. A. van Leeuwen, "Flavonoids: a review of probable mechanisms of action and potential applications," *The American Journal of Clinical Nutrition*, vol. 74, no. 4, pp. 418–425, 2001.

[25] C. Liang, M. E. Oest, and M. R. Prater, "Intrauterine exposure to high saturated fat diet elevates risk of adult-onset chronic diseases in C57BL/6 mice," *Birth Defects Research Part B: Developmental and Reproductive Toxicology*, vol. 86, no. 5, pp. 377–384, 2009.

[26] L. K. Stewart, J. L. Soileau, D. Ribnicky et al., "Quercetin transiently increases energy expenditure but persistently decreases circulating markers of inflammation in C57BL/6J mice fed a high-fat diet," *Metabolism*, vol. 57, pp. S39–S46, 2008.

[27] L. Rivera, R. Morón, M. Sánchez, A. Zarzuelo, and M. Galisteo, "Quercetin ameliorates metabolic syndrome and improves the inflammatory status in obese zucker rats," *Obesity*, vol. 16, no. 9, pp. 2081–2087, 2008.

[28] A. S. Strimpakos and R. A. Sharma, "Curcumin: preventive and therapeutic properties in laboratory studies and clinical trials," *Antioxidants & Redox Signaling*, vol. 10, no. 3, pp. 511–546, 2008.

[29] A. Asai and T. Miyazawa, "Dietary curcuminoids prevent high-fat diet-induced lipid accumulation in rat liver and epididymal adipose tissue," *The Journal of Nutrition*, vol. 131, no. 11, pp. 2932–2935, 2001.

[30] W. J. Spuyvander and E. Pretorius, "Is the use of resveratrol in the treatment and prevention of obesity premature?" *Nutrition Research Reviews*, vol. 22, no. 2, pp. 111–117, 2009.

[31] J. Burns, T. Yokota, H. Ashihara, M. E. J. Lean, and A. Crozier, "Plant foods and herbal sources of resveratrol," *Journal of Agricultural and Food Chemistry*, vol. 50, no. 11, pp. 3337–3340, 2002.

[32] U. Stervbo, O. Vang, and C. Bonnesen, "A review of the content of the putative chemopreventive phytoalexin resveratrol in red wine," *Food Chemistry*, vol. 101, no. 2, pp. 449–457, 2007.

[33] S.-J. Cho, U. J. Jung, and M.-S. Choi, "Differential effects of low-dose resveratrol on adiposity and hepatic steatosis in diet-induced obese mice," *British Journal of Nutrition*, vol. 108, no. 12, pp. 2166–2175, 2012.

[34] S. Kim, Y. Jin, Y. Choi, and T. Park, "Resveratrol exerts anti-obesity effects via mechanisms involving down-regulation of

adipogenic and inflammatory processes in mice," *Biochemical Pharmacology*, vol. 81, no. 11, pp. 1343–1351, 2011.

[35] M. Lagouge, C. Argmann, Z. Gerhart-Hines et al., "Resveratrol improves mitochondrial function and protects against metabolic disease by activating SIRT1 and PGC-1α," *Cell*, vol. 127, no. 6, pp. 1109–1122, 2006.

[36] S. Rom, V. Zuluaga-Ramirez, N. L. Reichenbach et al., "Secoisolariciresinol diglucoside is a blood-brain barrier protective and anti-inflammatory agent: implications for neuroinflammation," *Journal of Neuroinflammation*, vol. 27, no. 15, p. 25, 2018.

[37] J. L. Adolphe, S. J. Whiting, B. H. J. Juurlink, L. U. Thorpe, and J. Alcorn, "Health effects with consumption of the flax lignan secoisolariciresinol diglucoside," *British Journal of Nutrition*, vol. 103, no. 7, pp. 929–938, 2010.

[38] S. Jian, Y. Tang, Y. Xiao et al., "Flaxseed lignans alleviate high fat diet-induced hepatic steatosis and insulin resistance in mice: potential involvement of AMP-activated protein kinase," *Journal of Functional Foods*, vol. 24, pp. 482–491, 2016.

[39] L. Sun, Y. Wang, Y. Song et al., "Resveratrol restores the circadian rhythmic disorder of lipid metabolism induced by high-fat diet in mice," *Biochemical and Biophysical Research Communications*, vol. 458, no. 1, pp. 86–91, 2015.

[40] Y. Wang, B. Fofana, M. Roy et al., "Flaxseed lignan secoisolariciresinol diglucoside improves insulin sensitivity through upregulation of GLUT4 expression in diet-induced obese mice," *Journal of Functional Foods*, vol. 18, pp. 1–9, 2015.

[41] C. C. Yu, "Effects of oil preparation technology on the content of phenolic compounds and their antioxidant properties in flaxseed cake," Master's thesis, Jiangnan University, Wuxi, China, 2019.

[42] Y. Zhao, "Functional components of flaxseed and its application value in food industry," *ShanXi Food Industry*, vol. 2, pp. 31–33, 2005.

[43] C. Dzuvor, J. Taylor, C. Acquah, S. Pan, and D. Agyei, "Bioprocessing of functional ingredients from flaxseed," *Molecules*, vol. 23, no. 10, p. 2444, 2018.

[44] A. N. Martinchik, A. K. Baturi, V. V. Zubtsov, and V. I. Molofeev, "Nutritional value and functional properties of flaxseed," *Voprosy Pitaniia*, vol. 81, no. 3, pp. 4–10, 2012.

[45] S. Fukumitsu, K. Aida, N. Ueno, S. Ozawa, Y. Takahashi, and M. Kobori, "Flaxseed lignan attenuates high-fat diet-induced fat accumulation and induces adiponectin expression in mice," *British Journal of Nutrition*, vol. 100, no. 3, pp. 669–676, 2008.

[46] W. Zhang, X. Wang, Y. Liu et al., "Dietary flaxseed lignan extract lowers plasma cholesterol and glucose concentrations in hypercholesterolaemic subjects," *British Journal of Nutrition*, vol. 99, no. 6, pp. 1301–1309, 2008.

[47] J. Kang, J. Park, H.-L. Kim et al., "Secoisolariciresinol diglucoside inhibits adipogenesis through the AMPK pathway," *European Journal of Pharmacology*, vol. 820, pp. 235–244, 2018.

[48] A. Pan, W. Demark-Wahnefried, X. Ye et al., "Effects of a flaxseed-derived lignan supplement on C-reactive protein, IL-6 and retinol-binding protein 4 in type 2 diabetic patients," *British Journal of Nutrition*, vol. 101, no. 8, pp. 1145–1149, 2009.

[49] E. W. Gregg, Y. J. Cheng, B. L. Cadwell et al., "Secular trends in cardiovascular disease risk factors according to body mass index in US adults," *Journal of American Medical Associations*, vol. 293, no. 15, pp. 1868–1874, 2005.

[50] S. M. Grundy, "Adipose tissue and metabolic syndrome: too much, too little or neither," *European Journal of Clinical Investigation*, vol. 45, no. 11, pp. 1209–1217, 2015.

[51] F. B. Hillgartner, L. M. Salati, and A. G. Goodridge, "Physiological and molecular mechanisms involved in nutritional regulation of fatty acid synthesis," *Physiological Reviews*, vol. 75, no. 1, pp. 47–76, 1995.

[52] R. Gao, Q. Yu, Y. Shen et al., "Production, bioactive properties, and potential applications of fish protein hydrolysates: developments and challenges," *Trends in Food Science & Technology*, vol. 110, pp. 687–699, 2021.

[53] T. Yamauchi, J. Kamon, Y. Ito et al., "Cloning of adiponectin receptors that mediate antidiabetic metabolic effects," *Nature*, vol. 423, no. 6941, pp. 762–769, 2007.

[54] M. Awazawa, K. Ueki, K. Inabe et al., "Adiponectin suppresses hepatic SREBP1c expression in an AdipoR1/LKB1/AMPK dependent pathway," *Biochemical & Biophysical Research Communications*, vol. 382, no. 1, pp. 51–56, 2009.

[55] T. J. Bartness, C. K. Song, H. Shi, R. R. Bowers, and M. T. Foster, "Brain-adipose tissue cross talk," *Proceedings of the Nutrition Society*, vol. 64, no. 1, pp. 53–64, 2005.

Hindawi
Journal of Food Quality
Volume 2021, Article ID 5510779, 11 pages
https://doi.org/10.1155/2021/5510779

Research Article

Application of Calcium Chloride-Sodium Alginate to Improve the Texture of Quick-Frozen *Heracleum moellendorffii*

Xiao-mei Li,[1] Li-kun Ren,[1] Yang Yang,[1] Xin Bian,[1] Yu Fu,[2] Lian-cheng Zhao,[1] Zhu-jing Xing,[1] Yan-guo Shi,[1] Wojciech Piekoszewski,[3,4] and Na Zhang[1]

[1]*College of Food Engineering, Harbin University of Commerce, Harbin 150028, China*
[2]*College of Food Science, Southwest University, No. 2 Tiansheng Road, Beibei District, Chongqing 400715, China*
[3]*Department of Analytical Chemistry, Jagiellonian University, 30-386 Krakow, Poland*
[4]*School of Biomedicine, Far Eastern Federal University, FEFU Campus, Vladivostok, Russia*

Correspondence should be addressed to Na Zhang; foodzhangna@163.com

Received 7 January 2021; Revised 26 January 2021; Accepted 15 March 2021; Published 22 March 2021

Academic Editor: quancai sun

Heat-soak and quick freezing could deteriorate the texture of vegetables. In this work, it was found that calcium chloride-sodium alginate (SA) could improve the appearance, brittleness, and chewiness of processed *Heracleum moellendorffii* (HM), a kind of popular nutritious wild vegetable in China. The effect resulted from the increase of calcium content in the vegetable, which was closely related to the ratio of calcium chloride to SA, the concentration of texture retaining agent, and soaking time significantly ($P < 0.01$). The best way to maintain the texture was to soak HM in 4 g/L of calcium chloride-SA (mass ratio 1 : 2) at 50°C for 30 minutes. The calcium content was increased to 71.56 mg/100g, and the brittleness and chewiness were 4630 gf and 2583.33 gf, respectively. The microstructure found that calcium could adhere to an inherent position on the cell membrane and protected the sample from cell damage and chloroplast spilling from the cell during thawing and quick freezing. The results showed that calcium chloride-SA treatment may be a promising method to improve the texture of vegetables during quick-frozen storage.

1. Introduction

Heracleum moellendorffii is a perennial herbaceous herb of the Umbelliferae family. It is a particular hill potherb in Northeast China [1] with high levels of dietary fiber, amino acids, vitamins, and other nutrients [2]. Among them, the content of vitamin C is the most abundant and is more than ten times that of ordinary vegetables. Besides, some studies have confirmed that the species has high edible and medicinal value; for example, the blade can prevent high blood pressure, and the stem can improve heart disease and other diseases (rheumatism and headache) [3]. Thus, in recent years, HM has become more and more popular among the Chinese people because of its fine quality (e.g., verdant appearance, crispy taste, rich nutrition, and special aroma). Compared with other vegetables, it is usually regarded as a healthier foodstuff. HM is a wild vegetable that grows in forest districts, on river, lake shorelines, or hills [4]. It ripens in April and May and has a short period for the harvest, so it is necessary to take some strategies to preserve HM for the goal of year-round edible. Currently, the preservation techniques for seasonal vegetables are mainly based on quick-freezing preservation. However, there is a common problem with quick-freezing vegetables, which is the decreasing of brittleness and chewiness after thawing [5, 6]. Therefore, with the increase of people's enthusiasm for nutrition and taste properties [7], keeping the freshness of HM in the frozen environment and keeping its texture after thawing are crucial to extending its market.

Some authors have reported that freezing changed the microstructure of plant tissues such as cell turgor, cells lost water, and shrinkage [8, 9], which may lead to the soft texture and the declined brittleness and chewiness thawing. The large ice crystals formed by traditional freezing will cause mechanical damage to the cell membrane, thereby causing the water loss of cells [10]. Compared to traditional

freezing, quick freezing can form tiny ice crystals which shorten the time of maximum ice crystal generation, thereby reducing cell damage and water migration [11]. Moreover, the exogenous addition of a texture retaining agent can significantly relieve the cell damage caused by traditional freezing. The reason may be that the treatment of vegetables with a texture retaining agent before freezing can retain the inherent permeability of the vegetable cells to reduce cell damage. In the food industry, the exogenous calcium salt and exogenous pectin methylesterase (PME) were used as texture retaining agents together to catalyze the decomposition of pectin to form pectic acid [12]. Furthermore, pectic acid can react with Ca^{2+} to form calcium pectate, a molecular gel that can exist in the intercellular space, which retains the cell membrane in an inherent position after thawing, thereby enhancing the antiwrinkle behavior and antidestructive effect of cells [13]. Some studies also proved that calcium pectate has a great adhesion effect among the plant cell wall and cell membrane, which can prevent cell shrinkage and provide standby for tissues [14]. At present, apart from the addition of exogenous texture retaining agent, endogenous PME and Ca^{2+} have the same effect. The endogenously produced calcium pectate was safer and lower in cost than the exogenous PME, and the exogenous Ca^{2+} can activate endogenous PME more efficiently and produce calcium pectate more efficiently under heating conditions (Nipaporn et al., 2009). Therefore, the gel can retain the texture of the thawed vegetables to the maximum extent.

Nowadays, the commercially available frozen HM is processed by the traditional freezing method without texture protection [15], and the texture of HM is greatly reduced after thawing, which is greatly different from the sensory quality of fresh HM. On the contrary, the sensory quality of HM treated with texture retaining agents can retain to a large extent [9] (Chitra et al., 2010). However, little information is available about the influence of quick freezing and the protection effect of texture retaining agent on the texture of HM.

Therefore, the objective of this study was to evaluate the quality using microscopic (the increase of calcium and laser scanning confocal microscopy (LSCM)) and apparent measurements (crispiness and chewiness) to obtain the key pretreatment technology before the quick freezing of HM. This study can provide a theoretical basis for the texture protection of HM during quick freezing, and it has a practical guiding significance for the industrial production of the frozen storage of HM.

2. Materials and Methods

2.1. Materials and Chemicals. Fresh HM was provided by Dong-sheng Food Co., Ltd. (Beian, China), and selected according to the similar size for this study. Calcium lactate, calcium chloride, and sodium alginate (SA) were purchased from Yimeng Biotechnology Co., Ltd. (Zhejiang, China).

2.2. Screening of the Texture Retaining Agent. Calcium chloride, calcium lactate, and SA were chosen and compounded (the compound type texture retaining agent of calcium chloride-SA, calcium lactate-SA, and calcium chloride-calcium lactate) as texture retaining agents with 1 : 1 (g : g). The calcium content increase of HM was used as an indicator to estimate the texture retaining agent to confirm the optimum texture retaining agents for the following experiments. The HM soaked in water without texture retaining agents at 50°C ($n = 3$) was used as a negative control test. The HM was treated with the selected texture retaining agent. Then, the effects of compounding ratios of calcium chloride to SA, texture retaining agent concentrations, and soaking times on the calcium content increase, and the brittleness and chewiness of HM were investigated.

2.3. Determination of Calcium Components in HM. HM was soaked in the texture retaining agent (calcium chloride-SA) at 50°C for 30 min. Next, Ca^{2+} was applied to stimulate the activity of PME [16] and further catalyze the formation of calcium pectate gel polymer that can be dissolved by NaCl solution. The unsoaked samples were used as a control group. Finally, the calcium content increase was conducted according to the atomic absorption spectrophotometry described by [17], with some modifications. The samples of the control group and the test group were homogenized, and a certain amount (±0.01 g) of homogenate was weighed. Then, the dissolved calcium was extracted by 1 mol/L NaCl solution, volumed to a constant and filtered. The detailed parameters of the instrument were set as follows: slit: 0.5 nm, gas flow: 1.8 L/min, flame type: air-C_2H_2, and wavelength: 422.7 nm.

2.4. Determination of Brittleness and Chewiness. Texture properties of the HM stems soaked in calcium chloride-SA were assessed using a texture analyzer (New Plus Texture Analyzer, Isenso Intelligent Technology Co., Ltd., New York, USA), according to the method described by [18] with some modifications. The stems of the sample were processed into small cubic sections ($1.5 \times 1.5 \times 1.5$ cm^3) and then penetrated using a Volodkevich-bite probe to represent brittleness. For chewiness analysis, a P/0.5 probe was used with 50% deformation and the parameters were set as follows: the pretest speed of 2.0 mm/s, test speed of 1.0 mm/s, the trigger force of 5.0 g, and the time interval of 5 s.

2.5. Observation of HM Cells. The stem and leaves of the HM were cut into small segments of 4–5 cm and cooled to room temperature (25°C). Then, HM was soaked in the selected texture retaining solution (compound type compound mass ratio of 1 : 1) at 50°C for 10–15 min. Then, the peroxidase of HM was inactivated at 90°C high-temperature bleaching for color retention and then cooled to room temperature (25°C) with cold water. Finally, they were preserved at −24°C for further experiments.

The samples were divided into 2 groups for the next step. The details were as follows: unfrozen group (fresh samples, samples soaked in water at 50°C, and samples soaked in texture retaining agent at 50°C) and frozen group (fresh samples + frozen, samples soaked in water at 50°C + frozen,

and samples soaked in texture retaining agent at 50°C + frozen). A blade was used to cut a square with a side length of 1 cm on the stem and leaves of the HM and a pair of tweezers were used to remove the square skin. After that, the unfrozen samples and their thawed samples were subjected to the morphological observation of organelle chloroplast, separately. The fresh HM was used as a control. Chloroplasts were observed according to the method described by [19] with some modifications with the helium laser launcher of LSCM at 663 nm (TCS SP5, Leica Microsystems Co., Ltd., Frankfurt, Germany). The stems and leaves were examined at 75 μm and 50 μm magnification under incident light, respectively. Moreover, the temperature was set to −24°C during the measurement.

2.6. Statistical Analysis. The correlation analysis of calcium content increase, brittleness, and chewiness in the experiment was assessed by SPSS 13.0 (SPSS Inc., Chicago, IL, USA) and then got the correlation coefficient. The data in the paper were expressed as means ± standard deviation (SD) from at least three independent trials. Statistical significance of data was assessed by one-way ANOVA using SPSS 13.0. Significant differences ($P < 0.05$) between the average values were identified with the least significant difference procedure.

3. Results and Discussion

3.1. The Selection of Texture Retaining Agent. Texture properties are important in the assessment of consumer acceptability. The texture of HM refers to its sensory quality that includes brittleness and chewiness. Freezing is a major reason that causes texture change [20], such as softening phenomenon. Additionally, Agcam et al. reported that calcium salts can increase the PME activity of the samples, thus promoting the decomposition of pectin to react with Ca^{2+} to form calcium pectate gel, which can be enriched in the intercellular space [16], thereby reducing the deterioration of the sample texture. Therefore, in this paper, the level of the increase of calcium content was used as an indicator to explore the influence of texture retaining agents on the crispiness of HM. The results were shown in Table 1, the fresh sample did not detect the dissolved calcium, and the calcium content increase was regarded as zero.

Compared with No. 1, No. 2 and No. 3 had an increased content of calcium, but no significant difference was observed between the two groups ($P > 0.05$). In the experimental group, there is a significant difference in the calcium content increase of HM with different texture retaining agents ($P < 0.05$). No. 3 showed the most significant differences compared to the other groups ($P < 0.01$) and SA soaking had no impact on the calcium content increase. The calcium content increase in No. 4 was also lower. On the contrary, the calcium content increases significantly ($P < 0.05$) in No. 5, No. 6, and No. 7; however, there were no significant differences among the three groups ($P < 0.05$). The differences obtained among samples soaked in solutions with and without Ca^{2+} reflected the enhancing effect of Ca^{2+} on tissue structure. Moreover, the calcium content increase ($P < 0.05$) reached a maximum when the sample was soaked in calcium chloride-SA. This may be due to the synergistic effects of reagents [21]. Therefore, the texture retaining agent of calcium chloride-SA had the best effect on the texture of HM and was selected for further experiments.

3.2. Effect of Texture Retaining Agent on the Calcium Content Increase of HM. It can be seen from Figures 1(a)~1(c) that the increase of calcium content in the HM depended on the change of the condition of the texture retaining agent. In the case of a fixed amount of calcium chloride, when the proportion of SA increased, the calcium content increase was significantly improved ($P < 0.05$) (Figure 1(a)). And the highest calcium content increase was observed when the ratio of calcium chloride to SA was 1 : 2. Furthermore, as shown in Figure 1(b), when the texture retaining agent concentration was 4 g/L, the calcium content increase of HM was significantly higher than other concentrations ($P < 0.01$). Moreover, the influence of soaking time on the calcium content increase of HM was firstly increased and then decreased (Figure 1(c)) and the calcium content increase was the highest with the soaking time of 30 min.

These phenomena may be related to the following factors: firstly, SA has good gelation and viscosity property, and viscosity increases with the concentration of SA [22]. SA has a cross-linking effect with Ca^{2+}, and then SA can cooperate with Ca^{2+} to enter the tissue of samples or adhere to the intercellular space, which had a synergistic effect on the texture. Secondly, the appropriate concentration of SA was beneficial for Ca^{2+} to contact with PME and activate the PME to form calcium pectate, which could attach to the intercellular space [23]. Calcium pectate had enhanced gelation [20], thereby supporting the cell wall and retaining the brittleness of the HM. Because of these factors, higher levels of calcium gains were achieved in this work as compared with previous literature results. Another research [24] showed that when blueberries were treated with calcium sulfate, the calcium content was less than it in this experiment.

Simultaneously, as shown in Figure 1(c), the calcium content increase of HM increased gradually with the increase of soaking time, until the calcium content decreased after soaking for 30 min. The reason was that the stable temperature of PME is 35–50°C, and the tolerance time is 40 min. Soaking at 50°C for 30 min, PME can achieve the proper activity, which is beneficial to exert the best catalytic effect [25]. However, prolonging soaking time at 50°C will result in a significant loss of active site due to changes in the structure of the enzyme protein, leading to a significant decrease in the activity of PME, which will lead to a significant decline in the amount of calcium pectate and a significant decrease in calcium content increase ($P < 0.05$).

3.3. Effect of Texture Retaining Agent on the Texture of HM. The calcium pectinate in the cells can reflect the effect of the texture retaining agent and brittleness and chewiness can indicate changes in texture. In the previous studies,

Table 1: The effect of texture retaining agents on the calcium content increase.

Group no.	Group	Dissolved content (mg/100g)	Calcium content increase (mg/100g)
1	Fresh samples	Not detected	0
2	Sample soaked in water	23.71 ± 3.40^{a}	2.01 ± 0.62^{a}
3	SA	26.09 ± 4.12^{a}	2.38 ± 0.49^{a}
4	Calcium lactate	55.97 ± 5.48^{b}	32.26 ± 6.32^{b}
5	Calcium chloride	71.69 ± 7.86^{c}	47.98 ± 8.17^{c}
6	Calcium lactate-SA	74.91 ± 6.65^{c}	51.20 ± 5.94^{c}
7	Calcium lactate-calcium chloride	75.10 ± 10.13^{c}	51.39 ± 6.82^{c}
8	Calcium chloride-SA	92.98 ± 12.34^{d}	69.27 ± 10.03^{d}

Error bars indicate SD ($n = 3$). Different letters indicate significant differences ($P < 0.05$).

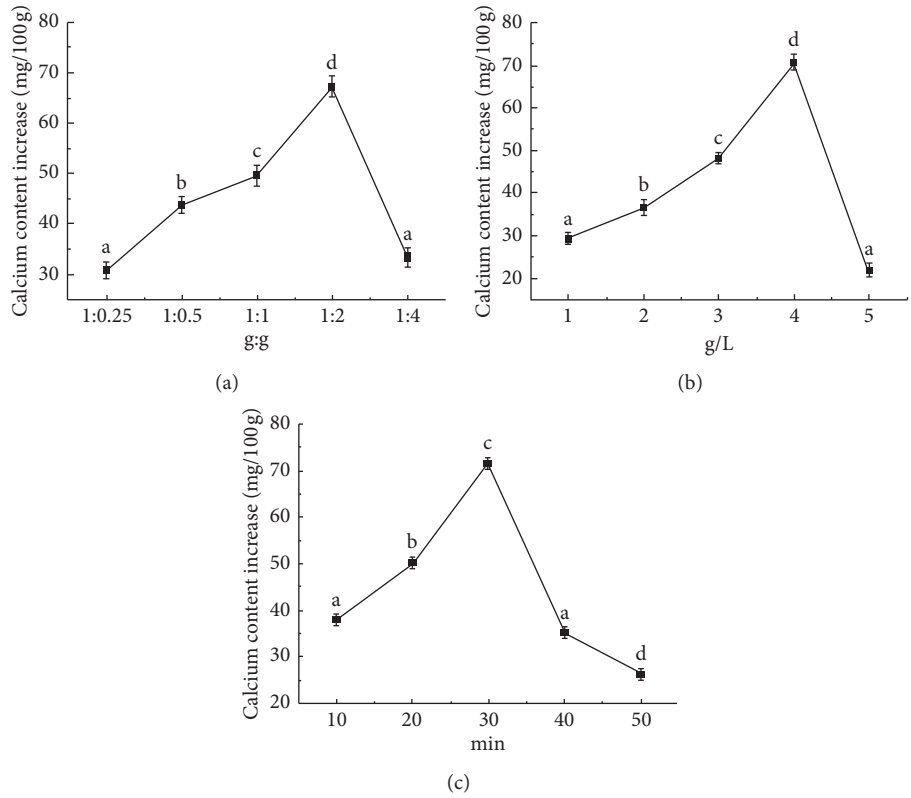

Figure 1: Effect of texture retaining agent (calcium chloride-sodium alginate (SA)) on calcium content increase of the *Heracleum moellendorffii* under different factors. (a) The effect of the ratio of calcium chloride to SA on the calcium content increase; (b) the effect of the concentration of the texture retaining agent on the calcium content increase; (c) the effect of the soaking time on the calcium content increase. Different letters within a line chart indicate significant differences ($P < 0.05$). Error bars indicate SD ($n = 3$).

brittleness and chewiness were usually used as the main indicators to evaluate the texture of HM (Prabhakaran et al., 2006). Brittleness is the force required to make HM cut off by incisors and chewiness is used to describe the force required when HM was chewed until swallowed.

The results of the effect of calcium chloride-SA compounding ratio on the texture of HM were listed in Table 2A. The results suggested the appropriate compound ratio was 1 : 2; at this time, the brittleness and chewiness of HM were the closest to the parameters of the fresh sample. This result corroborates the results of Figure 1. Thus, a suitable compound ratio of texture retaining agents can effectively keep the brittleness and chewiness which can be very close to fresh samples.

Also, it can be found that the changes in brittleness and chewiness were closely correlated with the changes in the concentration of texture retaining agents (Table 2B). As the concentration increased, the brittleness and chewiness of HM significantly increased ($P < 0.05$). When the concentration was 4 g/L, the calcium content increase was maximized. In contrast with the present study, Rico et al. noticed that appropriate calcium ion concentration can improve the shelf life of carrot by improving the texture quality of the sample [12]. Similarly, Gonzalez found that, after calcium ion treatment, there was a reduced disassembly of the structure (molecular network structure formed by calcium pectate gel) and also an improvement in brittleness and chewiness [26].

Table 2: Effect of texture retaining agent on the texture of the *Heracleum moellendorffii* under different factors.

Factor	Experimental group	Brittleness (gf)	Chewiness (gf)
A	1 : 025	2038 ± 84.31^{a}	1418.31 ± 50.89^{a}
	1 : 0.5	2521 ± 79.25^{b}	$1670.28 \pm 57.65^{a,b}$
	1 : 1	3044 ± 91.26^{c}	$1902.31 \pm 55.21^{b,d}$
	1 : 2	3810 ± 92.35^{d}	$2064.33 \pm 67.19^{c,d}$
	1 : 4	1077 ± 53.57^{e}	672.18 ± 34.11^{e}
B	1 g/L	1908 ± 67.32^{a}	927.61 ± 52.33^{a}
	2 g/L	2612 ± 73.89^{b}	1920.55 ± 70.13^{b}
	3 g/L	3726 ± 88.13^{c}	2187.92 ± 75.24^{c}
	4 g/L	4630 ± 87.26^{d}	2538.33 ± 81.60^{d}
	5 g/L	1911 ± 70.12^{a}	1101.65 ± 57.12^{e}
C	10 min	3067 ± 40.56^{a}	1556.36 ± 40.56^{a}
	20 min	3289 ± 58.22^{b}	1990.22 ± 52.24^{b}
	30 min	3890 ± 61.28^{c}	2278.15 ± 49.13^{c}
	40 min	$3301 \pm 52.36^{d,b}$	1817.64 ± 42.32^{b}
	50 min	2917 ± 48.27^{a}	1393.56 ± 48.69^{a}

[a]The texture retaining agent concentration factor experiment; [b]the proportional factor experiment of the texture retaining agent calcium chloride-sodium alginate; [c]the soaking time factor experiment. Error bars indicate SD ($n = 3$). Different letters indicate significant differences ($P < 0.05$).

An increase in soaking time improved the brittleness and chewiness of HM gradually until it reached 30 min. Sensory quality results after thawing were effective ($P < 0.01$). There was a positive correlation between soaking time and the activity of pectin methylesterase (PME). The higher the activity of PME, the more the calcium pectate gel formed in cells [27]. The presence of calcium pectate gel increased mechanical properties such as brittleness and chewiness due to the close connection between cells [28].

3.4. Analysis of the Correlation between Calcium Content, Brittleness, and Chewiness. The increase of calcium was used to express the chemical changes of HM and the texture of HM was represented by brittleness and chewiness, which together reflect the effect of texture retaining agent on HM. Thus, in this report, the correlation of calcium content, brittleness, and chewiness in the process of texture retaining of HM was investigated. As shown in Table 3, the correlation coefficient between calcium content, brittleness, and chewiness was 0.792, which was a significantly positive correlation ($P < 0.01$). The correlation coefficient between brittleness and chewiness was 0.930, which was a significantly positive correlation ($P < 0.05$). It can be explained that, in the process of texture retaining of HM, the change of calcium content was directly related to the brittleness and chewiness, and it also proved that the calcium content increase can enhance the brittleness and chewiness of HM. These effects showed that it is reasonable and feasible to select the change of calcium content, the crispness, and the chewiness index to evaluate the effect of the soaking of the HM before quick freezing on the crispness and chewiness after thawing. Further from both microscopic and apparent aspects, it reveals the mechanism and chemical essence of the texture retaining agent.

3.5. Microstructural Changes of HM under the Action of Texture Retaining Agent. Freezing can damage the organelles of stems and leaves of green plants, among which, chloroplast is a kind of organelle that is extremely sensitive to low temperature. In a low-temperature environment, the chloroplasts swell, causing disordered chloroplasts sorting and adhesion [29]. At the same time, the water in the cells forms ice crystals, which has a destructive effect on the cell membrane wall. After thawing, the cells lose water and shrink, which magnifies the problem of chloroplast sorting disorder and adhesion. The calcium pectate molecular gel adheres to the cell gap and supports the cell membrane wall, which can resist the mechanical damage of cells. Therefore, the microscopic observation method was used to observe and evaluate the changes in cell morphology before and after freezing treatment in Figures 2–5.

The changes in the position and state of chloroplasts in the cell walls and cell membrane of leaves epidermal cells [29] of HM were observed. Figures 2(a), 2(c), and 3(b) were not frozen and the untreated sample (Figure 2(a)) was a control group. The chloroplasts of each group were dispersed to the inner wall of the cells to varying degrees and were regularly granular. In contrast, the chloroplast morphology of frozen groups (Figures 2(b), 3(a), and 3(c)) changed to varying degrees, indicating that the freezing caused damage against the cells. Among them, Figure 3(a) only changed the chloroplasts of the cells with water soaking at 50°C, and the chloroplasts overflowed from the cells and adhered to the chloroplasts of other cells to form a network structure [30]. It indicated that the cell membrane and organelles were damaged by freezing after soaking in the water at 50°C [31]. Secondly, the chloroplasts of the cells aggregated in the fresh sample after freezing (Figure 2(b)) but no overflow occurred. In Figure 3(c), after 30 minutes of treatment by a 50°C texture retaining agent, the chloroplasts of cells were the smallest. Although there was some aggregation, the cell membrane structure was not destroyed and still observed to be granular. This result indicated that the addition of the texture retaining agent under the same condition can prevent the damage of the cell membrane and organelle caused by freezing, thereby affecting the texture of HM in nature.

In Figures 4 and 5, the changes in the position and state of chloroplasts in the cell walls and cell membrane of stems epidermal cells of HM could be observed by LSCM. Figures 4(b), 5(a), and 5(c) were frozen groups, and their chloroplasts had significantly more changes in the adhesion than the unfrozen group. In Figure 4(a), the chloroplasts were evenly dispersed in the inner wall of the cells and were regular particles. In contrast, although the chloroplasts in Figures 4(c) and 5(b) were dispersed in the inner wall in the form of particles, the degree of dispersion was not uniform. This was due to the strong peroxidase activity at 50°C, which caused an enzymatic reaction of chlorophyll in the cell [9, 32], resulting in a change in the degree of chloroplast dispersion. Among them, Figures 4(a), 4(c), and 5(b) were unfrozen groups, and the chloroplasts of the cells were dispersed in the cells with a

Table 3: Correlation analysis between calcium content increase, brittleness, and chewiness.

Index	Calcium content increase (mg/100g)	Brittleness (gf)	Chewiness (gf)
Calcium content increase (mg/100g)	1	0.792**	0.792**
Brittleness (gf)	0.792**	1	0.930**
Chewiness (gf)	0.792**	0.930**	1

**0.01 level (two-tailed), significant correlation.

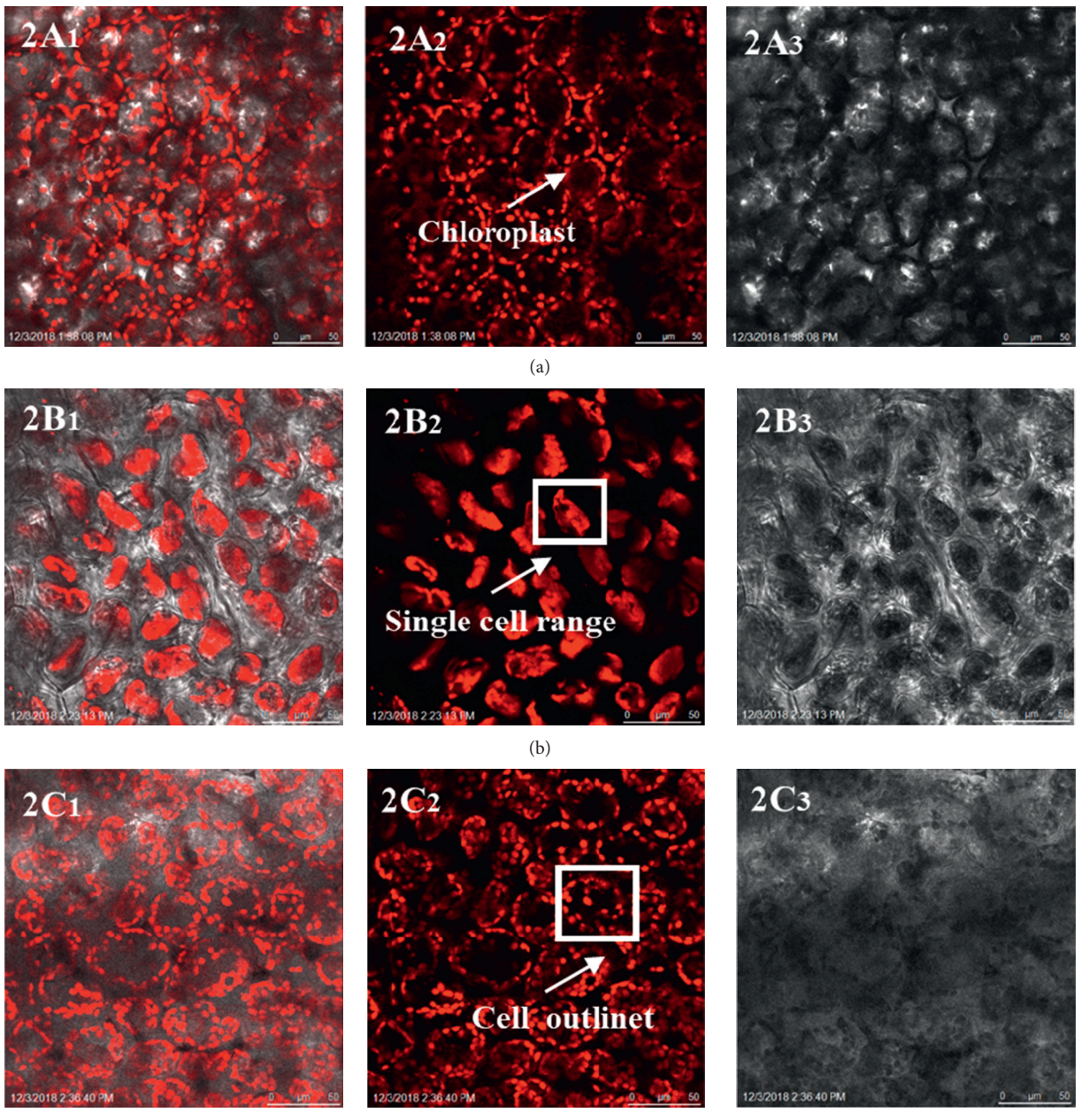

Figure 2: Microscopic observation of leaves epidermal cells of *Heracleum moellendorffii*. (a) A fresh sample; (b) a fresh sample after thawed; (c) a sample soaked in water at 50°C. The "index 1" represents the fluorescence and bright field superposition; the "index 2" represents the fluorescence; the "index 3" represents the bright field.

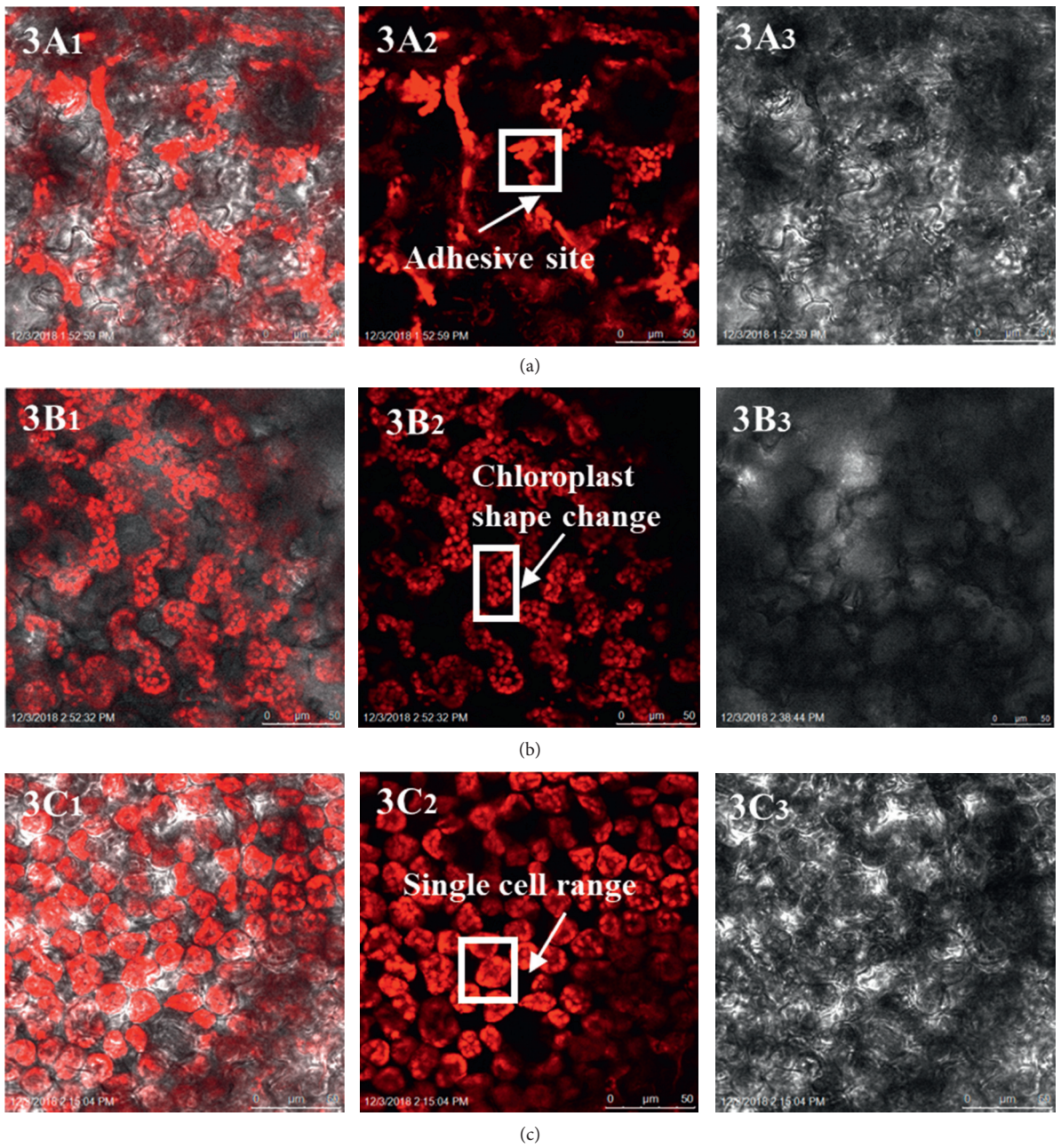

Figure 3: Microscopic observation of leaves epidermal cells of *Heracleum moellendorffii*. (a) A soaked sample in water after thawed; (b) a sample soaked with a texture retaining agent at 50°C; (c) a sample soaked with a texture retaining agent at 50°C after thawed. The "index 1" represents the fluorescence and bright field superposition; the "index 2" represents the fluorescence; the "index 3" represents the bright field.

granular shape. Among them, chloroplasts gathered but did not overflow, chloroplasts in Figure 5(a) overflowed from the cells and adhered to the chloroplasts of other cells to form a network structure, it showed that the cell membrane and cell wall were broken, the chloroplast in Figure 5(c) was the smallest, although there was a certain gather, the cell membrane structure was not destroyed, and the granular of chloroplasts could be observed. It meant that samples soaked by texture retaining agent before quick freezing could make the ice crystals in the cell fluid form quickly and small, which could prevent the cell membrane from damage. As can be seen from Figure 5(a), soaking in 50°C water caused the cell wall to rupture, which was more serious. This may be caused by a part of the chloroplasts overflowing into the water during the warm water treatment, and the texture retaining agent formed a gel network structure inside the texture to protect the chloroplast from overflowing [32]. Adding the texture retaining agent during soaking under the same conditions can reduce the rupture and damage of the cell

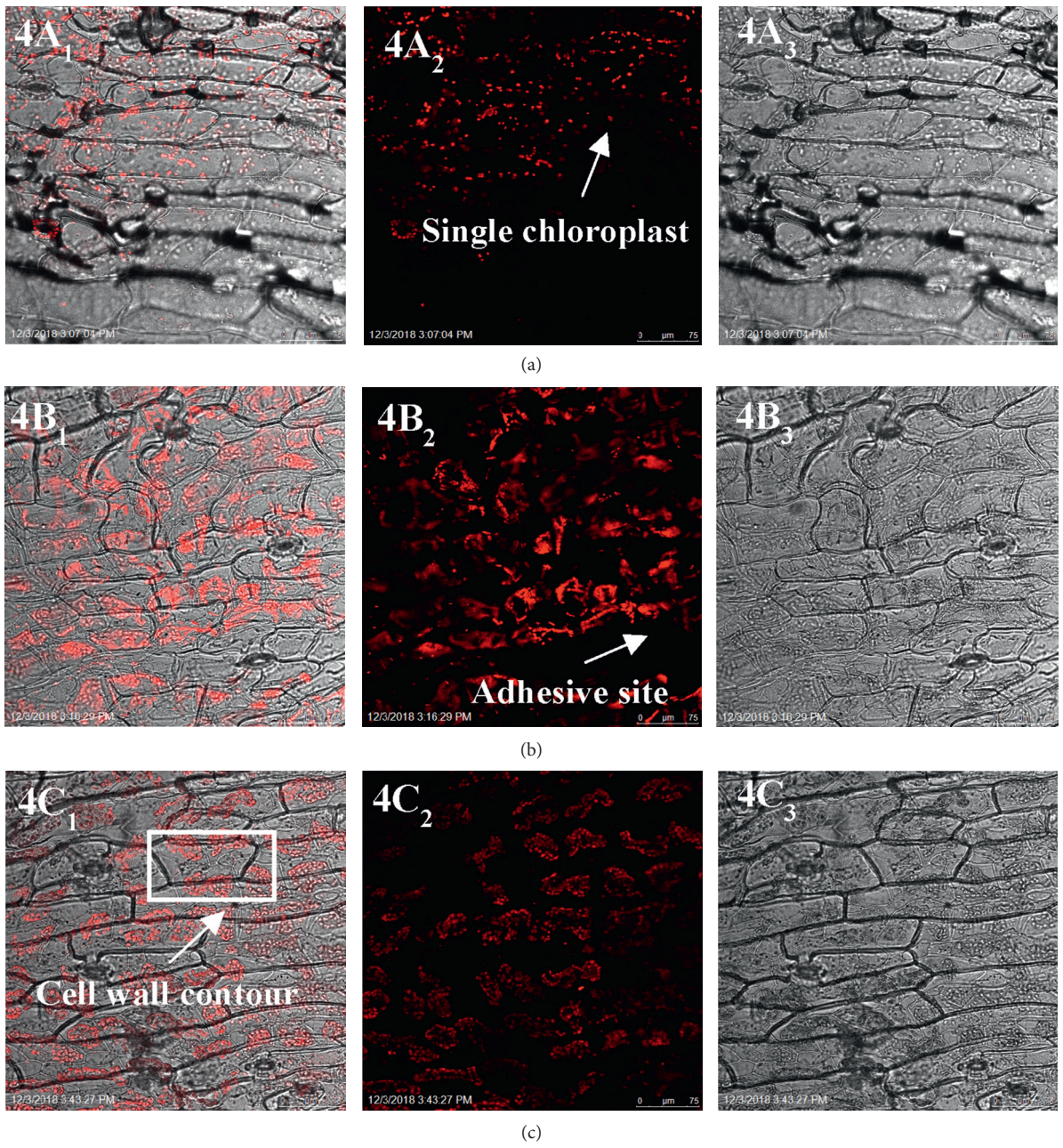

Figure 4: Microscopic observation of stems epidermal cells of *Heracleum moellendorffii*. (a) A fresh sample; (b) a fresh sample after thawed; (c) a sample soaked in water at 50°C; (d) a soaked sample in water after thawed; (e) a sample soaked with a texture retaining agent at 50°C; (f) a sample soaked with a texture retaining agent at 50°C. The "index 1" represents the fluorescence and bright field superposition; the "index 2" represents the fluorescence; the "index 3" represents the bright field.

membrane and cell wall caused by freezing. It showed that the compound SA-calcium chloride that formed calcium pectinate in the cells could enhance the support function of the cell wall and the ability to resist mechanical damage, thereby maintaining the brittleness and chewiness of HM to a certain extent in essence, and then had a significant positive effect on the texture of hill potherbs and the appearance of commodities.

In summary, changes in the position and adhesion between chloroplasts were microscopically observed in Figures 2 to 5. These results suggested the texture retaining agent had a synergistic effect on enhancing the brittleness and chewiness of HM. The microscopic gel material in the texture retaining agent was the key to enhancing the sensory quality. According to the experiments, it is the main reason to enhance sensory quality with the increased calcium content.

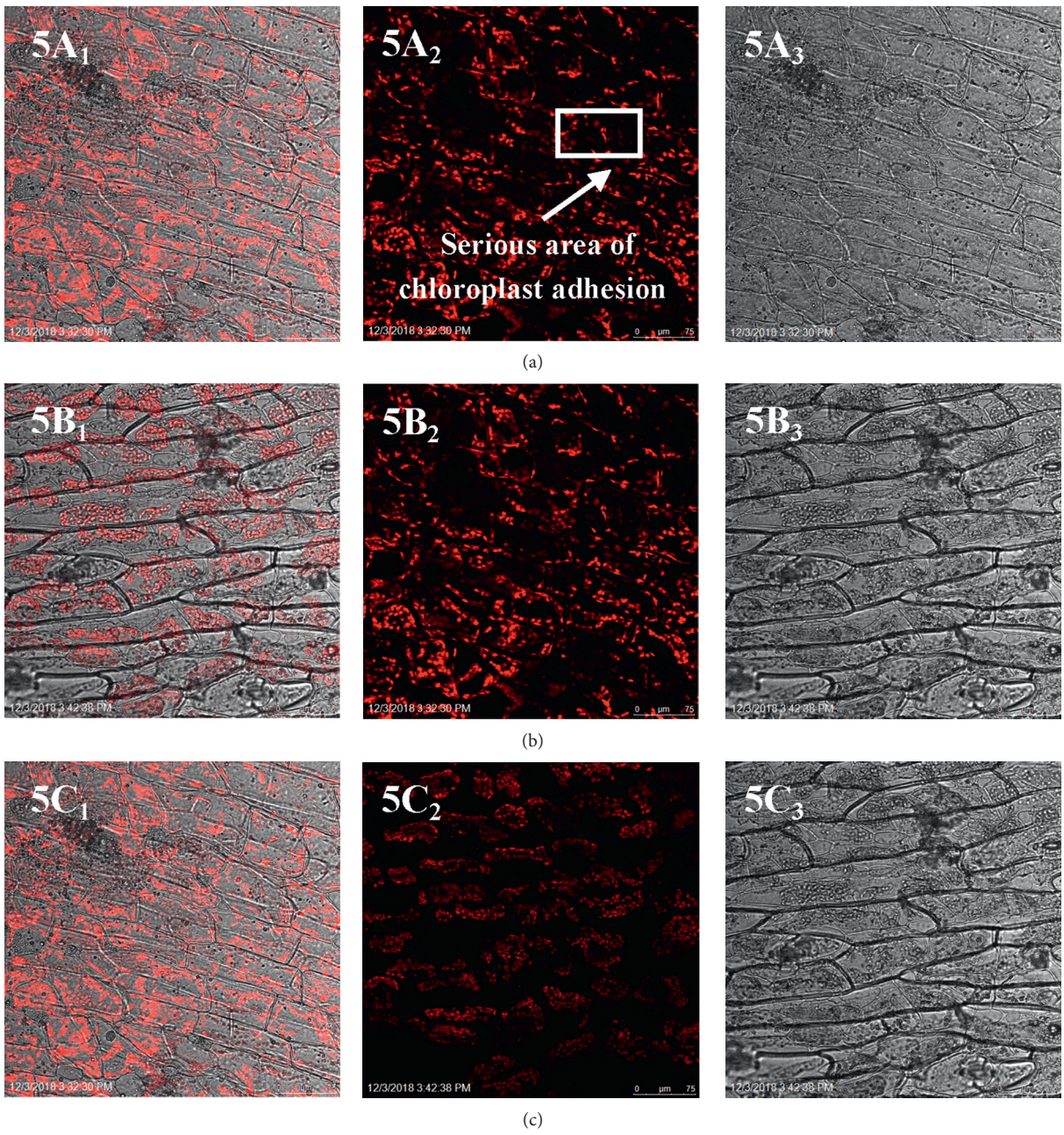

Figure 5: Microscopic observation of stems epidermal cells of *Heracleum moellendorffii*. (a) A soaked sample in water after thawed; (b) a sample soaked with a texture retaining agent at 50°C; (c) a sample soaked with a texture retaining agent at 50°C after thawed. The "index 1" represents the fluorescence and bright field superposition; the "index 2" represents the fluorescence; the "index 3" represents the bright field.

4. Conclusions

In this work, we selected a texture retaining agent and then determined its optimum treatment for HM, and the change of microstructure and sensory quality was analyzed. The calcium content increase was 71.56 mg in the 100g sample when the vegetable was soaking at 50°C for 30 minutes with a ratio of calcium chloride to SA (1 : 2). Correlation analysis showed that the microscopic calcium content increase was positively correlated with the brittleness and chewiness (correlation coefficient 0.792). Furthermore, the chloroplast morphology of the frozen group treated with texture retaining agent was well maintained. Most of the chloroplasts were in granular dispersion state, without overflow, with relatively small cell damage, suggesting that the texture (brittleness and mastication) was the closest to the fresh sample. The results confirmed that calcium chloride-SA can be used as a texture retaining agent during the quick-

freezing storage of HM, thereby providing an effective way to inhibit the texture change caused by frozen storage.

Data Availability

The authors confirm that the data supporting the findings of this study are available within the article.

Conflicts of Interest

The authors declare that they have no conflicts of interest.

Authors' Contributions

Xiao-mei Li and Yang Yang contributed equally to this work.

Acknowledgments

This work was financially supported by the National Natural Science Foundation (Grant nos. 32072258 and 31871747), the Major Science and Technology Program of Heilongjiang (Grant nos. 2019ZX08B02 and 2020ZX08B02), the Harbin University of Commerce "Young Innovative Talents" Support Program (Grant nos. 2019CX06 and 2020CX26), and the Central Financial Support for the Development of Local Colleges and Universities.

References

[1] M. Alam, B.-J. Seo, P. Zhao, and S.-H. Lee, "Anti-melanogenic activities of heracleum moellendorffii via ERK1/2-mediated MITF downregulation," *International Journal of Molecular Sciences*, vol. 17, no. 11, pp. 1844–1858, 2016.

[2] S. Liu, X. Jiang, Z. Liu, Y. Cheng, T. Sun, and X. Yu, "Mechanism of the breaking of seed dormancy by flower thinning in heracleum moellendorffii hance," *Journal of Plant Growth Regulation*, vol. 38, no. 3, pp. 870–882, 2019.

[3] S. Q. Diao, N. N. Zhu, and G. R. Sun, "Nutrients and processing characteristics of Spuriopimpinella brachycarpa (in Chinese)," *Journal of Northeast Forestry University*, vol. 38, pp. 48–50, 2010.

[4] H. Zhang, Y. Su, X. Wang et al., "Antidiabetic activity and chemical constituents of the aerial parts of Heracleum dissectum Ledeb," *Food Chemistry*, vol. 214, pp. 572–579, 2017.

[5] Y. Gao, Y. Liu, Z.-G. Wang, and H.-l. Zhang, "Chemical constituents of Heracleum dissectum and their cytotoxic activity," *Phytochemistry Letters*, vol. 10, pp. 276–280, 2014.

[6] M. Paciulli, T. Ganino, N. Pellegrini et al., "Impact of the industrial freezing process on selected vegetables - Part I. Structure, texture and antioxidant capacity," *Food Research International*, vol. 74, pp. 329–337, 2015.

[7] A. C. Dussault and E. Desaylniers, "Natural food," *Encyclopedia of Food and Agricultural Ethics*, vol. 80, no. September, pp. 1–11, 2013.

[8] T. Arunyanart, U. Siripatrawan, Y. Makino, and S. Oshita, "A new approach for the preservation of apple tissue by using a combined method of xenon hydrate formation and freezing," *Innovative Food Science & Emerging Technologies*, vol. 26, pp. 278–285, 2014.

[9] D. Li, Z. Zhu, and D.-W. Sun, "Effects of freezing on cell structure of fresh cellular food materials: a review," *Trends in Food Science & Technology*, vol. 75, pp. 46–55, 2018.

[10] D. J. Cosgrove, "Loosening of plant cell walls by expansins," *Nature*, vol. 407, no. 6802, pp. 321–326, 2000.

[11] Y. Karakurt and D. J. Huber, "Activities of several membrane and cell-wall hydrolases, ethylene biosynthetic enzymes, and cell wall polyuronide degradation during low-temperature storage of intact and fresh-cut papaya (Carica papaya) fruit," *Postharvest Biology and Technology*, vol. 28, no. 2, pp. 219–229, 2003.

[12] D. Rico, A. B. Martín-Diana, J. M. Frías, J. M. Barat, G. T. M. Henehan, and C. Barry-Ryan, "Improvement in texture using calcium lactate and heat-shock treatments for stored ready-to-eat carrots," *Journal of Food Engineering*, vol. 79, no. 4, pp. 1196–1206, 2007.

[13] A. Ortiz, J. Graell, and I. Lara, "Preharvest calcium applications inhibit some cell wall-modifying enzyme activities and delay cell wall disassembly at commercial harvest of 'Fuji Kiku-8′ apples," *Postharvest Biology and Technology*, vol. 62, no. 2, pp. 161–167, 2011.

[14] O. Yuliarti, S. Y. Chong, and K. K. T. Goh, "Physicochemical properties of pectin from green jelly leaf (Cyclea barbata Miers)," *International Journal of Biological Macromolecules*, vol. 103, pp. 1146–1154, 2017.

[15] G. Petzold, M. Caro, and J. Moreno, "Influence of blanching, freezing and frozen storage on physicochemical properties of broad beans (Vicia faba L)," *International Journal of Refrigeration*, vol. 40, pp. 429–434, 2014.

[16] E. Agcam, A. Akyıldız, and G. A. Evrendilek, "Effects of PEF and heat pasteurization on PME activity in orange juice with regard to a new inactivation kinetic model," *Food Chemistry*, vol. 165, pp. 70–76, 2014.

[17] D. B. Kiin-Kabari, S. Y. Giami, and B. Ndokiari, "Bioavailability of Mineral Nutrients in Plantain Based Product Enriched With Bambara Groundnut Protein Concentrate," *Journal of Food Research*, vol. 4, no. 4, pp. 74–80, 2015.

[18] M. S. Alamri, S. Hussain, A. Mohamed, and M. A. Osman, "Wheat flour solvent retention capacity, pasting and gel texture," *Quality Assurance and Safety of Crops and Foods*, vol. 8, no. 3, pp. 439–445, 2016.

[19] G. N. Chen, Z. F. Huang, R. Chen, J. Q. Lin, and L. J. Wang, "Fluorescence spectra and imaging of platymonas subcordiformis via LSCM (in Chinese)," *Spectroscopy and Spectral Analysis*, vol. 29, pp. 2330–2333, 2009.

[20] X. Guo, H. Duan, C. Wang, and X. Huang, "Characteristics of Two Calcium Pectinates Prepared from Citrus Pectin Using Either Calcium Chloride or Calcium Hydroxide," *Journal of Agricultural and Food Chemistry*, vol. 62, no. 27, pp. 6354–6361, 2014.

[21] Y. Wu, G. Zhao, C. Wei, S. Liu, Y. Fu, and X. Liu, "Effect of calcium chloride concentration on output force in electrical actuator made of sodium alginate gel," *IOP Conference Series: Materials Science and Engineering*, vol. 284, Article ID 012022, 2018.

[22] J. Ma, Y. Lin, X. Chen, B. Zhao, and J. Zhang, "Flow behavior, thixotropy and dynamical viscoelasticity of sodium alginate aqueous solutions," *Food Hydrocolloids*, vol. 38, pp. 119–128, 2014.

[23] T. E. Proseus and J. S. Boyer, "Calcium deprivation disrupts enlargement of Chara corallina cells: further evidence for the calcium pectate cycle," *Journal of Experimental Botany*, vol. 63, no. 10, pp. 3953–3958, 2012.

[24] P. Angeletti, H. Castagnasso, E. Miceli et al., "Effect of preharvest calcium applications on postharvest quality, softening and cell wall degradation of two blueberry (Vaccinium

corymbosum) varieties," *Postharvest Biology and Technology*, vol. 58, no. 2, pp. 98–103, 2010.

[25] R. Koshani, E. Ziaee, M. Niakousari, and M.-T. Golmakani, "Optimization of Thermal and Thermosonication Treatments on Pectin Methyl Esterase Inactivation of Sour Orange Juice (C itrus aurantium)," *Journal of Food Processing and Preservation*, vol. 39, no. 6, pp. 567–573, 2015.

[26] M. E. Gonzalez, J. A. Jernstedt, D. C. Slaughter, and D. M. Barrett, "Microscopic quantification of cell integrity in raw and processed onion parenchyma cells," *Journal of Food Science*, vol. 75, no. 7, pp. E402–E408, 2010.

[27] L. F. Goulao, J. Santos, I. de Sousa, and C. M. Oliveira, "Patterns of enzymatic activity of cell wall-modifying enzymes during growth and ripening of apples," *Postharvest Biology and Technology*, vol. 43, no. 3, pp. 307–318, 2007.

[28] D. Cantu, A. R. Vicente, J. M. Labavitch, A. B. Bennett, and A. L. T. Powell, "Strangers in the matrix: plant cell walls and pathogen susceptibility," *Trends in Plant Science*, vol. 13, no. 11, pp. 610–617, 2008.

[29] K. A. Fayez, D. E. M. Radwan, A. K. Mohamed, and A. M. Abdelrahman, "Fusilade herbicide causes alterations in chloroplast ultrastructure, pigment content and physiological activities of peanut leaves," *Photosynthetica*, vol. 52, no. 4, pp. 548–554, 2014.

[30] L. D. Bartolo, "Cell adhesion M//encyclopedia of membranes," 2014.

[31] T. Itakura, T. Suzuki, M. Watanabe, and H. Ando, "The influence of damage of cell membrane on softening of strawberry tissue due to freeze-thawing," *Acta Horticulturae*, vol. 1049, no. 1049, pp. 771–776, 2014.

[32] M. C. Beckerle, K. Burridge, G. N. Demartino, and D. E. Croall, "Colocalization of calcium-dependent protease II and one of its substrates at sites of cell adhesion," *Cell*, vol. 51, no. 4, pp. 569–577, 1987.

Hindawi
Journal of Food Quality
Volume 2021, Article ID 5571733, 12 pages
https://doi.org/10.1155/2021/5571733

Review Article

Antioxidative Stress Mechanisms behind Resveratrol: A Multidimensional Analysis

Tongyu Gu,[1] Nianmin Wang,[2] Tong Wu,[1] Qi Ge,[3] and Liang Chen [1]

[1]*School of Life Sciences, Jiangsu University, Zhenjiang 212013, Jiangsu, China*
[2]*School of Traditional Chinese Pharmacy, China Pharmaceutical University, Nanjing 211198, Jiangsu, China*
[3]*School of the Environment and Safety Engineering, Jiangsu University, Zhenjiang 212013, Jiangsu, China*

Correspondence should be addressed to Liang Chen; oochen@ujs.edu.cn

Received 11 January 2021; Revised 25 February 2021; Accepted 4 March 2021; Published 18 March 2021

Academic Editor: Shengbao Cai

Over the past decade, oxidative stress was shown to be a key factor for various diseases. The term "antioxidant" also rapidly gained attention worldwide, viewed as beneficial in disease prevention. Resveratrol (RSV), a natural polyphenol, is a plant antitoxin formed in response to harmful environmental factors such as infection and injury. This antitoxin is found in grapes, strawberries, peanuts, or herbal medicines and exhibits many pharmacological effects involved in antitumor, anti-inflammatory, antiaging, and antioxidation stress mechanisms. Recently, numerous *in vitro* and *in vivo* experiments have shown that RSV harbors antioxidative stress properties and can be used as an antioxidant. Here, we review the free radical scavenging ability, antioxidant properties, signaling pathways, expression and regulation of antioxidant enzymes, and oxidative stress-related diseases associated with RSV.

1. Introduction

Oxidative stress refers to an imbalance between the antioxidant defense system and the production of free radicals, leading to increased reactive oxygen species (ROS) and tissue damage. Possible consequences of oxidative damage result in diabetes mellitus [1], coronary heart disease [2], rheumatoid arthritis [3], and aging. Recently, a new article published in *Cell* uncovered that ROS accumulation in *Drosophila melanogaster* and mice with severe sleep deprivation caused oxidative stress, ultimately leading to death. However, this phenomenon is reversed by the administration of antioxidant compounds or by the targeted expression of antioxidant enzymes [4]. Even though it is unclear how the oxidative stress response triggers the disease, searching for a substance with antioxidant properties should be of focus to prevent the occurrence of diseases.

More recently, plant polyphenols have attracted the attention of many scholars. Plant polyphenols have been shown as beneficial to health by possessing antioxidant stress properties [5, 6]. In particular, resveratrol (RSV) has attracted a great deal of attention since it is a potential antioxidant that can be used in various applications. Numerous *in vivo* and *in vitro* experiments have shown that RSV exerts antitumor, anti-inflammatory, anticancer, antioxidant stress, and antiaging effects [7, 8]. The antioxidant effects of RSV were first discovered when treating cardiovascular diseases [9].

Presently, RSV has been shown to relieve cardiovascular, aging, and neurological diseases. However, RSV and its influence on diseases have not yet been systematically reviewed. Therefore, in this review article, we summarize the properties of RSV, signal pathways, and diseases related to oxidative stress to provide ideas for disease prevention.

2. Background

RSV is a secondary metabolite extracted from plant roots that contain multiple natural biological activities [10, 11]. Most RSV derives from the diet, such as grape products (red wine) [12], peanuts, and mulberries. The content of RSV is the greatest in grape wines, then chocolates, followed by peanuts, strawberries, and herbal medicines [13]. Even though RSV is abundant in fresh grape juice, it is susceptible

to degradation from heat exposure and processing. RSV exists in two forms including cis-resveratrol and trans-resveratrol (Figure 1). Under certain conditions, such as UV irradiation or low pH, the two isomers may convert into one another [14]. Generally, trans-resveratrol is more stable than cis-resveratrol.

Many studies have shown that RSV has both direct and indirect effects. RSV has been proved to be an effective antioxidant for scavenging free radicals, including superoxide radical (O^{2-}), hydroxyl radical (OH^-), hydrogen peroxide (H_2O_2), nitric oxide (NO), and nitrogen dioxide (NO_2) [15–18]. Based on its chemical structure, such as hydroxyl group on the ring and conjugated double bond system, RSV was proved to be an antioxidant. Wang et al. reported that replacing the hydrogen in three hydroxyl groups with CH_3 or removing the hydroxyl group leads to reduced antioxidant activity, indicating that $4'$ hydroxyl activity is essential [19, 20]. Another study analyzing the structure of RSV confirmed this observation [21]. The existence of a conjugated double bond can make the electron more delocalized [22]. Hydrogen atom transfer (HAT) and sequential proton loss electron transfer (SPLET) are the main mechanisms of RSV scavenging free radicals [23]. Based on crystal structure and ab initio calculation experiment, it was found that dynamic flip-flop motion could lead to the alternate formation of hydroxyl groups and break hydrogen bonds on adjacent phenolic oxygen, which can transfer up to three hydrogen atoms. The results indicated that the free radical scavenging activity of RSV was based on HAT [24]. The electrons are transferred to the free radicals by the HAT process to form phenoxy radicals, which can delocalize unpaired electrons on the whole molecule. The unpaired electrons of resveratrol radical are located at the position of 3, and 5 hydroxyl groups near position 4 were more stable, resulting in the formation of RSV quinone structure. After tautomerism rearrangement and intracellular nucleophilic attack on intermediate quinone, a dihydrofuran dimer was produced [25]. Leonard et al. used the ESR spin trap technique to measure hydroxyl radicals generated by the Fenton reaction as well as superoxide radicals produced by the xanthine/xanthine oxidase system to find that RSV reduced DMPO/OH^- and DMPO/O^{2-} in a concentration-dependent manner, proving that it has the ability to scavenge OH^-/O^{2-} [26]. Compared with butylated hydroxytoluene (BHT), butylated hydroxyanisole (BHA), tocopherol, and trolox, RSV has the activity of scavenging H_2O_2 *in vitro*, but its effect is lower than that of the standard [27]. Scavenging NO free radical is through a non-free radical mechanism and has a higher scavenging efficiency compared with catechin [17]. Combining with metal ions can exert its chelating activity and prevent an excessive generation of hydroxyl radicals and further oxidation [22]. Other studies showed that RSV scavenges free radicals using endogenous antioxidant enzymes [19, 28]. Among them, NADPH oxidase (O^{2-}), xanthine oxidase (O^{2-} and H_2O_2), mitochondrial respiratory chain enzyme (O^{2-}), and endothelial functional nitric oxide synthase (eNOS) (NO) can cause ROS production [29]. Endogenous antioxidant enzymes, as an antioxidant defense system, can effectively remove ROS and reduce the production of mitochondrial superoxide [30].

Currently, the fast absorption and low bioavailability of RSV are some disadvantages of using it in the clinic. In clinical trials, 25 mg of RSV showed a 70% absorption rate in 1 hour, with peak plasma metabolite levels reaching 2 μM. However, the bioavailability of RSV was only 1% [31]. This occurs since absorbed RSV easily combines with glucuronic acid or sulfate in the intestines or liver [32]. Therefore, the bioavailability of RSV needs to be improved in the future.

3. Antioxidative Stress Effects Associated with RSV

3.1. RSV and Free Radicals. Under normal conditions, antioxidant enzymes, such as catalase, superoxide dismutase, and glutathione-S-transferase, remove ROS produced during mitochondrial oxidative respiration. ROS are divided into free radicals (O^{2-} and OH^-) and non-free radicals (H_2O_2) [33]. However, when there is stimulation by harmful factors, such as ultraviolet radiation and chemical reagents, defense systems are damaged and contribute to excessive ROS accumulation, leading to an imbalance in oxidative stress [34]. In H_2O_2 and O^{2-} free radical activity scavenging experiments, the scavenging efficiency of 30 μg/mL of RSV reaches 19.5% and 71.8% for H_2O_2 and O^{2-}, respectively, indicating that RSV had a strong efficiency for free radical scavenging [27]. Palsamy et al. reported streptozotocin-(STZ-) induced oxidative stress in diabetic rats where O^{2-} and OH^- levels in the kidney were relatively high and significantly reduced after RSV administration, indicating that RSV effectively scavenged free radicals [35]. As reported in another paper, neurotoxin 1-methyl-4-phenyl-1.2.3.6-tetrahydropyridine (MPTP) induces oxidative stress in *Drosophila melanogaster*, leading to an accumulation of H_2O_2. However, when different concentrations of MPTP and RSV were administered together, H_2O_2 content significantly decreased, implying that it contains free radical scavenging properties [36]. Hence, it is important to eliminate excessive free radicals to balance oxidative stress levels and to reduce oxidative damage.

3.2. RSV and Lipid Peroxidation. When oxidative stress occurs, excessive ROS levels attack polyunsaturated fatty acids on cell membranes, resulting in liposome peroxidation and lipid peroxides [37]. Malondialdehyde (MDA), a major product of lipid peroxidation, is also an important indicator of measuring the degree of cell damage. Manna et al. pretreated U-937 cells with 5 μM of RSV for 4 h and then incubated cells with different concentrations of tumor necrosis factor (TNF) for 1 h. Results showed that TNF-induced lipid peroxidation in U-937 cells but RSV and TNF cotreatment completely inhibited lipid peroxidation [38]. Another study found that RSV inhibited lipid peroxidation more effectively than the antioxidant vitamins C and *E*, which was attributed to its high lipophilicity and hydrophilicity [39–41]. Palsamy et al. investigated levels of lipid peroxidation in healthy rats treated with RSV, rats with STZ-induced diabetes, and

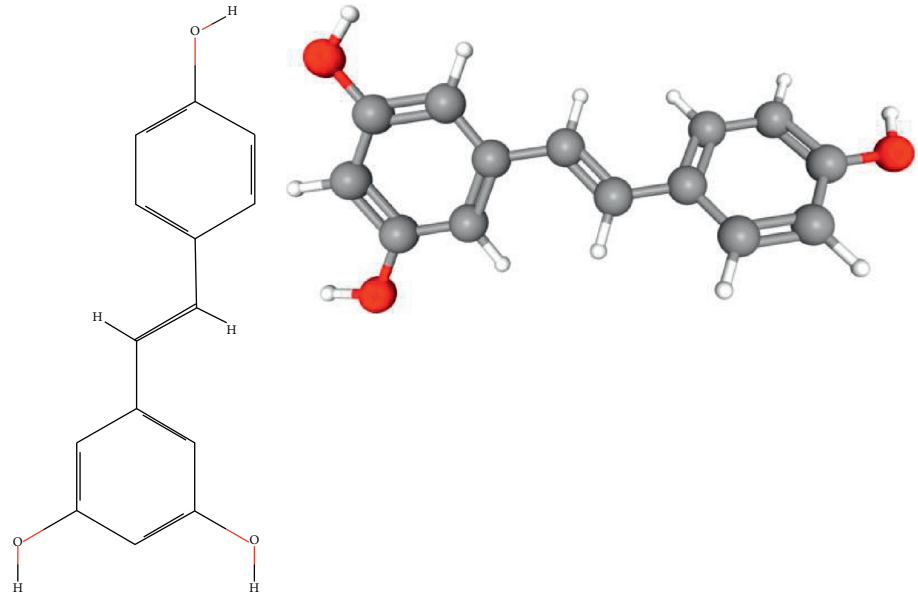

(a) (b)

Figure 1: The structure of resveratrol. (a) Chemical formula. (b) 3D structure diagram.

diabetic rats treated with RSV. Data revealed no significant differences in the RSV group and that MDA content in the diabetic group increased but then significantly decreased after the administration of RSV and eventually reached normal levels. This indicated that RSV inhibited lipid peroxidation induced by STZ [35]. These findings indicate that RSV has inhibitory properties on lipid peroxide formation.

3.3. RSV and Antioxidant Enzymes. The antioxidant system is mainly composed of antioxidant enzymes and nonenzymatic compounds [42]. Antioxidant enzymes include superoxide dismutase (SOD), catalase (CAT), and glutathione peroxidase (GPx). SOD and CAT are key scavengers for O^{2-} and H_2O_2 and are the first defense system in cells [43]. Superoxide dismutase (SOD) converts O^{2-} to hydrogen peroxide and then CAT or GPx degrades it into oxygen and water. When 35% ethanol was administered to mice for 6 weeks, MDA production was increased in the liver, and SOD, CAT, GPx, and other enzymatic activities were reduced. However, when 5 g/kg of RSV was added daily during ethanol treatment, MDA synthesis was inhibited and antioxidant enzymatic activity improved [44]. Chen et al. used C57BL/6J mice to confirm that RSV alleviated ethanol-induced oxidative stress and found that it enhanced SOD activity in HepG2 cells but did not affect CAT and GPx activities [45]. Nonenzymatic compounds mainly include glutathione (GSH), which directly scavenges free radicals or acts as a cofactor for glutathione-S-transferase. The ability to resist oxidative stress weakens if GSH content decreases [46, 47]. Liu et al. explored apoptosis of human umbilical vein endothelial cells (HUVECs) induced by hydrogen peroxide. RSV administration increased HUVEC activity and SOD significantly increased GSH content [48]. RSV significantly improves the activity of certain antioxidant enzymes and reduces damage caused by oxidative stress. Thus, RSV should be used in research revolving around the treatment of various diseases.

4. Antioxidant Stress Mechanisms of RSV

All organisms contain a complex antioxidant system, making it difficult to identify the exact molecular mechanisms behind RSV and its antioxidant mechanisms [49]. Findings indicate that RSV exerts its antioxidant stress characteristics mainly through several signal pathways and also activates antioxidant enzymes in these pathways. Table 1 summarizes the application of RSV antioxidant properties in the treatment of diseases. We will now highlight the important signal pathways associated with RSV.

4.1. Nrf2 Signaling Pathway. Nuclear factor-erythroid 2-related factor 2 (Nrf2) is a transcription factor that regulates the expression levels of antioxidant genes and protects cells from oxidative stress damage. The antioxidant effects linked to this pathway are linked to the activation of genes containing antioxidant response elements (ARE) [68]. Kelch-like ECH-associated protein *l* (KEAP1) is a regulatory protein that controls the activity of Nrf2. In the absence of external stimulation, Nrf2 is in the cytoplasm and binds to inactivated KEAP1. When ROS accumulates, there are conformational changes in KEAP1, making it disassociate from Nrf2 and translocate into the nucleus [69]. Musculoaponeurotic fibrosarcoma (Maf) protein forms a heterodimer with Nrf2 and then combines with ARE to enhance the expression of downstream phase II antioxidant genes, producing antioxidant enzymes [70]. The function of proteins produced by the activation of the Nrf2/ARE pathway is mainly to remove ROS as well as exogenous/endogenous

Table 1: Summary of the application of RSV antioxidant properties in the treatment of diseases.

Model	Types	Treatment time/ Dosage/Feeding regime	Disease	Beneficial effects	Mechanisms	Reference
Animal	Nonobese GK rats	10 weeks 20 mg/kg/day Intragastrical injection	Type 2 diabetes	MDA content ↓. Serum GPx activity ↓. Liver CAT activity ↓	Activated NF-κB signaling pathway	[50]
	Male SD rats	48 hours 10 mg/kg/day Intraperitoneal injection	Ischemic reperfusion injury	NOx, MDA content ↓. SOD, GSH, CAT activity ↑	Activated p38/MAPK	[51]
	Male Wistar rats	20 days 10 mg/kg/day Oral gavage	Periodontitis	iNOS expression ↓. OHdG expression ↑. NOx and nitrotyrosine formation ↓	Activated the SIRT1/ AMPK pathway	[52]
	Male Wistar albino rats	3 weeks 200 mg/kg/day Oral gavage	Rotenone-induced Parkinson	Striatal DA level ↑. CHOP, GRP78 mRNA expression ↓. Striatal caspase-3, xanthine oxidase activity ↓. Striatal IL-1β, PC levels ↓. Glutathione peroxidase activity ↑	Activated Nrf2/ antioxidant defense pathway	[53]
	Male Wistar rats	15 days 20 mg/kg/day Introgastric gavage	OHDA-induced Parkinson	TBARS, protein carbonyl levels ↓. Phospholipase A2 activity ↓. GPx, GR, CAT, and SOD activity ↑. COX-2 expression ↓	Activated Nrf2 signaling pathway	[54]
	C57BL/6 mice	24 hours 40 mg/kg/day Oral gavage	Aging	Nox2 and Nox4 expression ↓. SOD1 and SOD2 expression ↑	Activated AMPK and SIRT1	[55]
	Male ApoE-KO mice	7 days 30/100 mg/kg/day Oral gavage	Cardiovascular diseases	SOD1, SOD2, SOD3, CAT, GPx1 mRNA expression ↑. Nox2 and Nox4 expression↓. 2-HE and ethidium ↓. MDA and 3-nitrotyrosine ↓. GCH1 mRNA expression ↑	Activated SIRT1	[56]
	Male SAM	5 days 25/50/100 mg/kg/day Introgastric gavage	Aging	SOD activity ↑. SOD mRNA expression ↑. Gpx activity ↑MDA level ↓ mtDNA deletion ↓		[57]
	Adult male Wistar rats	10weeks 5/10/20 mg/kg/day Oral gavage	Alcohol-induced cognitive deficits	Acetylcholinesterase activity ↓. Nitrite level ↓. Lipid peroxide ↓. GSH, SOD, CAT activity ↑. TNF-a, IL-1β, NF-kβ, caspase-3 levels ↓		[58]
	Female Wistar rats	16 weeks 250 mg/kg/day Oral gavage	Alcoholic liver disease	Liver AST, ALT levels ↓ CAT, GPx enzyme activity ↑. MDA level ↓. CYP2E1 protein expression ↓. Caspase 3 activity ↓SOD1, SOD2, SOD3, CAT, GPx mRNA expression ↑		[59]
	Male Zucker rats	6 weeks 15/45 mg/kg/day Oral gavage	Nonalcoholic fatty liver disease	MDA level ↓. GSH/GSSH ↑. SOD activity ↑. ACO, CPT-Ia activity ↑		[60]

Table 1: Continued.

Model	Types	Treatment time/ Dosage/Feeding regime	Disease	Beneficial effects	Mechanisms	Reference
Cell	HT22 cell	12 hours 2.5-10 μM Not given	Glutamate-induced (2mM) Alzheimer and Parkinson	HO-1 expression ↑. The cytoprotective of HT22 cells ↓	Activated SIRT1 signaling pathway	[61]
	Oocytes	12 hours 0.5/1/5 μM Not given	Doxorubicin-induced compromised fertility	ROS level ↓. CAT, Sod1, Gpx3 mRNA levels ↑. DNA damage ↓		[62]
	Bronchial epithelial cell	7 days 100 mg/kg/days Intraperitoneal injection	HDM-induced asthma	Cell apoptosis ↓. ROS level ↓	Elevated the expression of SIRT1	[63]
	Metaphase II oocytes	15 days 50 mg/kg/day Intraperitoneal injection	Postovulatory oocyte aging	ROS level ↓. MtDNA copy number ↓. Mitochondrial function ↑	Coordinated SIRT1 and AMPK signaling pathways	[64]
	Vascular smooth muscle cells	24 hours 0-100 μM Not given	Age-related vascular disease	SM2-MHC protein expression ↑. Contractile capacity ↑		[65]
	Neuroblastoma (N2a) cells	48 hours 5 μM Not given	Alzheimer	Peroxiredoxins mRNA expression ↑. H_2O_2 level ↓. ATP level ↑. Lipid peroxidation production ↓	Activated Nrf2	[66]
	Human bronchial epithelial cells	24 hours 10 μM Not given	PQ-induced pulmonary fibrosis	Cell death, ROS production, mitochondrial damage ↓ TNFα, IL-6, TGFβ1 ↓		[67]

Abbreviation: MDA: malondialdehyde; GPx: glutathione peroxidase; CAT: catalase; NOx: nitrogen oxides; SOD: superoxide dismutase; GSH: glutathione; iNOS: nitric oxide synthase; OHdG: 8-hydroxy-2 deoxyguanosine; DA: dopamine; CHOP: C/EBP homologous protein; GRP78: glucose-regulated protein 78; PC: protein carbonyl Nox2: NADPH oxidase 2; Nox4: NADPH oxidase 4; SOD1: superoxide dismutase 1; SOD2: superoxide dismutase 2; 6-OHDA: 6-hydroxydopamine; TBARS: thiobarbituric acid reactive substances; GR: glutathione reductase; COX-2: cyclooxygenase-2; SM2-MHC: smooth muscle myosin heavy chain; ROS: reactive oxygen species; mtDNA: mitochondrial DNA; IL-1β: interleukin-1β; ApoE-KO: apolipoprotein *E* knockout; GCH1 : GTP cyclohydrolase 1 2-HE: 2-hydroxyethidium; HO-1: heme oxygenase; SAM: senescence-accelerated mice; H_2O_2: hydrogen peroxide; CYP2E1: cytochrome; P450 2E1 AST: aspartate aminotransferase; ALT: alanine aminotransferase; TNF: tumor necrosis factor; ACO: acyl-coenzyme A oxidase; CPT-Ia: carnitine palmitoyltransferase-Ia; PQ: paraquat; TGF: transforming growth factor; ↑: upregulation; ↓: downregulation.

harmful substances. Studies have demonstrated that RSV activates Nrf2 through cell signal pathways such as PI3K/AKT and AMPK. Iwasaki et al. found that RSV mitigates T-cell apoptosis induced by H_2O_2. RSV results in phosphorylation of Ser9 glycogen synthase kinase 3β (GSK3β) by activating AMP-activated protein kinase (AMPK) and induces the expression of Nrf2/ARE-dependent antioxidant genes, such as heme oxygenase-1 (HO-1) [71]. RSV also protects against PC12 cell death induced by H_2O_2, mainly through the activation of ERK and Akt, causing Nrf2 nuclear translocation and upregulation of HO-1 expression [72]. Another study revealed that cigarette smoke induces oxidative stress in alveolar epithelial cells, where RSV protects cells from damage through the activation of Nrf2, upregulation of glutamate-cysteine ligase (GCL) expression, and induction of GSH [73]. At the same time, studies have shown that Nrf2 plays a crucial role in the oxidative stress response to atherosclerosis [74], ischemia-reperfusion injury [75], and hypertension [76]. Even though there is work revealing that RSV activates Nrf2 and induces the expression of downstream antioxidant enzyme genes, these interactions are complex and warrant further investigation.

4.2. NF-κB Signaling Pathway. NF-κB is a nuclear transcription factor that binds to the κB site of the kappa light chain gene of B cells [77]. It is mainly involved in regulating the expression of genes during inflammation and apoptosis. Currently, various diseases, such as diabetes and cancer, are associated with dysregulation of NF-κB expression [78, 79]. Activation of the NF-κB pathway is mainly regulated by ROS [78], which has been verified in mice with type 2 diabetes. Activated NF-κB promotes the expression of proinflammatory cytokines, such as cyclooxygenase-2 (COX-2) and tumor necrosis factor-α (TNF-α) [80, 81]. RSV inhibits TNF and H_2O_2-induced NF-κB activation in a dose- and time-dependent manner, all of which were confirmed in different cell lines, including U937, Jurkat, and L4 cells [38]. Soufi et al. investigated STZ-induced diabetic male Wistar rats and administered 5 mg/kg of RSV daily for 4 weeks to determine antioxidative stress properties. Results revealed that RSV increased SOD activity, decreased the GSSH/GSH ratio, and significantly reduced retinal NF-κB activity and the apoptosis rate compared to diabetic control rats [82]. Therefore, effective regulation of NF-κB activity is essential and studies behind the effects of RSV on this pathway are worthy of future work.

4.3. SIRT1 Signaling Pathway. Identification and analysis from *in vivo* and *in vitro* studies have confirmed that sirtuins play a significant role in many cellular functions. A total of seven sirtuins have been identified in mammals. SIRT1 is involved in cell function regulation and depends on NAD^+ to regulate the deacetylation of different proteins, such as histones, p53, and FOXO [83–85]. Studies have shown that these seven sirtuins are involved in antioxidant stress and metabolic processes [86, 87], where DNA damage repair and protective effects of cell stress damage are mediated by SIRT1, SIRT2, and SIRT6 [87]. Some studies illustrated that RSV does not directly activate SIRT1 but inhibits cAMP to make phosphodiesterase nondegradable, leading to AMPK activation, an increase in NAD^+ levels, and SIRT1 activation [88]. Ungvari et al. reported the effects of RSV on hyperglycemia-induced mitochondrial oxidative stress in human coronary artery endothelial cells (CAECs). This work revealed that mtROS production and hydrogen peroxide levels were significantly reduced and MnSOD expression levels, GSH content, and SIRT1 activity were increased. Furthermore, the overexpression of SIRT1 diminished mtROS production and increased MnSOD expression. This effect was weakened after SIRT1 knockout [89]. Another work investigated the protective effects of RSV on Tilapia under low temperature stress. Findings revealed that mRNA expression levels of sirtuin homologs (sirt1, sirt2, sirt3, sirt5a, and sirt6) increased and catalase (cat), uncoupling protein 2 (ucp2) and superoxide dismutase (sod1, sod2, and sod3) levels were also increased [90]. SIRT1 primarily responds to oxidative stress by regulating FOXO transcription factors (such as FOXO1, FOXO3a, and FOXO4) and PGC-1a regulators, which form transcription complexes to enhance the expression of antioxidant enzymes and to scavenge ROS [91]. Furthermore, there may be an overlap or interaction between the activities of SIRT1 and NF-κB [92]. Regulation of SIRT1 signaling involves FOXO and PGC-1a, but the interaction between SIRT1, NF-κB, and Nrf2 signaling pathways has not been clearly identified (Figure 2). Thus, this aspect still needs further work in order to provide optimal solutions for disease treatment.

5. RSV and Oxidative Stress-Related Diseases

5.1. Neurodegenerative Diseases. The most common neurodegenerative diseases include Alzheimer's disease (AD) and Parkinson's disease (PD). By 2016, a total of 43.8 million people were diagnosed with dementia where 60% were caused by AD and 6 million were suffering from PD [93, 94]. According to statistics from Ray Dorsey and Nichols, 6.4 million and 3.2 million people passed away from dementia (including AD) and PD, respectively, in 2016 [94, 95]. Both AD and PD not only cause significant damage to health but also impact the social economy. Presently, there are both pharmacological and nonpharmacological treatments available for these diseases, but there is currently no cure [96]. Additionally, AD and PD are associated with oxidative damage and inflammation, so much research is concentrated on the therapeutic potential of antioxidants, such as RSV [97].

Oxidative stress is the most critical factor in the pathogenesis of AD. ROS accumulation leads to a decrease of antioxidant defense capacity and mitochondrial dysfunction, which ultimately causes neuronal damage. The neuroprotective effects of RSV have been proven in several AD models and are associated with increased SIRT1 activity [98–100]. RSV increases mRNA expression levels of CAT, SOD1, GST zeta 1, and SIRT1 as shown in lymphoblastic cell lines (LCLs) isolated from AD patients [101]. Learning and memory in rats with vascular dementia were explored by

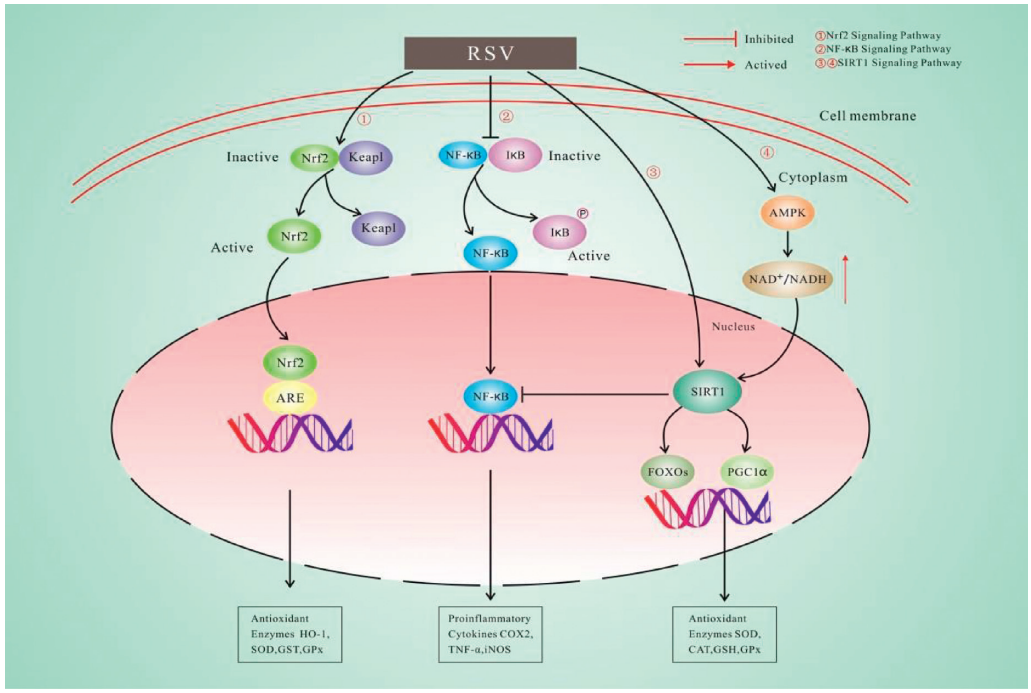

Figure 2: The signaling pathway of resveratrol to exert antioxidant properties.

Zhang et al., who found that SOD protein expression levels increased and MDA content decreased [102].

Mitochondrial dysfunction and oxidative stress are also causative factors in PD. The accumulation of oxidative stress caused by ROS can lead to neuronal death. Lindner et al. prepared RSV-loaded polysorbate80 (PS80) nanoparticles to observe the neuroprotective effects in PD mice. Results supported that the nanoparticle RVT reduced lipid peroxidation [103]. However, thus far, there are no clinical trials being performed investigating its safety. Therefore, efforts need to be made to fully understand the efficacy and safety of RSV for the treatment of AD and PD.

5.2. Aging. Aging is a programmed biological process caused by the interaction of genetic factors and adverse environmental factors. It is accompanied by changes such as increased inflammation, increased ROS, and mitochondrial function damage, as well as related chronic diseases. Among these, oxidative stress is one of the main causes of aging. RSV has been illustrated to extend lifespan in different animal models [104]. *In vitro* experiments showed that SIRT1 is associated with aging. In the H_2O_2-induced oxidative stress aging model, SIRT1 mRNA expression levels decreased and increased in a dose-dependent manner after RSV administration. In addition, the aging marker β-galactosidase also decreased [105]. Studies have also shown that RSV effects depend on the expression of antioxidant genes. Using RNAi technology to knock out SOD1 in *Drosophila melanogaster*, 200 μM of RSV increased the lifespan of female Sod1 RNAi flies to 9% under a standard diet [106]. Others believe that AMPK is the culprit of aging, since AMPK may activate FOXO and Nrf2 and inhibit NF-κB [107]. Afzal et al. found that various stress responses were induced in PREP cells, ROS levels decreased, and antioxidant capacity increased, indicating that RSV has potential in protecting cells from injury stress and also has potential in prolonging the lifespan. Furthermore, HP1γ, a marker of cell senescence, was significantly downregulated in treated cells [108]. Altogether, the antiaging properties of RSV are being thoroughly studied. Even though its clinical safety and efficacy have not yet been proven, RSV shows bright prospects in terms of antiaging strategies.

6. Conclusion

Over the past decade, the term "antioxidation" has become a hot topic on the Internet. Presently, the cosmetics and health care industries sell products using the term "antioxidant" in their ingredients. A polyphenol compound with natural activity, RSV shows the most potential and is a valuable commodity, as validated in various animal models. The antioxidant stress properties associated with RSV have been described in numerous animals and cell experiments [36, 80]. This article summarized the antioxidative stress properties of RSV, providing evidence that it can be used as a food additive that prevents disease and maintains health. Studies have shown that the basal diet supplemented with 400 mg/kg RSV can significantly improve feed utilization and growth performance of broilers [109]. The supplementation of 300 mg/kg and 600 mg/kg of RSV in the basic diet can significantly improve the activity of lactate

dehydrogenase, GPx activity, and its mRNA level, reduce MDA content, and improve the total antioxidant capacity of finishing pigs [110]. 25 mg of RSV from *Vitis vinifera*, taken as a standard dietary supplement for 12 weeks, was found to improve the quality of life associated with menopause in healthy women [111]. However, the low bioavailability of RSV is a property that needs to be further improved. Currently, many studies have confirmed that RSV nanoparticles have a greater ability to scavenge active free radicals (DPPH and ABTS+) and higher bioavailability and can further promote intestinal absorption. Li et al. synthesized a series of pyridoxine-resveratrol hybrids, where 12a, 12g, and 12l have better antioxidant activities and strong inhibitory effects on MAO-B, providing treatment direction of PD [112]. Fan et al. prepared RES-PPI nanoparticles to find that RSV enhanced thermal stability and did not degrade. In addition, its ability to remove DPPH and ABTS was enhanced [113]. This research broadens the application of RSV, but there are many problems that need to be solved before it can be used in the treatment of humans.

Abbreviation

RES: Resveratrol
ROS: Reactive oxygen species
ESR: Electron spin resonance
DMPO: 5,5-Dimethyl-1-pyrroline-N-oxide
H_2O_2: Hydrogen peroxide
SOD: Superoxide dismutase
CAT: Catalase
GPx: Glutathione peroxidase
MPTP: Methyl-4-phenyl-1.2.3.6-tetrahydropyridine
MDA: Malondialdehyde
TNF: Tumor necrosis factor
GSH: Glutathione
Nrf2: Nuclear factor-erythroid 2-related factor 2
ARE: Antioxidant response elements
KEAP1: Kelch-1ike ECH-associated protein l
AMPK: AMP-activated protein kinase
HO-1: Heme oxygenase-1
NF-κB: Nuclear factor-kappa B
SIRT1: Sirtuins
FOXO: Forkhead box
UCP2: Uncoupling protein 2
STZ: Streptozotocin nicotinamide.

Conflicts of Interest

The authors declare that there are no conflicts of interest regarding the publication of this paper.

Acknowledgments

This research was financially supported by the National Natural Science Foundation of China (Grant no. 31802140) and the Scientific Research Promotion Fund for the Talents of Jiangsu University (Grant no. 14JDG157).

References

[1] R. G. Larkins and M. E. Dunlop, "The link between hyperglycaemia and diabetic nephropathy," *Diabetologia*, vol. 35, no. 6, pp. 499–504, 1992.
[2] V. Shukla, S. K. Mishra, and H. C. Pant, "Oxidative stress in neurodegeneration," *Advances in Pharmacological Sciences*, vol. 2011, no. 1, 634 pages, Article ID 572634, 2011.
[3] G. Li, J. Fu, Y. Zhao, K. Ji, T. Luan, and B. Zang, "Alpha-lipoic acid exerts anti-inflammatory effects on lipopolysaccharide-stimulated rat mesangial cells via inhibition of nuclear factor kappa B (NF-κB) signaling pathway," *Inflammation*, vol. 38, no. 2, pp. 510–519, 2015.
[4] A. Vaccaro, Y. K. Dor, K. Nambara et al., "Sleep loss can cause death through accumulation of reactive oxygen species in the gut," *Cell*, vol. 181, no. 6, pp. 1307–1328, 2020.
[5] K. B. Pandey and S. I. Rizvi, "Plant polyphenols as dietary antioxidants in human health and disease," *Oxidative Medicine and Cellular Longevity*, vol. 2, no. 5, pp. 270–278, 2009.
[6] Y. Peng, R. Y. Gan, H. B. Li et al., "Absorption, metabolism, and bioactivity of vitexin: recent advances in understanding the efficacy of an important nutraceutical," *Critical Reviews in Food Science and Nutrition*, vol. 27, pp. 1–16, 2020.
[7] L. Frémont, "Biological effects of resveratrol," *Life Sciences*, vol. 66, no. 8, pp. 663–673, 2000.
[8] H. Wu, L. Chen, F. Zhu, X. Han, L. Sun, and K. Chen, "The cytotoxicity effect of resveratrol: cell cycle arrest and induced apoptosis of breast cancer 4T1 cells," *Toxins*, vol. 11, no. 12, pp. 731–751, 2019.
[9] A. A. Bertelli, L. Giovannini, D. Giannessi et al., "Antiplatelet activity of synthetic and natural resveratrol in red wine," *International Journal of Tissue Reactions*, vol. 17, no. 1, pp. 1–3, 1995.
[10] M. Takaoka, "The phenolic substances of white hellebore (veratrum grandiflorum loes fil.) II," *Nippon Kagaku Kaishi*, vol. 60, no. 12, pp. 1261–1264, 1939.
[11] R. Nakata, S. Takahashi, and H. Inoue, "Recent advances in the study on resveratrol," *Biological and Pharmaceutical Bulletin*, vol. 35, no. 3, pp. 273–279, 2012.
[12] J. Burns, T. Yokota, H. Ashihara, M. E. J. Lean, and A. Crozier, "Plant foods and herbal sources of resveratrol," *Journal of Agricultural and Food Chemistry*, vol. 50, no. 11, pp. 3337–3340, 2002.
[13] K. Pallauf, G. Rimbach, P. M. Rupp, D. Chin, and I. M.A. Wolf, "Resveratrol and lifespan in model organisms," *Current Medicinal Chemistry*, vol. 23, no. 41, pp. 4639–4680, 2016.
[14] C. Brent, L. A. Trela, and Waterhouse, "Resveratrol: Isomeric molar absorptivities and stability," *Journal of Agricultural and Food Chemistry*, vol. 44, no. 5, pp. 1253–1257, 1996.
[15] M. Valko, D. Leibfritz, J. Moncol, M. T. D. Cronin, M. Mazur, and J. Telser, "Free radicals and antioxidants in normal physiological functions and human disease," *The International Journal of Biochemistry & Cell Biology*, vol. 39, no. 1, pp. 44–84, 2007.
[16] J. H. Holthoff, K. A. Woodling, D. R. Doerge, S. T. Burns, J. A. Hinson, and P. R. Mayeux, "Resveratrol, a dietary polyphenolic phytoalexin, is a functional scavenger of peroxynitrite," *Biochemical Pharmacology*, vol. 80, no. 8, pp. 1260–1265, 2010.
[17] Y. Sueishi and M. Hori, "Nitric oxide scavenging rates of solubilized resveratrol and flavonoids," *Nitric Oxide*, vol. 29, pp. 25–29, 2013.

[18] S. Di Meo, T. T. Reed, P. Venditti, and V. M. Victor, "Role of ROS and RNS sources in physiological and pathological conditions," *Oxidative Medicine and Cellular Longevity*, vol. 2016, Article ID 1245049, 44 pages, 2016.

[19] M. Wang, J. Li, M. Rangarajan et al., "Antioxidative phenolic compounds from sage (salvia officinalis)," *Journal of Agricultural and Food Chemistry*, vol. 46, no. 12, pp. 4869–4873, 1998.

[20] L. A. Stivala, M. Savio, F. Carafoli et al., "Specific structural determinants are responsible for the antioxidant activity and the cell cycle effects of resveratrol," *Journal of Biological Chemistry*, vol. 276, no. 25, pp. 22586–22594, 2001.

[21] H. Cao, X. Pan, C. Li, C. Zhou, F. Deng, and T. Li, "Density functional theory calculations for resveratrol," *Bioorganic & Medicinal Chemistry Letters*, vol. 13, no. 11, pp. 1869–1871, 2003.

[22] M. A. Hussein, "A convenient mechanism for the free radical scavenging activity of resveratrol," *International Journal of Phytomedicine*, vol. 3, no. 4, pp. 459–469, 2011.

[23] A. Benayahoum, H. Amira-Guebailia, and O. Houache, "Homolytic and heterolytic O-H bond cleavage in trans-resveratrol and some phenantrene analogs: a theoretical study," *Computational and Theoretical Chemistry*, vol. 1037, pp. 1–9, 2014.

[24] F. Caruso, J. Tanski, A. Villegas-Estrada, and M. Rossi, "Structural basis for antioxidant activity oftrans-resveratrol: ab initio calculations and crystal and molecular structure," *Journal of Agricultural and Food Chemistry*, vol. 52, no. 24, pp. 7279–7285, 2004.

[25] S. Fabris, F. Momo, G. Ravagnan, and R. Stevanato, "Antioxidant properties of resveratrol and piceid on lipid peroxidation in micelles and monolamellar liposomes," *Biophysical Chemistry*, vol. 135, no. 1-3, pp. 76–83, 2008.

[26] S. S. Leonard, C. Xia, B.-H. Jiang et al., "Resveratrol scavenges reactive oxygen species and effects radical-induced cellular responses," *Biochemical and Biophysical Research Communications*, vol. 309, no. 4, pp. 1017–1026, 2003.

[27] İ. Gülçin, "Antioxidant properties of resveratrol: a structure-activity insight," *Innovative Food Science & Emerging Technologies*, vol. 11, no. 1, pp. 210–218, 2010.

[28] V.-L. Truong, M. Jun, and W.-S. Jeong, "Role of resveratrol in regulation of cellular defense systems against oxidative stress," *Biofactors*, vol. 44, no. 1, pp. 36–49, 2018.

[29] N. Xia, A. Daiber, U. Förstermann, and H. G. Li, "Antioxidant effects of resveratrol in the cardiovascular system," *British Journal of Pharmacology*, vol. 174, no. 12, pp. 1633–1646, 2017.

[30] C. Beauloye, L. Bertrand, S. Horman, and L. Hue, "AMPK activation, a preventive therapeutic target in the transition from cardiac injury to heart failure," *Cardiovascular Research*, vol. 90, no. 2, pp. 224–233, 2011.

[31] T. Walle, F. Hsieh, M. H. DeLegge, J. E. Oatis, and U. K. Walle, "High absorption but very low bioavailability of oral resveratrol in humans," *Drug Metabolism and Disposition*, vol. 32, no. 12, pp. 1377–1382, 2004.

[32] T. Walle, "Bioavailability of resveratrol," *Annals of the New York Academy of Sciences*, vol. 1215, no. 1, pp. 9–15, 2011.

[33] F. Q. Schafer and G. R. Buettner, "Redox environment of the cell as viewed through the redox state of the glutathione disulfide/glutathione couple," *Free Radical Biology and Medicine*, vol. 30, no. 11, pp. 1191–1212, 2001.

[34] S. Langård, "One hundred years of chromium and cancer: a review of epidemiological evidence and selected case reports," *American Journal of Industrial Medicine*, vol. 17, no. 2, pp. 189–215, 1990.

[35] P. Palsamy and S. Subramanian, "Resveratrol protects diabetic kidney by attenuating hyperglycemia-mediated oxidative stress and renal inflammatory cytokines via Nrf2-Keap1 signaling," *Biochimica Et Biophysica Acta-Molecular Basis of Disease*, vol. 1812, no. 7, 731 pages, 2011.

[36] A. O. Abolaji, A. O. Adedara, M. A. Adie, M. Vicente-Crespo, and E. O. Farombi, "Resveratrol prolongs lifespan and improves 1-methyl-4-phenyl-1,2,3,6-tetrahydropyridine-induced oxidative damage and behavioural deficits in Drosophila melanogaster," *Biochemical and Biophysical Research Communications*, vol. 503, no. 2, pp. 1042–1048, 2018.

[37] R. Nordmann, C. Ribière, and H. Rouach, "Implication of free radical mechanisms in ethanol-induced cellular injury," *Free Radical Biology and Medicine*, vol. 12, no. 3, pp. 219–240, 1992.

[38] S. K. Manna, A. Mukhopadhyay, and B. B. Aggarwal, "Resveratrol suppresses TNF-induced activation of nuclear transcription factors NF-κB, activator protein-1, and apoptosis: potential role of reactive oxygen intermediates and lipid peroxidation," *The Journal of Immunology*, vol. 164, no. 12, pp. 6509–6519, 2000.

[39] S. Chanvitayapongs, B. Draczynska-Lusiak, and A. Y. Sun, "Amelioration of oxidative stress by antioxidants and resveratrol in PC12 cells," *Neuroreport*, vol. 8, no. 6, pp. 1499–1502, 1997.

[40] S. Stojanovic, H. Sprinz, and O. Brede, "Efficiency and mechanism of the antioxidant action of trans-resveratrol and its analogues in the radical liposome oxidation," *Archives of Biochemistry and Biophysics*, vol. 391, no. 1, pp. 79–89, 2001.

[41] M. A. Murcia and M. Martínez-tomé, "Antioxidant activity of resveratrol compared with common food additives," *Journal of Food Protection*, vol. 64, no. 3, pp. 379–384, 2001.

[42] A. M. Pisoschi and A. Pop, "The role of antioxidants in the chemistry of oxidative stress: a review," *European Journal of Medicinal Chemistry*, vol. 97, no. 31, pp. 55–74, 2015.

[43] M. Kopff, I. Zakrzewska, J. Czernicki, J. Klem, and M. Strzelczyk, "Red cell superoxide dismutase and catalase activity in multiple sclerosis," *Acta Biochimica Polonica*, vol. 40, no. 1, pp. 154–157, 1993.

[44] A. Kasdallah-Grissa, B. Mornagui, E. Aouani et al., "Resveratrol, a red wine polyphenol, attenuates ethanol-induced oxidative stress in rat liver," *Life Sciences*, vol. 80, no. 11, pp. 1033–1039, 2007.

[45] W.-M. Chen, L.-H. Shaw, P.-J. Chang et al., "Hepatoprotective effect of resveratrol against ethanol-induced oxidative stress through induction of superoxide dismutase in vivo and in vitro," *Experimental and Therapeutic Medicine*, vol. 11, no. 4, pp. 1231–1238, 2016.

[46] M. Valko, "Free radicals and antioxidants in normal physiological functions and human disease," *The International Journal of Biochemistry*, vol. 39, no. 1, pp. 44–84, 2007.

[47] C. Espinosa-Diez, V. Miguel, D. Mennerich et al., "Antioxidant responses and cellular adjustments to oxidative stress," *Redox Biology*, vol. 6, pp. 183–197, 2015.

[48] L. Liu, L. Gu, Q. Ma, D. Zhu, and X. Huang, "Resveratrol attenuates hydrogen peroxide-induced apoptosis in human umbilical vein endothelial cells," *European Review for Medical and Pharmacological Sciences*, vol. 17, no. 1, pp. 88–94, 2013.

[49] H. Zhang and R. Tsao, "Dietary polyphenols, oxidative stress and antioxidant and anti-inflammatory effects," *Current Opinion in Food Science*, vol. 8, pp. 33–42, 2016.

[50] K. Szkudelska, M. Okulicz, I. Hertig, and T. Szkudelski, "Resveratrol ameliorates inflammatory and oxidative stress in type 2 diabetic goto-kakizaki rats," *Biomedicine & Pharmacotherapy*, vol. 125, Article ID 110026, 2020.

[51] S. Fu, R. Lv, L. Wang, H. Hou, H. Liu, and S. Shao, "Resveratrol, an antioxidant, protects spinal cord injury in rats by suppressing MAPK pathway," *Saudi Journal of Biological Sciences*, vol. 25, no. 2, pp. 259–266, 2018.

[52] N. Tamaki, R. Cristina Orihuela-Campos, Y. Inagaki, M. Fukui, T. Nagata, and H.-O. Ito, "Resveratrol improves oxidative stress and prevents the progression of periodontitis via the activation of the SirT1/AMPK and the Nrf2/antioxidant defense pathways in a rat periodontitis model," *Free Radical Biology and Medicine*, vol. 75, pp. 222–229, 2014.

[53] H. H. Gaballah, S. S. Zakaria, M. M. Elbatsh, and N. M. Tahoon, "Modulatory effects of resveratrol on endoplasmic reticulum stress-associated apoptosis and oxido-inflammatory markers in a rat model of rotenone-induced Parkinson's disease," *Chemico-Biological Interactions*, vol. 251, pp. 10–16, 2016.

[54] M. M. Khan, A. Ahmad, T. Ishrat et al., "Resveratrol attenuates 6-hydroxydopamine-induced oxidative damage and dopamine depletion in rat model of Parkinson's disease," *Brain Research*, vol. 1328, pp. 139–151, 2010.

[55] E. N. Kim, M. Y. Kim, J. H. Lim et al., "The protective effect of resveratrol on vascular aging by modulation of the renin-angiotensin system," *Atherosclerosis*, vol. 270, pp. 123–131, 2018.

[56] N. Xia, A. Daiber, A. Habermeier et al., "Resveratrol reverses endothelial nitric-oxide synthase uncoupling in apolipoprotein E knockout mice," *Journal of Pharmacology and Experimental Therapeutics*, vol. 335, no. 1, pp. 149–154, 2010.

[57] G. S. Liu, Z. S. Zhang, B. Yang, and W. He, "Resveratrol attenuates oxidative damage and ameliorates cognitive impairment in the brain of senescence-accelerated mice," *Life Sciences*, vol. 91, no. 17-18, pp. 872–877, 2012.

[58] V. Tiwari and K. Chopra, "Resveratrol abrogates alcohol-induced cognitive deficits by attenuating oxidative-nitrosative stress and inflammatory cascade in the adult rat brain," *Neurochemistry International*, vol. 62, no. 6, pp. 861–869, 2013.

[59] P. Y. He, Z. P. Hou, C. J. Song et al., "Resveratrol ameliorates experimental alcoholic liver disease by modulating oxidative stress," *Evidence-Based Complementary and Alternative Medicine*, vol. 2017, Article ID 4287890, 10 pages, 2017.

[60] S. Gómez-Zorita, A. Fernández-Quintela, M. T. Macarulla et al., "Resveratrol attenuates steatosis in obese zucker rats by decreasing fatty acid availability and reducing oxidative stress," *British Journal of Nutrition*, vol. 107, no. 2, pp. 202–210, 2012.

[61] D.-W. Kim, Y.-M. Kim, S.-D. Kang, Y.-M. Han, and H.-O. Pae, "Effects of resveratrol and trans-3,5,4'-trimethoxystilbene on glutamate-induced cytotoxicity, heme oxygenase-1, and sirtuin 1 in HT22 neuronal cells," *Biomolecules and Therapeutics*, vol. 20, no. 3, pp. 306–312, 2012.

[62] J. Han, H. Wang, T. Zhang et al., "Resveratrol attenuates doxorubicin-induced meiotic failure through inhibiting oxidative stress and apoptosis in mouse oocytes," *Aging*, vol. 12, no. 9, pp. 7717–7728, 2020.

[63] Y. Zhang, L. Guo, B. Y. Law et al., "Resveratrol decreases cell apoptosis through inhibiting DNA damage in bronchial epithelial cells," *International Journal of Molecular Medicine*, vol. 45, no. 6, pp. 1673–1684, 2020.

[64] Q.-X. Liang, Y.-H. Lin, C.-H. Zhang et al., "Resveratrol increases resistance of mouse oocytes to postovulatory aging in vivo," *Aging*, vol. 10, no. 7, pp. 1586–1596, 2018.

[65] A. M. Thompson, K. A. Martin, and E. M. Rzucidlo, "Resveratrol induces vascular smooth muscle cell differentiation through stimulation of SirT1 and AMPK," *PLoS One*, vol. 9, no. 1, Article ID e85495, 2014.

[66] M. Manczak, P. Mao, M. J. Calkins et al., "Mitochondria-targeted antioxidants protect against amyloid-β toxicity in alzheimer's disease neurons," *Journal of Alzheimer's Disease*, vol. 20, no. s2, pp. S609–S631, 2010.

[67] X. He, L. Wang, G. Szklarz, Y. Bi, and Q. Ma, "Resveratrol inhibits paraquat-induced oxidative stress and fibrogenic response by activating the nuclear factor erythroid 2-related factor 2 pathway," *Journal of Pharmacology and Experimental Therapeutics*, vol. 342, no. 1, pp. 81–90, 2012.

[68] T. M. Teixeira, D. C. Da Costa, A. C. Resende, C. O. Soulage, F. F. Bezerra, and J. B. Daleprane, "Activation of Nrf2-antioxidant signaling by 1,25-dihydroxycholecalciferol prevents leptin-induced oxidative stress and inflammation in human endothelial cells," *The Journal of Nutrition*, vol. 147, no. 4, pp. 506–513, 2017.

[69] E. B. Menshchikova, N. K. Zenkov, V. O. Tkachev, A. E. Lemza, and N. V. Kandalintseva, "Protective effect of ARE-Inducing phenol antioxidant TS-13 in chronic inflammation," *Bulletin of Experimental Biology and Medicine*, vol. 155, no. 3, pp. 330–334, 2013.

[70] X. Kou, M. Kirberger, Y. Yang, and N. Chen, "Natural products for cancer prevention associated with Nrf2-ARE pathway," *Food Science and Human Wellness*, vol. 2, no. 1, pp. 22–28, 2013.

[71] K. Iwasaki, P. D. Ray, B.-W. Huang, K. Sakamoto, T. Kobayashi, and Y. Tsuji, "Role of AMP-activated protein kinase in ferritin H gene expression by resveratrol in human T cells," *Biochemistry*, vol. 52, no. 30, pp. 5075–5083, 2013.

[72] C.-Y. Chen, J.-H. Jang, M.-H. Li, and Y.-J. Surh, "Resveratrol upregulates heme oxygenase-1 expression via activation of NF-E2-related factor 2 in PC12 cells," *Biochemical and Biophysical Research Communications*, vol. 331, no. 4, pp. 993–1000, 2005.

[73] A. Kode, S. Rajendrasozhan, S. Caito, S.-R. Yang, I. L. Megson, and I. Rahman, "Resveratrol induces glutathione synthesis by activation of Nrf2 and protects against cigarette smoke-mediated oxidative stress in human lung epithelial cells," *American Journal of Physiology-Lung Cellular and Molecular Physiology*, vol. 294, no. 3, pp. L478–L488, 2008.

[74] J. J. Boyle, M. Johns, J. Lo et al., "Heme induces heme oxygenase 1 via Nrf2," *Arteriosclerosis, Thrombosis, and Vascular Biology*, vol. 31, no. 11, pp. 2685–2691, 2011.

[75] Z. Cao, H. Zhu, L. Zhang, X. Zhao, J. L. Zweier, and Y. Li, "Antioxidants and phase 2 enzymes in cardiomyocytes: chemical inducibility and chemoprotection against oxidant and simulated ischemia-reperfusion injury," *Experimental Biology and Medicine*, vol. 231, no. 8, pp. 1353–1364, 2006.

[76] V. Malec, O. R. Gottschald, S. Li, F. Rose, W. Seeger, and J. Hänze, "HIF-1α signaling is augmented during intermittent hypoxia by induction of the Nrf2 pathway in NOX1-expressing adenocarcinoma A549 cells," *Free Radical Biology and Medicine*, vol. 48, no. 12, pp. 1626–1635, 2010.

[77] R. Sen and D. Baltimore, "Inducibility of κ immunoglobulin enhancer-binding protein NF-κB by a posttranslational mechanism," *Cell*, vol. 47, no. 6, pp. 921–928, 1986.

[78] M. J. Morgan and Z.-G. Liu, "Crosstalk of reactive oxygen species and NF-κB signaling," *Cell Research*, vol. 21, no. 1, pp. 103–115, 2011.

[79] S. Vallabhapurapu and M. Karin, "Regulation and function of NF-κB transcription factors in the immune system," *Annual Review of Immunology*, vol. 27, no. 1, pp. 693–733, 2009.

[80] X. Y. Zheng, S. Y. Zhu, S. F. Chang et al., "Protective effects of chronic resveratrol treatment on vascular inflammatory injury in streptozotocin-induced type 2 diabetic rats: role of NF-kappa B signaling," *European Journal of Pharmacology*, vol. 720, no. 1-3, pp. 147–157, 2013.

[81] R. Guo, B. Liu, K. Wang, S. Zhou, W. Li, and Y. Xu, "Resveratrol ameliorates diabetic vascular inflammation and macrophage infiltration in db/db mice by inhibiting the NF-κB pathway," *Diabetes and Vascular Disease Research*, vol. 11, no. 2, pp. 92–102, 2014.

[82] F. G. Soufi, D. Mohammad-Nejad, and H. Ahmadieh, "Resveratrol improves diabetic retinopathy possibly through oxidative stress - nuclear factor κB - apoptosis pathway," *Pharmacological Reports*, vol. 64, no. 6, pp. 1505–1514, 2012.

[83] R. A. Frye, "Phylogenetic classification of prokaryotic and eukaryotic Sir2-like proteins," *Biochemical and Biophysical Research Communications*, vol. 273, no. 2, pp. 793–798, 2000.

[84] S. Jarolim, J. Millen, G. Heeren, P. Laun, D. Goldfarb, and M. Breitenbach, "A novel assay for replicative lifespan in," *Fems Yeast Research*, vol. 5, no. 2, pp. 169–177, 2004.

[85] B. Chen, W. Zang, J. Wang et al., "The chemical biology of sirtuins," *Chemical Society Reviews*, vol. 44, no. 15, pp. 5246–5264, 2015.

[86] M. F. Oellerich and M. Potente, "FOXOs and sirtuins in vascular growth, maintenance, and aging," *Circulation Research*, vol. 110, no. 9, pp. 1238–1251, 2012.

[87] T. Nakagawa and L. Guarente, "Sirtuins at a glance," *Journal of Cell Science*, vol. 124, no. 6, pp. 833–838, 2011.

[88] S.-J. Park, F. Ahmad, A. Philp et al., "Resveratrol ameliorates aging-related metabolic phenotypes by inhibiting camp phosphodiesterases," *Cell*, vol. 148, no. 3, pp. 421–433, 2012.

[89] Z. Ungvari, N. Labinskyy, P. Mukhopadhyay et al., "Resveratrol attenuates mitochondrial oxidative stress in coronary arterial endothelial cells," *American Journal of Physiology-Heart and Circulatory Physiology*, vol. 297, no. 5, pp. H1876–H1881, 2009.

[90] M.-C. Wang, Y.-C. Wang, H.-W. Peng et al., "Resveratrol induces expression of metabolic and antioxidant machinery and protects tilapia under cold stress," *International Journal of Molecular Sciences*, vol. 21, no. 9, p. 3338, 2020.

[91] Y. Olmos, F. J. Sánchez-Gómez, B. Wild et al., "αSirT1 regulation of antioxidant genes is dependent on the formation of a FoxO3a/PGC-1α complex," *Antioxidants & Redox Signaling*, vol. 19, no. 13, pp. 1507–1521, 2013.

[92] S.-R. Yang, J. Wright, M. Bauter, K. Seweryniak, A. Kode, and I. Rahman, "Sirtuin regulates cigarette smoke-induced proinflammatory mediator release via RelA/p65 NF-κB in macrophages in vitro and in rat lungs in vivo: implications for chronic inflammation and aging," *American Journal of Physiology-Lung Cellular and Molecular Physiology*, vol. 292, no. 2, pp. L567–L576, 2007.

[93] M. G. Erkkinen, M.-O. Kim, and M. D. Geschwind, "Clinical neurology and epidemiology of the major neurodegenerative diseases," *Cold Spring Harbor Perspectives in Biology*, vol. 10, no. 4, Article ID a033118, 2018.

[94] E. Nichols, C. E. I. Szoeke, S. E. Vollset et al., "Global, regional, and national burden of alzheimer's disease and other dementias, 1990-2016: a systematic analysis for the global burden of disease study 2016," *Lancet Neurology*, vol. 18, no. 1, pp. 88–106, 2019.

[95] E. R. Dorsey, A. Elbaz, E. Nichols et al., "Global, regional, and national burden of Parkinson's disease, 1990-2016: a systematic analysis for the global burden of disease study 2016," *Lancet Neurology*, vol. 17, no. 11, pp. 939–953, 2018.

[96] A. D. Gitler, P. Dhillon, and J. Shorter, "Neurodegenerative disease: models, mechanisms, and a new hope," *Disease Models & Mechanisms*, vol. 10, no. 5, pp. 499–502, 2017.

[97] H. Zhang, L. Bai, J. He et al., "Recent advances in discovery and development of natural products as source for anti-Parkinson's disease lead compounds," *European Journal of Medicinal Chemistry*, vol. 141, pp. 257–272, 2017.

[98] D. Porquet, C. Griñán-Ferré, I. Ferrer et al., "Neuroprotective role of trans-resveratrol in a murine model of familial alzheimer's disease," *Journal of Alzheimer's Disease*, vol. 42, no. 4, pp. 1209–1220, 2014.

[99] T. Ahmed, S. Javed, S. Javed et al., "Resveratrol and alzheimer's disease: mechanistic insights," *Molecular Neurobiology*, vol. 54, no. 4, pp. 2622–2635, 2017.

[100] A. Freyssin, G. Page, B. Fauconneau, and A. Rioux Bilan, "Natural stilbenes effects in animal models of alzheimer's disease," *Neural Regeneration Research*, vol. 15, no. 5, pp. 843–849, 2020.

[101] M. Cosín-Tomàs, J. Senserrich, M. Arumí-Planas et al., "Role of resveratrol and selenium on oxidative stress and expression of antioxidant and anti-aging genes in immortalized lymphocytes from alzheimer's disease patients," *Nutrients*, vol. 11, no. 8, p. 1764, 2019.

[102] Y. Zhang, Y. Li, Y. Wang et al., "Effects of resveratrol on learning and memory in rats with vascular dementia," *Molecular Medicine Reports*, vol. 20, no. 5, pp. 4587–4593, 2019.

[103] G. D. Lindner, D. B. Santos, D. Colle et al., "Improved neuroprotective effects of resveratrol-loaded polysorbate 80-coated poly(lactide) nanoparticles in MPTP-induced parkinsonism," *Nanomedicine*, vol. 10, no. 7, pp. 1127–1138, 2015.

[104] K. S. Bhullar and B. P. Hubbard, "Lifespan and healthspan extension by resveratrol," *Biochimica Et Biophysica Acta-Molecular Basis of Disease*, vol. 1852, no. 6, pp. 1209–1218, 2015.

[105] C.-L. Kao, L.-K. Chen, Y.-L. Chang et al., "Resveratrol protects human endothelium from H2O2-induced oxidative stress and senescence via SirT1 activation," *Journal of Atherosclerosis and Thrombosis*, vol. 17, no. 9, pp. 970–979, 2010.

[106] C. Wang, C. T. Wheeler, T. Alberico et al., "The effect of resveratrol on lifespan depends on both gender and dietary nutrient composition in Drosophila melanogaster," *Age*, vol. 35, no. 1, pp. 69–81, 2013.

[107] A. Salminen and K. Kaarniranta, "AMP-activated protein kinase (AMPK) controls the aging process via an integrated signaling network," *Ageing Research Reviews*, vol. 11, no. 2, pp. 230–241, 2012.

[108] S. Afzal, S. Garg, D. Adiga et al., "Anti-stress, glial- and neuro-differentiation potential of resveratrol: characterization by cellular, biochemical and imaging assays," *Nutrients*, vol. 12, no. 3, p. 671, 2020.

[109] C. Zhang, L. Wang, X. H. Zhao, X. Y. Chen, L. Yang, and Z. Y. Geng, "Dietary resveratrol supplementation prevents transport-stress-impaired meat quality of broilers through maintaining muscle energy metabolism and antioxidant status," *Poultry Science*, vol. 96, no. 7, pp. 2219–2225, 2017.

[110] C. Zhang, J. Luo, B. Yu et al., "Dietary resveratrol supplementation improves meat quality of finishing pigs through changing muscle fiber characteristics and antioxidative status," *Meat Science*, vol. 102, pp. 15–21, 2015.

[111] S. Davinelli, G. Scapagnini, F. Marzatico, V. Nobile, N. Ferrara, and G. Corbi, "Influence of equol and resveratrol supplementation on health-related quality of life in menopausal women: a randomized, placebo-controlled study," *Maturitas*, vol. 96, pp. 77–83, 2017.

[112] W. Li, X. Yang, Q. Song et al., "Pyridoxine-resveratrol hybrids as novel inhibitors of MAO-B with antioxidant and neuroprotective activities for the treatment of Parkinson's disease," *Bioorganic Chemistry*, vol. 9710377 pages, 2020.

[113] Y. Fan, X. Zeng, J. Yi, and Y. Zhang, "Fabrication of pea protein nanoparticles with calcium-induced cross-linking for the stabilization and delivery of antioxidative resveratrol," *International Journal of Biological Macromolecules*, vol. 152, pp. 189–198, 2020.

Hindawi
Journal of Food Quality
Volume 2021, Article ID 5535476, 7 pages
https://doi.org/10.1155/2021/5535476

Research Article

Hypoglycemic Effect of Vitexin in C57BL/6J Mice and HepG2 Models

Weidong Xu,[1] **Jiayao Li**,[1] **Weipeng Qi**,[2] **and Ye Peng**[3]

[1]*School of Pharmacy, Jiangsu University, Zhenjiang, Jiangsu Province, China*
[2]*Department of Food Science, University of Massachusetts Amherst, Amherst, MA 01002, USA*
[3]*School of Food and Biological Engineering, Jiangsu University, Zhenjiang, Jiangsu Province, China*

Correspondence should be addressed to Ye Peng; leafypeng@outlook.com

Received 15 January 2021; Revised 30 January 2021; Accepted 22 February 2021; Published 11 March 2021

Academic Editor: Yan Zhang

Apigenin-8-C-glucoside (vitexin), a natural phytochemical contained in hawthorn, has been reported to have versatile beneficial bioactivities, such as antioxidation, anticancer property, and adipogenesis inhibition. The present research aimed to determine the influence of vitexin on insulin resistance elicited by HFD in mice and HepG2 cells. Vitexin markedly alleviated body weight gain and improved glucose and insulin intolerance induced by HFD. Vitexin partially normalized blood glucose, cholesterol, TNF-α, and hepatic lipid content. Moreover, vitexin recovered the reduced glucose uptake induced by glucosamine. The present results indicate that vitexin prevents HFD-induced insulin resistance.

1. Introduction

In recent years, incidence of type 2 diabetes has increased dramatically all over the world, and diabetes is usually accompanied by many systemic complications, such as heart, eye, and blood vessel diseases, which poses a great threat to patients [1]. The liver is an insulin-sensitive organ and plays an important role in maintaining glucose and lipid metabolism. Insulin resistance in the liver is closely linked with the occurrence and progression of type 2 diabetes [2]. In the liver, insulin resistance has been found to reduce glucose uptake and glycogen synthesis and to inhibit insulin signaling activation [3, 4]. HepG2 cells share the same lipid or glucose metabolism with normal hepatic cells [5]. In this metabolism, insulin activates an insulin receptor, and insulin receptor substrates are phosphorylated, which eventually leads to the activation of the PI3K/AKT pathway [6]. ER stress plays a critical role in the progression of liver insulin resistance [3]. ER stress promotes adipokine production and induces adipose tissue inflammation and dysfunction [7]. In the liver, ER stress interferes with hepatic glucose metabolism and impairs insulin sensitivity [8].

Vitexin is a natural flavonoid presenting in several consumable plants, such as hawthorn (*Crataegus pinnatifida*) and chayote (*Sechium edule*) [9, 10]. The plants have been historically used as Chinese medicine for curing toxification, intestinal inflammation, and digestive disorders three thousand years ago [11, 12]. Recently, a few studies reported that vitexin exhibits various bioactivities, including anti-inflammatory, anticancer, and antihypertension effects [13, 14]. Vitexin was shown to reduce the pro-hyperalgesic cytokine level, while enhancing the anti-hyperalgesic level [15]. Vitexin was also found to ameliorate streptozotocin- or lipopolysaccharide-induced damage of the pancreas and islet tissue via the upregulation of antioxidative factors, including Nrf2 and GPx [16]. Moreover, vitexin obtained from *Cynometra cauliflora* Linn. increased the translocation of GLUT4 from the cell cytoplasm to membrane, indicating its beneficial potential on glucose uptake [17]. Although the protection of the pancreas and the promotion of glucose uptake by vitexin may suggest its beneficial effects on glucose homeostasis, the information of vitexin on insulin resistance and hepatic ER stress response is scarce. Animal studies reported that HFD-induced obesity is closely associated with insulin resistance [18, 19]. Also, glucosamine has been

widely used to induce ER stress in vitro [4]. Thus, the present research aimed to determine vitexin's influence on HFD and glucosamine-elicited insulin resistance in C57BL/6J mice and in HepG2 cells.

2. Materials and Methods

2.1. Materials. HepG2 were bought from the Shanghai Cell Bank of the Chinese Academy of Sciences (Shanghai, China). Vitexin with purity ≥98% was purchased from Pufei De Biotech Co., Ltd. (Chengdu, Sichuan Province, China). FBS, DMEM, dimethyl sulfoxide, insulin, and glucosamine were purchased from Sigma-Aldrich (St. Louis, MO, USA). Glucose meter (GLM-75) and test strips were obtained from GlucoLeader (Beijing, China).

2.2. Animals and Diets. C57BL/6J male mice (10 week) were purchased from Jiangsu University Laboratory Animal Research Center (Jiangsu, China) and housed in the animal facility under standard conditions (12/12 h light-dark cycle). All animal experimental procedures were followed according to the Guide for the Care and Use of Laboratory Animals: Eighth Edition, ISBN-10: 0-309-15396-4, and the animal protocol was approved by the Jiangsu University Animal Ethics Committee. After a two-week adaptation, mice were separated into 3 groups (9 mice per group): LFD, HFD, and HFD + Vitexin (5 mg vitexin/kg BW/day) for 8 weeks. The HFD (60% of energy from fat, TP23400) and LFD (10% kcal from fat, TP23402) were from Trophic Animal Feed High-tech Co., Ltd. (Nantong, Jiangsu Province, China). The vitexin dose was based on a previous study [20].

At the end of the study, mice were fasted overnight before being sacrificed by CO_2 asphyxiation. Blood was collected by cardiac puncture. Serum was obtained from blood by centrifugation for 20 min at 2000 rpm. Part of the liver was fixed in buffered formalin (10%). The ITT and GTT were performed as previously described [21].

2.3. Serum Parameters and Liver Triglycerides Quantitation. The TG from the liver and serum and serum glucose levels were quantified using commercial kits according to manufacturers' instructions (Nanjing Jiancheng Bioengineering Institute, Nanjing, Jiangsu Province, China). The level of serum TNF-α was detected using the ELISA kits (FcMACS Co., Ltd, Nanjing, Jiangsu Province, China).

2.4. Cell Culture. HepG2 cells were maintained as previously reported [22]. After incubation with 18 mm glucosamine for 18 h to induce insulin resistance [4], the HepG2 cells were serum-starved for 2 h and then incubated with vitexin (20 μM) for 24 h, with 100 nM insulin added in the last 15 min. The vitexin and glucosamine concentrations were in accordance with previous publications [4, 20], and the concentrations had no influence on cell viability as determined by the MTT assay, as previously reported [23, 24]. Glucosamine was dissolved in PBS, and vitexin was dissolved in DMSO. All groups had the same amount of DMSO.

2.5. Glucose Uptake Assay. Glucose uptake measurement was performed with a fluorescent glucose derivative, 2-NBDG, as previously reported [25]. There were three treatment groups, i.e., Control, Glucosamine, and Glucosamine + Vitexin groups. Briefly, HepG2 cells were treated with or without 18 mM glucosamine for 18 h and starved in F-12K (5.5 mM glucose) serum-free media for 2 h. Then, cells were treated with or without 20 μM vitexin for 24 h following the treatment of 100 nM insulin for 15 min (serum-free medium). After washing, the fluorescent signal was quantified with a plate reader at excitation/emission of 465/540 nm (SpectraMax i3, Shanghai, China) and normalized by protein content (BCA protein assay kit, Beyotime Biotechnology Inc. Shanghai, China).

2.6. Statistical Analyses. Data were analyzed with one-way ANOVA (Tukey's multiple-range test) with SAS software (SAS Institute Inc., Cary, NC, USA). A $P < 0.05$ was considered statistically significant.

3. Results

3.1. Vitexin Decreased Body Weight in HFD-Treated Mice. As shown in Figure 1(a), the HFD group possessed higher body weight than the LFD and HFD + Vitexin groups during week 8. The HFD + Vitexin group had no significantly different body weight compared to the LFD group. All three groups had similar total food intake (Figure 1(b)).

3.2. Vitexin Improved Glucose Homeostasis. ITT and GTT were performed to determine the influence of vitexin on glucose metabolism, and results are shown in Figure 2. For the ITT, HFD-fed mice had a higher blood glucose level than mice fed with LFD at all points in time (Figure 2(a)). Compared to the HFD-fed mice, vitexin significantly reduced the HFD-induced blood glucose increase after 0, 15, 30, 60, and 120 minutes (Figure 2(a)). Similarly, HFD significantly increased the AUC of the ITT, and the AUC was significantly reduced by vitexin treatment (Figure 2(b)). For the GTT results, mice fed with a HFD had a significantly higher blood glucose level at 15, 30, and 60 minutes, as well as the AUC, than in the LFD group and the HFD + Vitexin group (Figures 2(c) and 2(d)). The results indicate that vitexin significantly alleviated insulin and glucose intolerance induced by the HFD.

3.3. Effects of Vitexin on Serum Markers. As shown in Table 1, in HFD-fed mice, the glucose and TG levels were significantly increased compared with the LFD-fed mice and were markedly decreased in the HFD + Vitexin group. In addition, vitexin reduced the HFD-induced TNF-α level. No differences were observed for the three parameters between the LFD and HFD + Vitexin groups.

3.4. Vitexin Reduced Liver Fat Content. The H&E staining results (Figure 3(a)) directly showed the difference of lipid content in the liver tissue in each group of mice. Mice fed with HFD had higher liver fat content than mice fed with the

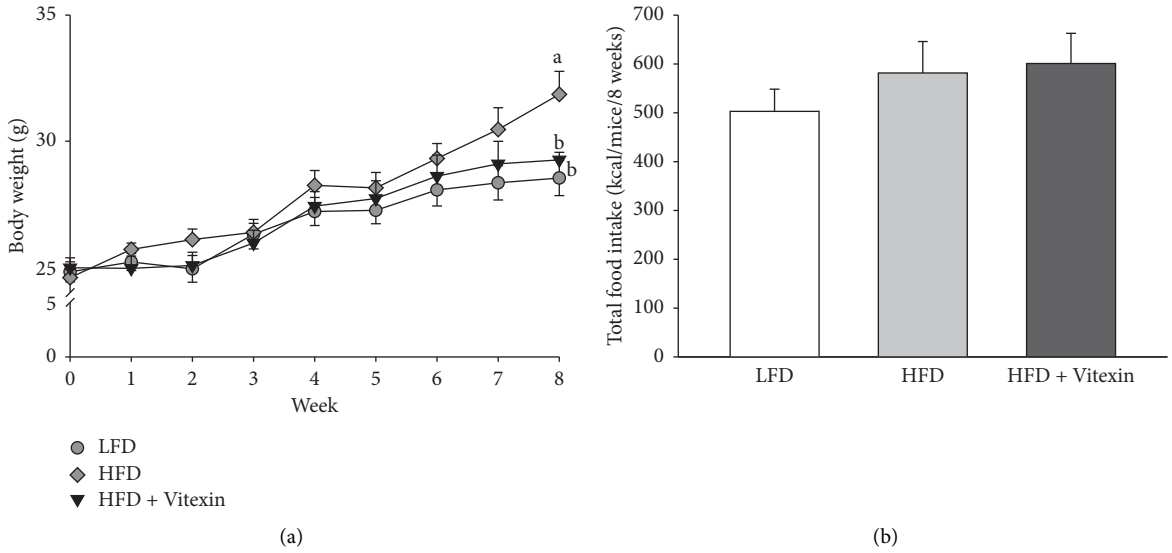

Figure 1: Influence of vitexin on body weight and food intake. Mice were fed with low-fat diet (LFD), high-fat diet (HFD), or HFD supplemented with 5 mg vitexin/kg BW/day (HFD + Vitexin) for 8 weeks. (a) Body weight monitored weekly; (b) total food intake. Numbers indicate mean ± SE ($n = 8 - 9$ for (a) and $n = 3$ for (b)). Means with different letters were significantly different at $P < 0.05$.

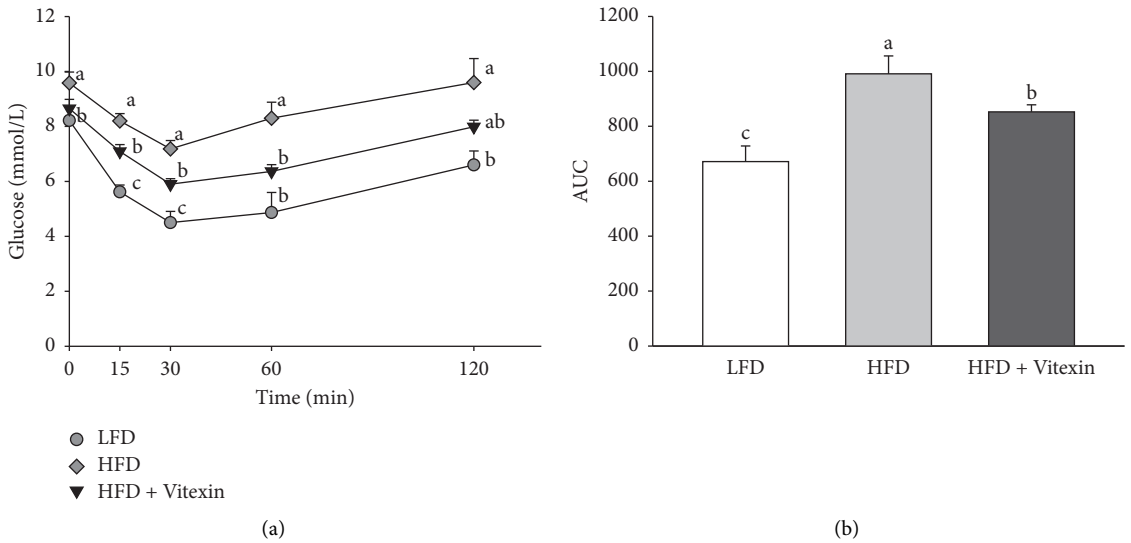

Figure 2: Continued.

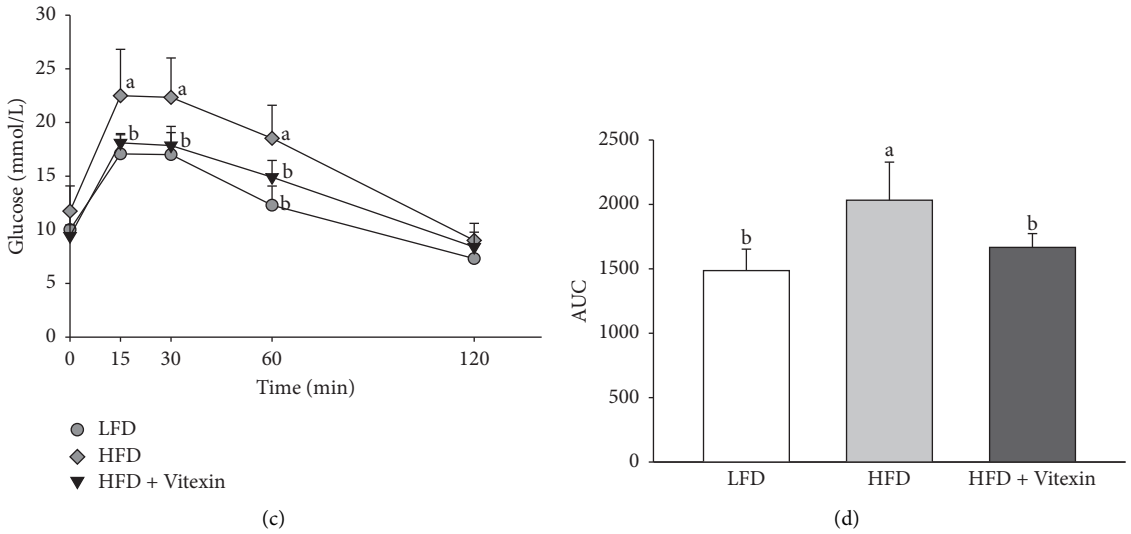

Figure 2: Influence of vitexin on insulin tolerance test (ITT) (a, b) and glucose tolerance test (GTT) (c, d). Mice were fed with low-fat diet (LFD), high-fat diet (HFD) or HFD supplemented with 5 mg vitexin/kg BW/day (HFD + Vitexin) for 8 weeks. Blood was collected from the tail vein, and glucose levels were determined at 0 min. Insulin (ITT) or glucose solutions (GTT) were subsequently administered by intraperitoneal injection, and the glucose level was further measured at 15, 30, 60, and 120 min after injection. Data were expressed as the mean ± SE ($n = 5 - 7$). Means with different letters were significantly different at $P < 0.05$.

Table 1: Serum parameters.

	LFD	HFD	HFD + Vitexin
Glucose (mg/dl)	162.0 ± 5.7	202.6 ± 4.3*	175.1 ± 9.6#
TG (mg/dl)	52.5 ± 5.0	80.3 ± 3.0*	66.3 ± 2.7#
TNF-α (pg/ml)	18.1 ± 2.9	49.3 ± 6.6*	31.9 ± 2.7#

Serum levels of glucose, TG, and proinflammatory cytokines including TNF-α in mice fed with a LFD, a HFD and a HFD with 5 mg/kg BW/day vitexin. LFD, low-fat diet; HFD, high-fat diet; HFD + Vitexin, high-fat diet plus vitexin at 5 mg/kg BW/day. Values represent means ± SE ($n = 8 - 9$). *$P < 0.05$ vs. LFD; #$P < 0.05$ vs. HFD.

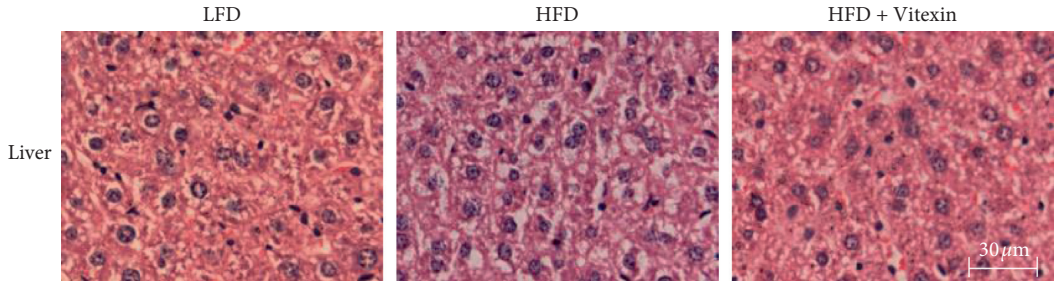

Figure 3: Continued.

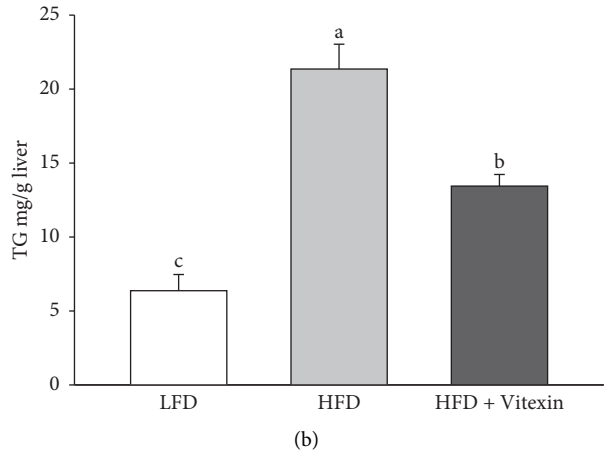

Figure 3: Effects of vitexin on liver morphology and triglyceride level. Mice were fed with low-fat diet (LFD), high-fat diet (HFD) or HFD containing 5 mg vitexin/kg BW/day (HFD + Vitexin) for 8 weeks. (a) Representative pictures of the liver after H&E staining; (b) liver triglyceride. Data were expressed as the mean ± SE ($n = 4$). Means with different letters were significantly different at $P < 0.05$.

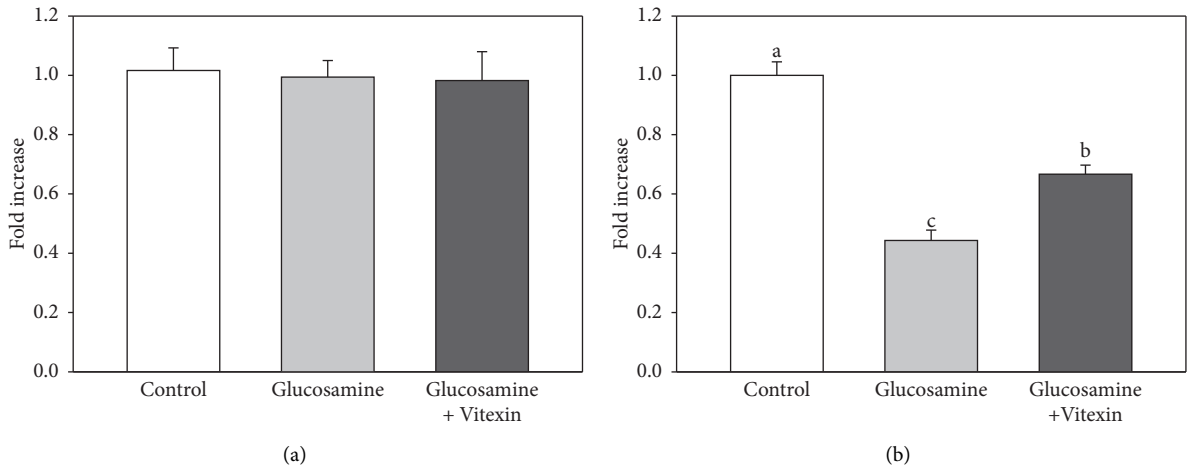

Figure 4: Influence of vitexin on cell viability and glucose uptake in HepG2 cells. (a) Cell viability; (b) triglyceride content. Numbers represent mean ± SE ($n = 3$). Means with different letters were significantly different at $P < 0.05$.

LFD, and the liver fat content was significantly reduced by vitexin treatment (Figure 3(b)).

3.5. Influence of Vitexin and Glucosamine on Cell Viability and Glucose Uptake in HepG2 Cells. Glucosamine (18 mM) and vitexin (20 μM) did not affect cell viability (Figure 4(a)). Reduced glucose uptake is an important marker of insulin resistance [26]. Glucosamine reduced glucose uptake by 56% compared to the control, while vitexin recovered glucose uptake by 50% compared to the glucosamine group (Figure 4(b)). These results suggested that vitexin alleviated glucose uptake reduction induced by glucosamine.

4. Discussion

Our present research demonstrated that vitexin improved HFD-induced insulin resistance in C57BL/6J male mice and recovered glucosamine-induced glucose uptake reduction.

In the present study, vitexin significantly recovered insulin tolerance and glucose tolerance impaired by HFD, and it increased glucose uptake reduced by glucosamine treatment, which are consistent with a previous study showing that oral administration of 1 to 200 mg vitexin/kg body weight effectively reduced the blood glucose level in sucrose-loaded mice [27, 28]. Excessive accumulation of fat and insulin resistance is closely linked with inflammation, as with excess TNF-α release [29]. Vitexin contained in mung bean extracts reduced the intramuscular TNF-α in KK-Ay diabetic mice [30]. Vitexin also inhibited TNF-α production in LPS-treated rats and pancreatic β-cells [31]. Consistent with the studies, the current research demonstrated that vitexin potently reduced the serum TNF-α level induced by a HFD in C57BL/6J mice.

Knowledge of serum vitexin concentration in human metabolism is limited, while the bioavailability of vitexin is relatively low [32]. The absolute bioavailability of vitexin is only around 4.9% when rats are orally administered with

30 mg/kg vitexin [33]. The vitexin concentration we used in the current *in vitro* study might be relatively high. Studies to increase vitexin's bioavailability are therefore necessary to better utilize vitexin as a functional food ingredient.

In summary, vitexin improved HFD-triggered insulin resistance and reduced hepatic fat accumulation in C57 BL/6J mice. Therefore, vitexin can be considered as a potential functional food ingredient which may be combined with preventive strategies to alleviate insulin resistance and type 2 diabetes.

Abbreviations

HFD:	High-fat diet
LFD:	Low-fat diet
HFD + vitexin:	HFD with 5 mg vitexin/kg BW/day
AKT:	Protein kinase B
AUC:	Area under the curve
DMEM:	Dubelco's modified Eagle's medium
FBS:	Fetal bovine serum
GPx:	Glutathione peroxidase
GTT:	Glucose tolerance test
ITT:	Insulin tolerance test
2-NBDG:	2-(N-(7-Nitrobenz-2-oxa-1,3-diazol-4-yl) amino)-2-deoxyglucose
PBS:	Phosphate-buffered saline
RIPA:	Radioimmunoprecipitation assay
TG:	Triglyceride
TNF-α:	Tumor necrosis factor.

Data Availability

The data used to support the findings of this study are available from the corresponding author upon request.

Conflicts of Interest

The authors declare that they have no conflicts of interest.

References

[1] N. M. Maruthur, "The growing prevalence of type 2 diabetes: increased incidence or improved survival?" *Current Diabetes Reports*, vol. 13, no. 6, pp. 786–794, 2013.

[2] M. H. Park and J.-S. P. Han, "Padina arborescens ameliorates hyperglycemia and dyslipidemia in C57BL/KsJ-db/db mice, a model of type 2 diabetes mellitus," *Journal of Medicinal Food*, vol. 18, no. 10, pp. 1088–1094, 2015.

[3] M. Flamment, E. Hajduch, P. Ferré, and F. Foufelle, "New insights into ER stress-induced insulin resistance," *Trends in Endocrinology & Metabolism*, vol. 23, no. 8, pp. 381–390, 2012.

[4] D. Zhu, Y. Wang, Q. Du, Z. Liu, and X. Liu, "Cichoric acid reverses insulin resistance and suppresses inflammatory responses in the glucosamine-induced HepG2 cells," *Journal of Agricultural and Food Chemistry*, vol. 63, no. 51, pp. 10903–10913, 2015.

[5] J. Xu, M. Ma, and W. M. Purcell, "Characterisation of some cytotoxic endpoints using rat liver and HepG2 spheroids as in vitro models and their application in hepatotoxicity studies. II. Spheroid cell spreading inhibition as a new cytotoxic marker," *Toxicology and Applied Pharmacology*, vol. 189, no. 2, pp. 112–119, 2003.

[6] P. J. Klover and R. A. Mooney, "Hepatocytes: critical for glucose homeostasis," *The International Journal of Biochemistry & Cell Biology*, vol. 36, no. 5, pp. 753–758, 2004.

[7] S. Ding, J. Jiang, Z. Wang et al., "Resveratrol reduces the inflammatory response in adipose tissue and improves adipose insulin signaling in high-fat diet-fed mice," *Peer-Reviewed journal*, vol. 6, Article ID e5173, 2018.

[8] M. Latreille, M.-K. Laberge, G. Bourret, L. Yamani, and L. Larose, "Deletion of Nck1 attenuates hepatic ER stress signaling and improves glucose tolerance and insulin signaling in liver of obese mice," *American Journal of Physiology-Endocrinology and Metabolism*, vol. 300, no. 3, pp. E423–E434, 2011.

[9] M. Liang, W. Xu, W. Zhang et al., "Quantitative LC/MS/MS method and in vivo pharmacokinetic studies of vitexin rhamnoside, a bioactive constituent on cardiovascular system from hawthorn," *Biomedical Chromatography*, vol. 21, no. 4, pp. 422–429, 2007.

[10] T. Siciliano, N. De Tommasi, I. Morelli, and A. Braca, "Study of flavonoids of Sechium edule(jacq) swartz (cucurbitaceae) different edible organs by liquid chromatography photodiode array mass spectrometry," *Journal of Agricultural and Food Chemistry*, vol. 52, no. 21, pp. 6510–6515, 2004.

[11] K. Ganesan and B. Xu, "A critical review on phytochemical profile and health promoting effects of mung bean (*Vigna radiata*)," *Food Science and Human Wellness*, vol. 7, no. 1, pp. 11–33, 2018.

[12] D. Kumar, V. Arya, Z. A. Bhat, N. A. Khan, and D. N. Prasad, "The genus crataegus: chemical and pharmacological perspectives," *Revista Brasileira de Farmacognosia*, vol. 22, no. 5, pp. 1187–1200, 2012.

[13] E. Díaz-de-Cerio, V. Verardo, A. Fernández-Gutiérrez, and A. M. Gómez-Caravaca, "New insight into phenolic composition of chayote (sechium edule (jacq.) sw.)," *Food Chemistry*, vol. 295, pp. 514–519, 2019.

[14] E. F. Vieira, O. Pinho, I. M. P. L. V. O. Ferreira, and C. Delerue-Matos, "Chayote (sechium edule): a review of nutritional composition, bioactivities and potential applications," *Food Chemistry*, vol. 275, pp. 557–568, 2019.

[15] S. M. Borghi, T. T. Carvalho, L. Staurengo-Ferrari et al., "Vitexin inhibits inflammatory pain in mice by targeting TRPV1, oxidative stress, and cytokines," *Journal of Natural Products*, vol. 76, no. 6, pp. 1141–1149, 2013.

[16] S. Nurdiana, Y. M. Goh, H. Ahmad et al., "Changes in pancreatic histology, insulin secretion and oxidative status in diabetic rats following treatment with Ficus deltoidea and vitexin," *BMC Complementary and Alternative Medicine*, vol. 17, p. 290, 2017.

[17] A. Seyedan, Z. Mohamed, M. A. Alshagga, S. Koosha, and M. A. Alshawsh, "Cynometra cauliflora Linn. Attenuates metabolic abnormalities in high-fat diet-induced obese mice," *Journal of Ethnopharmacology*, vol. 236, pp. 173–182, 2019.

[18] Z. Liu, I. Y. Patil, T. Jiang et al., "High-fat diet induces hepatic insulin resistance and impairment of synaptic plasticity," *PLoS One*, vol. 10, Article ID e0128274, 2015.

[19] Q. Sun, X. Xiao, Y. Kim et al., "Imidacloprid promotes high fat diet-induced adiposity and insulin resistance in male C57bl/6J mice," *Journal of Agricultural and Food Chemistry*, vol. 64, no. 49, pp. 9293–9306, 2016.

[20] Y. Peng, Q. Sun, W. Xu et al., "Vitexin ameliorates high fat diet-induced obesity in male C57BL/6J mice via the AMPK*x*-

mediated pathway," *Food & Function*, vol. 10, no. 4, pp. 1940–1947, 2019.

[21] Q. Sun, W. Qi, X. Xiao et al., "Imidacloprid promotes high fat diet-induced adiposity in female C57bl/6J mice and enhances adipogenesis in 3T3-L1 adipocytes via the AMPKα-mediated pathway," *Journal of Agricultural and Food Chemistry*, vol. 65, no. 31, pp. 6572–6581, 2017.

[22] J. S. Yang, W. Qi, R. Farias-Pereira et al., "Permethrin and ivermectin modulate lipid metabolism in steatosis-induced HepG2 hepatocyte," *Food and Chemical Toxicology*, vol. 125, pp. 595–604, 2019.

[23] L. Yuan, J. Lin, Y. Xu et al., "Deltamethrin promotes adipogenesis via AMPKα and ER stress-mediated pathway in 3T3- L1 adipocytes and *Caenorhabditis elegans*," *Food and Chemical Toxicology*, vol. 134, Article ID 110791, 2019.

[24] T. Mosmann, "Rapid colorimetric assay for cellular growth and survival: application to proliferation and cytotoxicity assays," *Journal of Immunological Methods*, vol. 65, no. 1-2, pp. 55–63, 1983.

[25] Y. Peng, Q. Sun, and Y. Park, "Chicoric acid promotes glucose uptake and Akt phosphorylation via AMP-activated protein kinase α-dependent pathway," *Journal of Functional Foods*, vol. 59, pp. 8–15, 2019.

[26] W. Y. Zhang, J.-J. Lee, I.-S. Kim, Y. Kim, and C.-S. Myung, "Stimulation of glucose uptake and improvement of insulin resistance by aromadendrin," *Pharmacology*, vol. 88, no. 5-6, pp. 266–274, 2011.

[27] C. Y. Choo, N. Y. Sulong, F. Man, and T. W. Wong, "Vitexin and isovitexin from the Leaves of Ficus deltoidea with in-vivo α-glucosidase inhibition," *Journal of Ethnopharmacology*, vol. 142, no. 3, pp. 776–781, 2012.

[28] W. Xu, M. Xiao, J. Li et al., "Hepatoprotective effects of di Wu Yang Gan: a medicinal food against CCl4-induced hepatotoxicity in vivo and in vitro," *Food Chemistry*, vol. 327, Article ID 127093, 2020.

[29] M. S. Ellulu, I. Patimah, H. Khaza'ai, A. Rahmat, and Y. Abed, "Obesity and inflammation: the linking mechanism and the complications," *Archives of Medical Science*, vol. 4, pp. 851–863, 2017.

[30] I. Kang, S. Choi, T. J. Ha et al., "Effects of mung bean (*Vigna radiata L.*) ethanol extracts decrease proinflammatory cytokine-induced lipogenesis in the KK-ay diabese mouse model," *Journal of Medicinal Food*, vol. 18, no. 8, pp. 841–849, 2015.

[31] F. Wang, J. Yin, Y. Ma, H. Jiang, and Y. Li, "Vitexin alleviates lipopolysaccharide-induced islet cell injury by inhibiting HMGB1 release," *Molecular Medicine Reports*, vol. 15, no. 3, pp. 1079–1086, 2017.

[32] H.-F. Xue, Z.-M. Ying, W.-J. Zhang, Y.-H. Meng, X.-X. Ying, and T.-G. Kang, "Hepatic, gastric, and intestinal first-pass effects of vitexin in rats," *Pharmaceutical Biology*, vol. 52, no. 8, pp. 967–971, 2014.

[33] Y. Wang, "Pharmacokinetics of vitexin in rats after intravenous and oral administration," *African Journal of Pharmacy and Pharmacology*, vol. 6, 2012.